FLOW-HABITAT RELATIONSHIPS FOR JUVENILE FALL/SPRING-RUN CHINOOK SALMON AND STEELHEAD/RAINBOW TROUT REARING IN THE YUBA RIVER

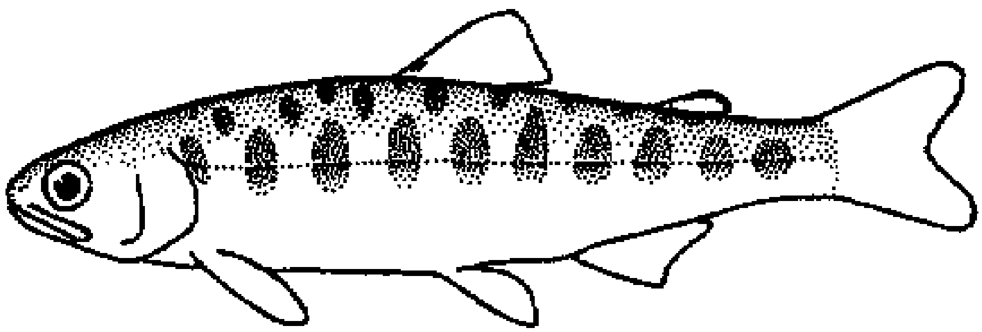

U. S. Fish and Wildlife Service
Sacramento Fish and Wildlife Office
2800 Cottage Way, Room W-2605
Sacramento, CA 95825

Prepared by staff of
The Energy Planning and Instream Flow Branch

FLOW-HABITAT RELATIONSHIPS FOR FALL/SPRING-RUN CHINOOK SALMON AND STEELHEAD/RAINBOW TROUT JUVENILE REARING IN THE YUBA RIVER

PREFACE

The following is the final report for the U.S. Fish and Wildlife Service's investigations on anadromous salmonid rearing habitat in the Yuba River between Englebright Dam and the Feather River, part of the Central Valley Project Improvement Act (CVPIA) Instream Flow Investigations, a 6-year effort which began in October, 2001.[1] Title 34, Section 3406(b)(1)(B) of the CVPIA, P.L. 102-575, requires the Secretary of the Interior to determine instream flow needs for anadromous fish for all Central Valley Project controlled streams and rivers, based on recommendations of the U.S. Fish and Wildlife Service after consultation with the California Department of Fish and Game. The purpose of these investigations is to provide scientific information to the U.S. Fish and Wildlife Service Central Valley Project Improvement Act Program to assist in developing such recommendations for Central Valley rivers.

Written comments or information can be submitted to and raw data in digital format can be obtained from:

Mark Gard, Senior Biologist
Energy Planning and Instream Flow Branch
U.S. Fish and Wildlife Service
Sacramento Fish and Wildlife Office
2800 Cottage Way, Room W-2605
Sacramento, CA 95825

Mark_Gard@fws.gov

[1] This program is a continuation of a 7-year effort, also titled the Central Valley Project Improvement Act Instream Flow Investigations, which ran from February 1995 through September 2001.

ACKNOWLEDGMENTS

The fieldwork described herein was conducted by Ed Ballard, Mark Gard, Rick Williams and Bill Pelle with assistance from Terry Adelsbach, Susan Hill, Jennifer Bain, Debbie Giglio, Jonathan Foster, Nick Hindman, Richard DeHaven, Steve Thomas and staff of the U.S. Bureau of Reclamation's Surveys and Mapping Branch. Data analysis and report preparation were performed by Ed Ballard, Mark Gard and Bill Pelle. Funding was provided by the Central Valley Project Improvement Act.

ABSTRACT

Flow-habitat relationships were derived for fall/spring-run Chinook salmon and steelhead/rainbow trout fry and juvenile rearing in the lower Yuba River between Englebright Dam and the Feather River. A 2-dimensional hydraulic and habitat model (River2D) was used for this study to model available habitat. Habitat was modeled for eight sites above Daguerre Point Dam and ten sites below Daguerre Point Dam which were representative of the mesohabitat types available in the two segments for fall/spring-run Chinook salmon and steelhead/rainbow trout fry and juvenile rearing. Bed topography was collected for these sites using a total station in dry and shallow portions of the sites and with an Acoustic Doppler Current Profiler (ADCP) in the deeper portions of the site. Additional data were collected to develop stage-discharge relationships at the upstream and downstream end of the sites as an input to River2D. Velocities measured at shallow locations in the site, along with velocities measured by the ADCP, were used to validate the velocity predictions of River2D. The raw topography data were refined by defining breaklines going up the channel along features such as thalwegs, tops of bars and bottoms of banks. A finite element computational mesh was then developed to be used by River2D for hydraulic calculations. River2D hydraulic data were calibrated by adjusting bed roughnesses until simulated water surface elevations matched measured water surface elevations. The calibrated files for each site were used in River2D to simulate hydraulic characteristics for 30 simulation flows. Habitat suitability criteria (HSC) were developed from depth, velocity, adjacent velocity and cover measurements collected at the locations of 178 fall/spring-Chinook salmon fry, 39 fall/spring-Chinook salmon juvenile, 195 steelhead/rainbow trout fry and 74 steelhead/rainbow trout juvenile observations. The horizontal locations of a subset of these observations, located in seven of the eighteen study sites, were measured with a total station to use in biological verification of the habitat models. Logistic regression was used to develop the HSC. Transferability tests were used to determine if HSC from the Sacramento River would transfer to fall/spring-Chinook salmon and steelhead/rainbow trout juveniles. Sacramento River cover HSC transferred to both species, depth HSC transferred only to steelhead/rainbow trout, and velocity and adjacent velocity HSC did not transfer to either species. Biological verification was accomplished by testing, with a one-tailed Mann-Whitney U test, whether the combined suitability predicted by River2D was higher at fry and juvenile locations versus at locations where fry and juveniles were absent. The biological verification did not show a significant difference between the suitability of occupied and unoccupied locations. The peak of the flow habitat relationship curves developed in this study are the following. In the Above Daguerre Segment, the 2-D model predicts the highest total WUA for fall/spring-run Chinook salmon fry at 4,300 cfs and for fall/spring-run Chinook salmon juveniles at 1,300 cfs. In the Above Daguerre Segment, the 2-D model predicts the highest total WUA for steelhead/rainbow trout fry at 400 cfs and for steelhead/rainbow trout juveniles at 1,000 cfs. In the Below Daguerre Segment, the 2-D model predicts the highest total WUA for fall/spring-run Chinook salmon fry rearing at 4,500 cfs and for fall/spring-run Chinook salmon juvenile rearing at 2,000 cfs. In the Below Daguerre Segment, the 2-D model predicts the highest total WUA for steelhead/rainbow trout fry rearing at 500 cfs and for steelhead/rainbow trout juvenile rearing at 2,000 cfs.

TABLE OF CONTENTS

LIST OF FIGURES

LIST OF TABLES

INTRODUCTION

In response to substantial declines in anadromous fish populations, the Central Valley Project Improvement Act provided for enactment of all reasonable efforts to double sustainable natural production of anadromous fish stocks including the four races of Chinook salmon (fall, late-fall, winter, and spring runs), steelhead, white and green sturgeon, American shad and striped bass. The Yuba River is a major tributary of the Feather River, located in the Sacramento River basin portion of the Central Valley of California. The Lower Yuba River, between Englebright Dam and the Feather River confluence, is a major contributor to anadromous salmonid production in the Central Valley and supports the largest stock of Chinook salmon that is not supplemented by hatcheries. The focus of this study was the Lower Yuba River, the only portion of the Yuba River accessible for spring and fall-run Chinook salmon and steelhead spawning and juvenile rearing. For the Yuba River downstream of Englebright Dam, the Central Valley Project Improvement Act Anadromous Fish Restoration Plan calls for improved flows for all life history stages of Chinook salmon and steelhead (U.S. Fish and Wildlife Service 1995) as a high priority action to restore anadromous fish populations in the Yuba River. Subsequently, Yuba County Water Agency, collaboratively with the National Marine Fisheries Service, the U.S. Fish and Wildlife Service, the California Department of Fish and Game and Non-Governmental Organizations, developed a comprehensive set of improved flow regimes, which now are the Flow Schedules of the Lower Yuba River Accord (HDR/SWRI 2007).

In June 2001, the U.S. Fish and Wildlife Service prepared a study proposal to identify the instream flow requirements for anadromous fish in certain streams within the Central Valley of California, including the Yuba River. The Yuba River was selected for study because of a number of factors, including the presence of listed threatened or endangered species, the number of target species or races, whether current instream flows were inadequate and if there was an upcoming hydroelectric project relicensing. The goal of this study was to produce models predicting habitat-discharge relationships in the Yuba River for fall/spring-run Chinook salmon and steelhead/rainbow trout rearing that meet, to the extent feasible, the levels of accuracy specified in the methods section. The tasks and their associated objectives are given in Table 1.

To develop a flow regime which will accommodate the habitat needs of anadromous species inhabiting streams, it is necessary to determine the relationship between streamflow and habitat availability for each life stage of each species. In this study, we apply the models and techniques contained within the Instream Flow Incremental Methodology (IFIM) to establish these relationships. The IFIM is a habitat-based tool developed by the U.S. Fish and Wildlife Service to assess instream flow problems (Bovee 1996). The decision variable generated by the IFIM is total habitat, in units of Weighted Useable Area (WUA), for each life stage (fry, juvenile and spawning) of each evaluation species (or race as applied to Chinook salmon). The process of computing habitat starts with developing a spatially-explicit index, based on hydrodynamic and habitat variables. The index is multiplied by area to compute WUA. Habitat incorporates both

Table 1. Study tasks and associated objectives.

Task	Objective
study segment selection	determine the number and aerial extent of study segments
habitat mapping	delineate the aerial extent and habitat type of mesohabitat units
field reconnaissance and study site selection	select study sites which adequately represent the mesohabitat types present in the study segments
transect placement (study site setup)	delineate the upstream and downstream boundaries of the study sites, coinciding with the boundaries of the mesohabitat units selected for study
hydraulic and structural data collection	collect the data necessary to develop stage-discharge relationships at the upstream and downstream boundaries of the site, to develop the site topography and cover distribution, and to use in validating the velocity predictions of the hydraulic model of the study sites
hydraulic model construction and calibration	predict depths and velocities throughout the study sites at a range of simulation flows
habitat suitability criteria data collection	collect depth, velocity, adjacent velocity and cover data for fall/spring-run Chinook salmon and steelhead/rainbow trout to be used in developing habitat suitability criteria
biological verification data collection	record the horizontal location of fry and juveniles within the study sites to use in the biological verification of the habitat models of the study sites
habitat suitability criteria development	develop indices to translate the output of the hydraulic models into habitat quality
biological verification	determine if the combined suitability of locations with fry and juveniles had higher suitability than those of unoccupied locations
habitat simulation	compute weighted useable area for each study site over a range of simulation flows using the habitat suitability criteria and the output of the hydraulic model

macro- and microhabitat features. Macrohabitat features include longitudinal changes in channel characteristics, base flow, water quality, and water temperature. Microhabitat features include the hydraulic and structural conditions (depth, velocity, substrate or cover) which define the actual living space of the organisms. The total habitat available to a species/life stage at any streamflow is the area of overlap between available microhabitat and suitable macrohabitat conditions.

Conceptual models are essential for establishing theoretical or commonly-accepted frameworks, upon which data collection and scientific testing can be interpreted meaningfully. A conceptual model of the link between rearing habitat and population change (Figure 1) may be described as follows (Bartholow 1996, Bartholow et al 1993, Williamson et al 1993). Changes in flows result in changes in depths and velocities. These changes, in turn, along with the distribution of cover,

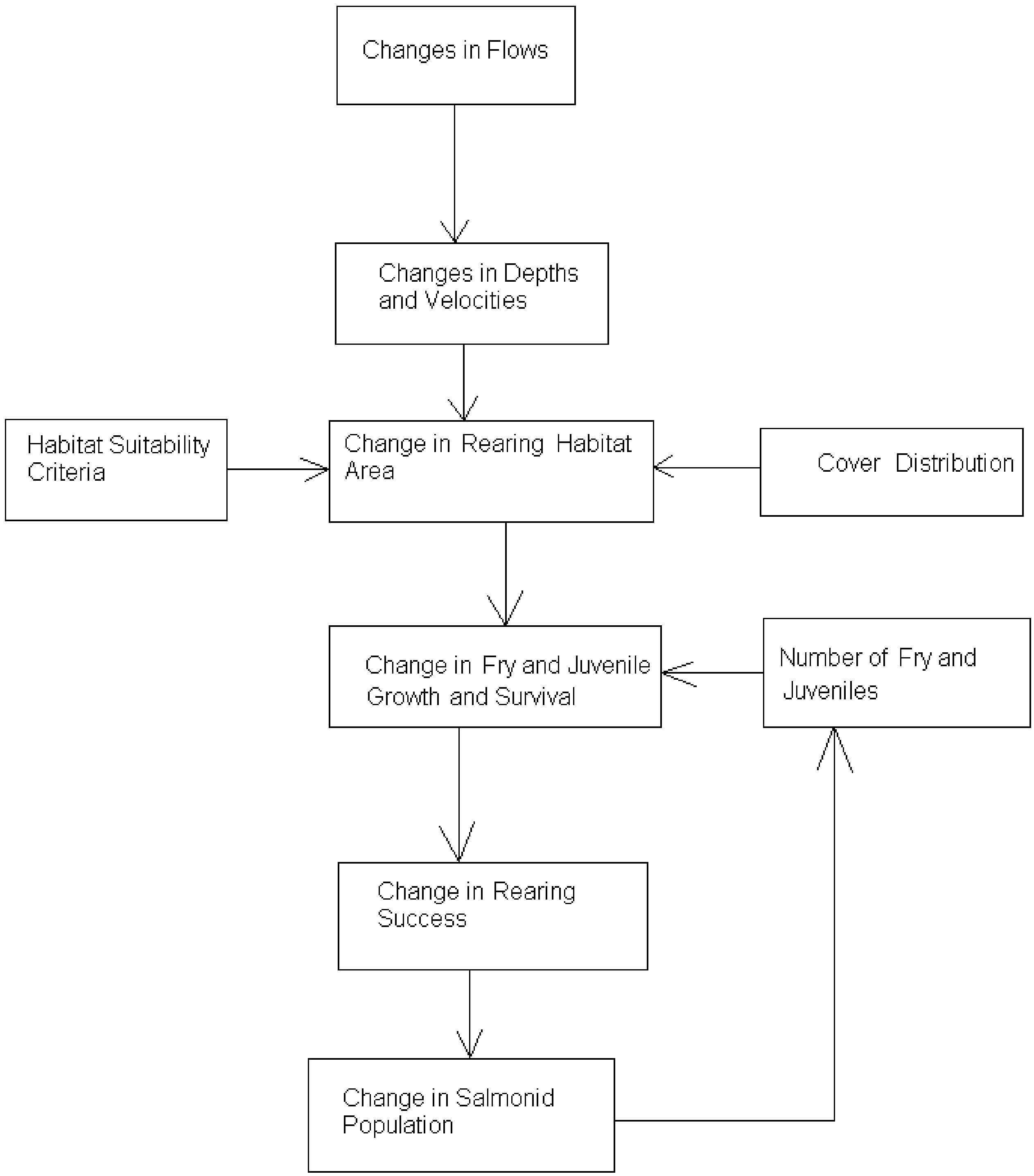

Figure 1. Conceptual model of the linkage between flow and salmonid populations.

alter the amount of habitat area for fry and juvenile rearing for anadromous salmonids. Changes in the amount of habitat for fry and juvenile rearing could affect rearing success through alterations in the conditions that favor fry and juvenile growth and promote survival. These alterations in rearing success could ultimately result in changes in salmonid populations. If a population is greatly under-seeded because of problems elsewhere (e.g., marine overharvest, pollution), instream flow is still needed to provide habitat for recovery. Instream flows should address the desired recovered population size because appropriation of water rights does not easily allow for adjusting flows upward to accommodate recovery once water rights have been allocated. It may not be reasonable to expect a population to track habitat or flows if the population is being depressed by other factors. When the other factors are alleviated, flows through habitat would impose a ceiling on the population.

There are a variety of alternative techniques available to quantify the functional relationship between flow and fry and juvenile rearing habitat availability, but they can be broken down into three general categories: 1) habitat modeling; 2) biological response correlations; and 3) demonstration flow assessment (Annear et al. 2002). Biological response correlations can be used to evaluate rearing habitat by examining juvenile production estimates at different flows (Hvidsten 1993). However, this method requires many years of data and it is difficult to separate out the effects of flows from year to year variation in escapement and other factors. Snorkel surveys are proposed to be conducted as part of the Lower Yuba River Accord. Although these data would be expected to provide insight into salmonid rearing habitat use, they would be too limited to use for determining instream flow needs. Demonstration flow assessments (CIFGS 2003) likewise use direct observation of river habitat conditions at several flows; at each flow, polygons of habitat are delineated in the field. Because the flow regime in the lower Yuba River is set by Federal Energy Regulatory Commission license requirements and water delivery demands made on the Yuba County Water Agency, demonstration flows cannot be conducted. Therefore, we chose to conduct habitat modeling for the lower Yuba River under a range of flows using data collected from representative study sites in the river. Modeling approaches are widely used to assess the effects of instream flows on fish habitat availability despite potential assumption, sampling, and measurement errors that, as in the other methods described above, can contribute to the uncertainty of results.

The range of Yuba River flows to be evaluated for management generally falls within the range of 150 cubic feet per second (cfs) downstream of Daguerre Point Dam (the lowest flow in the Yuba River Accord) and 400 cfs upstream of Daguerre Point Dam (the current State Water Resources Control Board minimum flow) to 4,170 cfs (the combined capacity of Narrows I and II). Accordingly, the range of study flows (400 to 4,500 cfs upstream Daguerre Point Dam and 150 to 4,500 cfs downstream of Daguerre Point Dam) encompasses the range of flows to be evaluated for management. The assumptions of this study are: 1) physical habitat is a limiting factor for salmonid populations in the Yuba River; 2) rearing habitat quality can be characterized by depth, velocity, adjacent velocity and cover; 3) the eighteen study sites are representative of anadromous salmonid rearing habitat in the Yuba River; and 4) theoretical equations of physical processes along with a description of stream bathymetry provide sufficient input to simulate velocity distributions through a study site.

METHODS

1. *Approach*

A two-dimensional hydraulic and habitat model, River2D Version 0.93 November 11, 2006 by P. Steffler, A. Ghanem, J. Blackburn and Z. Yang (Steffler and Blackburn 2002), was used for predicting Weighted Useable Area (WUA), instead of the Physical Habitat Simulation (PHABSIM[2]). River2D inputs include the bed topography and bed roughness, and the water surface elevation at the downstream end of the site. The amount of habitat present in the site is computed using the depths and velocities predicted by River2D, and the substrate and cover present in the site. River2D avoids problems of transect placement, since data are collected uniformly across the entire site (Gard 2009). River2D also has the potential to model depths and velocities over a range of flows more accurately than would PHABSIM because River2D takes into account upstream and downstream bed topography and bed roughness, and explicitly uses mechanistic processes (conservation of mass and momentum), rather than Manning's Equation and a velocity adjustment factor (Leclerc et al. 1995). Other advantages of River2D are that it can explicitly handle complex hydraulics, including transverse flows, across-channel variation in water surface elevations, and flow contractions/expansions (Ghanem et al. 1996, Crowder and Diplas 2000, Pasternack et al. 2004). With appropriate bathymetry data, the model scale is small enough to correspond to the scale of microhabitat use data with depths and velocities produced on a continuous basis, rather than in discrete cells. River2D, with compact cells, should be more accurate than PHABSIM, with long rectangular cells, in capturing longitudinal variation in depth, velocity and substrate. River2D should do a better job of representing patchy microhabitat features, such as gravel patches. The data for two-dimensional modeling can be collected with a stratified sampling scheme, with higher intensity sampling in areas with more complex or more quickly varying microhabitat features, and lower intensity sampling in areas with uniformly varying bed topography and uniform substrate. Bed topography and substrate mapping data can be collected at a very low flow, with the only data needed at high flow being water surface elevations at the up- and downstream ends of the site and flow, and edge velocities for validation purposes. In addition, alternative habitat suitability criteria, such as measures of habitat diversity, can be used.

[2] PHABSIM is the collection of one dimensional hydraulic and habitat models which can be used to predict the relationship between physical habitat availability and streamflow over a range of river discharges.

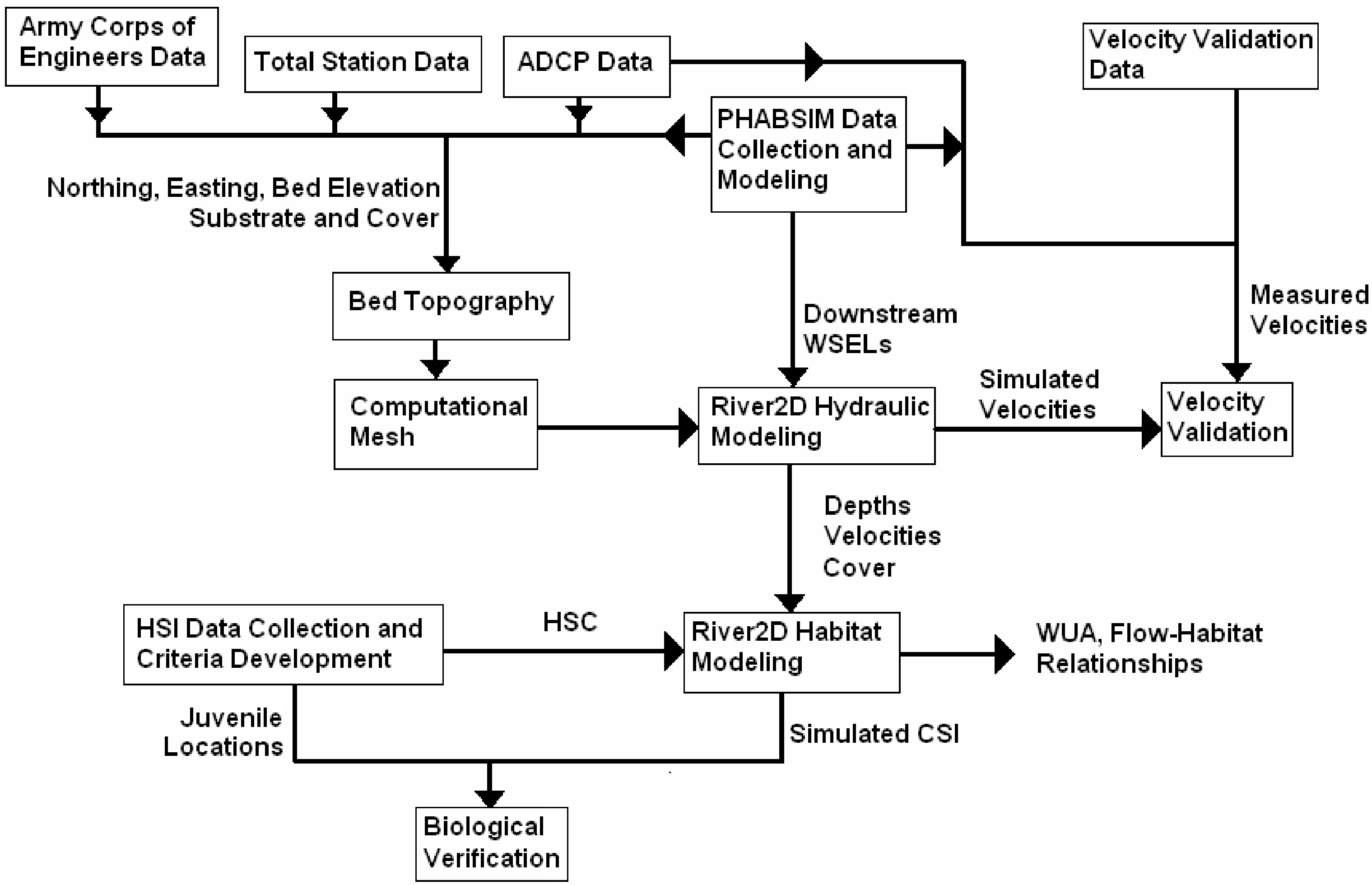

Figure 2. Flow diagram of data collection and modeling.

The upstream and downstream transects were modeled with the PHABSIM component of IFIM to provide water surface elevations as an input to the 2-D hydraulic and habitat model (River2D, Steffler and Blackburn 2002) used in this study (Figure 2). By calibrating the upstream and downstream transects with PHABSIM using the collected calibration water surface elevations (WSELs), we were able to predict the WSELs for these transects for the various simulation flows that were to be modeled using River2D. We calibrated the River2D models using the highest simulation flow. The highest simulation WSELs predicted by PHABSIM for the upstream and downstream transects were used for the upstream boundary condition (in addition to flow) and the downstream boundary condition. The PHABSIM-predicted WSEL for the upstream transect at the highest simulation flow was used to ascertain calibration of the River2D model at the highest simulation flow. After the River2D model was calibrated at the highest simulation flow, the WSELs predicted by PHABSIM for the downstream transect for each simulation flow were used as an input for the downstream boundary condition for River2D model production files for the simulation flows.

2. *Study Segment Delineation*

Study segments were delineated within the study reach of the Yuba River between Englebright Dam and the Feather River (Figure 3) based on differences in flow. Details on the methods used to delineate study segments are given in U.S. Fish and Wildlife Service (2010).

3. *Habitat Mapping*

Mesohabitat mapping was performed August 11-13, 2003. This work consisted of boating upstream from the confluence with the Feather River to the upstream end of the Narrows and hiking down from Englebright Dam to the upstream end of the Narrows, delineating the mesohabitat units. Using habitat typing protocols developed by the California Department of Fish and Game (CDFG) (Snider et al. 1992), the Yuba River was habitat mapped between the confluence with the Feather River and Englebright Dam. The CDFG habitat typing protocols designates 12 mesohabitat types: bar complex glides, bar complex pools, bar complex riffles, bar complex runs, flatwater glides, flatwater pools, flatwater riffles, flatwater runs, side channel glides, side channel pools, side channel riffles, and side channel runs (Table 2). Aerial photos were used in conjunction with direct observations to determine the aerial extent of each habitat unit. The location of the upstream and downstream boundaries of habitat units was recorded with a Global Positioning System (GPS) unit. The habitat units were also delineated on the aerial photos. Following the completion of the mesohabitat mapping on August 13, 2003, the mesohabitat types and number of habitat units of each habitat type in each segment were enumerated, and shapefiles of the mesohabitat units were created in a Geographic Information System (GIS) using the GPS data and the aerial photos. The area of each mesohabitat unit was computed in GIS from the above shapefiles.

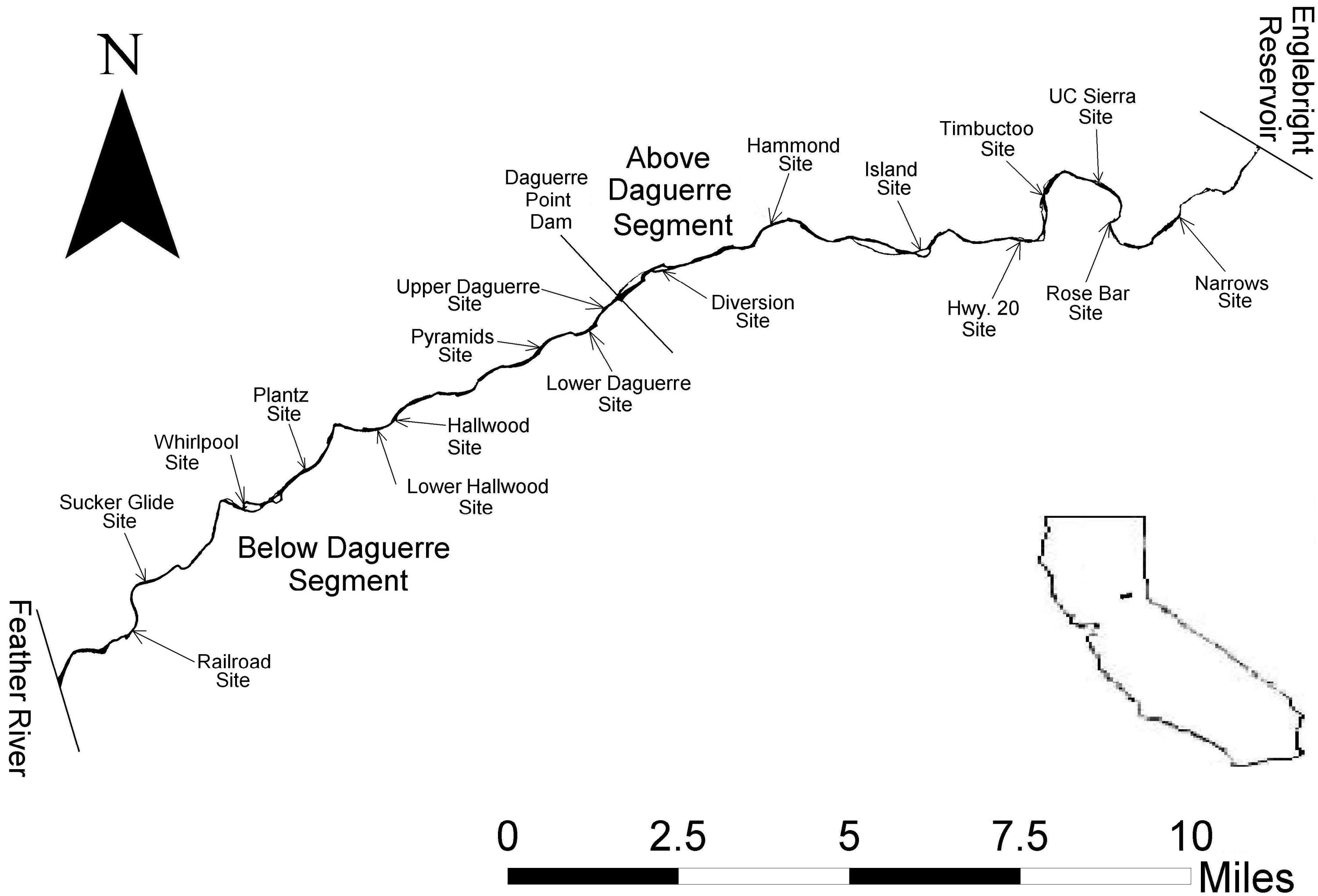

Figure 3. Yuba River stream segments and rearing study sites.

Table 2. Habitat type definitions.

Habitat Type	Definition
Bar Complex	Submerged and emergent bars are the primary feature, sloping cross-sectional channel profile.
Flatwater	Primary channel is uniform, simple and without gravel bars or channel controls, fairly uniform depth across channel.
Side Channel	Less than 20% of total flow.
Pool	Primary determinant is downstream control - thalweg gets deeper as go upstream from bottom of pool. Fine and uniform substrate, below average water velocity, above average depth, tranquil water surface.
Glide	Primary determinants are no turbulence (surface smooth, slow and laminar) and no downstream control. Low gradient, substrate uniform across channel width and composed of small gravel and/or sand/silt, depth below average and similar across channel width (but depth not similar across channel width for Bar Complex Glide), below average water velocities, generally associated with tails of pools or heads of riffles, width of channel tends to spread out, thalweg has relatively uniform slope going downstream.
Run	Primary determinants are moderately turbulent and average depth. Moderate gradient, substrate a mix of particle sizes and composed of small cobble and gravel, with some large cobble and boulders, above average water velocities, usually slight gradient change from top to bottom, generally associated with downstream extent of riffles, thalweg has relatively uniform slope going downstream.
Riffle	Primary determinants are high gradient and turbulence. Below average depth, above average velocity, thalweg has relatively uniform slope going downstream, substrate of uniform size and composed of large gravel and/or cobble, change in gradient noticeable.

4. *Field Reconnaissance and Study Site Selection*

Based on the results of habitat mapping, we selected eight juvenile habitat study sites that, together with the ten sites previously selected to study spawning habitat (U.S. Fish and Wildlife Service 2010), adequately represent the mesohabitat types present in each segment. The eight new study sites were placed in mesohabitat types that were not adequately represented in the ten previously selected study sites. Mesohabitat types were considered adequately represented by at least one mesohabitat unit of less common mesohabitat types and multiple mesohabitat units of more common mesohabitat types. As a result, the mesohabitat composition of the study sites, taken together, were roughly proportional to the mesohabitat composition of the entire reach. The eight new study sites were selected based on a stratified random selection method, where we randomly selected a habitat unit, out of all of the habitat units of that habitat type, for each habitat type which was not adequately represented in the spawning sites, to ensure unbiased selection of the study sites. On August 14, 2003, we visited the potential study sites that had been selected through this process to ascertain their suitability for 2-D modeling. Due to the logistical difficulties with accessing and transporting needed equipment above a large hydraulic barrier at the upper end of the Narrows (River Mile [RM] 22.6), the study sites were confined to downstream of that barrier. For the sites selected for modeling, the landowners along both riverbanks were identified and temporary entry permits were sent, accompanied by a cover letter, to acquire permission for entry onto their property during the course of the study.

5. *Transect Placement (study site set-up)*

Eight study sites (Figure 3) were established December 2003. Whenever possible, the study site boundaries (up- and downstream transects) were selected to coincide with the boundaries of the associated mesohabitat unit. The location of these boundaries was established during site setup by navigating to the points marked with the GPS unit during our mesohabitat mapping. In some cases, the upstream or downstream boundary had to be moved upstream or downstream to a location where the hydraulic conditions were more favorable to modeling (e.g., more linear direction of flow, more consistent water surface elevations from bank to bank).

For each study site, a transect was placed at the upstream and downstream end of the site. The downstream transect was modeled with PHABSIM to provide water surface elevations as an input to River2D. The upstream transect was used in calibrating River2D - bed roughnesses are adjusted until the WSEL at the top of the site predicted by River2D matches the WSEL predicted by PHABSIM. Transect pins (headpins and tailpins) were installed on each river bank above the 7,000 cfs water surface level using rebar driven into the ground and/or lag bolts placed in tree trunks. Survey flagging was used to mark the locations of each pin.

6. *Hydraulic and Structural Habitat Data Collection*

Vertical benchmarks were established at each site to serve as the reference elevations to which all elevations (streambed and water surface) were tied. Vertical benchmarks were tied together, using differential leveling, to achieve a level loop accuracy (ft) of at least 0.05 x (level loop distance [mi])$^{0.5}$. Vertical benchmarks consisted of lag bolts driven into trees or painted bedrock points. In addition, horizontal benchmarks (rebar driven into the ground) were established at each site for total station placement to serve as the reference locations to which all horizontal locations (northings and eastings) were tied when collecting bed topography data. The precise northing and easting coordinates and vertical elevations of two horizontal benchmarks were established for each site by the U.S. Bureau of Reclamation using real time kinematic survey-grade differential GPS. The elevations of these benchmarks were tied into the vertical benchmarks on our sites using differential leveling. Collection of site bed topography data relative to these values was used primarily to enable the incorporation of bed topography data collected for the Yuba River by the U.S. Army Corps of Engineers using photogrammetry and hydro-acoustic mapping.

Hydraulic and structural data collection began in December 2003 and was completed in April 2007. The precision and accuracy of the field equipment used for the hydraulic and structural data collection is given in Table 3. The data collected at the inflow and outflow transects included: 1) WSELs measured to the nearest 0.01 foot (0.003 m) at a minimum of three significantly different stream discharges using standard surveying techniques (differential leveling); 2) wetted streambed elevations determined by subtracting the measured depth from the surveyed WSEL at a measured flow; 3) dry ground elevations to points above bankfull discharge surveyed to the nearest 0.1 foot (0.031 m); 4) mean water column velocities measured at a mid-to-high-range flow at the points where bed elevations were taken; and 5) substrate[3] and cover classification at these same locations (Tables 4 and 5) and also where dry ground elevations were surveyed.

When conditions allowed, WSELs were measured along both banks and in the middle of each transect. Otherwise, the WSELs were measured along both banks. If the WSELs measured for a transect were within 0.1 foot (0.031 m) of each other, the WSELs at each transect were then derived by averaging the two to three values. If the WSEL differed by greater than 0.1 foot (0.031 m), the WSEL for the transect was selected based on which side of the transect we considered most representative of the flow conditions.

Depth and velocity measurements in portions of the transects with depths greater than 3 feet (0.91 meters) were made with a RD Instruments[R] Broad-Band Acoustic Doppler Current Profiler (ADCP)[4] mounted on a boat, while depths and velocity measurements in shallower areas were made by wading with a wading rod equipped with a Marsh-McBirney[R] model 2000 or Price AA velocity meter until the water became sufficiently deep to operate the ADCP (approximately 3 feet [0.91 meters]). The ADCP settings used are shown in Table 6. The distance intervals of each depth and velocity measurement from the headpin or tailpin were measured using a hand held laser range finder[5]. At the location of the last depth and velocity measurement made while wading, a buoy was placed to serve as a starting point for the ADCP. The boat was then positioned so that the ADCP started operation at the buoy, and water depth and velocity data were collected across the transect up to the location near the opposite bank where water depths of approximately 3 feet (0.91 meters) were reached. A buoy was placed at the location where ADCP operation ceased and the procedure used for measuring depths and velocities in shallow water was repeated until the far bank water's edge was reached. Additional details on the ADCP operation are given in Gard and Ballard (2003).

---

3 Substrate was only used to calculate bed roughness.

4 For a portion of the Narrows site data collected between the transects, we used a RD Instruments[R] Rio Grande ADCP.

5 The stations for the dry ground elevation measurements were also measured using the hand held laser range finder.

Table 3. Precision and accuracy of field equipment. The precision of the ADCP is the statistical uncertainty (1 σ) of the horizontal velocities, and varies depending on the depth cell size and mode. A blank means that that information is not available.

Equipment	Parameter	Precision	Accuracy
ADCP	Velocity	7.7 – 37 cm/s	0.2% ± 0.2 cm/s
ADCP	Depth		4%
Marsh-McBirney	Velocity		± 2% + 1.5 cm/s
Price AA	Velocity		± 6% at 7.6 cm/s to ± 1.5% at vel > 46 cm/s
Total Station	Slope Distance	± (5ppm + 5) mm	
Total Station	Angle		4 sec
Electronic Distance Meter	Slope Distance		1.5 cm
Autolevel	Elevation		0.3 cm
GPS	Horizontal Location		3 – 7 m

Table 4. Substrate codes, descriptors and particle sizes.

Code	Type	Particle Size (inches)
0.1	Sand/Silt	< 0.1 (0.25 cm)
1	Small Gravel	0.1 – 1 (0.25 – 2.5 cm)
1.2	Medium Gravel	1 – 2 (2.5 – 5 cm)
1.3	Medium/Large Gravel	1 – 3 (2.5 – 7.5 cm)
2.3	Large Gravel	2 – 3 (5 – 7.5 cm)
2.4	Gravel/Cobble	2 – 4 (5 – 10 cm)
3.4	Small Cobble	3 – 4 (7.5 – 10 cm)
3.5	Small Cobble	3 – 5 (7.5 – 12.5 cm)
4.6	Medium Cobble	4 – 6 (10 – 15 cm)
6.8	Large Cobble	6 – 8 (15 – 20 cm)
8	Large Cobble	8 – 10 (20 – 25 cm)
9	Boulder/Bedrock	> 12 (30 cm)
10	Large Cobble	10 – 12 (25 – 30 cm)

Table 5. Cover coding system.

Cover Category	Cover Code
No cover	0
Cobble	1
Boulder	2
Fine woody vegetation (< 1" diameter)	3
Fine woody vegetation + overhead	3.7
Branches	4
Branches + overhead	4.7
Log (> 1' diameter)	5
Log + overhead	5.7
Overhead cover (> 2' above substrate)	7
Undercut bank	8
Aquatic vegetation	9
Aquatic vegetation + overhead	9.7
Rip-rap	10

Substrate and cover classification was accomplished using underwater video equipment along the deepwater portion of the transects (generally those areas with depths greater than 10 feet [3.05 meters]) and visually in shallow water. The underwater video equipment consists of two waterproof remote cameras mounted on an aluminum frame with two 30-pound lead bombs. One camera was mounted facing forward, depressed at a 45° angle from the horizontal, and the second camera was mounted such that it faced directly down at a 90° angle from the horizontal. The camera mounted at a 45° angle was used for distinguishing changes in substrate size and cover types, while the camera mounted at 90° was used for assessing substrate size and cover type. The frame is attached to a cable/winch assembly, while a separate cable from the remote cameras is connected to two TV monitors on the boat. The two monitors are used by the winch operator to distinguish changes in substrate size and cover type and determine the substrate size and cover type. The substrate and cover were visually assessed by one observer based on a

Table 6. Configuration (CFG) files used for ADCP data. The first two (for the Rio Grande ADCP) or four (for the Broad-Band ADCP) characters of the ADCP traverse[6] designates which CFG file (containing the ADCP settings) was used for the traverses. WT is the water track transmit length. The first seven files were used with the Broad-Band ADCP, while the latter two files were used with the Rio Grande ADCP.

CFG File	Mode	Depth Cell Size (cm)	Depth Cell Number	Max Bottom Track (m)	Pings	WT	First Depth Cell (m)	Blanking Dist. (cm)
D45D	8	20	30	7.9	4	5	0.59	20
MD8A	8	20	15	7.9	4	5	0.49	10
MD4H	4	20	50	15.8	4	5	0.56	10
MD4G	4	20	50	11.9	4	5	0.56	10
MD4C	4	10	30	7.9	4	5	0.46	10
MD4A	4	20	15	7.9	4	5	0.56	10
MD1D	1	10	60	7.9	10	5	0.57	10
DF	1	20	40	7.9	4	5	0.37	10
VS	1	20	100	20.1	4	5	0.40	10

visually-estimated average of multiple grains (using a calibrated grid[7] on the monitor connected to the 90° camera) for the dominant particle size range for substrate (e.g., range of 2-4 inches) and for cover type. The substrate sizes and cover types were directly visually assessed by one observer based on a mental average of multiple grains, from the headpin or tailpin to the location along the transect where the water became too deep for further direct visual assessment. At each change in substrate size class or cover type, the distance from the headpin or tailpin was measured using a hand held laser range finder. A buoy was placed at the location where direct visual assessment stopped and assessment from that point was continued across the transect by boat using the video camera assembly, with the distances where substrate size or cover type changed again measured with the hand held laser range finder. A buoy was again dropped at the location along the transect near the opposite shore where substrate and cover could be directly visually assessed. The substrate and cover over the remaining distance from the buoy to the end

---

[6] A traverse refers to a set of data collected each time the ADCP is driven across the channel.

[7] The grid was calibrated so that, when the camera frame was 1 foot off the bottom, the smallest grid corresponded to a 2-inch substrate, the next largest grid corresponded to a 4-inch substrate, etc.

of the transect was assessed using the same visual methods used on the opposite bank. Additional details on the underwater video equipment operation are given in Gard and Ballard (2003).

Data collected between the transects included: 1) bed elevation; 2) northing and easting (horizontal location); 3) substrate; and 4) cover. These parameters were collected at enough points to characterize the bed topography, substrate and cover of the sites. We used two techniques to collect the data between the upstream and downstream transects: 1) for areas that were dry or shallow (less than 3 feet or 0.91 meters), bed elevation and horizontal location of individual points were obtained with a total station[8], while the cover and substrate were visually assessed by one observer based on a mental average of multiple grains at each point; and 2) in portions of the site with depths greater than 3 feet (0.91 meters), the ADCP was used in concert with the total station to obtain bed elevation and horizontal location. Specifically, the ADCP was run across the channel at 50 to 150-foot (15 to 45 m) intervals, with the initial and final horizontal location of each run measured by the total station. The WSEL of each ADCP run was measured with the level before starting the run. The WSEL of each run was then used together with the depths from the ADCP to determine the bed elevation of each point along the run. For sites where there was no U.S. Army Corps of Engineers raw hydroacoustic data upstream of the site, we collected a limited amount of ADCP traverse data upstream of the site to use for the upstream extension or used a one-channel-width artificial extension upstream of the top of the site.

For the collection of the substrate and cover data on the ADCP traverses for the sites, the initial and final locations of each deep bed elevation traverse were marked with buoys prior to the ADCP traverses. The deep substrate and cover data were collected immediately following the completion of the deep bed elevation data collection for a site, with buoys placed prior to the collection of the deep bed data and used during the collection of the deep substrate and cover data. For deepwater (generally greater than 10 feet (3.05 meters)) portions of the traverses, the underwater video and hand held laser range finder were then used to determine the substrate and cover along each traverse, so that substrate and cover values could be assigned to each point of the traverse. In shallower portions of the traverses, the substrate and cover were assessed by one observer based on the visually-estimated average of multiple grains at each point.

Velocities at each point measured by the ADCP were used to validate the 2-D model for deep areas within a site. To validate the velocities predicted by the 2-D model for shallow areas within a site, depth, velocity, substrate and cover measurements were collected along the right and left banks within each site by wading with a wading rod equipped with a Marsh-McBirney[R]

---

[8] A total station is an electronic/optical instrument used in modern surveying. The total station is an electronic theodolite (transit) integrated with an electronic distance meter (EDM) to read distances from the instrument to a particular point. Data from the total station consists of the horizontal angle, vertical angle and slope distance to each point.

model 2000 or a Price AA velocity meter. These validation velocities and the velocities measured on the transects described previously were collected at 0.6 of the depth for 20 seconds. The horizontal locations and bed elevations were recorded by sighting from the total station to a stadia rod and prism held at each point where depth and velocity were measured. A minimum of 25 representative points were measured along the length of each side of the river per site. Velocity data collected on the PHABSIM transects in depths of approximately 3 feet (0.91 meters) or less where the ADCP could not be utilized were also used to validate the velocities predicted for shallow areas within the site.

For sites where there was a gradual gradient change in the vicinity of the downstream transect, there could be a point in the thalweg downstream of the downstream transect that was higher than that measured at the downstream transect thalweg. This Stage of Zero Flow (SZF) downstream of the downstream transect acts as a control on the water surface elevations at the downstream transect. Because the true SZF is needed to accurately calibrate the water surface elevations on the downstream transect, this SZF in the thalweg downstream of the downstream transect was surveyed in using differential leveling.

7. *Hydraulic Model Construction and Calibration*

7.1. **PHABSIM WSEL Calibration**

All data were compiled and checked before entry into PHABSIM files for the upstream and downstream transects. American Standard Code for Information Interchange (ASCII) files of each ADCP traverse were produced using the Playback feature of the Transect program[9]. Each ASCII file was then imported into RHABSIM Version 2.0[10] to produce the bed elevations, average water column velocities, and stations (relative to the start of the ADCP traverse). RHABSIM was then used to output a second ASCII file containing this data. The second ASCII file was input into an Excel spreadsheet and combined with the velocity, depth, and station data collected in shallow water. We defined a statistic (R) to provide a quality control check of the velocity measured by the ADCP at a given station n, where $R = Vel_n/(Vel_{n-1} + Vel_{n+1})/2$ at station n[11]. R was calculated for each velocity where Vel_n, Vel_{n-1} and Vel_{n+1} were all greater than 1 foot/s (0.31 m/s) for each ADCP data set. Based on data collected using a Price AA velocity

---

9 The Transect program is the software used to receive, record and process data from the ADCP.

10 RHABSIM is a commercially produced software (Payne and Associates 1998) that incorporates the modeling procedures used in PHABSIM.

11 n - 1 refers to the station immediately before station n and n + 1 refers to the station immediately after station n.

meter on the Lower American River, the acceptable range of R was set at 0.5-1.6. All verticals with R values less than 0.5 or greater than 1.6 were deleted from each ADCP data set. We also deleted velocities where Vel_n was less than 1.00 ft/s (0.305 m/s) and Vel_{n-1} and Vel_{n+1} were greater than 2.00 feet/s (0.610 m/s), and where Vel_n had one sign (negative or positive) and Vel_{n-1} and Vel_{n+1} had the opposite sign (when the absolute value of all three velocities were greater than 1.00 ft/s [0.305 m/s]); these criteria were also based on the Lower American River data set. The traverse for each transect which had the flow closest to the gaged flow, determined from U.S. Geological Survey gage readings, was selected for use in the PHABSIM files. Flows were calculated for each ADCP traverse, including the data collected in shallow water.

A table of substrate and cover ranges/values was created to determine the substrate and cover for each vertical/cell (e.g., if the substrate size class was 2-4 inches on a transect from station 50 to 70, all of the verticals with station values between 50 and 70 were given a substrate coding of 2.4). Dry bed elevation data in field notebooks were entered into the spreadsheet to extend the bed profile up the banks above the WSEL of the highest flow to be modeled. An ASCII file produced from the spreadsheet was run through the FLOMANN program (written by Andy Hamilton, U.S. Fish and Wildlife Service, 1998) to get the PHABSIM input file and then translated into RHABSIM files. A separate PHABSIM file was constructed for each study site. A total of four or five sets of measured WSELs were used, all being checked as a quality control check to ensure that the WSELs from the upstream transect were greater than the WSELs from the downstream transect. The slope for each transect was computed for each WSEL flow as the difference in WSELs between the two transects divided by the distance between the two. The slope used for each transect was calculated by averaging the slopes computed for each flow. If WSELs were available for several closely spaced flows, the WSEL that corresponded with the velocity set or the WSEL collected at the lowest flow was used in the PHABSIM files. Flow/flow regressions were performed for sites which did not include the entire Yuba River flow, using the flows measured with a wading rod and Price AA or Marsh-McBirney flow meter in the site and the corresponding gage total flows for the dates that the site flows were measured. The regressions were developed from three or four sets of flows. Calibration flows in the PHABSIM files were the flows calculated from gage readings or from the above flow/flow regressions.

The SZF, an important parameter used in calibrating the stage-discharge relationship, was determined for each transect and entered into the PHABSIM file. In habitat types without backwater effects (e.g., riffles and runs), this value generally represents the lowest point in the streambed across a transect. However, if a transect directly upstream contains a lower bed elevation than the adjacent downstream transect, the SZF for the downstream transect applies to both. In some cases, data collected in between the transects showed a higher thalweg elevation than either transect; in these cases the higher thalweg elevation was used as the SZF for the upstream transect. For downstream transects in habitat types with a backwater effect, we used the U.S. Army Corps of Engineers hydro-acoustic mapping data downstream of the study site to determine the SZF for the downstream transect (the highest point on the thalweg downstream of the study site).

The first step in the calibration procedure was to determine the best approach for WSEL simulation. Initially, the *IFG4* hydraulic model (Milhous et al. 1989) was run on the PHABSIM file to compare predicted and measured WSELs. This model produces a stage-discharge relationship using a log-log linear rating curve calculated from at least three sets of measurements taken at different flows. Besides *IFG4*, two other hydraulic models are available in PHABSIM to predict stage-discharge relationships. These models are: 1) *MANSQ*, which operates under the assumption that the geometry of the channel and the nature of the streambed controls WSELs; and 2) *WSP*, the water surface profile model, which calculates the energy loss between transects to determine WSELs. *MANSQ*, like *IFG4*, evaluates each transect independently. *WSP* must, by nature, link at least two adjacent transects. *IFG4*, the most versatile of these models, is considered to have worked well if the following criteria are met: 1) the beta value (a measure of the change in channel roughness with changes in streamflow) is between 2.0 and 4.5; 2) the mean error in calculated versus measured discharges is less than 10%; 3) there is no more than a 25% difference for any calculated versus measured discharge; and 4) there is no more than a 0.1 foot (0.031 m) difference between measured and simulated WSELs[12]. *MANSQ* is considered to have worked well if the second through fourth of the above criteria are met, and if the beta value parameter used by *MANSQ* is within the range of 0 to 0.5. The first *IFG4* criterion is not applicable to *MANSQ*. *WSP* is considered to have worked well if the following criteria are met: 1) the Manning's n value used falls within the range of 0.04 - 0.07; 2) there is a negative log-log relationship between the reach multiplier and flow; and 3) there is no more than a 0.1 foot (0.031 m) difference between measured and simulated WSELs. The first three *IFG4* criteria are not applicable to *WSP*. For sites located within the backwater effects of the Feather River, we used a modification of *IFG4* with a log-log linear rating curve calculated from a multiple regression of WSELs versus both Yuba River and Feather River flows. We considered the multiple regression to work well if there is no more than a 0.1 foot (0.031 meters) difference between measured and simulated WSELs. For sites that we were not able to calibrate with any of the three PHABSIM models, we used an alternative downstream boundary condition in River2D, as discussed below under River2D Model Calibration.

Velocity Adjustment Factors (VAFs) were examined for all of the simulated flows as a potential indicator of problems with the stage-discharge relationship. The acceptable range of VAF values is 0.2 to 5.0 and the expected pattern for VAFs is a monotonic increase with an increase in flows.

7.2. **River2D Model Construction**

After completing the PHABSIM calibration process to arrive at the simulation WSELs that will be used as inputs to the River2D model, the next step is to construct the River2D model using the collected bed topography data. The data from the ADCP traverses made to characterize the bed

---

[12] The first three criteria are from U.S. Fish and Wildlife Service (1994), while the fourth criterion is our own.

topography of the sites between the transects for input to the 2-D model were processed for input into an Excel spreadsheet in the same manner described above for the ADCP data on the transects. We applied the same quality criteria to the velocities from these ADCP traverses as described above for the velocity data collected on the transects, with the velocities not meeting the quality control criteria deleted from each ADCP data set.

The bed elevation of each point along the ADCP traverse was calculated as the difference between the WSEL shot at the location of the traverse and the depth at each point. The distance along each ADCP traverse, in concert with initial and final horizontal locations, was used to compute the horizontal location of each point along the traverse. The station along each PHABSIM transect, in concert with the horizontal locations of the headpins and tailpins of the transects, was used to compute the horizontal location of each vertical of the PHABSIM transects. Substrate and cover were assigned to each point along each ADCP traverse in the same manner as described above for the transects.

The data from the ADCP traverses were combined in Excel with the total station data and the PHABSIM transect data to create the input files (bed and cover) for the 2-D modeling program. We also incorporated bed topography data collected for the Yuba River by the U.S. Army Corps of Engineers using hydroacoustic mapping and photogrammetry. The accuracy of the hydroacoustic data were 1 foot (0.31 m) horizontal and 0.1 foot (0.031 m) vertical, while the accuracy of the photogrammetry data were 3 feet (0.91 m) horizontal and 1 foot (0.31 m) vertical (Scott Stonestreet, U.S. Army Corps of Engineers, personal communication). We used the raw hydroacoustic data and the 2-foot (0.61 m) contour photogrammetry data. We used the U.S. Army Corps of Engineers data to develop the bed topography upstream of most study sites to improve the accuracy of the flow distribution at the upstream end of the sites. Using this data, we extended the bed topography at least one and a half channel widths upstream of the upstream transect. For sites where the upstream transect was located near the upstream end of a split channel, we added an artificial extension one channel-width-long upstream of the top of the site to enable the flow to be distributed by the model when it reached the study area, thus minimizing the influence of boundary conditions on the flow distribution at the upstream transect and within the study site. For sites where there was no U.S. Army Corps of Engineers raw hydroacoustic data upstream of the site, we used the limited amount of ADCP traverse data collected upstream of the site to develop the upstream extension. For sites where we added a downstream extension to improve velocity simulations, we also extended the bed topography downstream of the downstream transect approximately one channel width using the U.S. Army Corps of Engineers raw hydroacoustic data.

The bed files contain the horizontal location (northing and easting), bed elevation and initial bed roughness value for each point, while the cover files contain the horizontal location, bed elevation and the cover for each point. The initial bed roughness value for each point was determined from the substrate and cover codes for that point and the corresponding bed roughness values in Table 7 with the bed roughness value computed as the sum of the substrate bed roughness value and the cover bed roughness value. The bed roughness values for substrate

Table 7. Initial bed roughness values.

Substrate Code	Bed Roughness (m)	Cover Code	Bed Roughness (m)
0.1	0.05	0.1	0
1	0.1	1	0
1.2	0.2	2	0
1.3	0.25	3	0.11
2.3	0.3	3.7	0.2
2.4	0.4	4	0.62
3.4	0.45	4.7	0.96
3.5	0.5	5	1.93
4.6	0.65	5.7	2.59
6.8	0.9	7	0.28
8	1.25	8	2.97
9	0.05, 0.76, 2[13]	9	0.29
10	1.4	9.7	0.57
		10	3.05

in Table 7 were computed as five times the average particle size[14]. The bed roughness values for cover in Table 7 were computed as five times the average cover size, where the cover size was measured on the Sacramento River on a representative sample of cover elements of each cover-type. The bed and cover files were exported from Excel as ASCII files.

---

[13] For substrate code 9, we used bed roughnesses of 0.76 and 2, respectively, for cover codes 1 and 2, and a bed roughness of 0.05 for all other cover codes. The bed roughness value for cover code 1 (cobble) was estimated as five times the assumed average size of cobble (6 inches [0.15 m]). The bed roughness values for cover code 2 (boulder) was estimated as five times the assumed median size of boulders (1.3 feet [0.4 m]). Bed roughnesses of zero were used for cover codes 1 and 2 for all other substrate codes, since the roughness associated with the cover was included in the substrate roughness.

[14] Five times the average particle size is approximately the same as 2 to 3 times the d85 particle size, which is recommended as an estimate of bed roughness height (Yalin 1977).

A utility program, R2D_BED (Steffler 2002), was used to define the study area boundary and to refine the raw topographical data TIN (triangulated irregular network) by defining breaklines[15] going up the channel along features such as thalwegs, tops of bars and bottoms of banks. The first step in refining the TIN was to conduct a quality assurance/quality control process, consisting of a point-by-point inspection to eliminate quantitatively wrong points, and a qualitative process where we checked the features constructed in the TIN against aerial photographs to make sure we had represented landforms correctly. Breaklines were also added along lines of constant elevation.

An additional utility program, R2D_MESH (Waddle and Steffler 2002), was used to define the inflow and outflow boundaries to improve the fit between the mesh and the final bed file and to improve the quality of the mesh, as measured by the Quality Index (QI) value. The QI is a measure of how much the least equilateral mesh element deviates from an equilateral triangle. An ideal mesh (all equilateral triangles) would have a QI of 1.0. A QI value of at least 0.2 is considered acceptable (Waddle and Steffler 2002). The final step with the R2D_MESH software was to generate the computational (cdg) file.

7.3. **River2D Model Calibration**

Once a River2D model has been constructed, calibration is then required to determine that the model is reliably simulating the flow-WSEL relationship that was determined through the PHABSIM calibration process using the measured WSELs. The cdg files were opened in the River2D software, where the computational bed topography mesh was used together with the WSEL at the bottom of the site, the flow entering the site, and the bed roughnesses of the computational mesh elements to compute the depths, velocities and WSELs throughout the site. The basis for the current form of River2D is given in Ghanem et al. (1995). The computational mesh was run to steady state at the highest flow to be simulated, and the WSELs predicted by River2D at the upstream end of the site were compared to the WSELs predicted by PHABSIM at the upstream transect. Calibration was considered to have been achieved when the WSELs predicted by River2D at the upstream transect were within 0.1 foot (0.031 m) of the WSEL predicted by PHABSIM. In cases where the simulated WSELs at the highest simulation flow varied across the channel by more than 0.1 foot (0.031 m), we used the highest measured flow within the range of simulated flows for River2D calibration. The bed roughnesses of the computational mesh elements were then modified by multiplying them by a constant bed roughness multiplier (BR Mult) until the WSELs predicted by River2D at the upstream end of the site matched the WSELs predicted by PHABSIM at the top transect. The minimum groundwater depth, used by the model to determine if nodes are wet (surface water) or dry

[15] Breaklines are a feature of the R2D_Bed program which force the TIN of the bed nodes to linearly interpolate bed elevation and bed roughness values between the nodes on each breakline and force the TIN to fall on the breaklines (Steffler 2002).

(groundwater), was adjusted to a value of 0.05 m to increase the stability of the model. The values of all other River2D hydraulic parameters were left at their default values (upwinding coefficient = 0.5, groundwater transmissivity = 0.1, groundwater storativity = 1, and eddy viscosity parameters $\varepsilon_1 = 0.01$, $\varepsilon_2 = 0.5$ and $\varepsilon_3 = 0.1$)[16].

For sites where we were unable to calibrate with PHABSIM, we used the depth-unit discharge relationship boundary condition for the downstream transect. This boundary condition uses the equation:

$$q = Kh^m, \qquad (1)$$

where q = unit discharge, h = depth and K and m are constants. We used the default value of 1.666 for m and varied the value of K until the simulated downstream WSEL matched the WSEL measured at the downstream transect. We then calibrated the upstream transect using the methods described above, varying the Bed Roughness Multiplier (BR Mult) until the simulated WSEL at the upstream transect matched the measured WSEL at the upstream transect.

An additional step was needed for sites with a downstream extension to develop a relationship between the WSEL at the downstream boundary and the WSEL predicted by PHABSIM at the downstream transect for the simulation flows. For such sites, we tried different WSELs for the downstream boundary at the highest simulation flow until we found a WSEL for the downstream boundary that resulted in a WSEL predicted by RIVER2D at the downstream transect which matched the WSEL predicted by PHABSIM for the downstream transect. The same process was repeated at the lowest simulation flow and an intermediate simulation flow, with the WSEL predicted by RIVER2D at the downstream transect compared to the WSEL predicted by PHABSIM at the downstream transect for these two flows. We then developed a linear relationship between flow and the difference between the WSEL specified at the downstream boundary and the WSEL at the downstream transect, using the data from these three flows. This relationship was then used to determine what to subtract from the WSEL predicted by PHABSIM at the downstream transect for each simulation flow to generate the WSEL to be used for the downstream boundary for each simulation flow.

---

[16] Exceptions to this are given in the results.

A stable solution will generally have a solution change[17] (Sol Δ) of less than 0.00001 and a net flow (Net Q) of less than 1% (Steffler and Blackburn 2002). In addition, solutions for low gradient streams should usually have a maximum Froude Number (Max F) of less than one[18]. Finally, the WSEL predicted by the 2-D model should be within 0.1 foot (0.031 m) of the WSEL measured at the upstream transects[19].

7.4. River2D Model Velocity Validation

Velocity validation is the final step in the preparation of the hydraulic models for use in habitat simulation. Velocities predicted by River2D were compared with measured velocities to determine the accuracy of the model's predictions of mean water column velocities. The measured velocities used were those measured at the upstream and downstream transects, the velocities measured during collection of the deep bed topography with the ADCP, and the 50 measurements taken between the transects. The criterion used to determine whether the model was validated was whether the correlation coefficient (R) between measured and simulated velocities was greater than 0.6. A correlation of 0.5 to 1.0 is considered to have a large effect (Cohen 1992). The model would be in question if the simulated velocities deviated from the measured velocities to the extent that the correlation between measured and simulated velocities fell below 0.6.

7.5. River2D Model Simulation Flow Runs

After the River2D model was calibrated, the flow and downstream WSEL in the calibrated cdg file were changed to simulate the hydraulics of the site at the simulation flows. The cdg file for each flow contained the WSEL predicted by PHABSIM at the downstream transect at that flow. Each cdg file was run in River2D to steady state. Again, a stable solution will generally have a Sol Δ of less than 0.00001 and a Net Q of less than 1%. In addition, solutions should usually have a Max F of less than one.

---

[17] Solution change is the relative overall change in the solution variables over the latest time step (Steffler and Blackburn 2002).

[18] Maximum Froude number refers to the highest Froude number found in a given site at a given flow. This criterion is based on the assumption that flow in low gradient streams is usually subcritical, where the Froude number is less than one (Peter Steffler, personal communication).

[19] We have selected this standard because it is a standard used by the U.S. Fish and Wildlife Service for PHABSIM (U. S. Fish and Wildlife Service 2000).

8. *Habitat Suitability Criteria (HSC) Data Collection*

Habitat suitability criteria (HSC) are used within 2-D habitat modeling to translate hydraulic and structural elements of rivers into indices (HSIs) of habitat quality (Bovee 1986). HSC refer to the overall functional relationships that are used to convert depth, velocity and cover values into habitat quality (HSI). HSI refers to the independent variable in the HSC relationships. The primary habitat variables which were used to assess physical habitat suitability for Chinook salmon and steelhead/rainbow trout fry and juvenile rearing were depth, velocity, cover and adjacent velocity[20].

Traditionally, criteria are created from observations of fish use by fitting a nonlinear function to the frequency of habitat use for each variable (depth, velocity, and cover). One concern with this technique is the effect of availability of habitat on the observed frequency of habitat use. For example, if a cover type is relatively rare in a stream, fish will be found primarily not using that cover type simply because of the rarity of that cover type, rather than because they are selecting areas without that cover type. Guay et al. (2000) proposed a modification of this technique where depth, velocity, and cover data are collected both in locations where juveniles are present and in locations where juveniles are absent, and a logistic regression is used to develop the criteria. This approach is employed in this study.

HSC data collection for Chinook salmon and steelhead/rainbow trout fry and juvenile (YOY) rearing was conducted September 2003 - September 2005. Data were collected along banks by snorkeling and by SCUBA in the deep water portion of the habitat units. We also collected depth, velocity, adjacent velocity and cover data on locations which were not occupied by YOY Chinook salmon and steelhead/rainbow trout (unoccupied locations). This was done so that we could apply the method presented in Guay et al. (2000) to explicitly take into account habitat availability in developing HSC criteria, without using preference ratios (use divided by availability).

---

[20] Adjacent velocity can be an important habitat variable as fish, particularly fry and juveniles, frequently reside in slow-water habitats adjacent to faster water where invertebrate drift is conveyed (Fausch and White 1981). Both the residence and adjacent velocity variables are important for fish to minimize the energy expenditure/food intake ratio and maintain growth. The adjacent velocity was measured where the velocity was the highest within 2 feet (0.61 meters) on either side of the residence location. Two feet (0.61 meters) was selected based on a mechanism of turbulent mixing transporting invertebrate drift from fast-water areas to adjacent slow-water areas where fry and juvenile salmon and steelhead/rainbow trout reside, taking into account that the size of turbulent eddies is approximately one-half of the mean river depth (Terry Waddle, USGS, personal communication), and assuming that the mean depth of the Yuba River is around 4 feet (1.22 meters) (i.e., 4 feet x ½ = 2 feet).

Before going out into the field, a data book was prepared with one line for each unoccupied location where depth, velocity, cover and adjacent velocity would be measured. Each line had a distance from the bank, with a range of 0.5 to 10 feet (0.15 to 3.05 m) by 0.5 foot (0.15 m) increments, with the values produced by a random number generator. In areas where we were able to sample up to 20 feet (6.10 m) from the bank, we doubled the above distances.

When conducting snorkel surveys adjacent to the bank, one person snorkeled upstream along the bank and placed a weighted, numbered tag at each location where YOY Chinook salmon or steelhead/rainbow trout were observed. The snorkeler recorded the tag number, the species, the cover code[21] and the number of individuals observed in each 10-20 mm size class on a Poly Vinyl Chloride (PVC) wrist cuff. Water temperature, the average and maximum distance from the water's edge that was sampled, cover availability in the area sampled (percentage of the area with different cover types) and the length of bank sampled (measured with a 300-foot-long tape [91 m]) was also recorded. The cover coding system used is shown in Table 5.

A 300-foot-long (91 m) tape was put out with one end at the location where the snorkeler finished and the other end where the snorkeler began. Three people went up the tape, one with a stadia rod and data book and the other two with wading rods and velocity meters. At every 20-foot (6 m) interval along the tape, the person with the stadia rod measured out the distance from the bank given in the data book. If there was a tag within 3 feet (0.91 m) of the location, "tag within 3" was recorded on that line in the data book and the people proceeded to the next 20-foot (6 m) mark on the tape, using the distance from the bank on the next line. If the location was beyond the sampling distance, based on the information recorded by the snorkeler, "beyond sampling distance[22]" was recorded on that line and the recorder went to the next line at that same location, repeating until reaching a line with a distance from the bank within the sampling distance. If there was no tag within 3 feet (0.91 m) of that location, one of the people with the wading rod measured the depth, velocity, adjacent velocity and cover at that non-use location. Depth was recorded to the nearest 0.1 ft (0.031 m) and average water column velocity and adjacent velocity were recorded to the nearest 0.01 ft/s (0.003 m/s). Another individual retrieved the tags, measured the depth and mean water column velocity at the tag location, measured the adjacent velocity for the location, and recorded the data for each tag number. Data taken by the snorkeler and the measurer were combined for each tag location.

---

[21] If there was no cover elements (as defined in Table 5) within 1 foot (0.30 meters) horizontally of the fish location, the cover code was 0.1 (no cover).

[22] Beyond sampling distance refers to the distance out from the bank that the snorkeler was able to sample for fish. For example, for most of the 300 feet (91 m) of bank sampled, the snorkeler may have been able to look for fish up to 20 feet (6 m) out from the bank, but there may have been a short portion of the bank where, due to fast and deep conditions, the snorkeler had to hug the bank and thus was only able to see 10 feet (3 m) out from the bank. In such a location, an unoccupied measurement that was specified as, for example, 20 feet (6 m) from the bank, would have been denoted as "beyond sampling distance" in the databook.

These procedures were modified for several periods (November - December 2004, July - September 2005), to increase the number of observations of fish greater than 60 mm standard length (SL). At these times, tags were only placed for salmonids greater than 60 mm SL. We would generally snorkel all the way upstream along the bank through one habitat unit, then float downstream approximately 50-100 feet (15-30 m) away from the bank, looking for salmonids greater than 60 mm SL, until we reached the downstream end of the next habitat unit downstream of the first habitat unit, and repeat this process. We would continuously snorkel both banks of the Yuba River, going upstream, until we saw salmonids greater than 60 mm SL. At that point, we would drop a tag at the fish location and put out 100 feet (30 m) of tape, roughly centered on the location of the tag. We would then collect unoccupied observations, as described above, at every 20 feet (6 m) along the tape. With the exception of the 100-foot (30 m) reaches in which unoccupied observations were collected, the only datum that was recorded was the total length of each habitat unit sampled. During these periods, sampling away from the bank was limited to floating back down through habitat units, except for one SCUBA survey conducted in August of 2005.

SCUBA surveys of deep water mesohabitat areas were conducted by first anchoring a rope longitudinally upstream through the area to be surveyed to facilitate upstream movement by the divers and increase diver safety. Two divers entered the water at the downstream end of the rope and proceeded along the rope upstream using climbing ascenders. One diver concentrated on surveying the water below and to the side, while the other diver concentrated on surveying the water above and to the side. When a YOY salmon or steelhead/rainbow trout was observed, a weighted buoy was placed by the divers at the location of the observation. The cover code and the number of individuals observed in each 10-20 mm size class were then recorded on a PVC wrist cuff. Water temperature, cover availability in the area sampled (percentage of the area with different cover types) and the length of river sampled (based on the length of the rope) were also recorded.

After the dive was completed, the ADCP was turned on (to record unoccupied depth and velocity data) as we started to pull in the rope after the dive. The boat followed the course of the dive as the rope was pulled back into the boat. If there were any observations during the dive, the ADCP was stopped 3 feet (0.91 meters) before the location of the observation and started again 3 feet (0.91 meters) after the location of the observation. For each occupied location, individuals in the boat retrieved each buoy and measured the water velocity and depth over that location with the ADCP, making at least 12 observations. For each set of data collected using the ADCP for a juvenile fish observation, the depth and velocity averaged from the observations are considered the depth and velocity, while the highest mean water column velocity is considered the adjacent velocity. The ADCP was turned off at the location where the dive ended.

9.   *Biological Verification Data Collection*

Biological verification data were collected to test the hypothesis that the compound suitability predicted by the River2D model is higher at locations where fry or juveniles were present than in locations where fry or juveniles were absent. The compound suitability is the product of the depth suitability, the velocity suitability, the adjacent velocity suitability and the cover suitability. The collected biological verification data were the horizontal locations of fry and juveniles. The horizontal locations of Chinook salmon and steelhead/rainbow trout fry and juveniles found during surveys were recorded by sighting from the total station to a stadia rod and prism. Depth, velocity, adjacent velocity, and cover type as described in the previous section on habitat suitability criteria data collection were also measured. The horizontal locations of where fry or juveniles were not present (unoccupied locations) were also recorded with the total station. The hypothesis that the compound suitability predicted by the River2D model is higher at locations where fry and juveniles were present than in locations where fry and juveniles were absent was statistically tested with a one-tailed Mann-Whitney U test (Gard 2006, Gard 2009, McHugh and Budy 2004).

10.   *Habitat Suitability Criteria (HSC) Development*

It is well-established in the literature (Knapp and Preisler 1999, Parasiewicz 1999, Geist et al. 2000, Guay et al. 2000, Tiffan et al. 2002, McHugh and Budy 2004) that logistic regressions are appropriate for developing habitat suitability criteria. For example, McHugh and Budy (2004) state (page 90):

> "More recently, and based on the early recommendations of Thielke (1985), many researchers have adopted a multivariate logistic regression approach to habitat suitability modeling (Knapp and Preisler 1999; Geist et al. 2000; Guay et al. 2000)."

Accordingly, logistic regression has been employed in the development of the habitat suitability criteria (HSC) in this study. Criteria were developed by using a logistic regression procedure, with presence or absence of YOY as the dependent variable and depth, velocity, cover and adjacent velocity as the independent variables, with all of the data (in both occupied and unoccupied locations) used in the regression.

For the SCUBA data, a random number generator was used to select ADCP measurements of depth and velocity for unoccupied locations. The number of unoccupied cells selected for each site was the lesser of either 10 percent of the total distance (feet) sampled or 30 percent of the total number of ADCP points. Cover was assigned to all of the observations in proportion to which they were observed during the dive. The adjacent velocity for each unoccupied location was the largest of the three following values: the depth-averaged velocity at the location immediately prior to the unoccupied location, the depth-averaged velocity at the unoccupied location, and the depth-averaged velocity at the location immediately after the unoccupied location.

All YOY Chinook salmon observed were classified by race according to a table provided by CDFG (Frank Fisher, Red Bluff, 1994) correlating race with life stage periodicity and total length. However, based on Earley and Brown (2004) and McReynolds et al.'s (2004) findings that most known spring-run Chinook salmon YOY from Sacramento River tributaries would be classified as fall-run by the CDFG race table, we are considering all YOY classified by the race table as fall-run to be some combination of spring and fall-run (hereafter referred to as fall/spring-run). It is likely we would find the same results as Earley and Brown (2004) and McReynolds et al. (2004) for the Yuba River. Data were also compiled on the length of each mesohabitat and cover type sampled to try to have equal effort in each mesohabitat and cover type and ensure that each location was only sampled once at the same flow to avoid problems with pseudo-replication.

Separate salmonid YOY rearing HSC are typically developed for different size classes of YOY (typically called fry and juvenile). Since we recorded the size classes of the YOY, we were able to investigate three different options for the size used to separate fry from juveniles: <40 mm versus > 40 mm, <60 mm versus >60 mm, and <80 mm versus >80 mm. We used Mann-Whitney U tests to test for differences in depth, velocity and adjacent velocity, and Pearson's test for association to test for differences in cover, for the above categories of fry versus juveniles. Separate fry and juvenile HSC could be developed for each species (Chinook salmon and steelhead/rainbow trout). To determine if there were differences between species, we used Mann-Whitney U tests to test for differences in depth, velocity and adjacent velocity, and used Pearson's test for association to test for differences in cover, for fry and juveniles. We used nonparametric tests because the data was not normally distributed. Mann-Whitney U tests are generally used for continuous variables, such as depth, velocity and adjacent velocity, while Pearson's test for association is generally used for categorical variables, such as cover.

Generally, at least 150 observations are needed to develop habitat suitability criteria (Bovee 1986). In cases where we had less than 150 observations, we used the procedure described by Thomas and Bovee (1993) to determine if Sacramento River Chinook salmon rearing criteria (US Fish and Wildlife Service 2005) would transfer to Yuba River salmonids. The procedure involves two one-sided χ^2 tests (Conover 1971) using counts of occupied and unoccupied cells in each of three suitability classifications (optimum, useable and unsuitable) to determine if there is non-random selection for optimum habitat over useable habitat, and for suitable (optimum plus useable) over unsuitable habitat. Two null hypotheses are tested: 1) optimum cells will be occupied in the same proportion as useable cells; and 2) suitable cells will be occupied in the same proportion as unsuitable cells. For a set of HSC to be considered transferable, both null hypotheses must be rejected at the 0.05 level of significance. The test procedures require a minimum of 55 occupied and 200 unoccupied cells to avoid either the erroneous acceptance of non-transferable HSC or rejection of transferable HSC (Thomas and Bovee, 1993).

Suitability classifications for depth, mean water column velocity, adjacent velocity, and cover for the Sacramento River Chinook salmon rearing criteria were determined as follows. The optimum range for a variable was defined as the interval encompassing suitabilities greater than 0.75 for the Sacramento River criteria. The suitable range for a variable was defined as the interval containing suitabilities greater than 0.1[23]. Thus, the useable range for a variable encompassed the interval between suitabilities of 0.1 and 0.75, and the unsuitable range was suitabilities less than 0.1. Separate transferability tests were conducted for each parameter. Suitable counts were obtained by combining the optimum and useable counts. The counts were cross classified in two 2 x 2 contingency tables: one to test suitable versus unsuitable classifications and one to test optimum versus useable counts. Test statistics were then calculated from each table using the test statistic for one-sided χ^2 tests given as

$$T = [N^{0.5} (ad-bc)]/[(a+b)(c+d)(a+c)(b+d)]^{0.5}, \qquad (2)$$

where a = number of occupied optimum (or suitable) cells; b = number of occupied useable (or unsuitable) cells; c = number of unoccupied optimum (or suitable) cells; d = number of unoccupied useable (or unsuitable) cells; and N = total number of cells. The null hypothesis is rejected at the 0.05 level of significance (indicating transferability) if $T \geq 1.6449$.

In cases where the Sacramento River Chinook salmon criteria did not transfer to Yuba River salmonids, we developed the Yuba River criteria using Yuba River data of less than 150 observations[24]. For cases where the Sacramento River Chinook salmon did transfer to Yuba River salmonids, we used the Sacramento River Chinook salmon criteria, modified by restricting non-zero suitability to the range of occupied values observed in the Yuba River.

In cases where we had at least 150 observations from the Yuba River, we used a polynomial logistic regression (SYSTAT 2002), with dependent variable frequency (with a value of 1 for occupied locations and 0 for unoccupied locations) and independent variable depth or velocity, to develop depth and velocity HSI. The logistic regression fits the data to the following expression:

$$\text{Frequency} = \frac{\text{Exp}\,(I + J * V + K * V^2 + L * V^3 + M * V^4)}{1 + \text{Exp}\,(I + J * V + K * V^2 + L * V^3 + M * V^4)}, \qquad (3)$$

where Exp is the exponential function; I, J, K, L and M are coefficients calculated by the logistic regression; and V is velocity or depth. The logistic regressions were conducted in a sequential fashion, where the first regression tried was a fourth order regression. If any of the coefficients or the constant were not statistically significant at p = 0.05, the associated terms were dropped

23 The derivation of the 0.75 and 0.1 values is given in U.S. Fish and Wildlife Service (1997).

24 In this circumstance, this was the only option we had to develop criteria.

from the regression equation, and the regression was repeated. The results of the regression equations were rescaled so that the highest value of suitability was 1.0. The resulting HSC were modified by truncating at the slowest/shallowest and deepest/fastest ends, so that the next shallower depth or slower velocity value below the shallowest observed depth or the slowest observed velocity had a SI value of zero, and so that the next larger depth or faster velocity value above the deepest observed depth or the fastest observed velocity had an SI value of zero; and eliminating points where interpolation from retained points resulted in the same HSI value at the eliminated point.

Because adjacent velocities were highly correlated with velocities, a logistic regression of the following form was used to develop adjacent velocity criteria:

$$\text{Frequency} = \frac{\text{Exp}\,(I + J * V + K * V^2 + L * V^3 + M * V^4 + N * AV)}{1 + \text{Exp}\,(I + J * V + K * V^2 + L * V^3 + M * V^4 + N * AV)}, \qquad (4)$$

where Exp is the exponential function; I, J, K, L, M and N are coefficients calculated by the logistic regression; V is velocity and AV is adjacent velocity. The I and N coefficients from the above regression were then used in the following equation:

$$HSI = \frac{\text{Exp}\,(I + N * AV)}{1 + \text{Exp}\,(I + N * AV)}. \qquad (5)$$

We computed values of equation (4) for the range of occupied adjacent velocities, and rescaled the values so that the largest value was 1.0. We used a linear regression on the rescaled values to determine, using the linear regression equation, HSI_0 (the HSI where the AV is zero) and AV_{LIM} (the AV at which the HSI is 1.0). The final adjacent velocity criteria started at HSI_0 for an adjacent velocity of zero, ascended linearly to an HSI of 1.0 at an adjacent velocity of AV_{LIM} and stayed at an HSI of 1.0 for adjacent velocities greater than AV_{LIM}.

To evaluate whether we spent equal effort sampling areas with and without woody cover, we have developed two different groups of cover codes based on snorkel surveys we conducted on the Sacramento River: Cover Group 1 (cover codes 3.7, 4, 4.7, 5.7, 7 and 9.7), and Cover Group 0 (all other cover codes). In U.S. Fish and Wildlife Service (2005), which describes the derivation of these two cover groups, we had addressed the availability of cover in developing the Sacramento River criteria using the following process: 1) ranking the sites sampled in descending order by the percentage of cover group 1; 2) calculating the cumulative feet sampled of cover groups 0 and 1 going down through the sites until we reached an equal number of cumulative feet of cover groups 0 and 1 sampled; and 3) continuing the development of cover criteria using only the above subset of sites. This process allowed us to maximize the amount of area sampled to include in development of the cover criteria while equalizing the amount of area sampled in cover groups 0 and 1. We were unable to use this process on the Yuba River because of the low amount of cover group 1 present in the Yuba River. Instead, we developed the Yuba River cover criteria using a logistic regression analysis. For a categorical independent variable, the result of a logistic regression is the percentage of occupied locations (number of occupied locations / (number of occupied locations + number of unoccupied locations)) for each category of the independent variable.

The first step in the development of the cover criteria was to group cover codes within each species, so that there were no significant differences within the groups and a significant difference between the groups, using Pearson’s test for association. We excluded cover codes from this analysis that had a total (occupied plus unoccupied) of two or fewer observations. We combined together the occupied and unoccupied observations in each group of cover types and calculated the percentage of occupied locations for each group. The HSI for each group was calculated by dividing the percent of occupied locations in each group by the percent of occupied locations in the group with the highest percent of occupied locations. This procedure normalized the HSI, so that the maximum HSI value was 1.0. The HSI for cover codes that had a total of two or fewer observations was determined based on the Sacramento River cover criteria.

11. *Biological Verification*

We determined the combined habitat suitability predicted by River2D at each fry and juvenile observation location in the sites where fall/spring-run Chinook salmon and steelhead/rainbow trout fry and juvenile locations were recorded with total station and prism. We ran the River2D cdg files at the flows present in the study sites for the dates that the biological verification data were collected. We used the horizontal location measured for each observation to determine the location of each observation in the River2D sites. We used the horizontal locations recorded with the total station where fry or juveniles were not present for the unoccupied points. We used one-tailed Mann-Whitney U tests (Zar 1984) to determine whether the combined suitability predicted by River2D was higher at locations where fry or juveniles were present versus locations where fry or juveniles were absent.

12. *Habitat Simulation*

The final step was to simulate available habitat for each site. Preference curve files were created containing the digitized fry and juvenile rearing HSC developed for the Yuba River fall/spring-run Chinook salmon and steelhead/rainbow trout. The final cdg files, the cover file and the preference curve file were used in River2D to calculate the combined suitability of depth, velocity and cover for each site. The resulting data were exported into a comma-delimited file for each flow, species, life stage, and each mesohabitat type present in each site. These files were then run through a GIS post-processing software[25] to incorporate the adjacent velocity criteria into the habitat suitability, and to calculate the WUA values for each mesohabitat type in each site over the desired range of flows for all eighteen sites. The total WUA for each segment was calculated using the following equation:

$$\text{Segment WUA} = \Sigma\,(\text{Ratio}_i * \Sigma\ \text{Mesohabitat Unit}_{i,j}\ \text{WUA}), \qquad (6)$$

where Ratio_i is the ratio of the total area of habitat type_i present in a given segment to the area of habitat type_i that was modeled in that segment and Mesohabitat $\text{Unit}_{i,j}$ WUA is the WUA for mesohabitat unit_j of habitat type_i that was modeled in that segment.

RESULTS

1. *Study Segment Delineation*

We established one segment between Englebright Dam (river mile 24.1) and Daguerre Point Dam (river mile 11.4) (hereafter termed Above Daguerre Segment) and a second segment between Daguerre Point Dam and the confluence with the Feather River at Marysville (hereafter termed river mile 0) (Below Daguerre Segment). Details on the results of the study segment delineation are given in U.S. Fish and Wildlife Service (2010).

2. *Habitat Mapping*

A total of 130 mesohabitat units were mapped for the segment upstream of Daguerre Point Dam and 90 mesohabitat units for the segment downstream of Daguerre Point Dam. Table 8 summarizes the habitat types, area and numbers of each type recorded during the habitat mapping process, while Appendix A gives a complete list of the habitat units.

3. *Field Reconnaissance and Study Site Selection*

The reconnaissance work narrowed the list of potential sites to the eight additional juvenile rearing sites that were modeled (Table 9, Appendix B). The eight additional juvenile rearing sites are as follows from upstream to downstream: Narrows, Rosebar, Diversion, Lower Hallwood, Whirlpool, Side Channel, Sucker Glide, and Railroad. Three of the new juvenile

---

[25] The software calculates the adjacent velocity for each node, then uses the adjacent velocity criteria to calculate the adjacent velocity suitability index for that node. This index is then multiplied by the combined depth, velocity and cover suitability indices. This product is then multiplied by the area represented by each node to calculate the WUA for each node, with the WUA for all nodes summed to determine the total WUA for each mesohabitat type, flow, life stage and species.

Table 8. Yuba River mesohabitat mapping results by segment.

Mesohabitat Type	Upstream of Daguerre Point Dam		Downstream of Daguerre Point Dam	
	Area (1000 m^2)	Number of Units	Area (1000 m^2)	Number of Units
Bar Complex Riffle (BCRi)	73.5	17	94.6	14
Bar Complex Run (BCRu)	631.8	19	379.3	24
Bar Complex Glide (BCG)	193.5	12	361.7	17
Bar Complex Pool (BCP)	159.6	15	120.5	14
Flat Water Riffle (FWRi)	1.6	2	0	0
Flat Water Run (FWRu)	49.0	6	6.2	1
Flat Water Glide (FWG)	18.6	1	73.4	4
Flat Water Pool (FWP)	78.7	8	173.9	6
Side Channel Riffle (SCRi)	11.0	12	1.5	1
Side Channel Run (SCRu)	46.8	19	11.3	5
Side Channel Glide (SCG)	5.5	3	2.1	2
Side Channel Pool (SCP)	34.5	15	1.4	2
Cascade (C)	1.1	1	0	0

rearing study sites were located between the Narrows and Daguerre Point Dam (Narrows, Rosebar, and Diversion) and the remaining five were located downstream of Daguerre Point Dam between Daguerre Point Dam and the confluence with the Feather River (Lower Hallwood, Whirlpool, Side Channel, Sucker Glide, and Railroad). The mesohabitat composition of the study sites versus the entire segments are given in Table 10.

Table 9. Sites selected for modeling fall/spring-run Chinook salmon and steelhead/rainbow trout rearing. Lack of a number in parenthesis indicates one unit for that mesohabitat type in the site.

Site Name	Reach	Site Mesohabitat Types
Narrows	Above	FWP, FWRu
Rose Bar	Above	BCP
U.C. Sierra	Above	BCRi, BCG, BCP, SCRi (2), SCRu, SCP
Timbuctoo	Above	BCRu (2), BCRi (2), BCG, BCP, SCRu (3), SCRi, SCG, SCP
Highway 20	Above	BCRi, BCP, BCG, SCRu, SCRi
Island	Above	BCRu, BCG, BCP (2), SCRu, SCRi
Hammond	Above	BCRu
Diversion	Above	BCRu
Upper Daguerre	Below	BCRu(2), BCRi
Lower Daguerre	Below	BCRu, BCRi
Pyramids	Below	BCRu, BCRi, BCG
Hallwood	Below	BCRu, BCRi
Lower Hallwood	Below	BCP, BCG
Plantz	Below	BCRu, BCG
Whirlpool	Below	BCP
Side-Channel	Below	SCRu, SCP
Sucker Glide	Below	FWG
Railroad	Below	FWRu, FWP

The study site boundaries (up- and downstream transects) were selected to coincide with the upstream and downstream ends of the mesohabitat unit. The exceptions to the above were: 1) Narrows; 2) Rosebar; 3) Whirlpool; 4) Side-Channel; and 5) Railroad. The Narrows upstream transect was moved 650 feet (198 meters) downstream of the top of the Flat Water Run because of the presence of a large cascade at that location. The Rosebar upstream transect was moved 200 feet (61 meters) upstream of the top of the habitat unit and the downstream transect was moved 585 feet (178 meters) downstream of the bottom downstream of the bottom of the habitat unit to locations where the hydraulic conditions were more favorable (e.g., more linear direction of flow, more consistent water surface elevations from bank to bank). The Whirlpool upstream transect was moved 430 feet (131 meters) upstream of the top of the unit to a location where the hydraulic conditions were more favorable. The Whirlpool downstream transect was moved 140 feet (43 meters) upstream of the bottom of the unit to keep the study site within the confines of the smaller channel of the split channel that was present in this area of the river. The Side-Channel site upstream transect was moved upstream 35 feet (11 meters) from the top of the Side-

Table 10. Yuba River segment and study site mesohabitat composition (percent area).

Mesohabitat Type	Upstream of Daguerre Point Dam		Downstream of Daguerre Point Dam	
	Segment	Sites	Segment	Sites
Bar Complex Riffle (BCRi)	5.6%	7.0%	7.7%	16.4%
Bar Complex Run (BCRu)	48.3%	31.4%	30.9%	51.8%
Bar Complex Glide (BCG)	14.8%	24.1%	29.5%	18.6%
Bar Complex Pool (BCP)	12.2%	11.3%	9.8%	2.4%
Flat Water Riffle (FWRi)	0.1%	0	0	0
Flat Water Run (FWRu)	3.7%	2.2%	0.5%	1.1%
Flat Water Glide (FWG)	1.4%	0	6.0%	6.1%
Flat Water Pool (FWP)	6.0%	10.1%	14.2%	2.4%
Side Channel Riffle (SCRi)	1.2%	3.2%	0.1%	0
Side Channel Run (SCRu)	3.6%	8.5%	0.9%	1.0%
Side Channel Glide (SCG)	0.4%	0.2%	0.2%	0
Side Channel Pool (SCP)	2.6%	2.0%	0.1%	0.3%
Cascade (C)	0.1%	0	0	0

Channel Run and the downstream transect was moved 85 feet (26 meters) of the Side-Channel Pool. In both cases, the transects were moved to a location where the hydraulic conditions were more favorable. The Railroad upstream transect was moved 165 feet (50 meters) upstream of the top of the habitat unit. This transect was also moved to a location where the hydraulic conditions were more favorable.

4. *Hydraulic and Structural Habitat Data Collection*

All sites met the standard for level loops (Table 11). Water surface elevations were measured at high (2,908-3,270 cfs), medium (1,220-2,036 cfs) and low (516-970 cfs) flows for the eight study sites. The number and density of the points collected for each site is given in Table 12 and shown in Appendix C. There were no U.S. Army Corps of Engineers raw hydroacoustic data upstream of the Narrows or Side Channel sites. As a result, we collected five ADCP traverses within the first 160 feet (48.77 meters) upstream of the Narrows site for use as the upstream extension, and used a one-channel-width artificial extension upstream of the Side Channel site.

5. *Hydraulic Model Construction and Calibration*

5.1. PHABSIM WSEL Calibration

The gaged calibration flows, determined from U.S. Geological Survey (USGS) gage readings[26], are given in Table 13, and the ADCP traverses selected for use in PHABSIM files are shown in Table 14. The flow/flow regressions used for Diversion, Whirlpool and Side-Channel sites are given in Table 15. Calibration flows for Diversion, Whirlpool, and Side-Channel sites (Table 16) were computed from the total discharge in Table 13 and the appropriate regression equation in Table 15. A total of four sets (Narrows**,** Rosebar, Diversion, Sucker Glide, and Railroad) or five sets (Lower Hallwood (downstream transect) and Whirlpool) of measured WSELs were used in the WSEL calibration. In the case of Lower Hallwood, the upstream transect was the same as the downstream transect of the Hallwood spawning study site and the calibration used for that transect in the spawning study was applied here. See U.S. Fish and Wildlife (2010) for more details on the Hallwood spawning study site and transects. The SZFs used for each transect are given in Appendix D, Table 1. Calibration flows in the PHABSIM files are given in Appendix D. For a majority of the transects, *IFG4* met the criteria described in the methods section for *IFG4* (Appendix D). In the case of Rosebar site, we used the right bank WSELs for the downstream transect and the left bank WSELs for the upstream transect for the 1,942 and 2,908 flows because there was a difference of >0.1 feet (0.03 meters) between the right bank and left bank WSELs. The WSELs were selected based on which side appeared to be most representative for the transects at those flows. In the case of the Lower Hallwood downstream transect, we could only meet the *IFG4* criteria with the upper three flows.

The Side-Channel site transects could not be calibrated with *IFG4* or *MANSQ*. This was apparently due to changing backwater effects from a beaver dam occurring between collection of WSELs on January 18 and February 24 in 2004. The influence of this beaver dam changed over the course of the study as the result of a high flow event that occurred on February 18, 2004,

---

[26] For the Above Daguerre Segment, we used the sum of the flows from the Smartville (USGS gage number 11418000) and Deer Creek (USGS gage number 11418500) gages. For the Below Daguerre Segment, we used the Marysville gage (USGS gage number 11421000).

Table 11. Level loop error results.

Site Name	Level Loop Distance (mi)	Level loop error (ft)	
		Allowable error	Actual error
Narrows	0.760 (1.216 km)	0.04 (0.012 m)	0.03 (0.009 m)
Rose Bar	0.427 (0.684 km)	0.03 (0.009 m)	0.02 (0.006 m)
Diversion	0.465 (0.744 km)	0.03 (0.009 m)	0.00 (0.00 m)
Lower Hallwood	0.765 (1.224 km)	0.04 (0.012 m)	0.01 (0.003 m)
Whirlpool	0.312 (0.500 km)	0.03 (0.009 m)	0.00 (0.00 m)
Side-Channel	Not measured	Unknown	Unknown[27]
Sucker Glide	0.231 (0.370 km)	0.02 (0.006 m)	0.00 (0.00 m)
Railroad	Not measured	Unknown	0.00 (0.00 m)

Table 12. Number and density of data points collected for each site. The Army Corps of Engineers (ACE) supplied us with bed topography data derived from photogrammetry and hydro-acoustic mapping.

	USFWS	USFWS	USFWS	ACE	
Site Name	Number of Points on Transect	Points Between Transects Collected with Total Station	Points Between Transects Collected with ADCP	Number of Points Between Transects	Density of Points (points/ 100 m^2)
Narrows	64	1,911	971	618	9.71
Rosebar	98	1,867	343	189	11.26
Diversion	79	878	---	43	5.62
Lower Hallwood	72	1,840	149	94	4.34
Whirlpool	76	1,020	35	66	7.67
Side-Channel	66	659	---	38	27.80
Sucker Glide	58	522	308	147	7.39
Railroad	67	307	150	29	6.36

[27] There was no level loop for this site because the vertical benchmarks were tied together with one backsight and one foresight.

Table 13. Gage measured calibration flows for the eight study sites (cfs).

Date	Narrows	Rosebar	Diversion	Lower Hallwood	Whirlpool	Side-Channel	Sucker Glide	Railroad
12/4/2003			832					
12/16/2003	1,942	1,942						
12/18/2003					1,220	1,220		
1/12/2004								
1/14/2004				1,930	1,930	1,930		
1/15/2004			2,036					
2/11/2004	1,890						1,920	1,920
2/24/2004	2,908	2,908	2,908	3,270	3,270	3,270	3,270	3,270
7/26/2004				970	970	970	970	
7/27/2004								962
8/23/2004		1,493	1,493					
9/8/2004					516		516	516
9/9/2004	734	734		516				

Table 14. ADCP files used in PHABSIM files.

Date	Site Name	Transect Number	File Name	USFWS Measured Q	% Difference from Gage Measured Q
2/11/2004	Narrows	1	MD45D155	1,513	21%
2/11/2004	Narrows	2	MD4G075	1,767	6.5%
2/10/2004	Rosebar	1	MD4C351	1,785	7%
2/10/2004	Rosebar	2	MD8A703	2,013	4%
2/11/2004	Sucker Glide	1	MD8A713	2,003	4%
2/11/2004	Sucker Glide	2	MD8A714	1,957	2%
2/11/2004	Railroad	1	MD8A706	2,139	8.6%
2/11/2004	Railroad	2	MD8A710	1,829	7%

Table 15. Flow/flow regression equations.

Study Site	XS #	Flow Range	Regression Equation	R^2-value
Diversion	all	400-4,500	Diversion Q = 10 ^ (-1.654 + 1.342 x log (Q))	0.998
Whirlpool	all	150-1,200	Whirlpool Q = -69.135 +0.247 x Q	0.991
Whirlpool	all	1,300-4,500	Whirlpool Q = -224.523 +0.372 x Q	0.999
Side-Channel	all	150-4,500	Sidechannel Q = 10 ^ (-63.011 + 0.0587 x log (Q))	0.967

Table 16. Calibration flows for the Diversion, Whirlpool and Side-channel sites (cfs).

Date	Diversion	Whirlpool	Side-Channel
12/4/2003	193		
12/18/2003		231	
1/14/2004		494	37
1/15/2004	610		
2/24/2004	985	993	132
7/26/2004		171	2.3
8/23/2004	403		
9/8/2004		59	

which temporarily removed most of the beaver dam. We were unable to use *WSP* to calibrate this site since *WSP* requires the input of a stage-discharge relationship at a transect downstream of the transect of interest. For the Side-Channel downstream transect, there was no transect downstream of it. Since we were unable to calibrate this site with any of the three PHABSIM models, we used an alternative downstream boundary condition in River2D, as discussed below under River2D Model Calibration.

Both Railroad transects could not be calibrated using *IFG4* or *MANSQ*. After considering the close proximity of this site (at RM 1.4) to the confluence with the Feather River, we found that there was a backwater effect resulting from the Feather River. As a result, we needed to develop a relationship between the WSELs at this site and the flows of both the Yuba and Feather Rivers[28]. We used a multiple regression formula for the upstream and downstream transects that uses four flows from the Yuba and Feather Rivers for the same dates. This formula is as follows:

$$\text{Log(WSEL – SZF)} = A + B \times \text{Log(Yuba River Flow)} + C \times \text{Log(Feather River Flow)} \qquad (7)$$

For the downstream transect, SZF = 90.7, A = -0.896, B = 0.334, and C = 0.148 (r^2 = 0.996, p = 0.06). For the upstream transect, SZF = 90.7, A = -0.894, B = 0.329, and C = 0.152 (r^2 = 0.996, p = 0.06). For both transects, the simulated WSELs differed from the measured WSELs by a maximum of 0.11 feet (0.03 meters) (Appendix D).

Velocity Adjustment Factors (VAFs) were examined for all of the simulated flows (Appendix E). None of the transects deviated significantly from the expected pattern of VAFs, with the exception of the highest flow VAF for both Railroad site transects. In addition, VAF values (ranging from 0.14 to 3.62) were within an acceptable range of 0.2 to 5.0, with the exception of the lowest flow VAF for both Railroad transects. The lowest flow VAFs for the Railroad upstream and downstream transects of 0.18 and 0.14, respectively, were slightly below the acceptable range. For Side-Channel site, we were unable to develop stage-discharge relationships using *IFG4*, *MANSQ*, or *WSP* which prevented us from evaluating VAF patterns for the site.

5.2. **River2D Model Construction**

For the Narrows site, we extended the bed topography downstream of the downstream transect approximately one channel width. We did this to improve the velocity simulation for the Narrows site. The bed topography for each site is shown in Appendix F. The meshes for all sites had QI values of at least 0.30, meeting the criterion of having a QI value of at least 0.2 (Appendix G). The percentage of the original bed nodes for which the meshes differed by less than 0.1 foot (0.031 m) from the elevation of the original bed nodes ranged from 72% to 95% (Appendix G). The average mesh resolution was 1.2 nodes/m^2.

5.3. **River2D Model Calibration**

Calibration was conducted at the highest simulation flow, 4,500 cfs (127.4 m^3/s), for Narrows, Rosebar, Lower Hallwood, and Railroad sites. In the cases of Diversion and Sucker Glide, we used the highest measured flow within the range of simulated flows because the simulated WSELs at the highest simulation flow of 4,500 cfs varied across the channel by more than 0.1 foot (0.031 m), thus resulting in the River2D simulated WSELs differing from the PHABSIM

---

[28] Flows for the Feather River were from gage readings for the Gridley gage (USGS gage number 11407150). Current flow data for this gage is available at: http://cdec.water.ca.gov/cgi-progs/queryDaily?GRL

simulated WSELs by more than 0.1 foot (0.031 m). Diversion site at the highest measured flow had WSELs on the two banks that differed by more than 0.1 foot (0.031 m). Side-Channel site was calibrated at the highest measured flow within the range of simulated flows because we were unable to develop stage-discharge relationships for this site using PHABSIM. For this site, we used the depth-unit discharge relationship boundary condition for the downstream boundary, arriving at a value of 0.8 for K.

The calibrated cdg files all had a Sol Δ of less than 0.000001 (meeting the criterion for this measure), with the net Q for all sites less than 1%, with the exception of Railroad site (Appendix G). The calibrated cdg file for all study sites, with the exception of Diversion, Sucker Glide, and Railroad, had a maximum Froude Number greater than 1 (Appendix G). Six of the eight study sites had calibrated cdg files within 0.1 foot (0.031 m) of the PHABSIM or measured WSELs (for those sites using the WSEL for the highest measured flow within the range of simulation flows). Narrows and Lower Hallwood had maximum WSEL values that exceeded the 0.1 foot (0.031 m) criterion but Lower Hallwood had average WSELs that were well within that criterion value (Appendix G). In the case of Lower Hallwood case, the WSELs next to the locations of the left and right banks within the model were all within the 0.1 foot (0.031 m) criterion value. However, in the case of Narrows, the WSELs next to the locations of the left bank within the model were within the 0.1 foot (0.031 m) criterion value, but exceeded that criterion value next to the right bank.

5.4. **River2D Model Velocity Validation**

The correlation between predicted and measured velocities ranged from moderate to moderately strong (Appendix H), with there being some significant differences between individual measured and predicted velocities. The hydraulic models for Rosebar, Diversion, Lower Hallwood, Whirlpool, and Side-Channel sites were validated, since the correlation between the predicted and measured velocities was greater than 0.6 for these sites. However, we were unable to validate the velocity simulation of the original hydraulic models for Narrows, Sucker Glide, and Railroad sites, since the correlation values were considerably less than 0.6. For these three sites, we tried adding a downstream extension to see if it would improve the velocity simulation. The downstream extension resulted in a substantially better velocity simulation for the Narrows site (correlation of 0.65), as compared to this site without a downstream extension (correlation of 0.42). For Sucker Glide and Railroad sites, the downstream extensions resulted in a slightly worse velocity simulation (correlations of 0.471 and 0.40, respectively), as compared to these sites without downstream extensions (correlations of 0.475 and 0.45, respectively). Accordingly, we did not use downstream extensions for these two sites. As a result, the models for these sites are in question.

In general, the simulated and measured cross-channel velocity profiles at the upstream and downstream transects (Appendix H[29]) were relatively similar in shape. Unless noted, the simulated velocities for the eight sites were relatively similar to the measured velocities for the transects and deep bed ADCP traverses, with some differences in magnitude that fall within the range of variation in the ADCP velocity measurements. Please note that for the sites where deep traverses were performed, there is a map in Appendix H that displays the locations of the transects and deep bed traverses. This map follows the figures showing the velocity profiles for each transect.

In the case of the Side-Channel downstream (XS1) and upstream (XS2) transects, River2D under-predicted the velocities across most of the channel and over-predicted the velocities on the north side of the channel. For the Whirlpool downstream transect, River2D under-predicted the velocities toward the west side of the channel and over-predicted the velocities for the upstream (XS2) transect on the south side of the channel.

River2D over or under-predicted the velocities on one or both sides of the channel for the following deep beds[30]: Narrows Deep Beds A-G, I, J, M, N, Q-U, W, X-AB, AD-AH, AM, AN, AS, AT, AV, AW, BA-BC, BE-BI, BK, BM-BQ, BT, BV, BW, CA-CD, and CF; Rosebar Deep Beds B-E, G, H, M, O, P, Q, and T; Lower Hallwood Deep Beds A, E, G, H, and J-L; Whirlpool Deep Beds B and C; Sucker Glide Deep Beds A-E, G, H, J, L, M, and N; and Railroad Deep Beds A-H (Appendix H).

5.5. River2D Model Simulation Flow Runs

An example hydraulic model output is given in Appendix I. The simulation flows were 400 cfs to 2,100 cfs by 100 cfs increments and 2,100 cfs to 4,500 cfs by 200 cfs increments for the study sites in the Above Daguerre Segment and 150 cfs to 2,100 cfs by 100 cfs increments, 2,100 cfs to 2,900 cfs by 200 cfs increments and 2,900 cfs to 4,500 cfs by 400 cfs increments for the study sites in the Below Daguerre Segment[31]. The lowest simulated flow for the Above Daguerre Segment was 40% of the lowest measured flow. The lowest simulated flow for the Below Daguerre Segment (150 cfs) was the lowest specified flow in the Yuba River Accord. For the Side-Channel site, we used a minimum groundwater depth of 0.005 for flows of 1,800 cfs or less, and used the default minimum groundwater depth of 0.05 for flows greater than 1,800 cfs. The production cdg files all had a Sol Δ of less than 0.00001, but the net Q was greater than 1% for 7

---

[29] Velocities were plotted versus easting for transects that were oriented primarily east-west, while velocities were plotted versus northing for transects that were primarily north-south.

[30] Deep beds refers to the data collected with the ADCP between the transects.

[31] The lowest simulation flow for Whirlpool site was 300 cfs and the lowest simulation flow for Side-Channel site was 900 cfs because there was no flow in these sites for total Yuba River flows less than the above flows.

flows for Narrows, 1 flow for Lower Hallwood, 10 flows for Side-Channel, 11 flows for Sucker Glide, and 4 flows for Railroad (Appendix J). The maximum Froude Number exceeded one for all of the simulated flows for Rosebar, Side-Channel, Sucker Glide, and Railroad sites. The maximum Froude Number exceeded one for 29 out of the 30 simulated flows for Narrows, 11 out of 30 simulated flows for Diversion, 23 out of 30 simulated flows for Lower Hallwood, and 15 out 28 simulated flows for Whirlpool (Appendix J).

6. *Habitat Suitability Criteria Data Collection*

The sampling dates and Yuba River flows are shown in Table 17. We collected 469 measurements of cover and 468 measurements of depth, velocity and adjacent velocity where YOY Chinook salmon and steelhead/rainbow trout were observed. All but 8 of these measurements were made near the river banks. There were 244 observations of Chinook salmon and 258 observations of steelhead/rainbow trout[32]. There were 82 observations of fish less than 40 mm, 311 observations of 40-60 mm fish, 78 observations of 60-80 mm fish and 39 observations of fish greater than 80 mm. A total of 6.1 miles of near-bank habitat and 1.4 miles of mid-channel habitat were sampled. Table 18 summarizes the number of feet of different mesohabitat types sampled and Table 19 summarizes the number of feet of different cover types sampled. We snorkeled upstream through an additional 21.6 miles (34.8 kilometers) of near-bank habitat and downstream through 6.9 miles (11.1 kilometers) of mid-channel habitat in November to December 2004 and in July to September 2005. While snorkeling this additional habitat during both these time periods, we did not observe any salmonids greater than 60 mm SL and did not collect any unoccupied data. Table 20 summarizes the number of feet of different mesohabitat types snorkeled in November to December 2004 and in July to September 2005 and the results of these surveys.

We sampled 27,239 feet (8302 meters) of cover group 0 and 4,856 feet (1480 meters) of cover group 1 in near-bank habitats, and 7,091 feet (2161 meters) of cover group 0 and 405 feet (123 meters) of cover group 1 in mid-channel habitats. Depths at locations where YOY Chinook salmon and steelhead/ rainbow trout were observed ranged from 0.2 to 18.4 feet (0.06 to 5.61 meters), while velocities ranged from 0 to 3.98 ft/s (0 to 1.21 m/s) and adjacent velocities ranged from 0 to 4.80 ft/s (0 to 1.46 m/s). SCUBA was used for sampling in September 2003 to September 2004 and in August 2005.

We made 1,624 measurements for unoccupied observations (1,385 in shallow areas and 239 in deep areas), with depths ranging from 0 to 42.2 feet (0 to 12.86 meters), velocities ranging from 0 to 5.56 ft/s (0 to 1.69 m/s) and adjacent velocities ranging from 0 to 6.51 ft/s (0 to 1.98 m/s). Depth and velocity were measured for all 1,624 unoccupied locations, and adjacent velocity was

---

[32] These numbers total more than 469 because many of the observations included both Chinook salmon and steelhead/rainbow trout YOY and only one measurement was made per group of closely associated individuals.

Table 17. Chinook salmon and steelhead/rainbow trout YOY HSC sampling dates and flows.

Sampling Dates	Yuba River Flows (cfs) Upstream of Daguerre Point Dam	Downstream of Daguerre Point Dam
September 8-11, 2003	820	536
November 3-6, 2003	938	590
January 26-29, 2004	2,128	2,157
March 22-24, 2004	2,311	2,450
May 17-20, 2004	2,234	1,560
July 12-15, 2004	2,005	1,015
September 20-23, 2004	707	508
November 15-18, 2004	829	522
December 13-16, 2004	760	679
February 7-10, 2005	940	901
July 11-14, 2005	2,827	1,685
August 8-11, 2005	1,699	722
September 6-9, 2005	848	853

measured at 1,623 locations. Cover was not collected at one unoccupied location. We collected unoccupied observations for all of the 6.1 miles (9.8 kilometers) of near-bank habitat sampled and for all but 1500 feet (457.2 meters) of the mid-channel habitat sampled with SCUBA.

7. *Biological Verification Data Collection*

We conducted biological verification surveys on eight study sites. However, fry and juvenile fall/spring-run Chinook salmon and/or steelhead/rainbow trout were observed only in five of those sites. The horizontal locations of Chinook salmon and steelhead/rainbow trout fry and juveniles and unoccupied locations found during surveys listed in Table 21 were recorded by sighting from the total station to a stadia rod and prism. Table 22 shows the numbers of fall/spring-run Chinook salmon and/or steelhead/rainbow trout fry and juveniles that were observed and horizontal locations recorded using total station in each of these five sites. Note

Table 18. Distances (feet and meters) sampled for juvenile salmonid HSC data - mesohabitat types. Bar Complex and Flatwater Pools were typically the only habitat types that were deep enough to sample with SCUBA. Distances in this table include only areas where unoccupied data were collected, and include all areas sampled in September 2003 to September 2004 and February 2005, but only areas where fish > 60 mm SL were found for November to December 2004 and July to September 2005.

Mesohabitat Type	**Near-bank Habitat Distance Sampled (ft, m)**		**Mid-channel Habitat Distance Sampled (ft, m)**	
Bar Complex Glide	5,780	1762	300	91
Bar Complex Pool	4,205	1282	4,140	1262
Bar Complex Riffle	2,344	714	0	0
Bar Complex Run	12,296	3748	0	0
Flatwater Glide	1,080	329	0	0
Flatwater Pool	1,400	427	3,055	931
Flatwater Riffle	0	0	0	0
Flatwater Run	330	101	0	0
Side-Channel Glide	699	213	0	0
Side-Channel Pool	915	279	0	0
Side-Channel Riffle	220	67	0	0
Side-Channel Run	2,826	861	0	0

that we sampled one of these five sites (Timbuctoo) three times and sampled another of the five sites (Hammond) twice. In both cases, different portions of the site were sampled each time. We were limited by time constraints in the number of sites and dates that we could conduct the biological verification surveys.

8. *Habitat Suitability Criteria Development*

The results of the Mann-Whitney U tests and Pearson's test for association to test for differences between fry and juvenile salmonids (Table 23) showed significant differences (at p = 0.05) between fry and juvenile habitat use for all four variables for the <60 mm versus >60 mm criteria to separate fry from juveniles. In contrast, there were no significant differences (at p = 0.05) for adjacent velocity for the <40 mm versus > 40 mm criteria and for all parameters except depth for the <80 mm versus > 80 mm criteria. Hereafter, fry refers to YOY less than 60 mm, while juvenile refers to YOY greater than 60 mm.

Table 19. Distances (feet and meters) sampled for juvenile salmonid HSC data - cover types. Data in this table are for the same areas sampled for which data are given in Table 15.

Cover Type	Near-bank Habitat Distance Sampled (ft, m)		Mid-channel Habitat Distance Sampled (ft, m)	
None	9,625	2,934	3,941	1,201
Cobble	10,872	3,314	449	137
Boulder	4,472	1,363	2,025	617
Fine Woody	4,193	1,278	80	25
Branches	1,507	459	224	68
Log	297	91	78	24
Overhead	809	247	0	0
Undercut	3	0.9	0	0
Aquatic Vegetation	261	80	548	167
Rip Rap	56	17	150	46
Overhead + instream	3,732	1,138	384	117

Table 20. Distances (feet and meters) snorkeled in November to December 2004 and in July to September 2005 where we didn't observe any salmonids greater than 60 mm SL and where we did not collect any unoccupied data.

Mesohabitat Type	Near-bank Habitat Distance Sampled (ft, m)		Mid-channel Habitat Distance Sampled (ft, m)	
Bar Complex Glide	2,223	678	5,559	1,694
Bar Complex Pool	17,859	5,443	9,660	2,944
Bar Complex Riffle	2,190	668	1,550	472
Bar Complex Run	36,482	11,120	5,761	1,756
Flatwater Glide	1,944	593	420	128
Flatwater Pool	13,982	4,262	0	0
Flatwater Riffle	0	0	0	0
Flatwater Run	200	61	0	0
Side-Channel Glide	3,228	984	1,673	510
Side-Channel Pool	2,932	894	1,529	466
Side-Channel Riffle	0	0	0	0
Side-Channel Run	13,103	3,994	10,186	3,105

Table 21. Date, study site, mesohabitat number, mesohabitat type and flow for juvenile steelhead/rainbow trout and fall/spring Chinook salmon surveys where biological verification data were collected.

Date	Study Site	MHU #	MHU Type	Flow (cfs)
11/3/2003	Upper Daguerre	86	BCRI	607
11/3/2003	Upper Daguerre	87	BCRU	607
11/4/2003	U.C. Sierra	180	SCRU	945
11/4/2003	U.C. Sierra	178	BCG	945
11/6/2003	Timbuctoo	158	SCRU	917
11/6/2003	Timbuctoo	160	SCRU	917
11/6/2003	Timbuctoo	161	SCP	917
1/28/2004	Island	130	BCG	2,252
3/22/2004	Railroad	11	FWP	2,510
3/23/2004	Side-Channel	30	SCRU	2,430
3/23/2004	Side-Channel	31	SCP	2,430
5/18/2004	Lower Daguerre	83	BCRU	1,560
5/19/2004	Hammond	112	BCRU	1,540
7/14/2004	Timbuctoo	170	SCRU	2,022
7/15/2004	Timbuctoo	168	BCG	1,963
9/21/2004	Hammond	112	BCRU	708

The results of the Mann-Whitney U tests and Pearson's test for association to test for differences between Chinook salmon and steelhead/rainbow trout indicate significant differences (at p = 0.05) between species for fry for velocity and adjacent velocity and for juveniles for depth (See χ^2 values in Table 23) and for both fry and juveniles for cover (see C values in Table 24), but there were no significant differences (at p = 0.05) between species for fry for depth or for juveniles for velocity and adjacent velocity. Since the p-value for depth for fry was only slightly larger than 0.05, we developed separate criteria for Chinook salmon and steelhead/rainbow fry rearing to reduce Type II error. For juveniles, we lumped together data for both species for velocity and adjacent velocity, but split the data between species for depth and cover.

Table 22. Observation results for biological verification surveys.

Date	Site	Chinook Fry	Chinook Juvenile	Steelhead/ Rainbow Trout Fry	Steelhead/ Rainbow Trout Juvenile
11/6/2003	Timbuctoo			28	1
12/28/2004	Island	3			
3/23/2004	Side-Channel	17	3		
5/18/2004	Lower Daguerre	5	1		
5/19/2004	Hammond	5	1	6	1
7/14/2004	Timbuctoo	19		20	
7/15/2004	Timbuctoo	19		17	
9/21/2004	Hammond	2			

Table 23. Differences in YOY salmonid habitat use as a function of size.

Variable	<40 mm Versus > 40 mm	<60 mm Versus > 60 mm	< 80 mm Versus > 80 mm
Depth	$\chi^2 = 36.07$, $p < 0.000001$, n = 83, 408	$\chi^2 = 61.51$, $p < 0.000001$, n = 109, 371	$\chi^2 = 24.08$, $p = 0.000001$, n = 39, 437
Velocity	$\chi^2 = 7.42$, $p = 0.0064$, n = 83, 408	$\chi^2 = 18.82$, $p = 0.000014$, n = 109, 371	$\chi^2 = 0.13$, $p = 0.71$, n = 39, 437
Adjacent Velocity	$\chi^2 = 1.92$, $p = 0.16$, n = 83, 408	$\chi^2 = 20.65$, $p = 0.000005$, n = 109, 371	$\chi^2 = 1.07$, $p = 0.30$, n = 39, 437
Cover	C = 21, p = 0.03, n = 83, 409	C = 40, p = 0.00003, n = 372, 109	C = 17, p = 0.12, n = 39, 437

Based on the CDFG race table, fall/spring-run Chinook salmon fry are present between October 16 and June 29[33]. As a result, we only used unoccupied data collected between October 16 and June 29 (835 observations) to develop fall/spring-run Chinook salmon fry depth, velocity, adjacent velocity and cover criteria, for the time periods when we collected occupied data on fry (September 2003 to September 2004 and February 2005). We observed steelhead/rainbow trout fry in the Yuba River between May and January, Chinook salmon juveniles in the Yuba River between March and September, and steelhead/rainbow trout juveniles in the Yuba River between May and December. As a result, we only used unoccupied data collected between May and January (1,154 observations) to develop steelhead/rainbow trout fry depth, velocity, adjacent

33 We did not observe any fall/spring-run Chinook salmon outside of this time period.

Table 24. Differences in YOY habitat use as a function of species.

Variable	< 60 mm Fish	> 60 mm Fish
Depth	χ^2 = 3.51, p = 0.061, n = 178, 195	χ^2 = 22.42, p = 0.00002, n = 39, 74
Velocity	χ^2 = 20.74, p = 0.000005, n = 178, 195	χ^2 = 0.97, p = 0.32, n = 39, 74
Adjacent Velocity	χ^2 = 19.05, p = 0.000013, n = 178, 195	χ^2 = 0.43, p = 0.43, n = 39, 74
Cover	C = 90, p = 1.5 x 10^{-14}, n = 179, 195	C = 20.6, p = 0.008, n = 39, 74

velocity and cover criteria, for the time periods when we collected occupied data on fry (September 2003 to September 2004 and February 2005). Further, we only used unoccupied data collected between May and December (1,168 observations) to develop steelhead/rainbow trout juvenile depth and cover criteria, and unoccupied data collected between March and September (968 observations) to develop Chinook salmon juvenile depth and cover criteria. We used all of the unoccupied observations when we combined together juveniles of both species, since juveniles are present year-round. The number of occupied and unoccupied locations for each parameter, species and life-stage are shown in Table 25.

For the transferability tests of juvenile salmonids velocity and adjacent velocity, and Chinook salmon and steelhead/rainbow trout juvenile depth and cover, the optimum ranges from the Sacramento River Chinook salmon juvenile rearing criteria were 1.2 to 3.8 feet (0.37 to 1.16 meters), velocities of 0.15 to 0.74 ft/s (0.05 to 0.23 m/s), adjacent velocities of greater than or equal to 3.00 ft/s (0.91 m/s), and cover codes of 3.7, 4, 4.7, 5, 5.7 and 8. The suitable ranges were 0.4 to 7.6 feet (0.12 to 2.32 meters), velocities of 0 to 1.65 ft/s (0 to 0.50 m/s), adjacent velocities of greater than or equal to 0.05 ft/s (0.02 m/s), and all cover codes. Since there were not any Sacramento River cover codes that were unsuitable, we were only able to conduct the optimum/useable transferability test for cover. The distribution of the Yuba River juvenile salmonid observations, relative to the Sacramento River optimum and suitable ranges, are shown in Figures 4 to 9. The results of the transferability tests (Table 26) were that the Sacramento River juvenile Chinook salmon cover criteria transferred to both Yuba River juvenile Chinook salmon and juvenile steelhead/rainbow trout, that the Sacramento River juvenile Chinook salmon depth criteria transferred to Yuba River juvenile steelhead/rainbow trout but not to Yuba River juvenile Chinook salmon, and that the Sacramento River juvenile Chinook salmon velocity and adjacent velocity criteria did not transfer to Yuba River juvenile salmonids. We modified the Sacramento River juvenile depth criteria to use with Yuba River juvenile steelhead/rainbow trout

Table 25. Number of occupied and unoccupied locations.

		Depth	Velocity	Adjacent Velocity	Cover
Chinook salmon fry	**Occupied**	178	178	178	179
	Unoccupied	835	835	834	835
Steelhead/rainbow trout fry	**Occupied**	195	195	195	195
	Unoccupied	1,154	1,154	1,154	1,153
Juvenile salmonid	**Occupied**	N/A	109	109	N/A
	Unoccupied	N/A	1,624	1,623	N/A
Chinook salmon juvenile	**Occupied**	39	N/A	N/A	39
	Unoccupied	968	N/A	N/A	967
Steelhead/rainbow trout juvenile	**Occupied**	74	N/A	N/A	74
	Unoccupied	1,168	N/A	N/A	1,167

by setting suitability equal to zero for depths less than 0.5 ft (the minimum depth at which we found juvenile steelhead/rainbow trout) and greater than 15 ft (4.57 m) (the maximum depth at which we found juvenile steelhead/rainbow trout).

The coefficients for the final logistic regressions for depth and velocity for each species and size class are shown in Table 27. The p values for all of the non-zero coefficients in Table 26 were less than 0.05, as were the p values for the overall regressions. The logistic regression equation for Chinook fry depth initially peaked at 1.2 feet (0.37 meters), reached a minimum at 10 to 10.1 feet (3.05 to 3.08 meters), and then reached a maximum at 18.4 feet (5.61 meters) (the maximum depth for Chinook fry). There were 2 occupied (1%) and 51 unoccupied (6%) locations with depths greater than 10.1 feet (3.08 meters). As a result, we set the SI to 0.02 (the SI value from the logistic regression at 10.1 feet (3.08 meters)) for depths of 10.1 to 18.4 feet (3.08 to 5.61 meters).

The logistic regression equation for juvenile Chinook salmon depth initially peaked at 3.4 feet (1.04 meters), reached a minimum SI of 0.22 at 7.6 to 8.6 feet (2.32 to 2.62 meters), and then increased to a SI of 0.55 at 11.8 feet (3.60 meters) (the maximum depth at which we found juvenile Chinook salmon in the Yuba River). There were 3 occupied (8%) and 78 unoccupied (8%) locations with depths greater than 8.6 feet (2.62 meters). As a result, we set the SI to 0.22 for depths of 7.6 to 11.8 feet (2.32 to 3.60 meters).

We were unable to use a logistic regression to develop velocity criteria for juvenile salmonids. Following the logistic regression procedure described in the methods, only the constant had a p-value less than 0.05. When the constant was excluded from the logistic regression, the four logistic regression coefficients were less than 0.05, but the regression equation was inconsistent with the observed data. Specifically, this logistic regression equation resulted in suitability reaching zero at 1.5 ft/s (0.46 m/s), even though 19 percent (21 of 109) of the occupied locations had velocities of greater than 1.5 ft/s (0.46 m/s). For velocities up to 2.55 ft/s, the frequency

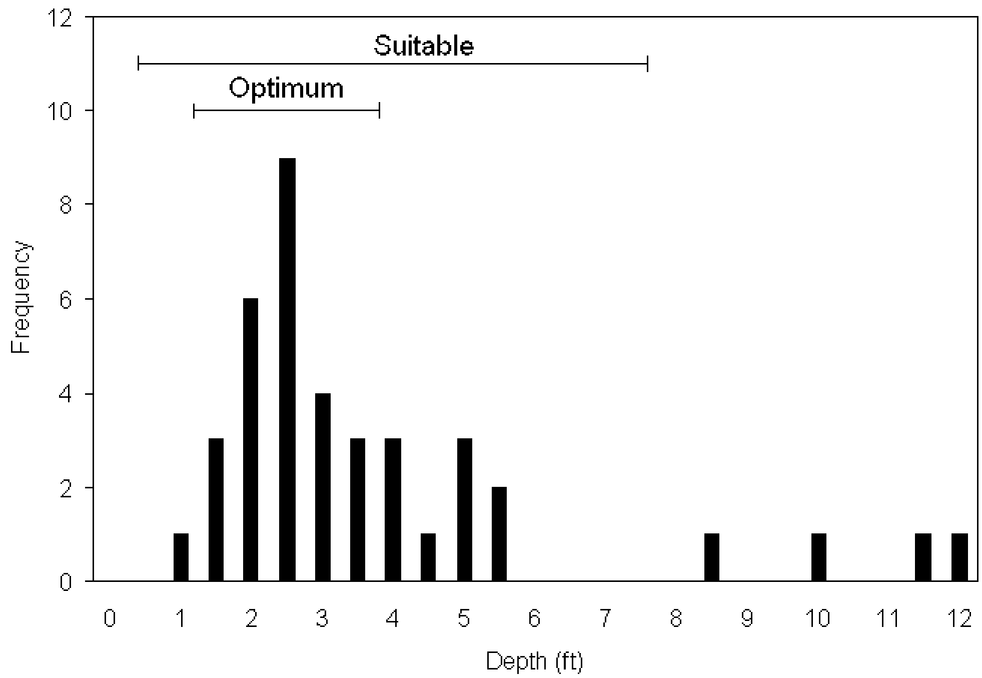

Figure 4. Optimum and suitable ranges of Sacramento River juvenile Chinook salmon depth HSC (horizontal lines) tested against Yuba River juvenile Chinook salmon observations (vertical bars).

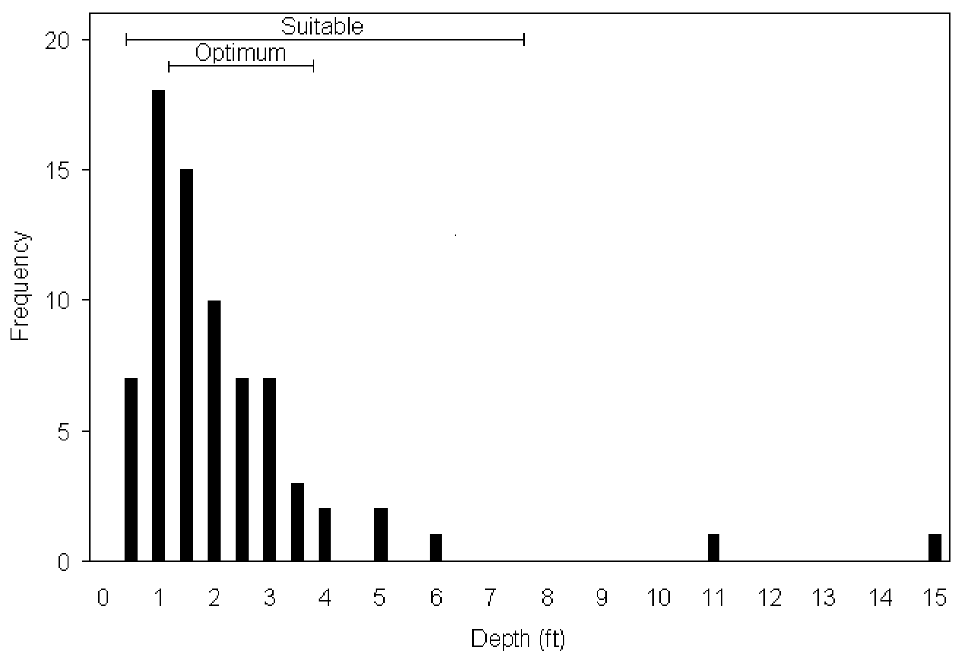

Figure 5. Optimum and suitable ranges of Sacramento River juvenile Chinook salmon depth HSC (horizontal lines) tested against Yuba River juvenile steelhead/rainbow trout observations (vertical bars).

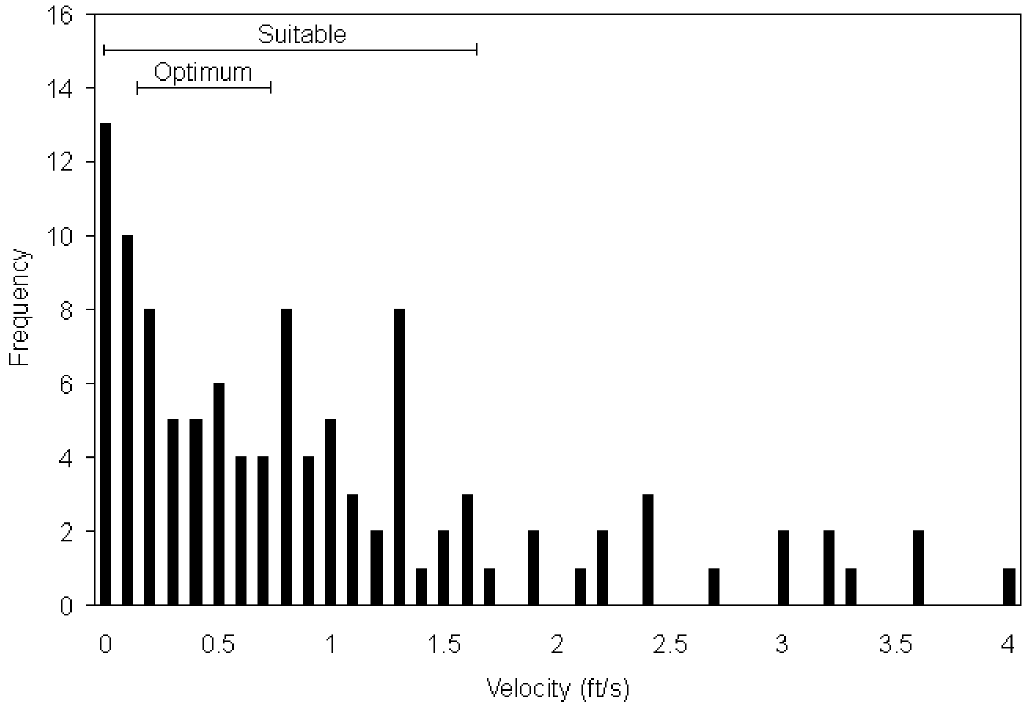

Figure 6. Optimum and suitable ranges of Sacramento River juvenile Chinook salmon velocity HSC (horizontal lines) tested against Yuba River juvenile salmonid observations (vertical bars).

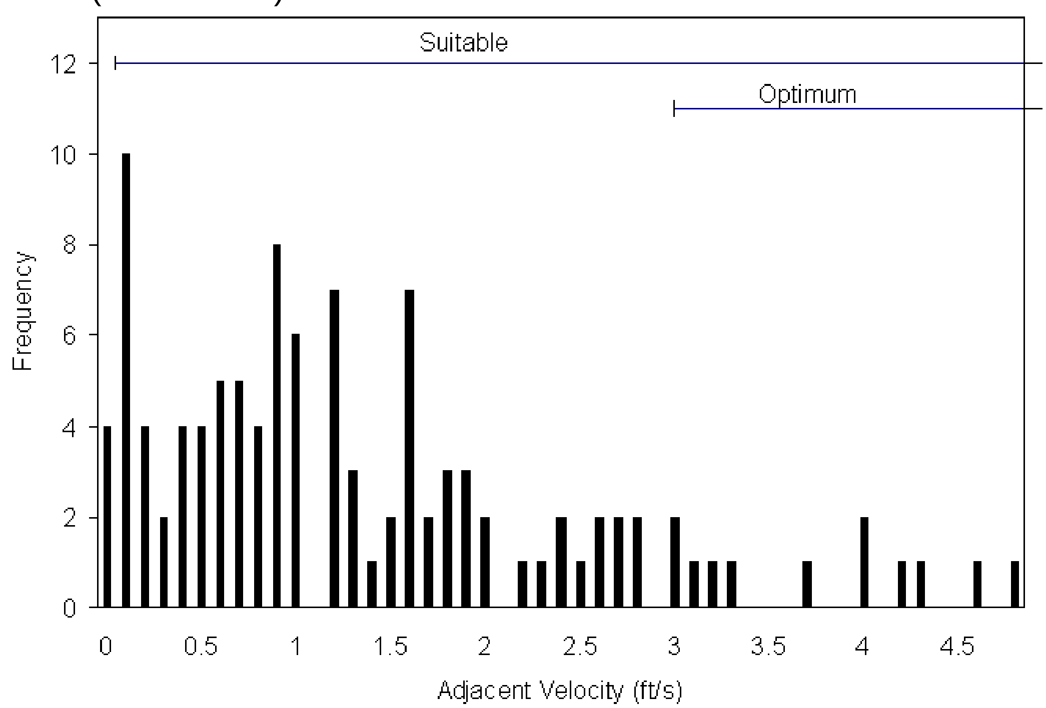

Figure 7. Optimum and suitable ranges of Sacramento River juvenile Chinook salmon adjacent velocity HSC (horizontal lines) tested against Yuba River juvenile salmonid observations (vertical bars).

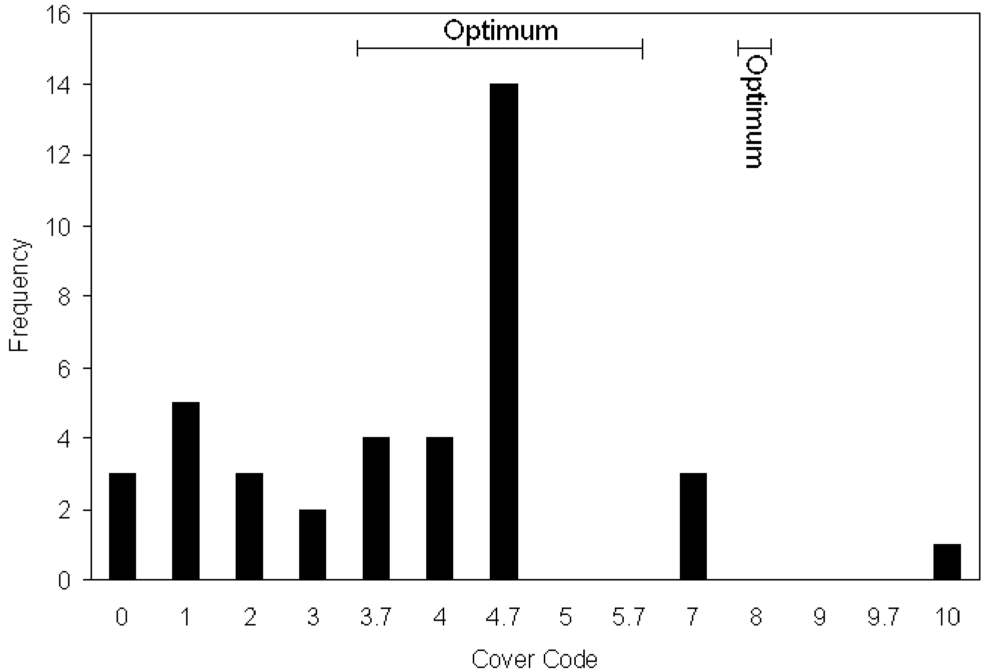

Figure 8. Optimum values of Sacramento River juvenile Chinook salmon cover HSC (horizontal lines) tested against Yuba River juvenile Chinook salmon observations (vertical bars). All cover codes were suitable in the Sacramento River juvenile criteria.

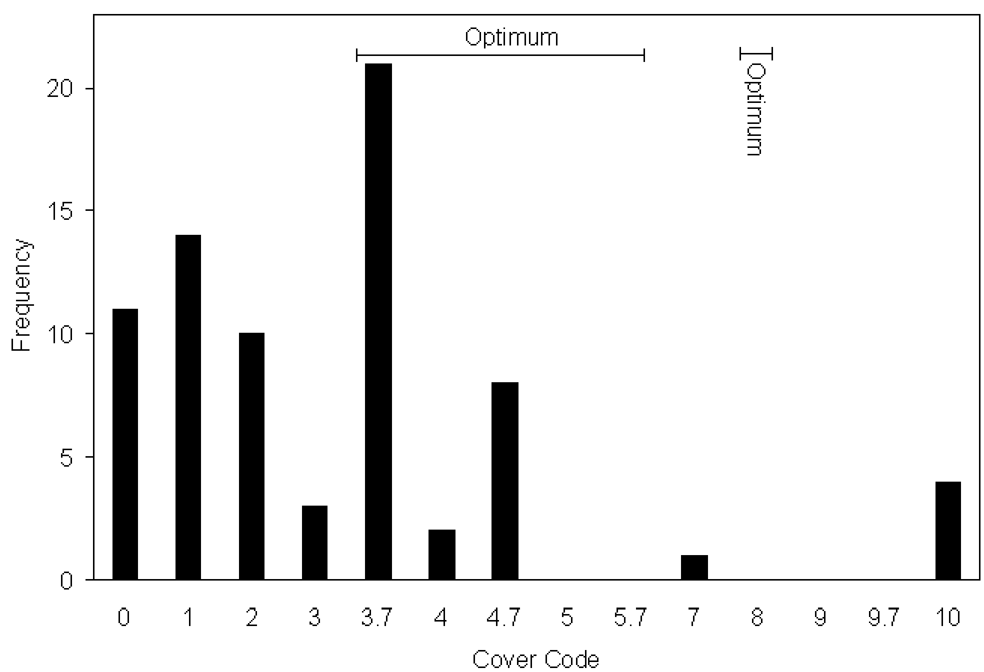

Figure 9. Optimum values of Sacramento River juvenile Chinook salmon cover HSC (horizontal lines) tested against Yuba River juvenile steelhead/rainbow trout observations (vertical bars). All cover codes were suitable in the Sacramento River juvenile criteria.

Table 26. Results of transferability tests. Sacramento River juvenile Chinook salmon cover criteria transferred to both Yuba River juvenile Chinook salmon and juvenile steelhead/rainbow trout, Sacramento River juvenile Chinook salmon depth criteria transferred to Yuba River juvenile steelhead/rainbow trout but not to Yuba River juvenile Chinook salmon, and Sacramento River juvenile Chinook salmon velocity and adjacent velocity criteria did not transfer to Yuba River juvenile salmonids.

Species	Parameter	Optimum/Useable Test	Suitable/Unsuitable Test
Chinook salmon	Depth	$T = 2.52$, p = 0.01	$T = 0.996$, p = 0.16
Chinook salmon	Cover	$T = 9.46$, p =1.6×10^{-21}	N/A
Steelhead/rainbow trout	Depth	$T = 2.63$, p = 0.004	$T = 2.83$, p = 0.002
Steelhead/rainbow trout	Cover	$T = 8.68$, p = 1.9×10^{-18}	N/A
Salmonid	Velocity	$T = -1.02$, p = 0.85	$T = 0.53$, p = 0.30
Salmonid	Adjacent Velocity	$T = 0.65$, p = 0.26	$T = -0.266$, p = 0.60

Table 27. Logistic regression coefficients. A coefficient or constant value of zero indicates that term or the constant was not used in the logistic regression, because the p-value for that coefficient or for the constant was greater than 0.05. The coefficients in this table were determined from Equation 2. The p values for all of the non-zero coefficients were less than 0.05, as were the p values for the overall regressions.

Species/life stage	Parameter	I	J	K	L	M	R^2
Chinook salmon fry	depth	-1.5946	0.68638	-0.326879	0.028827	-0.000702	0.06
Chinook salmon fry	velocity	-0.9490	0	-2.111003	0.978349	-0.122900	0.09
Steelhead/rainbow trout fry	depth	-2.4204	1.40089	-0.492838	0.040801	-0.000975	0.07
Steelhead/rainbow trout fry	velocity	-1.5340	0	-0.208349	0	0	0.03
Chinook salmon juvenile	depth	-9.1580	5.34456	-1.330538	0.125920	-0.004031	0.13

distribution of juvenile salmonids and steelhead/rainbow trout fry is similar (Figure 10). In contrast, above 2.55 ft/s (0.78 m/s), there was only one observation of steelhead/rainbow trout fry. For velocities less than or equal to 2.55 ft/s (0.78 m/s), there was no significant difference between velocities used by juvenile salmonids and steelhead/rainbow trout fry (Mann-Whitney U test, p = 0.18, n = 100, 194).

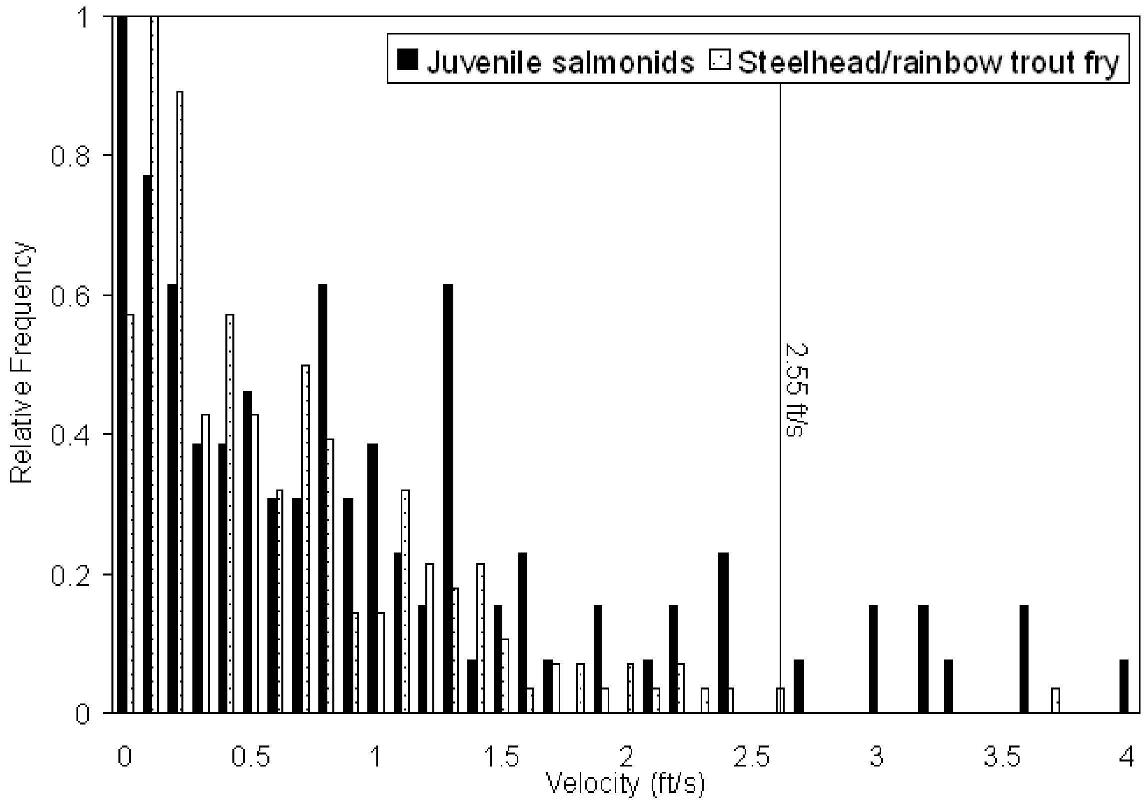

Figure 10. Comparison of relative frequency distribution of juvenile salmonid and steelhead/rainbow trout fry velocities. The relative frequencies for each life stage were calculated by rescaling the frequencies so that the highest relative frequency for each life stage had a value of 1.0.

Accordingly, we used the steelhead/rainbow trout fry velocity criteria for juvenile salmonids up to 2.55 ft/s (0.78 m/s), and then kept a constant suitability for velocities of 2.55 to 3.98 ft/s (0.78 to 1.21 m/s) (the maximum velocity at which we observed juvenile salmonids). The final depth and velocity criteria, reflecting the combined effects of the frequency distributions of occupied and unoccupied locations, are shown in Figures 11 through 17 and Appendix K.

Adjacent velocities were highly correlated with velocities (Table 28). For fall/spring-run fry, the [J * V] term was dropped from the regressions because the p-value for J was greater than 0.05. For steelhead/rainbow trout fry adjacent velocity, the [J * V] and [$M * V^4$] terms were dropped from the regressions because the p-values for J and M were greater than 0.05. For juvenile salmonid adjacent velocity, the [J * V], [$L * V^3$] and [$M * V^4$] terms were dropped from the regressions because the p-values for J, L and M were greater than 0.05. The p-values for the remaining coefficients were less than 0.05, as were the overall p values for the four logistic regressions. The I and N coefficients from equation 3 are given in Table 28. The results of equation 4 and the derivation of the final adjacent velocity criteria (Appendix K) are shown in Figures 18 to 20.

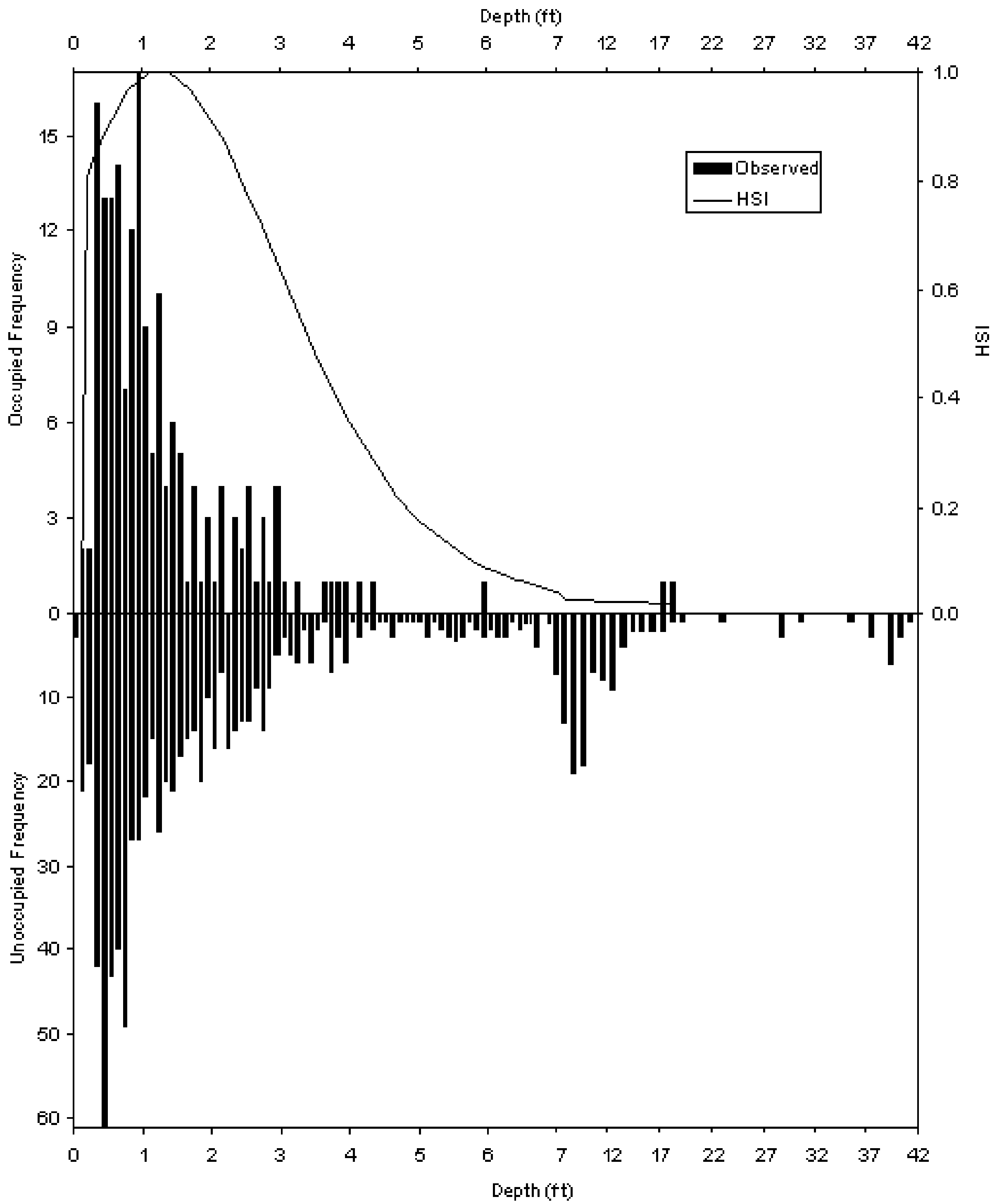

Figure 11. Fall/spring-run Chinook salmon fry rearing depth HSC. The HSC show that fall/spring-run Chinook salmon fry rearing has a non-zero suitability for depths of 0.2 to 18.4 feet (0.06 to 5.61 meters) and an optimum suitability at depths of 1.1 to 1.4 feet (0.34 to 0.43 meters).

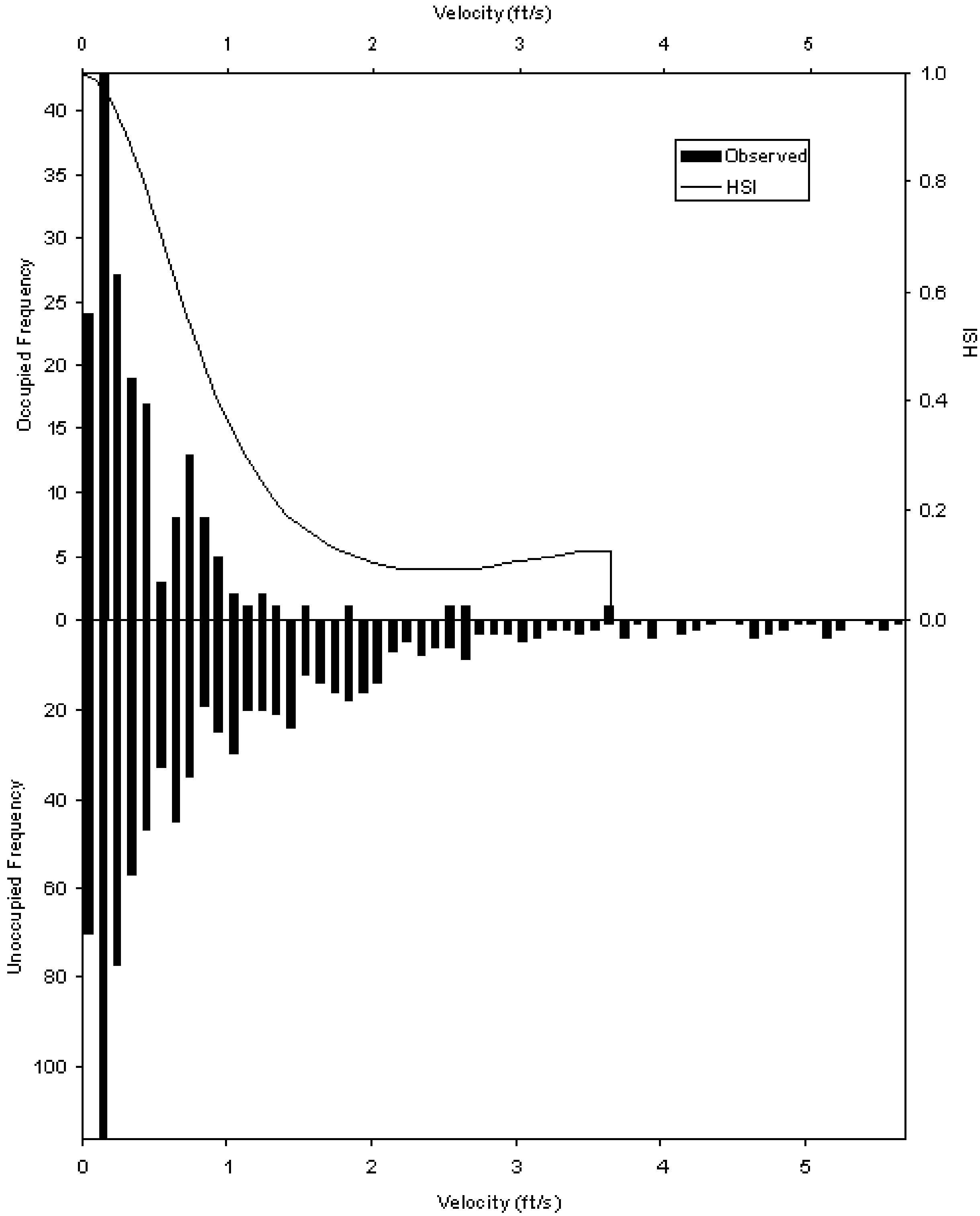

Figure 12. Fall/spring-run Chinook salmon fry rearing velocity HSC. The HSC show that fall/spring-run Chinook salmon fry rearing has a non-zero suitability for velocities of 0 to 3.62 feet/sec (1.10 meters/sec) and an optimum suitability at a velocity of zero.

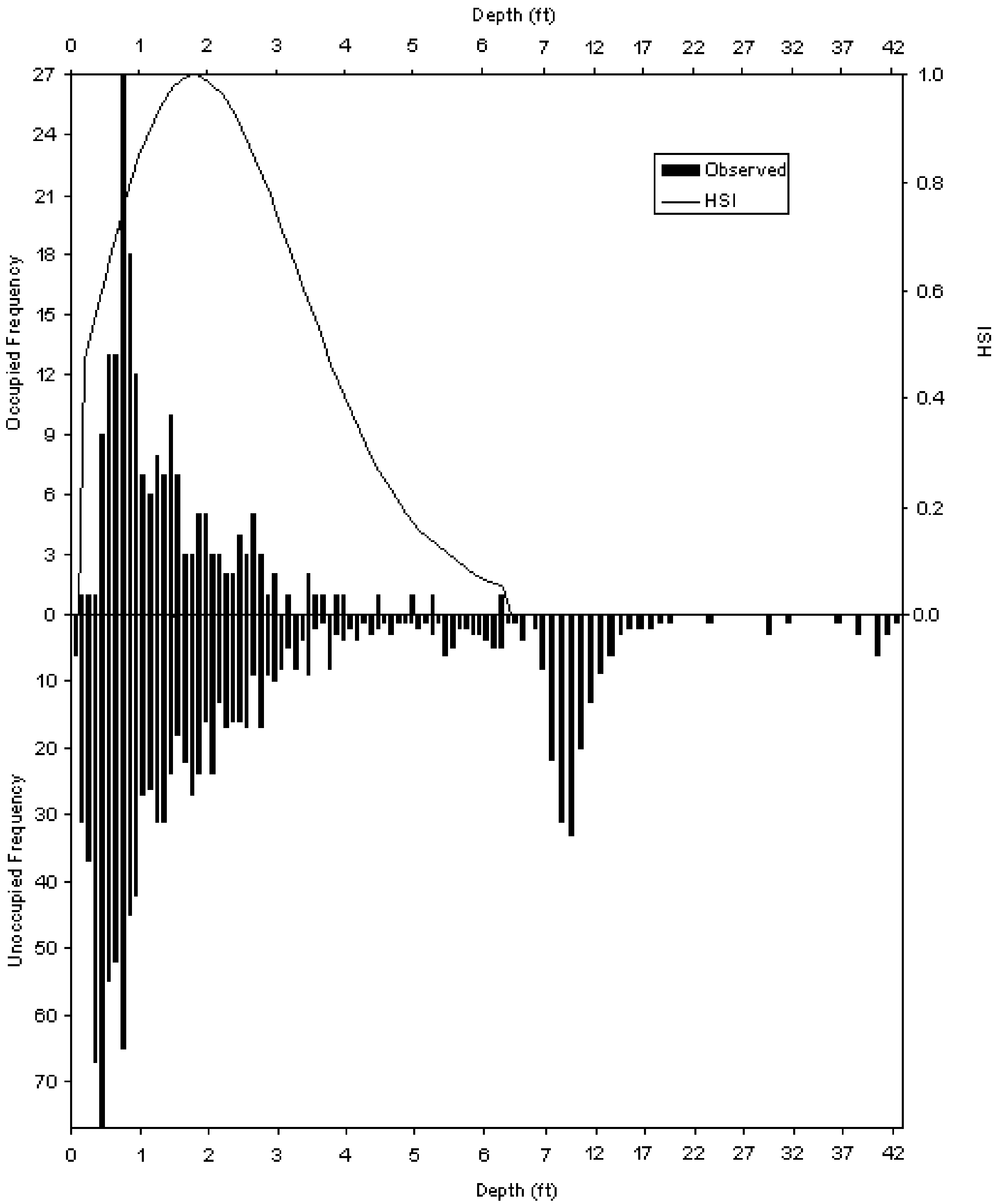

Figure 13. Steelhead/rainbow trout fry rearing depth HSC. The HSC show that steelhead/rainbow trout fry rearing has a non-zero suitability for depths of 0.2 to 6.3 feet (0.06 to 1.92 meters) and an optimum suitability at depths of 1.7 to 1.9 feet (0.52 to 0.58 meters).

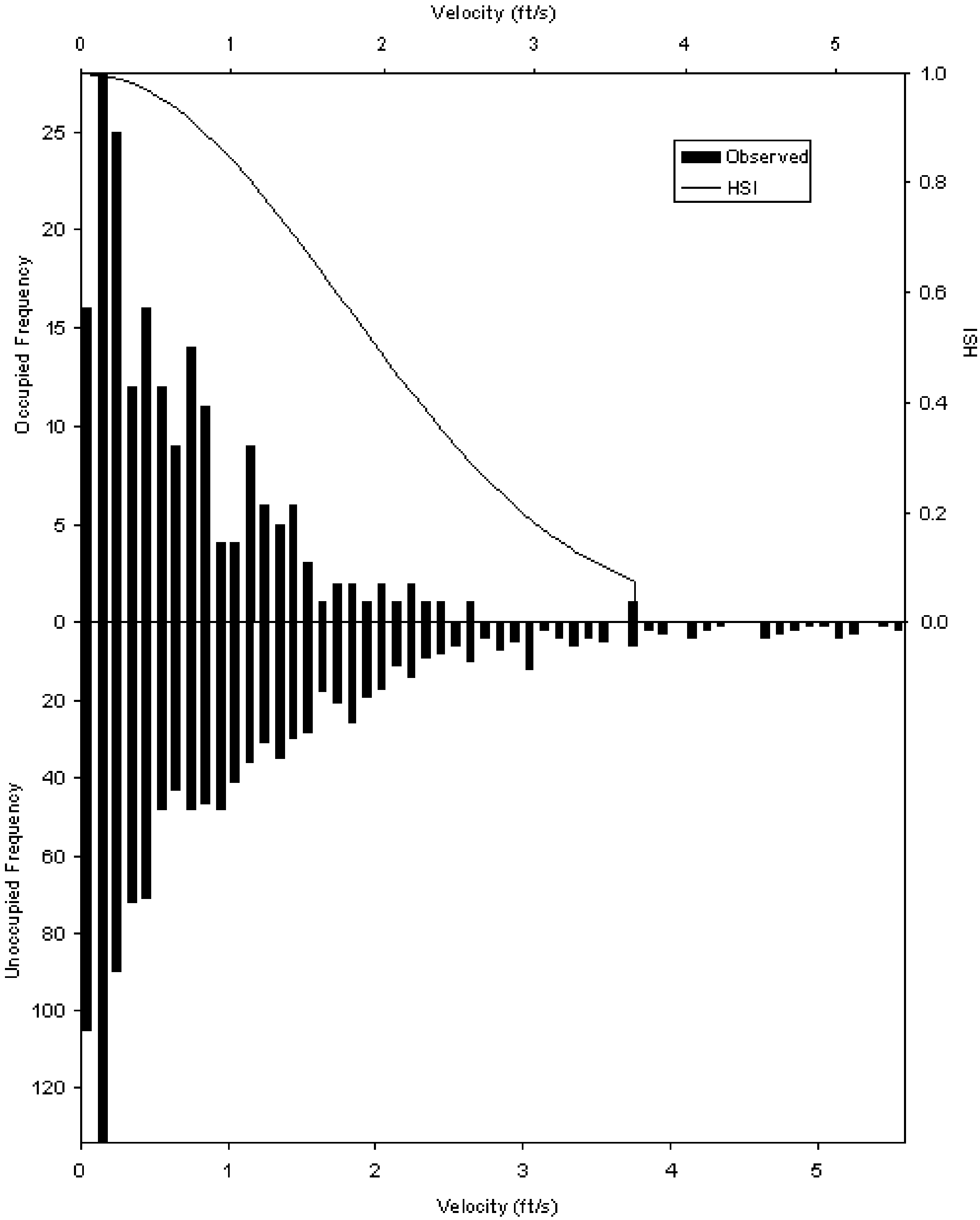

Figure 14. Steelhead/rainbow trout fry rearing velocity HSC. The HSC show that steelhead/rainbow trout fry rearing has a non-zero suitability for velocities of 0 to 3.66 feet/sec (0 to 1.12 meters/sec) and an optimum suitability at velocities of 0 to 0.1 feet/sec (0 to 0.03 meters/sec).

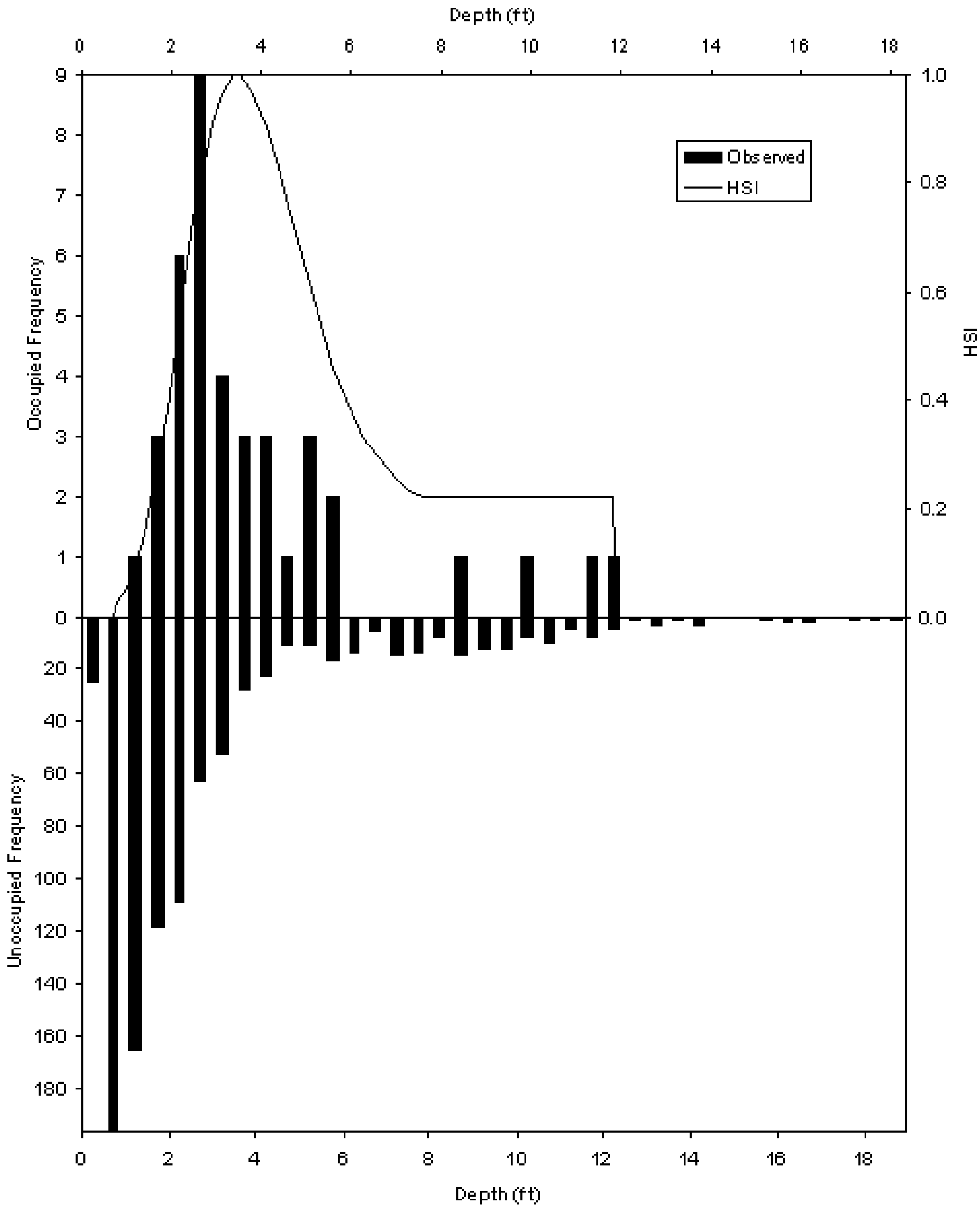

Figure 15. Fall/spring-run Chinook salmon juvenile rearing depth HSC. The HSC show that fall/spring-run Chinook salmon juvenile rearing has a non-zero suitability for depths of 0.2 to 11.8 feet (0.06 to 3.60 meters) and an optimum suitability at depths of 3.4 to 3.5 feet (1.04 to 1.07 meters).

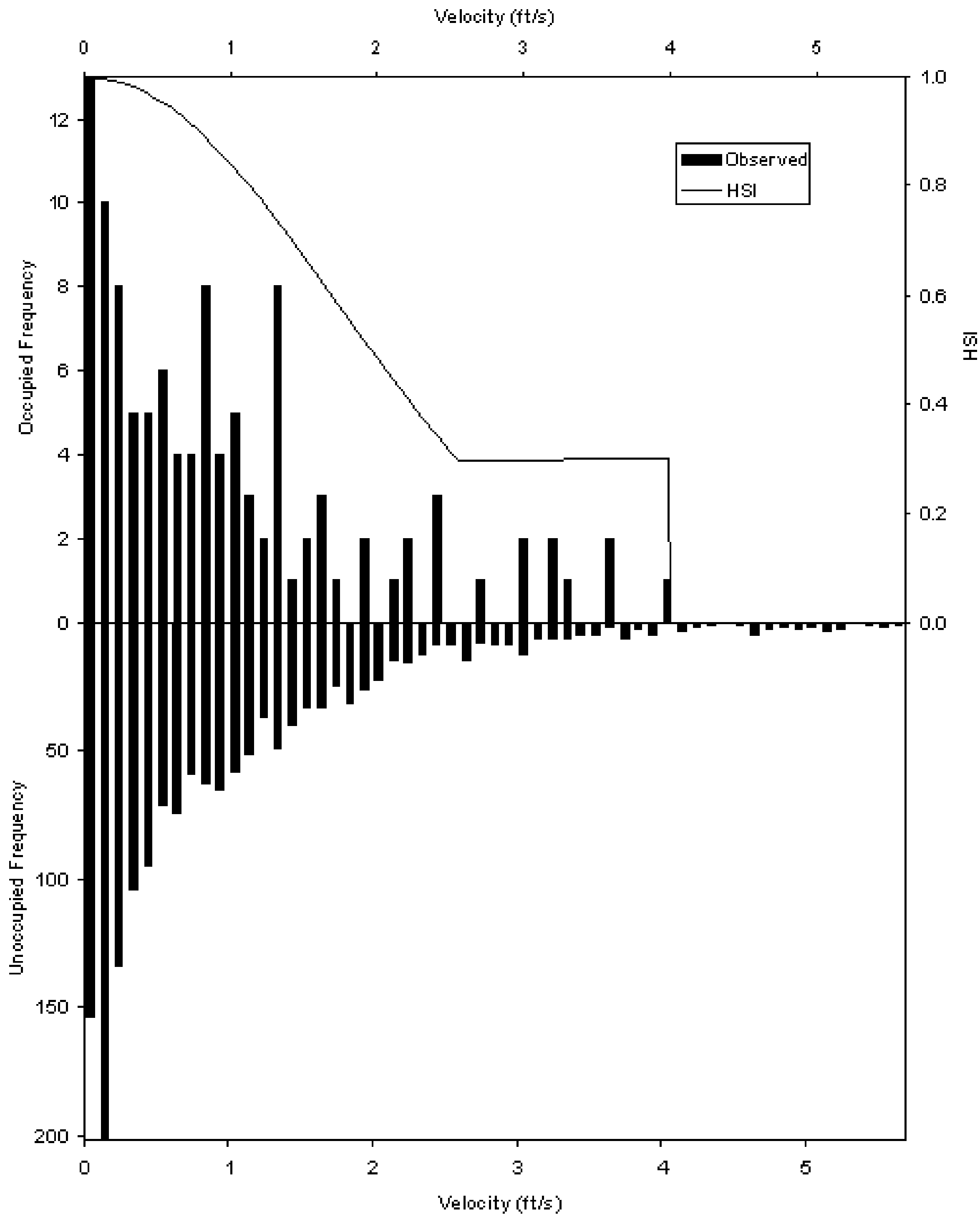

Figure 16. Fall/spring-run Chinook salmon and steelhead/rainbow trout juvenile rearing velocity HSC. The HSC show that fall/spring-run Chinook salmon and steelhead/rainbow trout juvenile rearing has a non-zero suitability for velocities of 0 to 3.98 feet/sec (0 to 1.21 meters/sec) and an optimum suitability at velocities of 0 to 0.1 feet/sec (0 to 0.03 meters/sec).

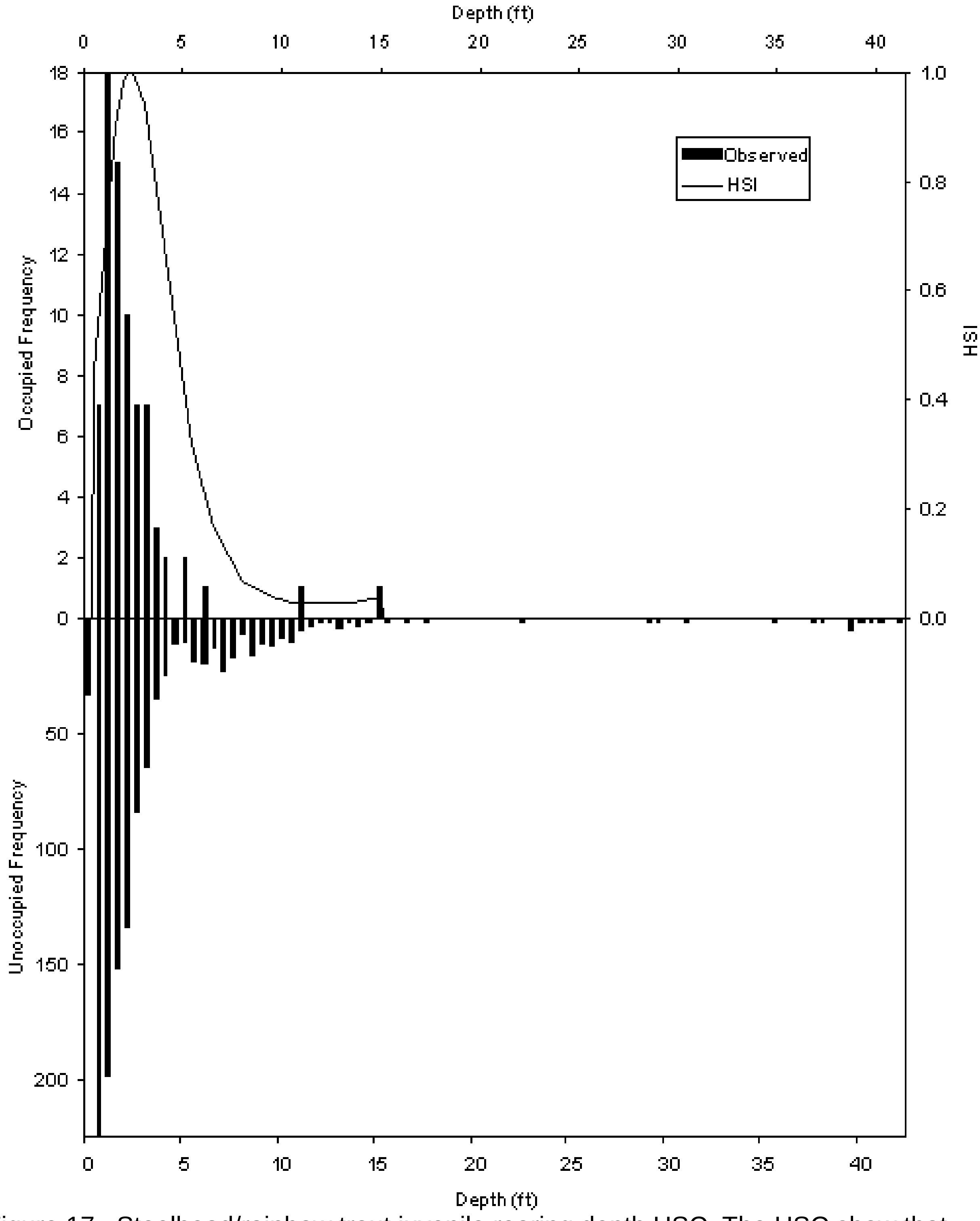

Figure 17. Steelhead/rainbow trout juvenile rearing depth HSC. The HSC show that steelhead/rainbow trout juvenile rearing has a non-zero suitability for depths of 0.2 to 15.0 feet (0.06 to 4.57 meters) and an optimum suitability at depths of 2.2 to 2.5 feet (0.67 to 0.76 meters).

Table 28. Adjacent velocity logistic regression coefficients and R^2 values. The R^2 values are McFadden's Rho-squared values. The coefficients in this table were determined from Equation 3.

Species/Life Stage	Velocity/Adjacent Velocity Correlation	I	N	R^2
Chinook fry	0.94	-1.119996	0.489388	0.09
Steelhead/rainbow trout fry	0.93	-1.789983	0.537042	0.04
Juvenile salmonids	0.93	-3.084743	0.513841	0.01

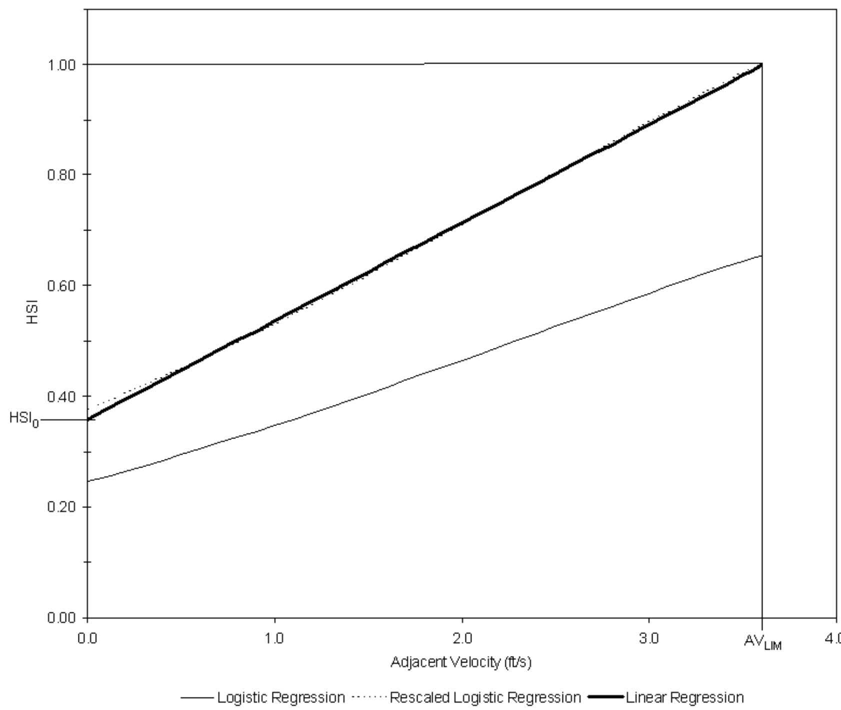

Figure 18. Fall/spring-run Chinook salmon fry rearing adjacent velocity HSC.

The initial analysis of cover used the occupied and unoccupied observations in Table 24. For fall/spring-run Chinook salmon fry, there was a total of two or less observations for cover codes 5 (log) and 8 (undercut bank). For steelhead/rainbow trout fry, there was a total of two or less observations for cover codes 5, 5.7 (log plus overhead), 8 and 9.7 (aquatic vegetation plus overhead). The statistical tests are presented in Tables 29 and 30. For Table 29, an asterisk indicates that presence/absence of fish for those cover codes were significantly different at p = 0.05. For Table 30, an asterisk indicates that fish presence/absence was significantly different between groups at p = 0.05. Our analysis indicated that there were four distinct groups (A, B, C and D) of cover types for fall/spring-run Chinook salmon fry and four distinct groups for

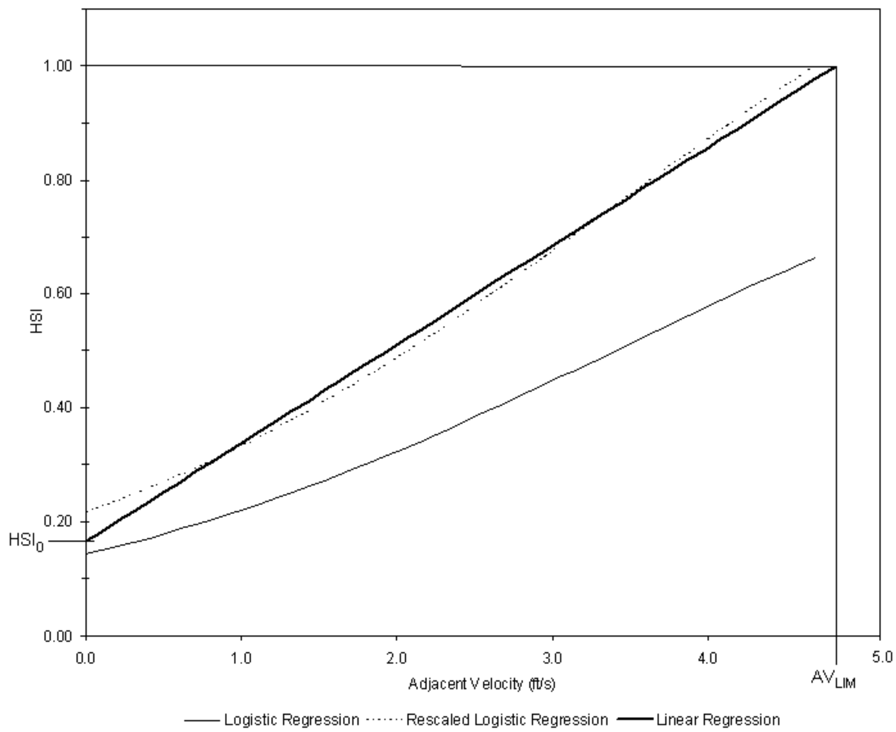

Figure 19. Steelhead/rainbow trout fry rearing adjacent velocity HSC.

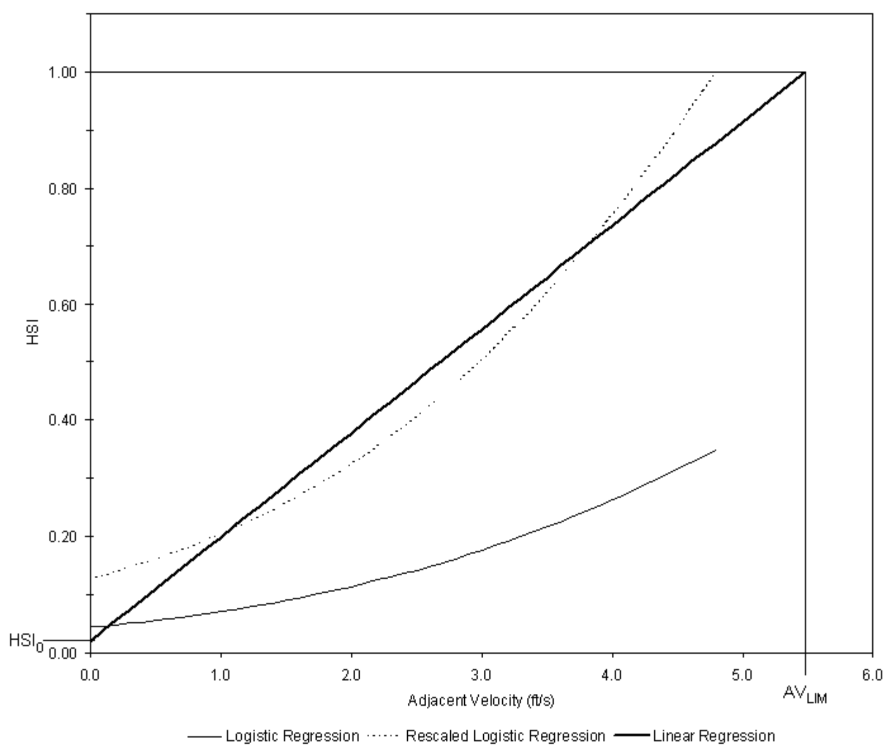

Figure 20. Fall/spring-run Chinook salmon and steelhead/rainbow trout juvenile rearing adjacent velocity HSC.

Table 29. Statistical tests of difference between cover codes for all cover codes and for groups of cover codes. An asterisk indicates that presence/absence of fish (occupied versus unoccupied) for those cover codes were significantly different at p = 0.05.

Species	Cover Codes	c-value
Chinook salmon	4.7, 3.7, 5.7, 4, 10, 3, 9, 7, 1, 0.1, 2, 9.7	192 *
Chinook salmon	4.7, 3.7, 5.7 (log + overhead), 4	2.40
Chinook salmon	10 (rip-rap), 3 (fine woody)	0.0036
Chinook salmon	9, 7 (overhead cover), 1 (cobble)	0.71
Chinook salmon	0.1, 2, 9.7(aquatic vegetation + overhead)	4.94
Steelhead/rainbow trout	3.7, 10, 4.7, 4, 1, 7, 3, 2, 0.1, 9	105 *
Steelhead/rainbow trout	3.7, 10, 4.7 (branches + overhead)	0.79
Steelhead/rainbow trout	4 (branches), 1	0.01
Steelhead/rainbow trout	7, 3, 2 (boulder)	1.95
Steelhead/rainbow trout	0.1 (no cover), 9 (aquatic vegetation)	1.40

Table 30. Statistical tests of differences between the cover code groups shown in Table 29. An asterisk indicates that fish presence/absence (occupied versus unoccupied) was significantly different between Groups at p = 0.05.

	Cover Codes In Group				
Species	Group A	Group B	Group C	Group D	c-value
Chinook salmon	4.7, 3.7, 5.7, 4	10, 3	9, 7, 1	0.1, 2, 9.7	189 *
Steelhead/rainbow trout	3.7, 10, 4.7	4, 1	7, 3, 2	0.1, 9	101 *

steelhead/rainbow trout fry. This was the minimum number of groups for which there were significant differences between groups but no significant differences among the cover codes in each group. For fall/spring-run Chinook salmon fry, we assigned cover codes 5 and 8 the same suitability as cover codes 4.7 (branches plus overhead), 3.7 (fine woody plus overhead), 5.7 and 4 (branches), since the Sacramento River cover criteria had the same suitability for all six of these cover codes. For steelhead/rainbow trout fry, we assigned cover codes 5, 5.7 and 8 the same suitability as cover codes 3.7, 10 (rip-rap) and 4.7, since the Sacramento River cover criteria had the same suitability for cover codes 3.7, 4.7, 5, 5.7 and 8. In addition, we assigned cover code 9.7 the same suitability as cover code 9 (aquatic vegetation), since there were no occupied and two unoccupied locations for cover code 9.7, indicating that this cover code should have a low suitability. As discussed above, the Sacramento River cover criteria were used for both fall/spring-run Chinook salmon and steelhead/rainbow trout juveniles. The final cover HSC values for both species and life stages are shown in Figures 21 to 23 and in Appendix K.

9. *Biological Verification*

The fry or juvenile locations for Island site were not included in the analysis as a result of the total station horizontal angle being set incorrectly. This caused the juvenile observations to have the wrong horizontal locations. There was no significant difference in the combined habitat suitability predicted by the 2-D model (Figure 24) for locations with fall/spring-run Chinook fry (median = 0.094, n = 33) than for locations without fry (median = 0.081, n = 52), based on the one-tailed Mann-Whitney U test (U = 667.5, p = 0.086). The location of the fall/spring-run Chinook fry is shown in Appendix M. The one fall/spring Chinook fry location that the 2-D model predicted had a combined suitability of zero, out of the total of 70 fall/spring Chinook fry locations (3.0%), had a combined suitability of zero due to River2D predicting the location was dry.

The combined habitat suitability predicted by the 2-D model for locations with fall/spring-run Chinook juveniles was significantly higher for locations with juveniles (median = 0.358, n = 5) than for locations without juveniles (median = 0.011, n = 23), based on the one-tailed Mann-Whitney U test (U = 16, p = 0.013). The results for this test are admittedly weak, due to the small juvenile sample size. The 2-D model predicted a combined suitability of greater than zero for all five locations. Figures showing the frequency distributions of combined habitat suitability for locations with and without juveniles were not created for this analysis due to small sample size. The location of the fall/spring-run Chinook juveniles is shown in Appendix M. The small sample size used in the analysis was due to a combination of limitations on conducting the biological verification surveys due to time constraints and the scarcity of fall/spring-run Chinook juvenile observations encountered during the course of the study. With such a small occupied sample size, there could have been biases imposed by selection, methods used, time or other factors.

There was no significant difference in the combined habitat suitability predicted by the 2-D model (Figure 25) for locations with steelhead/rainbow trout fry (median = 0.036, n = 71) than for locations without fry (median = 0.048, n = 98), based on the one-tailed Mann-Whitney U test (U = 3582.5, p = 0.741). The location of the steelhead/rainbow fry is shown in Appendix M. Of the 16 steelhead/rainbow fry locations that the 2-D model predicted had a combined suitability of zero, out of the total of 71 steelhead/rainbow fry locations (22.5%), 15 locations had a combined suitability of zero due to River2D predicting the locations were dry. The 1 remaining location

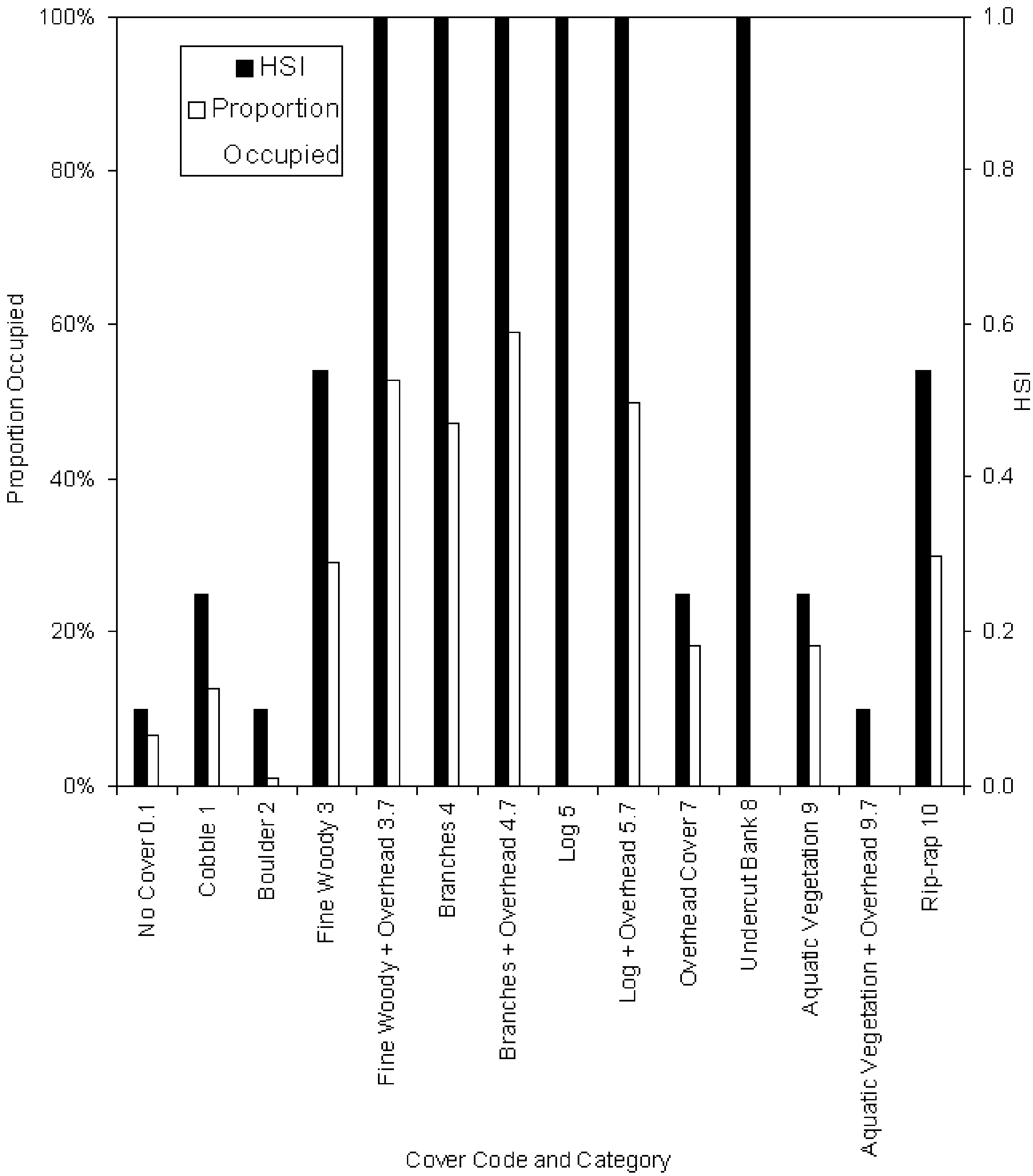

Figure 21. Fall/spring-run Chinook salmon fry rearing cover HSC. Data for the cover categories Log and Undercut Bank were not used in developing the HSC because there were a total (occupied plus unoccupied) of two or less observations for these cover categories.

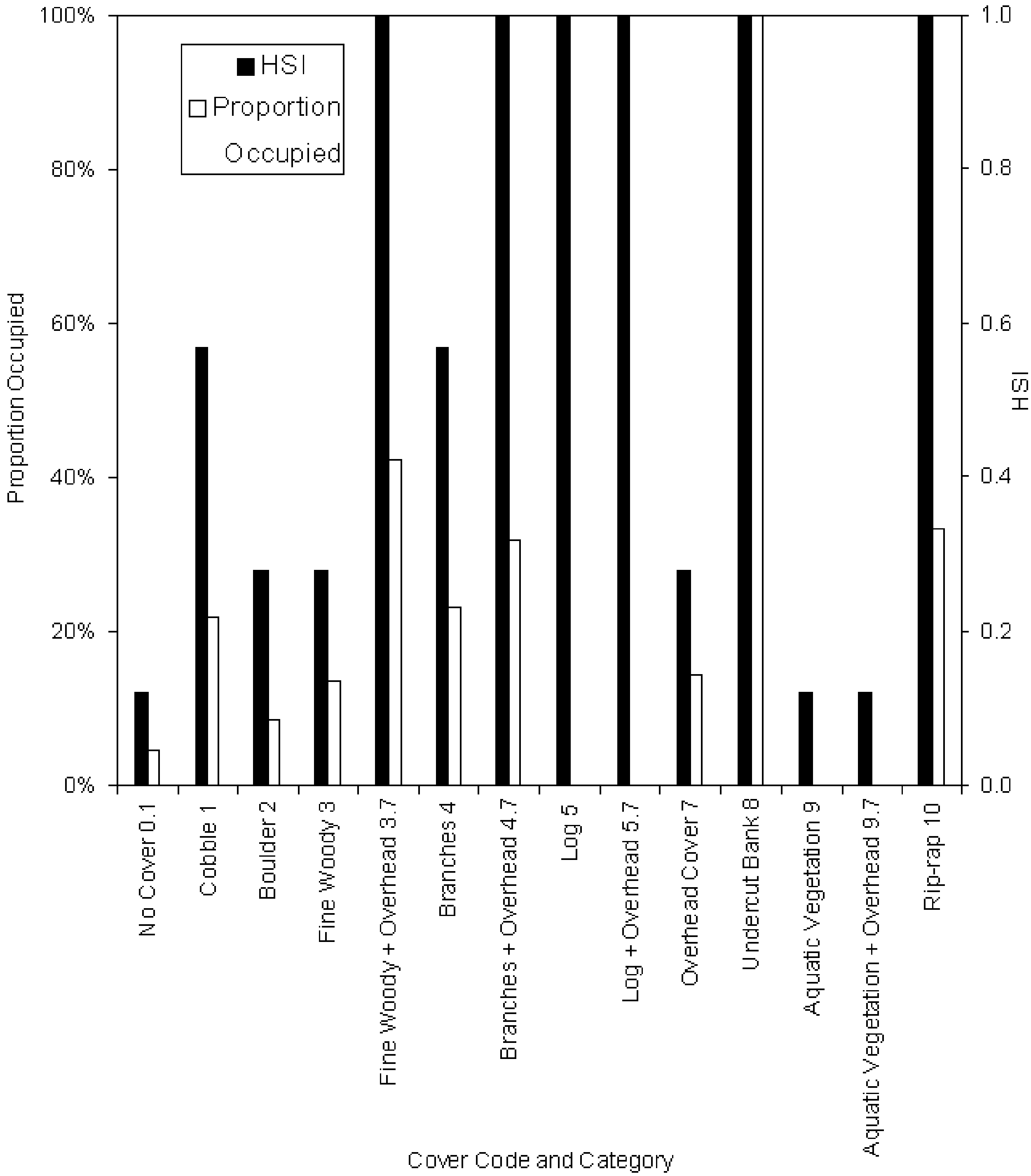

Figure 22. Steelhead/rainbow trout fry rearing cover HSC. Data for the cover categories Log, Log + Overhead, Undercut Bank and Aquatic Vegetation + Overhead were not used in developing the HSC because there were a total (occupied plus unoccupied) of two or less observations for these cover categories.

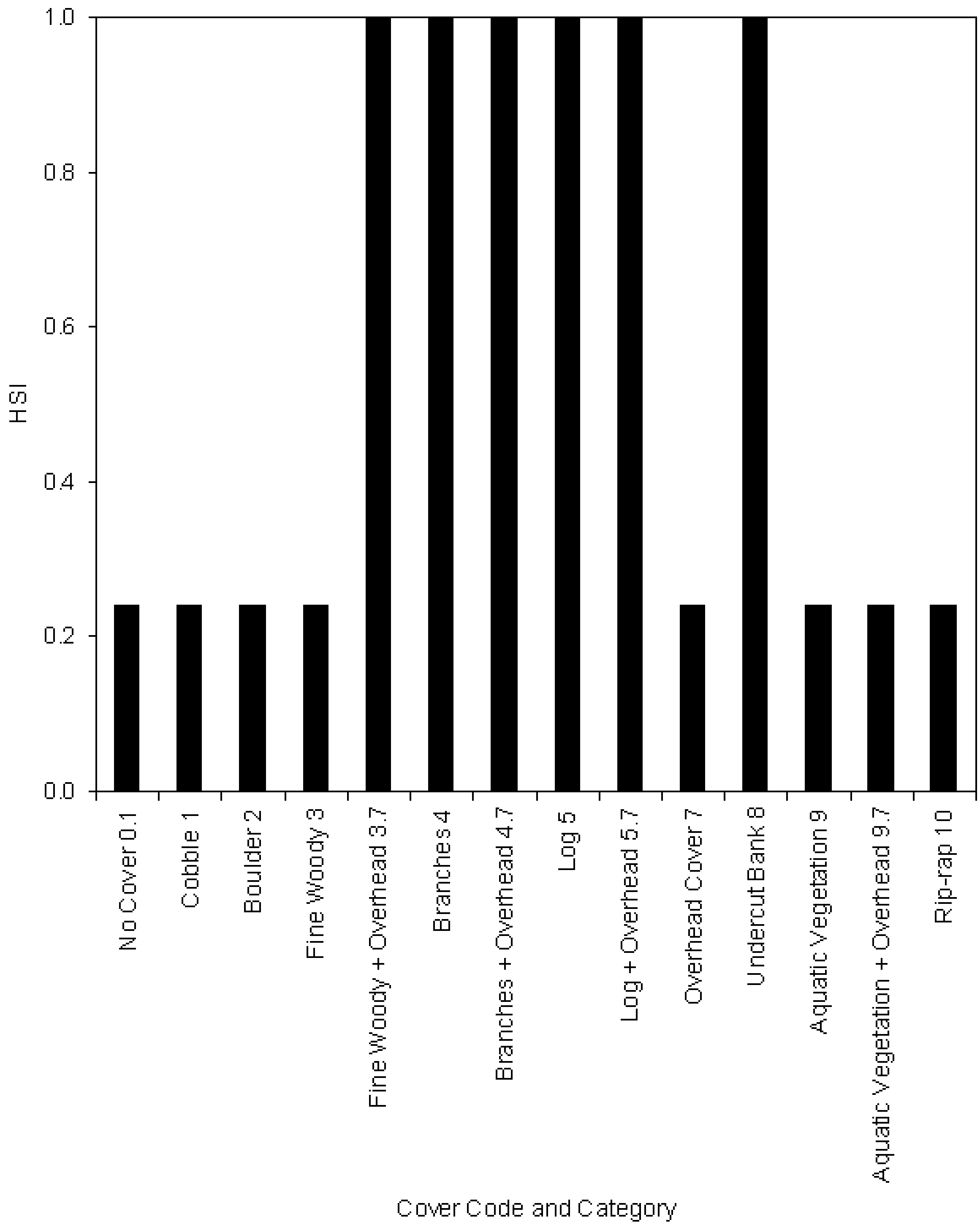

Figure 23. Fall/spring-run Chinook salmon and steelhead/rainbow trout juvenile rearing cover HSC. The cover observations for these species and life stage are shown in Figures 8 and 9.

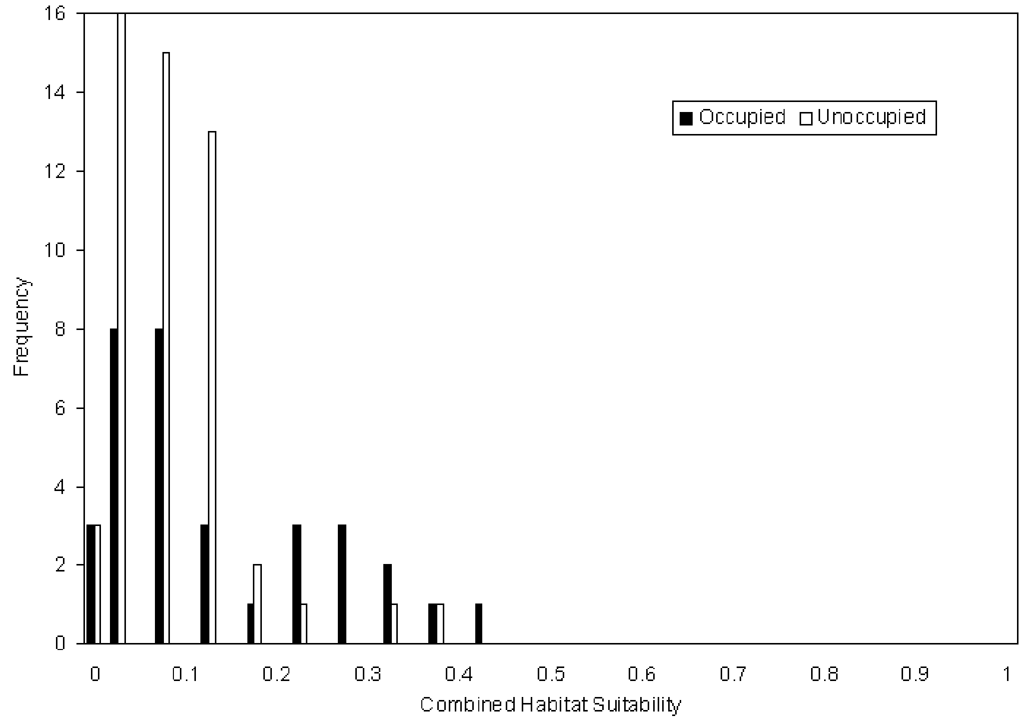

Figure 24. Combined suitability for 2-D model locations with (occupied) and without (unoccupied) fall/spring-run Chinook fry.

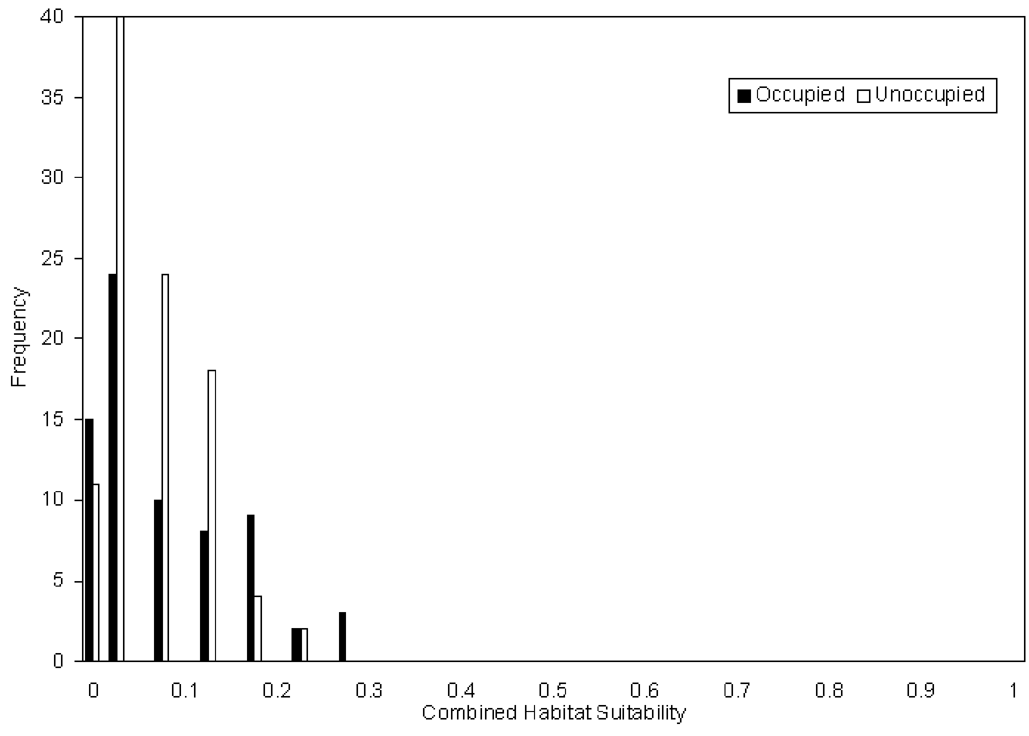

Figure 25. Combined suitability for 2-D model locations with (occupied) and without (unoccupied) steelhead/rainbow trout fry.

with a combined suitability of zero had two of the three mesh nodes for that location in the artificial upstream extension. It appears to have received a resulting value of zero due to the fact that the substrate and cover for the upstream boundary are automatically assigned a value of zero.

There was no significant difference in the combined habitat suitability predicted by the 2-D model for locations with steelhead/rainbow trout juveniles (median = 0.019, n = 3) and for locations without juveniles (median = 0.017, n = 80), based on the one-tailed Mann-Whitney U test (U = 138, p = 0.66). One of the three occupied locations was predicted by the 2-D model to have a combined suitability of zero. This one location had a combined suitability of zero due to River2D predicting that this location was dry. Figures showing the frequency distributions of combined habitat suitability for locations with and without juveniles were not created for this analysis due to small sample size. The location of the steelhead/rainbow juveniles is shown in Appendix M. The small sample size used in the analysis was due to a combination of limitations on conducting the biological verification surveys due to time constraints and the scarcity of steelhead/rainbow trout juvenile observations encountered during the course of the study. With such a small occupied sample size, there could have been biases imposed by selection, methods used, time or other factors.

10. *Habitat Simulation*

The WUA values calculated for each site are contained in Appendix L. The ratios of the total area of each habitat type present in a given segment to the area of each habitat type that was modeled in that segment are given in Table 31. Flow-habitat relationships, by species, life stage and segment, are depicted in Figures 26 – 33, given in Appendix L and summarized in Table 32.

DISCUSSION

1. *Habitat Mapping*

Traditionally habitat mapping is done in a linear fashion going downstream. The two-dimensional habitat mapping used in this study is more consistent with a two-dimensional-based hydraulic and habitat modeling of habitat availability. In addition (Figure 34) two-dimensional habitat mapping better captures the complexity of mesohabitat units in the Yuba River. The geomorphically-based habitat classification system used in this study (Snider et al. 1992) provides significant benefits versus a more traditional habitat mapping system based on depths and velocities. Specifically, since the Snider et al. (1992) system is not dependent on flow-varying parameters, habitat mapping does not change with flows. The hierarchical nature of the habitat classification system used in this study is particularly well suited to capturing the habitat complexity of alluvial streams, since it includes major channel features (bar-complex, flatwater and side-channel) in addition to the pool, riffle, run and glide habitat types used in more traditional habitat mapping systems. The field-based habitat mapping using a combination of aerial photos and GPS, followed by GIS digitizing of the habitat units, allowed us to cost-

Table 31. Ratio of habitat areas in segment to habitat areas in modeled sites. Entries with an asterisk indicate that the habitat type was not modeled in that reach.

Habitat Type	Above Daguerre	Below Daguerre
Flatwater Glide	*	5.95
Flatwater Pool	2.08	34.89
Flatwater Riffle	*	*
Flatwater Run	5.92	2.60
Bar Complex Glide	2.34	9.28
Bar Complex Pool	3.74	23.68
Bar Complex Riffle	2.86	2.79
Bar Complex Run	8.84	3.49
Side Channel Pool	4.55	2.18
Side Channel Riffle	1.27	*
Side Channel Run	1.46	5.64
Side Channel Glide	8.97	*

Table 32. Summary of flow-habitat relationship results. Numbers given in this table are the flow (cfs) with the highest total WUA.

Species	Life Stage	Above Daguerre	Below Daguerre
Chinook salmon	Fry	4,300	4,500
Chinook salmon	Juvenile	1,300	2,000
Steelhead/rainbow trout	Fry	400	500
Steelhead/rainbow trout	Juvenile	1,000	2,000

effectively delineate the aerial extent of habitat units with an adequate degree of accuracy (from the GPS data). With the GPS data and aerial photo overlays, we were able to successfully identify the aerial extent of the habitat units in GIS.

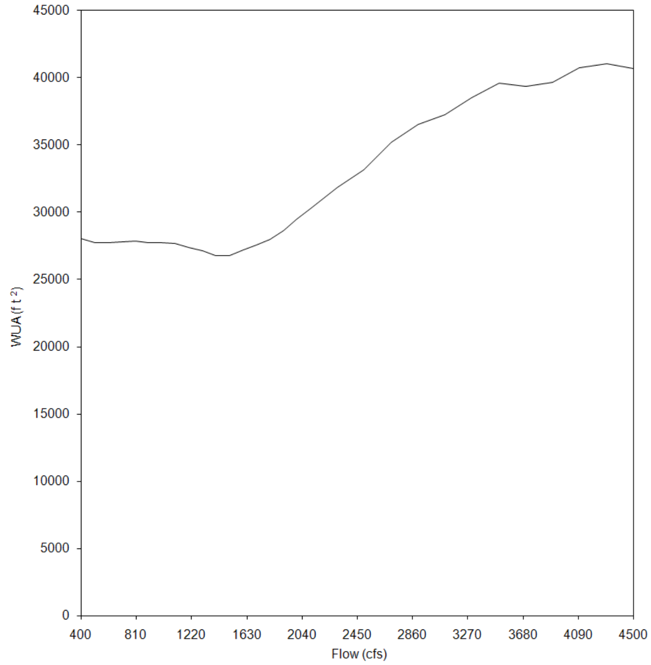

Figure 26. Fall/spring-run Chinook salmon fry rearing flow-habitat relationship above Daguerre Point Dam. The flow with the maximum fall/spring-run Chinook salmon fry rearing habitat was 4,300 cfs.

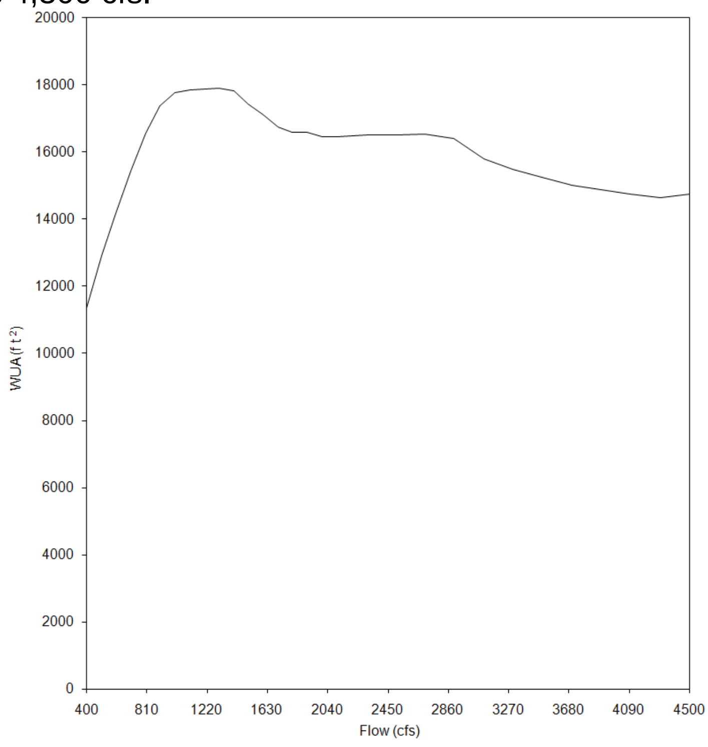

Figure 27. Fall/spring-run Chinook salmon juvenile rearing flow-habitat relationship above Daguerre Point Dam. The flow with the maximum fall/spring-run Chinook salmon juvenile rearing habitat was 1,300 cfs.

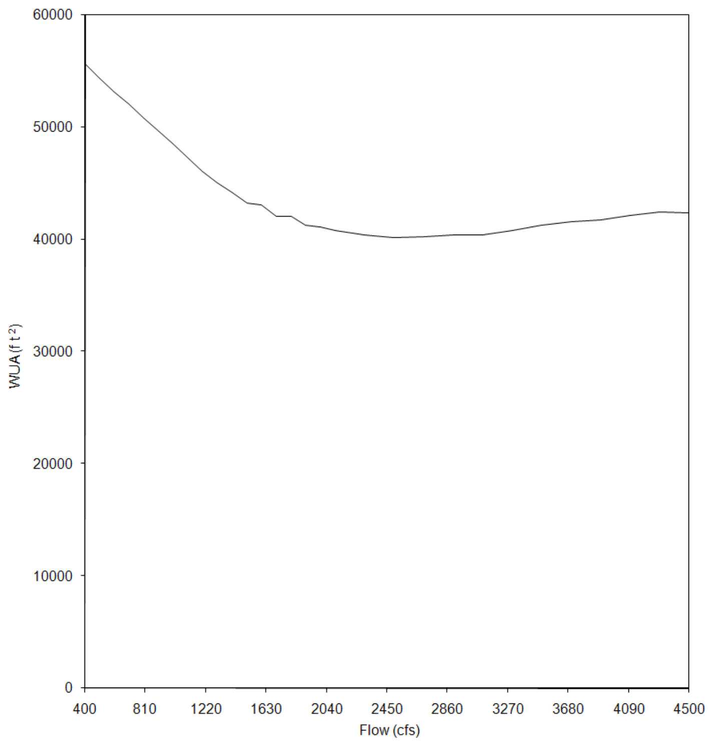

Figure 28. Steelhead/rainbow trout fry rearing flow-habitat relationship above Daguerre Point Dam. The flow with the maximum steelhead/rainbow trout fry rearing habitat was 400 cfs.

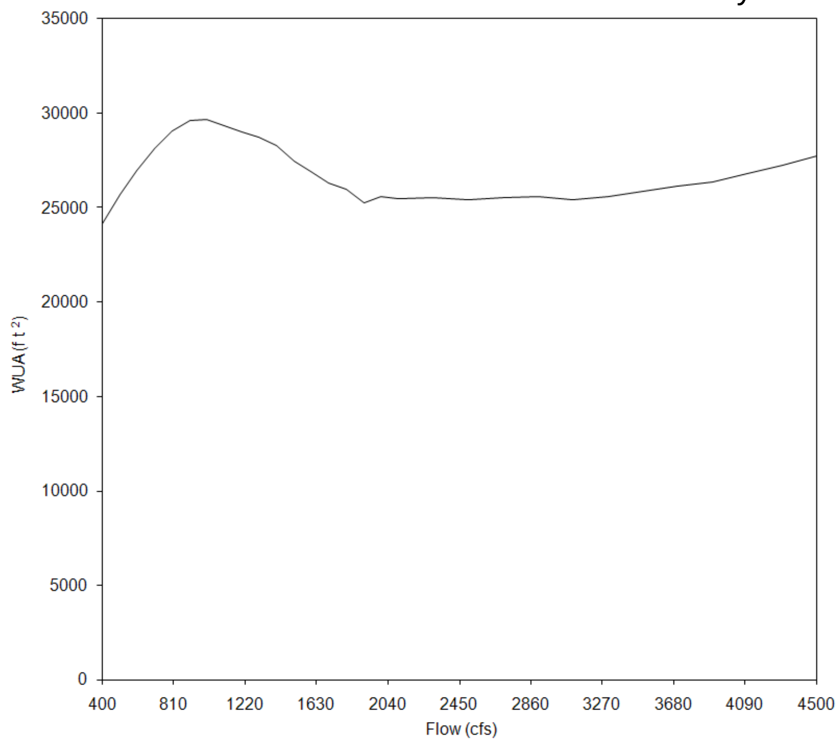

Figure 29. Steelhead/rainbow trout juvenile rearing flow-habitat relationship above Daguerre Point Dam. The flow with the maximum steelhead/rainbow trout juvenile rearing habitat was 1,000 cfs.

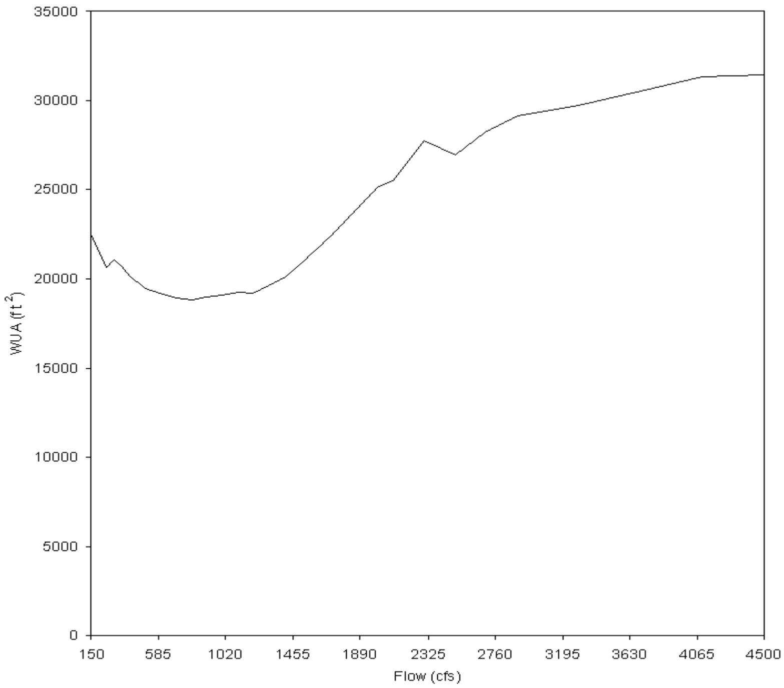

Figure 30. Fall/spring-run Chinook salmon fry rearing flow-habitat relationship below Daguerre Point Dam. The flow with the maximum fall/spring-run Chinook salmon fry rearing habitat was 4,500 cfs.

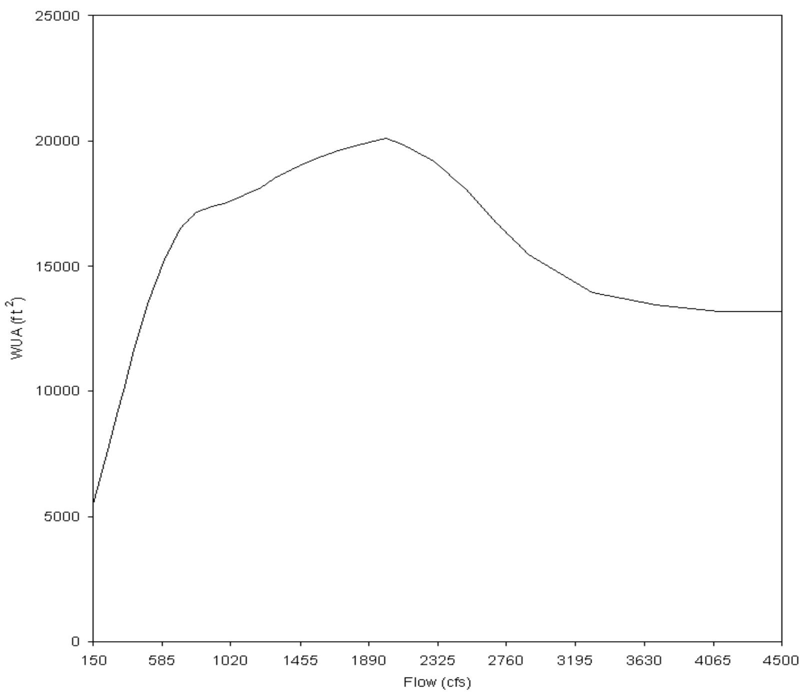

Figure 31. Fall/spring-run Chinook salmon juvenile rearing flow-habitat relationship below Daguerre Point Dam. The flow with the maximum fall/spring-run Chinook salmon juvenile rearing habitat was 2,000 cfs.

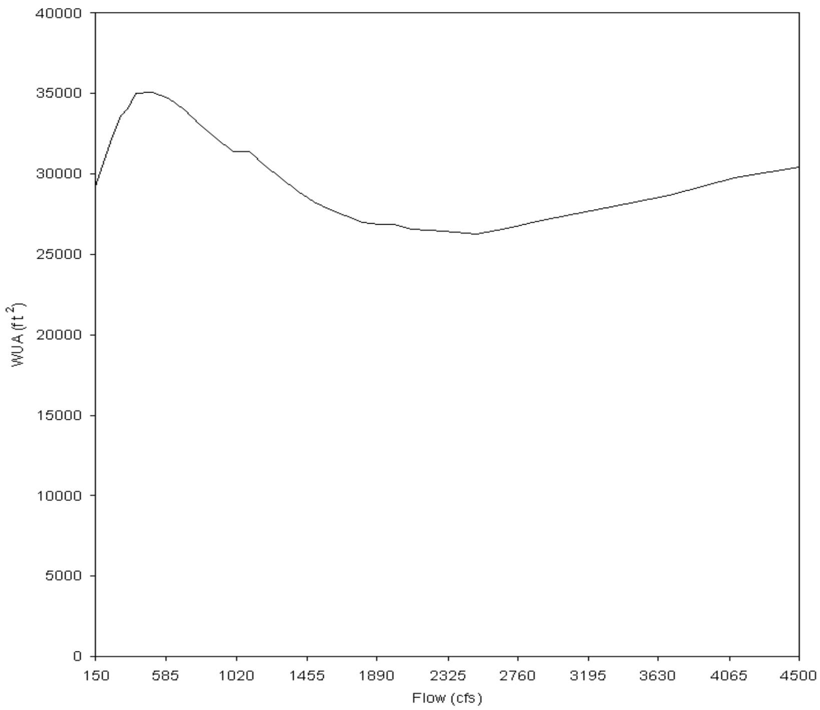

Figure 32. Steelhead/rainbow trout fry rearing flow-habitat relationship below Daguerre Point Dam. The flow with the maximum steelhead/rainbow trout fry rearing habitat was 500 cfs.

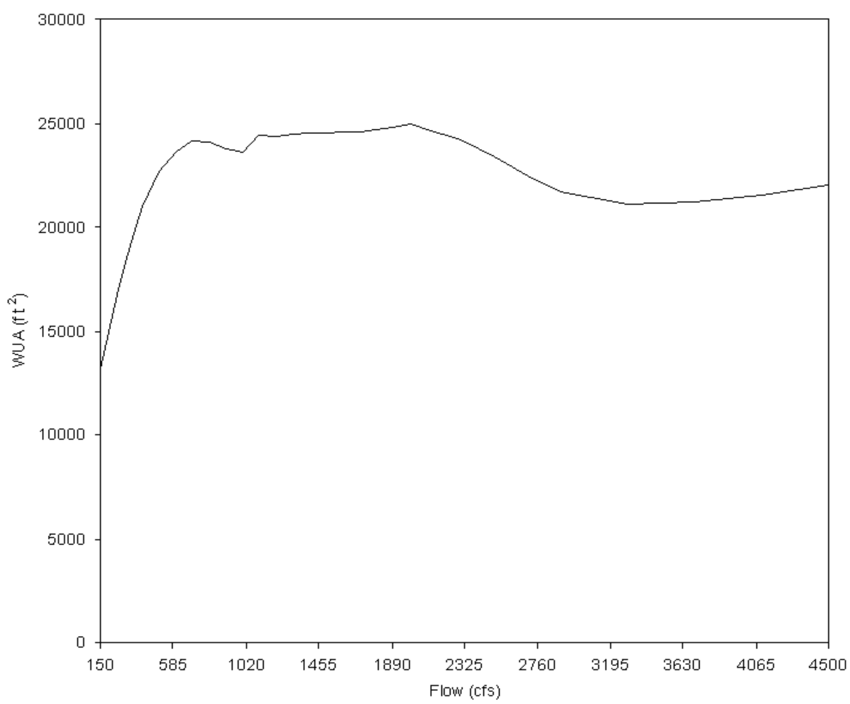

Figure 33. Steelhead/rainbow trout juvenile rearing flow-habitat relationship below Daguerre Point Dam. The flow with the maximum steelhead/rainbow trout juvenile rearing habitat was 2,000 cfs.

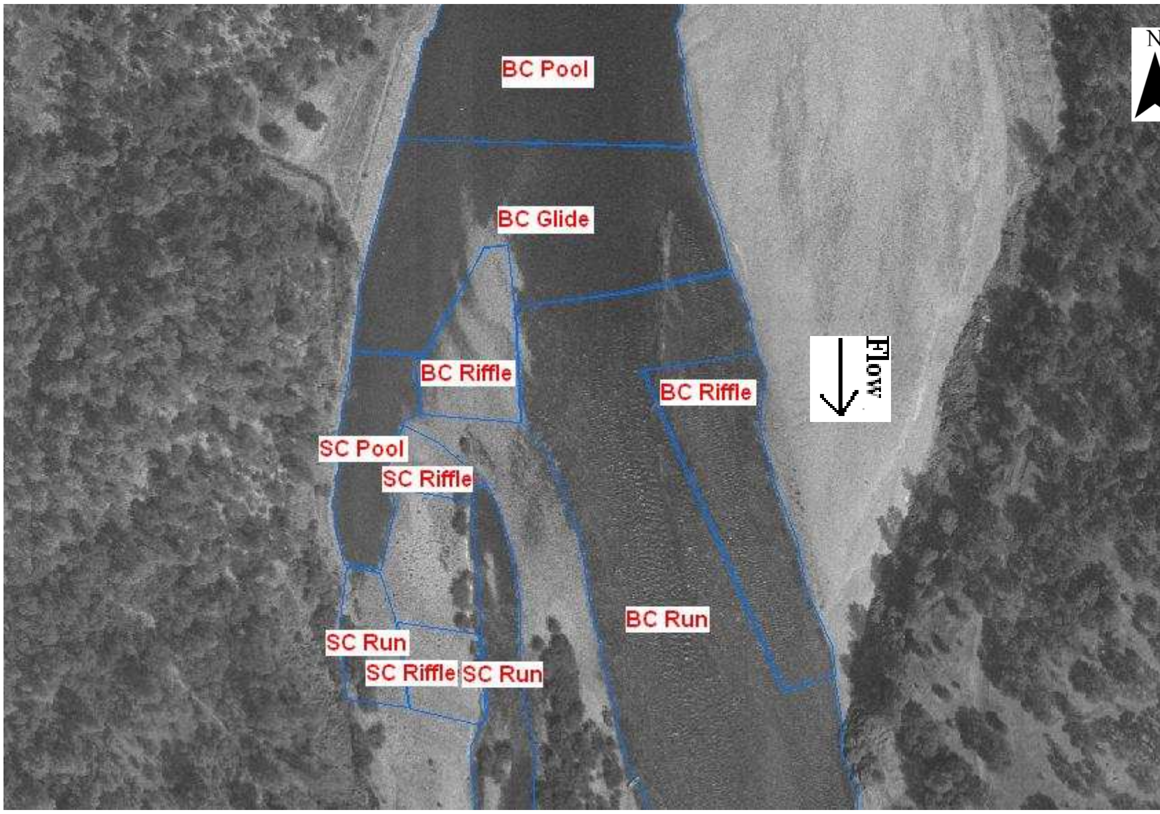

Scale: 1:2595

Figure 34. Detail of habitat mapping of a portion of the Timbuctoo study site.

2. *Field Reconnaissance and Study Site Selection*

We chose to use the ten spawning sites to model juvenile rearing habitat because it increased the area of river modeled for juvenile rearing habitat. Not doing so would have meant that fewer habitat units would have used to calculate juvenile habitat. Otherwise, we would have needed to spend a significantly greater amount of effort on juvenile rearing by establishing additional juvenile study sites in the same habitat types as were in the spawning sites. The only drawback of using the spawning sites is that they were not randomly selected.

3. *Hydraulic and Structural Habitat Data Collection*

Incorporating the U.S. Army Corps of Engineers data allowed greater refinement of the bed topography for each study site. Establishing the precise northing and easting coordinates and elevations of our horizontal benchmarks using dual frequency survey-grade differential GPS and tying in our vertical benchmarks to the elevations of the horizontal benchmarks also enabled establishing the location and orientation of the sites and their bed elevations and water surface elevations relative to data that is concurrently being collected by other entities. This will facilitate the sharing and comparison of data for the various studies being conducted on the Yuba River. All of the measurements were accurate to 1 foot (0.31 m) horizontally and 0.1 foot (0.031 m) vertically; therefore, we believe that measurement error would have a minimal effect on the final result.

4. *Hydraulic Model Construction and Calibration*

4.1. **PHABSIM WSEL Calibration**

We decided that the multiple regression WSEL calibration for Railroad was acceptable, despite there being more than a 0.1 foot (0.031 m) difference between measured and simulated WSELs. Specifically, the maximum difference between measured and simulated WSELs of 0.11 feet (0.033 m) was much less than the maximum difference with *IFG4* and *MANSQ*, and reflected the additional errors implicit in predicting WSELs from two different flows (from the Yuba and Feather Rivers), versus Predicting WSELs from only one flow. We did not regard the slightly low VAF values for the lowest simulation flow of 150 cfs for Railroad upstream and downstream transects, nor the deviation from the expected pattern of VAFs for the highest simulation flow of 4,500 cfs for Railroad upstream and downstream transects, as problematic since RHABSIM was only used to simulate WSELs and not velocities.

4.2. **River2D Model Construction**

The U.S. Army Corps of Engineers data incorporated into the bed topography allowed greater refinement of the bed topography for each study site. In most cases, the portions of the mesh where there was greater than a 0.1 foot (0.031 m) difference between the mesh and final bed file were in steep areas; in these areas, the mesh would be within 0.1 foot (0.031 m) vertically of the bed file within 1.0 foot (0.31 m) horizontally of the bed file location. Given that we had a 1-foot (0.31 m) horizontal level of accuracy, such areas would have an adequate fit of the mesh to the bed file.

4.3. **River2D Model Calibration**

Narrows and Lower Hallwood sites' simulated WSELs at the calibration flow differed by more than 0.1 foot (0.031 m) in some places along the upstream transect. We were uncertain which model was responsible for the discrepancies between the WSELs predicted by River2D and PHABSIM. In the case of Narrows, the results from River2D may be somewhat questionable, given that the average value exceeded 0.1 foot (0.031 m). However, for Narrows and Lower Hallwood sites, the WSELs next to the locations of the left and right banks within the model were all within the 0.1 foot (0.031 meters) criterion value in the final calibration. The PHABSIM simulated WSELs and the measured WSELs used for calibrating the cdg files were based on WSEL measurements taken next to the left and right banks. For higher gradient portions of the Yuba River, the WSEL going across the river will differ by more than 0.1 foot (0.031 m) at some flows, with up to a 0.23 foot (0.070 m) measured difference in WSEL between the two banks in some areas, such as the Rosebar site. We accepted the calibration results at the highest simulation flow for the Narrows and Lower Hallwood sites because all our WSEL measurements were made next to the left and right banks (Appendix G). Although the maximum WSEL values for Lower Hallwood site's upstream transect exceeded the 0.1 foot (0.031 m) criterion, Lower Hallwood had an average WSEL that was well within that criterion value (Appendix G).

We attribute the maximum difference of 0.29 feet (0.09 meters) between the WSEL simulated by River2D and PHABSIM at 4,500 cfs for the Narrows upstream transect to inaccuracies in the bed topography upstream of the site. Specifically, the lack of Army Corps of Engineers hydroacoustic data upstream of the site and the limited amount of ADCP data we collected upstream of the site likely resulted in an inaccurate simulation of WSELs at the upstream transect. Alternatively, the actual WSEL in the middle of the Narrows upstream transect at 4,500 cfs may have been 0.29 feet (0.09 meters) lower than the WSELs on the left and right banks. We have no way of testing this alternative, since we did not measure WSELs for that transect away from the left and right banks, because most of the transect was over 6 feet (1.83 meters) deep, with an average depth of over 20 feet (6.10 meters). The measured WSELs are not consistent with the above alternative, since at all flows, the left and right bank WSELs differed by a maximum of 0.03 feet (0.01 meters). Based on the previous discussion, we decided the calibration for Lower Hallwood site was acceptable, with the likelihood that Narrows was also acceptable.

We felt that it would be more accurate to calibrate Diversion and Sucker Glide sites using the measured WSELs for the highest flow within the range of simulated flows. Our general rule is that it is more accurate to calibrate sites using the WSELs simulated by PHABSIM at the highest simulation flow because the River2D model is more sensitive to the bed roughness multiplier at higher flows, versus lower flows. However, when we have decided, as for these sites, that the simulation of the WSEL at the upstream transect at the highest simulation flow by PHABSIM is inaccurate, it no longer makes sense to calibrate River2D using the WSELs simulated by PHABSIM at the highest simulation flow. In these cases, we use the fall-back option of calibrating River2D using the WSELs measured at the highest flow within the range of simulation flows.

We considered the solution to be acceptable for the study site cdg files which had a maximum Froude Number greater than one. Although the Froude Number did exceed one at a few nodes, the vast majority of the site had Froude Numbers less than one. The nodes with Froude Numbers greater than one were located either at the water's edge or where water depth was extremely shallow, typically approaching zero. A high Froude Number at a very limited number of nodes at water's edge or in very shallow depths would be expected to have an insignificant effect on the model results. The calibration for Railroad, where the net Q was greater than 1%, was still considered to have a stable solution since the net Q was not changing and the net Q was less than 5%. In comparison, the accepted level of accuracy for USGS gages is generally 5%. Thus, the difference between the flows at the upstream and downstream boundary (net Q) is within the same range as the accuracy for USGS gages, and so we accepted the results for this site.

4.4. **River2D Model Velocity Validation**

As noted in the results section, we were unable to validate the velocity predictions for the hydraulic models of Sucker Glide and Railroad sites (Figure 3). As a result, there is greater uncertainty in the habitat modeling results for these sites than for the remaining sites. We were left with two alternatives: 1) to throw out these sites and represent flatwater habitat in the Below Daguerre segment by bar complex habitat; or 2) to use the sites. We believe that it would be more accurate to model rearing habitat in the Below Daguerre segment using these sites because if we threw out these sites, the rearing habitat would not include results from flatwater habitat types, which comprise 21 percent of the area of the Yuba River between Daguerre Dam and the confluence with the Feather River. We believe that the errors associated with simulated velocities for these sites are less than the errors that would be associated with representing flatwater habitats by bar complex habitats.

Differences in magnitude in most cases are likely due to: (1) aspects of the bed topography of the site that were not captured in our data collection; (2) operator error during data collection, i.e., the probe was not facing precisely into the direction of current; (3) range of natural velocity variation at each point over time (i.e. noise) resulting in some measured data points at the low or high end of the velocity range averaged in the model simulations; and (4) the measured velocities being the component of the velocity in the downstream direction, while the velocities predicted by the 2-D model were the absolute magnitude of velocity[34]. As shown by the figures in Appendix H, we attribute many of the differences between measured and predicted velocities to noise in the measured velocity measurements; specifically, for the transects, the simulated velocities typically fell within the range of the measured velocities of the three or more ADCP traverses made on each transect. The 2-D model integrates effects from the surrounding elements at each point. Thus, point measurements of velocity can differ from simulated values simply due to the local area integration that takes place. As a result, the area integration effect noted above will produce somewhat smoother lateral velocity profiles than the observations.

For the Side-Channel site, we attribute the differences between the measured and simulated velocities for both transects to the lack of Army Corps of Engineers raw hydroacoustic data upstream of the site. The actual topography upstream of the site likely resulted in less of the flow going on the north side of the channel and more of the flow going through the remainder of the channel. Because the actual topography upstream of the study site was not included in the bed topography of the model, the influence of this topography was not reflected in the velocities simulated by the River2D model of the study site. Since the site was relatively short, the effect of the topography upstream of the site propagated all the way through the site, affecting the velocity distribution at the downstream transect. The River2D model sets velocities at the

---

[34] For areas with transverse flow, this would result in the 2-D model appearing to over-predict velocities even if it was accurately predicting the velocities.

upstream boundary proportional to depth. The fastest modeled velocities at the upstream boundary were at the thalweg, while the actual topography upstream of the site resulted in relatively low velocities at the thalweg at the upstream end of the site.

For Whirlpool site, we attribute the differences between the measured and simulated velocities for the downstream transect to an eddy generated by River2D on the east side of the channel (Figure 35), which was not present in the measured data. The presence of this eddy resulted inRiver2D underestimating the velocities on the east side of the channel; to achieve a mass balance, this resulted in overestimating the velocities for the west side of the channel. We were unable to improve the prediction of velocities at the downstream end of Whirlpool site by adding a downstream extension onto the hydraulic model because the downstream end of Whirlpool site was located at the downstream end of a split channel. We attribute the differences between the measured and simulated velocities for the upstream transect at the Whirlpool site to the use of relatively low density Army Corps of Engineers data to produce the channel topography upstream of the upstream transect. We believe that a small-scale feature upstream of the upstream transect, that influenced the water velocities in that area, was not accurately characterized or was missing from the model bed topography.

For those deep beds where River2D over or under-predicted the velocities on one or both sides of the channel for the following deep beds, we attribute this to either errors in the bed topography that did not properly characterize features that resulted in faster/slower velocities, or errors in the ADCP measurements of velocity. Narrows Deep Beds A-G, I, J, M, N, Q-U, W, X-AB, AD-AH, AM, and AN are good examples of where the bed topography was likely not sufficiently accurately characterized in the model. The upper portion of the Narrows site had very irregular topography as a result of bedrock and boulder formations; in this situation, it would have required an extremely high density of bed topography points to accurately characterize the bed topography for this site.

Modeled velocities were lower than measured velocities across most of the channel for Sucker Glide Deep Beds D, E and N; we attribute this to errors in the ADCP velocity measurements (being too high). Specifically, the calculated discharges for Sucker Glide Deep Beds D, E and N were, respectively, 1,632, 1,746 and 1,499 cfs, versus the actual total river discharge of 1,250 cfs. Modeled velocities were higher than measured velocities for Lower Hallwood Deep Beds J to L; we attribute this to errors in the ADCP measurements (being too low). For example, the calculated discharges for Lower Hallwood Deep Beds J to L (which crossed most of the wetted channel) were 698, 645 and 487 cfs, respectively, versus the actual total discharge of 1,060 cfs.

4.5. **River2D Model Simulation Flow Runs**

We initially ran the Side-Channel site simulation cdg files with a minimum groundwater depth of 0.05. However, we discovered that for Side-Channel site flows of less than 35.7 cfs (corresponding to total river flows of less than 1,900 cfs), a minimum groundwater depth of 0.05 resulted in a Net Q of greater than 1 percent. We attributed this to the extremely shallow nature

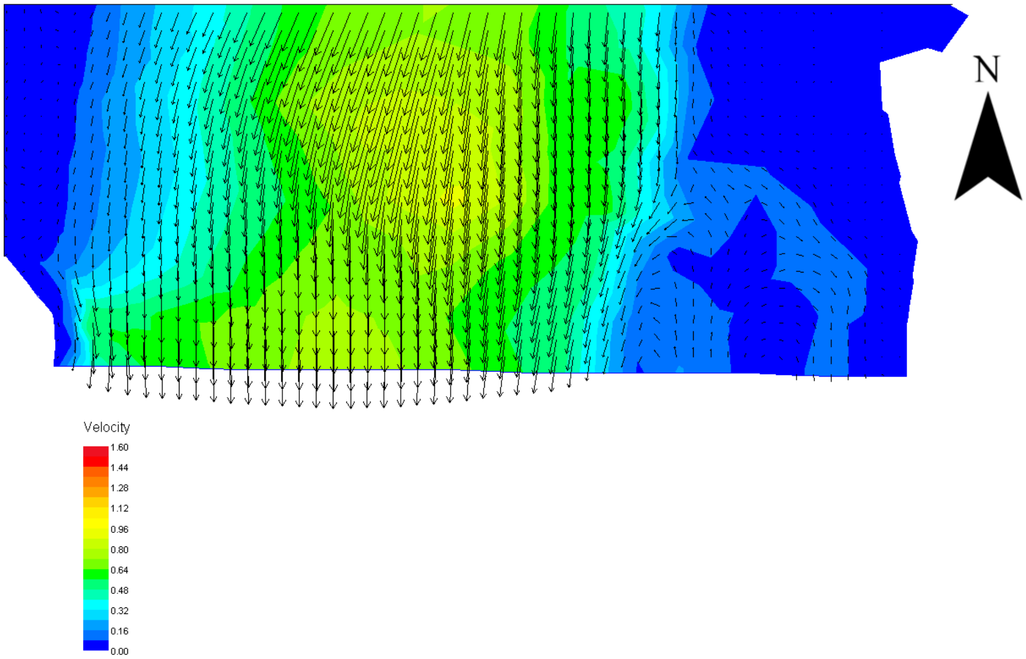

Scale: 1:438

Figure 35. Detail of velocity simulation for the downstream-most portion of Whirlpool site at a flow of 1,220 cfs. Units of velocity are m/s.

of this site at low flows, where a substantial percentage of the site had water depths less than 0.05 m. Accordingly, for Side-Channel site flows of less than 35.7 cfs, we used a minimum groundwater depth of 0.005. The lower minimum groundwater depth, for most of the simulation flows, reduced the Net Q and thus resulted in a more stable solution.

The simulation flow run cdg files for Narrows (with the exception of 500 cfs, 800 cfs and 1,000-1,100 cfs), Lower Hallwood, Side-Channel (with the exception of 800-900 cfs), Sucker Glide (with the exceptions of 150 and 400-1,000 cfs), and Railroad sites, where the net Q was greater than 1%, were still considered to have a stable solution since the net Q was not changing and the net Q in all cases was less than 5%. In comparison, the accepted level of accuracy for USGS gages is generally 5%. Thus, the difference between the flows at the upstream and downstream boundary (net Q) is within the same range as the accuracy for USGS gages, and so we accepted the results for this site. In the cases of the four Narrows cdg files, the two Side-Channel cdg files, and the eight Sucker Glide cdg files where the net Q significantly exceeded the 5% level, there is more uncertainty in the results for these production files. We still used these files to avoid gaps in the flow-habitat relationships for these sites. In the case of the Side-Channel 800 cfs cdg file, the net Q difference of 374% was so high that we eliminated this flow from the simulation flow runs. At a total flow of 800 cfs, the flow in the site was mostly subsurface and the habitat present would not be available to juvenile salmonids, since it would be isolated from the main channel (Figure 36). For the Side-Channel site at a total flow of 900 cfs, we attribute

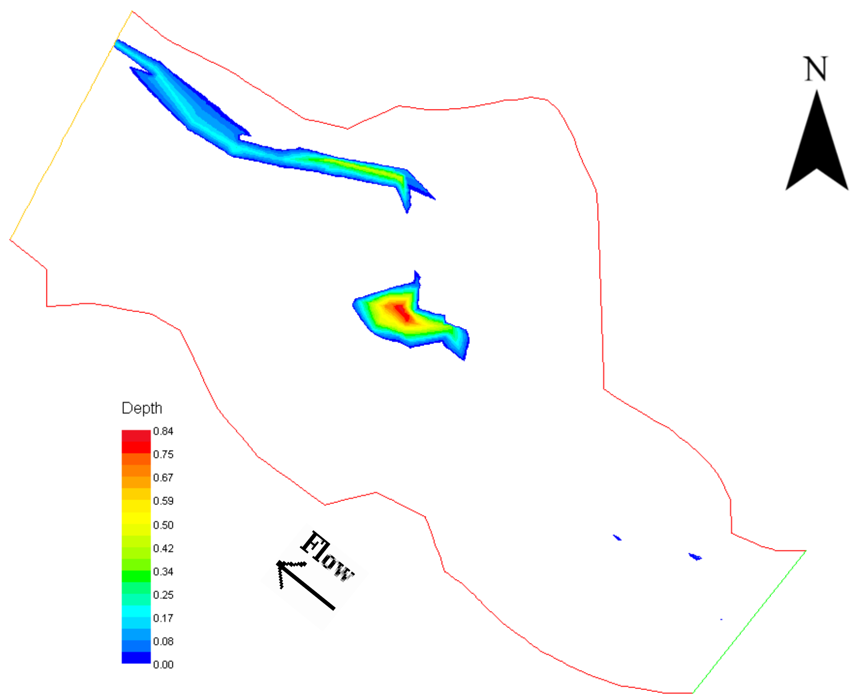

Scale: 1:1152

Figure 36. Detail of depth simulation for Side-Channel site at a site flow of 0.2 cfs, corresponding to a total flow of 800 cfs. Uncolored area connotes the region of subsurface flow. Units of depth are m.

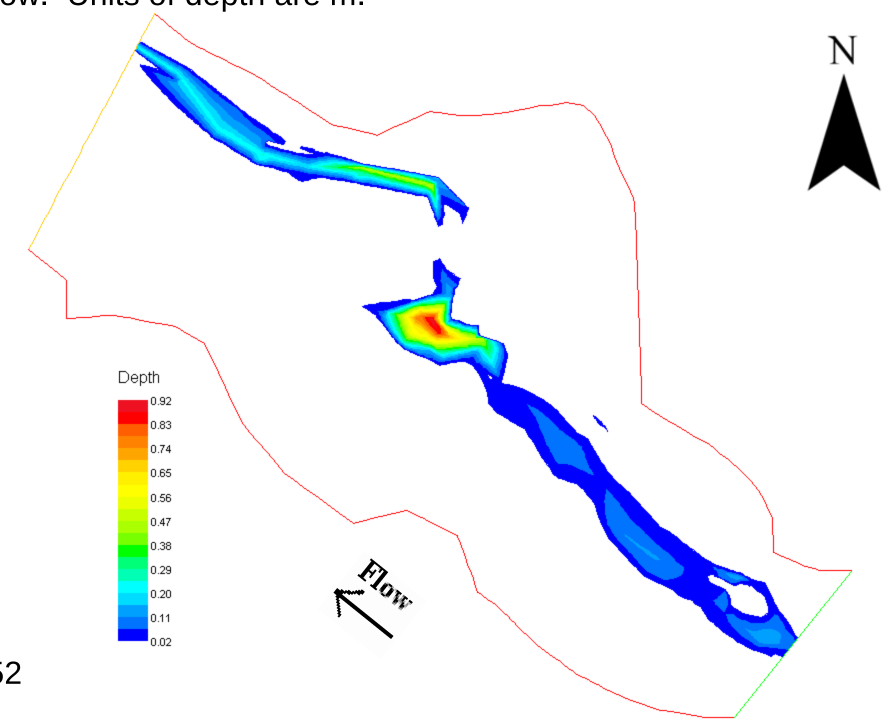

Scale: 1:1152

Figure 37. Detail of depth simulation for Side-Channel site at a site flow of 1.2 cfs, corresponding to a total flow of 900 cfs. Uncolored area connotes the region of subsurface flow. Units of depth are m.

the high net Q value (20.67%) to the flow being subsurface all the way across the channel at the hydraulic control within the site (Figure 37). In contrast to the other total river flows of less than 1,900 cfs at this site, the simulation for a total flow of 900 cfs with a minimum groundwater depth of 0.05 resulted in a lower Net Q (4.8%) than for the minimum groundwater depth of 0.005 used to simulate this flow. The higher net Q's in Sucker Glide site likely resulted from an error in the bed topography in the vicinity of the downstream boundary causing an eddy in the hydraulic model.

One of the purposes for adding a downstream extension to the Narrows site was to eliminate an eddy at the downstream boundary that was present in the original hydraulic model for this site. With the downstream extension, there was still an eddy present at the downstream extension at 500 cfs, but not at 800, 1000 or 1100 cfs. We attribute the net Q's greater than 5 percent for Narrows 800 and 1000 cfs to an error in the model's calculation of net Q. When the total outflow is calculated from the difference in cumulative discharge at the left and right water's edge at the downstream boundary, the actual net Q value for the Narrows site at 800 and 1000 cfs were, respectively, 3.6 and 4.8 percent. While there was a similar error for 1100 cfs, the total outflow calculated from the difference in cumulative discharge at the left and right water's edge at the downstream boundary resulted in a net outflow of 8.3%.

Although a majority of the simulation flow files had Max F values that exceeded 1, we considered these production runs to be acceptable since the Froude Number was only greater than one at a few nodes, with the vast majority of the area within the site having Froude Numbers less than one. Again, as described in River2D Model Calibration discussion, these nodes were located either at the water's edge or where water depth was extremely shallow, typically approaching zero. A high Froude number at a very limited number of nodes at water's edge or in very shallow depths would be expected to have an insignificant effect on the model results. In addition, there were limited portions of a few of the sites, such as portions of the upper end of Narrows where water was passing over the top of boulders, where there actually was supercritical flow, where a Max F value of greater than 1 would be expected.

5. *Habitat Suitability Criteria (HSC) Data Collection*

Despite considerable effort, sampling 36 miles of channel, we were only able to make 39 observations of Chinook salmon greater than 60 mm and 74 observations of steelhead/rainbow trout greater than 60 mm. In contrast, sampling the Sacramento River, we made 133 observations of fall-run Chinook salmon greater than 60 mm while sampling 24.4 miles of channel (U.S. Fish and Wildlife Service 2005). Similarly, sampling Clear Creek we made 173 observations of fall-run Chinook salmon greater than 60 mm while sampling 2.4 miles of channel (U.S. Fish and Wildlife Service 2007). We do not know if our paucity of observations on the Yuba River was due to very low densities of Chinook salmon and steelhead/rainbow trout greater than 60 mm, or if most juvenile salmonids greater than 60 mm detected us and fled before we had the opportunity to observe them. The latter appears more likely, given the large numbers of both juvenile Chinook salmon and steelhead/rainbow trout greater than 60 mm that are captured in the screw traps on the Yuba River (Massa 2004) and the coefficients of variation (4 to 173 percent) seen between replicate snorkel surveys for juvenile steelhead in the Yuba River (Bratovich et al. 2003). We believe that the low numbers of juvenile salmonids greater than 60 mm that we observed likely reflects a limitation of using snorkel survey methods in the Yuba River to collect HSI data for juvenile salmonids greater than 60 mm. It is difficult to directly compare our results with those from Beak (1989). Beak (1989) had 500 observations of juvenile fall-run Chinook salmon, but they defined each fish as one observation. In contrast, we defined each group of fish as one observation; the 39 observations that we had of Chinook salmon greater than 60 mm comprised a total of 213 fish greater than 60 mm. Each observation in our study represented between 1 and 300 fish, with a median of 3 fish per observation. In addition, Beak (1989) defined juveniles as being greater than 50 mm, while we defined juveniles as being greater than 60 mm.

6. *Habitat Suitability Criteria (HSC) Development*

The R^2 values in Tables 26 and 27 in general reflect the large degree of overlap in occupied and unoccupied depths and velocities (Figures 11 – 17). Low R^2 values are the norm in logistic regression, particularly in comparison with linear regression models (Hosmer and Lemeshow 2000). The R^2 values in this study were significantly lower than those in Knapp and Preisler (1999), Geist et al. (2000) and Guay et al. (2000), which had R^2 values ranging from 0.49 to 0.86. We attribute this difference to the fact that the above studies used a multivariate logistic regression which included all of the independent variables. It would be expected that the proportion of variance (R^2 value) explained by the habitat suitability variables would be apportioned among depth, velocity, adjacent velocity and cover. For example, McHugh and Budy (2004) had much lower R^2 values, in the range of 0.13 to 0.31, for logistic regressions with only one independent variable.

The logistic regressions clearly showed that there was a significant influence of depth and velocity on use or nonuse with the range of overlapping conditions, since the p-values for the logistic regressions and the p-values for the individual terms of the logistic regressions were all less than 0.05. Accordingly, we believe that depth and velocity do not act as boundary conditions for use, where suitability is optimal within a given range of depth and velocities, given that all other rearing conditions are suitable (i.e., adjacent velocity and cover). Binary criteria (i.e. either optimal or unsuitable) are generally biologically unrealistic – they either overestimate the habitat value of marginal conditions if the binary criteria are broadly defined (for example, setting suitability equal to one for any depths and velocities where the original HSI value was greater than 0.1) or completely discount the habitat value of marginal conditions. The latter case would be biologically unrealistic since many fry and juveniles would be in areas which would be considered completely unsuitable from the binary criteria.

Rubin et al. (1991) present a similar method to logistic regression using fish density instead of presence-absence, and using an exponential polynomial regression, rather than a logistic regression. Rubin et al. (1991) selected an exponential polynomial regression because the distribution of counts of fish resembles a Poisson distribution. We did not use this method for the following reasons: 1) we had low confidence in the accuracy of our estimates of the number of fish in each observation; and 2) while it is reasonable to assume that a school of fish represents higher quality habitat than one fish, it is probably unreasonable to assume that, for example, 100 fish represents 100 times better habitat than one fish. A more appropriate measure of the effects of the number of fish on habitat quality would probably be to select some measure like log (number of fish + 1), so that 1-2 fish would represent a value of one, 3-30 fish would represent a value of two and 31-315 fish would represent a value of three[35]. We are not aware of any such measure in the literature, nor are we aware of how we could determine what an appropriate measure would be.

It should be noted that the regressions were fit to the raw occupied and unoccupied data, rather than to the frequency histograms shown in Figures 11 through 17. In general, the criteria track the occupied data, but drop off slower than the occupied data due to the frequency of the unoccupied data also dropping over the same range of depths and velocities. In general, the velocity criteria more closely tracked the occupied frequencies than the depth criteria, indicating that the limited availability of deeper conditions has a larger effect on YOY habitat use than the availability of faster conditions. The lower availability of intermediate depths, versus shallow depths, constrains YOY habitat use largely to shallow depths. With greater availability of intermediate depths YOY habitat use would be expected to be highest at intermediate depths, consistent with the HSC. HSI values for relatively rare cover types, such as riprap, may be influenced by the limited number of observations. However, since these cover types are relatively rare, the HSI values for these cover types would be expected to have a minimal effect on the overall flow-habitat relationships.

The HSC from this study for depth, velocity, adjacent velocity and cover varied with life stage and species (Figures 38 – 41). Consistent with the scientific literature (Gido and Propst 1999, Sechnick et al. 1986, Baltz and Moyle 1984 and Moyle and Vondracek 1985), our data showed that larger fish select deeper and faster conditions than smaller fish, although for steelhead/rainbow trout, the higher suitability of faster velocities was only shown for velocities greater than 2.55 ft/s (0.78 m/s). The criteria also show a consistent preference for composite cover (instream woody plus overhead – cover codes 3.7, 4.7 and 5.7). Composite cover likely is an important aspect of juvenile salmonid habitat because it reduces the risk of both piscivorous and avian predation. The cover criteria also suggest that cobble cover is more important for steelhead/rainbow trout fry than for steelhead/rainbow trout juveniles or Chinook salmon fry or juveniles. This is consistent with our observations that steelhead/rainbow trout fry were sometime observed coming out of or going under cobble substrate during our snorkel surveys.

---

[35] The largest number of fish that we had in one observation was 300 fish.

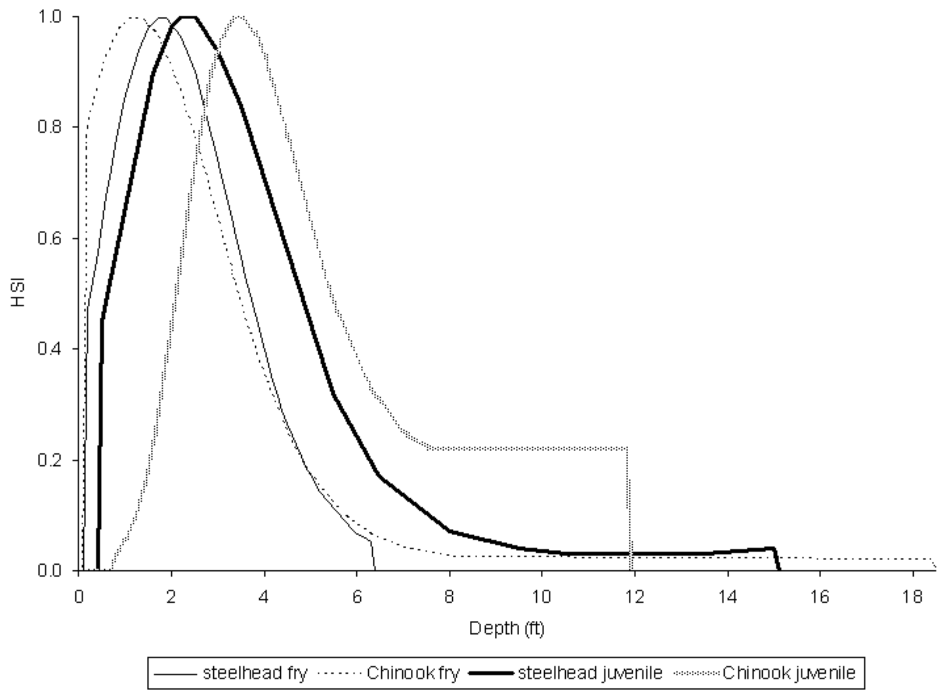

Figure 38. Comparison of depth HSC from this study. These criteria indicate that the optimum depths for juvenile fish are greater than those for fry, particularly for Chinook salmon.

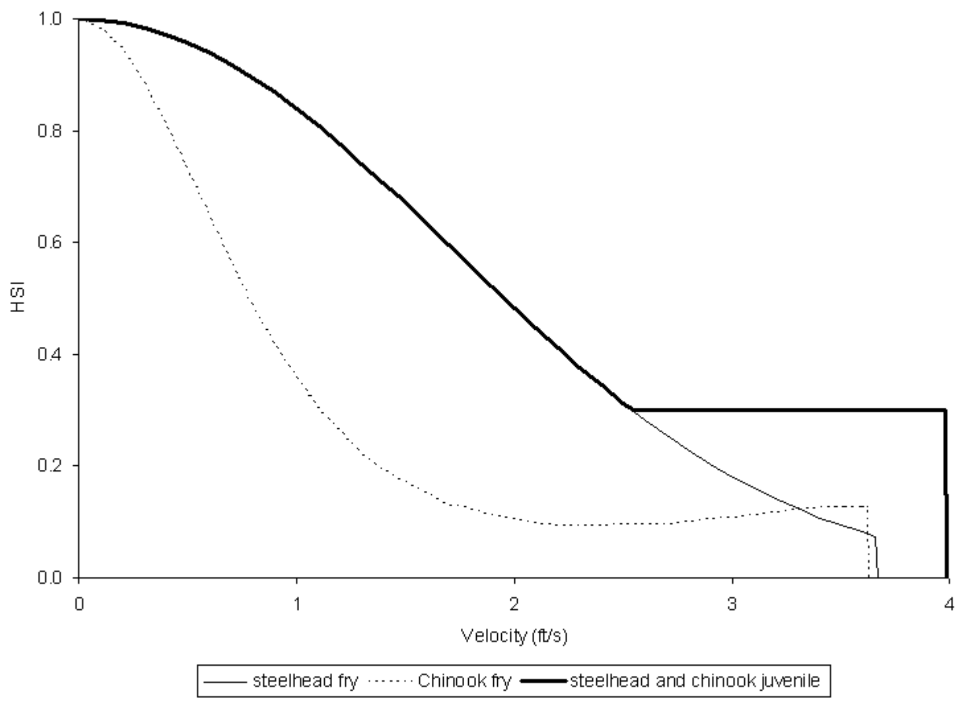

Figure 39. Comparison of velocity HSC from this study. These criteria indicate that there was a slower rate of decline of suitability with increasing velocity for steelhead/rainbow trout fry and both Chinook and steelhead/rainbow trout juveniles than for Chinook salmon fry.

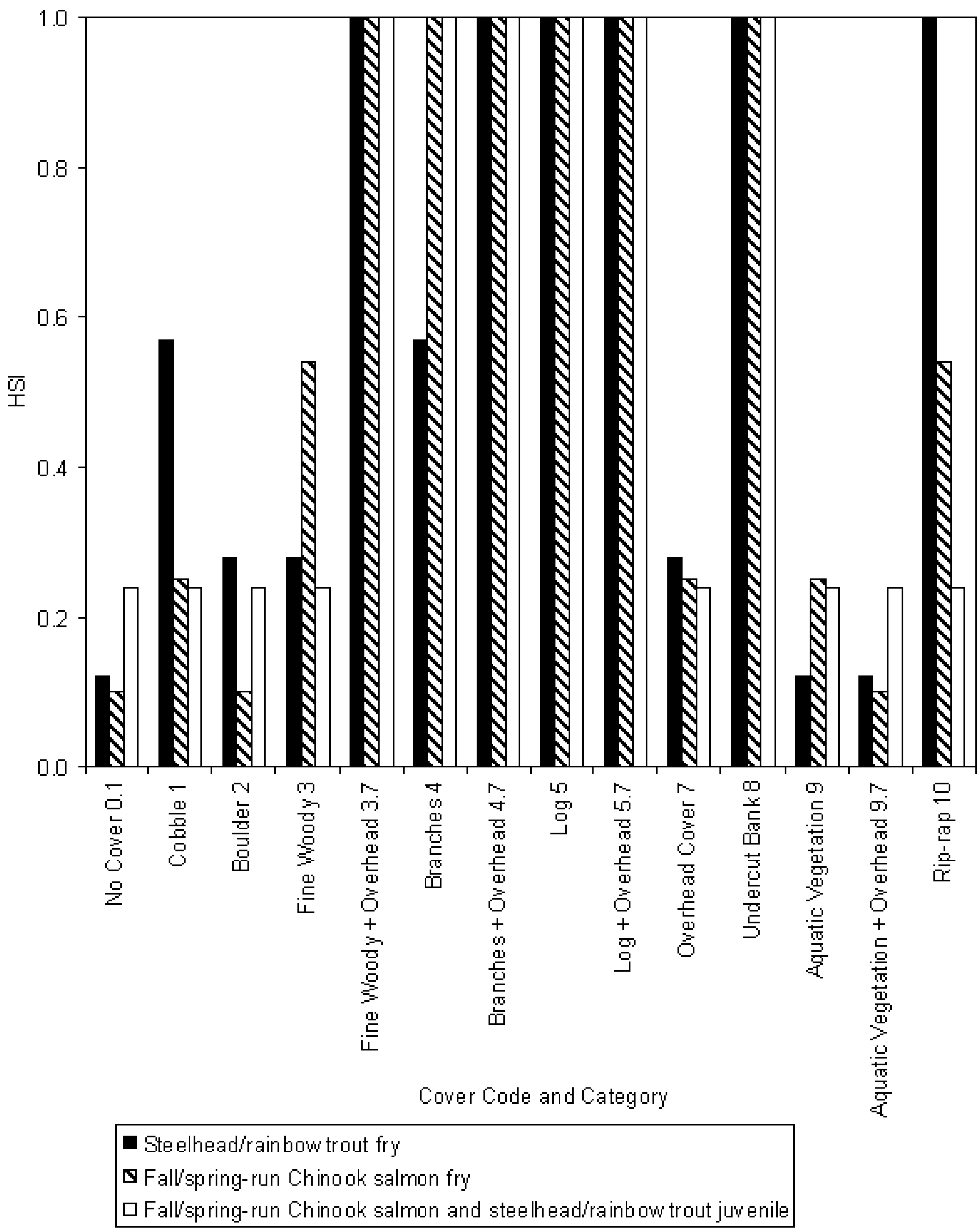

Figure 40. Comparison of cover HSC from this study. These criteria indicate that no cover had a lower suitability for fry than juveniles, but that there was a consistent preference for composite cover (instream woody plus overhead – cover codes 3.7, 4.7 and 5.7).

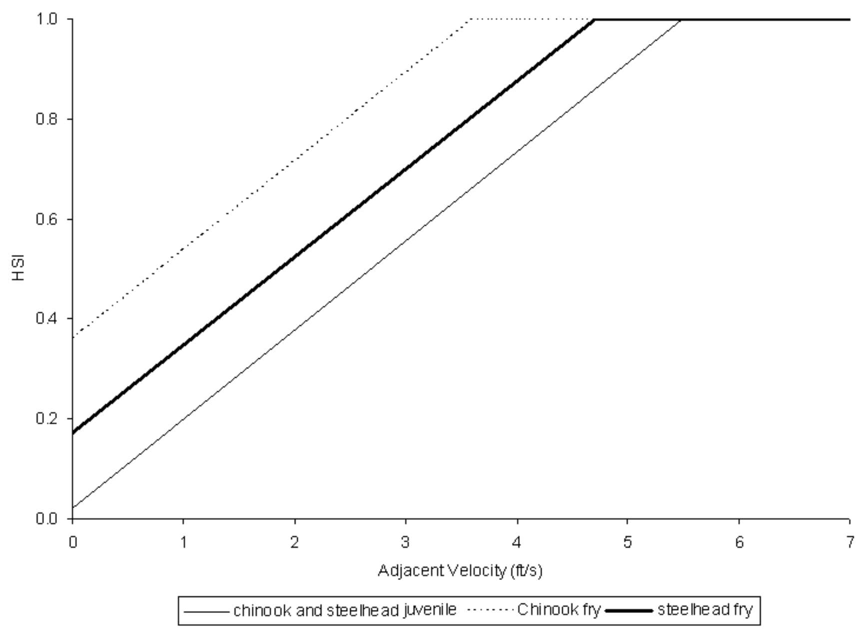

Figure 41. Comparison of adjacent velocity HSC from this study. These criteria indicate that turbulent mixing transporting invertebrate drift from fast-water areas to adjacent slow-water areas was most important for Chinook and steelhead juveniles and least important for Chinook fry.

The limit to the suitability of the Chinook juvenile depth criteria, reaching zero at 11.9 feet (3.63 meters), versus the Chinook fry criteria, which does not reach zero until 18.5 feet (5.64 meters), likely reflects the small number of occupied observations that we were able to collect for juvenile Chinook. With a larger sample size, we would have expected to have made at least one observation of juvenile Chinook salmon in depths greater than 11.9 feet (3.63 meters). For example, on the Sacramento River (Gard 2006), we found juvenile Chinook salmon in depths of up to 23.7 feet (7.22 meters).

We compared the criteria from this study with the criteria from other studies (Figures 42 - 52). For fall/spring-run Chinook salmon fry and juvenile depth and velocity, we compared the criteria from this study with those of Beak (1989) on the Yuba River and California Department of Water Resources (2005) on the Feather River. For steelhead/rainbow trout fry and juvenile depth and velocity, we compared our HSC to those from the Feather (California Department of Water Resources 2005) and Trinity (Hampton 1997) rivers[36]. With the exception of Chinook salmon fry, we compared all of the depth and velocity criteria with those from Bovee (1978), since these

[36] These were the only other steelhead fry and juvenile HSC developed in California that we were able to identify. Beak (1989) did not develop criteria for steelhead/rainbow trout.

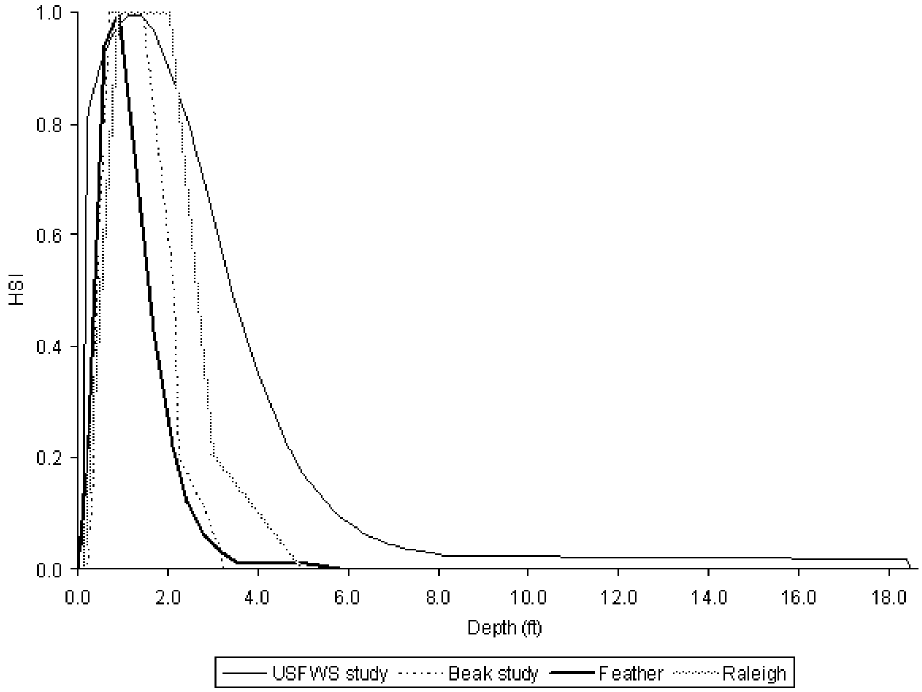

Figure 42. Comparison of fall/spring-run Chinook salmon fry depth HSC from this study with other fall-run Chinook salmon fry depth HSC. The criteria from this study show non-zero suitability, albeit at low values, for deeper conditions than the other criteria.

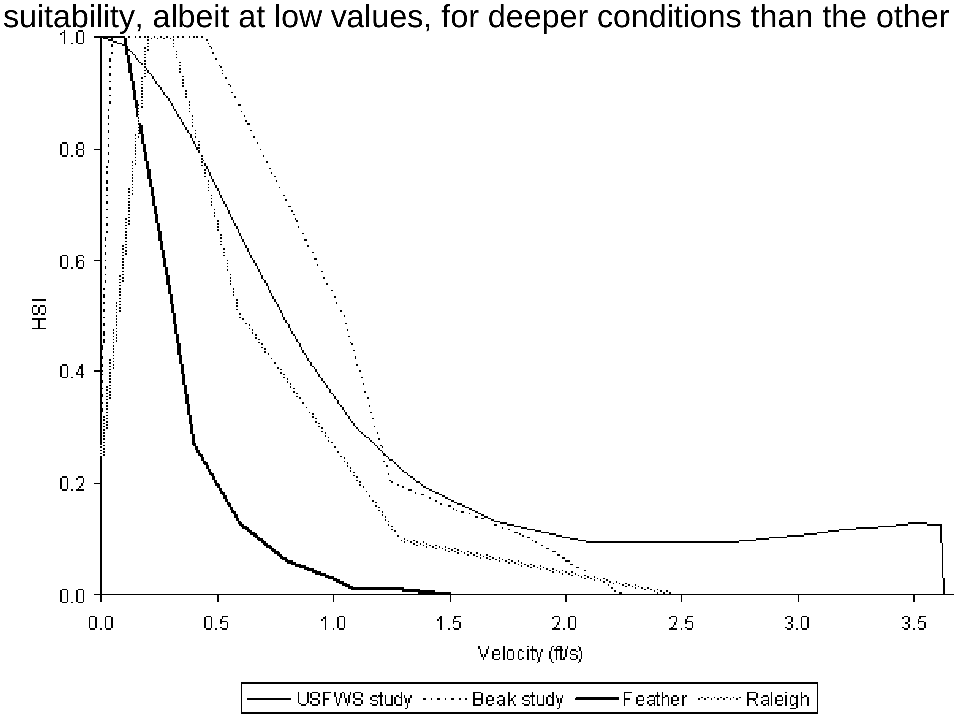

Figure 43. Comparison of fall/spring-run Chinook salmon fry velocity HSC from this study with other fall-run Chinook salmon fry velocity HSC. The criteria from this study show non-zero suitability, albeit at low values, for faster conditions than other criteria.

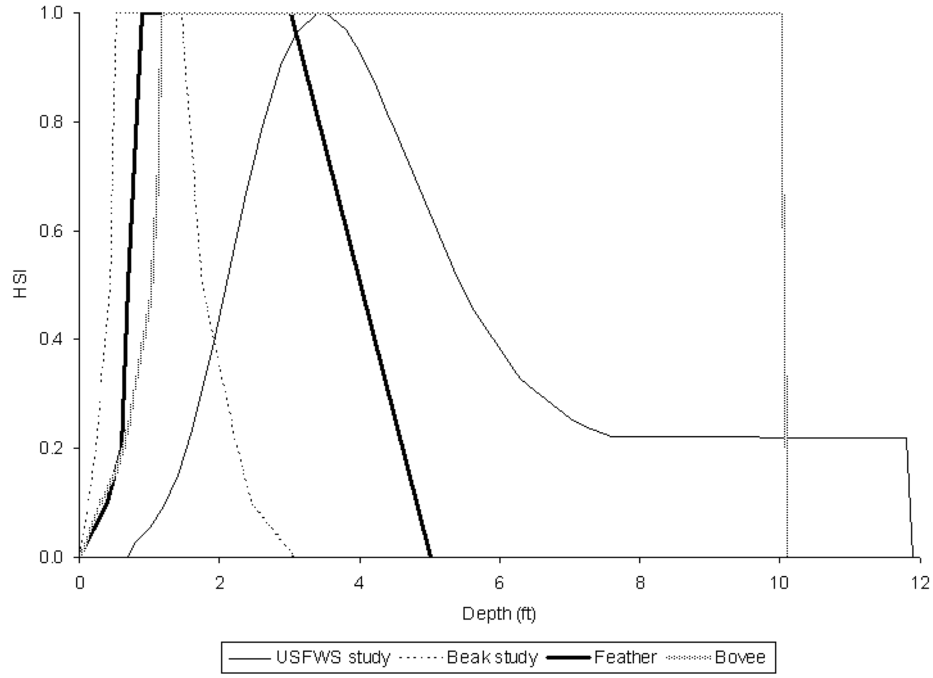

Figure 44. Comparison of fall/spring-run Chinook salmon juvenile depth HSC from this study with other fall-run Chinook salmon juvenile depth HSC. The criteria from this study reaches an optimum depth at deeper conditions than the other criteria.

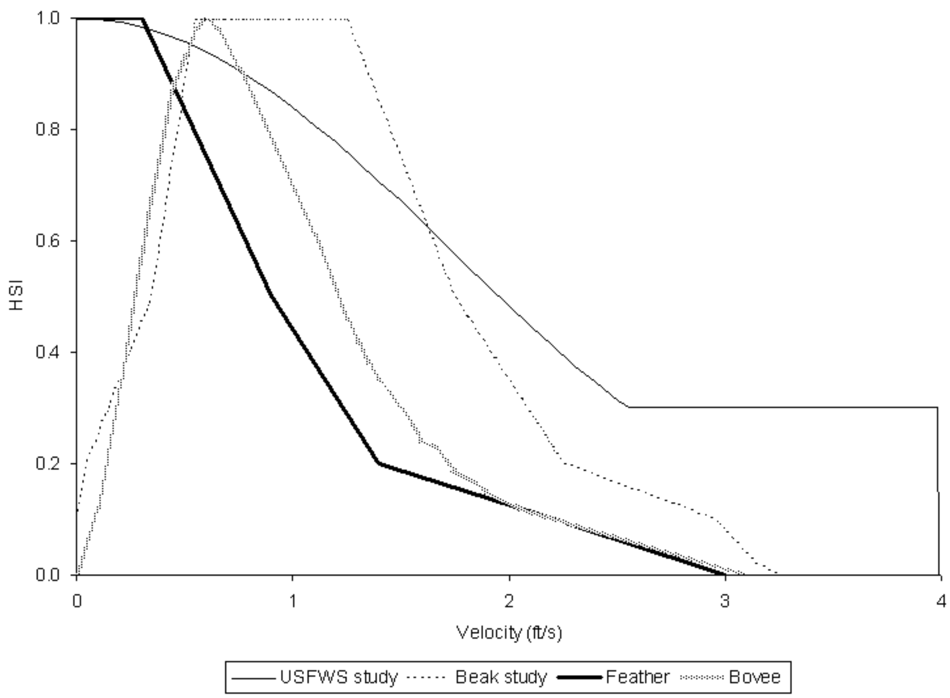

Figure 45. Comparison of fall/spring-run Chinook salmon juvenile velocity HSC from this study with other fall-run Chinook salmon juvenile velocity HSC. The criteria from this study show non-zero suitability for faster conditions than other criteria.

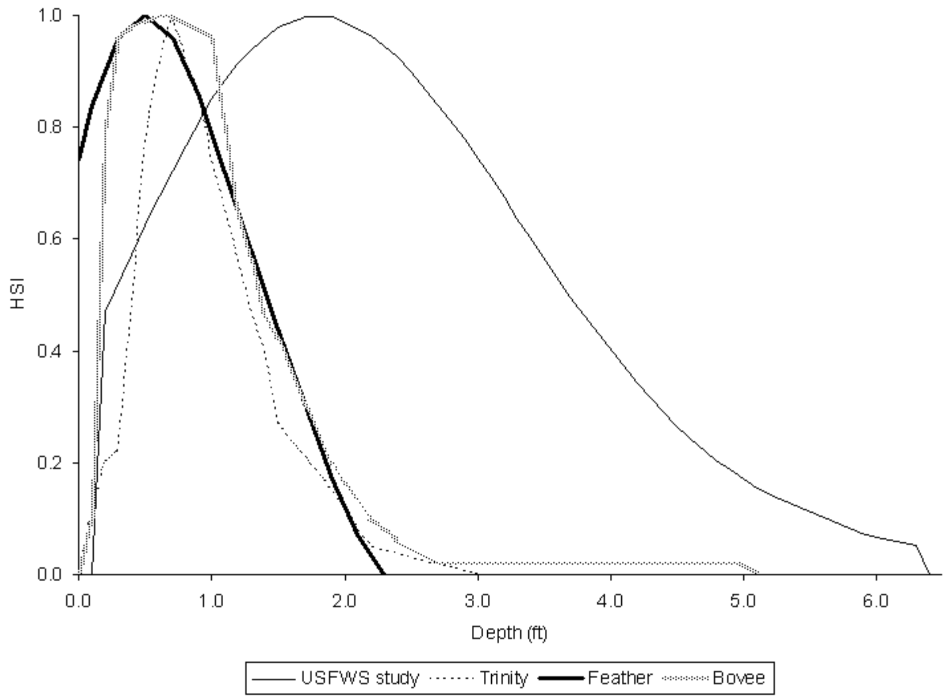

Figure 46. Comparison of steelhead/rainbow trout fry depth HSC from this study with other steelhead fry depth HSC. The criteria from this study show steelhead/rainbow trout fry preferring deeper conditions than other criteria.

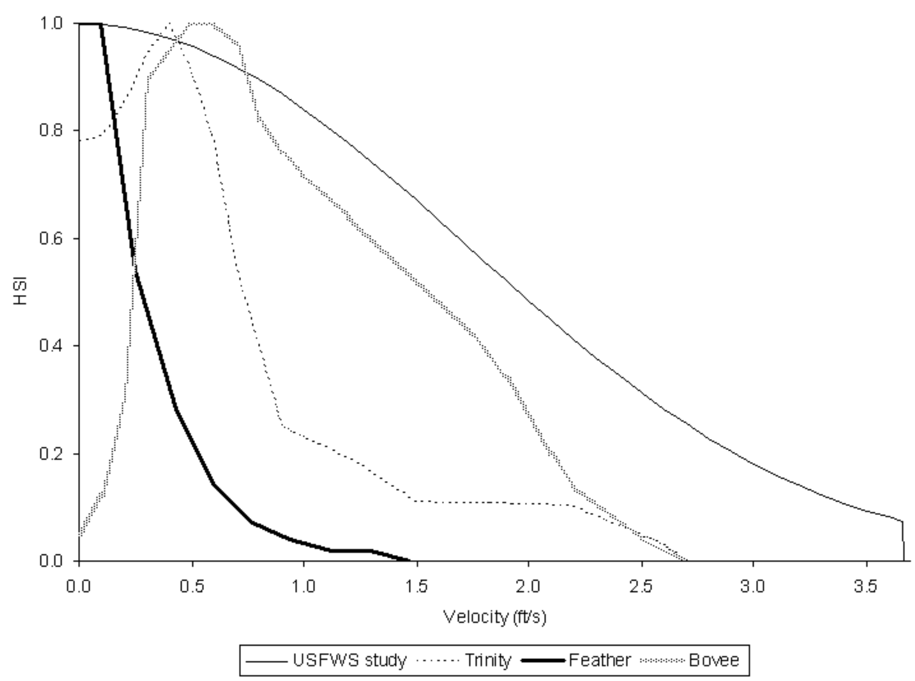

Figure 47. Comparison of steelhead/rainbow trout fry velocity HSC from this study with other steelhead fry velocity HSC. The criteria from this study show non-zero suitability extending to faster conditions than other criteria.

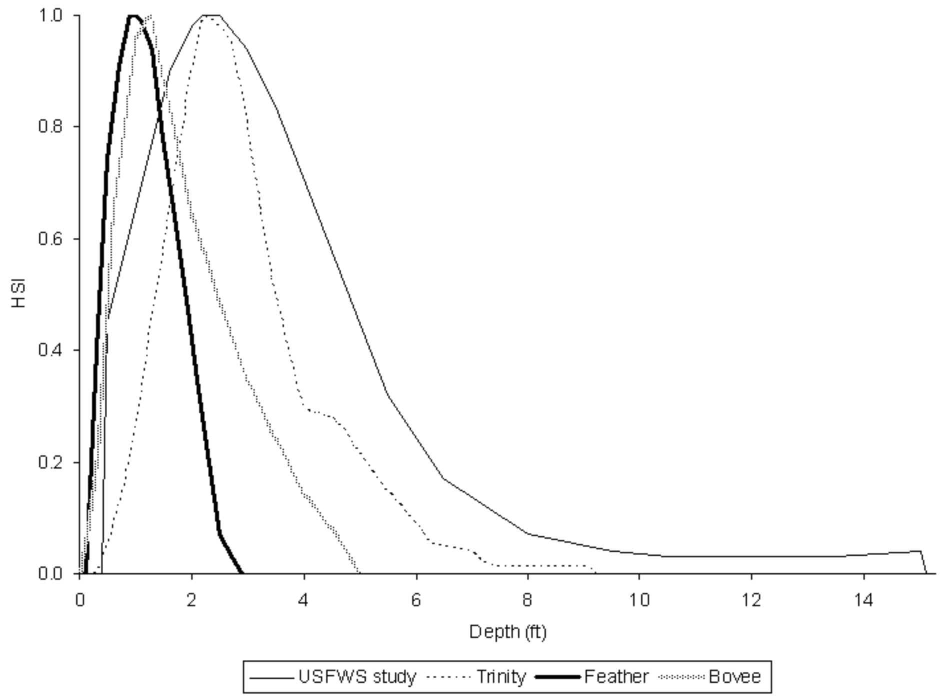

Figure 48. Comparison of steelhead/rainbow trout juvenile depth HSC from this study with other steelhead juvenile depth HSC. The criteria from this study show non-zero suitability, albeit at low values, for deeper conditions than the other criteria.

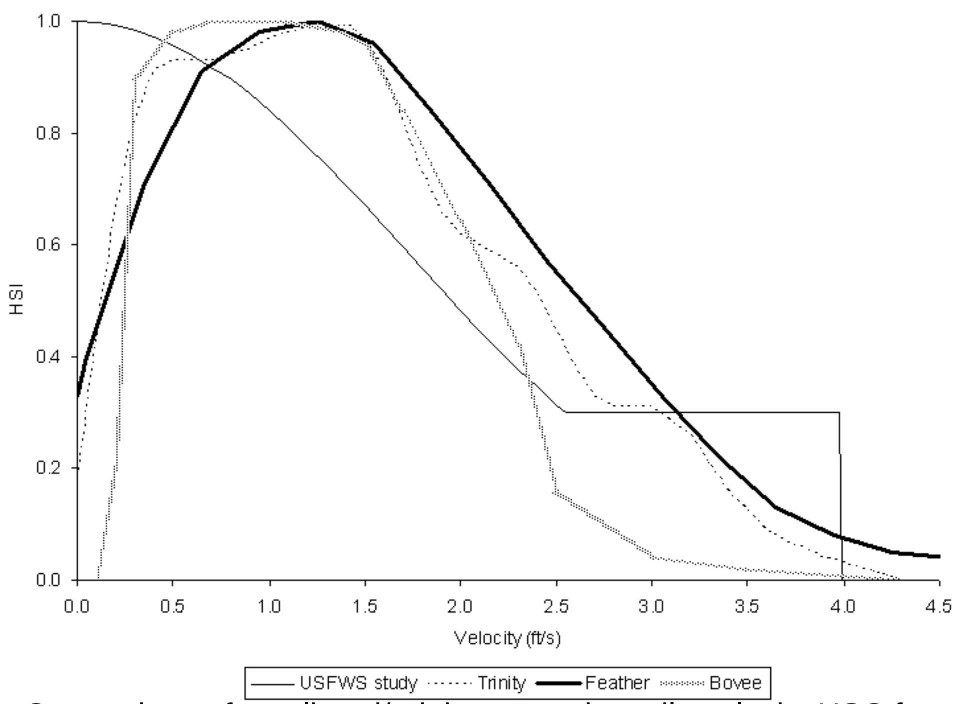

Figure 49. Comparison of steelhead/rainbow trout juvenile velocity HSC from this study with other steelhead juvenile velocity HSC. The criteria from this study show an optimal velocity at a lower value than for other criteria.

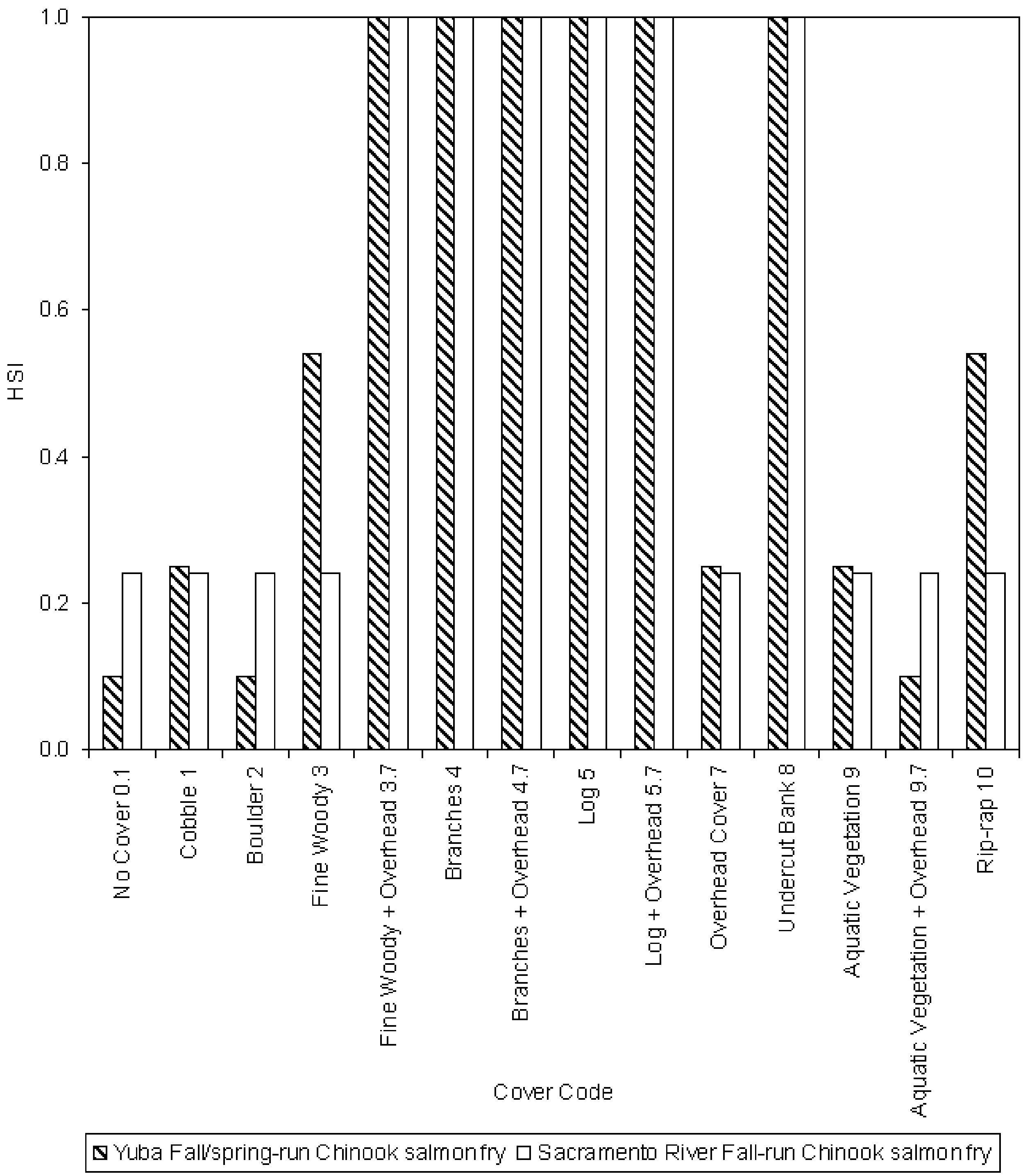

Figure 50. Comparison of fall/spring-run Chinook salmon fry cover HSC from this study with other fall-run Chinook salmon fry cover HSC. These criteria indicate a consistent preference for composite cover (instream woody plus overhead).

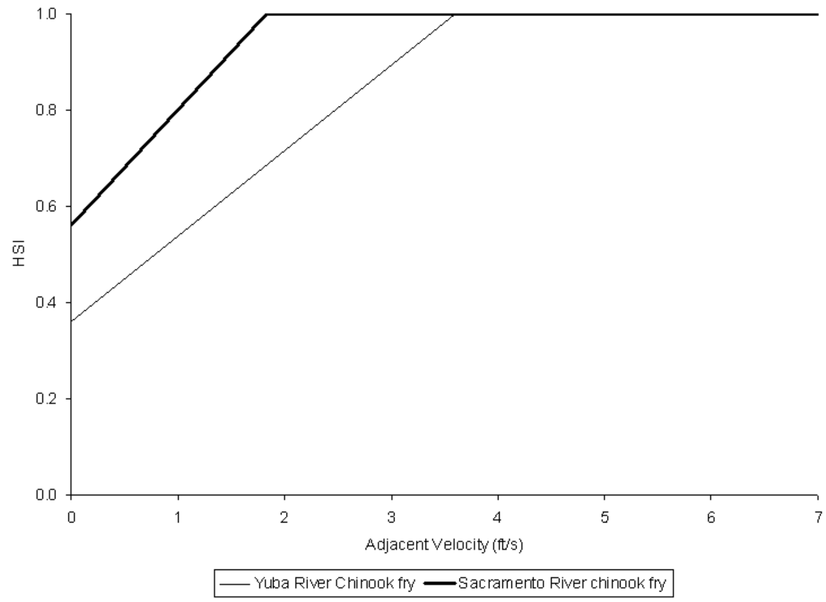

Figure 51. Comparison of fall/spring-run Chinook salmon fry adjacent velocity HSC from this study with other fall-run Chinook salmon fry adjacent velocity HSC. The criteria indicate that turbulent mixing transporting invertebrate drift from fast-water areas to adjacent slow-water areas was more important for Yuba River Chinook fry than for Sacramento River Chinook fry.

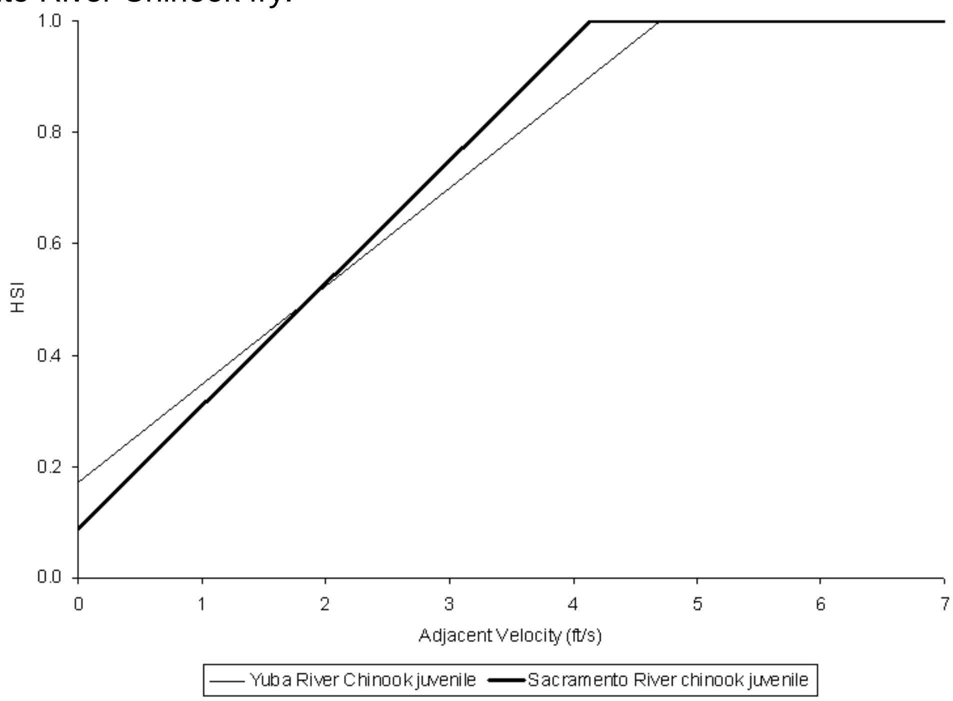

Figure 52. Comparison of fall/spring-run Chinook salmon juvenile adjacent velocity HSC from this study with other fall-run Chinook salmon juvenile adjacent velocity HSC. The Yuba and Sacramento River criteria are quite similar.

criteria are commonly used in instream flow studies as reference criteria. Since Bovee (1978) does not have criteria for Chinook salmon fry, we used another commonly cited reference criteria (Raleigh et al. 1986).

For cover, we were limited to comparing the criteria from this study to criteria we had developed on other studies which used the same, unique cover coding system. We compared the fall/spring-run Chinook salmon fry criteria from this study to those we had developed for fall-run Chinook salmon on the Sacramento River (Gard 2006). We were not able to compare the fall/spring-run Chinook salmon juvenile criteria from this study to those developed for the Sacramento River (Gard 2006), since we already have adopted the Sacramento River cover criteria for this study, as discussed in the Results – Habitat Suitability Criteria Development section. We have not previously developed criteria for steelhead/rainbow trout fry or juvenile rearing.

For adjacent velocity, the only other HSC we were able to identify for Chinook salmon fry or juvenile rearing were the criteria we developed on the Sacramento River (Gard 2006). We have not previously developed criteria for steelhead/rainbow trout fry or juvenile rearing, nor were we able to identify any other adjacent velocity HSC that had been developed for steelhead/rainbow trout fry or juvenile rearing.

The fall/spring-run Chinook salmon fry and juvenile and steelhead/rainbow trout juvenile depth criteria show non-zero suitability, albeit at low values, for deeper conditions than the criteria from other studies. We attribute this to the use of SCUBA sampling to collect fry and juvenile rearing HSC data in deeper water. Typically, criteria data for fry and juvenile anadromous salmonids are only collected using snorkel surveys, on the assumption that fry and juvenile anadromous salmonids will not be found in deeper water. In contrast, we found that fry and juvenile anadromous salmonids will use deeper water with suitable velocities. The depth criteria for steelhead/rainbow trout fry differed more substantially from other criteria, with an optimal suitability at 1.7 to 1.9 feet (0.52 to 0.58 meters), versus at 0.5 to 0.7 feet (0.15 to 0.21 meters) for other criteria. We attribute this to the use of a logistic regression to address availability, and that the other criteria, developed using use data, underestimate the suitability of deeper conditions (in the range of 1.5 to 6 feet (0.46 to 1.83 meters) because they do not take availability into account. In addition, we observed steelhead/rainbow trout fry in deeper conditions than for other criteria; we had seven percent of our observations in water ≥ 3 feet (0.91 meters), while both the Feather and Trinity River HSC had zero suitability for depths ≥ 3 feet (0.91 meters).

The fall/spring-run Chinook salmon fry velocity criteria show non-zero suitability, albeit at low values, for faster conditions than the other criteria. We attribute this to the fact that we observed fall/spring-run Chinook salmon fry at higher velocities than for other criteria; we had observations at velocities as high as 3.62 feet/sec (1.10 meters/sec), while both the Feather River and Beak (1989) HSC had zero suitability for velocities greater than 2.24 feet/sec (0.68 meters/sec). Similarly, our fall/spring-run Chinook salmon juvenile and steelhead/rainbow trout fry velocity criteria show non-zero suitability for faster conditions than other criteria. We attribute this to the fact that we observed fall/spring-run Chinook salmon juveniles and steelhead/rainbow trout fry at higher velocities than for other criteria. For fall/spring-run Chinook salmon juveniles, we had observations at velocities as high as 3.98 feet/sec (1.21 meters/sec), while both the Feather River and Beak (1989) HSC had zero suitability for velocities greater than 3.24 feet/sec (0.99 meters/sec). For steelhead/rainbow trout fry, we had observations at velocities as high as 3.66 feet/sec (1.12 meters/sec), while both the Feather and Trinity River HSC had zero suitability for velocities greater than 2.69 feet/sec (0.82 meters/sec). Our fall/spring-run Chinook salmon and steelhead/rainbow trout juvenile velocity HSC showed an optimal velocity at a lower value than for other criteria. We attribute this to having to use the steelhead/rainbow trout fry velocity HSC for fall/spring-run Chinook salmon and steelhead/rainbow trout juveniles, for velocities less than 2.55 feet/sec (0.78 meters/sec). The very similar frequency distribution of occupied and unoccupied velocities for fall/spring-run Chinook salmon and steelhead/rainbow trout juveniles resulted in a logistic regression that showed that there was no significant influence of velocity on use or nonuse. Accordingly, we could have used a binary velocity criteria for fall/spring-run Chinook salmon and steelhead/rainbow trout juveniles, but decided that the use of the steelhead/rainbow trout fry velocity HSC for velocities less than 2.55 feet/sec (0.78 meters/sec) was more appropriate, given the lack of a significant difference between velocities used by juvenile salmonids and steelhead/rainbow trout fry for velocities less than 2.55 feet/sec (0.78 meters/sec).

The consistency between the Yuba and Sacramento River Chinook salmon fry cover HSC, relative to preference for composite cover (instream woody plus overhead), and the Chinook salmon juvenile adjacent velocity criteria supports the importance of these two habitat characteristics for anadromous juvenile salmonid rearing. While cover is frequently used for anadromous juvenile salmonid rearing, the simplicity of the cover categories (typically no cover, object cover, overhead cover and object plus overhead cover) misses the importance of woody composite cover for anadromous juvenile salmonid rearing. The concept of adjacent velocity criteria was included in the original PHABSIM software, through the HABTAV program (Milhous et al. 1989), but has rarely been implemented, and has been envisioned as primarily applying to adult salmonids, where the fish reside in low-velocity areas, but briefly venture into adjacent fast-velocity areas to feed on invertebrate drift. In both this study and our Sacramento River study (US Fish and Wildlife Service 2005), we have developed the adjacent velocity criteria based on an entirely different mechanism, namely the transport of invertebrate drift from fast-water areas to adjacent slow-water areas where fry and juvenile salmonids reside via turbulent mixing. We believe that this is an important aspect of anadromous juvenile salmonid rearing habitat that has been overlooked in previous studies. The Yuba River Chinook salmon fry adjacent velocity criteria show a lower suitability for an adjacent velocity of zero and a higher adjacent velocity at which the suitability reaches one. This indicates that the transport of invertebrate drift from fast-water areas to adjacent slow-water areas via turbulent mixing was more important for Yuba River Chinook fry than for Sacramento River Chinook fry.

7. *Biological Verification*

In general, our biological verification was unsuccessful due to the low number of fry and juvenile fall/spring-run Chinook salmon and juvenile steelhead/rainbow trout observed. This resulted in a low number of occupied locations (33, 5 and 3 for, respectively, the above three species/life stages) that could be included in the comparisons, and a consequent low power of the Mann-Whitney U test for these species/life stages. In this regard, Thomas and Bovee (1993) found in the analogous transferability test that the power of the test was significantly reduced if the number of occupied locations was less than 45. We did not use a parametric test because the assumption of normality of parametric tests was violated, as shown in Figures 24 to 25, indicating the appropriateness of nonparametric tests. A large unbalanced sample size was appropriate for the Mann-Whitney U test to reduce type II errors, since unoccupied depths, velocities and substrates have a much greater range of values than occupied depths, velocities and substrates, and thus did not bias results. Analogously, Thomas and Bovee (1993) found that a minimum of 55 occupied and 200 unoccupied locations were required to reduce type II errors.

The limited performance of River2D in predicting the CSI of occupied locations likely is related to errors due to: 1) the predictive accuracy of the HSC; and 2) the predictive accuracy of the hydraulic modeling. Errors in the habitat predictions for occupied locations for River2D can be due to inadequate detail in mapping cover distribution, insufficient data collected to correctly map the bed topography of the site, or effects of the bed topography upstream of the study site not being included in the model. To assess the relative magnitude of errors due to the predictive accuracy of the HSC and the predictive accuracy of the hydraulic modeling, we calculated a combined habitat suitability of occupied and unoccupied locations using the measured depth, velocity, adjacent velocity and cover data, which we will refer to as “measured combined habitat suitability”. The measured combined habitat suitability was significantly higher for occupied versus unoccupied locations for fall/spring-run Chinook fry and juveniles and for steelhead/rainbow trout fry, but there was no significant difference between the measured combined habitat suitability of occupied and unoccupied locations for steelhead/rainbow trout juveniles (Table 33). We plotted the frequency distribution of measured combined habitat suitability for locations with and without fall/spring-run Chinook (Figure 53) and steelhead/rainbow trout (Figure 54) fry to graphically illustrate the difference in measured combined habitat suitability between occupied and unoccupied locations**.** Since occupied locations had a significantly greater measured combined habitat suitability than unoccupied locations for those life stages/species with larger occupied sample sizes (fall/spring-run Chinook and steelhead/rainbow trout fry), while there was no significant difference (Results – Biological Verification) between the combined habitat suitability predicted by the River2D model for these life stages/races, we believe that the failure of the biological verification was primarily due to errors in predictive accuracy of the hydraulic modeling. While many of the occupied points were located in areas with higher suitability than unoccupied locations, some occupied points were located where the suitability was poor or where there was dry land in the model. We attribute these results primarily to a point density which was inadequate to accurately characterize the bed topography and the cover. Errors in bed topography were certainly the primary cause of modeled

Table 33. Results of Mann-Whitney tests using combined habitat suitability index (CSI) calculated from measured depths, velocities, adjacent velocities and cover.

			Mann-Whitney U test	
Species/Life Stage	Median occupied CSI	Median unoccupied CSI	U statistic	p-value
Chinook fry	0.199 (n = 33)	0.058 (n = 52)	398	0.000034
Steelhead/rainbow trout fry	0.135 (n = 71)	0.034 (n = 98)	1729	< 0.000001
Chinook juveniles	0.123 (n = 5)	0.005 (n = 23)	15	0.0099
Steelhead/rainbow trout juveniles	0.007 (n = 3)	0.024 (n = 80)	139	0.64

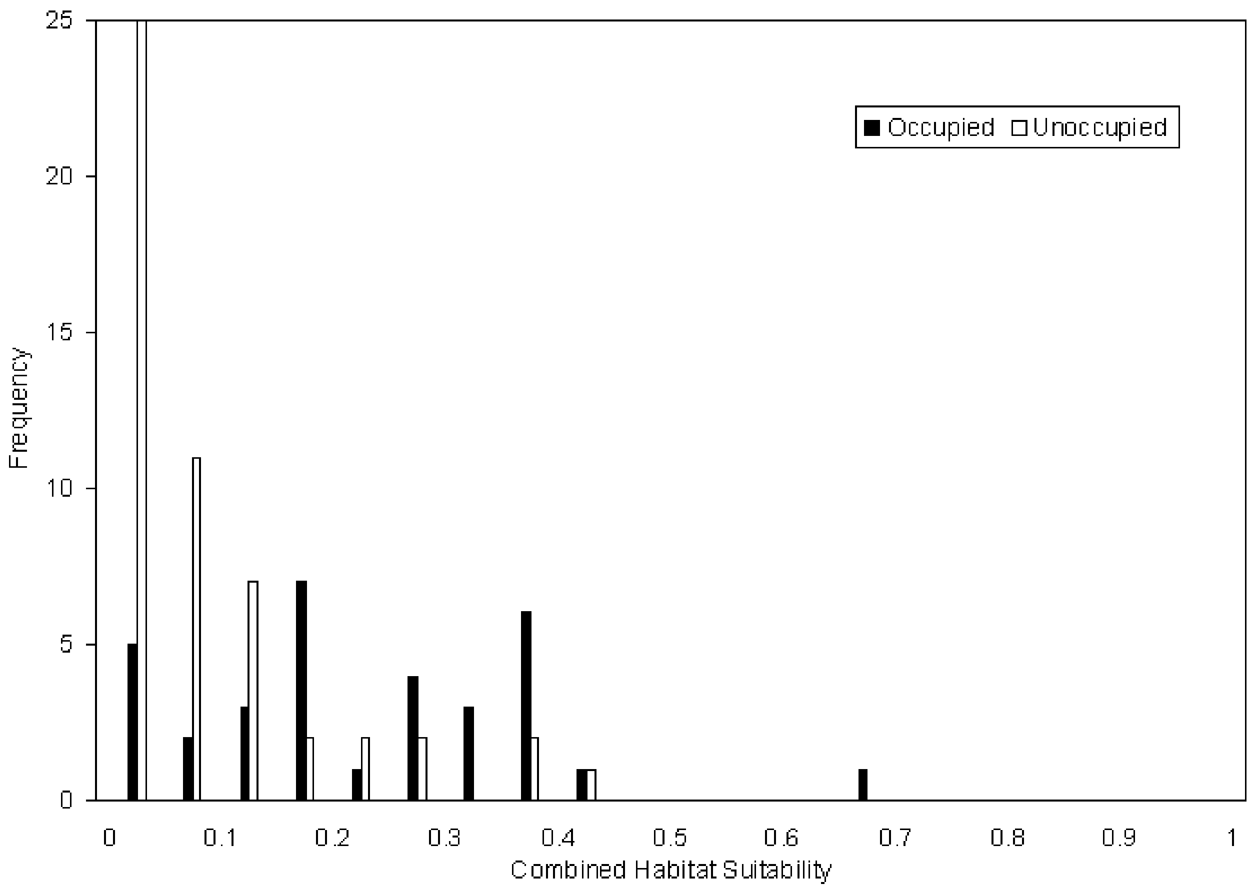

Figure 53. Combined habitat suitability calculated from measured depths, velocities, adjacent velocities and cover for locations with (occupied) and without (unoccupied) fall/spring-run Chinook fry.

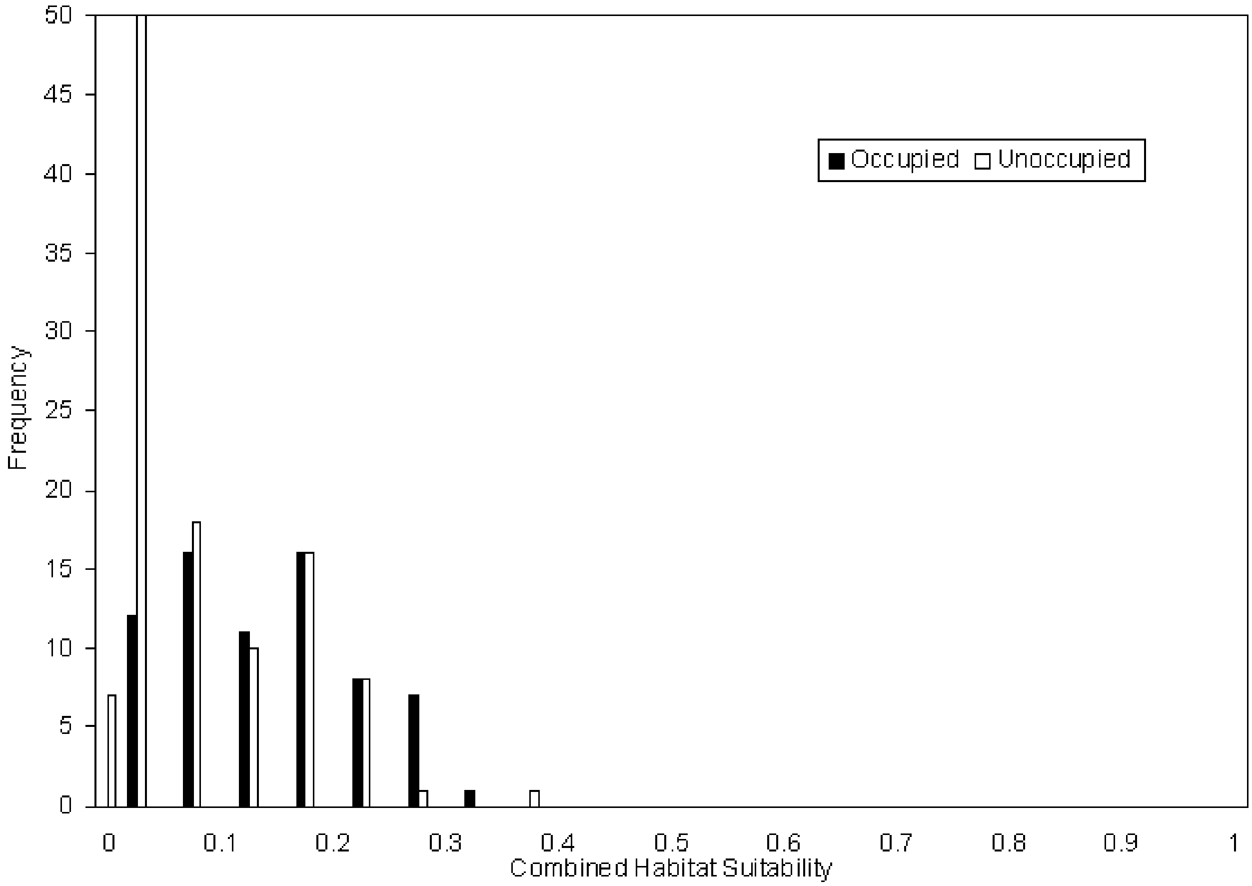

Figure 54. Combined habitat suitability calculated from measured depths, velocities, adjacent velocities and cover for locations with (occupied) and without (unoccupied) steelhead/rainbow trout fry.

dry land where it was actually wet. Errors in bed topography likely resulted in modeled unsuitable velocities in some of the locations where juveniles were observed. A very high density of bed topography and cover points would likely be needed to arrive at a better fit between juvenile observations and habitat suitability.

The biological verification results for Timbuctoo steelhead/rainbow trout fry at 917 cfs (Appendix M) illustrates another error of the hydraulic model that contributed to the failure of the biological verification. Specifically, 11 out of the 15 steelhead/rainbow trout fry occupied locations where River2D predicted zero suitability were found in a side channel run habitat unit that had entirely subsurface inflow at 917 cfs (Figure 55). It is likely that River2D predicted too low a flow in this habitat unit because of insufficient predicted subsurface flow. While River2D can generate subsurface flow (as illustrated by the non-zero velocities in this habitat unit shown in Figure 55), the accuracy of River2D to simulate subsurface flow is likely low, since subsurface flow is primarily included in the River2D model to address wetting/drying during model runs.

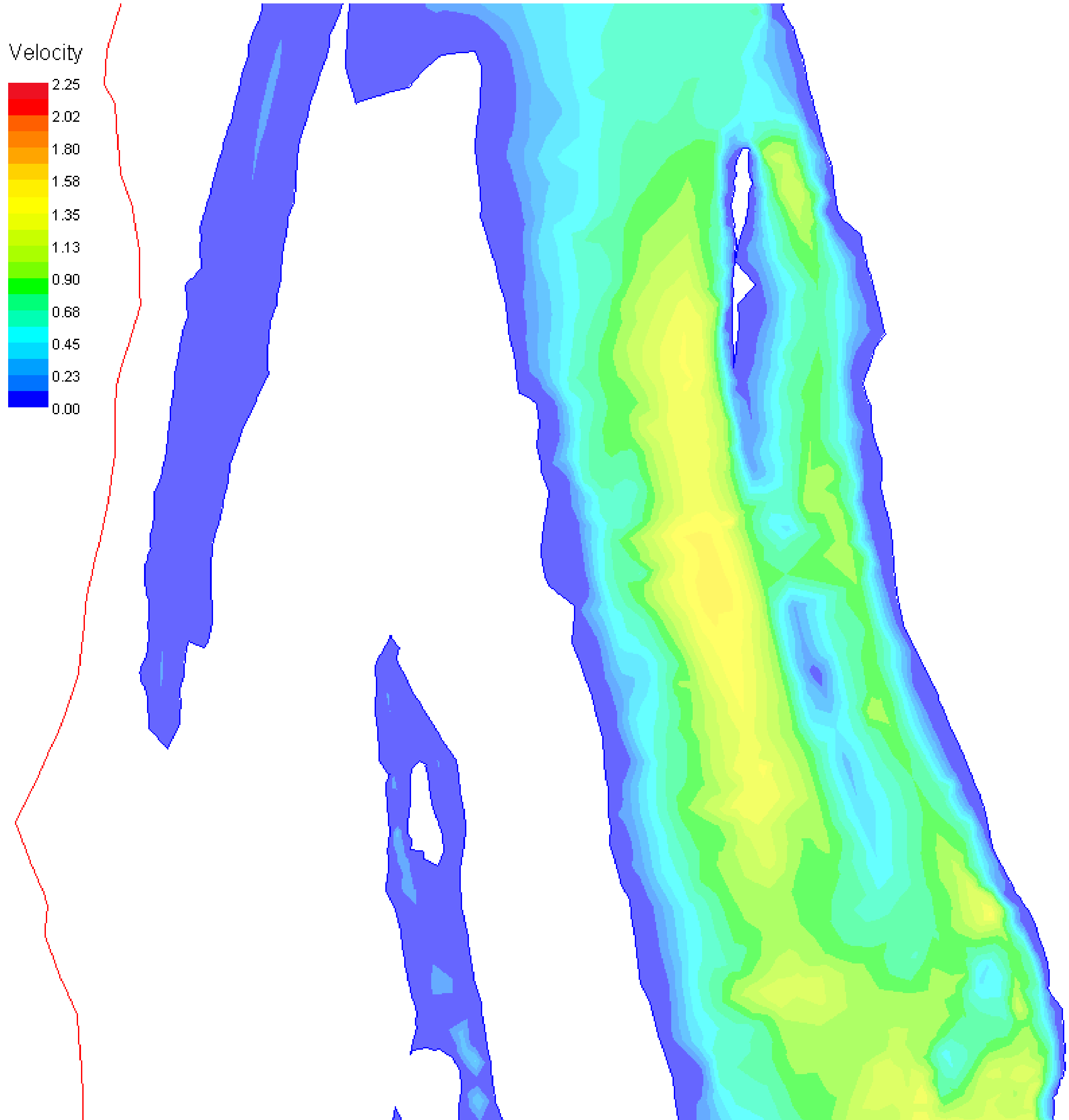

Scale: 1:1342

Figure 55. Detail of velocity simulation at a total river flow of 917 cfs for the portion of the Timbuctoo site including the side-channel run habitat unit with 11 locations of steelhead/rainbow trout fry that River2D predicted were dry. Note the non-zero velocities in the side-channel run, indicating that River2D was generating subsurface flow into the upstream end of the habitat unit.

The performance of River2D in this situation might have been improved by trying a larger groundwater transmissivity value. When data from this habitat unit are excluded from the biological verification test, there still is no significant difference between the steelhead/rainbow trout fry combined habitat suitability predicted by River2D for occupied (median = 0.056, n = 54) and unoccupied (median = 0.048, n = 82) locations. However, the p-value from the one-tailed Mann-Whitney U test in this case (0.19) is much lower than when data from the above habitat unit are included in the analysis (p = 0.74), indicating that the hydraulic modeling error for this habitat unit had a large effect on the failure of the biological validation for steelhead/rainbow trout fry.

The statistical tests used in this report for biological verification differ from those used in Guay et al. (2000). In Guay et al. (2000), biological verification was accomplished by testing for a statistically significant positive relationship between fish densities, calculated as the number of fish per area of habitat with a given range of habitat suitability (i.e. 0 to 0.1), and habitat quality indexes. We were unable to apply this approach in this study because of the low number of fry and juveniles and low area of habitat with high values of habitat quality. As a result, the ratio of fry and juvenile numbers to area of habitat for high habitat quality values exhibits significant variation simply due to chance. Both the number of fry and juveniles and amount of habitat at high values of habitat quality is quite sensitive to the method used to calculate combined suitability. When combined suitability is calculated as the product of the individual suitabilities, as we did in this study and is routinely done in instream flow studies, very low amounts of high quality habitat will be predicted. For example, if depth, velocity, adjacent velocity and cover all have a high suitability of 0.9, the combined suitability would be only 0.66. In contrast, Guay et al. (2000) calculated combined suitability as the geometric mean of the individual suitabilities; for the above example, the combined suitability calculated as a geometric mean would be 0.9.

The plots of combined suitability of fry and juvenile locations in Appendix M are similar to the methods used for biological verification in Hardy and Addley (2001). In general, Hardy and Addley (2001) report a much better agreement between fry and juvenile locations and areas with high suitability than what we found in this study. We attribute the differences between our study and Hardy and Addley (2001) to the following two factors: 1) Hardy and Addley (2001) present results for an entire study site, while our results are just for the portion of the site that we sampled; and 2) Hardy and Addley (2001) calculated combined suitability as the geometric mean of the individual suitabilities, while we calculated combined suitability as the product of the individual suitabilities. The combination of the above two factors results in the plots in Hardy and Addley (2001) having large areas with zero suitability (away from the channel margins) and smaller areas of high suitabilities near the channel margins where fish were located. However, Hardy and Addley (2001) did report lower quality simulation results for juvenile steelhead, as a result of insufficient bed topography detail, particularly around boulder clusters.

8. *Habitat Simulation*

There was considerable inter-site variation in the flow-habitat relationships (Appendix L). Sites that did not include the entire river flow (Whirlpool and Side-Channel) reached the maximum amount of habitat for fall/spring-run Chinook salmon fry at or near the highest simulation flow (4,500 cfs), while other sites which did include the entire river flow (Sucker Glide) had the maximum amount of habitat for fall/spring-run Chinook salmon fry at the lowest simulation flow (150 cfs). We attribute the variation from site to site to complex interactions of the combinations of availability and suitability of depth, velocity, adjacent velocity and cover, as they vary with flow. The overall flow-habitat relationships for each segment (Figures 26 – 33) capture the inter-site variability in flow-habitat relationships by weighting the amount of habitat for each mesohabitat unit in each site by the proportion of each mesohabitat type present within each segment.

An earlier study (Beak 1989) also modeled fall-run Chinook salmon fry and juvenile rearing habitat in the Yuba River. The results from our study predict substantially less habitat for juvenile Chinook salmon at low flows and a peak amount of habitat at higher flows for both fry and juvenile Chinook salmon than did Beak (1989) (Figures 56 – 59). However, the difference between studies in the flow with the peak amount of habitat varied by reach. We attribute the differences between our study and Beak (1989) to the following: 1) the Beak (1989) study used HSC generated only from use data, as opposed to the criteria generated with logistic regression in this study; 2) the Beak (1989) study did not use cover or adjacent velocity criteria; and 3) the use of PHABSIM in the Beak (1989) study, versus 2-D modeling in this study. We believe that these differences likely biased the flow-habitat results in the Beak (1989) study towards lower flows, since the HSC, generated only from use data and without cover or adjacent velocity criteria, were biased towards slower and shallower conditions. In contrast, our study reduces biases due to availability and includes the important juvenile habitat components of cover and adjacent velocity. We attribute the difference in magnitude of the results from this study versus Beak (1989) primarily to a combination of a broader range of suitable depths and velocities and the use of adjacent velocity criteria in this study. A broader range of suitable depths and velocities will result in more habitat. In contrast, a fourth habitat suitability index parameter will tend to result in overall lower amounts of habitat, since the combined suitability index is calculated as the product of the individual suitability indices. The effects of adjacent velocity are most pronounced at low flows, where a large proportion of the channel has low adjacent velocities, and thus low suitability for this parameter. Thus, the results of this study are a more accurate assessment of the relationship between flow and anadromous salmonid fry and juvenile rearing habitat than the results of Beak (1989).

A basic assumption of all instream flow studies is that a stream is in dynamic equilibrium. When a channel is in dynamic equilibrium, there is an approximate balance between sediment supply and transport, so that the channel pattern and cross-sectional profile of the entire stream is consistent (Bovee 1996). For a stream in dynamic equilibrium, it would be expected that large flow events would not result in a significant change in flow-habitat relationships. Recent high

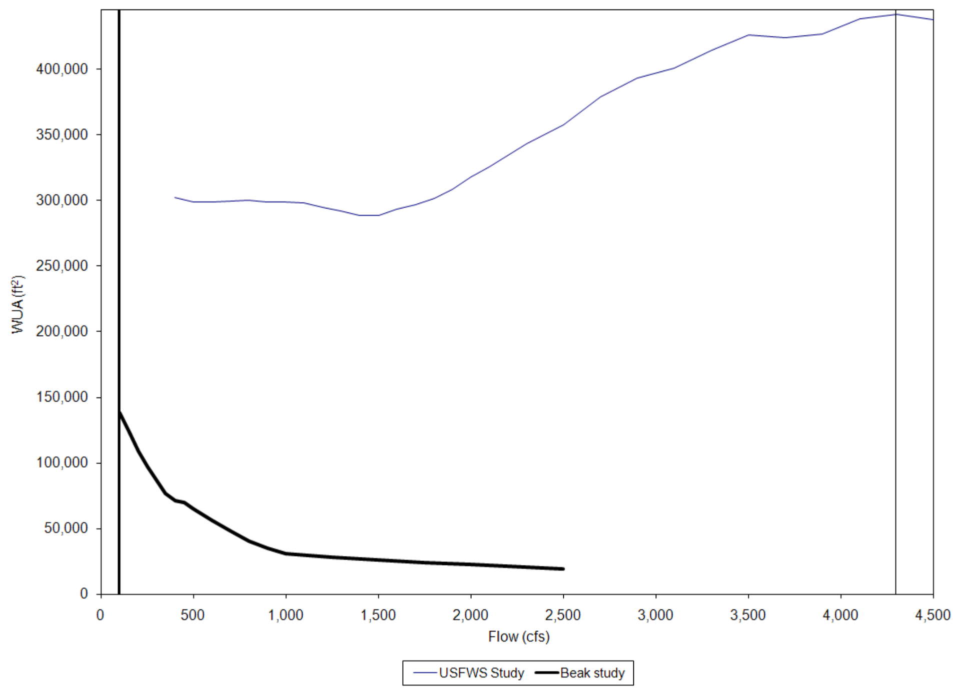

Figure 56. Comparison of Chinook salmon fry flow-habitat relationship above Daguerre Point Dam from this study and the Beak (1989) study. This study predicted more habitat at all flows and the peak habitat at a higher flow than the Beak (1989) study.

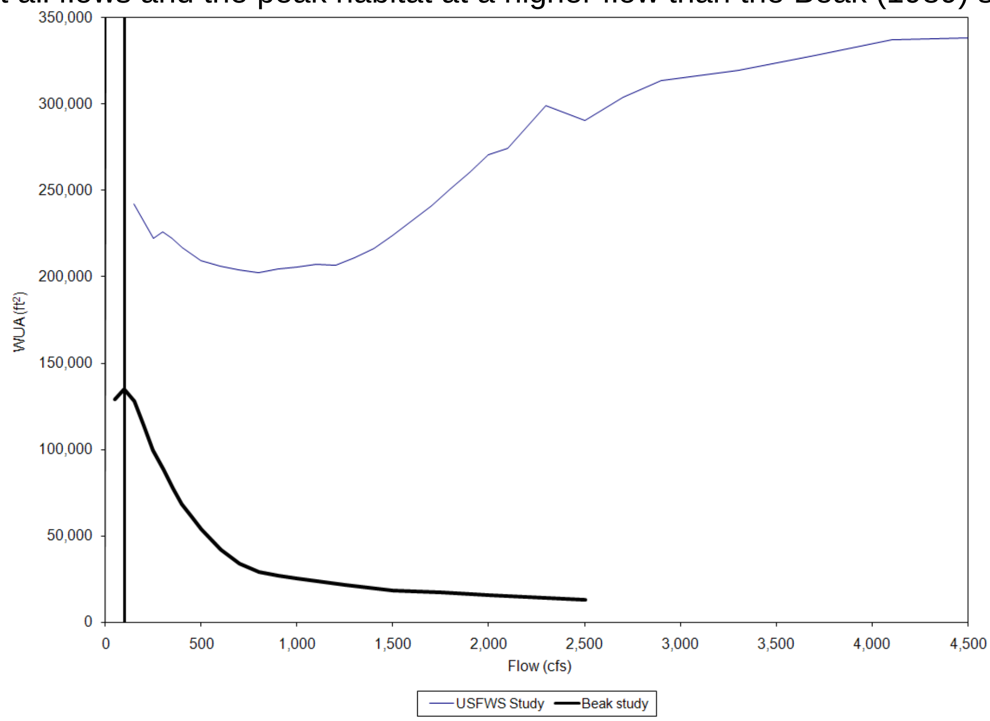

Figure 57. Comparison of Chinook salmon fry flow-habitat relationship below Daguerre Point Dam from this study and the Beak (1989) study. This study predicted more habitat at all flows and the peak habitat at a higher flow than the Beak (1989) study.

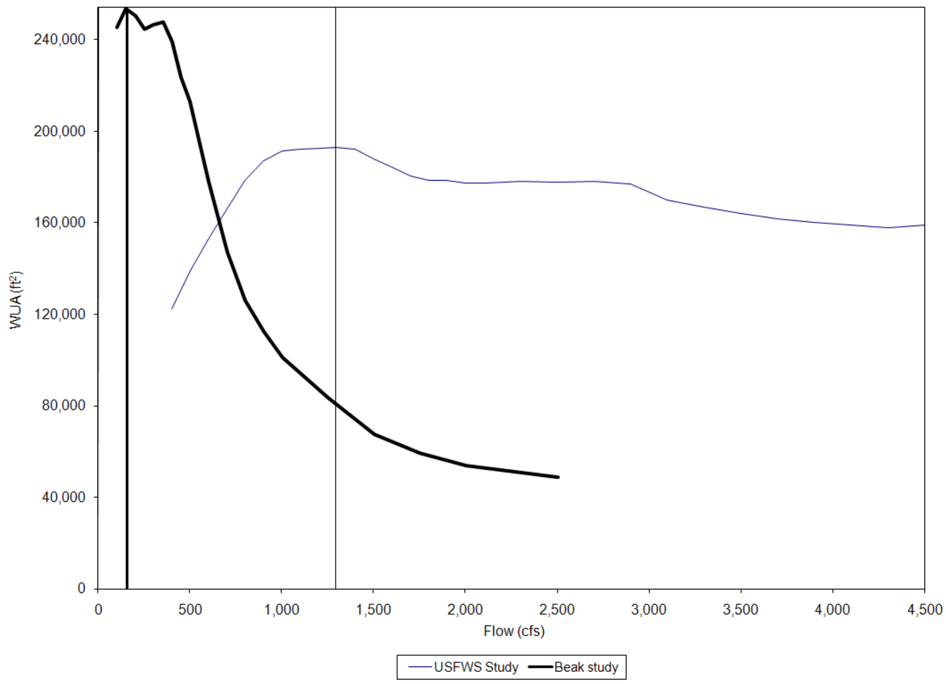

Figure 58. Comparison of Chinook salmon juvenile flow-habitat relationship above Daguerre Point Dam from this study and the Beak (1989) study. This study predicted less habitat at low flows and the peak habitat at a higher flow than the Beak (1989) study.

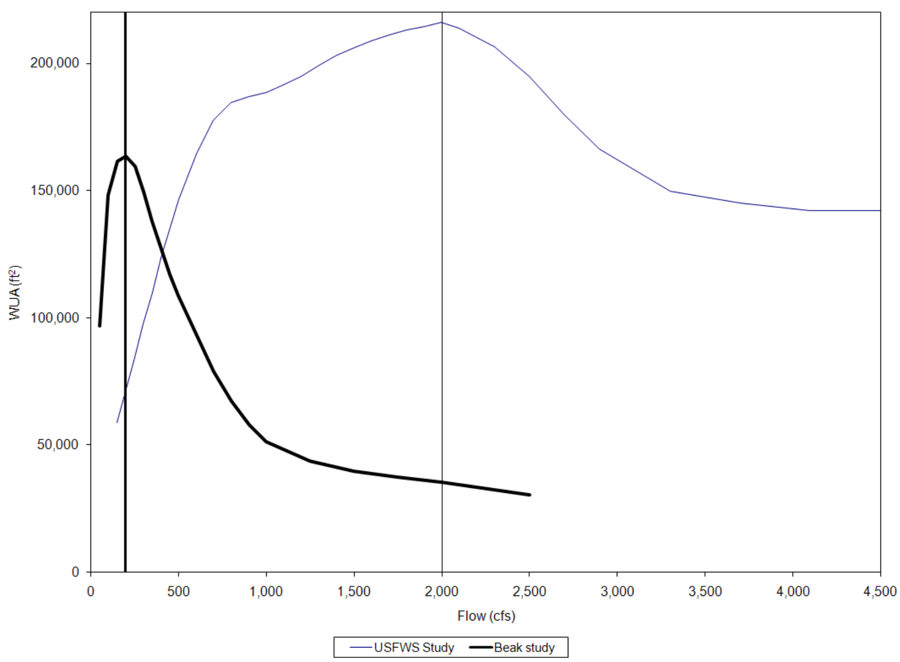

Figure 59. Comparison of Chinook salmon juvenile flow-habitat relationship below Daguerre Point Dam from this study and the Beak (1989) study. This study predicted less habitat at low flows and the peak habitat at a higher flow than the Beak (1989) study.

flows on the Yuba River (Figure 60) have resulted in some channel changes (Pasternack 2007). While we do not have direct evidence that the Yuba River is in dynamic equilibrium, our findings on the American River that the January 1997 flood did not result in a substantial change in chinook salmon or steelhead spawning flow-habitat relationships (US Fish and Wildlife Service 2000) offer support that the results of this study are still applicable to the Yuba River.

The flow-habitat model developed in this study is predictive for flows ranging from 400 to 4,500 cfs above Daguerre Point Dam and from 150 to 4,500 cfs below Daguerre Point Dam. The results of this study are intended to focus on management actions with a temporal scale of one month and do not include an analysis of habitat during peak events (e.g., flows above 4,500 cfs). In the Yuba River, these events are largely associated with flood control releases from Englebright Dam. However, it should be noted that the data collected in this study could be used to simulate rearing habitat up to 11,000 cfs above Daguerre Point Dam and 13,500 cfs below Daguerre Point Dam. If there was sufficient interest in simulating rearing habitat at flows between 4,500 and 11,000 to 13,500 cfs, an additional report could be prepared presenting such results.

The combination of the velocity and adjacent velocity criteria generally limit fry and juvenile habitat to a band along the channel margins. With increasing flows, this band of habitat moves up the banks, resulting in fry and juvenile WUA not changing much with flow (Figures 26 to 33), especially upstream of Daguerre Point Dam. The most significant limitation of fry and juvenile habitat in the Yuba River, particularly upstream of Daguerre Point Dam, is the limited amount of available instream woody cover (Figure 61). The greater increase in Chinook salmon fry and juvenile WUA with flow downstream of Daguerre Point Dam, versus upstream of Daguerre Point Dam, can be attributed to a combination of: 1) the greater abundance of instream woody cover downstream of Daguerre Point Dam; 2) the generally greater inundation of instream woody cover at higher flows; and 3) the high suitability of instream woody cover for fry and juvenile Chinook salmon. In contrast, the lower abundance of instream woody cover upstream of Daguerre Dam and higher suitability of cobble cover for steelhead/rainbow trout fry, versus Chinook salmon fry, results in the flow-habitat relationship for steelhead/rainbow trout fry upstream of Daguerre Point Dam having a maximum value at the lowest simulated flow (Figure 28).

Evaluation of such alternative hydrograph management scenarios should also consider the flow-habitat relationships for Chinook salmon and steelhead/rainbow trout spawning, reported separately (U.S. Fish and Wildlife Service 2010), and water temperature modeling information. Habitat is more likely to be limiting fall-run Chinook salmon populations, versus spring-run Chinook salmon or steelhead/rainbow trout populations, due to the substantially larger population size of fall-run Chinook salmon. Thus, in evaluating flow needs of anadromous fish in the fall, increased flows above Daguerre Dam would likely have beneficial effects on fall-run Chinook salmon spawning, but likely would have no adverse effect on steelhead/rainbow trout fry rearing, since steelhead/rainbow trout fry densities are likely low enough to not be limited by

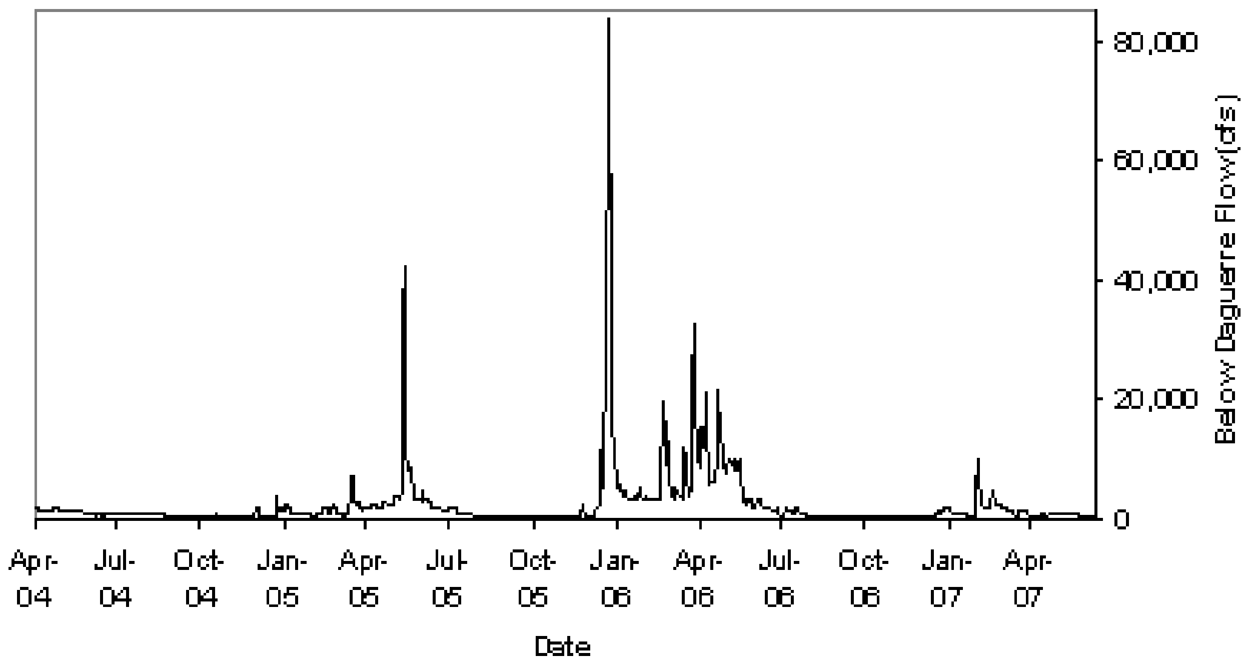

Figure 60. Yuba River flows below Daguerre Point Dam subsequent to the completion of most of the data collection for this study. High flows in May 2005 and January and April 2006 resulted in some channel changes in the Yuba River.

available habitat. In addition, the relatively flat flow-habitat relationships for fry and juvenile rearing makes it likely that the main benefits of altered flow regimes would be for spawning habitat.

9. *Factors Causing Uncertainty*

Factors causing uncertainty in the flow-habitat relationships include: 1) effects of high flows in May 2005 and January and April 2006; 2) extrapolation from the study sites to the entire Yuba River; 3) transmission losses (reduced streamflow due to infiltration into groundwater) in the segment upstream of Daguerre Point Dam in the fall in dry years; 4) errors in velocity simulation; 5) errors in bathymetry data; 6) computational mesh element size and density of bed topography data; 7) errors in velocity measurements used to develop habitat suitability criteria; 8) differences between sampled versus population habitat suitability criteria data; and 9) potential biases in juvenile criteria due to survey techniques. Assuming dynamic equilibrium, we hypothesize that the high flows in May 2005 and January and April 2006 did not significantly alter the flow-habitat relationships. The validity of the assumption of dynamic equilibrium for the Yuba River could be tested by comparing flow-habitat relationships from Professor Greg Pasternack's topography data for the UC Sierra site, which was collected prior to the May 2005 high flows, between the May 2005 and January 2006 high flows and after the January 2006 high flows

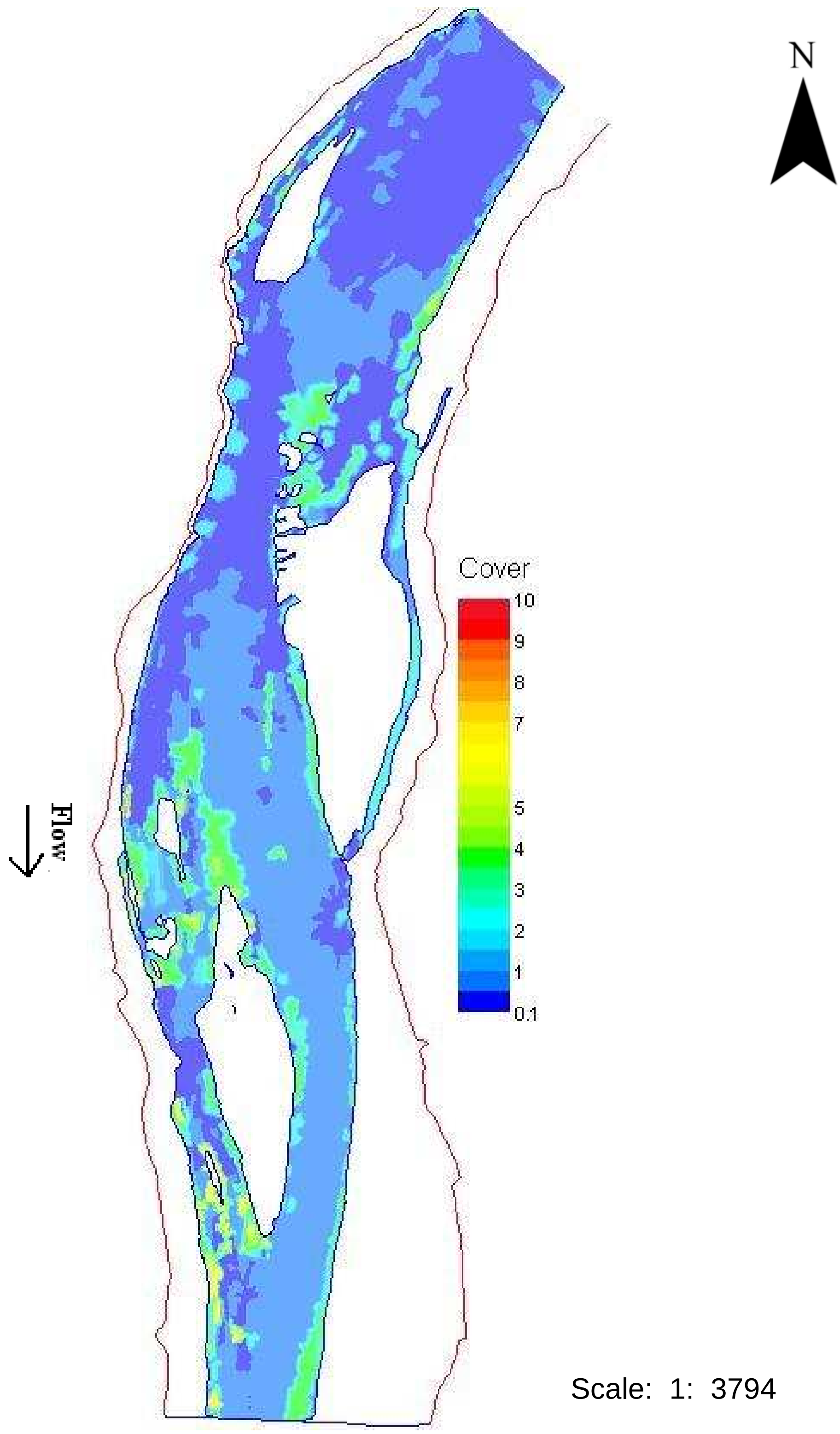

Figure 61. Cover distribution data for wetted portion of Timbuctoo study site at 4,500 cfs.

(Pasternack 2007) – if the flow-habitat relationships from these three datasets had a similar shape, this would support the assumption that the Yuba River is in dynamic equilibrium. Overall, we do not feel that there are any significant limitations of the model.

Based on the number of study sites and the percentage of mesohabitat area found in the study sites, we believe that there is a low level of uncertainty associated with the extrapolation from the study sites to the entire Yuba River. Except for pools in the Below Daguerre segment, at least 11 percent of the area of all mesohabitat types was located within the study sites. Both data from Professor Greg Pasternak and from this study suggest that there may be transmission losses (on the order of 10 percent) in the fall of dry years in the segment upstream of Daguerre Dam. There are two potential consequences to the transmission losses for the segment upstream of Daguerre Point Dam: 1) we may have underestimated the stage at the bottom of the sites for lower flows, which would result in an overestimate of velocities; and 2) additional releases would be needed from Englebright Dam in the fall of dry years to get the flow that would result in the amount of habitat predicted in this report in the segment upstream of Daguerre Point Dam.

There is a greater level of uncertainty for the velocity predictions of the models for the Sucker Glide and Railroad sites than for the remaining sixteen sites, since we were unable to validate the velocity predictions for these sites. We believe that over or under-predicted velocities at all sites would have a minimal effect on the overall flow-habitat relationships, given the high correlation between measured and predicted velocities. Specifically, the effects of over-predicted velocities would be cancelled out by the effect of under-predicted velocities, given the lack of bias in velocity predictions. The overall flow-habitat relationship is driven by the change in the distribution of depths and velocities with flow. The distribution of velocities would not be affected by over or under-predicted velocities because over-predicted velocities would have the opposite effect on the distribution of velocities as under-predicted velocities. Similarly, we believe that errors in bed bathymetry data, which would cause over-prediction or under-prediction of depths, would have a minimal effect on the overall flow-habitat relationships. Specifically, the effects of over-predicted depths would be cancelled out by the effect of under-predicted depths. The overall flow-habitat relationship is driven by the change in the distribution of depths and velocities with flow. The distribution of depths would not be affected by over or under-predicted depths because over-predicted depths would have the opposite effect on the distribution of depths as under-predicted depths.

The effects of discretization size and density of bed topography data on the flow-habitat relationships given in Appendix L are unknown but likely minor. The magnitude of these effects could be investigated by comparing the flow-habitat relationships for the UC Sierra Site in Appendix L with flow-habitat relationships that could be generated by hydraulic modeling of Professor Greg Pasternack's bed topography data (with a point density of 0.64 points/m^2) for the UC Sierra site collected prior to May 2005 (Moir and Pasternack 2008).

Errors in velocity measurements used to develop habitat suitability criteria would likely be a minor source of uncertainty on the flow-habitat relationships given in Appendix L. Since errors in velocity measurement are random and not biased, effects of positive errors in velocity measurements would be cancelled out by the effect of negative errors in velocity measurements. The overall velocity habitat suitability curve is driven by the distribution of velocities. The distribution of velocities would not be affected by positive or negative errors in velocity measurements because positive errors in velocity measurements would have the opposite effect on the distribution of velocities as negative errors in velocity measurements.

The most likely source of uncertainty in the flow-habitat relationships given in Appendix L is the potential for difference between sampled versus population habitat suitability criteria data. Due to the smaller sample size for juvenile HSC data versus fry HSC data, there is likely higher uncertainty in the flow-habitat relationships for juveniles than for fry. The uncertainty from this factor could be quantified by a bootstrap analysis of the sampled HSC data to develop 95 percent confidence limit HSC, which could be applied to the hydraulic models of the eighteen study sites to determine 95 percent confidence limits for the flow-habitat relationships given in Appendix L.

If juveniles were detecting the snorkelers and fleeing before we could observe them to collect HSC data, the HSC data could be biased towards fish that are more in the open, versus fish that are closer to cover. In addition, the lower detection rates that we had for SCUBA, versus snorkeling, could be partially due it being easier for fish to evade SCUBA divers, versus snorkelers. The likely effect of such biases would be to overestimate the habitat value of no cover and underestimate the habitat value of deeper conditions. We are unable to quantify what effect such biases would have on the resulting flow-habitat relationships, other than it would tend to shift the peak of the curve to higher flows.

CONCLUSION

This study achieved the objective of predicting physical habitat in the Yuba River for fall/spring-run Chinook salmon and steelhead/rainbow trout fry and juvenile rearing over a range of stream flows. The results of this study are intended to support or revise the flow recommendations in the Introduction. The results of this study, showing varying relationships between flow and habitat, depending on species, life stage and stream segment, may be consistent with the flow recommendations in the Introduction. The results of this study can be used to evaluate 720 different hydrograph management scenarios (each of the 30 simulation flows for each of the two segments[37] in each of the 12 rearing months). For example, increasing flows from 400 cfs to 1,300 cfs upstream of Daguerre Point Dam in September would result in an increase of 59.4% of habitat during this month for fall/spring-run Chinook salmon juvenile rearing in this segment.

[37] Flows downstream of Daguerre Point Dam can to some extent be modified independent of flows upstream of Daguerre Point Dam by changes in the amount of flow diverted at Daguerre Point Dam.

Based on the conceptual model presented in the introduction, this increase in rearing habitat could increase juvenile survival which could result in an increase in fall/spring-run Chinook salmon populations.

REFERENCES

Annear, T., I. Chirholm, H. Beecher, A. Locke, P. Aarestad, N. Burkhart, C. Coomer, C. Estes, J. Hunt, R. Jacobson, G. Jobsis, J. Kauffman, J. Marshall, K. Mayes, C. Stalnaker and R. Wentworth. 2002. Instream Flows for Riverine Resource Stewardship. Instream Flow Council, Cheyenne, Wyoming.

Baltz, D.M. and P.B. Moyle. 1984. Segregation by species and size classes of rainbow trout, *Salmo gairdneri*, and Sacramento Sucker, *Catostomus occidentalis*, in three California streams. Environmental Biology of Fishes 10: 101-110.

Bartholow, J.M. 1996. Sensitivity of a salmon population model to alternative formulations and initial conditions. Ecological Modeling 88:215-226.

Bartholow, J.M., J.L. Laake, C.B. Stalnaker and S.C. Williamson. A salmonid population model with emphasis on habitat limitations. Rivers 4(4):265-279.

Beak Consultants Inc. 1989. Yuba River fisheries investigations, 1986-1988. Appendix B. The relationship between stream discharge and physical habitat as measured by weighted useable area for fall run Chinook salmon (*Oncorhynchus tshawytscha*) in the lower Yuba River, California. Prepared for State of California Resources Agency, Department of Fish and Game.

Bovee, K.D. 1978. Probability of use criteria for the family salmonidae. Instream Flow Information Paper 4. U.S. Fish and Wildlife Service FWS/OBS-78/07. 80 pp.

Bovee, K.D. 1986. Development and evaluation of habitat suitability criteria for use in the Instream Flow Incremental Methodology. Instream Flow Information Paper 21. U. S. Fish and Wildlife Service Biological Report 86(7). 235 pp.

Bovee, K.D., editor. 1996. The Complete IFIM: A Coursebook for IF 250. U.S. Geological Survey, Fort Collins, CO.

Bratovich, P., J. Perez-Comas, T. Duster, J. Piñero, B. Mitchell and D. Maniscalco. 2003. Draft Evaluation of 2002 Yuba River Water Transfers. January 2003. Prepared for Yuba County Water Agency by Surface Water Resources, Inc. and Jones & Stokes.

California Department of Water Resources. 2005. Phase 2 report addendum evaluation of project effects on instream flows and fish habitat, SP F-16, Oroville Facilities Relicensing FERC Project No. 2100. California Department of Water Resources, Sacramento, CA.

Clackamas Instream Flow/Geomorphology Subgroup (CIFGS). 2003. Estimating salmonid habitat availability in the lower oak grove fork using expert habitat mapping, summary of methods and preliminary results. Report prepared by McBain and Trush Inc., Arcata, California, for Clackamas Instream Flow/Geomorphology Subgroup, March 5, 2003.

Cohen, J. 1992. Quantitative methods in psychology: A power primer. Psychological Bulletin 112(1): 155-159.

Conover, W.J. 1971. Practical Nonparametric Statistics. Wiley, New York. p 493.

Crowder, D.W. and Diplas P. 2000. Using two-dimensional hydrodynamic models at scales of ecological importance. Journal of Hydrology. 230: 172-191.

Earley, J.T. and M. Brown. 2004. Accurately estimating abundance of juvenile spring Chinook salmon in Battle and Clear Creeks. In: Getting Results: Integrating Science and Management to Achieve System-Level Responses. 3rd Biennial CALFED Bay-Delta Program Science Conference Abstracts. October 4-6, 2004. Sacramento, CA.

Fausch, K.D. and R.J. White. 1981. Competition between brook trout (*Salvelinus fontinalis*) and brown trout (*Salmo trutta*) for positions in a Michigan stream. Canadian Journal of Fisheries and Aquatic Sciences 38: 1220-1227.

Gard, M. 2006. Changes in salmon spawning and rearing habitat associated with river channel restoration. International Journal of River Basin Management 4: 201-211.

Gard, M. and E. Ballard. 2003. Applications of new technologies to instream flow studies in large rivers. North American Journal of Fisheries Management 23: 1114-1125.

Gard, M. 2006. Changes in salmon spawning and rearing habitat associated with river channel restoration. International Journal of River Basin Management 4: 201-211.

Gard, M. 2009. Comparison of spawning habitat predictions of PHABSIM and River2D models. International Journal of River Basin Management 7:55-71.

Geist, D.R., J. Jones, C.J. Murray and D.D. Dauble. 2000. Suitability criteria analyzed at the spatial scale of redd clusters improved estimates of fall Chinook salmon (*Oncorhynchus tshawytscha*) spawning habitat use in the Hanford Reach, Columbia River. Canadian Journal of Fisheries and Aquatic Sciences 57: 1636-1646.

Ghanem, A., P. Steffler, F. Hicks and C. Katopodis. 1995. Two-dimensional modeling of flow in aquatic habitats. Water Resources Engineering Report 95-S1, Department of Civil Engineering, University of Alberta, Edmonton, Alberta. March 1995.

Ghanem, A., P. Steffler, F. Hicks and C. Katopodis. 1996. Two-dimensional hydraulic simulation of physical habitat conditions in flowing streams. Regulated Rivers: Research and Management. 12: 185-200.

Gido, K.B. and D.L. Propst. 1999. Habitat use and association of native and nonnative fishes in the San Juan River, New Mexico and Utah. Copeia 1999: 321-332.

Guay, J.C., D. Boisclair, D. Rioux, M. Leclerc, M. Lapointe and P. Legendre. 2000. Development and validation of numerical habitat models for juveniles of Atlantic salmon (*Salmo salar*). Canadian Journal of Fisheries and Aquatic Sciences 57: 2065-2075.

Hampton, M. 1997. Microhabitat suitability criteria for anadromous salmonids of the Trinity River. U.S. Fish & Wildlife Service, Arcata, CA.

Hardy, T.B. and R.C. Addley. 2001. Evaluation of interim instream flow needs in the Klamath River, phase II, final report. Prepared for U.S. Department of the Interior. Institute for Natural Systems Engineering, Utah Water Research Laboratory, Utah State University, Logan, Utah.

HDR/SWRI. 2007. Final Environmental Impact Report/Environmental Impact Statement for the Proposed Lower Yuba River Accord. Prepared for the California Department of Water Resources, Yuba County Water Agency and the U.S. Bureau of Reclamation. October 2007. HDR/SWRI: Sacramento, CA.

Hosmer, D.W. and S. Lemeshow. 2000. Applied Logistic Regression, Second Edition. John Wiley and Sons, Inc, New York.

Hvidsten, H.B. 1993. High winter discharge after regulation increases production of Atlantic salmon, *Salmo salar,* smolts in the River Orkla, Norway. Pages 175-177 in: R.J. Gibson and R.E. Cutting, editors. Production of Juvenile Atlantic Salmon, *Salmo salar*, in Natural Waters. Special Publication of the Canadian Journal of Fisheries and Aquatic Sciences 118.

Knapp, R.A. and H.K. Preisler. 1999. Is it possible to predict habitat use by spawning salmonids? A test using California golden trout (*Oncorhynchus mykiss aguabonita*). Canadian Journal of Fisheries and Aquatic Sciences 56: 1576-1584.

Leclerc, M., A. Boudreault, J.A. Bechara and G. Corfa. 1995. Two-dimensional hydrodynamic modeling: a neglected tool in the instream flow incremental methodology. Transactions of the American Fisheries Society. 124(5): 645-662.

Massa, D.A. 2004. Yuba River juvenile Chinook salmon, *Oncorhynchus tshawytsha*, and juvenile Central Valley steelhead trout, *Oncorhynchus mykiss*, life history survey, annual data report 2003-2004. California Department of Fish and Game, Rancho Cordova, CA.

McHugh, P. and P. Budy. 2004. Patterns of spawning habitat selection and suitability for two populations of spring chinook salmon, with an evaluation of generic verses site-specific suitability criteria. Transactions of the American Fisheries Society 133: 89-97.

McReynolds, T., P. Ward and C. Harvey-Arrison. 2004. Utility of juvenile salmon growth models for discrimination of Central Valley spring-run Chinook in California. In: Getting Results: Integrating Science and Management to Achieve System-Level Responses. 3rd Biennial CALFED Bay-Delta Program Science Conference Abstracts. October 4-6, 2004. Sacramento, CA.

Milhous, R.T., M.A. Updike and D.M. Schneider. 1989. Physical habitat simulation system reference manual - version II. Instream Flow Information Paper No. 26. U. S. Fish and Wildlife Service Biological Report 89(16).

Moir, H.J. and G.B. Pasternack. 2008. Relationships between mesoscale morphological units, stream hydraulics and Chinook salmon (*Oncorhynchus tshawytscha*) spawning habitat on the Lower Yuba River, California. Geomorphology in press.

Moyle, P.B. and B. Vondracek. 1985. Persistence and structure of the fish assemblage in a small California stream. Ecology 66: 1-13.

Parasiewicz, P. 1999. A hybrid model – assessment of physical habitat conditions combining various modeling tools. In: Proceedings of the Third International Symposium on Ecohydraulics, Salt Lake City, Utah.

Pasternack, G.B. 2007. The importance of flow-convergence routing for maintaining riffles and pools on large, regulated, gravel-bed rivers. Geological Society of America, Abstracts with Programs 39:6:34.

Pasternack G.B., C.L. Wang and J.E. Merz. 2004. Application of a 2D hydrodynamic model to design of reach-scale spawning gravel replenishment on the Mokelumne River, California. River Research and Applications. 20(2): 202-225.

Payne and Associates. 1998. RHABSIM 2.0 for DOS and Window's User's Manual. Arcata, CA: Thomas R. Payne and Associates.

Raleigh, R.F., W.J. Miller and P.C. Nelson. 1986. Habitat suitability index models and instream flow suitability curves: Chinook salmon. United States Fish and Wildlife Service, Biological Report 82(10.122). 64pp.

Rubin, S.P., T.C. Bjornn and B. Dennis. 1991. Habitat suitability curves for juvenile chinook salmon and steelhead development using a habitat-oriented sampling approach. Rivers 2(1):12-29.

Sechnick, C.W., R.F. Carline, R.A. Stein and E.T. Rankin. 1986. Habitat selection by smallmouth bass in response to physical characteristics of a simulated stream. Transactions of the American Fisheries Society 115: 314-321.

Snider, W.M., D.B. Christophel, B.L. Jackson and P.M. Bratovich. 1992. Habitat characterization of the Lower American River. California Department of Fish and Game, Sacramento, CA.

Steffler, P. 2002. River2D_Bed. Bed Topography File Editor. User's manual. University of Alberta, Edmonton, Alberta. 32 pp. http://www.River2D.ualberta.ca/download.htm

Steffler, P. and J. Blackburn. 2002. River2D: Two-dimensional Depth Averaged Model of River Hydrodynamics and Fish Habitat. Introduction to Depth Averaged Modeling and User's Manual. University of Alberta, Edmonton, Alberta. 120 pp. http://www.River2D.ualberta.ca/download.htm

SYSTAT. 2002. SYSTAT 10.2 Statistical Software. SYSTAT Software Inc., Richmond, CA.

Thielke, J. 1985. A logistic regression approach for developing suitability-of-use functions for fish habitat. Pages 32-38 in F.W. Olson, R.G. White, and R.H. Hamre, editors. Proceedings of the symposium on small hydropower and fisheries. American Fisheries Society, Western Division and Bioengineering Section, Bethesda, Maryland.

Thomas, J.A. and K.D. Bovee. 1993. Application and testing of a procedure to evaluate transferability of habitat suitability criteria. Regulated Rivers: Research & Management 8: 285-294.

Tiffan, K.E., R.D. Garland and D.W. Rondorf. 2002. Quantifying flow-dependent changes in subyearling fall Chinook salmon rearing habitat using two-dimensional spatially explicit modeling. North American Journal of Fisheries Management 22: 713-726.

U.S. Fish and Wildlife Service. 1994. Using the computer based physical habitat simulation system (PHABSIM). Fort Collins, CO: U.S. Fish and Wildlife Service.

U. S. Fish and Wildlife Service. 1995. Working paper on restoration needs: habitat restoration actions to double natural production of anadromous fish in the Central Valley of California. Volume 1. May 9, 1995. Prepared for the U. S. Fish and Wildlife Service under the direction of the Anadromous Fish Restoration Program Core Group. U.S. Fish and Wildlife Service, Stockton, CA.

U. S. Fish and Wildlife Service. 1997. Identification of the instream flow requirements for fall-run Chinook salmon spawning in the Merced River. U.S. Fish and Wildlife Service, Sacramento, CA.

U.S. Fish and Wildlife Service. 2000. Effects of the January 1997 flood on flow-habitat relationships for steelhead and fall-run Chinook salmon in the Lower American River. U.S. Fish and Wildlife Service, Sacramento, CA.

U. S. Fish and Wildlife Service. 2005. Flow-habitat relationships for Chinook salmon rearing in the Sacramento River between Keswick Dam and Battle Creek. U.S. Fish and Wildlife Service, Sacramento, CA.

U. S. Fish and Wildlife Service. 2007. Identification of the instream flow requirements for anadromous fish in the streams within the central valley of California. Annual progress report fiscal year 2007. U.S. Fish and Wildlife Service, Sacramento, CA.

U. S. Fish and Wildlife Service. 2010. Flow-habitat relationships for spring and fall-run Chinook salmon and steelhead/rainbow trout spawning in the Yuba River. U.S. Fish and Wildlife Service, Sacramento, CA.

Waddle, T. and P. Steffler. 2002. R2D_Mesh - Mesh Generation Program for River2D Two Dimensional Depth Averaged Finite Element. Introduction to Mesh Generation and User's manual. U.S. Geological Survey, Fort Collins, CO. 32 pp. http://www.River2D.ualberta.ca/download.htm

Williamson, S.C., J.M. Bartholow and C.B. Stalnaker. 1993. Conceptual model for quantifying pre-smolt production from flow-dependent physical habitat and water temperature. Regulated Rivers: Research and Management 8:15-28.

Yalin, M.S. 1977. Mechanics of Sediment Transport. Pergamon Press, New York.

Zar, J.H. 1984. Biostatistical Analysis, Second Edition. Prentice-Hall, Inc., Englewood Cliffs, NJ.

APPENDIX A
HABITAT MAPPING DATA

Habitat distribution identified in the Yuba River study reach confluence with Feather River (RM 0) to Englebright Dam (RM 24.1)

Mesohabitat Unit #	Mesohabitat Type	Mesohabitat Unit Area (m^2)	River mile
1	Flatwater Pool	81,387	0 - 0.6
2	Flatwater Glide	15,377	0.6 – 0.7
3	Flatwater Pool	17,042	0.7 – 0.8
4	Bar Complex Glide	12,045	0.8 – 0.9
5	Bar Complex Riffle	5,668	0.9 – 1.0
6	Bar Complex Pool	24,406	1.0 – 1.2
7	Bar Complex Glide	3,006	1.2
8	Bar Complex Pool	4,826	1.2 – 1.3
9	Bar Complex Run	3,045	1.3
10	Bar Complex Glide	8,216	1.3 – 1.4
11	Flatwater Pool	5,452	1.4
12	Flatwater Run	6,247	1.4 – 1.5
13	Bar Complex Riffle	1,567	1.5
14	Bar Complex Pool	14,953	1.5 – 1.7
15	Flatwater Pool	4,630	1.7 – 1.8
16	Bar Complex Glide	9,922	1.8 – 1.9
17	Flatwater Pool	28,276	1.9 – 2.2
18	Flatwater Glide	12,975	2.2 – 2.4
19	Flatwater Pool	37,124	2.4 – 2.8
20	Bar Complex Pool	8,123	2.8 – 2.9
21	Bar Complex Run	15,840	2.9 – 3.2
22	Flatwater Glide	21,473	2.3 – 3.4
23	Bar Complex Glide	39,403	3.4 – 3.9
24	Bar Complex Run	27,556	3.9 – 4.2
25	Bar Complex Riffle	5,870	4.2 – 4.3
26	Bar Complex Run	7,339	4.3 – 4.4
27	Side Channel Glide	629	4.3
28	Side Channel Run	656	4.3
29	Side Channel Pool	762	4.3
30	Side Channel Run	1,377	4.3 – 4.4
31	Side Channel Pool	602	4.4
32	Side Channel Run	757	4.4
33	Bar Complex Glide	12,798	4.4 – 4.5
34	Bar Complex Pool	4,485	4.5
35	Bar Complex Run	16,673	4.5 – 4.8
36	Bar Complex Riffle	5,268	4.8 – 4.9
37	Bar Complex Run	20,091	4.4 – 4.8
38	Bar Complex Pool	1,887	4.5

Mesohabitat Unit #	Mesohabitat Type	Mesohabitat Unit Area (m^2)	River mile
39	Bar Complex Riffle	2,419	4.8
40	Bar Complex Pool	12,442	4.9 – 5.0
41	Side Channel Run	6,224	5.0 – 5.1
42	Bar Complex Glide	3,760	5.0
43	Side Channel Glide	1,470	5.1
44	Side Channel Run	2,287	5.1 – 5.2
45	Side Channel Riffle	1,505	5.2
46	Bar Complex Pool	2,229	5.0
47	Bar Complex Run	11,627	5.0 – 5.2
48	Bar Complex Run	8,367	5.0 – 5.1
49	Bar Complex Glide	58,233	5.1 – 5.6
50	Bar Complex Run	15,880	5.6 – 5.7
51	Bar Complex Glide	39,195	5.7 – 6.1
52	Bar Complex Pool	6,767	6.1 – 6.2
53	Bar Complex Run	24,596	6.2 – 6.4
54	Bar Complex Glide	5,172	6.4
55	Bar Complex Pool	5,797	6.4 – 6.5
56	Bar Complex Run	16,627	6.5 – 6.7
57	Bar Complex Glide	9,269	6.7 – 6.8
58	Bar Complex Run	13,917	6.8 – 7.0
59	Bar Complex Riffle	15,888	7.0
60	Bar Complex Glide	21,700	7.0 – 7.3
61	Bar Complex Pool	3,606	7.3
62	Bar Complex Run	9,583	7.3 – 7.5
63	Bar Complex Riffle	7,351	7.4 – 7.5
64	Bar Complex Glide	17,185	7.5 – 7.6
65	Bar Complex Pool	12,449	7.6 – 7.8
66	Bar Complex Riffle	8,967	7.7 – 7.9
67	Bar Complex Run	2,810	7.8 – 7.9
68	Bar Complex Glide	34,402	7.8 – 8.1
69	Bar Complex Run	7,176	8.1 – 8.3
70	Bar Complex Riffle	9,408	8.2 – 8.3
71	Bar Complex Run	17,022	8.3 – 8.4
72	Bar Complex Riffle	5,172	8.4 – 8.5
73	Bar Complex Run	9,365	8.5 – 8.7
74	Bar Complex Glide	22,516	8.5 – 8.8
75	Bar Complex Run	7,393	8.8 – 8.9
76	Bar Complex Riffle	2,082	8.9
77	Flatwater Glide	23,586	8.9 – 9.1
78	Bar Complex Run	39,515	9.1 – 9.6
79	Bar Complex Glide	23,351	9.6 – 9.7

Mesohabitat Unit #	Mesohabitat Type	Mesohabitat Unit Area (m^2)	River mile
80	Bar Complex Run	18,815	9.7 – 9.9
81	Bar Complex Riffle	13,877	9.8 – 10.0
82	Bar Complex Glide	41,556	9.9 – 10.4
83	Bar Complex Run	47,567	10.4 – 10.9
84	Bar Complex Riffle	8,419	10.8 – 10.9
85	Bar Complex Run	22,512	10.9 – 11.2
86	Bar Complex Riffle	2,649	11.1 – 11.2
87	Bar Complex Run	5,552	11.2
88	Bar Complex Pool	8,067	11.2 – 11.3
89	Bar Complex Run	10,393	11.3 – 11.4
90	Bar Complex Pool	10,417	11.4
Daguerre Point Dam (RM 11.4)			
91	Bar Complex Run	24,440	11.4 – 11.6
92	Flatwater Glide	18,639	11.6 – 11.7
93	Bar Complex Run	20,203	11.7 – 11.9
94	Bar Complex Riffle	13,865	11.8 – 12.0
95	Side Channel Pool	15,861	11.4 – 11.7
96	Side Channel Run	257	11.7
97	Side Channel Pool	33	11.7
98	Side Channel Run	79	11.7
99	Side Channel Riffle	110	11.7
100	Side Channel Pool	4,483	11.7 – 11.9
101	Side Channel Run	460	11.9
102	Side Channel Pool	468	11.9 – 12.0
103	Side Channel Glide	101	12.0
104	Side Channel Run	143	12.0
105	Bar Complex Glide	7,326	11.9 – 12.0
106	Bar Complex Run	38,642	12.0 – 12.4
108	Bar Complex Run	9,426	12.2 – 12.3
109	Bar Complex Glide	3,132	12.1 – 12.2
110	Bar Complex Riffle	3,412	12.1
111	Bar Complex Glide	22,825	12.3 – 12.6
112	Bar Complex Run	206,390	12.6 – 14.5
113	Bar Complex Riffle	6,837	13.6 – 13.7
114	Bar Complex Riffle	3,379	14.3
115	Bar Complex Riffle	9,548	14.5 – 14.6
116	Bar Complex Glide	17,035	14.6 – 14.7
117	Bar Complex Run	72,461	14.7 – 15.5
118	Side Channel Run	17,990	15.4 – 15.8
119	Bar Complex Glide	21,037	15.5 – 15.8
120	Bar Complex Run	18,275	15.8 – 16.0

Mesohabitat Unit #	Mesohabitat Type	Mesohabitat Unit Area (m^2)	River mile
107	Side Channel Glide	5,035	15.9 – 16.1
121	Side Channel Run	2,977	15.9
122	Side Channel Pool	651	15.8 – 15.9
123	Side Channel Riffle	920	15.7
124	Bar Complex Riffle	4,650	16.0 – 1.61
125	Bar Complex Glide	19,566	16.1 – 16.2
126	Bar Complex Pool	12,619	16.2 – 16.3
127	Bar Complex Run	17,792	16.3 – 16.6
128	Side Channel Run	6,742	16.3 – 16.5
129	Side Channel Riffle	2,883	16.5 – 16.6
130	Bar Complex Glide	12,688	16.6 – 16.7
131	Bar Complex Pool	14,172	16.7 – 16.8
132	Bar Complex Glide	6,834	16.8 – 16.9
133	Side Channel Run	759	16.8 – 16.9
134	Side Channel Pool	768	16.9
135	Bar Complex Run	89,953	16.9 – 18.2
136	Bar Complex Pool	1,389	17.2 – 17.3
137	Side Channel Run	491	17.3
138	Bar Complex Riffle	1,942	17.3
139	Bar Complex Riffle	3,393	18.0 – 18.1
140	Bar Complex Pool	2,380	18.2
141	Side Channel Run	3,347	18.1
142	Side Channel Riffle	2,098	18.2
143	Bar Complex Glide	8,384	18.2 – 18.3
144	Bar Complex Pool	6,280	18.3 – 18.4
145	Side Channel Pool	2,642	18.4
146	Side Channel Run	994	18.4 – 18.5
147	Side Channel Pool	1,045	18.5
148	Side Channel Run	1,013	18.5
149	Side Channel Riffle	2,108	18.5
150	Bar Complex Run	23,517	18.4 – 18.4
151	Bar Complex Riffle	3,136	18.7
152	Bar Complex Run	24,113	18.7 – 19.0
153	Bar Complex Riffle	3,240	18.9 – 19.0
154	Side Channel Pool	1,580	18.9 – 19.0
155	Side Channel Run	886	18.9
156	Side Channel Riffle	870	18.9
157	Side Channel Riffle	526	19.0
158	Side Channel Run	2,180	18.9 – 19.0
159	Side Channel Riffle	515	18.9
160	Side Channel Run	329	18.8

Mesohabitat Unit #	Mesohabitat Type	Mesohabitat Unit Area (m^2)	River mile
161	Side Channel Pool	504	18.8
162	Side Channel Run	3,706	18.7 – 18.8
163	Side Channel Glide	386	18.7
164	Bar Complex Riffle	1,567	19.0
165	Bar Complex Glide	6,726	19.0
166	Bar Complex Pool	15,645	19.0 – 19.2
167	Bar Complex Riffle	6,713	19.1 – 19.2
168	Bar Complex Glide	38,122	19.2 – 19.5
169	Side Channel Pool	375	19.3
170	Side Channel Run	1,046	19.3
171	Side Channel Pool	1,021	19.2
172	Bar Complex Pool	17,117	19.4 – 19.6
173	Bar Complex Run	9,501	19.6 – 19.7
174	Bar Complex Pool	3,797	19.7 – 19.8
175	Bar Complex Run	22,427	19.7 – 20.1
176	Side Channel Riffle	79	20.0
177	Bar Complex Riffle	2,200	20.1
178	Bar Complex Glide	29,780	20.1 – 20.3
179	Side Channel Pool	2,110	20.0 – 20.1
180	Side Channel Run	2,045	20.1 – 20.2
181	Side Channel Riffle	670	20.1
182	Side Channel Riffle	158	20.2
183	Bar Complex Pool	24,010	20.3 – 20.6
184	Bar Complex Run	2,766	20.6
185	Bar Complex Pool	5,907	20.6 – 20.7
186	Bar Complex Run	5,386	20.7 – 20.8
187	Bar Complex Pool	5,896	20.8 – 20.9
188	Bar Complex Run	20,419	20.9 – 21.2
189	Bar Complex Riffle	1,234	21.1 – 21.2
190	Side Channel Pool	602	21.1 – 21.2
191	Side Channel Riffle	72	21.2
192	Bar Complex Pool	4,575	21.2 – 21.3
193	Bar Complex Run	4,025	21.3
194	Bar Complex Riffle	2,640	21.3 – 21.4
195	Bar Complex Run	7,928	21.4
196	Bar Complex Pool	11,200	21.4 – 21.6
197	Bar Complex Riffle	1,165	21.5 – 21.6
198	Bar Complex Run	14,130	21.5 – 21.7
199	Bar Complex Pool	6,691	21.7 – 21.8
200	Bar Complex Riffle	4,547	21.8
201	Bar Complex Pool	27,881	21.8 – 22.1

Mesohabitat Unit #	Mesohabitat Type	Mesohabitat Unit Area (m^2)	River mile
202	Flatwater Pool	35,283	22.1 – 22.4
203	Flatwater Run	10,313	22.4 – 22.6
204	Cascade	1,129	22.6 – 22.7
205	Flatwater Run	10,425	22.7 – 23.0
206	Side Channel Run	1,341	22.9
207	Side Channel Pool	2,209	22.9 – 23.0
208	Flatwater Pool	4,918	23.0
209	Flatwater Riffle	365	23.0
210	Flatwater Pool	3,062	23.0 – 23.1
211	Flatwater Pool	354	23.1
212	Flatwater Run	4,459	23.1 – 23.2
213	Flatwater Riffle	1,251	23.2
214	Flatwater Pool	5,195	23.2
215	Flatwater Run	4,774	23.3
216	Flatwater Pool	14,924	23.3 – 23.5
217	Flatwater Run	8,283	23.5 – 23.7
218	Flatwater Pool	9,958	23.7 – 23.8
219	Flatwater Run	10,738	23.8 – 24.0
220	Flatwater Pool	5,050	24.0 – 24.1

Shapefiles for the above mesohabitat units are available in electronic format upon request from:

Mark Gard, Senior Biologist
Energy Planning and Instream Flow Branch
U.S. Fish and Wildlife Service
Sacramento Fish and Wildlife Office
2800 Cottage Way, Room W-2605
Sacramento, CA 95825

Mark_Gard@fws.gov

APPENDIX B
STUDY SITE AND TRANSECT LOCATIONS

NARROWS STUDY SITE

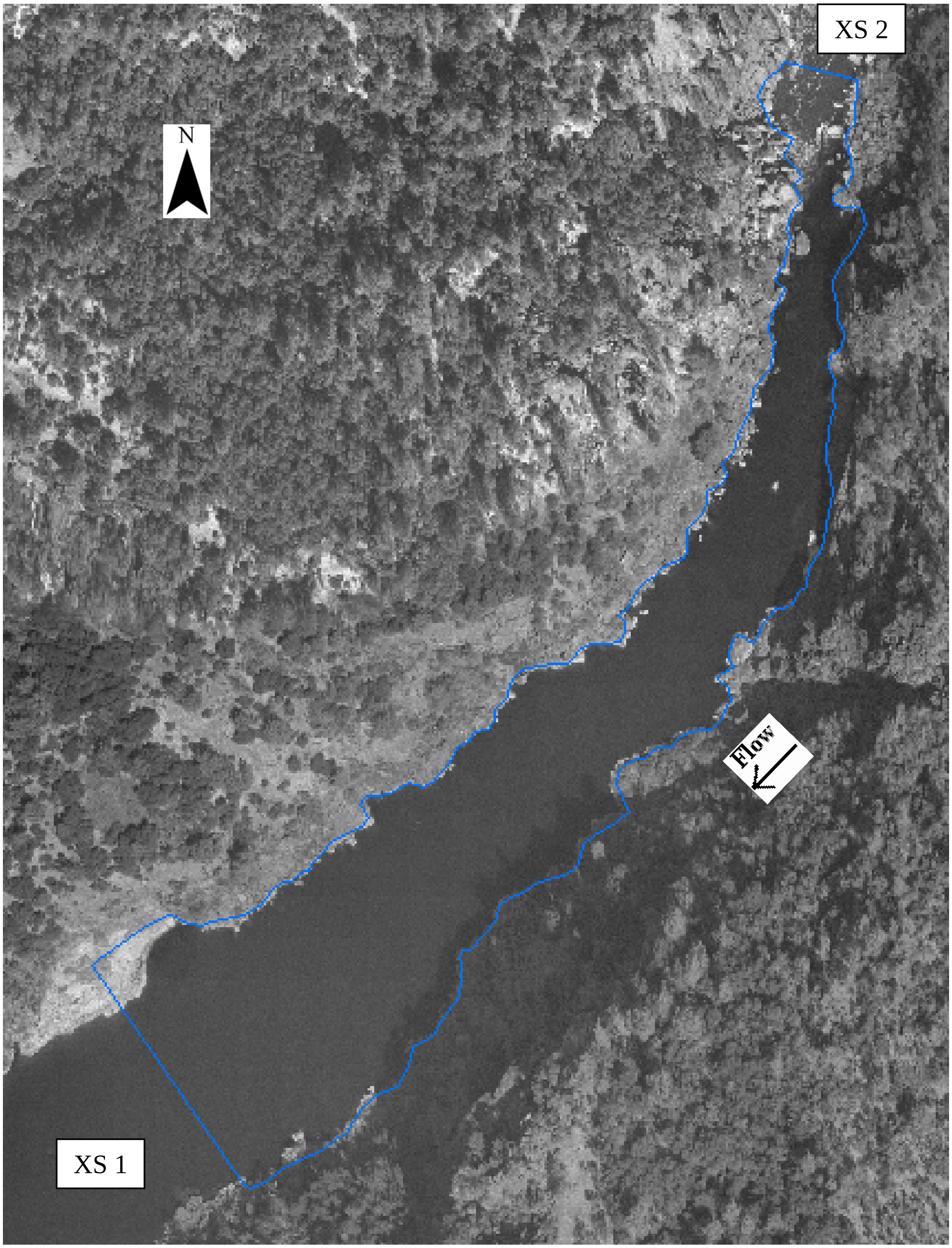

Scale: 1:2791

ROSEBAR STUDY SITE

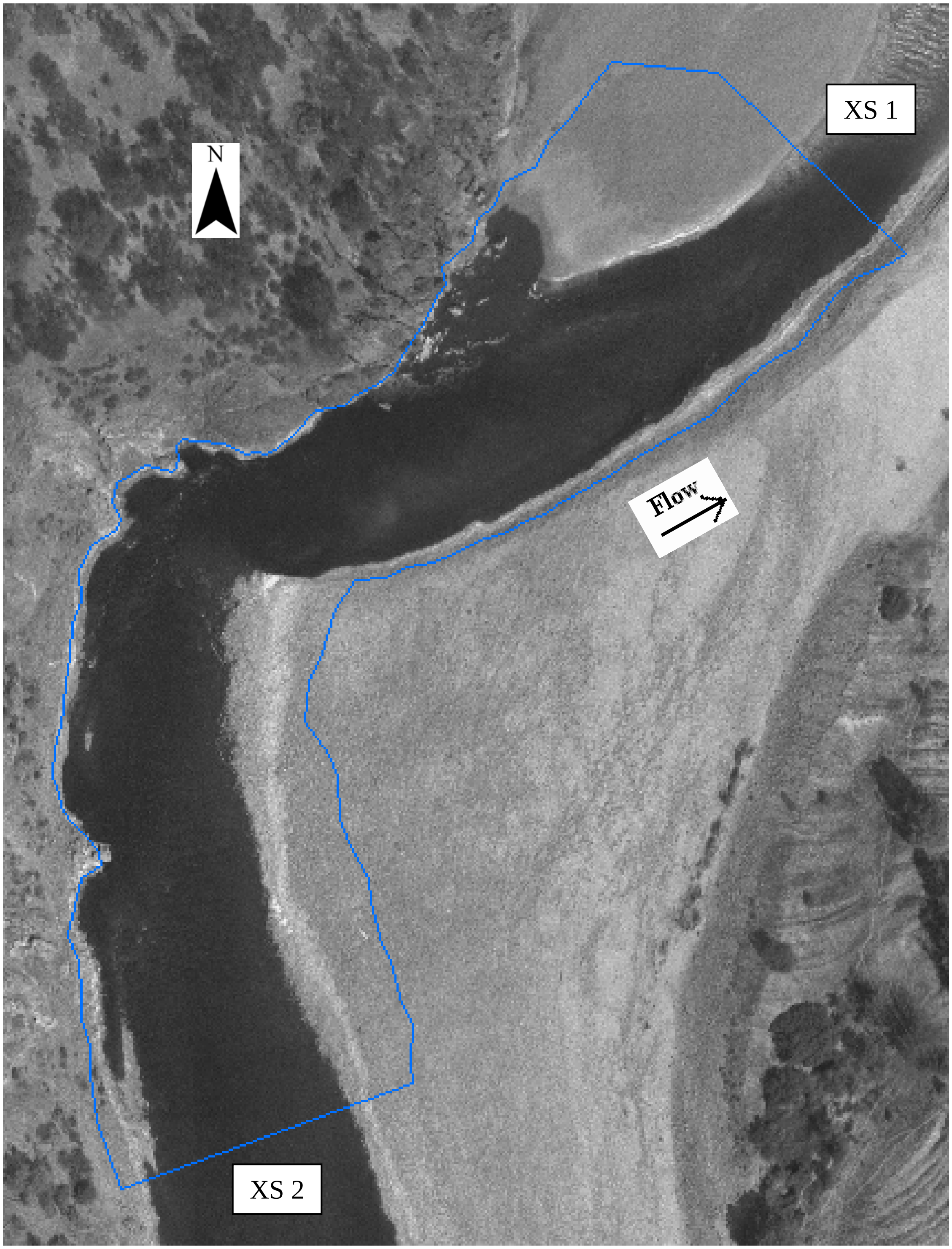

Scale: 1:1772

DIVERSION STUDY SITE

Scale: 1:1078

LOWER HALLWOOD STUDY SITE

Scale: 1:2003

WHIRLPOOL STUDY SITE

Scale: 1: 977

USFWS, SFWO, Energy Planning and Instream Flow Branch
Yuba River Rearing Report
October 8, 2010

SIDE-CHANNEL STUDY SITE

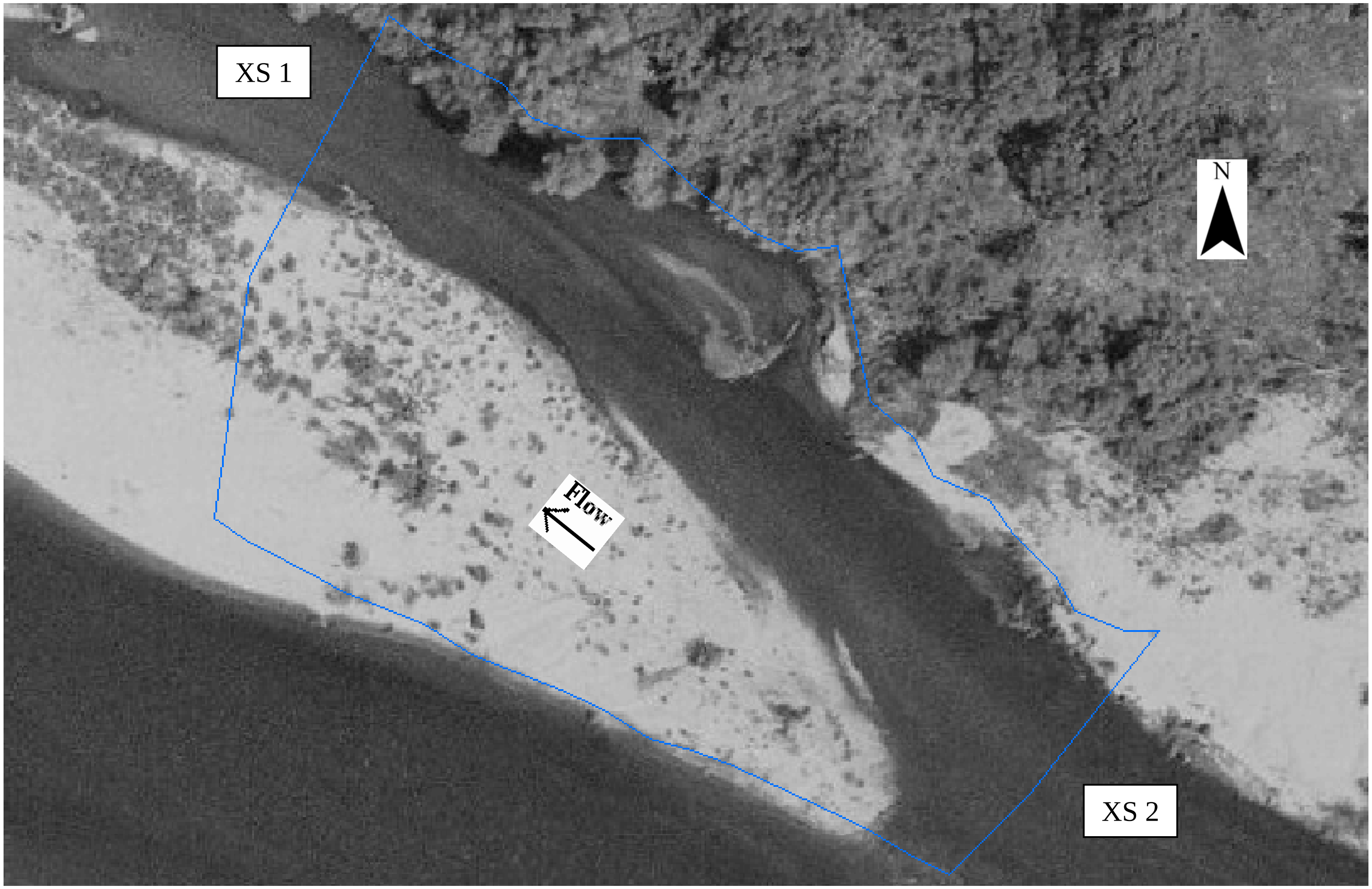

Scale: 1:782

SUCKER GLIDE STUDY SITE

Scale: 1:1129

RAILROAD STUDY SITE

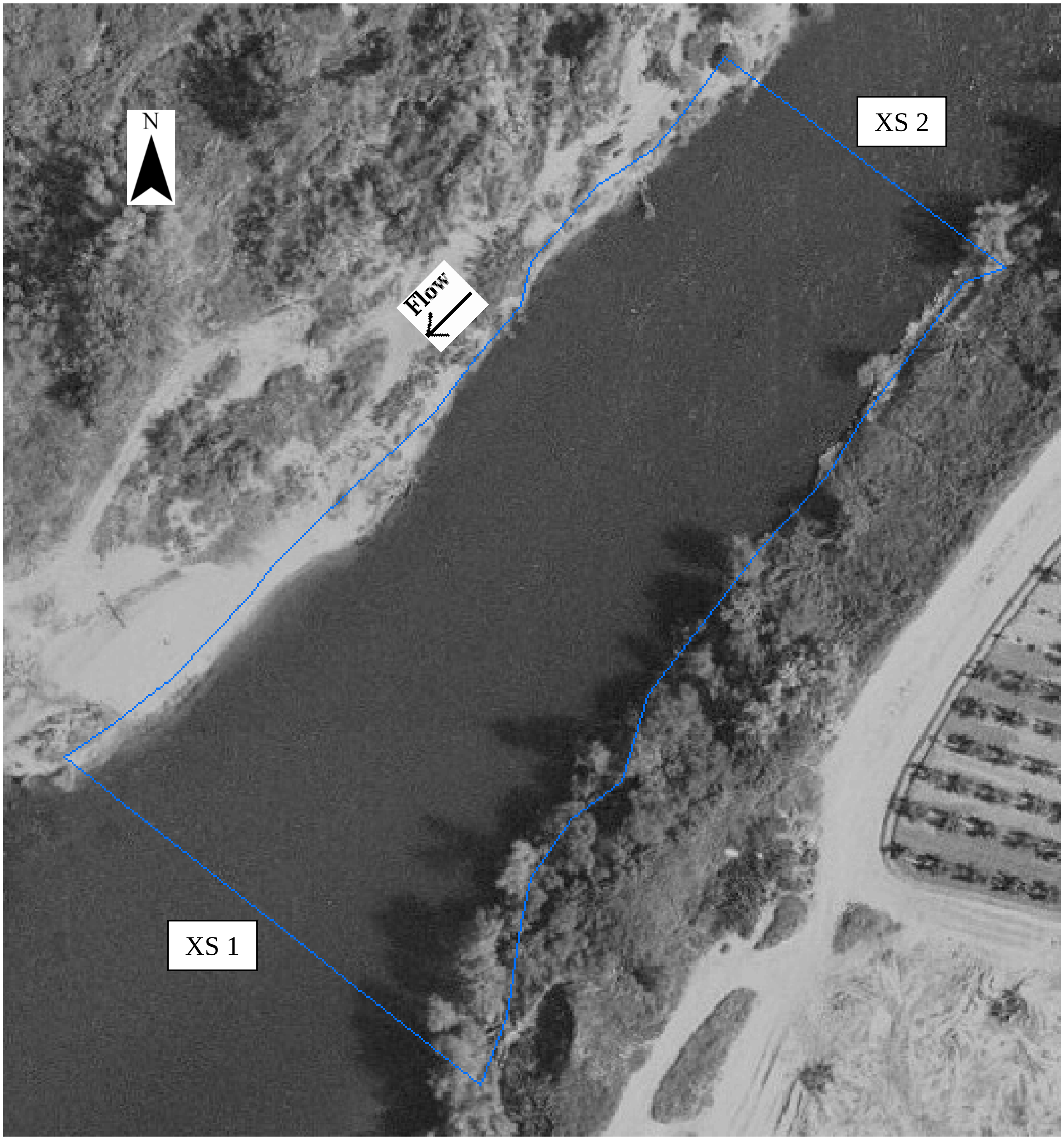

Scale: 1:927

APPENDIX C
BED TOPOGRAPHY POINT LOCATIONS

NARROWS STUDY SITE

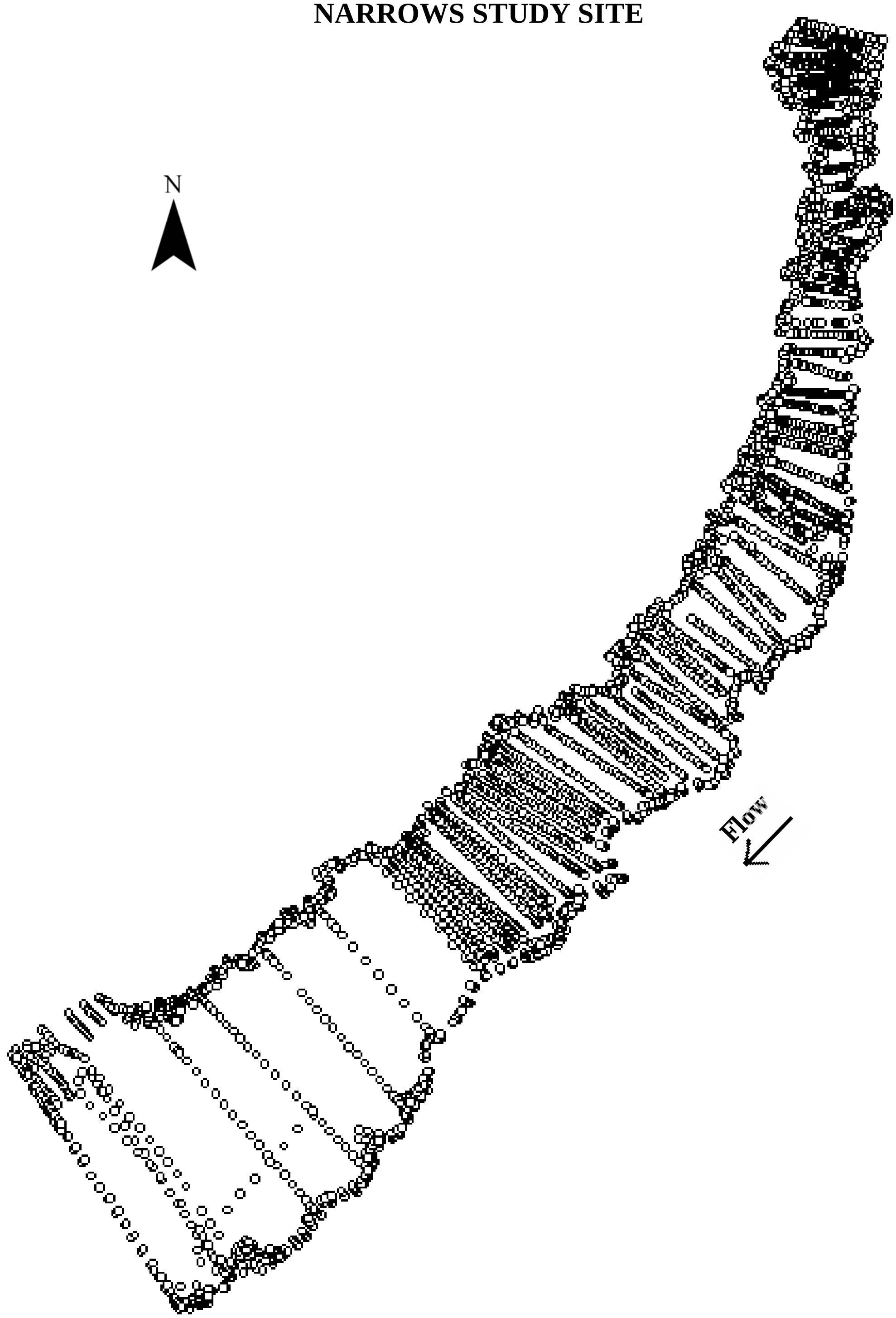

Scale: 1:2791

ROSEBAR STUDY SITE

Scale: 1:1646

DIVERSION STUDY SITE

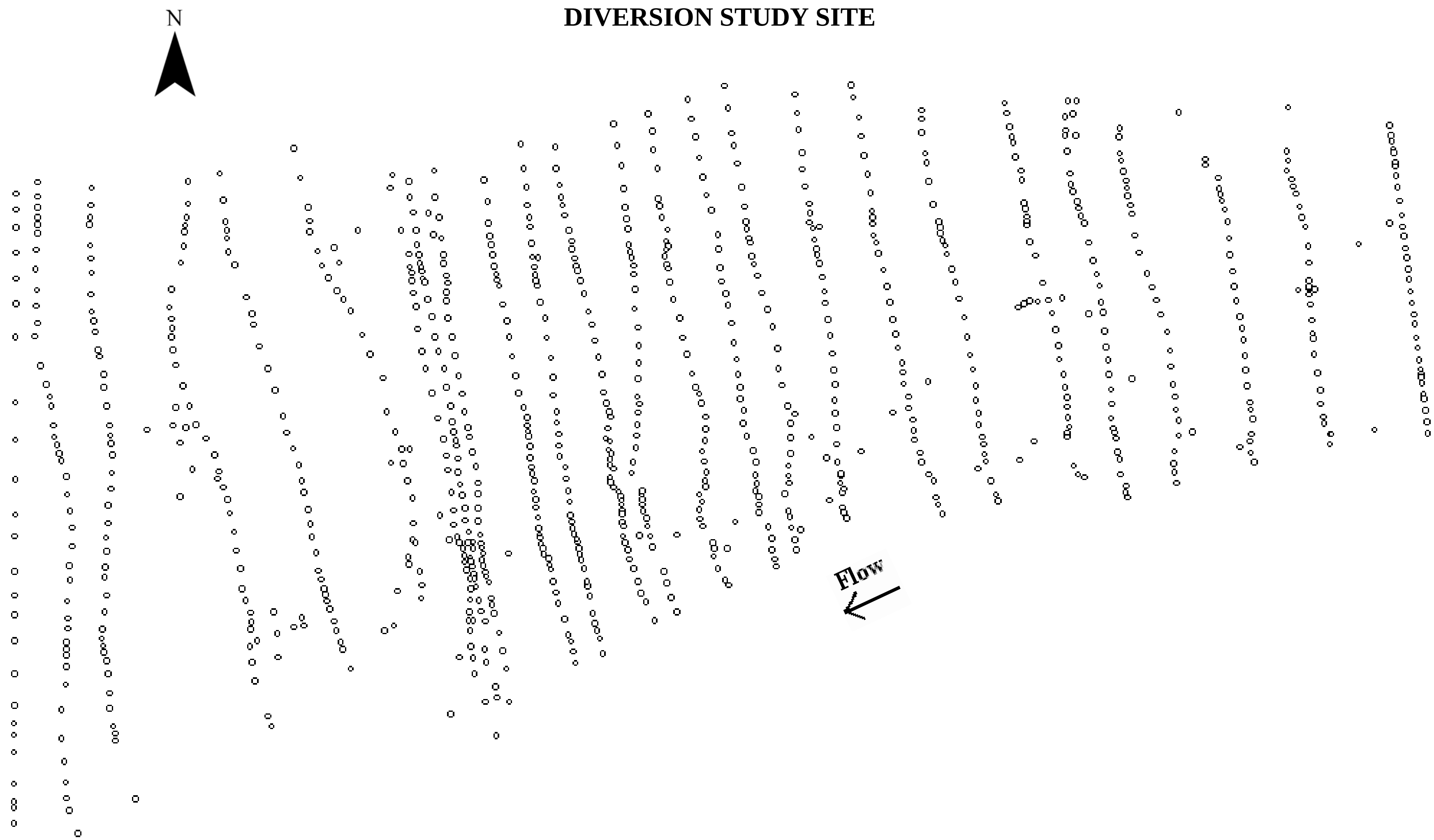

Scale: 1:960

LOWER HALLWOOD STUDY SITE

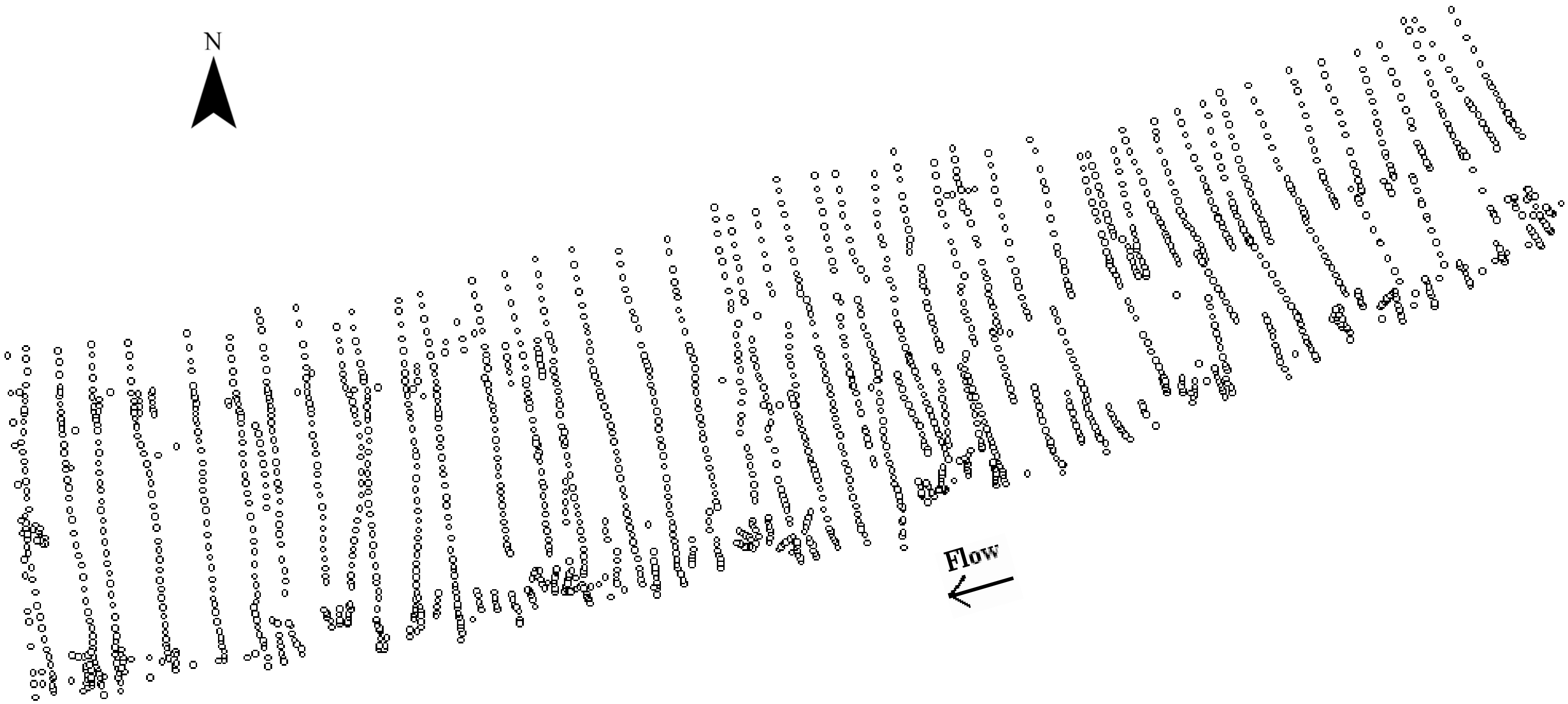

Scale: 1:1878

WHIRLPOOL STUDY SITE

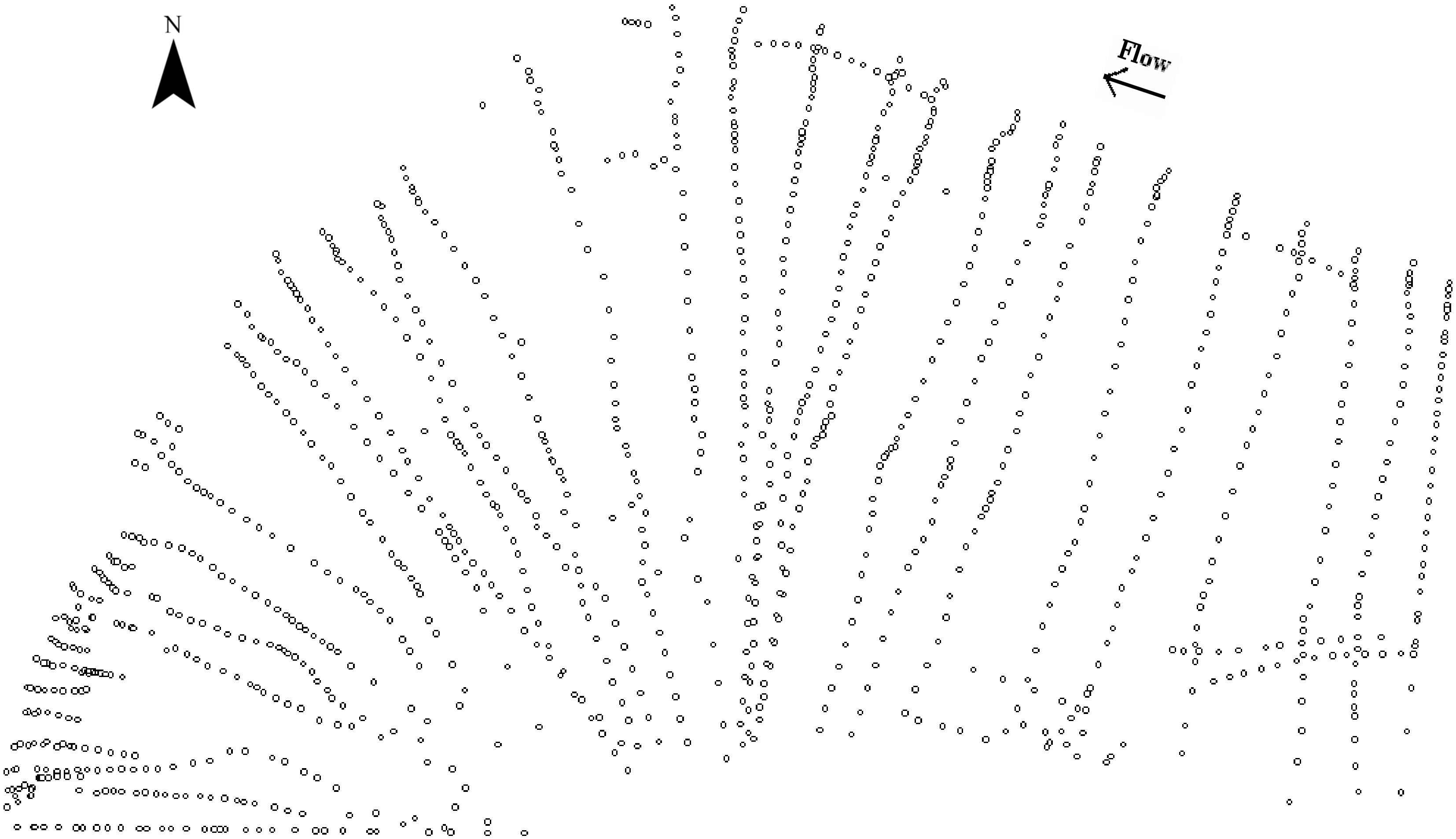

Scale: 1:896

SIDE-CHANNEL STUDY SITE

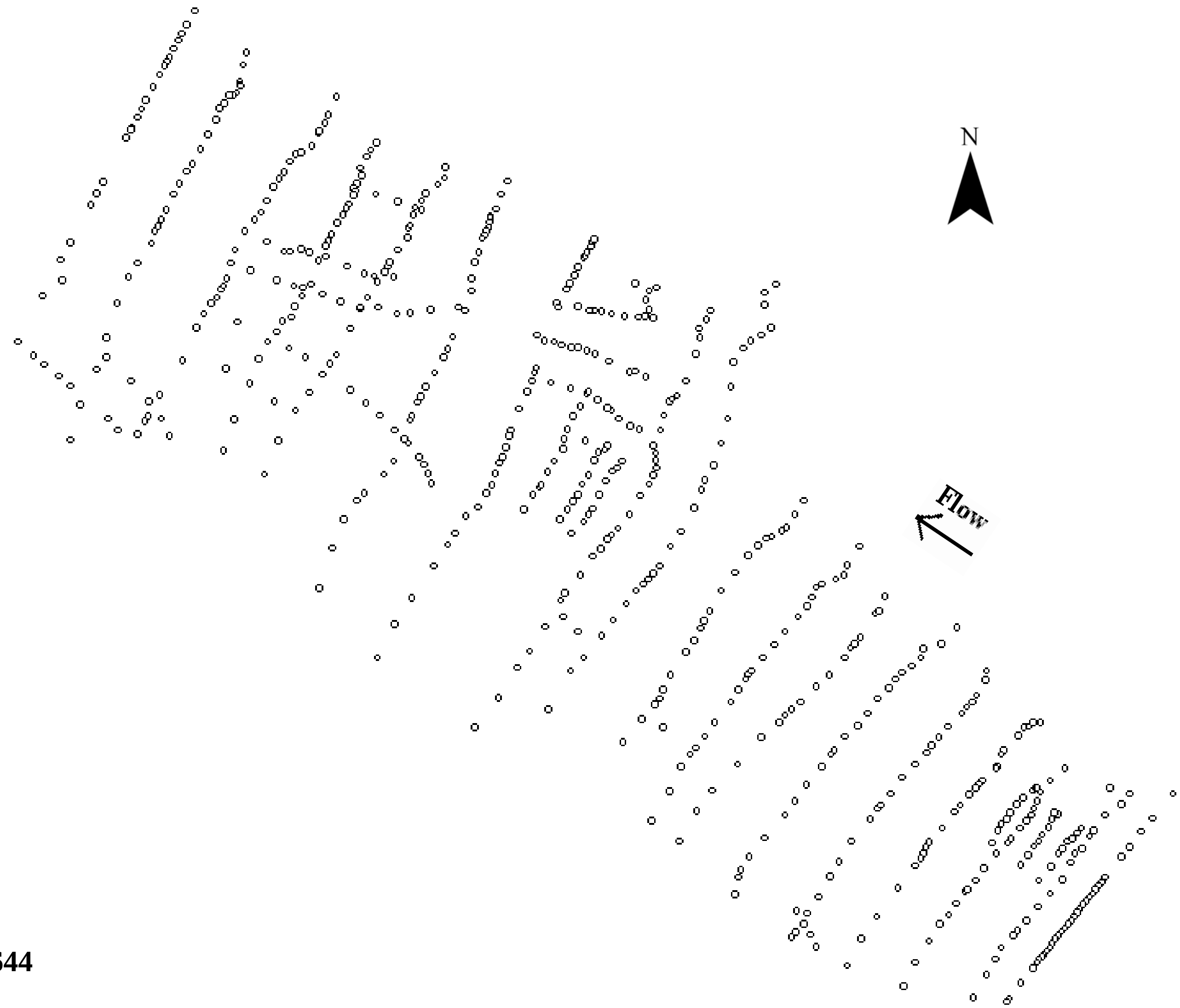

Scale: 1:644

SUCKER GLIDE STUDY SITE

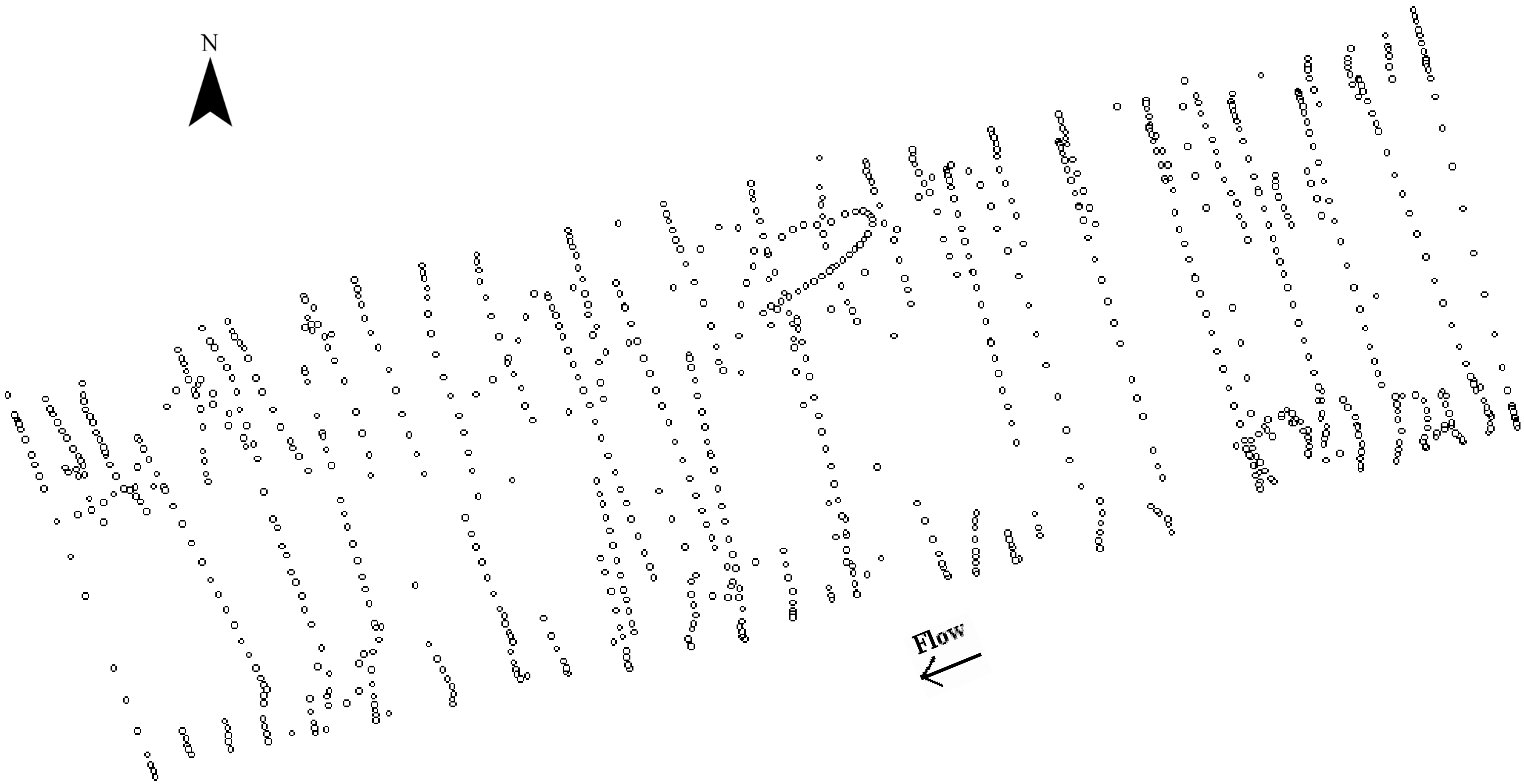

Scale: 1:985

RAILROAD STUDY SITE

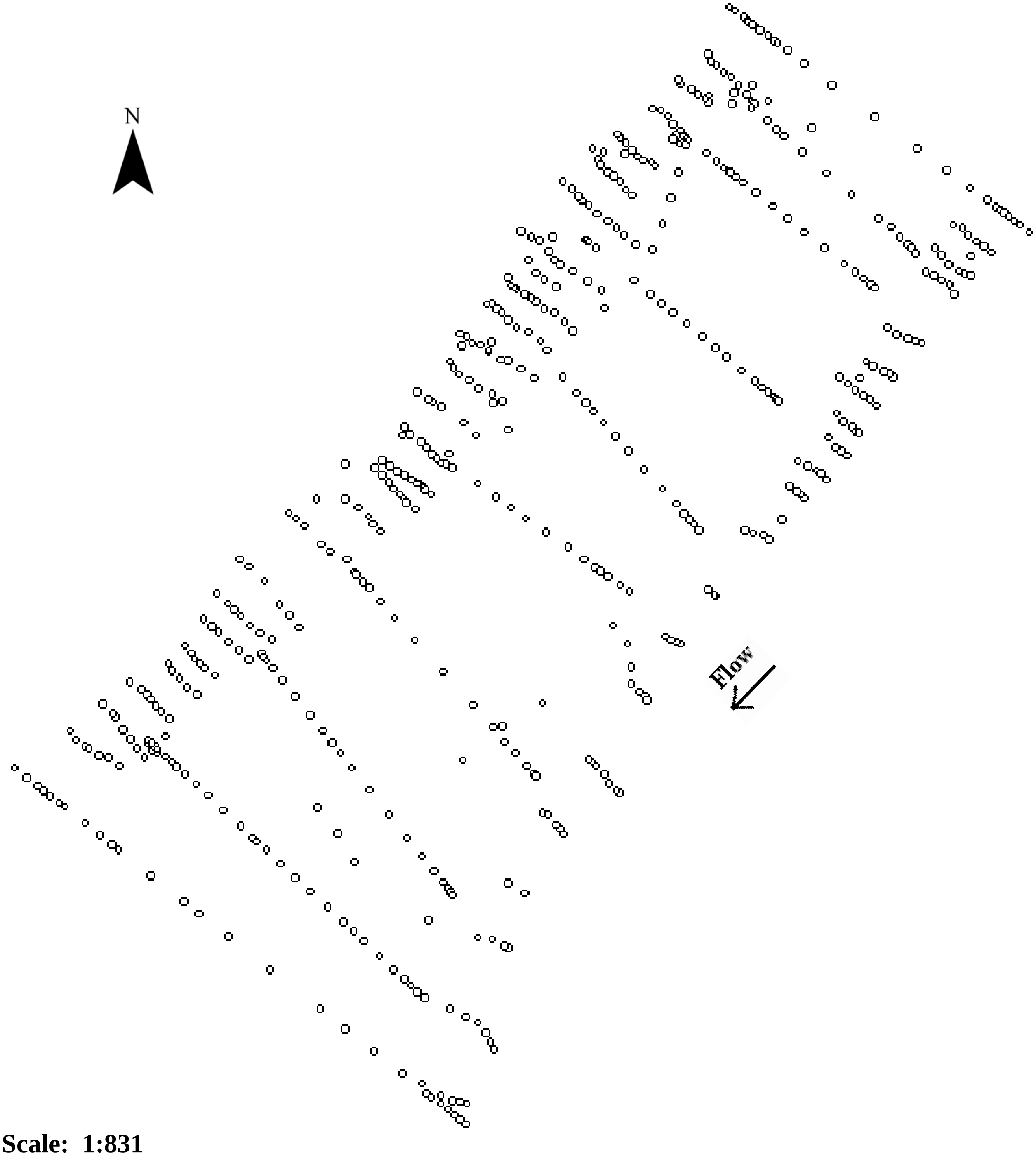

Scale: 1:831

APPENDIX D
RHABSIM WSEL CALIBRATION

Stage of Zero Flow Values

Study Site	XS # 1 SZF	XS # 2 SZF
Narrows	91.0	91.0
Rose Bar	87.2	93.9
Diversion	89.5	91.0
Lower Hallwood	92.2	95.1
Side Channel	92.3	93.2
Whirlpool	92.4	95.5
Sucker Glide	85.7	88.1
Railroad	90.7	90.7

Calibration Methods and Parameters Used

Study Site	XS #	Flow Range (cfs)	Calibration Flows (cfs)	Method	Parameters
Narrows	1, 2	400-4,500	734, 1,890, 1,942, 2,908	IFG4	- - -
Rosebar	1, 2	400-4,500	734, 1,493, 1,942, 2,908	IFG4	- - -
Diversion	1, 2	400-4,500	862, 1,493, 2,036, 2,908	IFG4	- - -
Lower Hallwood	1	150-1,900	516, 970, 1,930	MANSQ	β = 0.165, CALQ = 1,930 cfs
Lower Hallwood	1	2,000-4,500	970, 1,930, 3,270	IFG4	- - -
Whirlpool	1, 2	150-4,500	516, 970, 1,220, 1,930, 3,270	IFG4	- - -
Side-Channel	1,2	800-4,500	3,270	River2D	K = 0.8
Sucker Glide	1	150-4,500	516, 970, 1,920, 3,270	IFG4	- - -
Sucker Glide	2	150-4,500	516, 970, 1,920, 3,270	MANSQ	β = 0.380, CALQ = 516 cfs
Railroad	1	150-4,500	516, 962, 1,920, 3,270	Multiple Regression	A = -0.896, B = 0.334, C = 0.152
Railroad	2	150-4,500	516, 962, 1,920, 3,270	Multiple Regression	A = -0.894, B = 0.329, C = 0.152

Narrows Study Site

	BETA	%MEAN	Calculated vs Given Discharge (%)				Difference (measured vs. pred. WSELs)			
XS	COEFF.	ERROR	734	1,890	1,942	2,908	734	1,890	1,942	2,908
1	2.79	2.9	1.38	0.72	4.98	4.56	0.01	0.01	0.10	0.03
2	2.19	1.1	0.13	2.18	2.06	0.05	0.00	0.06	0.06	0.00

Rosebar Study Site

	BETA	%MEAN	Calculated vs Given Discharge (%)				Difference (measured vs. pred. WSELs)			
XS	COEFF.	ERROR	734	1,493	1,942	2,908	734	1,493	1,942	2,908
1	2.45	2.4	2.25	5.00	1.09	1.50	0.03	0.09	0.02	0.04
2	2.40	2.5	2.67	5.36	0.39	2.11	0.03	0.07	0.01	0.04

Diversion Study Site

	BETA	%MEAN	Calculated vs Given Discharge (%)				Difference (measured vs. pred. WSELs)			
XS	COEFF.	ERROR	862	1,492	2,036	2,908	862	1,492	2,036	2,908
1	3.95	9.5	10.8	14.2	6.0	7.4	0.07	0.09	0.04	0.07
2	2.74	7.1	9.0	14.3	1.0	4.8	0.05	0.09	0.01	0.05

Lower Hallwood Study Site

	BETA	%MEAN	Calculated vs Given Discharge (%)			Difference (measured vs. pred. WSELs)		
XS	COEFF.	ERROR	516	970	1,930	516	970	1,930
1	---	10.0	18.0	12.0	0.0	0.10	0.10	0.00

	BETA	%MEAN	Calculated vs Given Discharge (%)			Difference (measured vs. pred. WSELs)		
XS	COEFF.	ERROR	970	1,930	3,270	970	1,930	3,270
1	2.07	1.3	0.9	2.0	1.0	0.01	0.03	0.02

Whirlpool Study Site

	BETA	%MEAN	Calculated vs Given Discharge (%)					Difference (measured vs. pred. WSELs)				
XS	COEFF.	ERROR	516	970	1,220	1,930	3,270	516	970	1,220	1,930	3,270
1	3.68	3.5	1.6	0.3	6.7	7.4	1.6	0.01	0.00	0.06	0.07	0.02
2	2.90	2.0	1.7	3.3	1.5	1.7	1.7	0.01	0.02	0.01	0.10	0.02

Sucker Glide Study Site

	BETA	%MEAN	Calculated vs Given Discharge (%)				Difference (measured vs. pred. WSELs)			
XS	COEFF.	ERROR	516	970	1,920	3,270	516	970	1,920	3,270
1	2.64	0.6	0.7	0.9	0.2	0.5	0.01	0.02	0.01	0.01
2	---	2.3	0.0	4.1	3.1	1.8	0.00	0.08	0.07	0.05

Railroad Study Site

	BETA	%MEAN	Calculated vs Given Discharge (%)				Difference (measured vs. pred. WSELs)			
XS	COEFF.	ERROR	516	970	1,920	3,270	516	970	1,920	3,270
1	---	---	---	---	---	---	0.01	0.11	0.10	0.08
2	---	---	---	---	---	---	0.00	0.08	0.11	0.06

APPENDIX E
VELOCITY ADJUSTMENT FACTORS

Narrows Study Site

Discharge	Velocity Adjustment Factors Xsec 1	Xsec 2
400	0.37	0.28
600	0.52	0.40
800	0.66	0.52
1,000	0.80	0.64
1,200	0.93	0.75
1,400	1.05	0.86
1,600	1.17	0.96
1,800	1.28	1.06
2,000	1.39	1.17
2,300	1.55	1.31
2,500	1.65	1.41
2,900	1.85	1.60
3,300	2.03	1.78
3,700	2.21	1.96
4,100	2.38	2.13
4,500	2.54	2.30

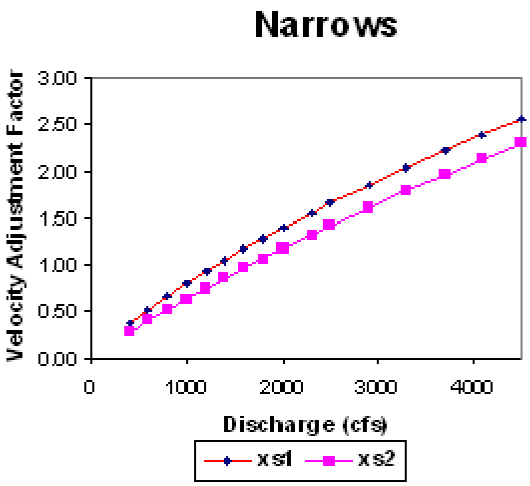

Rosebar Study Site

Discharge	Velocity Adjustment Factors Xsec 1	Xsec 2
400	0.86	0.66
600	0.90	0.75
800	0.93	0.81
1,000	0.96	0.86
1,200	0.99	0.90
1,400	1.01	0.94
1,600	1.03	0.97
1,800	1.05	1.00
2,000	1.07	1.02
2,300	1.10	1.05
2,500	1.11	1.07
2,900	1.14	1.10
3,300	1.17	1.13
3,700	1.20	1.16
4,100	1.22	1.18
4,500	1.24	1.20

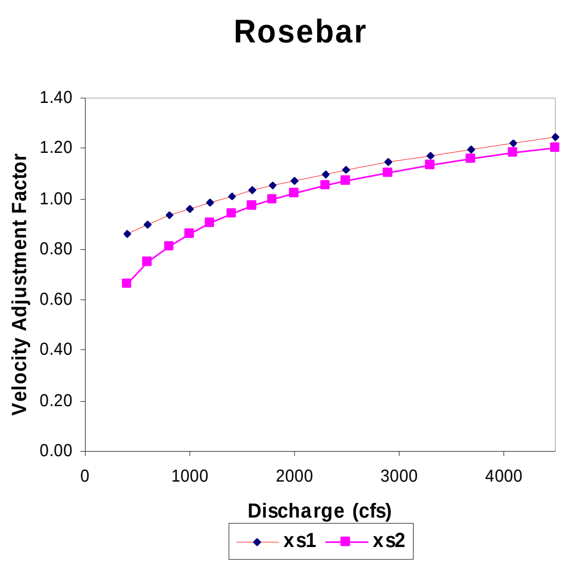

Diversion Study Site

	Velocity Adjustment Factors	
Discharge	Xsec 1	Xsec 2
400	0.41	0.69
600	0.51	0.75
800	0.59	0.80
1,000	0.68	0.84
1,200	0.75	0.88
1,400	0.82	0.92
1,600	0.89	0.95
1,800	0.95	0.98
2,000	1.01	1.00
2,300	1.10	1.04
2,500	1.16	1.06
2,900	1.27	1.11
3,300	1.37	1.15
3,700	1.47	1.18
4,100	1.57	1.22
4,500	1.66	1.25

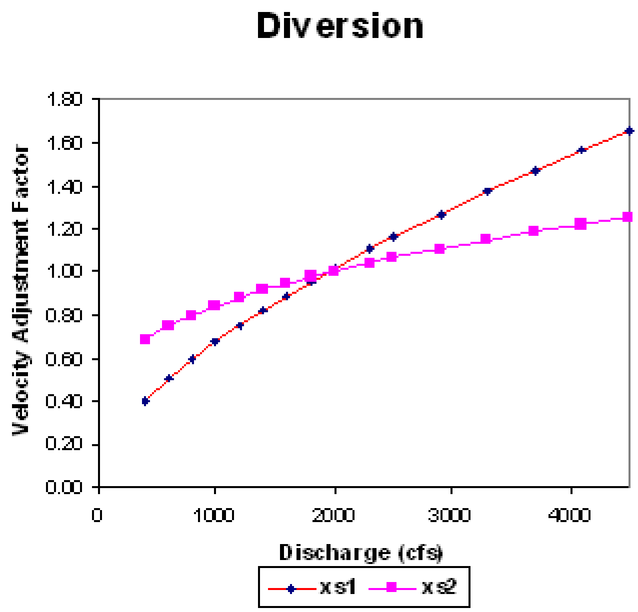

Lower Hallwood Study Site

	Velocity Adjustment Factors
Discharge	Xsec 1
150	0.65
300	0.72
400	0.76
600	0.81
800	0.84
1,000	0.87
1,200	0.90
1,400	0.92
1,600	0.94
1,800	0.96
2,000	0.95
2,300	0.95
2,700	0.95
3,300	0.96
4,100	0.97
4,500	0.98

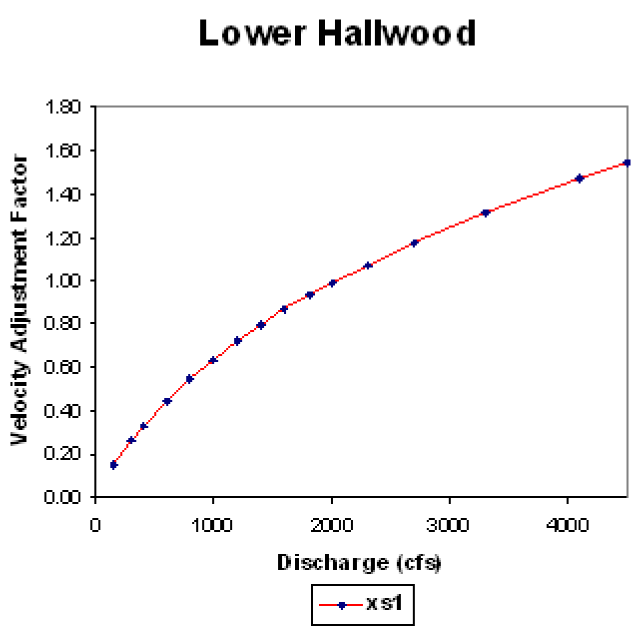

Whirlpool Study Site

Discharge	Velocity Adjustment Factors Xsec 1	Xsec 2
300	1.19	1.02
400	1.35	1.15
600	1.60	1.37
800	1.81	1.54
1,000	1.99	1.69
1,200	2.14	1.83
1,400	2.28	1.95
1,600	2.40	2.06
1,800	2.52	2.16
2,000	2.63	2.26
2,300	2.78	2.39
2,700	2.96	2.55
3,300	3.20	2.77
4,100	3.49	3.03
4,500	3.62	3.15

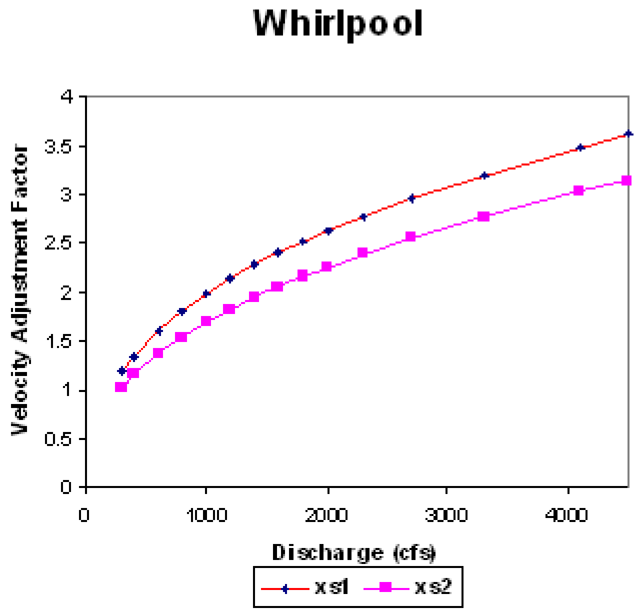

Sucker Glide Study Site

Discharge	Velocity Adjustment Factors Xsec 1	Xsec 2
150	0.54	0.34
300	0.63	0.45
400	0.67	0.51
600	0.75	0.60
800	0.80	0.68
1,000	0.85	0.74
1,200	0.89	0.80
1,400	0.93	0.85
1,600	0.96	0.90
1,800	0.99	0.94
2,000	1.02	0.99
2,300	1.06	1.04
2,700	1.11	1.11
3,300	1.18	1.21
4,100	1.25	1.32
4,500	1.28	1.37

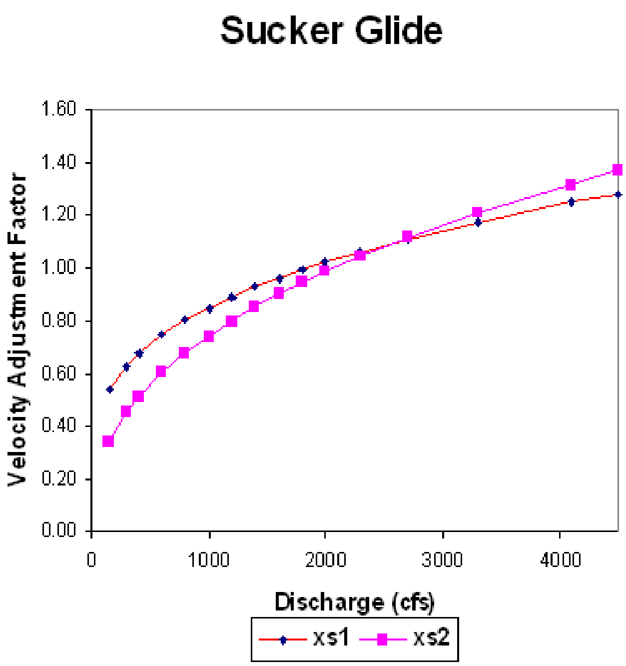

Railroad Study Site

Discharge	Velocity Adjustment Factors Xsec 1	Xsec 2
150	0.18	0.14
300	0.28	0.25
400	0.32	0.31
600	0.40	0.42
800	0.47	0.52
1,000	0.53	0.61
1,200	0.58	0.69
1,400	0.63	0.77
1,600	0.68	0.85
1,800	0.74	0.94
2,000	0.78	1.01
2,300	0.87	1.14
2,700	0.95	1.28
3,300	1.10	1.50
4,100	1.28	1.79
4,500	1.13	1.68

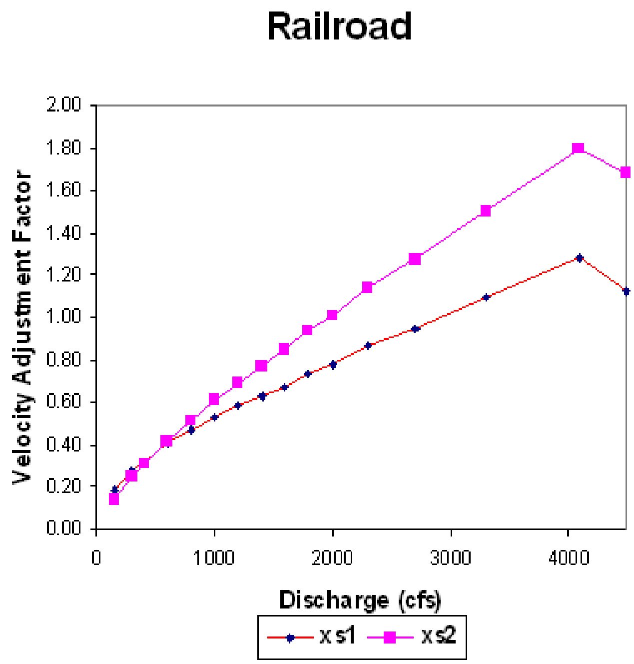

APPENDIX F
BED TOPOGRAPHY OF STUDY SITES

NARROWS STUDY SITE

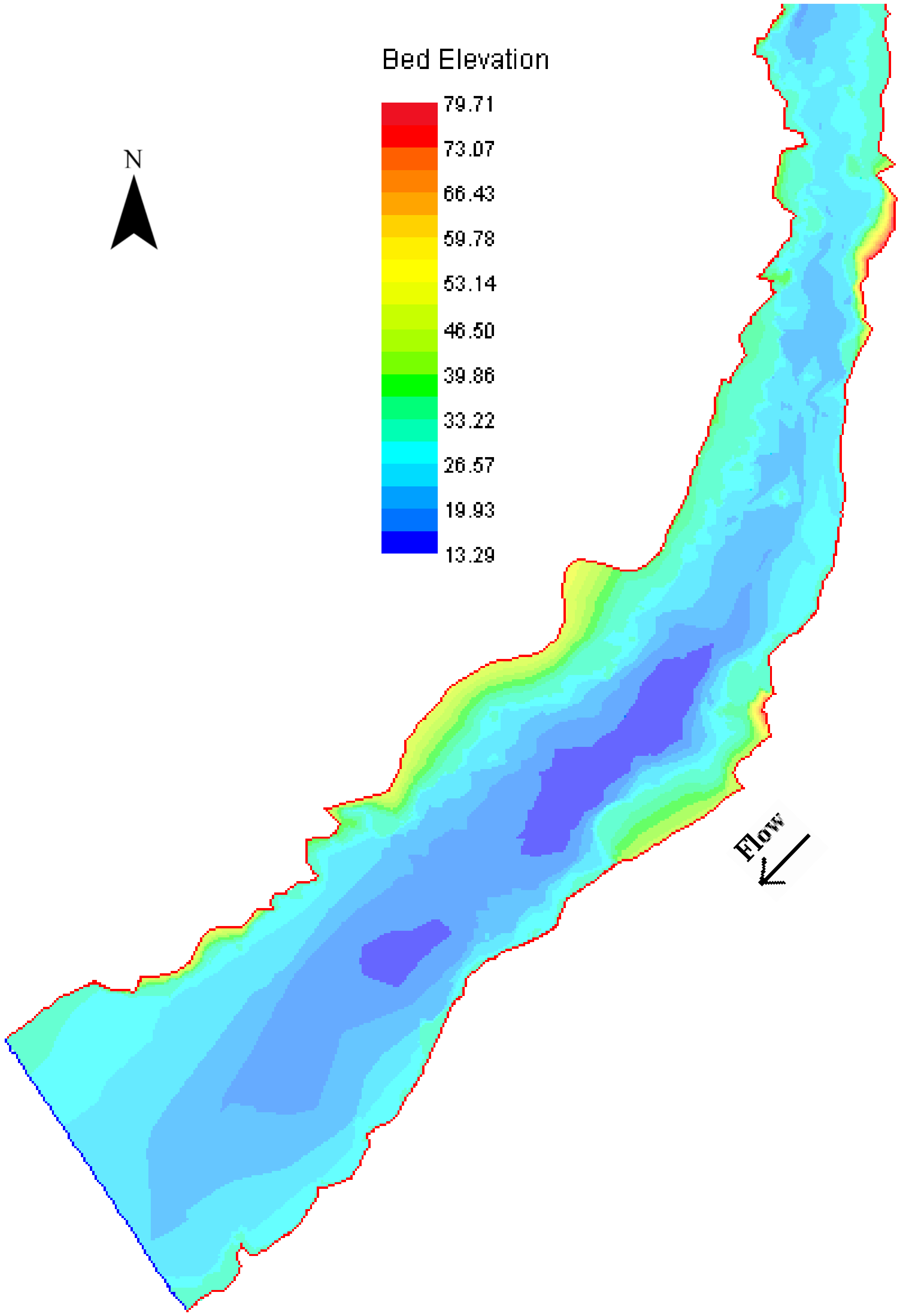

Scale: 1:2695

Units of Bed Elevation are in meters, in 10 equal increments from the lowest to the highest bed elevation in the site.

ROSEBAR STUDY SITE

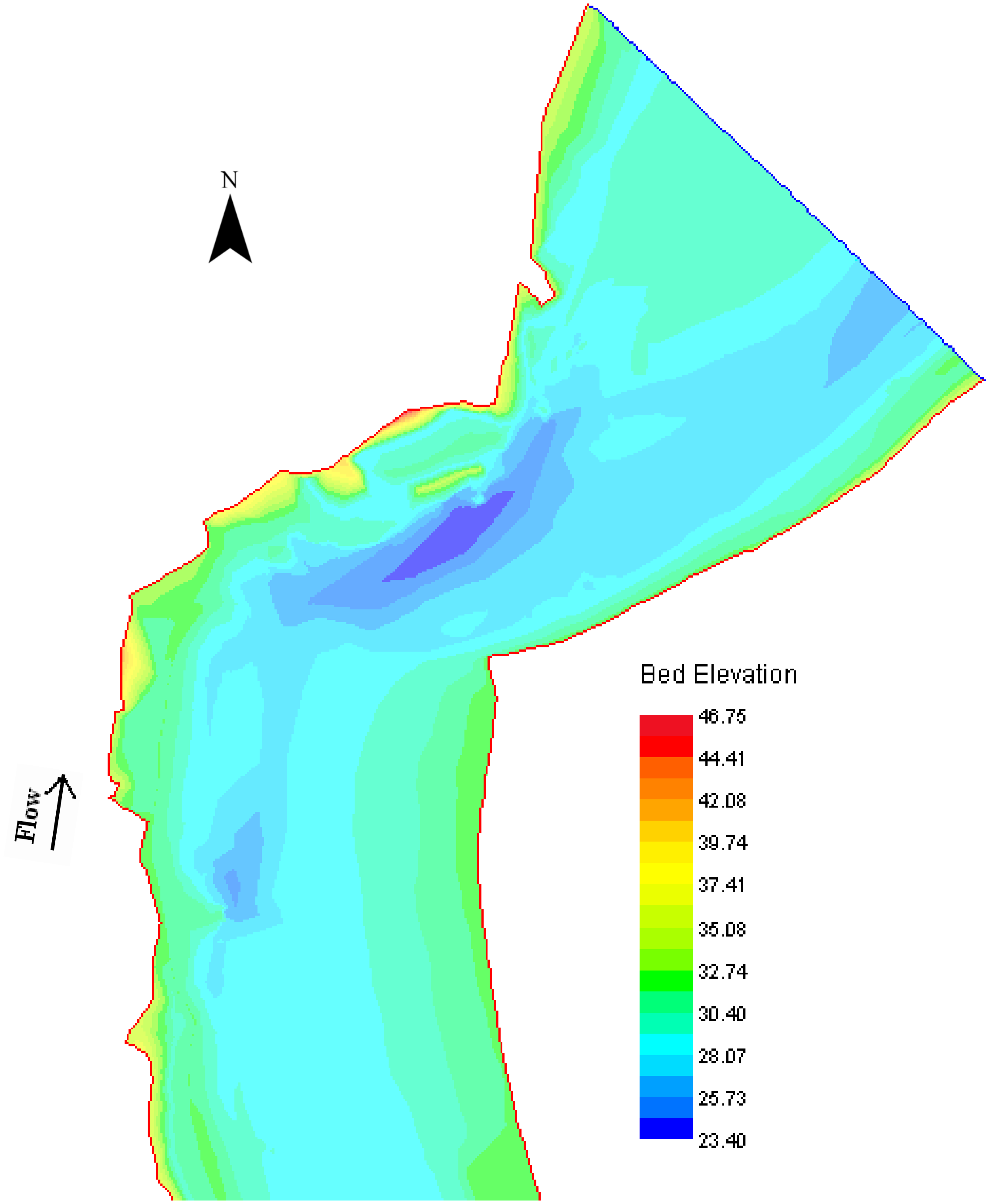

Scale: 1:1536

Units of Bed Elevation are in meters, in 10 equal increments from the lowest to the highest bed elevation in the site.

DIVERSION STUDY SITE

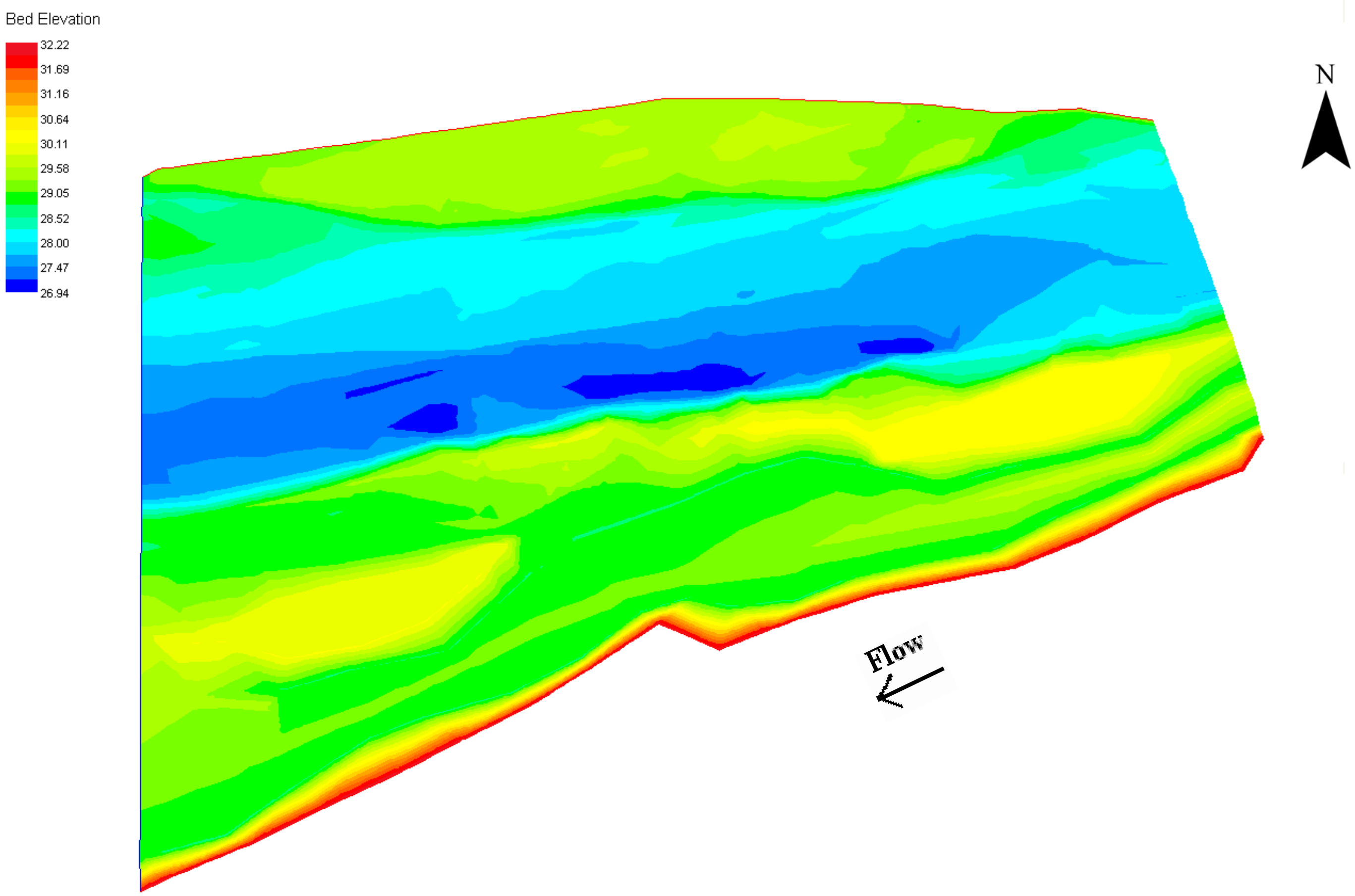

Scale: 1:1024

Units of Bed Elevation are in meters, in 10 equal increments from the lowest to the highest bed elevation in the site.

LOWER HALLWOOD STUDY SITE

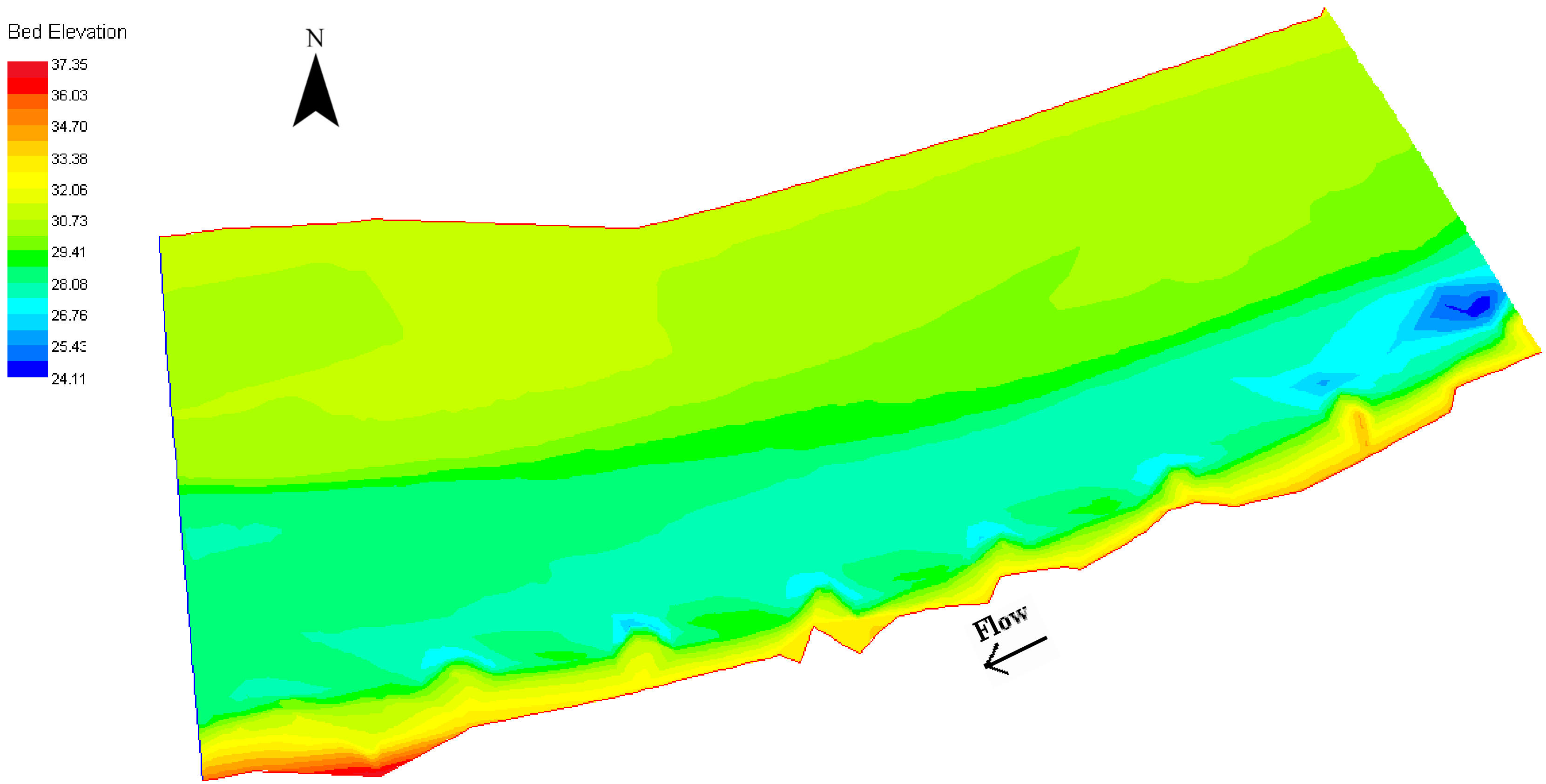

Scale: 1:1252

Units of Bed Elevation are in meters, in 10 equal increments from the lowest to the highest bed elevation in the site.

WHIRLPOOL STUDY SITE

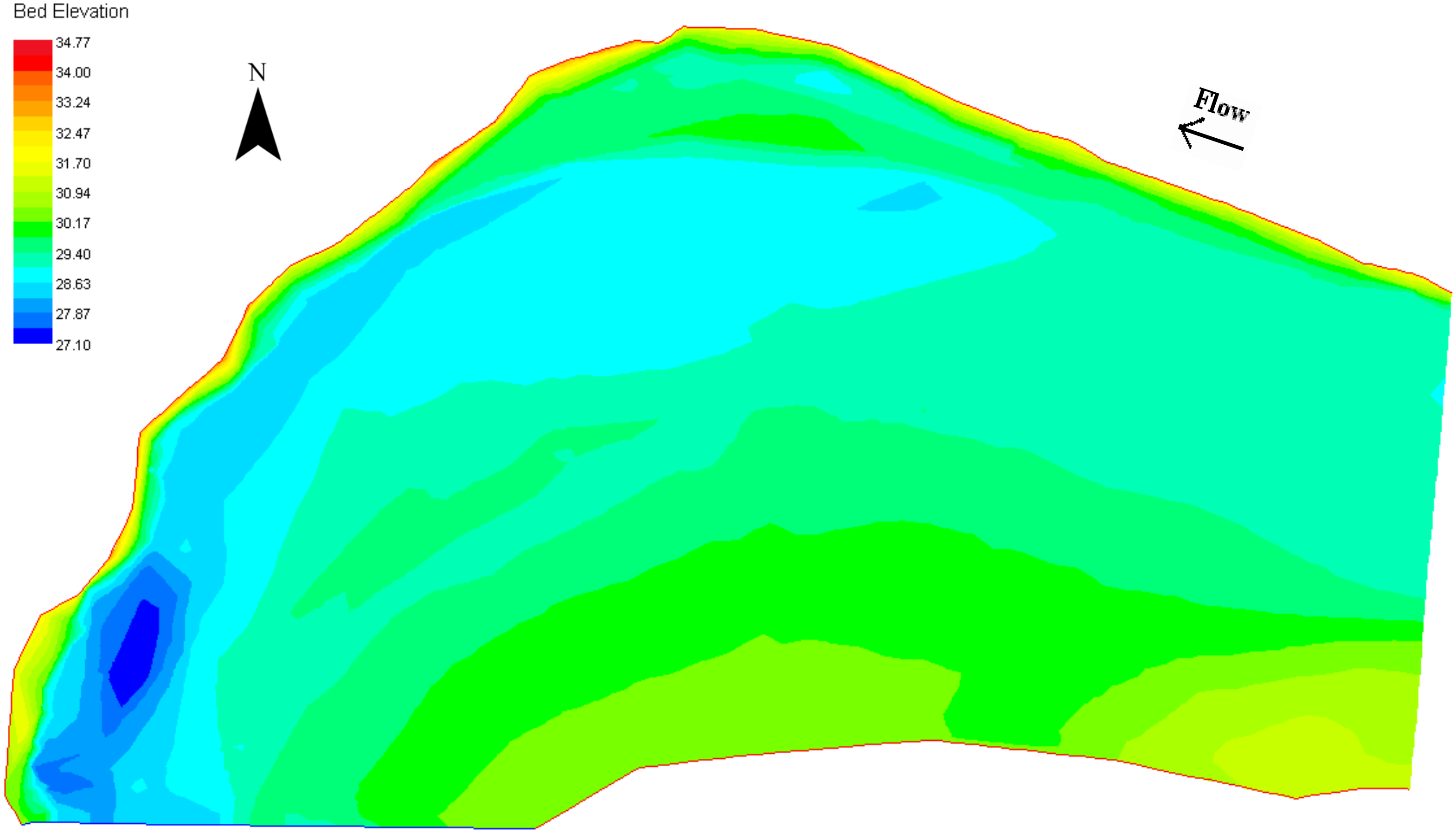

Scale: 1:935

Units of Bed Elevation are in meters, in 10 equal increments from the lowest to the highest bed elevation in the site.

SIDE-CHANNEL STUDY SITE

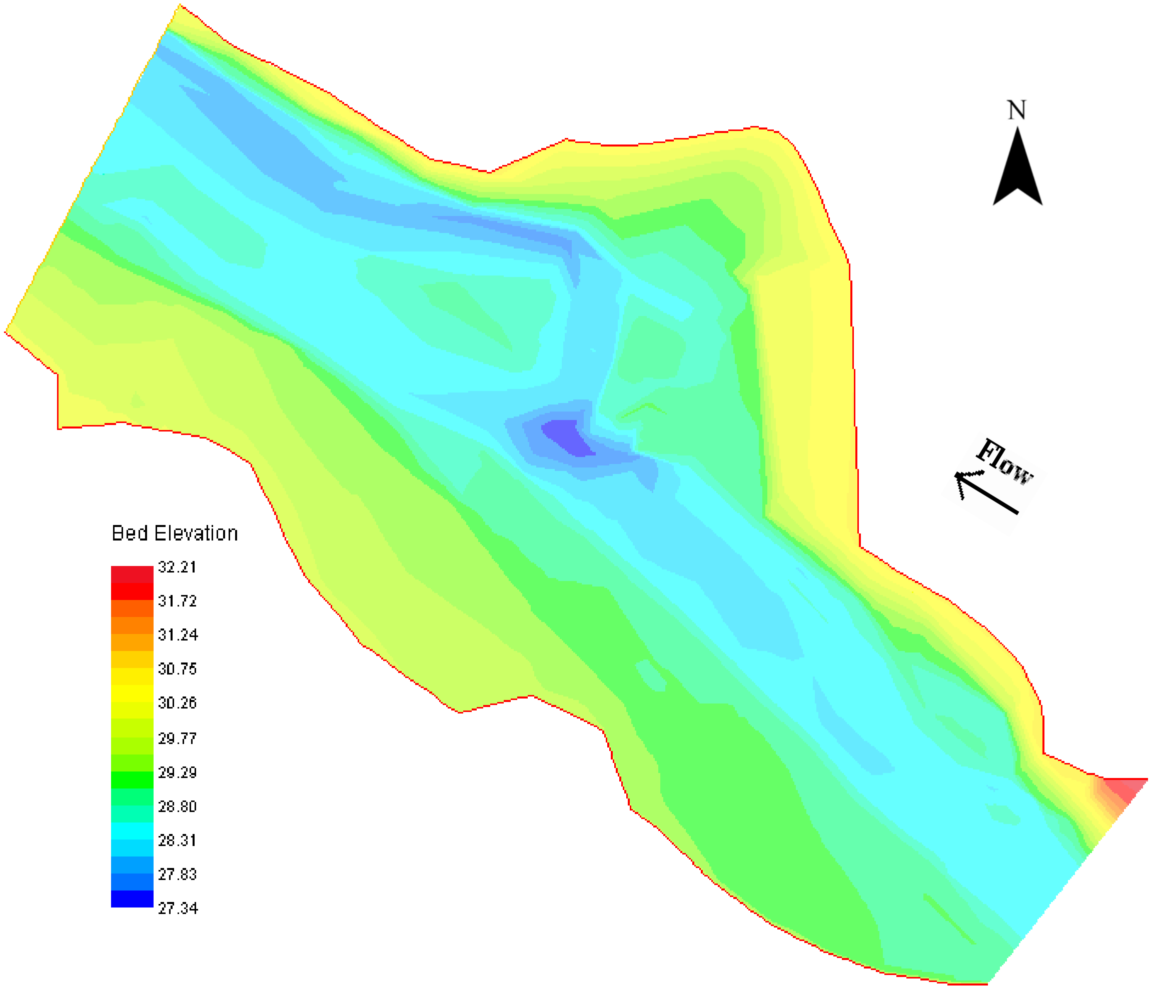

Scale: 1:663

Units of Bed Elevation are in meters, in 10 equal increments from the lowest to the highest bed elevation in the site.

SUCKER GLIDE STUDY SITE

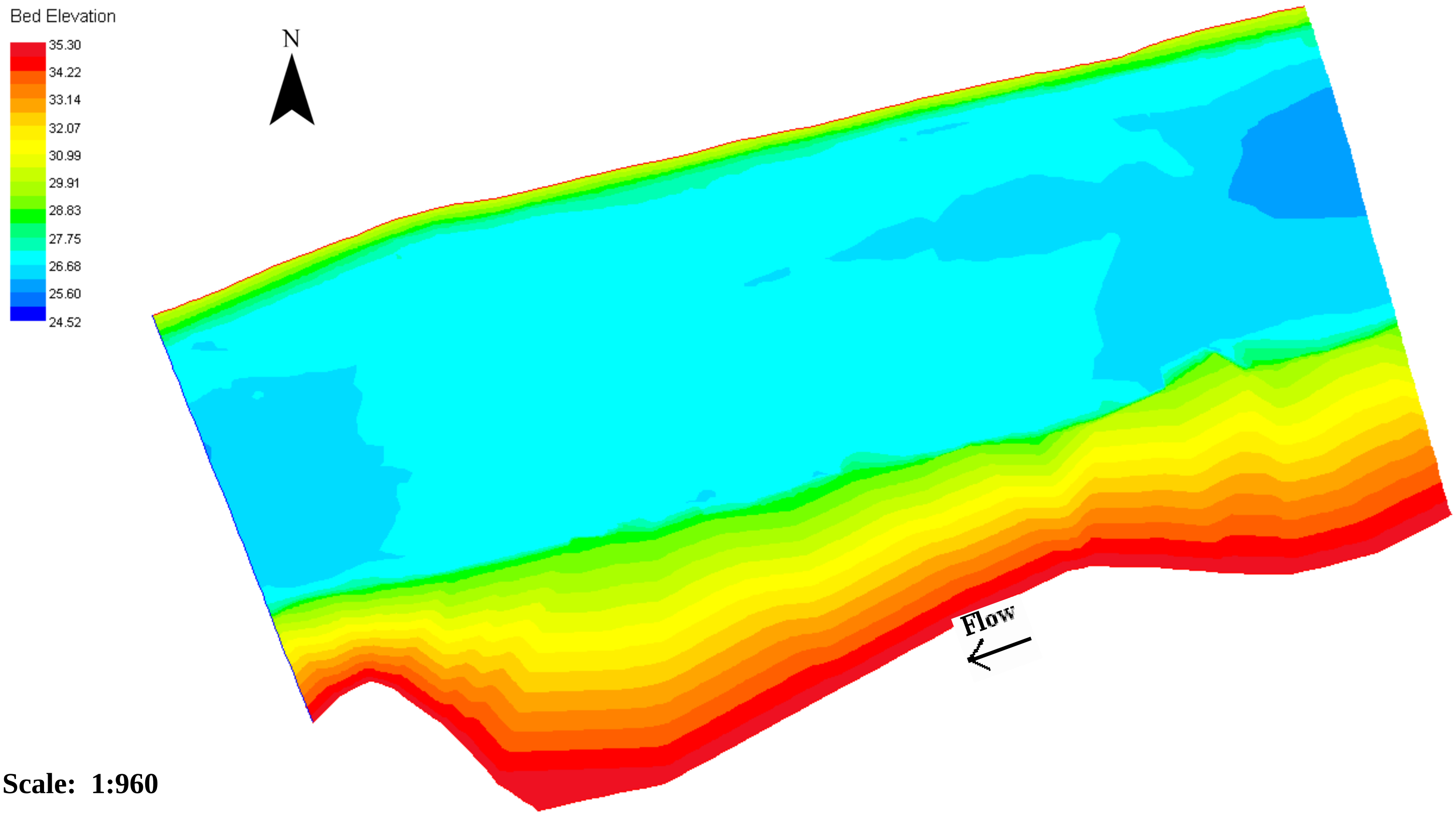

Scale: 1:960

Units of Bed Elevation are in meters, in 10 equal increments from the lowest to the highest bed elevation in the site.

RAILROAD STUDY SITE

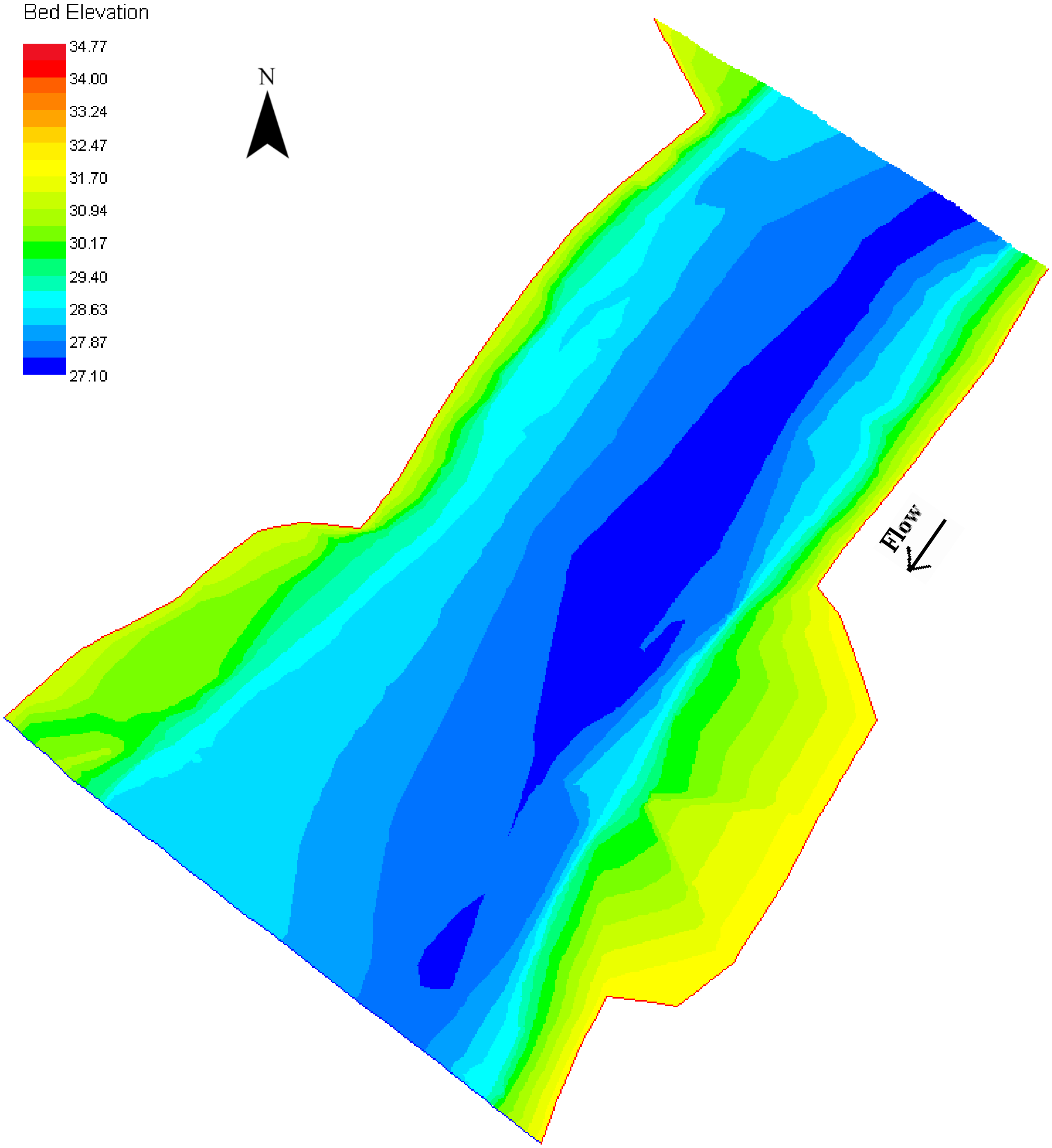

Scale: 1:730

Units of Bed Elevation are in meters, in 10 equal increments from the lowest to the highest bed elevation in the site.

APPENDIX G
2-D WSEL CALIBRATION

Calibration Statistics

Site Name	**Cal Q (cfs)**	**% Nodes within 0.1'**	**Nodes**	**QI**	**Net Q**	**Sol Δ**	**Max F**
Narrows	4,500	72%	46,061	0.30	0.00%	<.000001	6.56
Rosebar	4,500	84%	31,461	0.30	0.15%	.000002	6.00
Diversion	2,908	92%	7,221	0.31	0.07%	.000008	0.83
Lower Hallwood	4,500	91%	18,581	0.30	0.43%	.000006	1.51
Whirlpool	4,500	95%	8,231	0.30	0.46%	.000006	1.23
Side-Channel	3,270	94%	7,243	0.30	0.05%	<.000001	1.27
Sucker Glide	3,270	88%	13,303	0.31	0.16%	.000007	0.43
Railroad	4,500	87%	17,265	0.32	1.51%	.000004	0.64

Narrows Site

XSEC	Br Multiplier	Difference (measured vs. pred. WSELs, feet) Average	Standard Deviation	Maximum
2	1.0	0.11	0.09	0.25
2 LB	1.0	0.02	0.12	0.10
2 RB	1.0	0.20	0.05	0.25
1	1.0	0.07	0.01	0.08

Rosebar Site

XSEC	Br Multiplier	Difference (measured vs. pred. WSELs, feet) Average	Standard Deviation	Maximum
2	0.75	0.01	0.06	0.09

Diversion Site

XSEC	Br Multiplier	Difference (measured vs. pred. WSELs, feet) Average	Standard Deviation	Maximum
2	0.3	0.03	0.03	0.07
2 LB	0.3	0.02	0.02	0.07
2 RB	0.3	0.06	0.01	0.09

Lower Hallwood Site

XSEC	Br Multiplier	Difference (measured vs. pred. WSELs, feet) Average	Standard Deviation	Maximum
2	0.55	0.03	0.05	0.12
2 LB	0.55	0.03	0.04	0.07
2 RB	0.55	0.05	0.01	0.05

Whirlpool Site

XSEC	Br Multiplier	Difference (measured vs. pred. WSELs, feet) Average	Standard Deviation	Maximum
2	0.7	0.04	0.02	0.07

Side-channel Site

XSEC	Br Multiplier	Difference (measured vs. pred. WSELs, feet) Average	Standard Deviation	Maximum
1	3.0	0.04	0.02	0.09
2	3.0	0.05	0.02	0.07

Sucker Glide Site

XSEC	Br Multiplier	Difference (measured vs. pred. WSELs, feet) Average	Standard Deviation	Maximum
2	0.3	0.03	0.005	0.04
2 LB	0.3	0.03	0.003	0.04
2 RB	0.3	0.02	0.006	0.03

Railroad Site

XSEC	Br Multiplier	Difference (measured vs. pred. WSELs, feet) Average	Standard Deviation	Maximum
2	1.0	0.05	0.02	0.09

APPENDIX H
VELOCITY VALIDATION STATISTICS

Site Name	Number of Observations	Correlation Between Measured and Simulated Velocities
Narrows	2,464	0.65
Rosebar	383	0.73
Diversion	92	0.62
Lower Hallwood	209	0.72
Whirlpool	126	0.76
Side-Channel	92	0.64
Sucker Glide	340	0.47
Railroad	234	0.45

Measured Velocities less than 3 ft/s

Difference (measured vs. pred. velocities, ft/s)

Site Name	Number of Observations	Average	Standard Deviation	Maximum
Narrows	2,418	0.43	0.48	3.03
Rosebar	174	1.29	1.24	5.33
Diversion	59	0.75	0.68	2.82
Lower Hallwood	188	0.56	0.49	2.45
Whirlpool	114	0.54	0.47	1.96
Side-Channel	85	0.53	0.36	2.04
Sucker Glide	285	0.67	0.52	2.31
Railroad	205	0.75	0.57	2.14

All differences were calculated as the absolute value of the difference between the measured and simulated velocity.

Measured Velocities greater than 3 ft/s

Percent difference (measured vs. pred. velocities)

Site Name	Number of Observations	Average	Standard Deviation	Maximum
Narrows	46	25%	19%	88%
Rosebar	209	22%	20%	122%
Diversion	33	18%	19%	63%
Lower Hallwood	21	8%	6%	24%
Whirlpool	12	16%	10%	40%
Side-Channel	7	30%	9%	47%
Sucker Glide	55	45%	17%	74%
Railroad	29	49%	18%	80%

All differences were calculated as the absolute value of the difference between the measured and simulated velocity.

Narrows Study Site

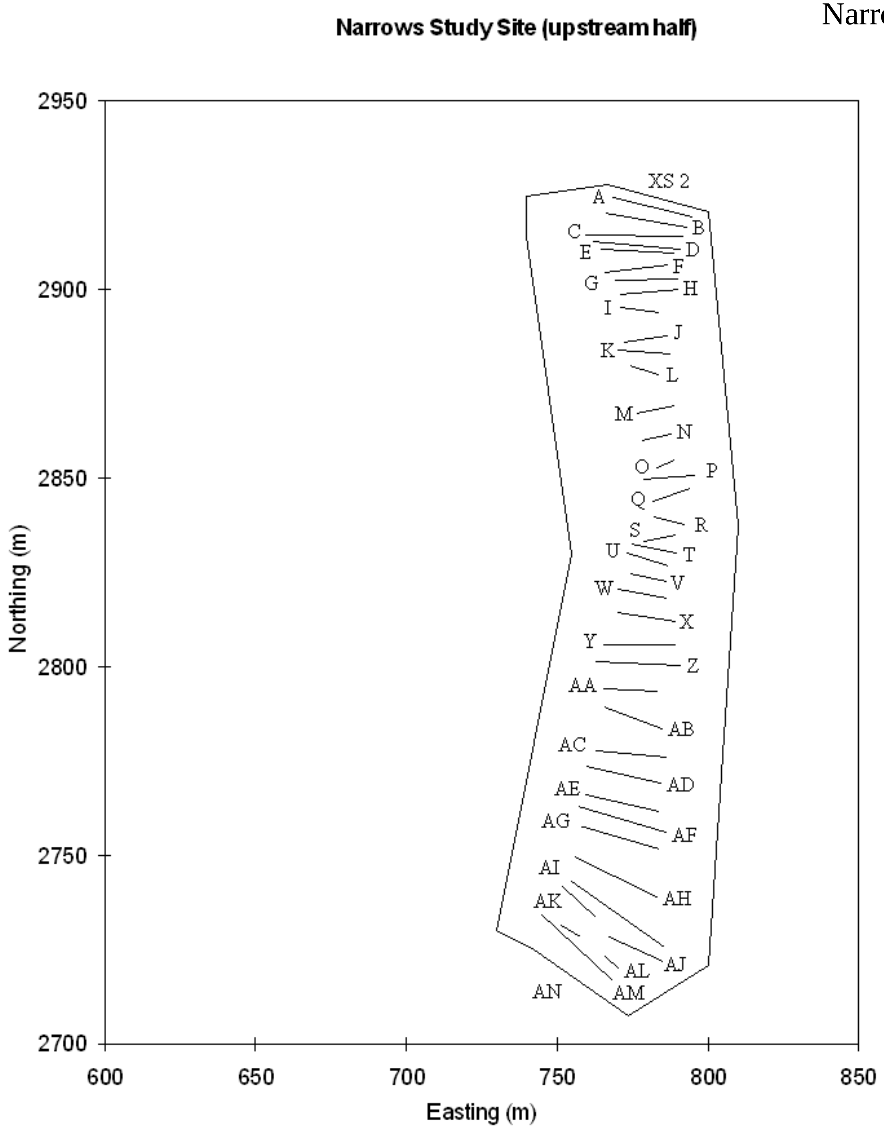

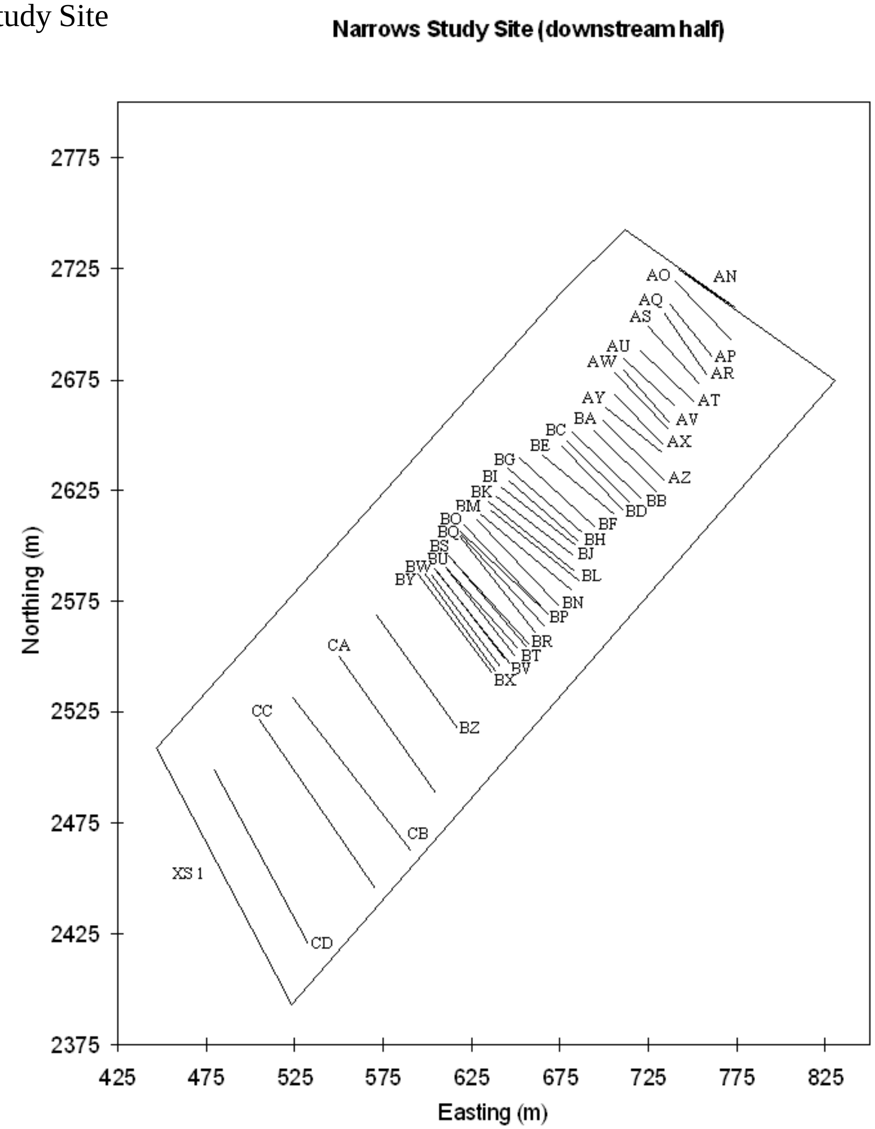

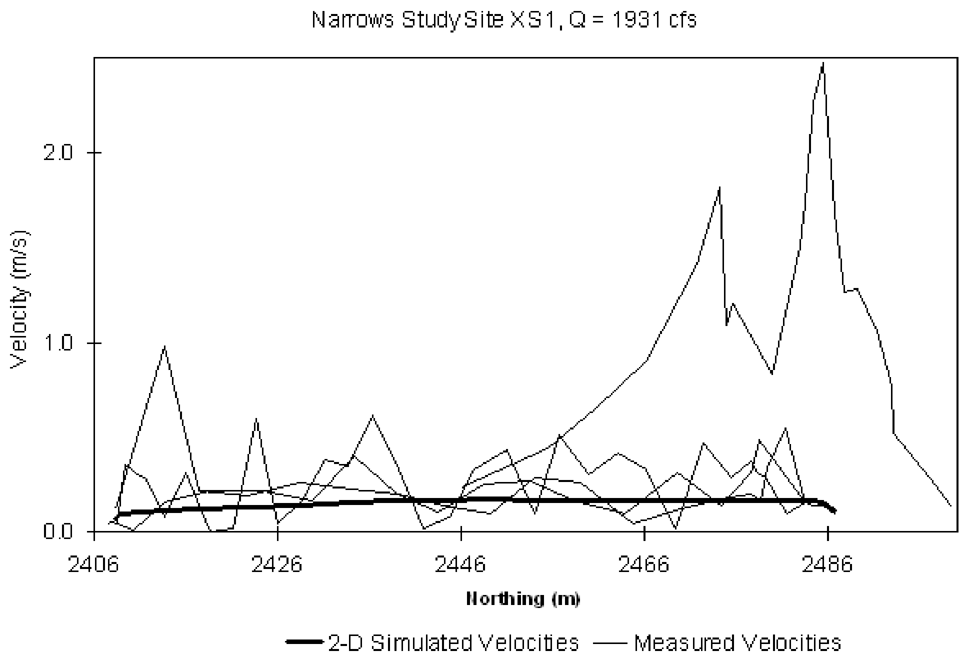
Narrows Study Site XS1, Q = 1931 cfs
Velocity (m/s)
2.0
1.0
0.0
2406
2426
2446
2466
2486
Northing (m)
2-D Simulated Velocities
Measured Velocities

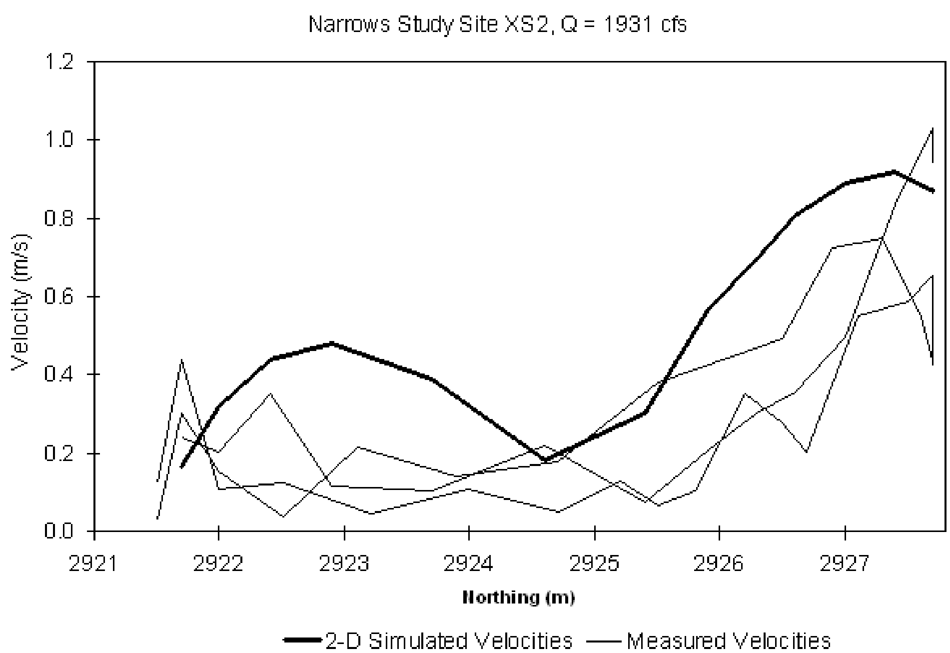
Narrows Study Site XS2, Q = 1931 cfs
Velocity (m/s)
1.2
1.0
0.8
0.6
0.4
0.2
0.0
2921
2922
2923
2924
2925
2926
2927
Northing (m)
2-D Simulated Velocities
Measured Velocities

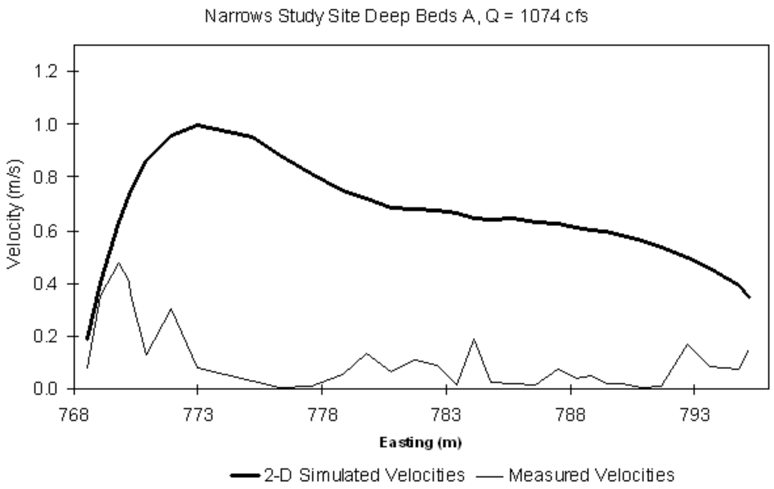
Narrows Study Site Deep Beds A, Q = 1074 cfs
Velocity (m/s)
Easting (m)
2-D Simulated Velocities
Measured Velocities

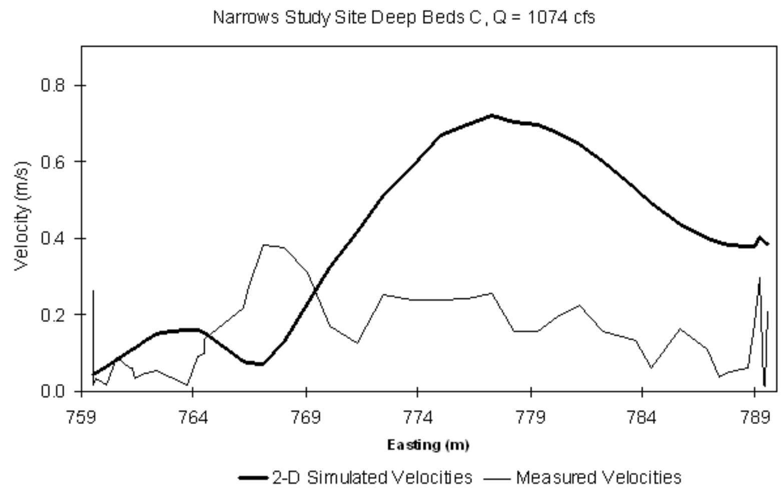
Narrows Study Site Deep Beds C, Q = 1074 cfs
Velocity (m/s)
Easting (m)
2-D Simulated Velocities
Measured Velocities

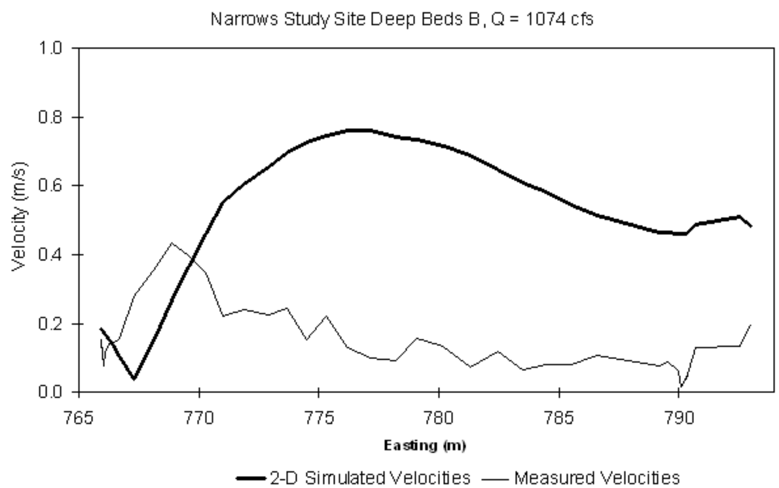
Narrows Study Site Deep Beds B, Q = 1074 cfs
Velocity (m/s)
Easting (m)
2-D Simulated Velocities
Measured Velocities

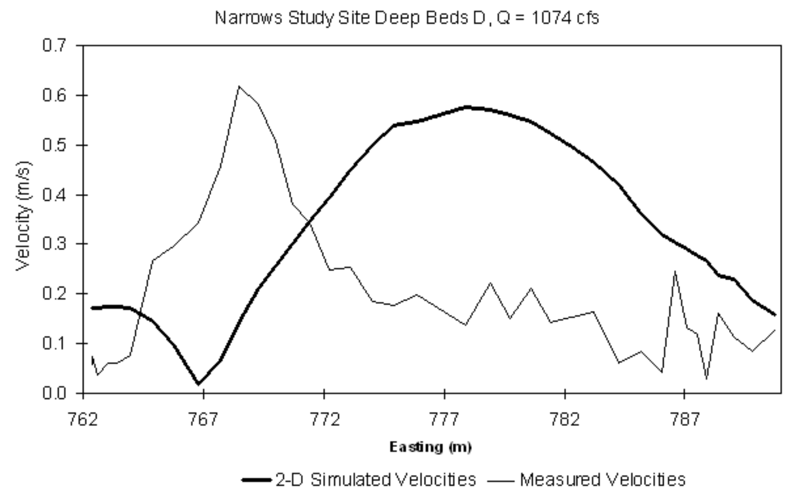
Narrows Study Site Deep Beds D, Q = 1074 cfs
Velocity (m/s)
Easting (m)
2-D Simulated Velocities
Measured Velocities

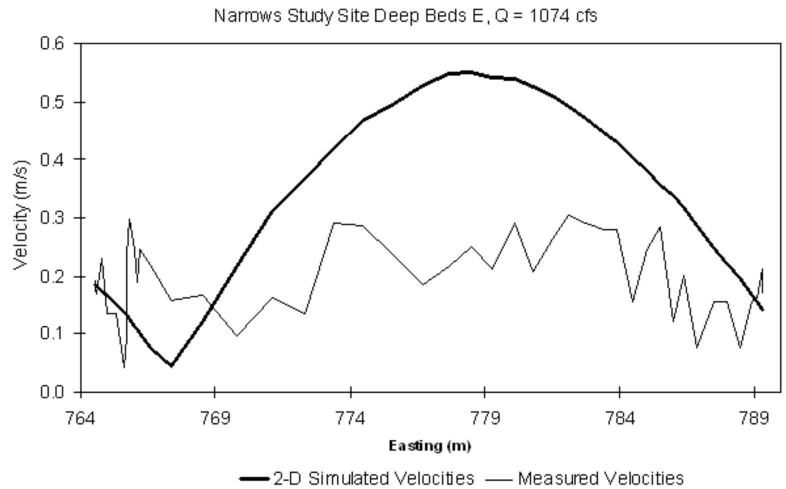
Narrows Study Site Deep Beds E, Q = 1074 cfs
Velocity (m/s)
0.6
0.5
0.4
0.3
0.2
0.1
0.0
764
769
774
779
784
789
Easting (m)
2-D Simulated Velocities
Measured Velocities

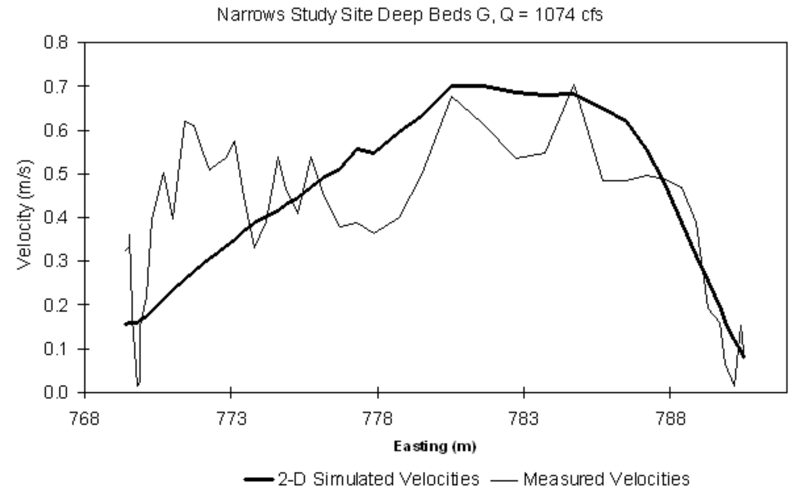
Narrows Study Site Deep Beds G, Q = 1074 cfs
Velocity (m/s)
0.8
0.7
0.6
0.5
0.4
0.3
0.2
0.1
0.0
768
773
778
783
788
Easting (m)
2-D Simulated Velocities
Measured Velocities

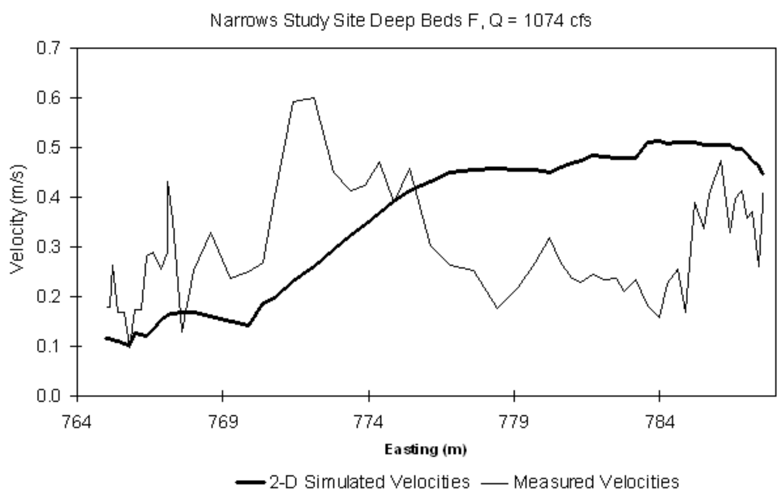
Narrows Study Site Deep Beds F, Q = 1074 cfs
Velocity (m/s)
0.7
0.6
0.5
0.4
0.3
0.2
0.1
0.0
764
769
774
779
784
Easting (m)
2-D Simulated Velocities
Measured Velocities

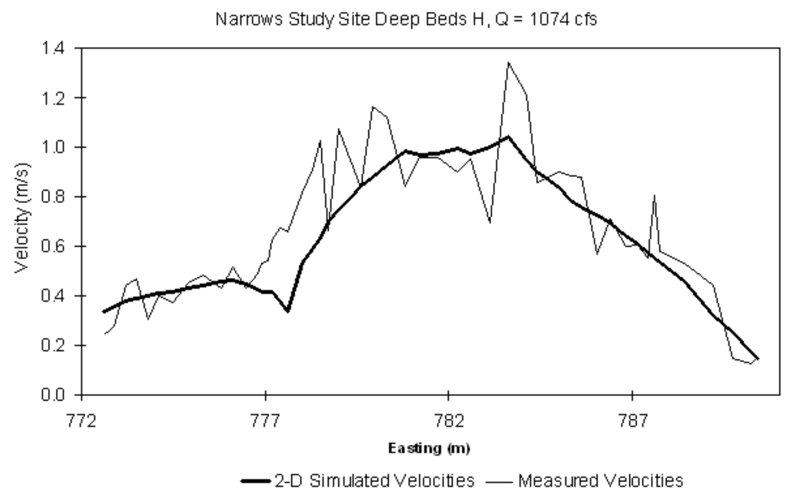
Narrows Study Site Deep Beds H, Q = 1074 cfs
Velocity (m/s)
1.4
1.2
1.0
0.8
0.6
0.4
0.2
0.0
772
777
782
787
Easting (m)
2-D Simulated Velocities
Measured Velocities

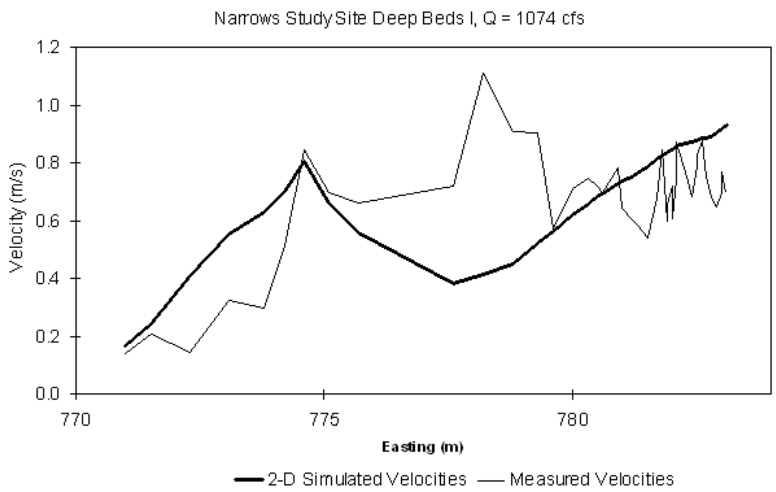
Narrows Study Site Deep Beds I, Q = 1074 cfs
Velocity (m/s)
Easting (m)
2-D Simulated Velocities
Measured Velocities

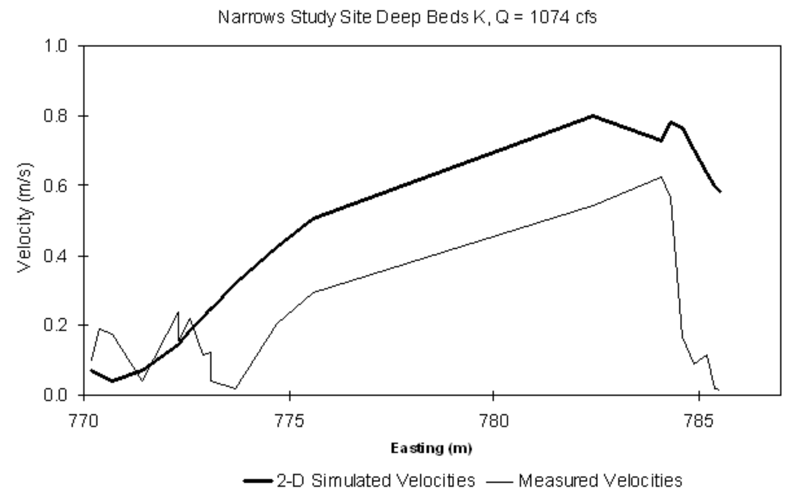
Narrows Study Site Deep Beds K, Q = 1074 cfs
Velocity (m/s)
Easting (m)
2-D Simulated Velocities
Measured Velocities

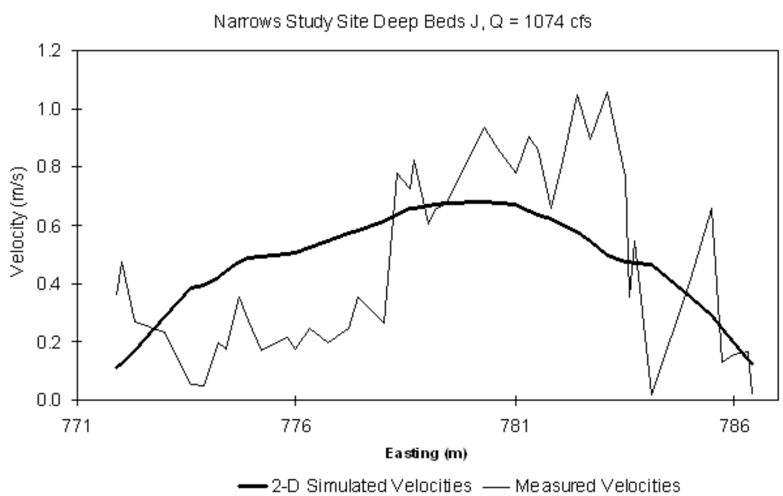
Narrows Study Site Deep Beds J, Q = 1074 cfs
Velocity (m/s)
Easting (m)
2-D Simulated Velocities
Measured Velocities

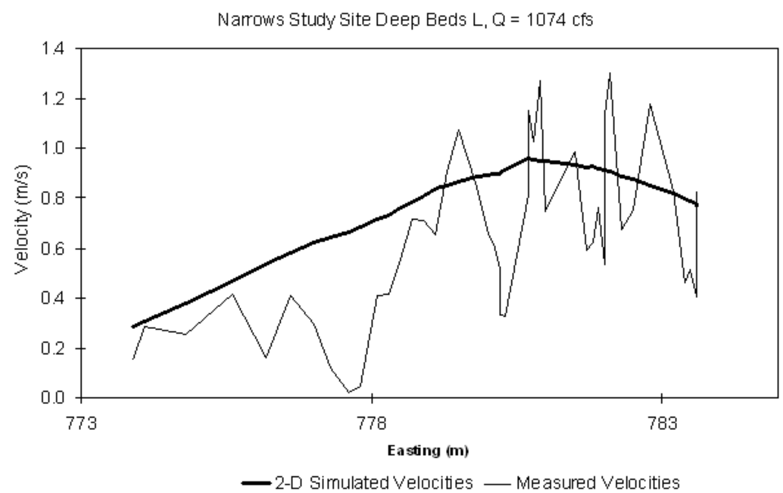
Narrows Study Site Deep Beds L, Q = 1074 cfs
Velocity (m/s)
Easting (m)
2-D Simulated Velocities
Measured Velocities

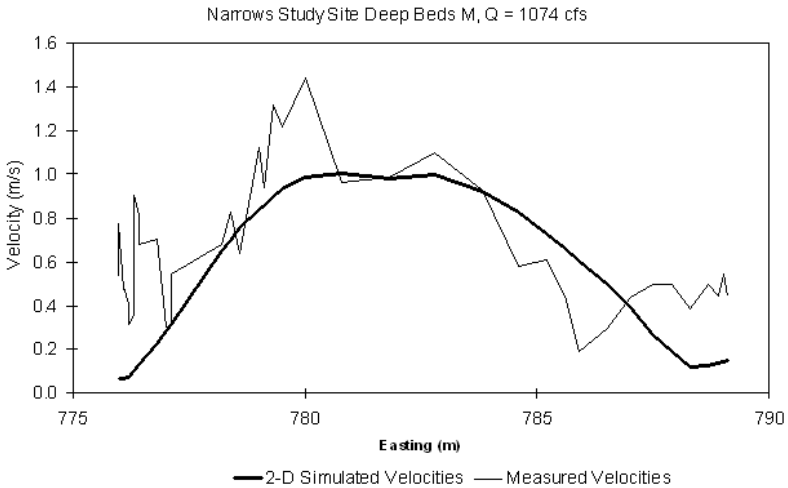
Narrows Study Site Deep Beds M, Q = 1074 cfs
Velocity (m/s)
1.6
1.4
1.2
1.0
0.8
0.6
0.4
0.2
0.0
775
780
785
790
Easting (m)
2-D Simulated Velocities
Measured Velocities

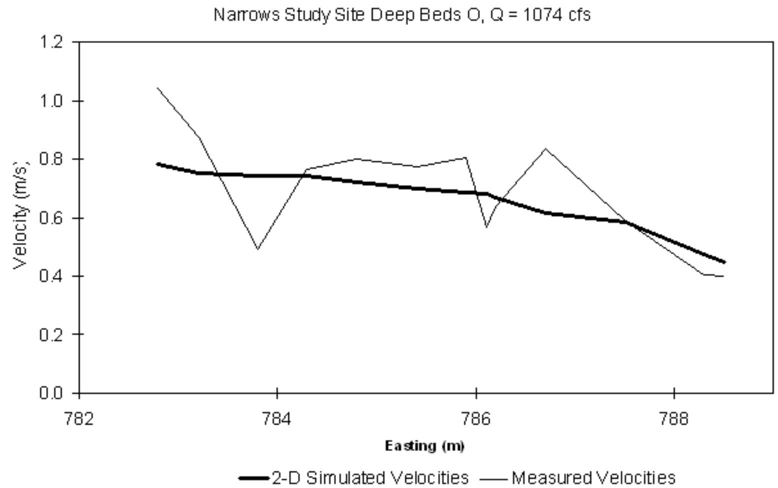
Narrows Study Site Deep Beds O, Q = 1074 cfs
Velocity (m/s)
1.2
1.0
0.8
0.6
0.4
0.2
0.0
782
784
786
788
Easting (m)
2-D Simulated Velocities
Measured Velocities

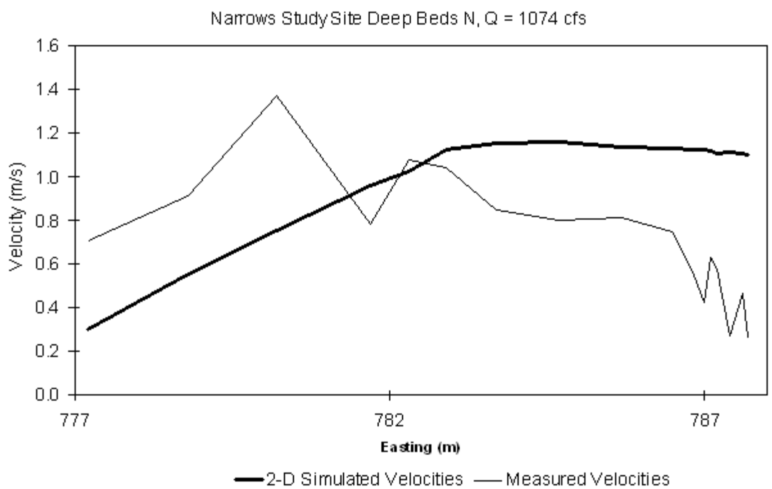
Narrows Study Site Deep Beds N, Q = 1074 cfs
Velocity (m/s)
1.6
1.4
1.2
1.0
0.8
0.6
0.4
0.2
0.0
777
782
787
Easting (m)
2-D Simulated Velocities
Measured Velocities

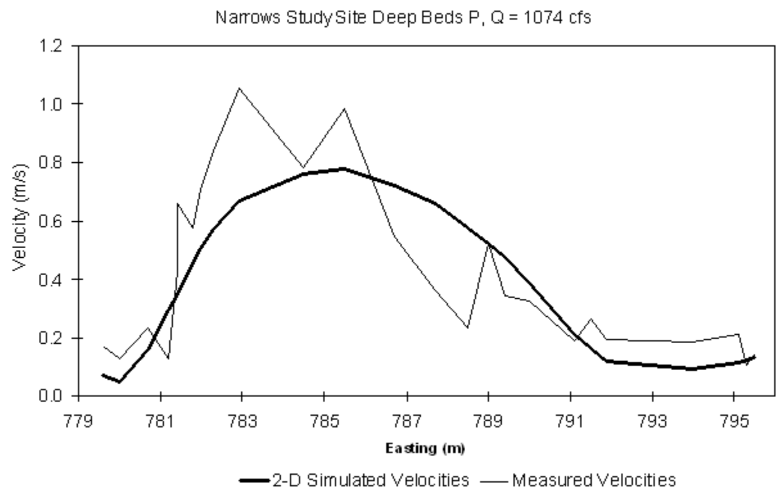
Narrows Study Site Deep Beds P, Q = 1074 cfs
Velocity (m/s)
1.2
1.0
0.8
0.6
0.4
0.2
0.0
779
781
783
785
787
789
791
793
795
Easting (m)
2-D Simulated Velocities
Measured Velocities

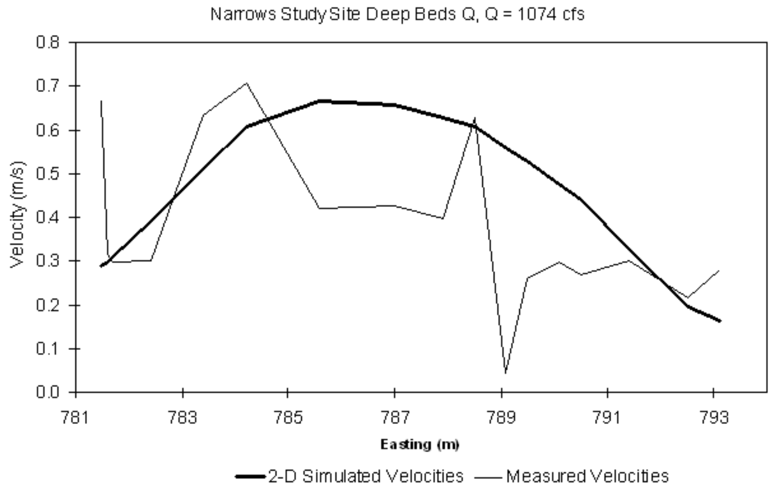
Narrows Study Site Deep Beds Q, Q = 1074 cfs
Velocity (m/s)
Easting (m)
2-D Simulated Velocities
Measured Velocities

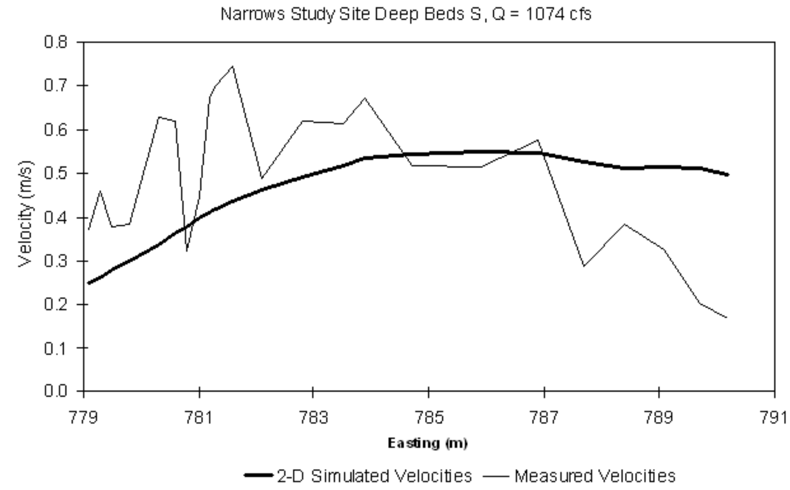
Narrows Study Site Deep Beds S, Q = 1074 cfs
Velocity (m/s)
Easting (m)
2-D Simulated Velocities
Measured Velocities

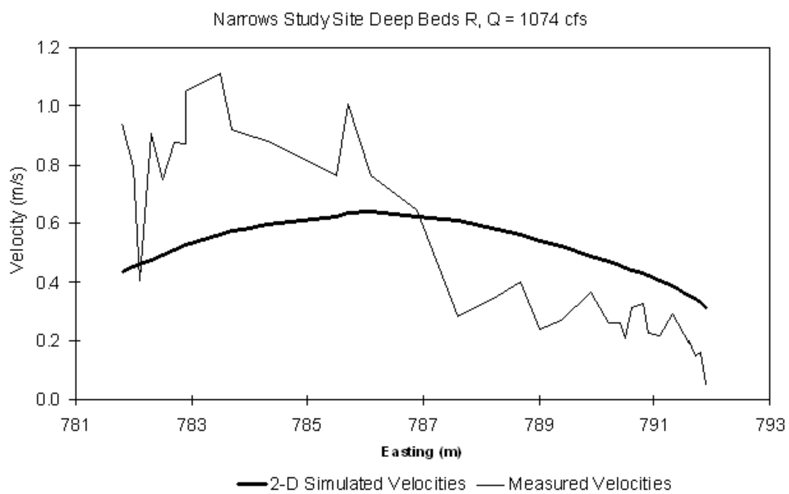
Narrows Study Site Deep Beds R, Q = 1074 cfs
Velocity (m/s)
Easting (m)
2-D Simulated Velocities
Measured Velocities

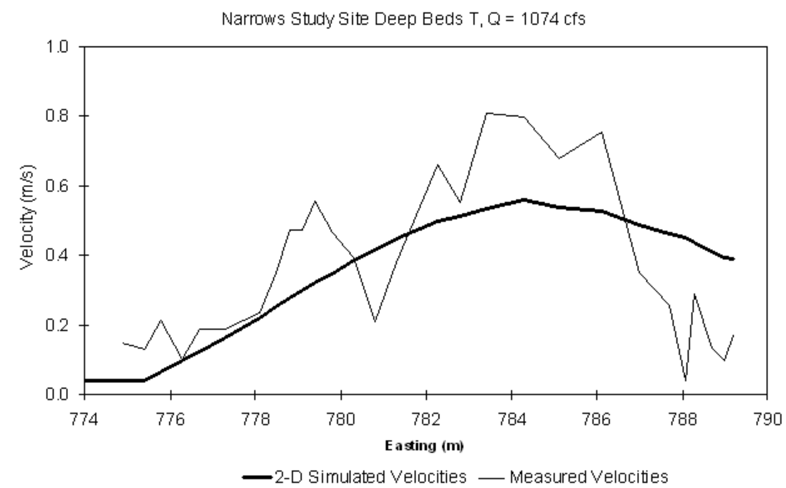
Narrows Study Site Deep Beds T, Q = 1074 cfs
Velocity (m/s)
Easting (m)
2-D Simulated Velocities
Measured Velocities

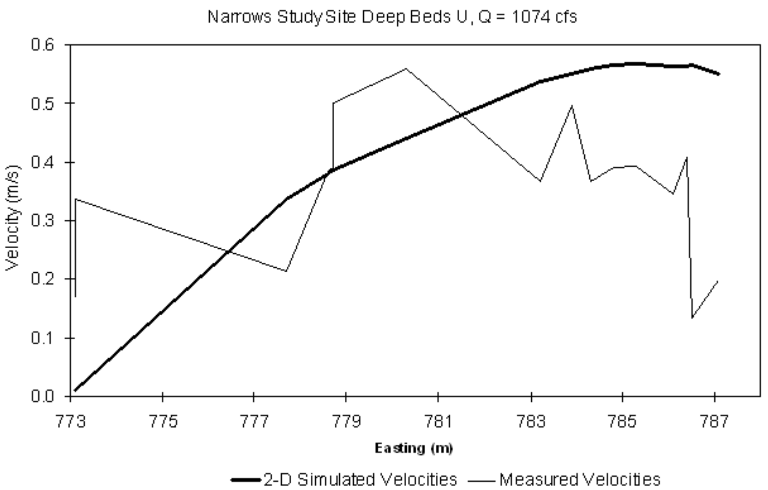
Narrows Study Site Deep Beds U, Q = 1074 cfs
Velocity (m/s)
0.0
0.1
0.2
0.3
0.4
0.5
0.6
773
775
777
779
781
783
785
787
Easting (m)
2-D Simulated Velocities
Measured Velocities

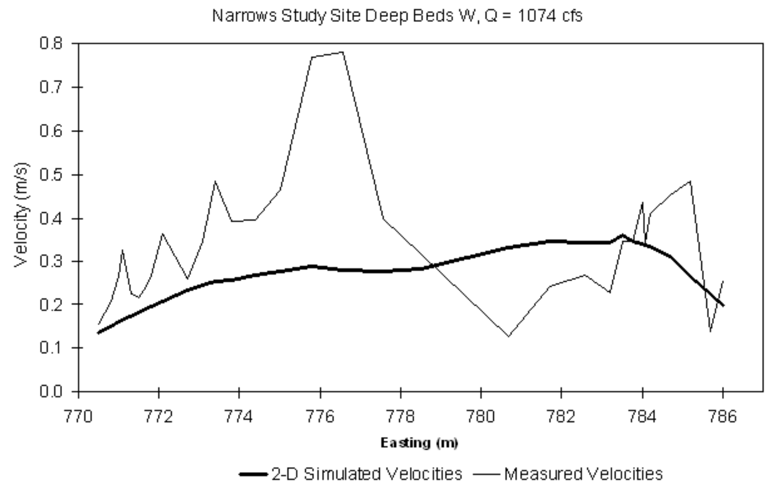
Narrows Study Site Deep Beds W, Q = 1074 cfs
Velocity (m/s)
0.0
0.1
0.2
0.3
0.4
0.5
0.6
0.7
0.8
770
772
774
776
778
780
782
784
786
Easting (m)
2-D Simulated Velocities
Measured Velocities

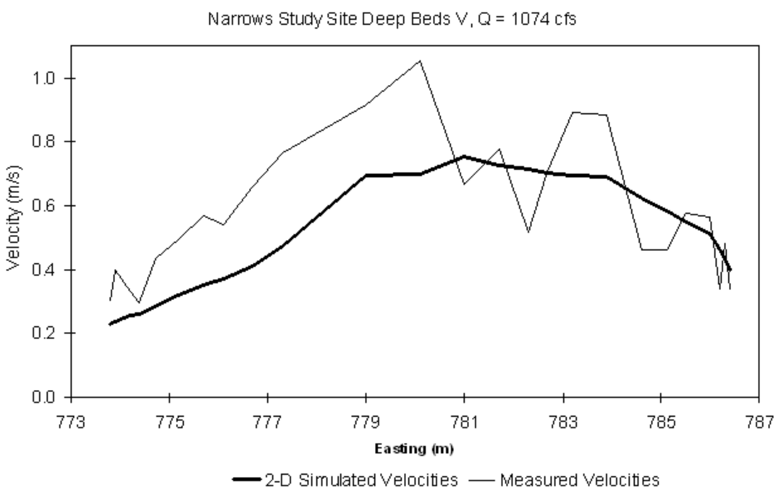
Narrows Study Site Deep Beds V, Q = 1074 cfs
Velocity (m/s)
0.0
0.2
0.4
0.6
0.8
1.0
773
775
777
779
781
783
785
787
Easting (m)
2-D Simulated Velocities
Measured Velocities

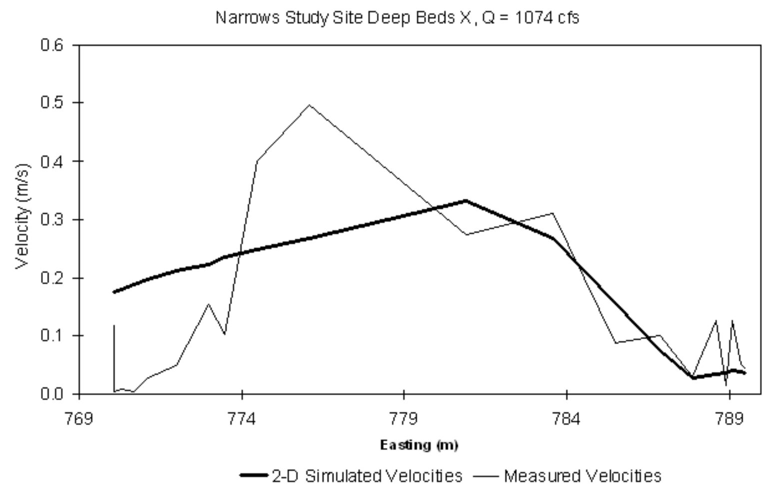
Narrows Study Site Deep Beds X, Q = 1074 cfs
Velocity (m/s)
0.0
0.1
0.2
0.3
0.4
0.5
0.6
769
774
779
784
789
Easting (m)
2-D Simulated Velocities
Measured Velocities

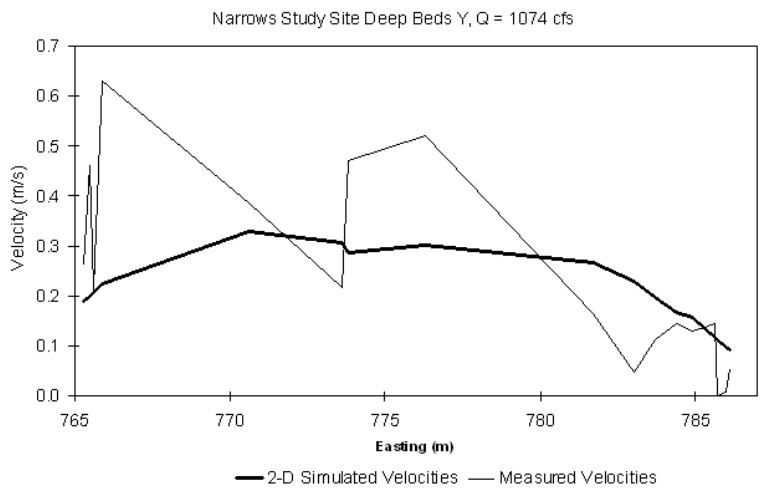
Narrows Study Site Deep Beds Y, Q = 1074 cfs
Velocity (m/s)
0.7
0.6
0.5
0.4
0.3
0.2
0.1
0.0
765
770
775
780
785
Easting (m)
2-D Simulated Velocities
Measured Velocities

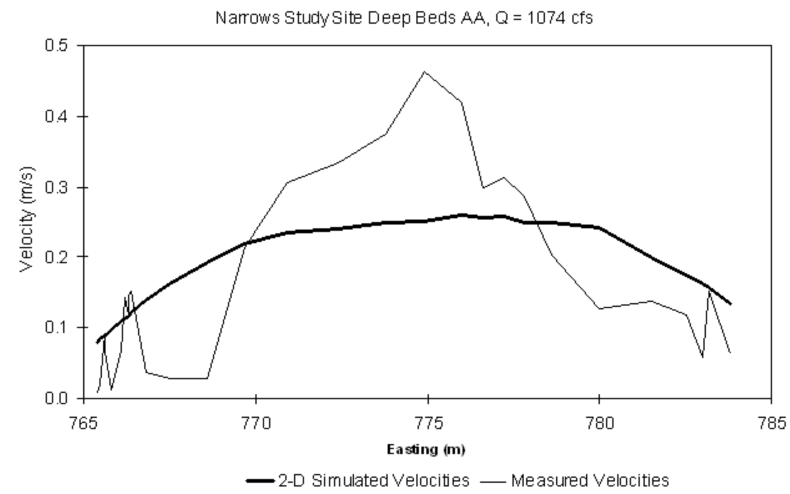
Narrows Study Site Deep Beds AA, Q = 1074 cfs
Velocity (m/s)
0.5
0.4
0.3
0.2
0.1
0.0
765
770
775
780
785
Easting (m)
2-D Simulated Velocities
Measured Velocities

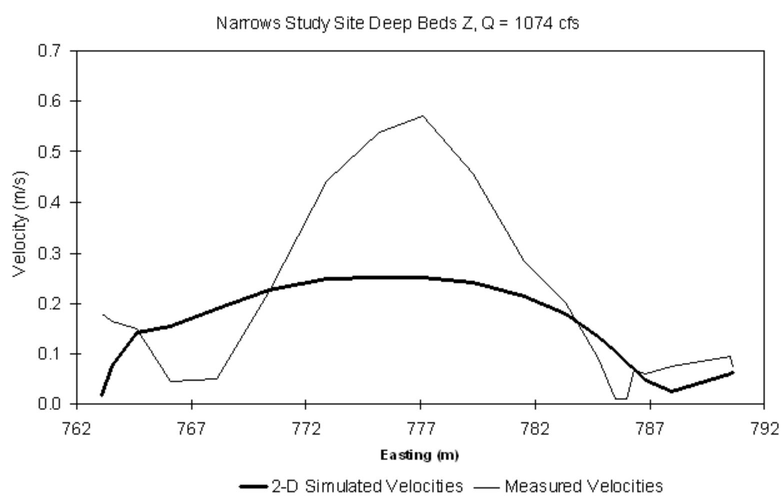
Narrows Study Site Deep Beds Z, Q = 1074 cfs
Velocity (m/s)
0.7
0.6
0.5
0.4
0.3
0.2
0.1
0.0
762
767
772
777
782
787
792
Easting (m)
2-D Simulated Velocities
Measured Velocities

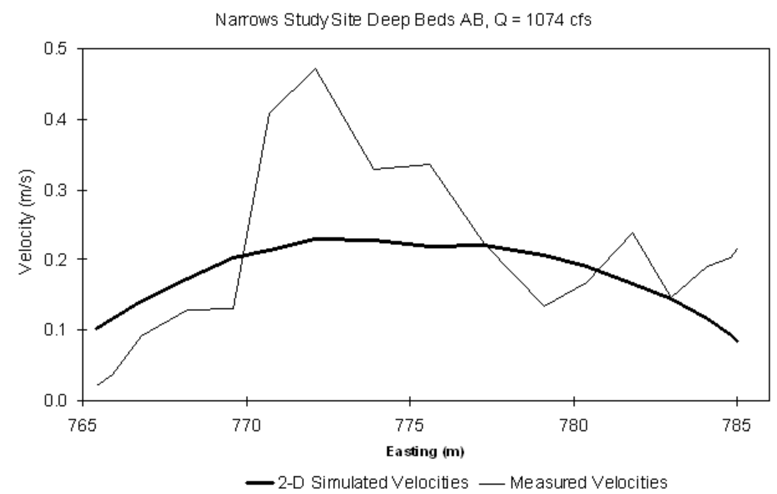
Narrows Study Site Deep Beds AB, Q = 1074 cfs
Velocity (m/s)
0.5
0.4
0.3
0.2
0.1
0.0
765
770
775
780
785
Easting (m)
2-D Simulated Velocities
Measured Velocities

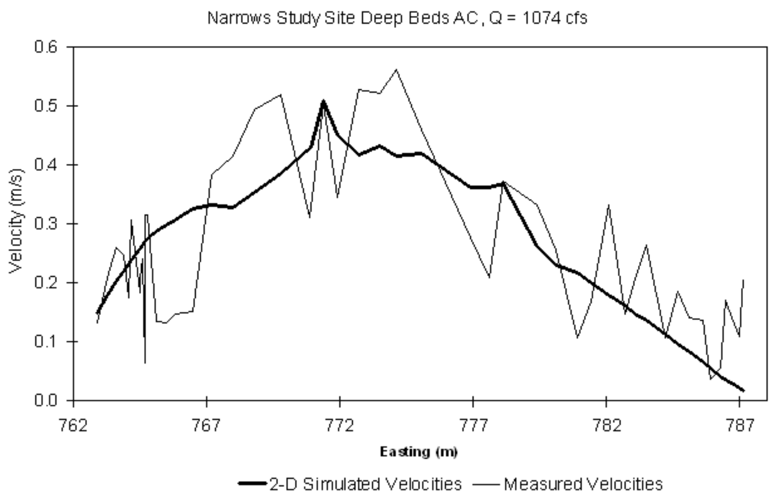
Narrows Study Site Deep Beds AC, Q = 1074 cfs
Velocity (m/s)
0.6
0.5
0.4
0.3
0.2
0.1
0.0
762
767
772
777
782
787
Easting (m)
2-D Simulated Velocities
Measured Velocities

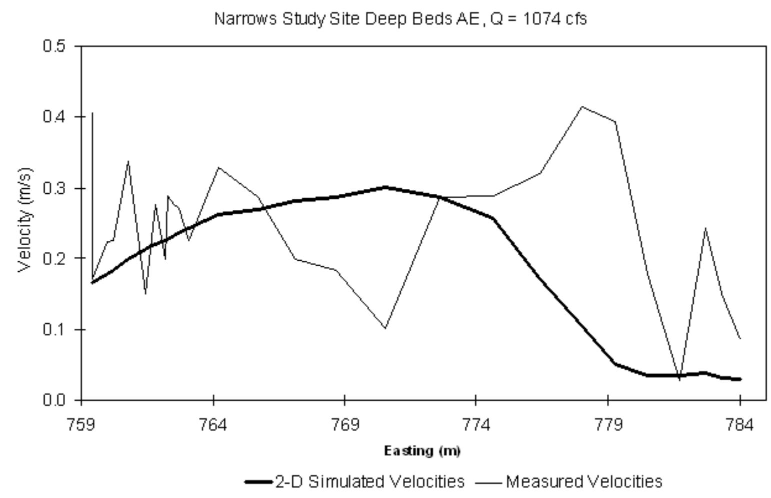
Narrows Study Site Deep Beds AE, Q = 1074 cfs
Velocity (m/s)
0.5
0.4
0.3
0.2
0.1
0.0
759
764
769
774
779
784
Easting (m)
2-D Simulated Velocities
Measured Velocities

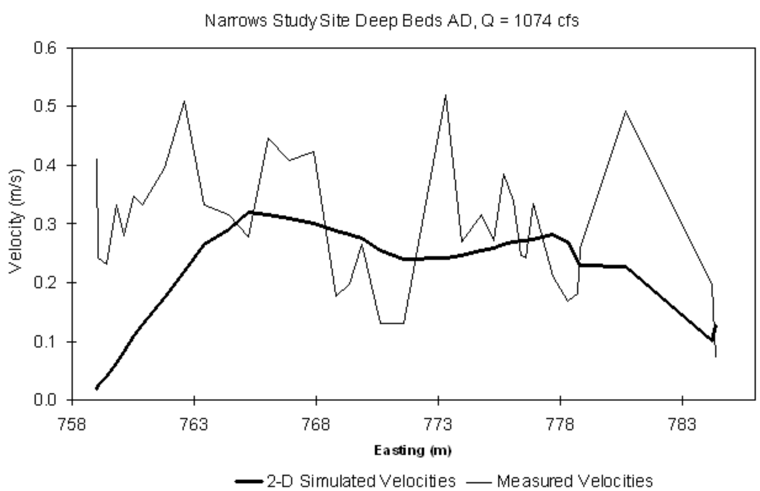
Narrows Study Site Deep Beds AD, Q = 1074 cfs
Velocity (m/s)
0.6
0.5
0.4
0.3
0.2
0.1
0.0
758
763
768
773
778
783
Easting (m)
2-D Simulated Velocities
Measured Velocities

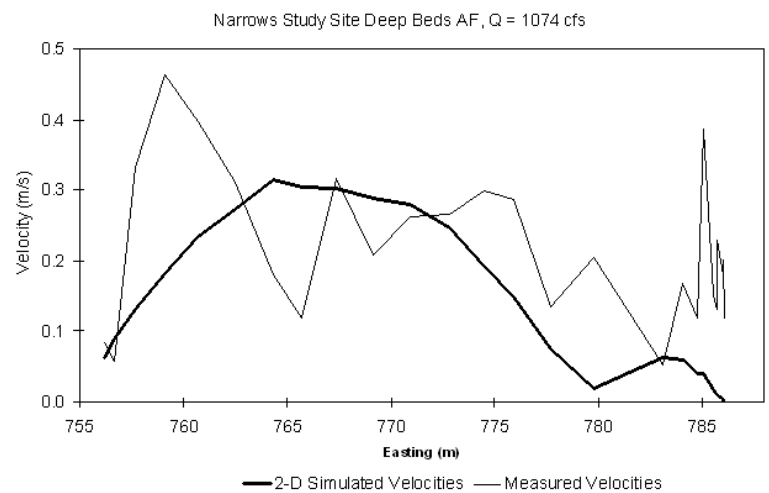
Narrows Study Site Deep Beds AF, Q = 1074 cfs
Velocity (m/s)
0.5
0.4
0.3
0.2
0.1
0.0
755
760
765
770
775
780
785
Easting (m)
2-D Simulated Velocities
Measured Velocities

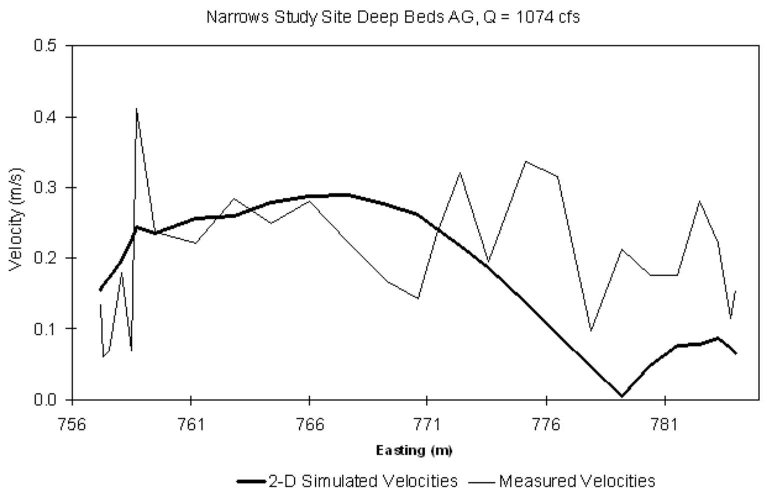
Narrows Study Site Deep Beds AG, Q = 1074 cfs
Velocity (m/s)
0.5
0.4
0.3
0.2
0.1
0.0
756
761
766
771
776
781
Easting (m)
2-D Simulated Velocities
Measured Velocities

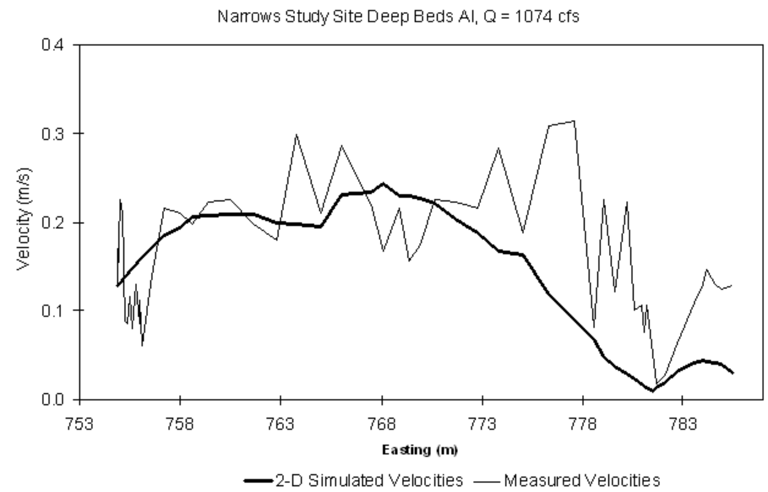
Narrows Study Site Deep Beds AI, Q = 1074 cfs
Velocity (m/s)
0.4
0.3
0.2
0.1
0.0
753
758
763
768
773
778
783
Easting (m)
2-D Simulated Velocities
Measured Velocities

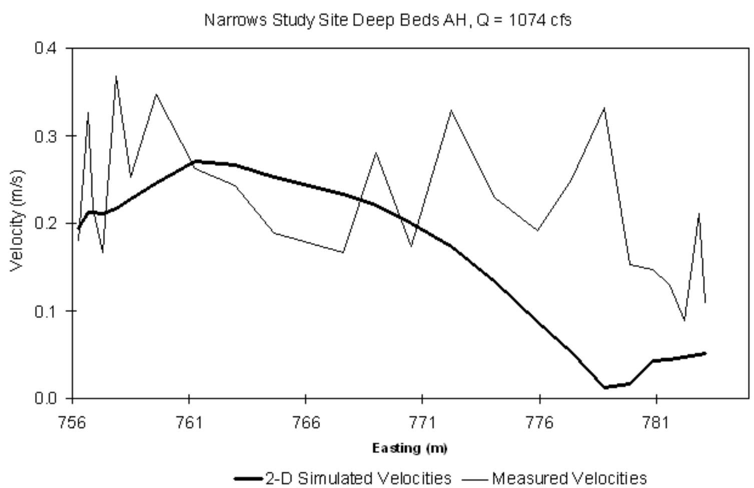
Narrows Study Site Deep Beds AH, Q = 1074 cfs
Velocity (m/s)
0.4
0.3
0.2
0.1
0.0
756
761
766
771
776
781
Easting (m)
2-D Simulated Velocities
Measured Velocities

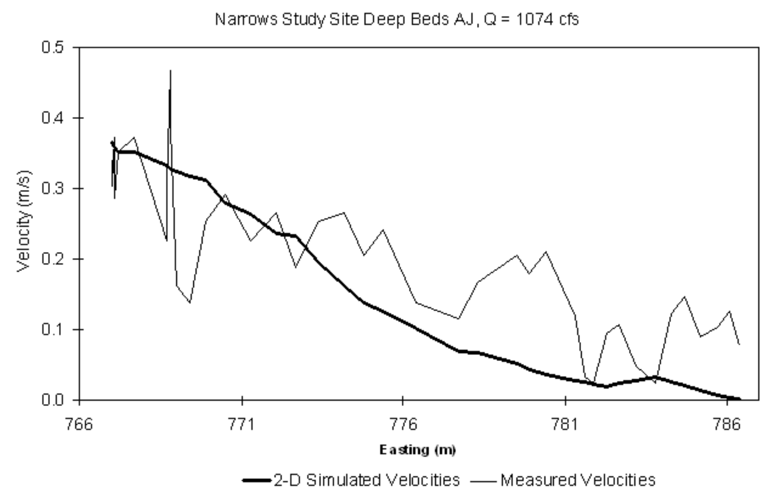
Narrows Study Site Deep Beds AJ, Q = 1074 cfs
Velocity (m/s)
0.5
0.4
0.3
0.2
0.1
0.0
766
771
776
781
786
Easting (m)
2-D Simulated Velocities
Measured Velocities

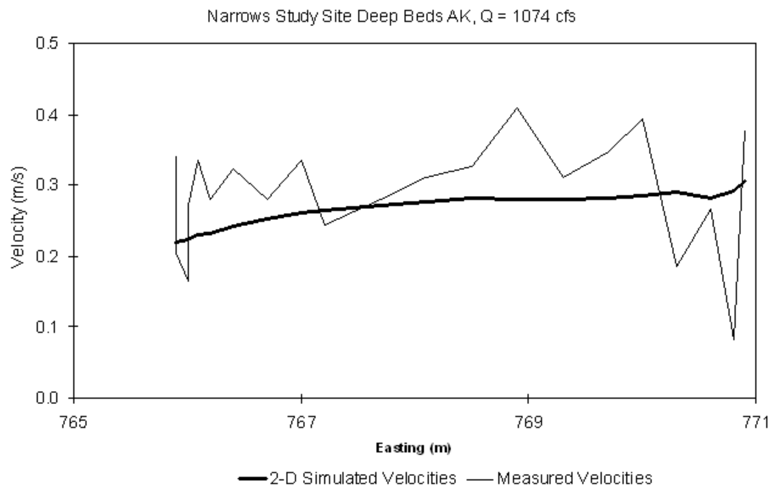
Narrows Study Site Deep Beds AK, Q = 1074 cfs
Velocity (m/s)
Easting (m)
2-D Simulated Velocities
Measured Velocities

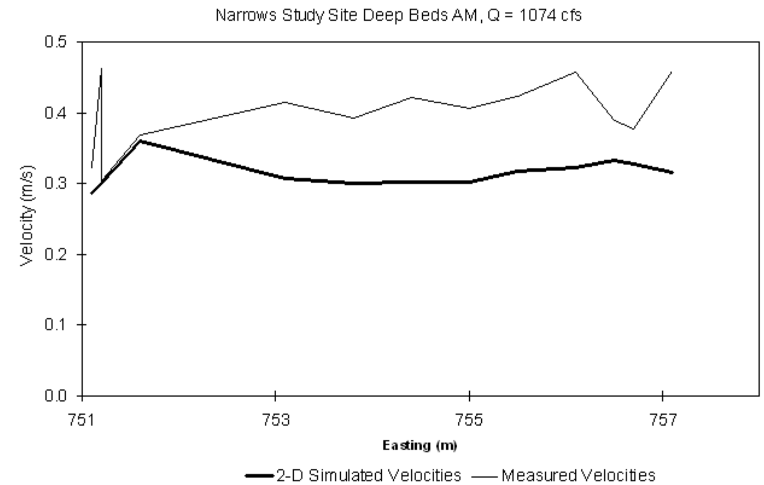
Narrows Study Site Deep Beds AM, Q = 1074 cfs
Velocity (m/s)
Easting (m)
2-D Simulated Velocities
Measured Velocities

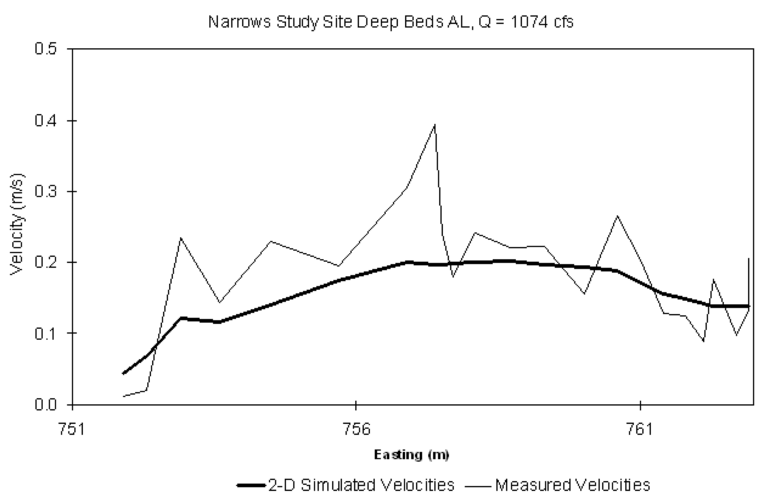
Narrows Study Site Deep Beds AL, Q = 1074 cfs
Velocity (m/s)
Easting (m)
2-D Simulated Velocities
Measured Velocities

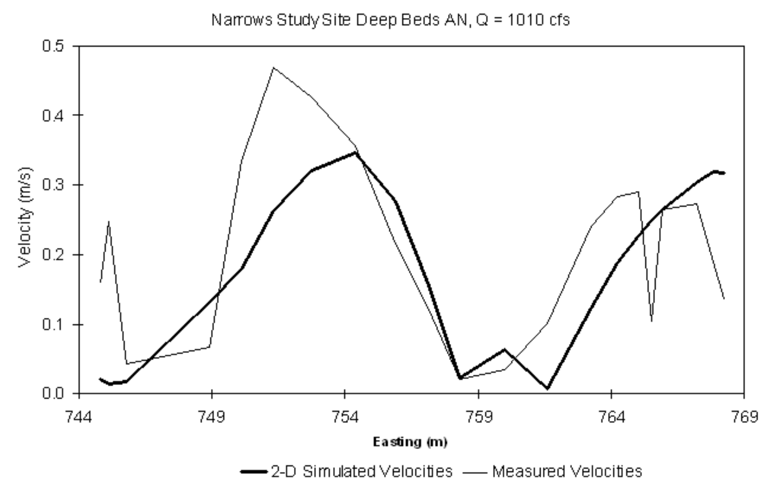
Narrows Study Site Deep Beds AN, Q = 1010 cfs
Velocity (m/s)
Easting (m)
2-D Simulated Velocities
Measured Velocities

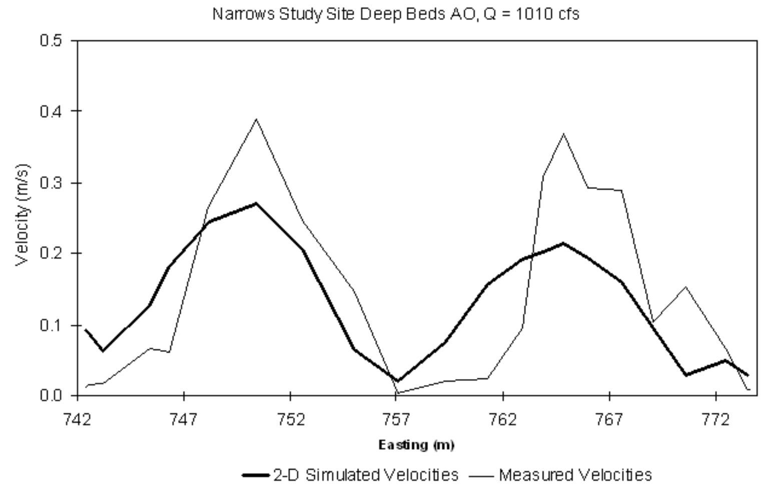
Narrows Study Site Deep Beds AO, Q = 1010 cfs
Velocity (m/s)
0.5
0.4
0.3
0.2
0.1
0.0
742
747
752
757
762
767
772
Easting (m)
2-D Simulated Velocities
Measured Velocities

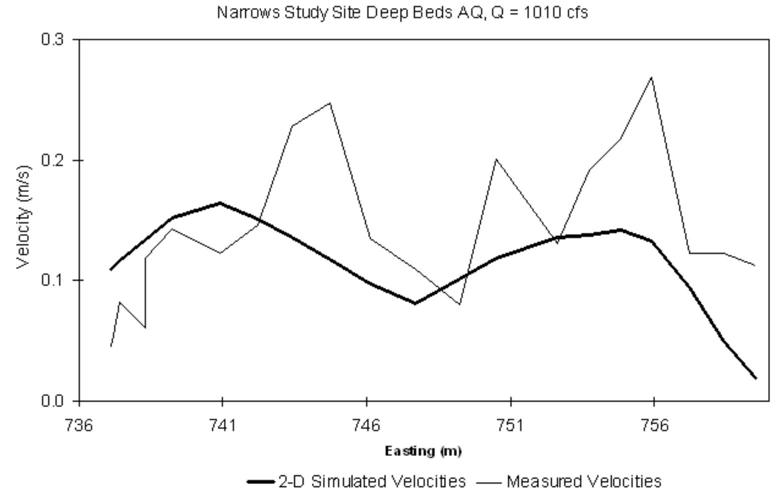
Narrows Study Site Deep Beds AQ, Q = 1010 cfs
Velocity (m/s)
0.3
0.2
0.1
0.0
736
741
746
751
756
Easting (m)
2-D Simulated Velocities
Measured Velocities

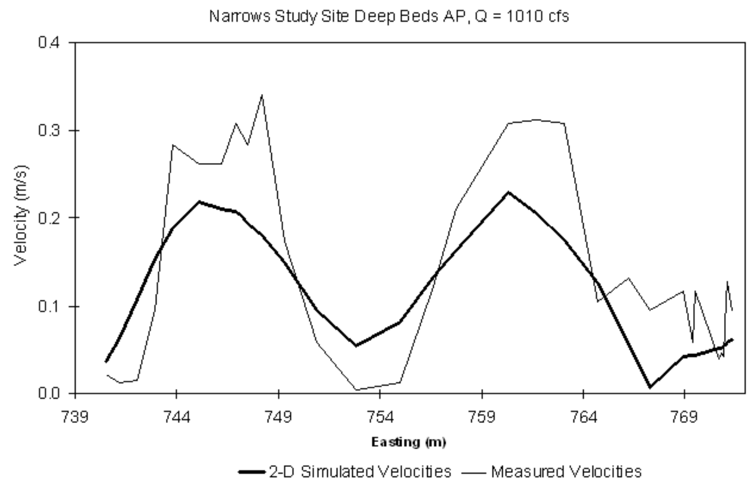
Narrows Study Site Deep Beds AP, Q = 1010 cfs
Velocity (m/s)
0.4
0.3
0.2
0.1
0.0
739
744
749
754
759
764
769
Easting (m)
2-D Simulated Velocities
Measured Velocities

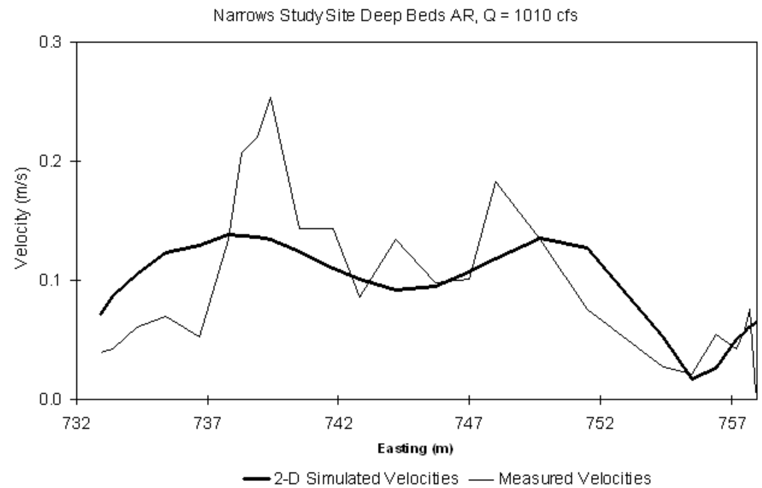
Narrows Study Site Deep Beds AR, Q = 1010 cfs
Velocity (m/s)
0.3
0.2
0.1
0.0
732
737
742
747
752
757
Easting (m)
2-D Simulated Velocities
Measured Velocities

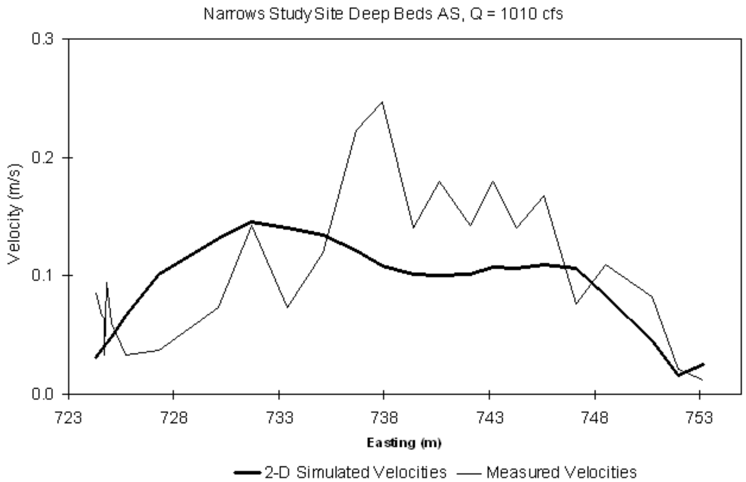
Narrows Study Site Deep Beds AS, Q = 1010 cfs
Velocity (m/s)
0.3
0.2
0.1
0.0
723
728
733
738
743
748
753
Easting (m)
2-D Simulated Velocities
Measured Velocities

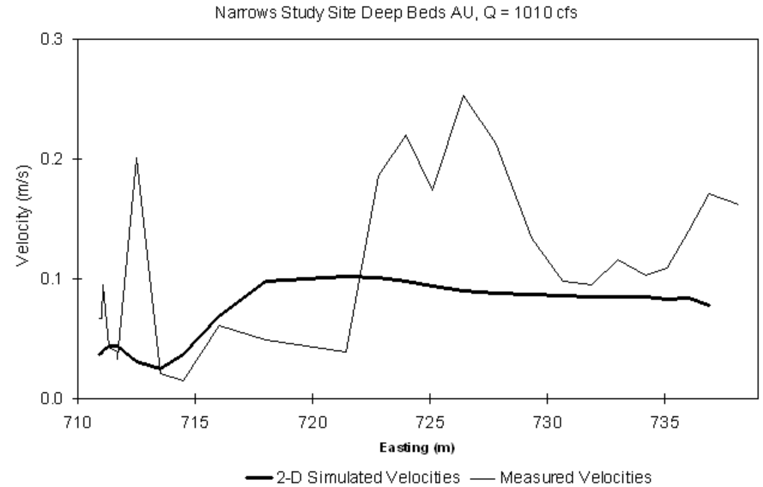
Narrows Study Site Deep Beds AU, Q = 1010 cfs
Velocity (m/s)
0.3
0.2
0.1
0.0
710
715
720
725
730
735
Easting (m)
2-D Simulated Velocities
Measured Velocities

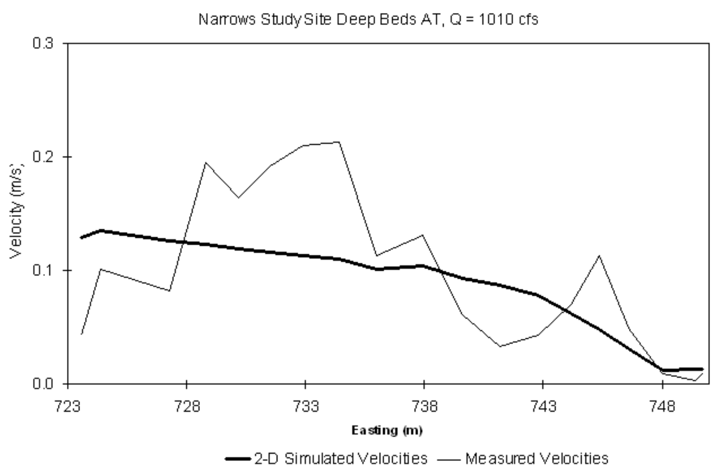
Narrows Study Site Deep Beds AT, Q = 1010 cfs
Velocity (m/s)
0.3
0.2
0.1
0.0
723
728
733
738
743
748
Easting (m)
2-D Simulated Velocities
Measured Velocities

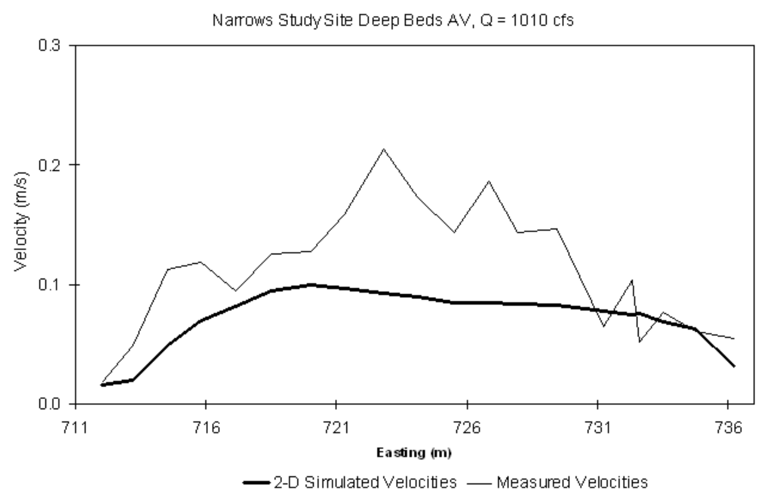
Narrows Study Site Deep Beds AV, Q = 1010 cfs
Velocity (m/s)
0.3
0.2
0.1
0.0
711
716
721
726
731
736
Easting (m)
2-D Simulated Velocities
Measured Velocities

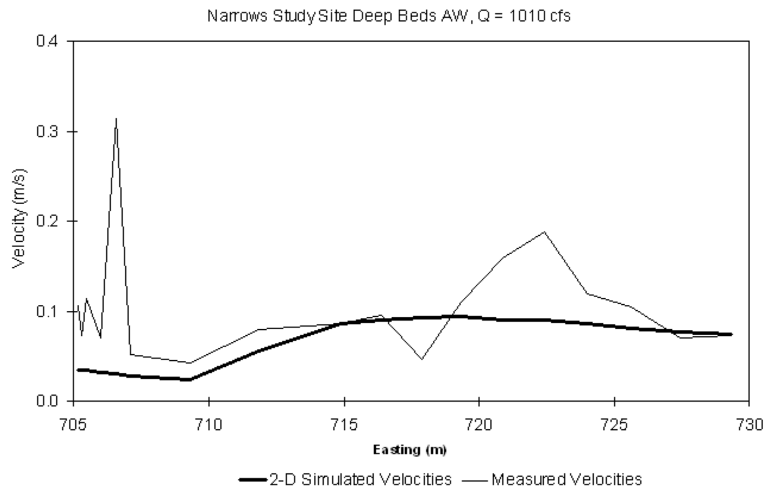
Narrows Study Site Deep Beds AW, Q = 1010 cfs
Velocity (m/s)
0.4
0.3
0.2
0.1
0.0
705
710
715
720
725
730
Easting (m)
2-D Simulated Velocities
Measured Velocities

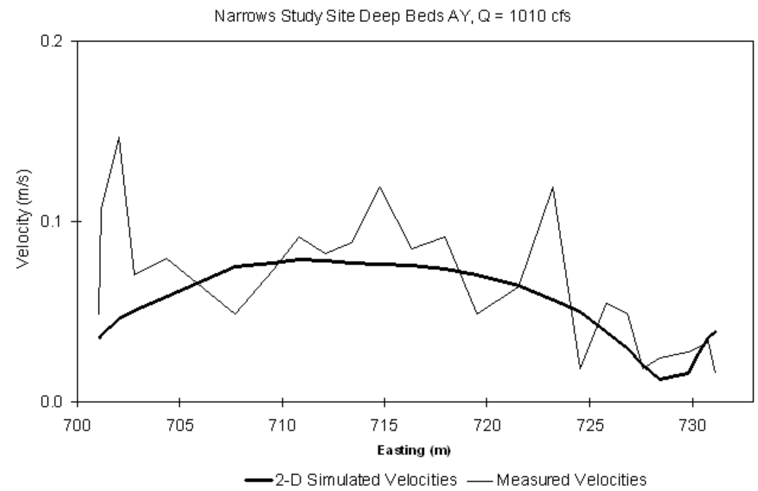
Narrows Study Site Deep Beds AY, Q = 1010 cfs
Velocity (m/s)
0.2
0.1
0.0
700
705
710
715
720
725
730
Easting (m)
2-D Simulated Velocities
Measured Velocities

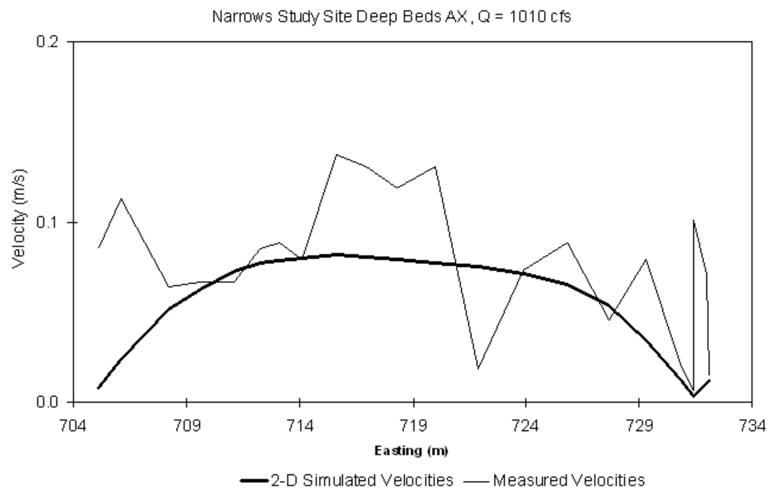
Narrows Study Site Deep Beds AX, Q = 1010 cfs
Velocity (m/s)
0.2
0.1
0.0
704
709
714
719
724
729
734
Easting (m)
2-D Simulated Velocities
Measured Velocities

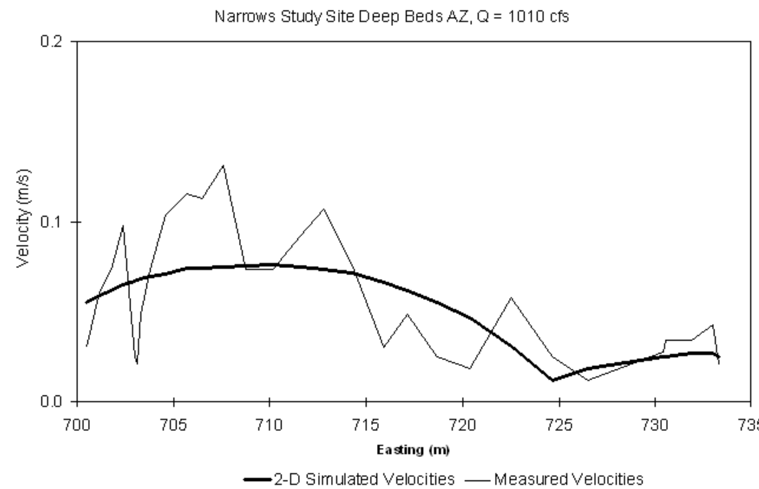
Narrows Study Site Deep Beds AZ, Q = 1010 cfs
Velocity (m/s)
0.2
0.1
0.0
700
705
710
715
720
725
730
735
Easting (m)
2-D Simulated Velocities
Measured Velocities

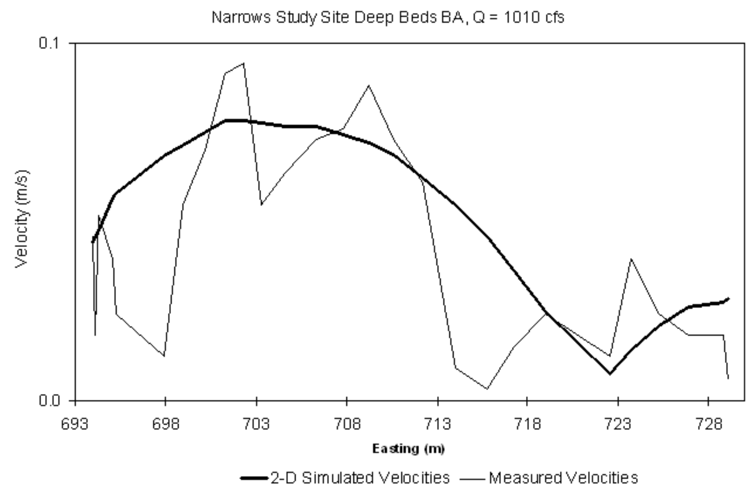
Narrows Study Site Deep Beds BA, Q = 1010 cfs
Velocity (m/s)
Easting (m)
2-D Simulated Velocities
Measured Velocities

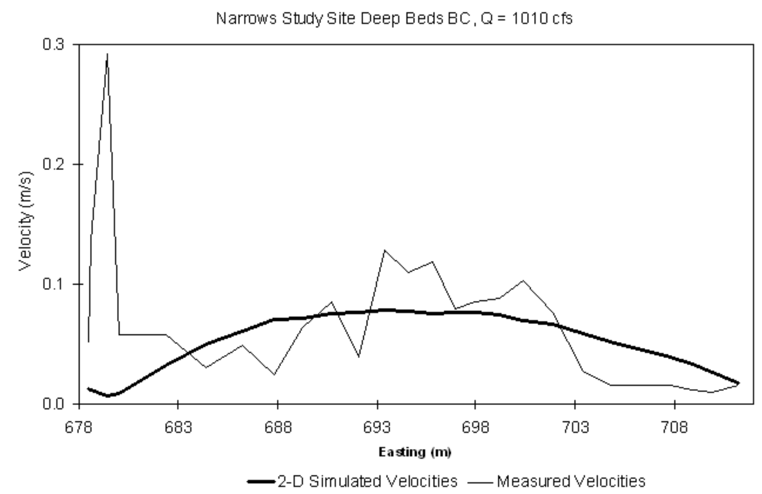
Narrows Study Site Deep Beds BC, Q = 1010 cfs
Velocity (m/s)
Easting (m)
2-D Simulated Velocities
Measured Velocities

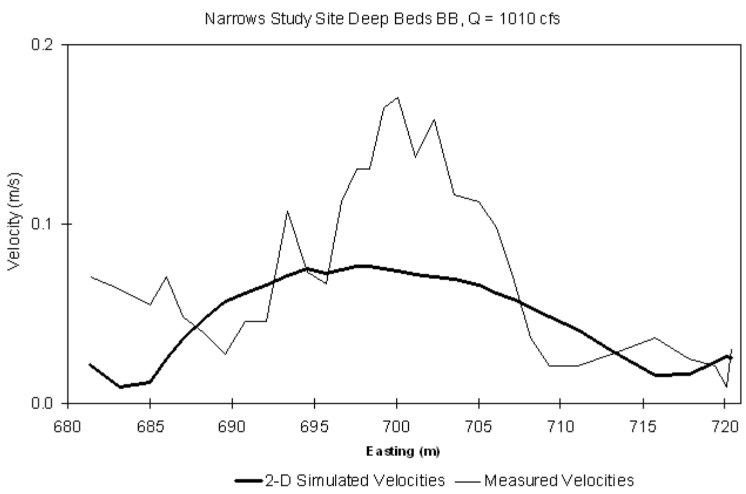
Narrows Study Site Deep Beds BB, Q = 1010 cfs
Velocity (m/s)
Easting (m)
2-D Simulated Velocities
Measured Velocities

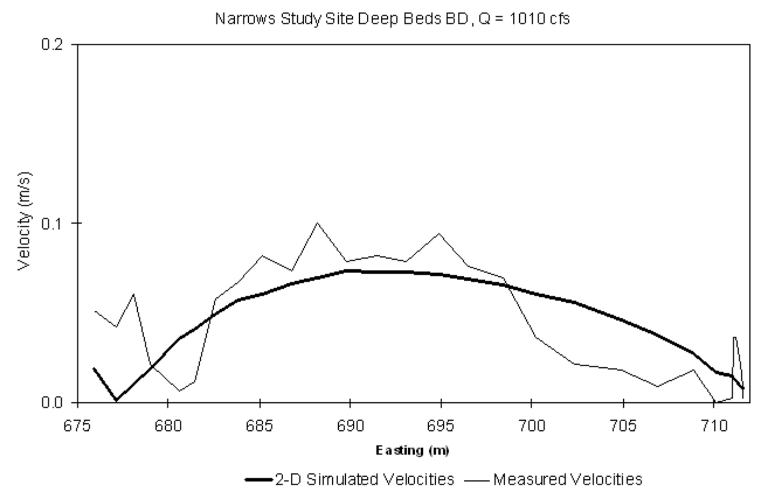
Narrows Study Site Deep Beds BD, Q = 1010 cfs
Velocity (m/s)
Easting (m)
2-D Simulated Velocities
Measured Velocities

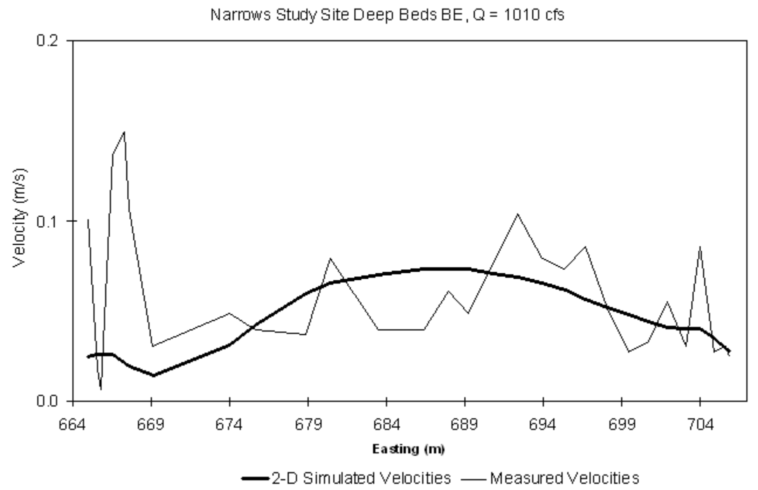

Narrows Study Site Deep Beds BE, Q = 1010 cfs
Velocity (m/s)
0.0
0.1
0.2
664
669
674
679
684
689
694
699
704
Easting (m)
2-D Simulated Velocities
Measured Velocities

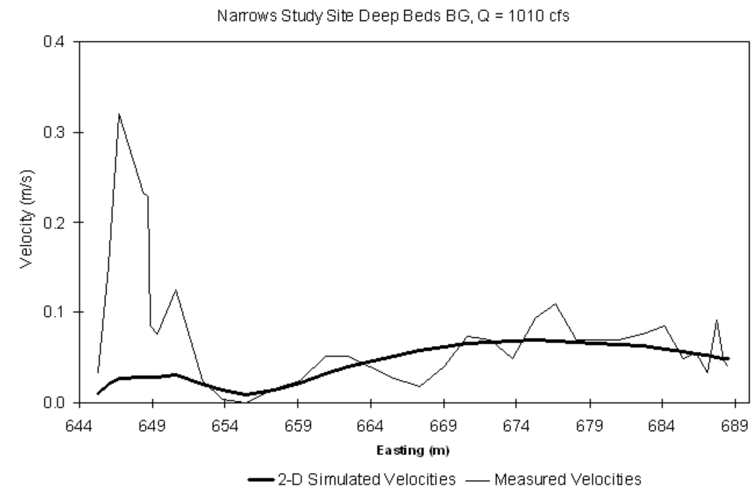

Narrows Study Site Deep Beds BG, Q = 1010 cfs
Velocity (m/s)
0.0
0.1
0.2
0.3
0.4
644
649
654
659
664
669
674
679
684
689
Easting (m)
2-D Simulated Velocities
Measured Velocities

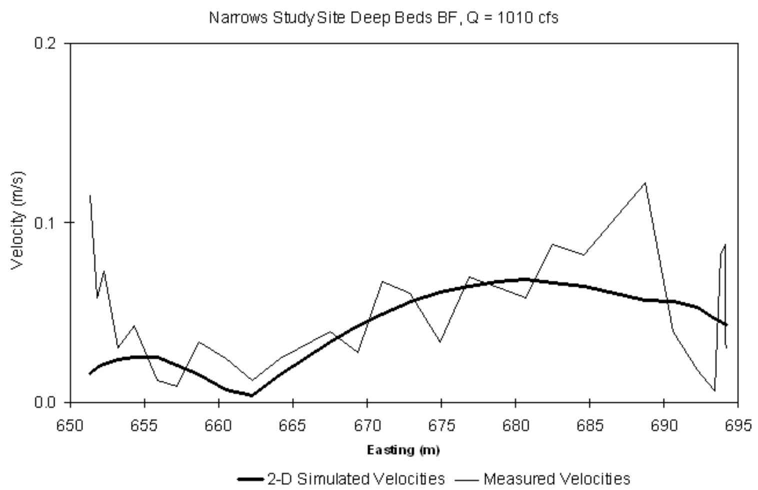

Narrows Study Site Deep Beds BF, Q = 1010 cfs
Velocity (m/s)
0.0
0.1
0.2
650
655
660
665
670
675
680
685
690
695
Easting (m)
2-D Simulated Velocities
Measured Velocities

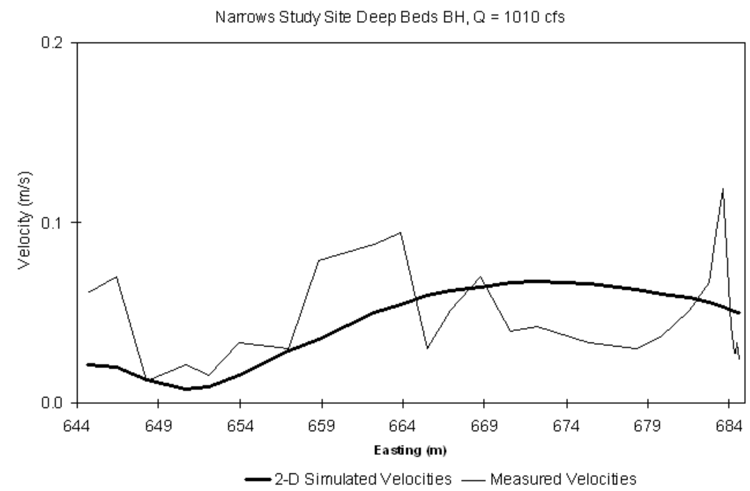

Narrows Study Site Deep Beds BH, Q = 1010 cfs
Velocity (m/s)
0.0
0.1
0.2
644
649
654
659
664
669
674
679
684
Easting (m)
2-D Simulated Velocities
Measured Velocities

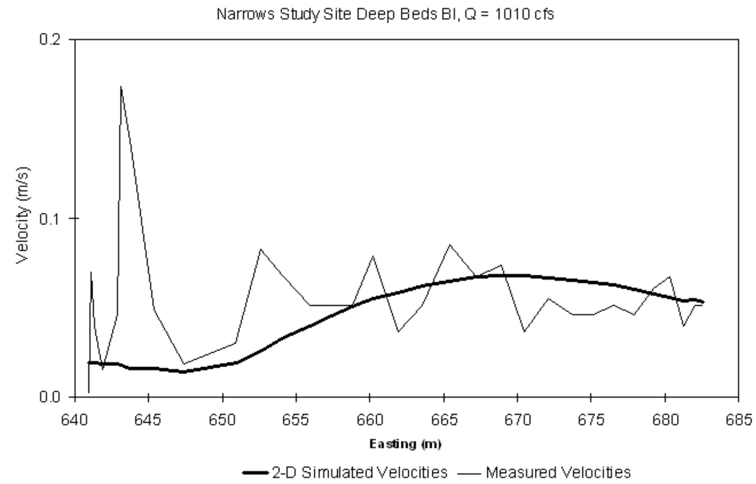
Narrows Study Site Deep Beds BI, Q = 1010 cfs
Velocity (m/s)
0.2
0.1
0.0
640
645
650
655
660
665
670
675
680
685
Easting (m)
2-D Simulated Velocities
Measured Velocities

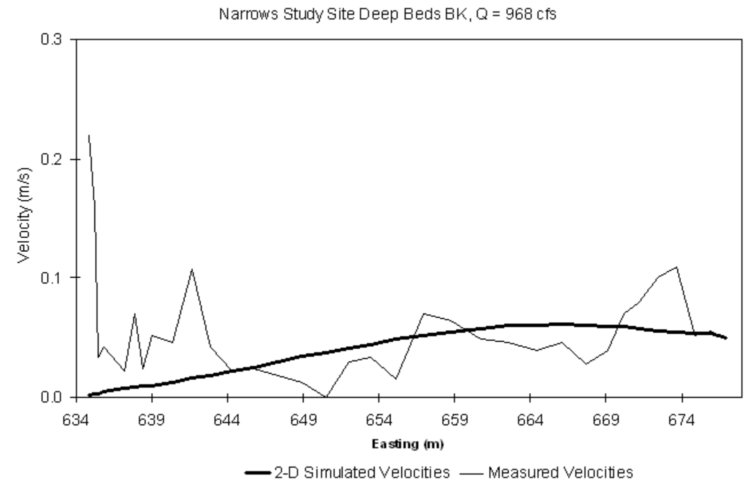
Narrows Study Site Deep Beds BK, Q = 968 cfs
Velocity (m/s)
0.3
0.2
0.1
0.0
634
639
644
649
654
659
664
669
674
Easting (m)
2-D Simulated Velocities
Measured Velocities

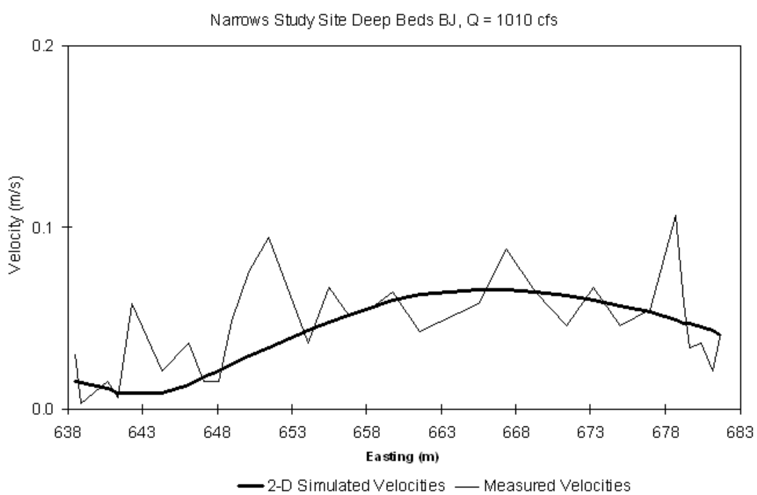
Narrows Study Site Deep Beds BJ, Q = 1010 cfs
Velocity (m/s)
0.2
0.1
0.0
638
643
648
653
658
663
668
673
678
683
Easting (m)
2-D Simulated Velocities
Measured Velocities

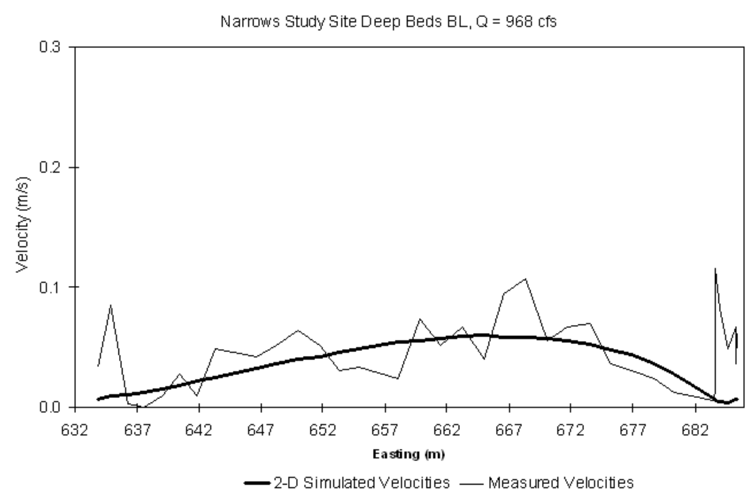
Narrows Study Site Deep Beds BL, Q = 968 cfs
Velocity (m/s)
0.3
0.2
0.1
0.0
632
637
642
647
652
657
662
667
672
677
682
Easting (m)
2-D Simulated Velocities
Measured Velocities

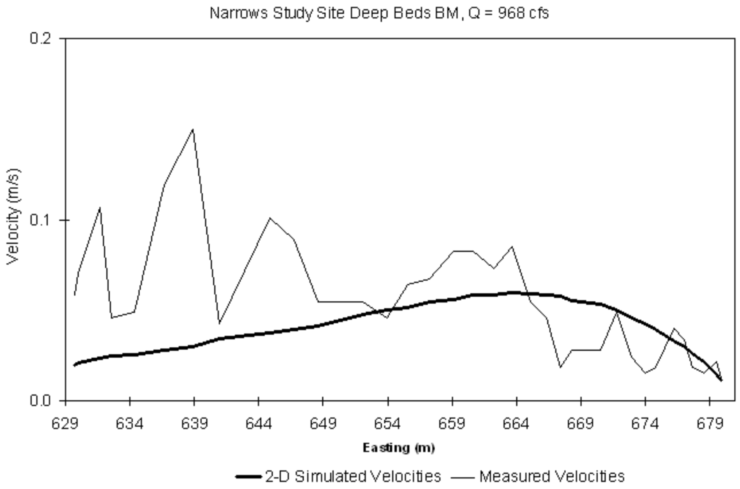
Narrows Study Site Deep Beds BM, Q = 968 cfs
Velocity (m/s)
0.2
0.1
0.0
629
634
639
644
649
654
659
664
669
674
679
Easting (m)
2-D Simulated Velocities
Measured Velocities

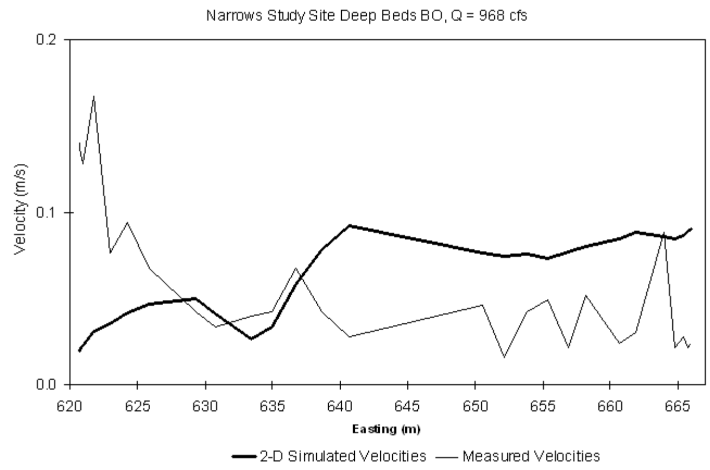
Narrows Study Site Deep Beds BO, Q = 968 cfs
Velocity (m/s)
0.2
0.1
0.0
620
625
630
635
640
645
650
655
660
665
Easting (m)
2-D Simulated Velocities
Measured Velocities

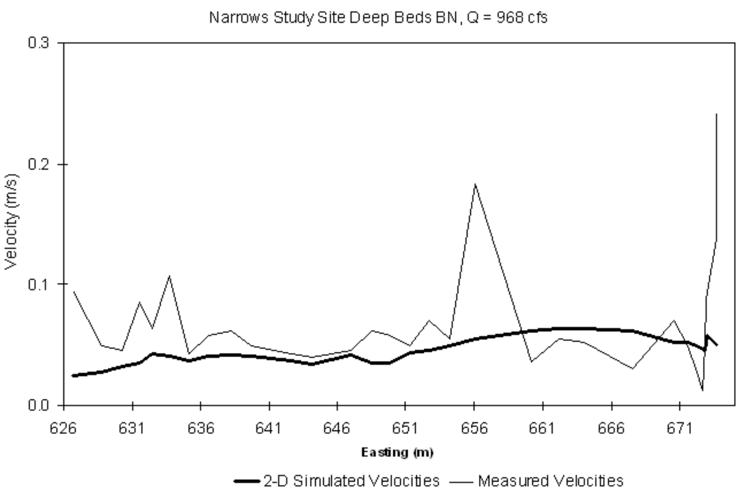
Narrows Study Site Deep Beds BN, Q = 968 cfs
Velocity (m/s)
0.3
0.2
0.1
0.0
626
631
636
641
646
651
656
661
666
671
Easting (m)
2-D Simulated Velocities
Measured Velocities

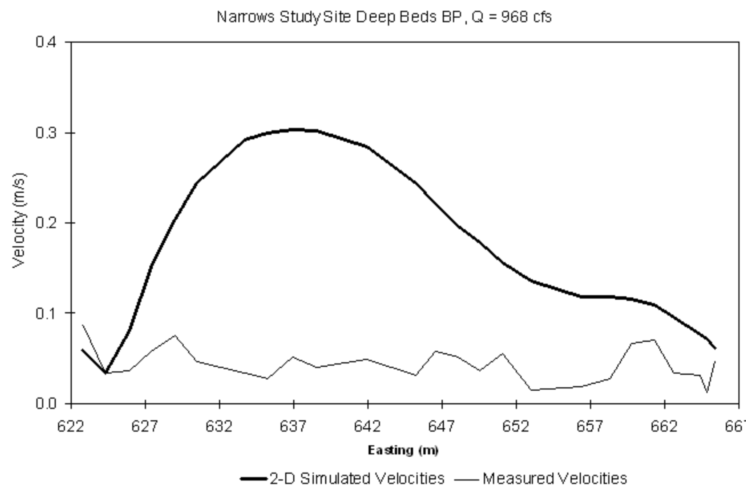
Narrows Study Site Deep Beds BP, Q = 968 cfs
Velocity (m/s)
0.4
0.3
0.2
0.1
0.0
622
627
632
637
642
647
652
657
662
667
Easting (m)
2-D Simulated Velocities
Measured Velocities

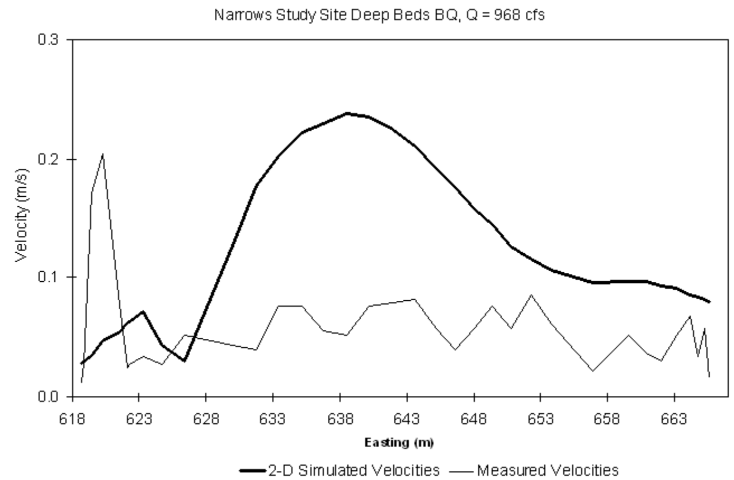
Narrows Study Site Deep Beds BQ, Q = 968 cfs
Velocity (m/s)
Easting (m)
2-D Simulated Velocities
Measured Velocities

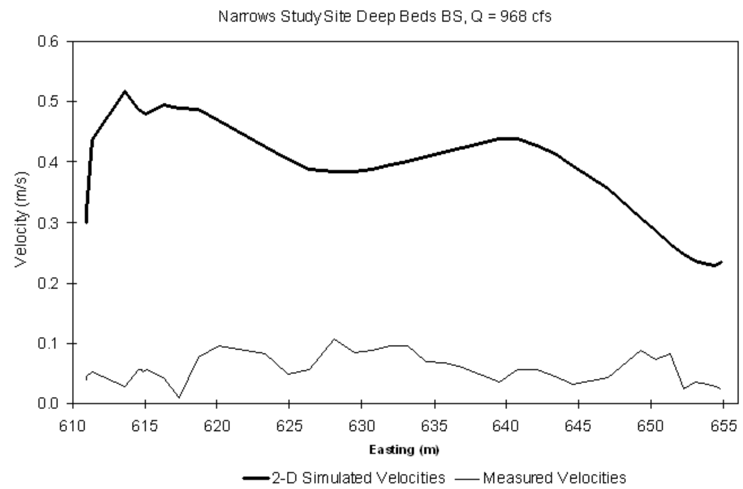
Narrows Study Site Deep Beds BS, Q = 968 cfs
Velocity (m/s)
Easting (m)
2-D Simulated Velocities
Measured Velocities

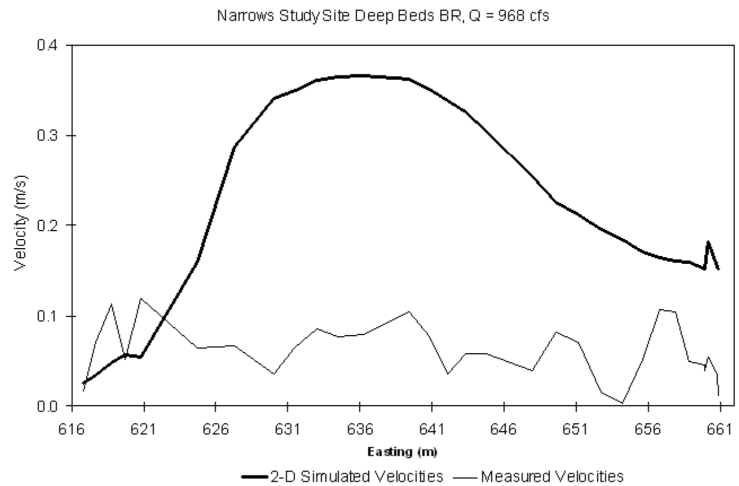
Narrows Study Site Deep Beds BR, Q = 968 cfs
Velocity (m/s)
Easting (m)
2-D Simulated Velocities
Measured Velocities

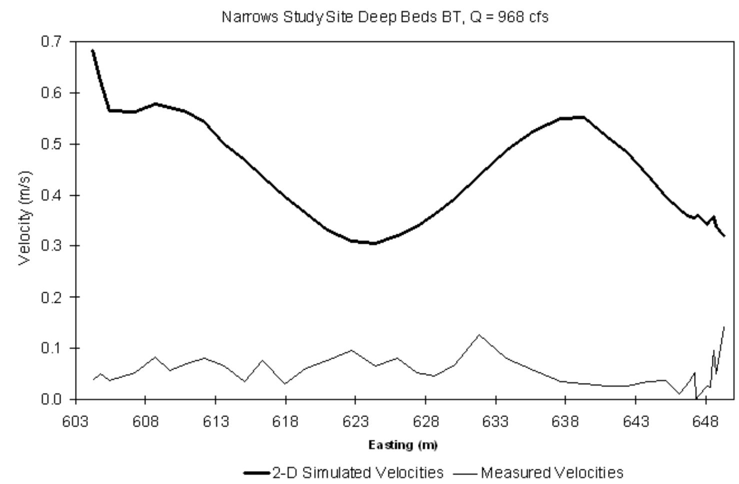
Narrows Study Site Deep Beds BT, Q = 968 cfs
Velocity (m/s)
Easting (m)
2-D Simulated Velocities
Measured Velocities

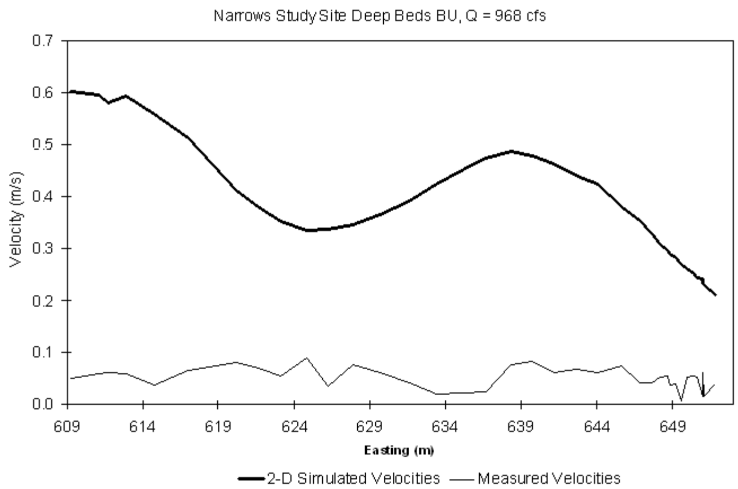
Narrows Study Site Deep Beds BU, Q = 968 cfs
Velocity (m/s)
0.0
0.1
0.2
0.3
0.4
0.5
0.6
0.7
609
614
619
624
629
634
639
644
649
Easting (m)
2-D Simulated Velocities
Measured Velocities

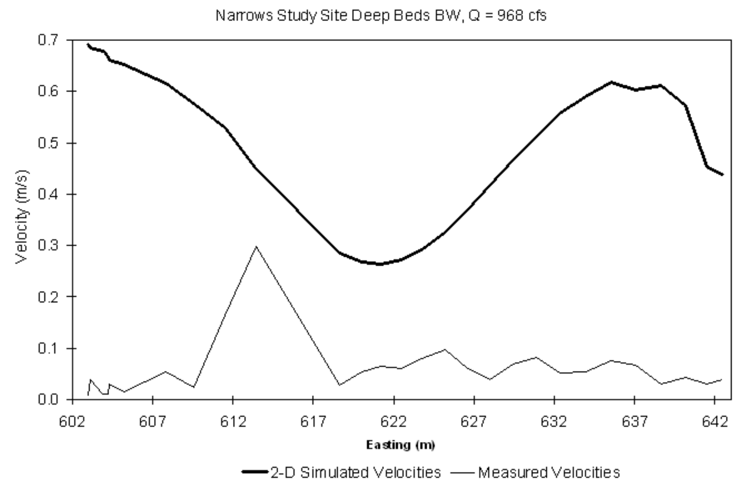
Narrows Study Site Deep Beds BW, Q = 968 cfs
Velocity (m/s)
0.0
0.1
0.2
0.3
0.4
0.5
0.6
0.7
602
607
612
617
622
627
632
637
642
Easting (m)
2-D Simulated Velocities
Measured Velocities

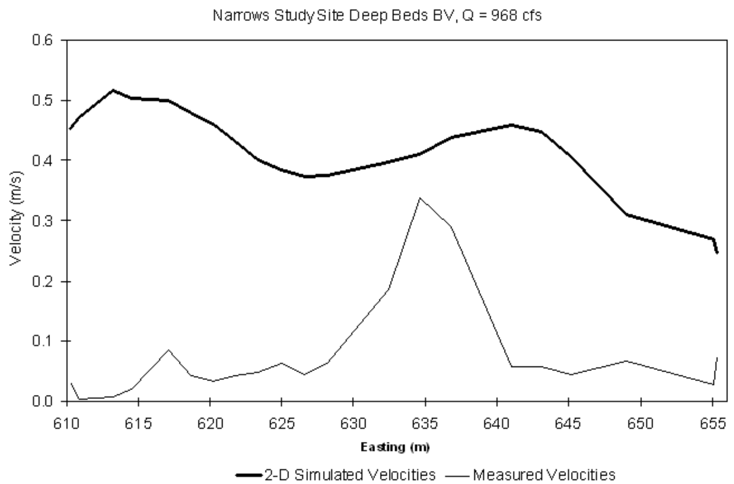
Narrows Study Site Deep Beds BV, Q = 968 cfs
Velocity (m/s)
0.0
0.1
0.2
0.3
0.4
0.5
0.6
610
615
620
625
630
635
640
645
650
655
Easting (m)
2-D Simulated Velocities
Measured Velocities

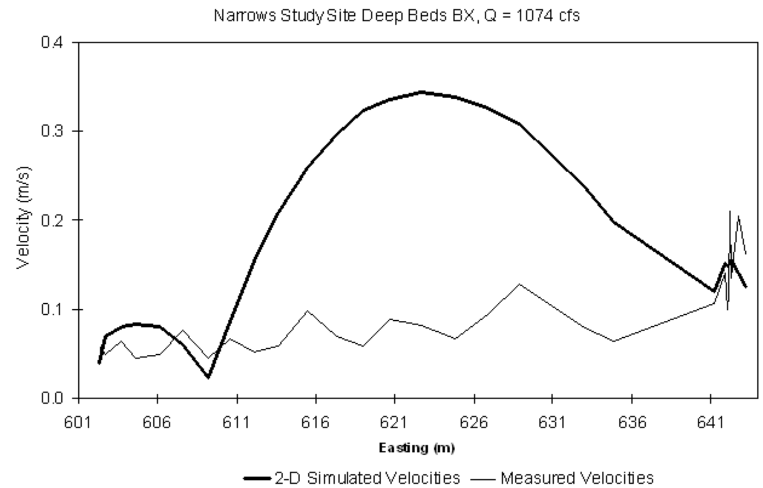
Narrows Study Site Deep Beds BX, Q = 1074 cfs
Velocity (m/s)
0.0
0.1
0.2
0.3
0.4
601
606
611
616
621
626
631
636
641
Easting (m)
2-D Simulated Velocities
Measured Velocities

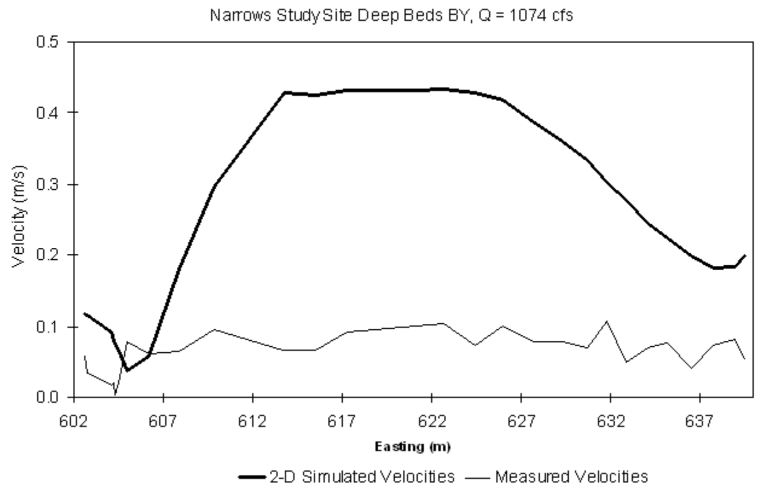
Narrows Study Site Deep Beds BY, Q = 1074 cfs
Velocity (m/s)
0.5
0.4
0.3
0.2
0.1
0.0
602
607
612
617
622
627
632
637
Easting (m)
2-D Simulated Velocities
Measured Velocities

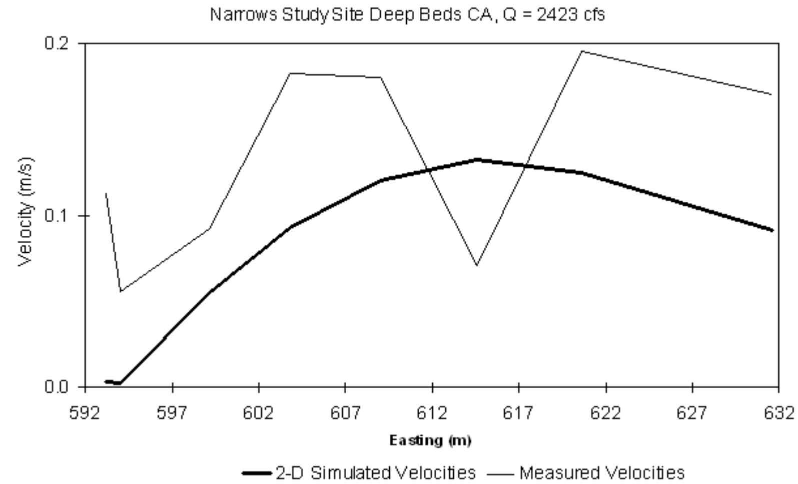
Narrows Study Site Deep Beds CA, Q = 2423 cfs
Velocity (m/s)
0.2
0.1
0.0
592
597
602
607
612
617
622
627
632
Easting (m)
2-D Simulated Velocities
Measured Velocities

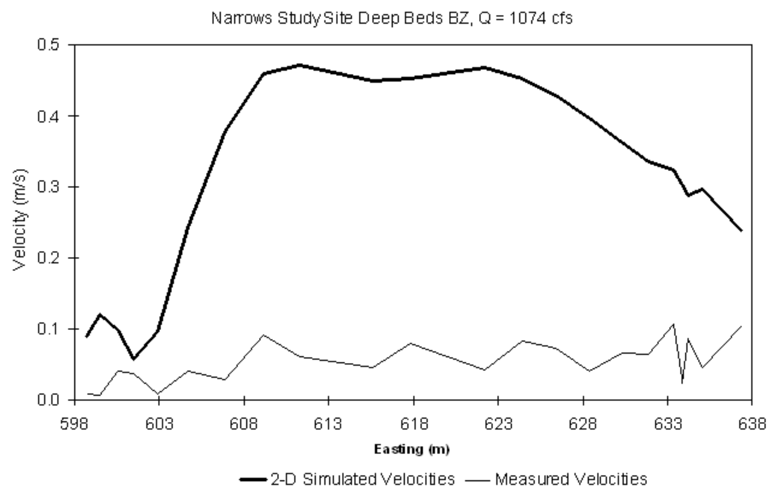
Narrows Study Site Deep Beds BZ, Q = 1074 cfs
Velocity (m/s)
0.5
0.4
0.3
0.2
0.1
0.0
598
603
608
613
618
623
628
633
638
Easting (m)
2-D Simulated Velocities
Measured Velocities

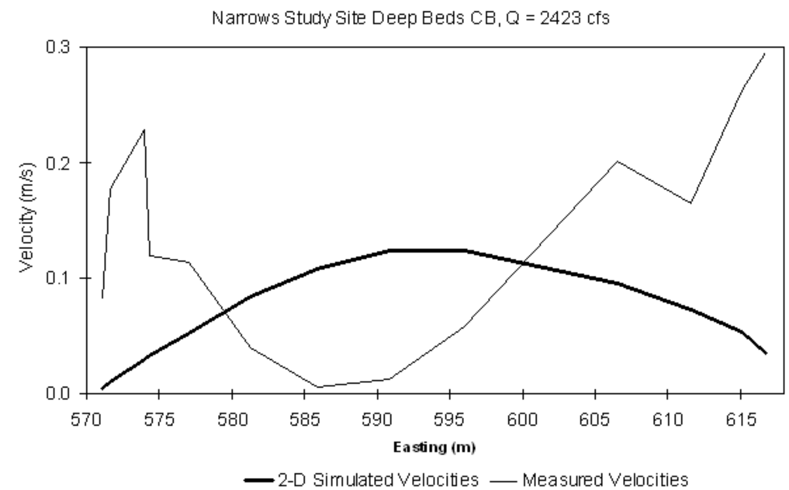
Narrows Study Site Deep Beds CB, Q = 2423 cfs
Velocity (m/s)
0.3
0.2
0.1
0.0
570
575
580
585
590
595
600
605
610
615
Easting (m)
2-D Simulated Velocities
Measured Velocities

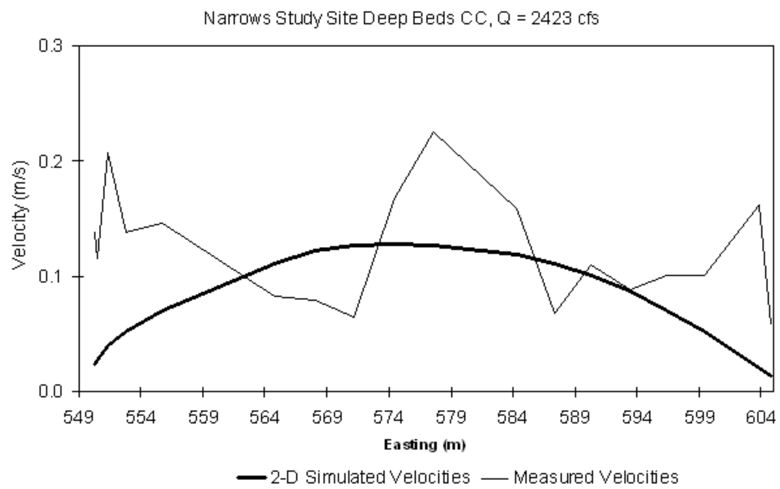
Narrows Study Site Deep Beds CC, Q = 2423 cfs
Velocity (m/s)
0.0
0.1
0.2
0.3
549
554
559
564
569
574
579
584
589
594
599
604
Easting (m)
2-D Simulated Velocities
Measured Velocities

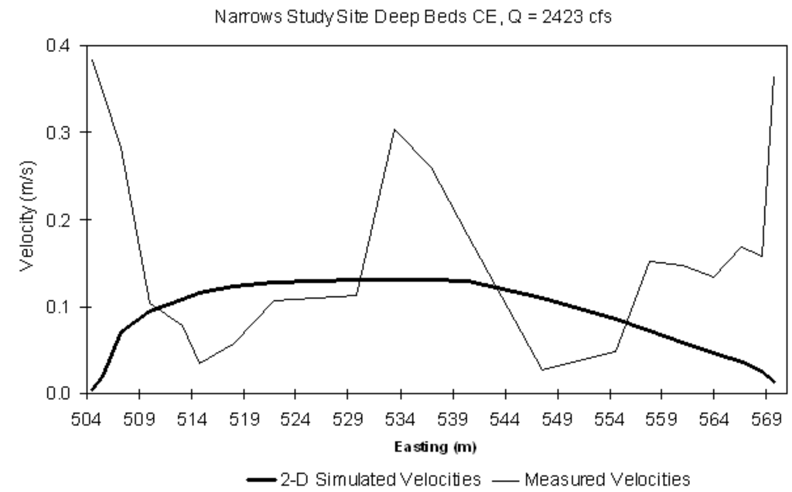
Narrows Study Site Deep Beds CE, Q = 2423 cfs
Velocity (m/s)
0.0
0.1
0.2
0.3
0.4
504
509
514
519
524
529
534
539
544
549
554
559
564
569
Easting (m)
2-D Simulated Velocities
Measured Velocities

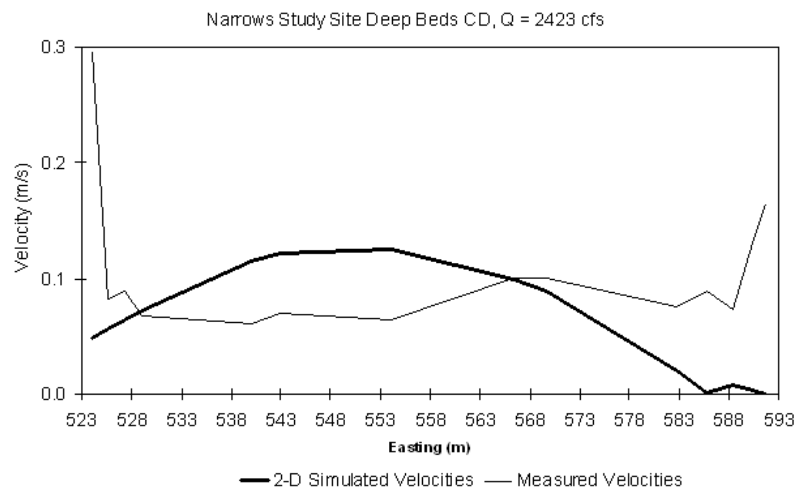
Narrows Study Site Deep Beds CD, Q = 2423 cfs
Velocity (m/s)
0.0
0.1
0.2
0.3
523
528
533
538
543
548
553
558
563
568
573
578
583
588
593
Easting (m)
2-D Simulated Velocities
Measured Velocities

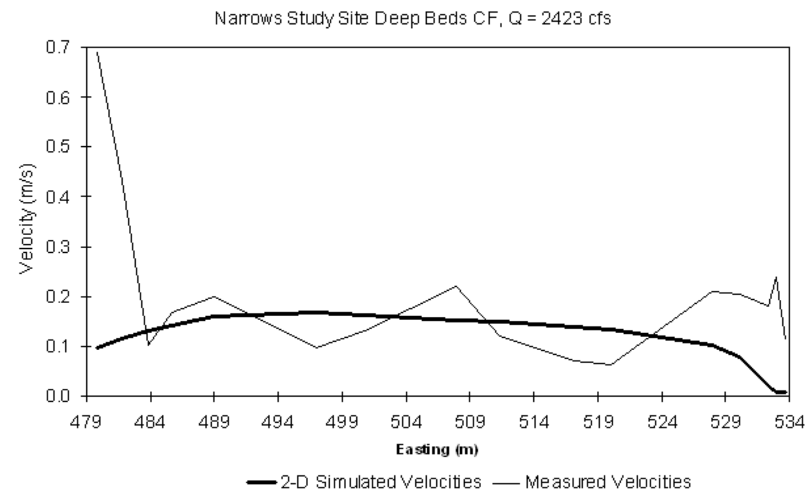
Narrows Study Site Deep Beds CF, Q = 2423 cfs
Velocity (m/s)
0.0
0.1
0.2
0.3
0.4
0.5
0.6
0.7
479
484
489
494
499
504
509
514
519
524
529
534
Easting (m)
2-D Simulated Velocities
Measured Velocities

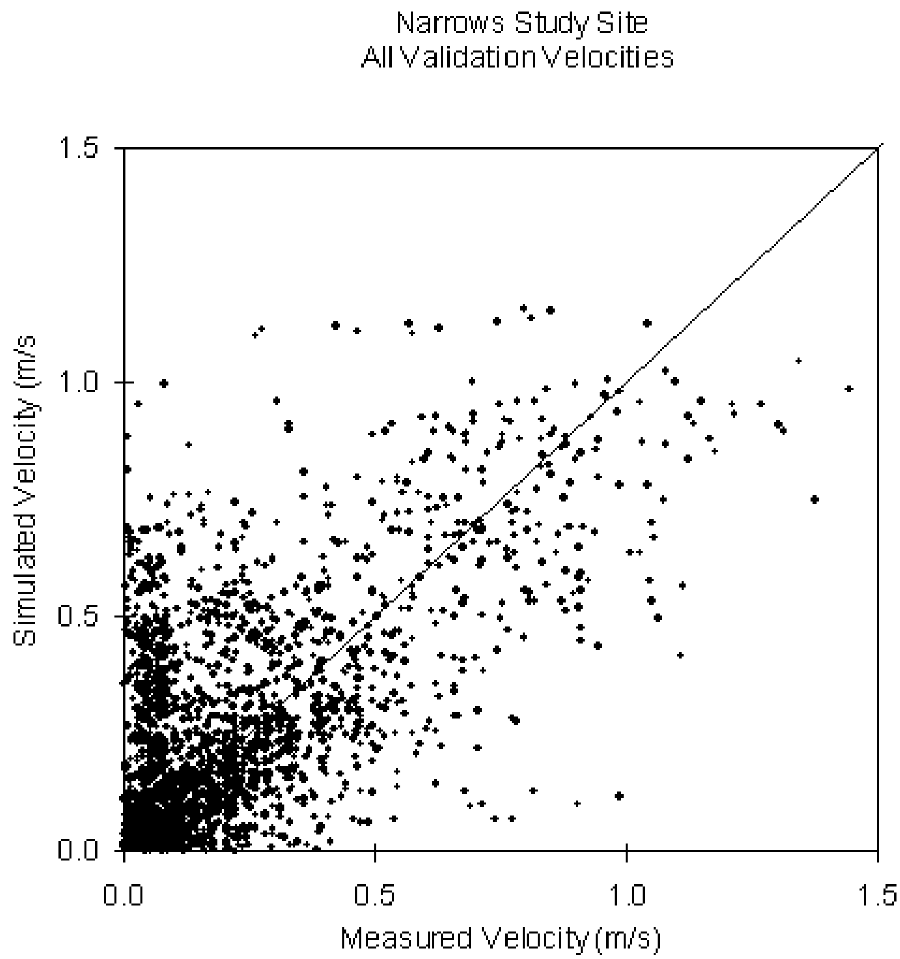
Narrows Study Site
All Validation Velocities
1.5
1.0
0.5
0.0
Simulated Velocity (m/s)
0.0
0.5
1.0
1.5
Measured Velocity (m/s)

Rosebar Study Site

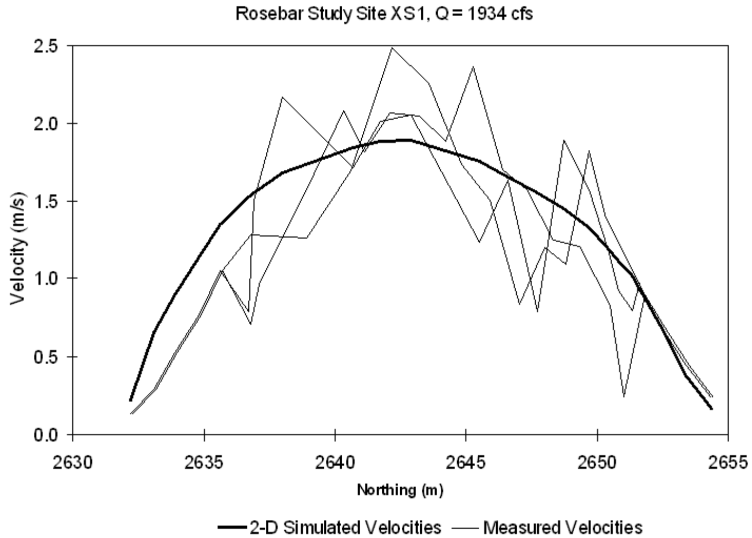

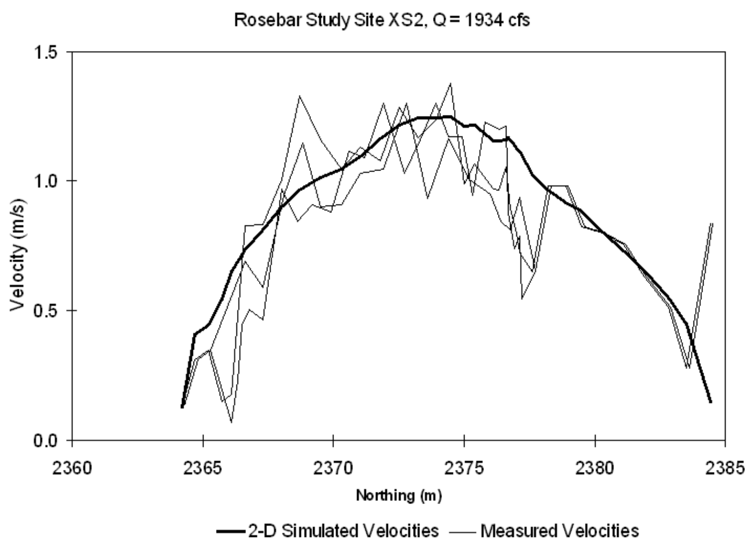

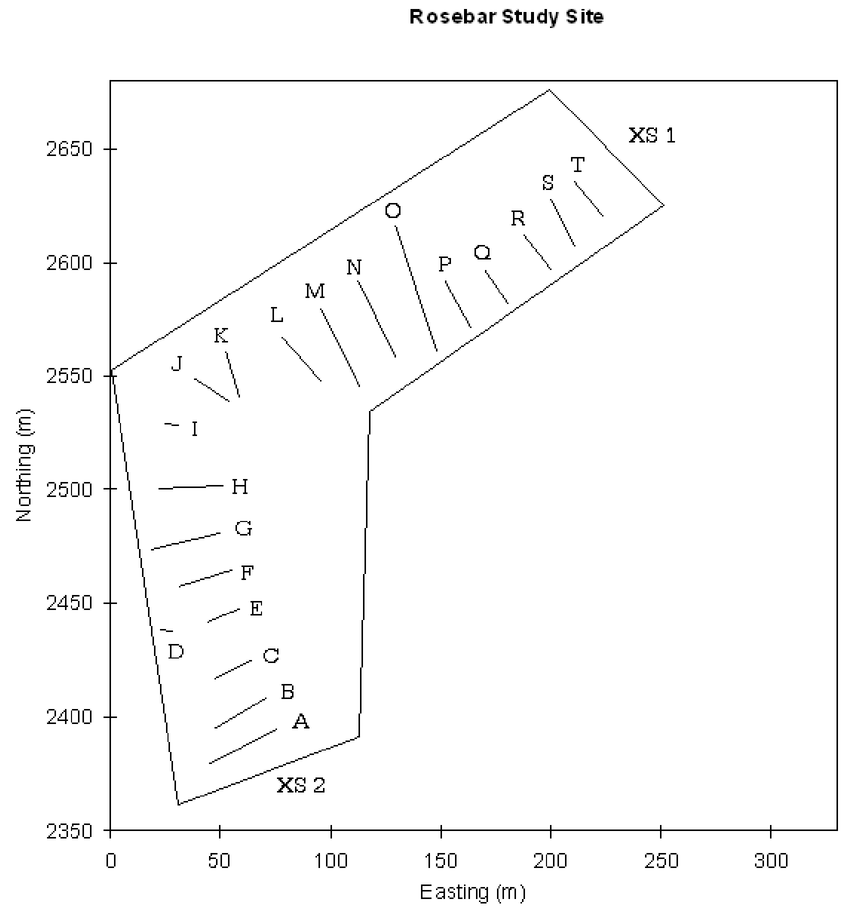

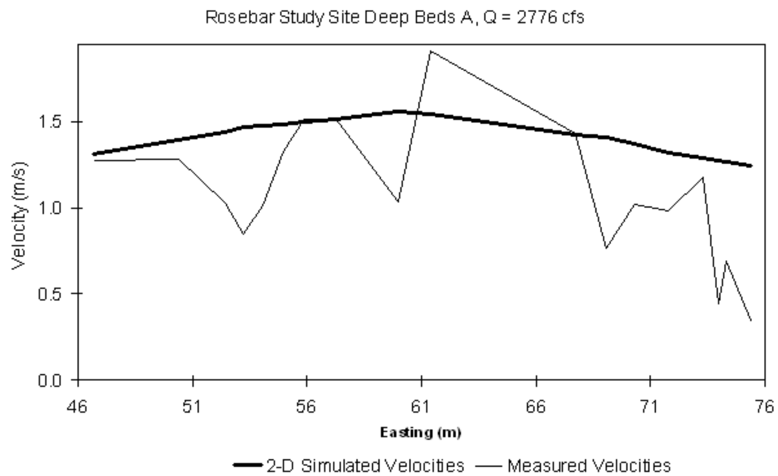
Rosebar Study Site Deep Beds A, Q = 2776 cfs
Velocity (m/s)
0.0
0.5
1.0
1.5
46
51
56
61
66
71
76
Easting (m)
2-D Simulated Velocities
Measured Velocities

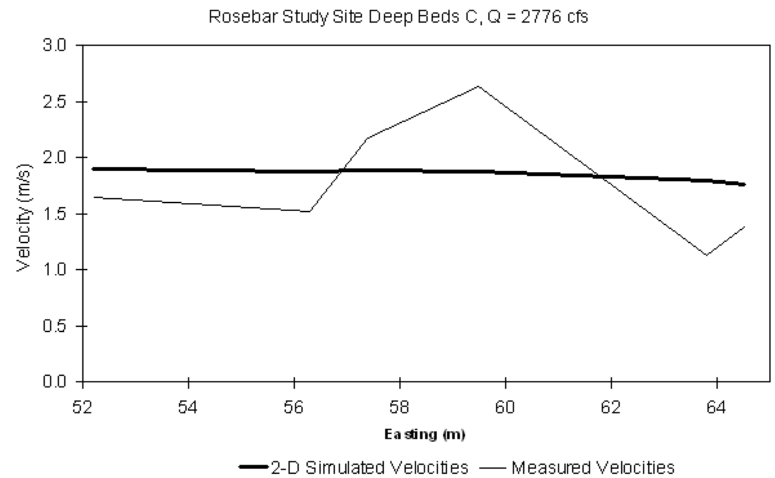
Rosebar Study Site Deep Beds C, Q = 2776 cfs
Velocity (m/s)
0.0
0.5
1.0
1.5
2.0
2.5
3.0
52
54
56
58
60
62
64
Easting (m)
2-D Simulated Velocities
Measured Velocities

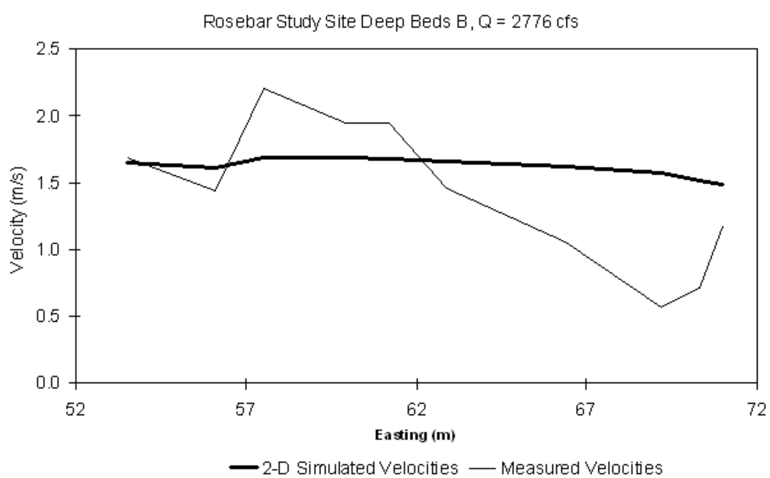
Rosebar Study Site Deep Beds B, Q = 2776 cfs
Velocity (m/s)
0.0
0.5
1.0
1.5
2.0
2.5
52
57
62
67
72
Easting (m)
2-D Simulated Velocities
Measured Velocities

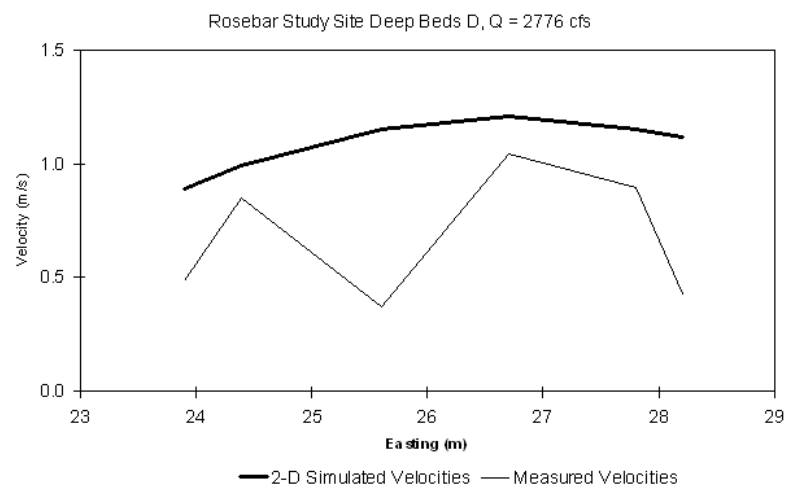
Rosebar Study Site Deep Beds D, Q = 2776 cfs
Velocity (m/s)
0.0
0.5
1.0
1.5
23
24
25
26
27
28
29
Easting (m)
2-D Simulated Velocities
Measured Velocities

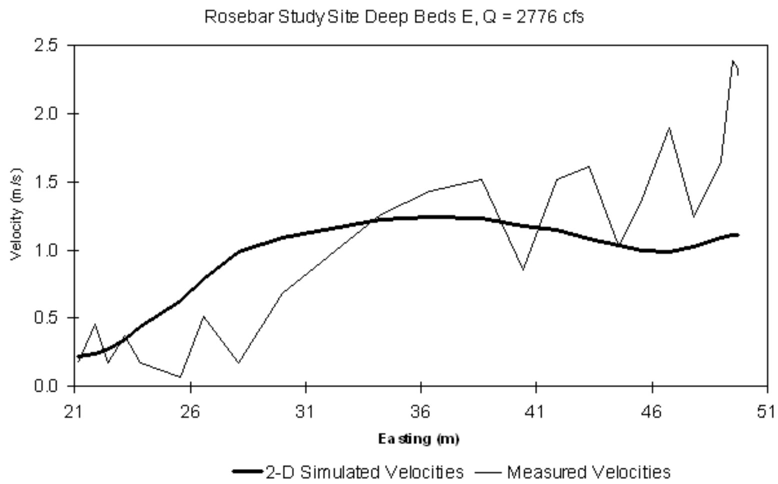
Rosebar Study Site Deep Beds E, Q = 2776 cfs
Velocity (m/s)
Easting (m)
2-D Simulated Velocities
Measured Velocities

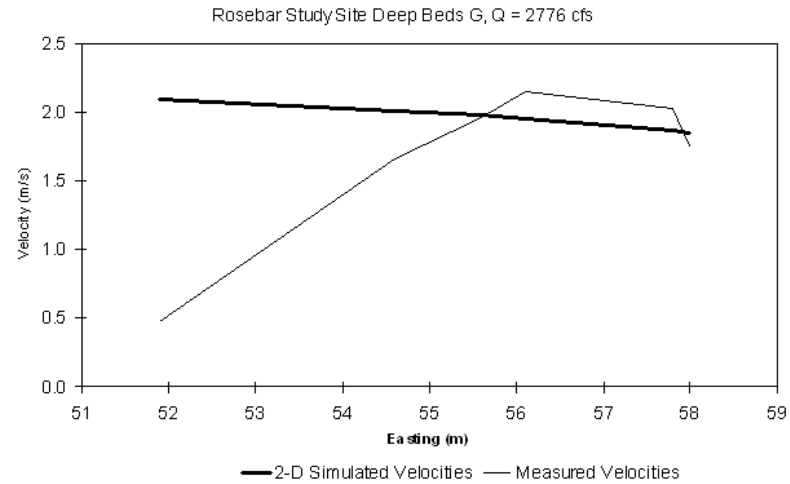
Rosebar Study Site Deep Beds G, Q = 2776 cfs
Velocity (m/s)
Easting (m)
2-D Simulated Velocities
Measured Velocities

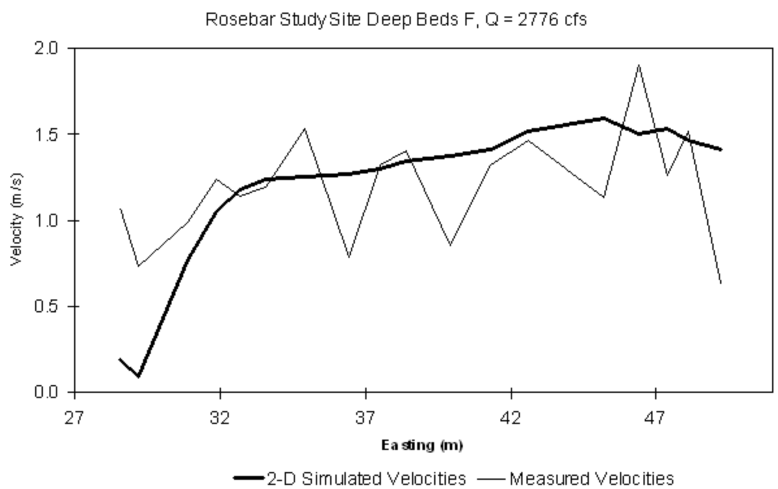
Rosebar Study Site Deep Beds F, Q = 2776 cfs
Velocity (m/s)
Easting (m)
2-D Simulated Velocities
Measured Velocities

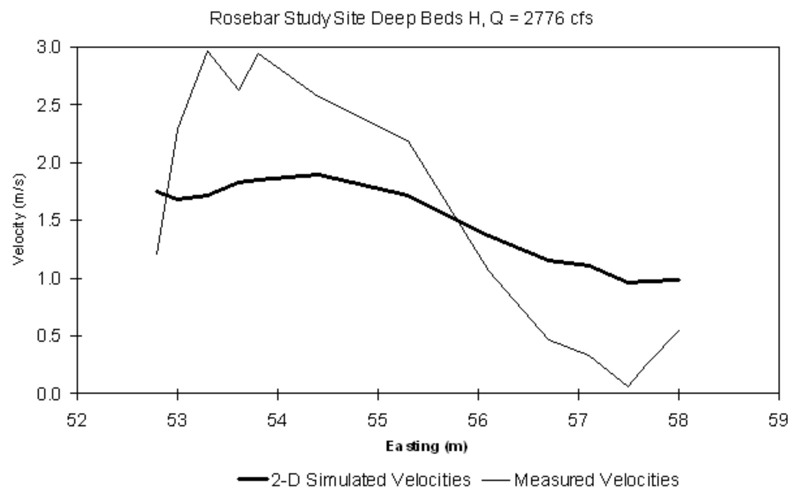
Rosebar Study Site Deep Beds H, Q = 2776 cfs
Velocity (m/s)
Easting (m)
2-D Simulated Velocities
Measured Velocities

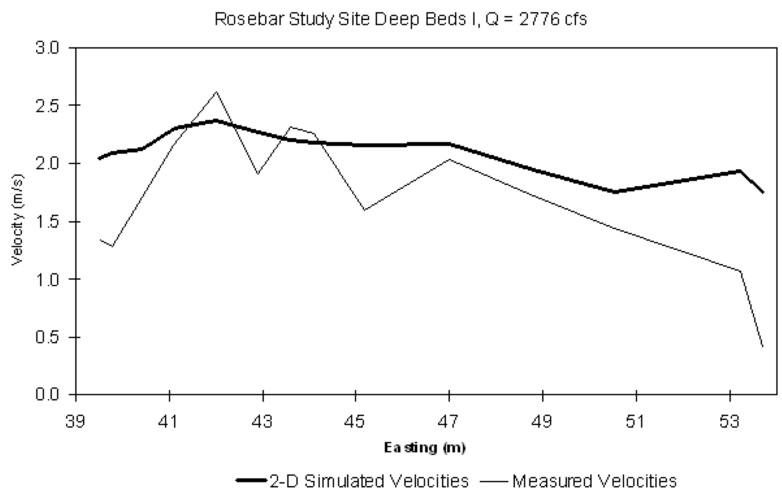
Rosebar Study Site Deep Beds I, Q = 2776 cfs
Velocity (m/s)
3.0
2.5
2.0
1.5
1.0
0.5
0.0
39
41
43
45
47
49
51
53
Easting (m)
2-D Simulated Velocities
Measured Velocities

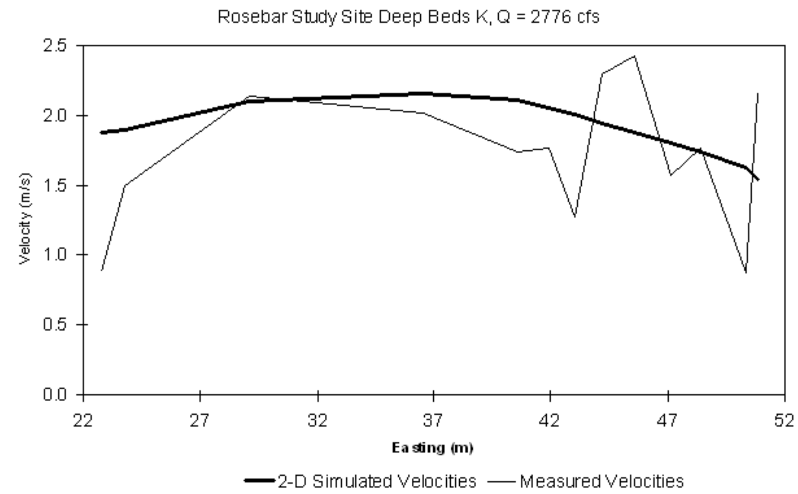
Rosebar Study Site Deep Beds K, Q = 2776 cfs
Velocity (m/s)
2.5
2.0
1.5
1.0
0.5
0.0
22
27
32
37
42
47
52
Easting (m)
2-D Simulated Velocities
Measured Velocities

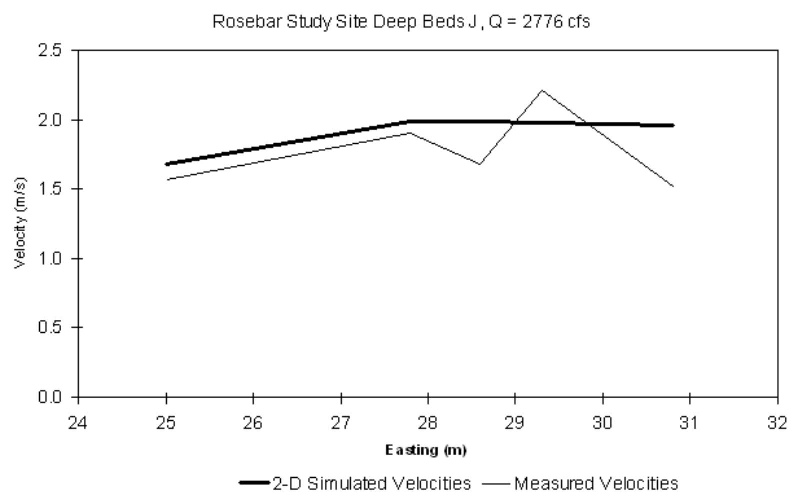
Rosebar Study Site Deep Beds J , Q = 2776 cfs
Velocity (m/s)
2.5
2.0
1.5
1.0
0.5
0.0
24
25
26
27
28
29
30
31
32
Easting (m)
2-D Simulated Velocities
Measured Velocities

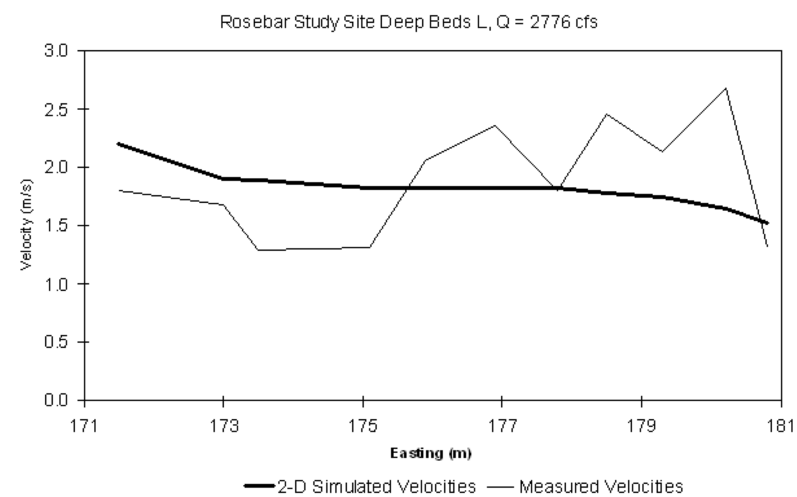
Rosebar Study Site Deep Beds L, Q = 2776 cfs
Velocity (m/s)
3.0
2.5
2.0
1.5
1.0
0.5
0.0
171
173
175
177
179
181
Easting (m)
2-D Simulated Velocities
Measured Velocities

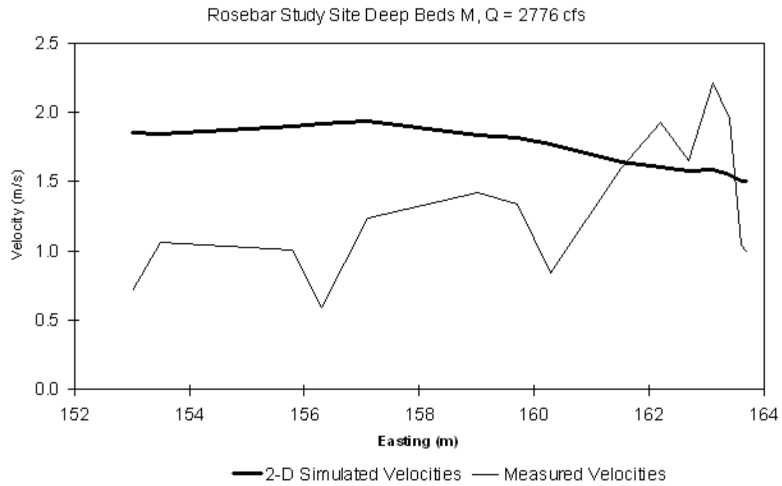
Rosebar Study Site Deep Beds M, Q = 2776 cfs
Velocity (m/s)
Easting (m)
2-D Simulated Velocities
Measured Velocities

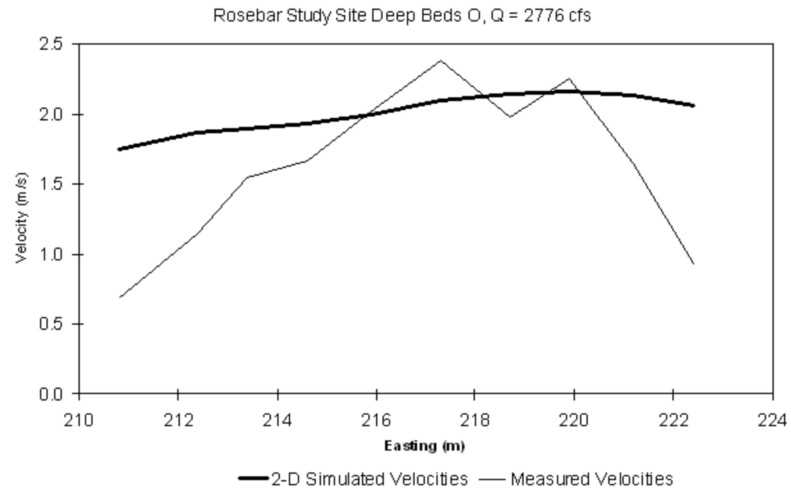
Rosebar Study Site Deep Beds O, Q = 2776 cfs
Velocity (m/s)
Easting (m)
2-D Simulated Velocities
Measured Velocities

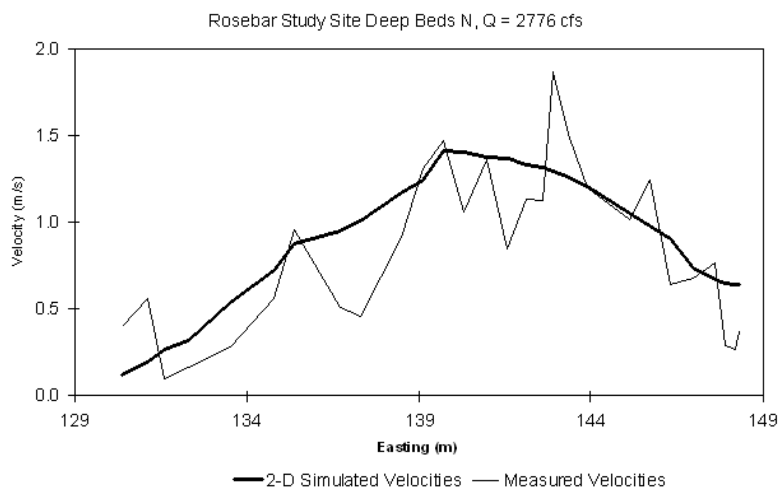
Rosebar Study Site Deep Beds N, Q = 2776 cfs
Velocity (m/s)
Easting (m)
2-D Simulated Velocities
Measured Velocities

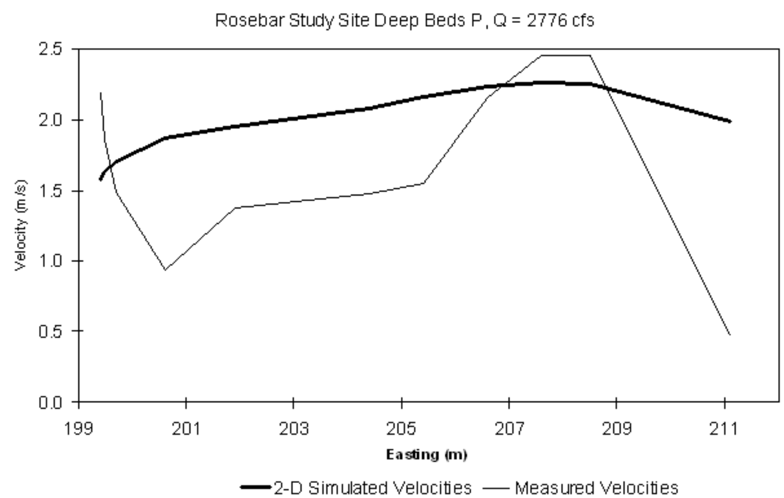
Rosebar Study Site Deep Beds P, Q = 2776 cfs
Velocity (m/s)
Easting (m)
2-D Simulated Velocities
Measured Velocities

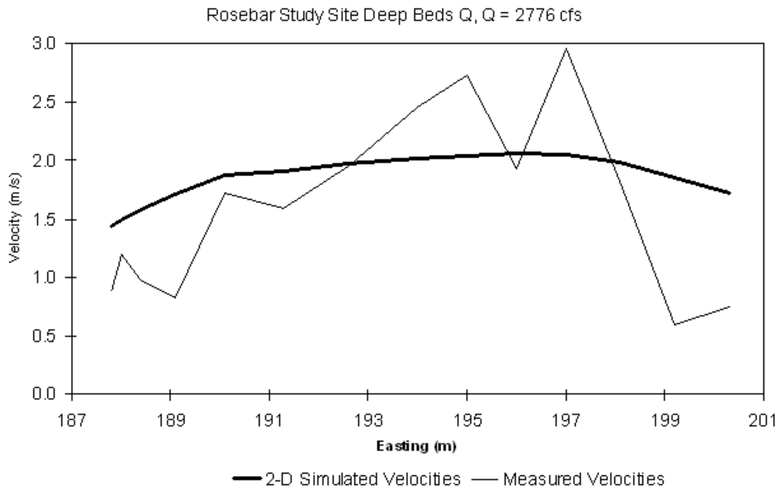
Rosebar Study Site Deep Beds Q, Q = 2776 cfs
Velocity (m/s)
Easting (m)
2-D Simulated Velocities
Measured Velocities

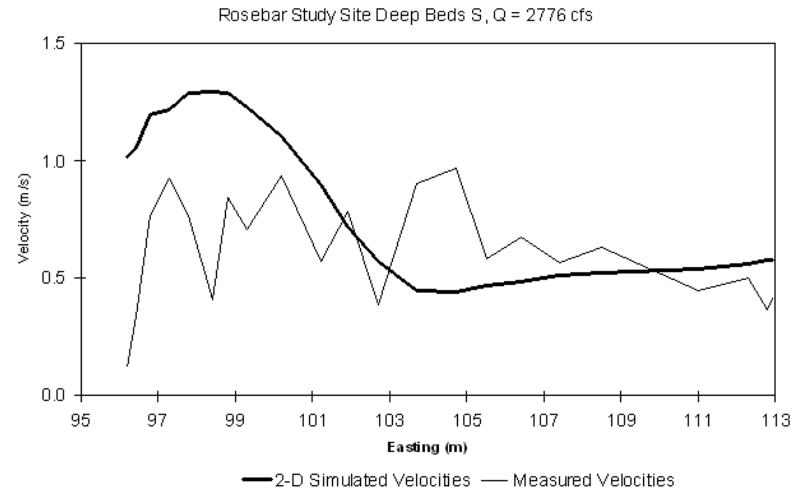
Rosebar Study Site Deep Beds S, Q = 2776 cfs
Velocity (m/s)
Easting (m)
2-D Simulated Velocities
Measured Velocities

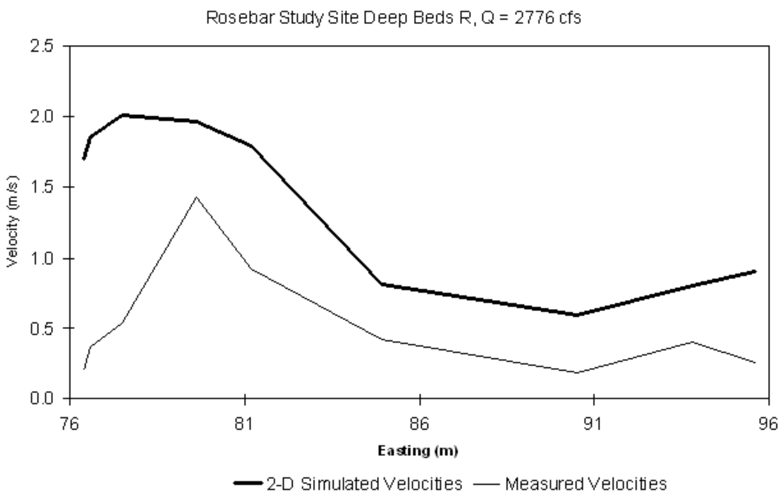
Rosebar Study Site Deep Beds R, Q = 2776 cfs
Velocity (m/s)
Easting (m)
2-D Simulated Velocities
Measured Velocities

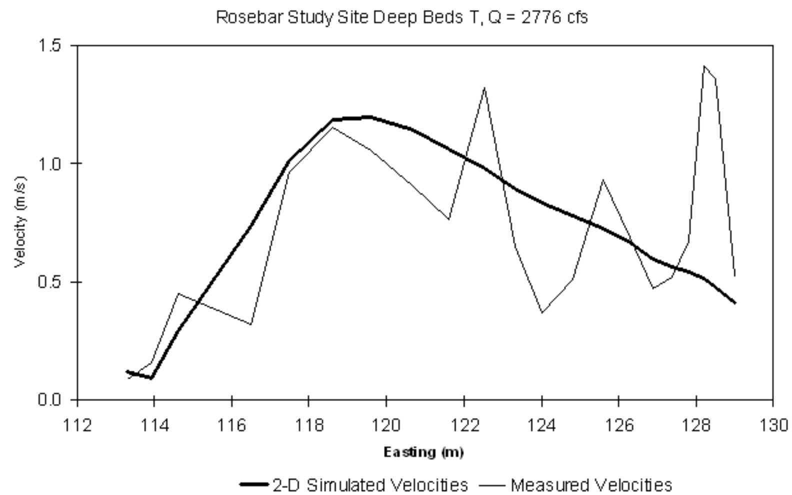
Rosebar Study Site Deep Beds T, Q = 2776 cfs
Velocity (m/s)
Easting (m)
2-D Simulated Velocities
Measured Velocities

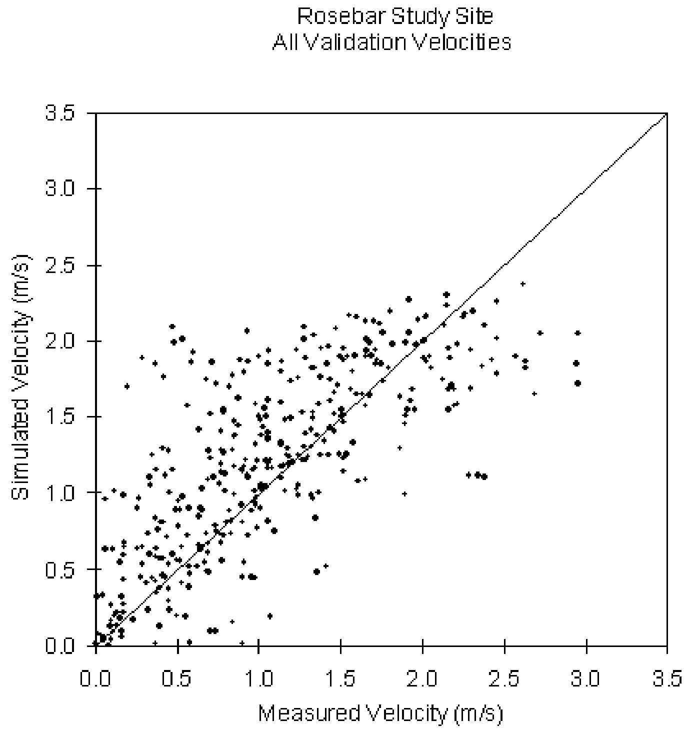
Rosebar Study Site
All Validation Velocities
Simulated Velocity (m/s)
Measured Velocity (m/s)
0.0
0.5
1.0
1.5
2.0
2.5
3.0
3.5

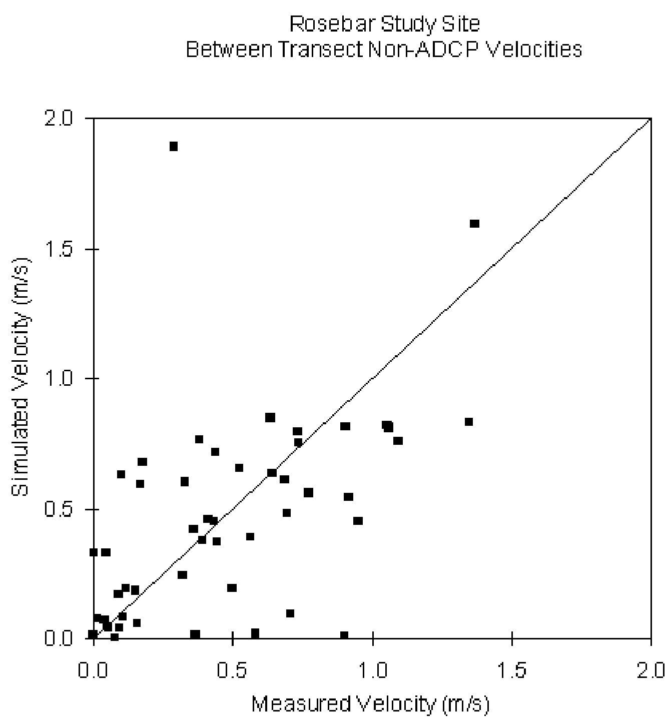
Rosebar Study Site
Between Transect Non-ADCP Velocities
Simulated Velocity (m/s)
Measured Velocity (m/s)
0.0
0.5
1.0
1.5
2.0

Diversion Study Site

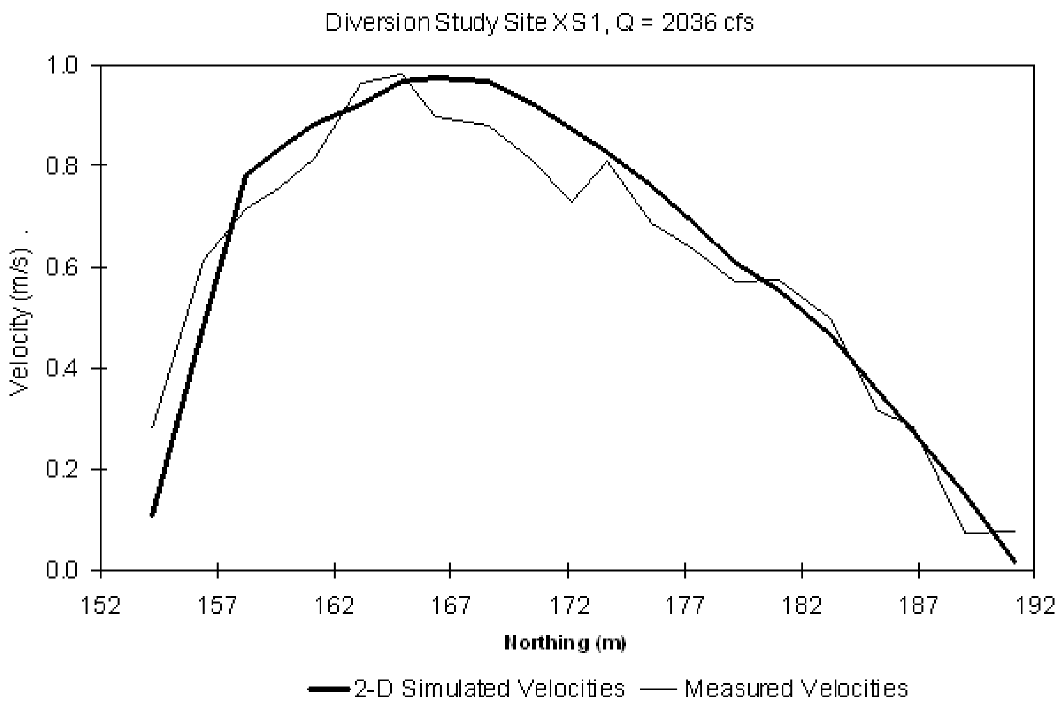

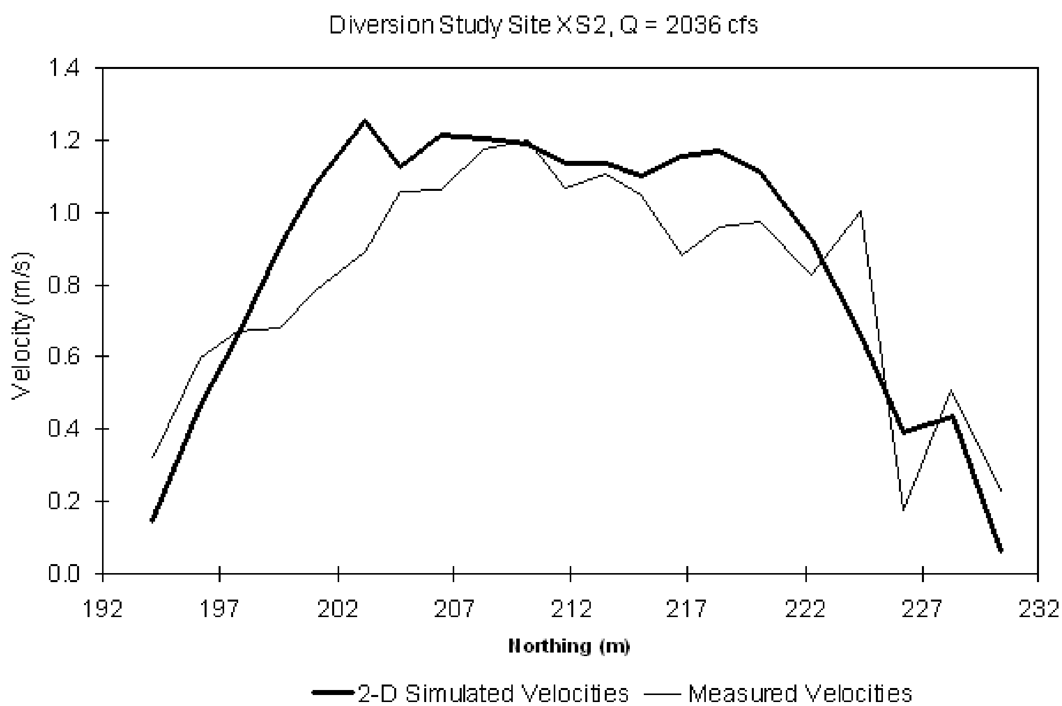

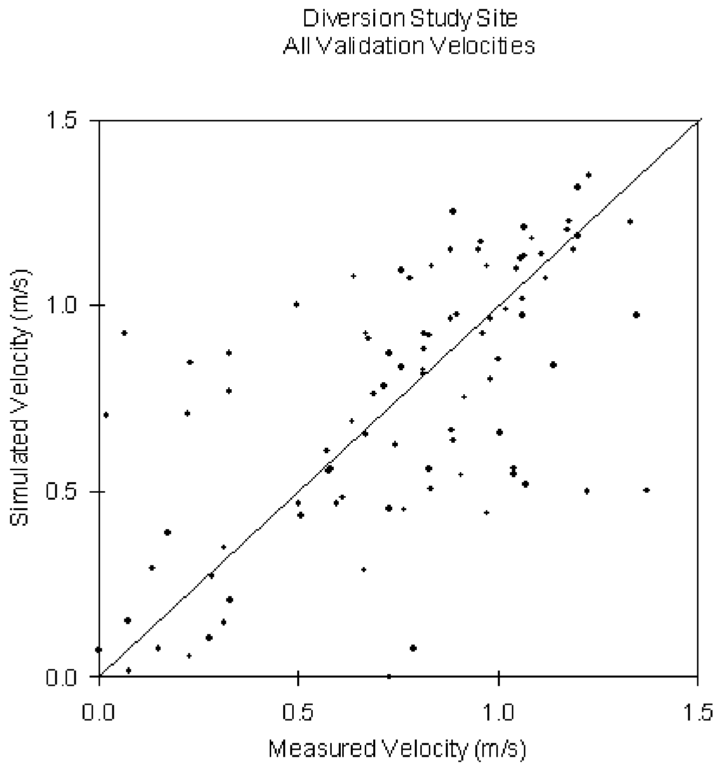
Diversion Study Site
All Validation Velocities
Simulated Velocity (m/s)
Measured Velocity (m/s)
0.0
0.5
1.0
1.5

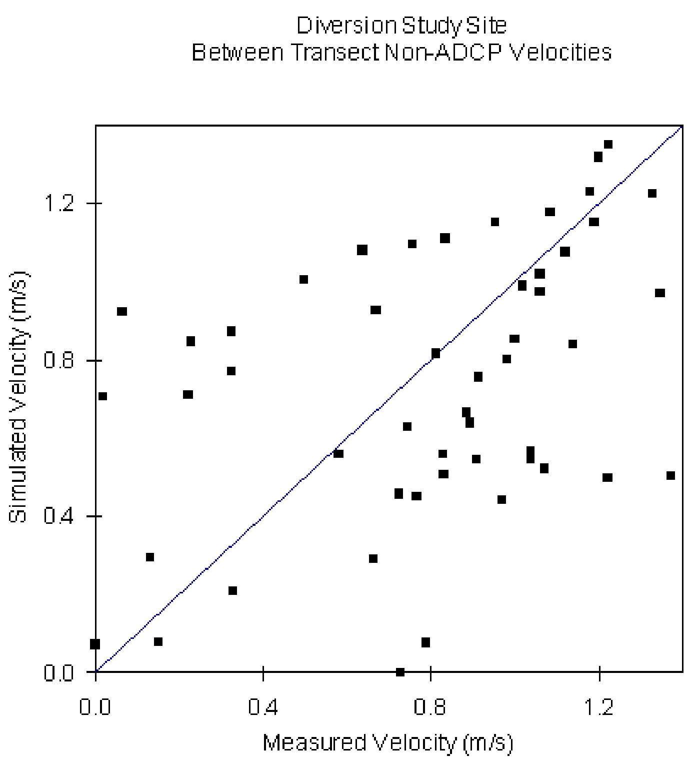
Diversion Study Site
Between Transect Non-ADCP Velocities
Simulated Velocity (m/s)
Measured Velocity (m/s)
0.0
0.4
0.8
1.2

Lower Hallwood Study Site

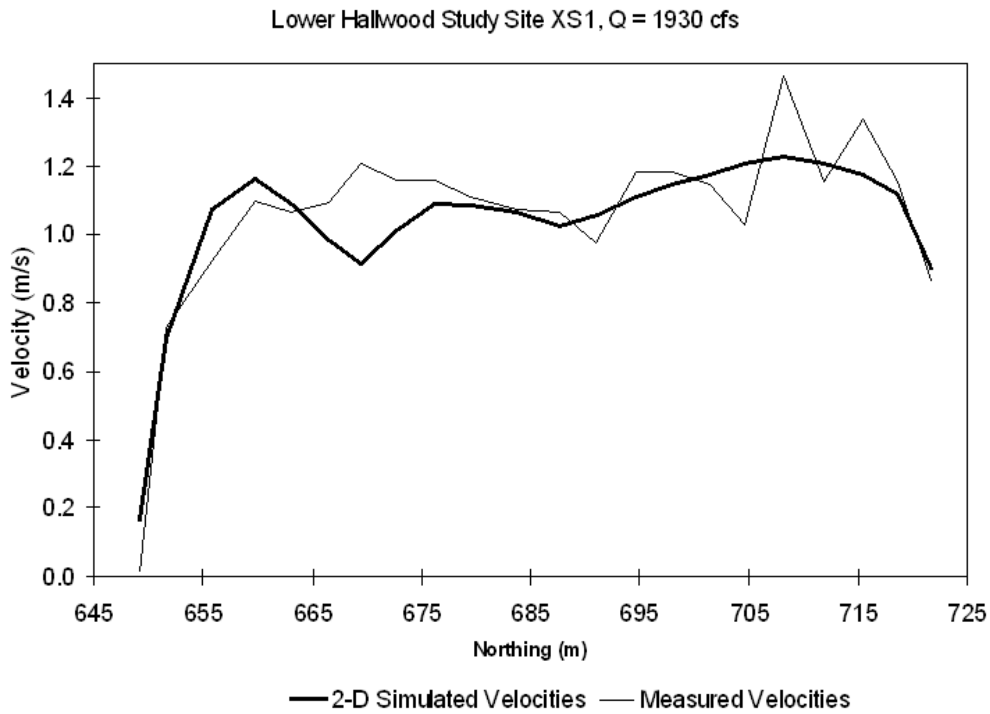

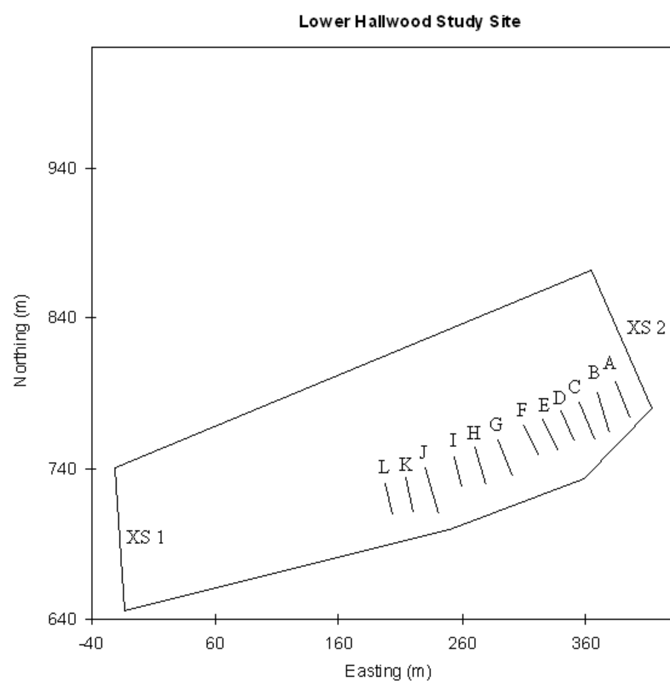

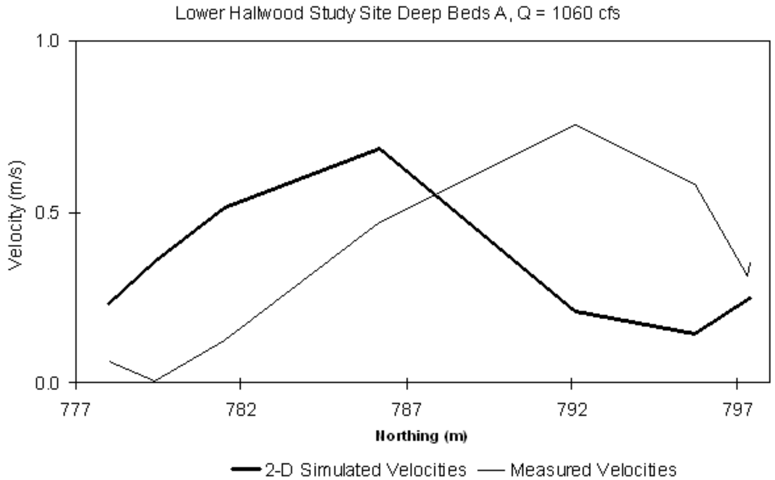
Lower Hallwood Study Site Deep Beds A, Q = 1060 cfs
Velocity (m/s)
Northing (m)
2-D Simulated Velocities
Measured Velocities

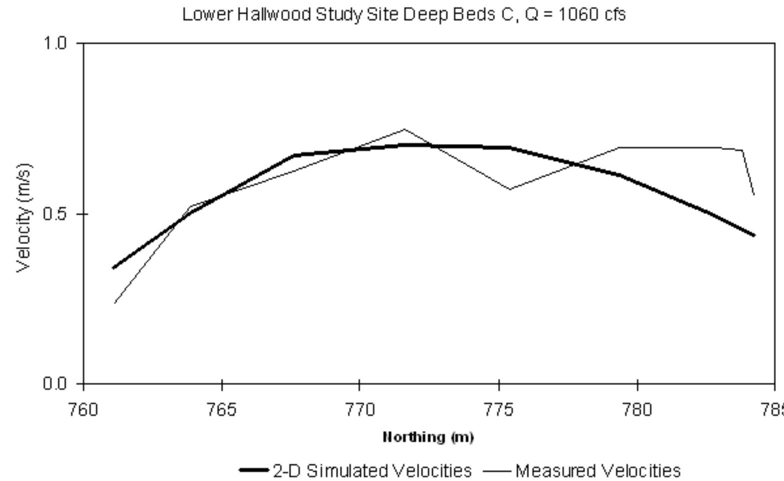
Lower Hallwood Study Site Deep Beds C, Q = 1060 cfs
Velocity (m/s)
Northing (m)
2-D Simulated Velocities
Measured Velocities

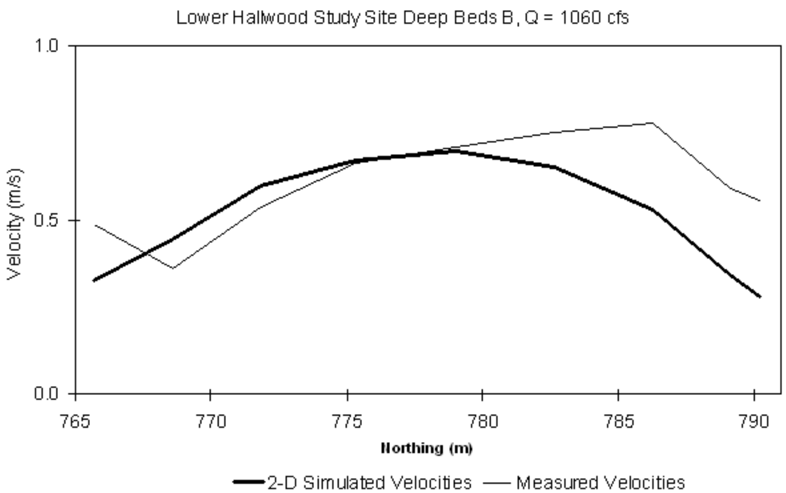
Lower Hallwood Study Site Deep Beds B, Q = 1060 cfs
Velocity (m/s)
Northing (m)
2-D Simulated Velocities
Measured Velocities

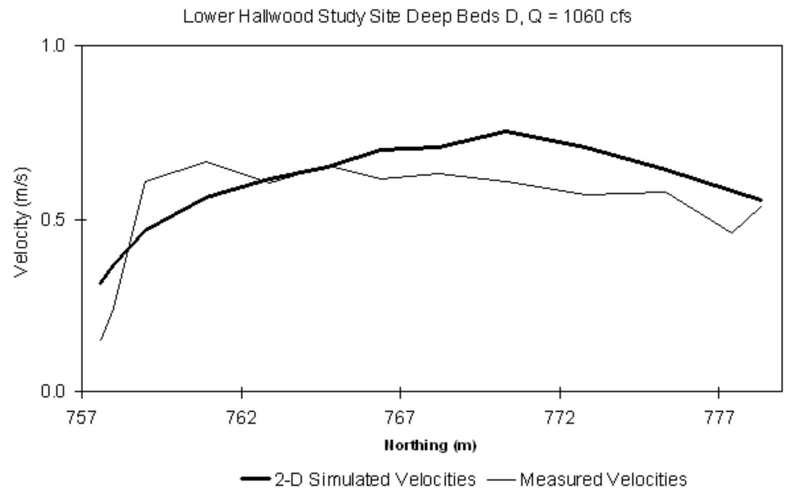
Lower Hallwood Study Site Deep Beds D, Q = 1060 cfs
Velocity (m/s)
Northing (m)
2-D Simulated Velocities
Measured Velocities

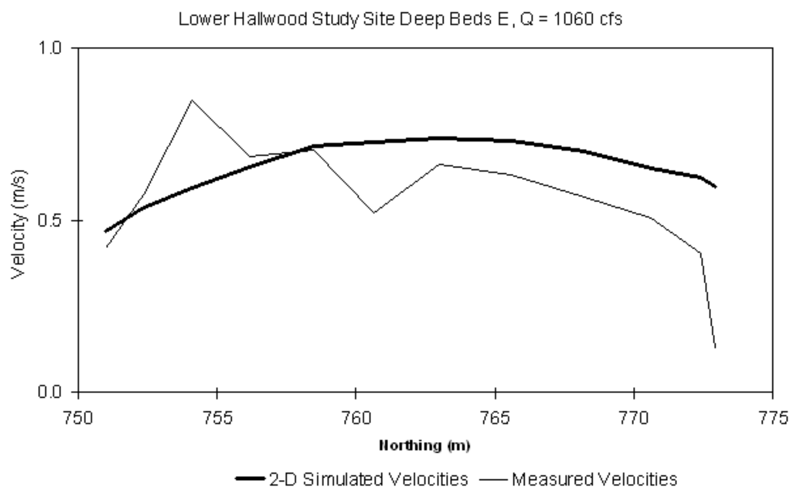
Lower Hallwood Study Site Deep Beds E, Q = 1060 cfs
Velocity (m/s)
1.0
0.5
0.0
750
755
760
765
770
775
Northing (m)
2-D Simulated Velocities
Measured Velocities

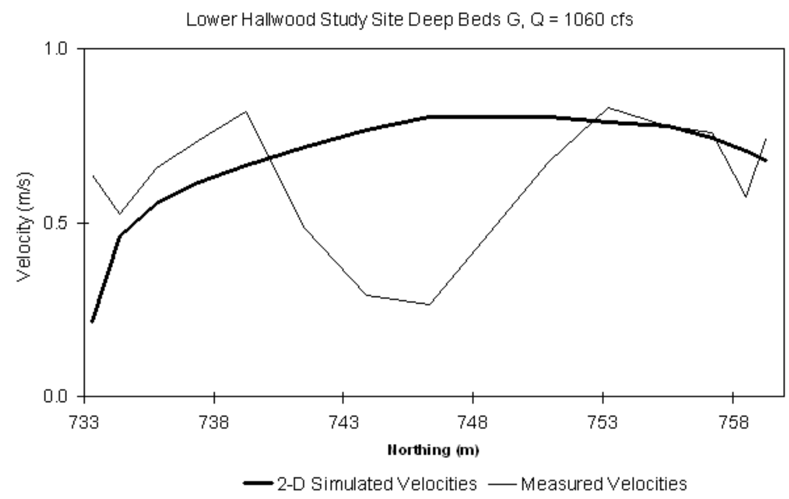
Lower Hallwood Study Site Deep Beds G, Q = 1060 cfs
Velocity (m/s)
1.0
0.5
0.0
733
738
743
748
753
758
Northing (m)
2-D Simulated Velocities
Measured Velocities

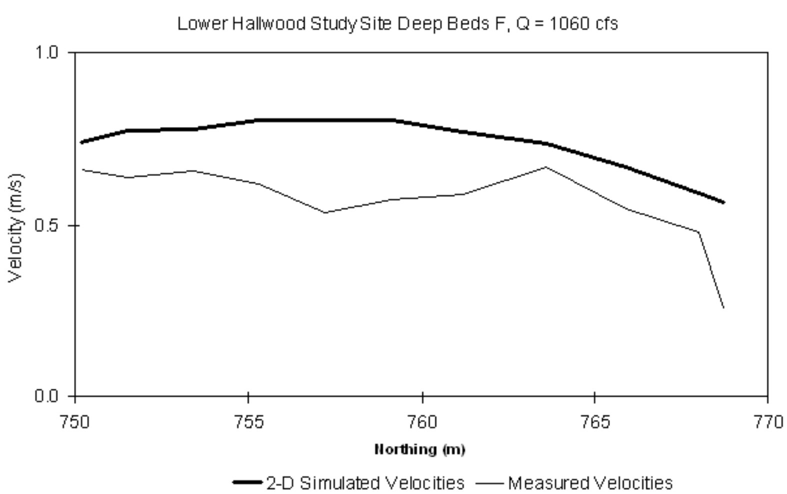
Lower Hallwood Study Site Deep Beds F, Q = 1060 cfs
Velocity (m/s)
1.0
0.5
0.0
750
755
760
765
770
Northing (m)
2-D Simulated Velocities
Measured Velocities

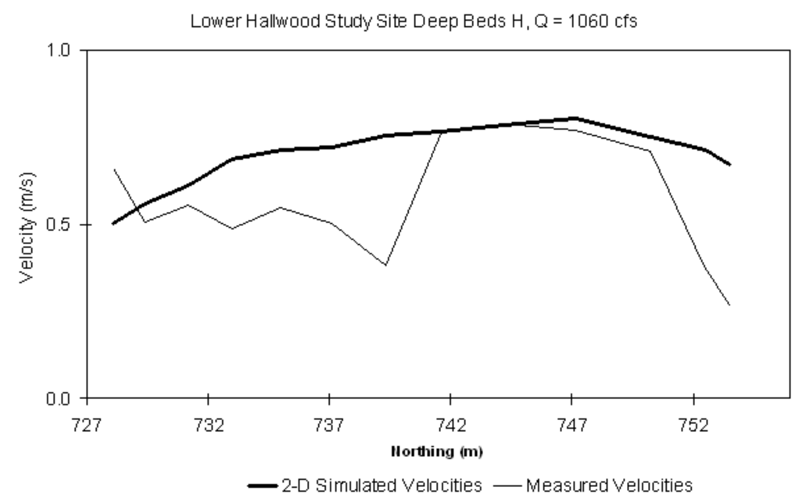
Lower Hallwood Study Site Deep Beds H, Q = 1060 cfs
Velocity (m/s)
1.0
0.5
0.0
727
732
737
742
747
752
Northing (m)
2-D Simulated Velocities
Measured Velocities

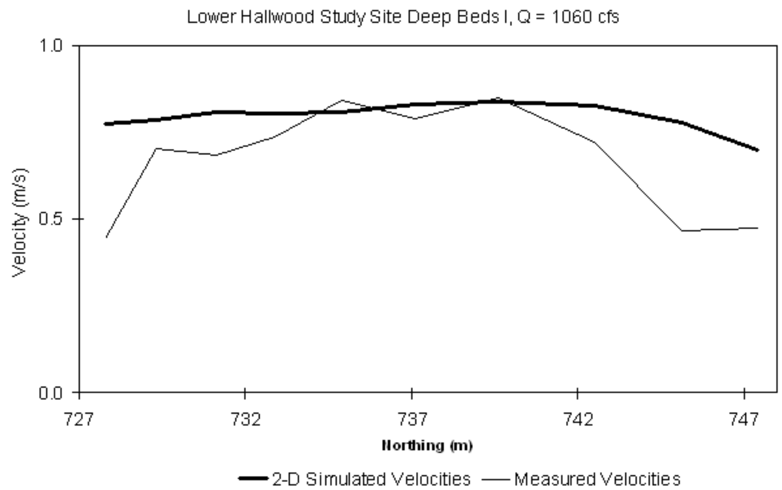
Lower Hallwood Study Site Deep Beds I, Q = 1060 cfs
Velocity (m/s)
1.0
0.5
0.0
727
732
737
742
747
Northing (m)
2-D Simulated Velocities
Measured Velocities

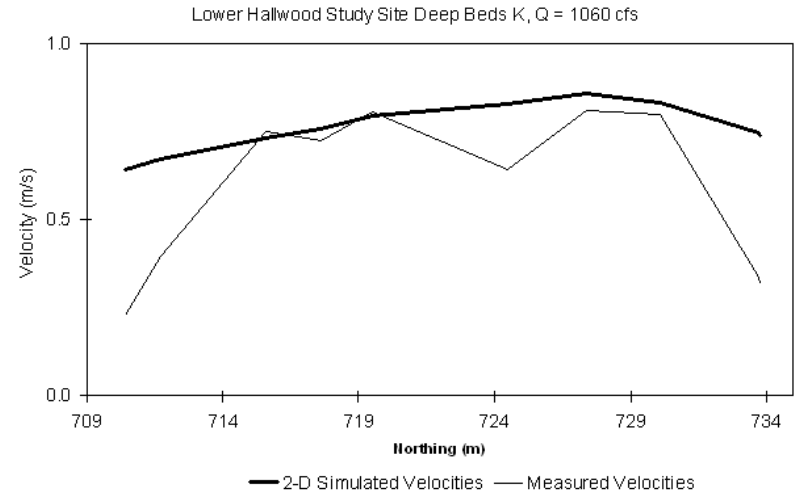
Lower Hallwood Study Site Deep Beds K, Q = 1060 cfs
Velocity (m/s)
1.0
0.5
0.0
709
714
719
724
729
734
Northing (m)
2-D Simulated Velocities
Measured Velocities

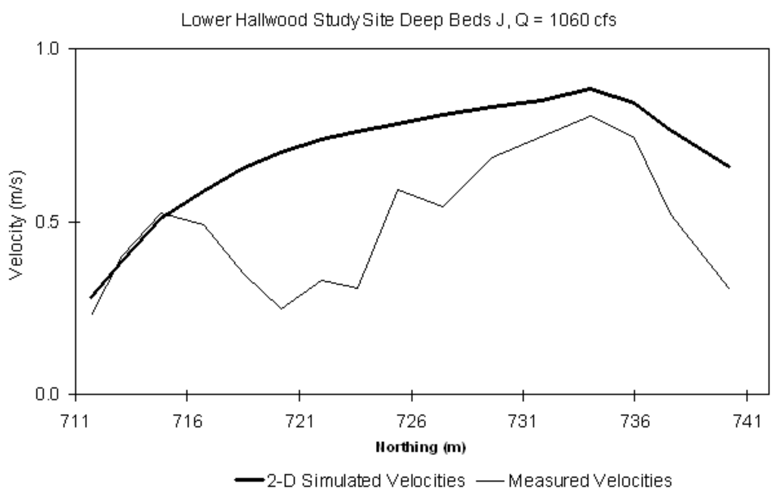
Lower Hallwood Study Site Deep Beds J, Q = 1060 cfs
Velocity (m/s)
1.0
0.5
0.0
711
716
721
726
731
736
741
Northing (m)
2-D Simulated Velocities
Measured Velocities

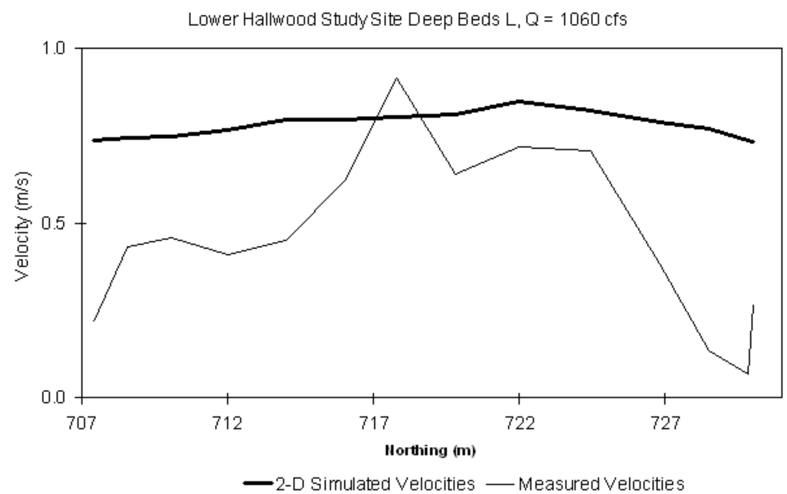
Lower Hallwood Study Site Deep Beds L, Q = 1060 cfs
Velocity (m/s)
1.0
0.5
0.0
707
712
717
722
727
Northing (m)
2-D Simulated Velocities
Measured Velocities

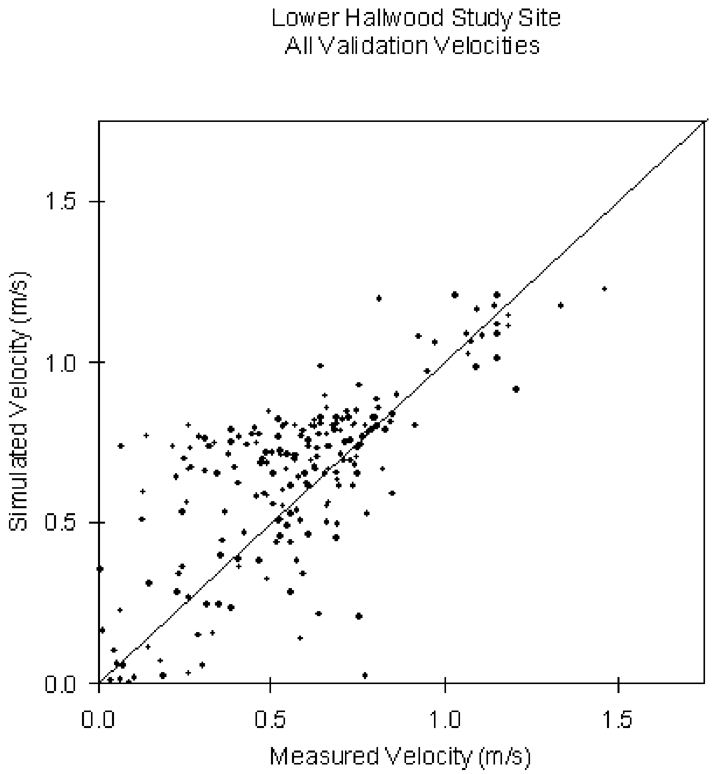
Lower Hallwood Study Site
All Validation Velocities
Simulated Velocity (m/s)
Measured Velocity (m/s)
0.0
0.5
1.0
1.5

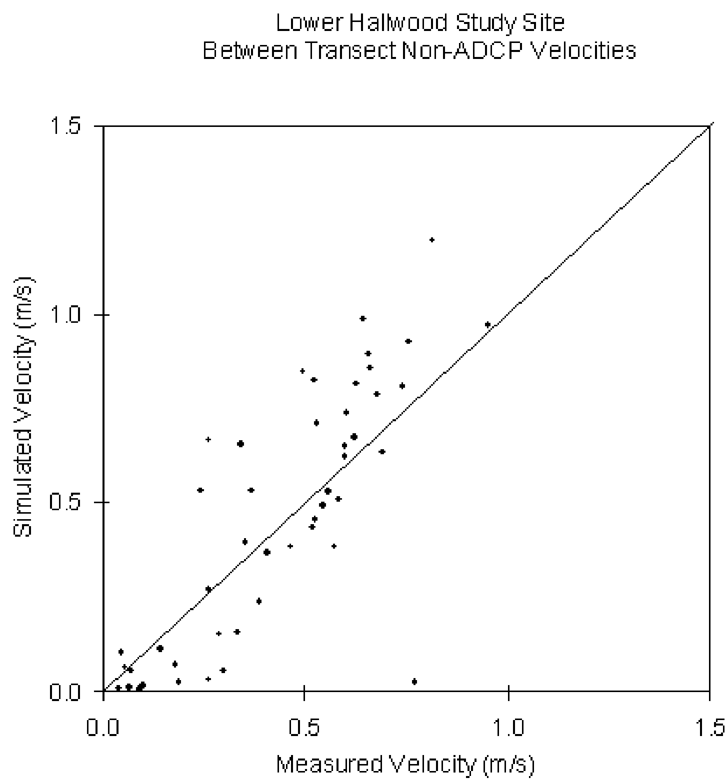
Lower Hallwood Study Site
Between Transect Non-ADCP Velocities
Simulated Velocity (m/s)
Measured Velocity (m/s)
0.0
0.5
1.0
1.5

Whirlpool Study Site

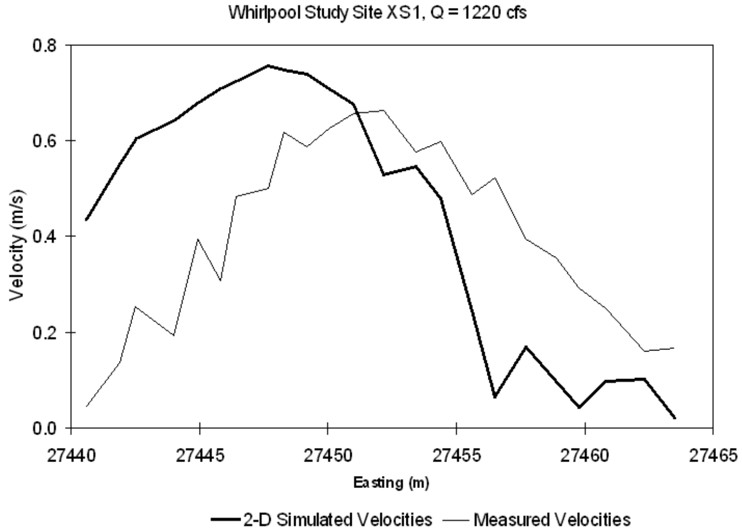

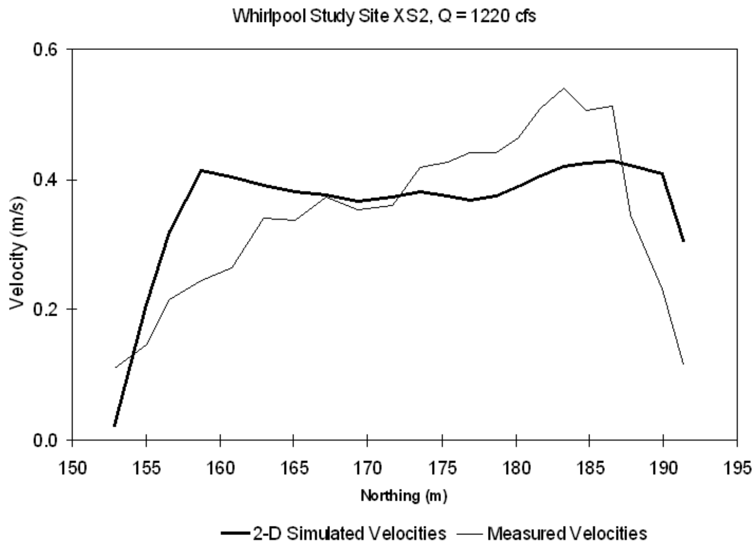

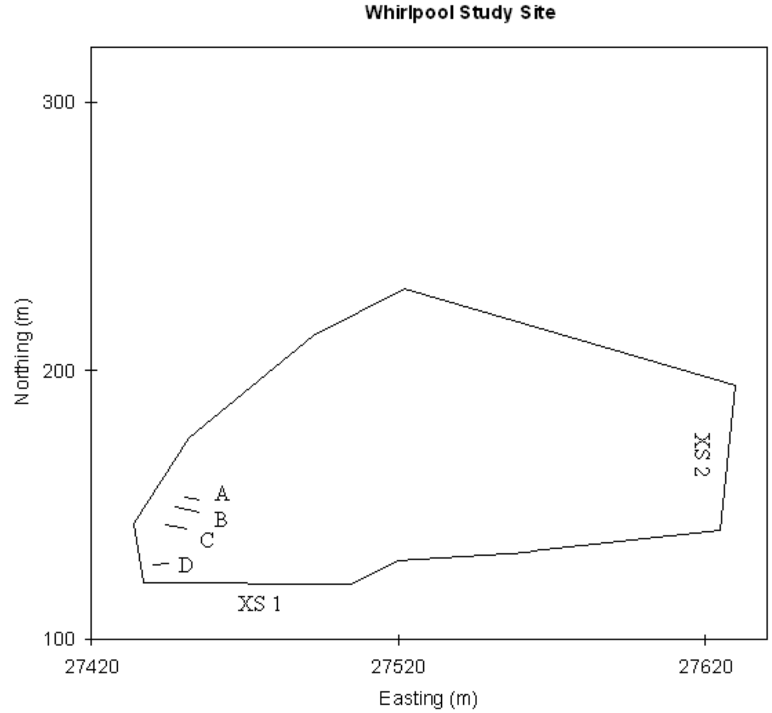

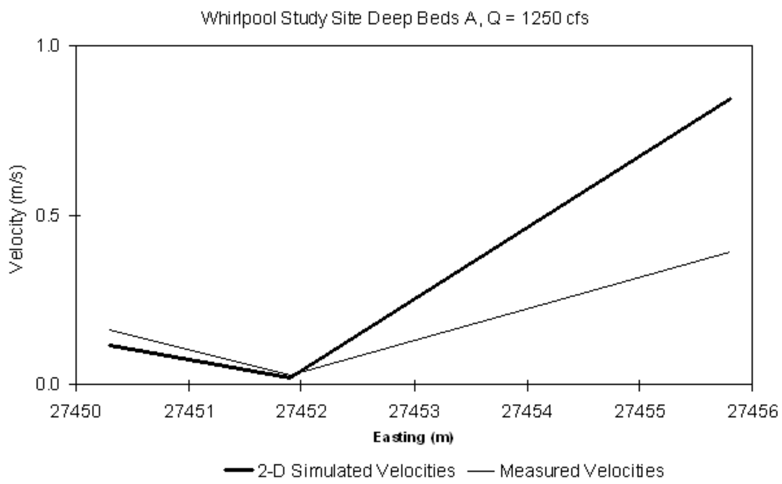
Whirlpool Study Site Deep Beds A, Q = 1250 cfs
1.0
0.5
0.0
Velocity (m/s)
27450
27451
27452
27453
27454
27455
27456
Easting (m)
2-D Simulated Velocities
Measured Velocities

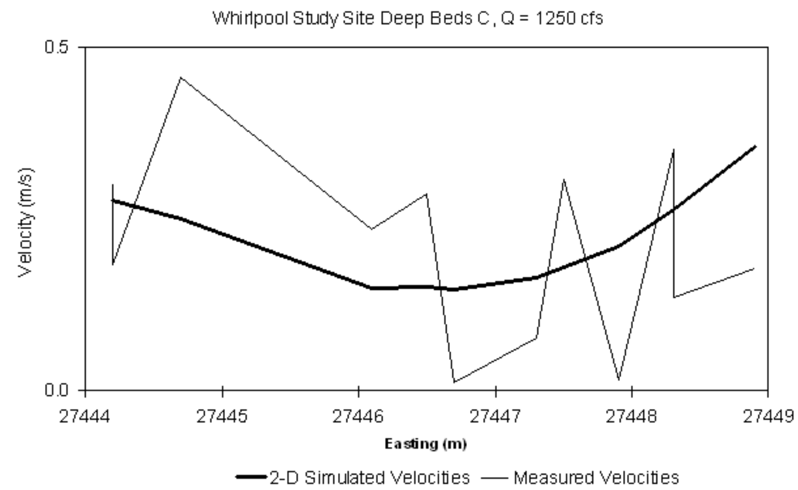
Whirlpool Study Site Deep Beds C, Q = 1250 cfs
0.5
0.0
Velocity (m/s)
27444
27445
27446
27447
27448
27449
Easting (m)
2-D Simulated Velocities
Measured Velocities

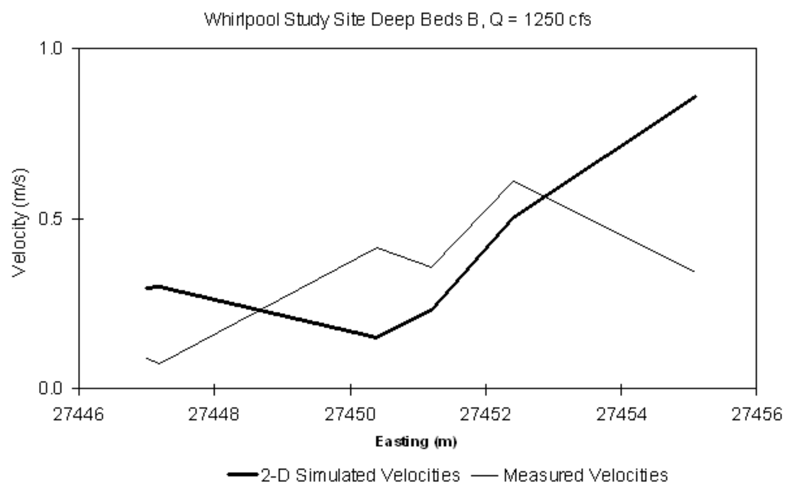
Whirlpool Study Site Deep Beds B, Q = 1250 cfs
1.0
0.5
0.0
Velocity (m/s)
27446
27448
27450
27452
27454
27456
Easting (m)
2-D Simulated Velocities
Measured Velocities

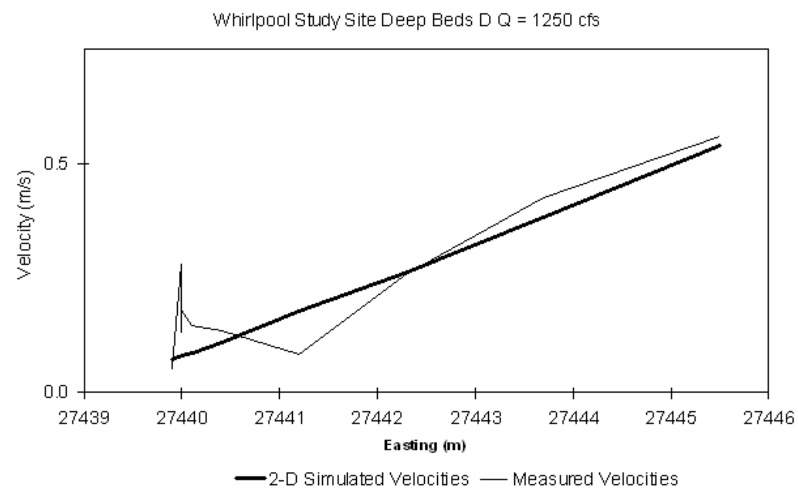
Whirlpool Study Site Deep Beds D Q = 1250 cfs
0.5
0.0
Velocity (m/s)
27439
27440
27441
27442
27443
27444
27445
27446
Easting (m)
2-D Simulated Velocities
Measured Velocities

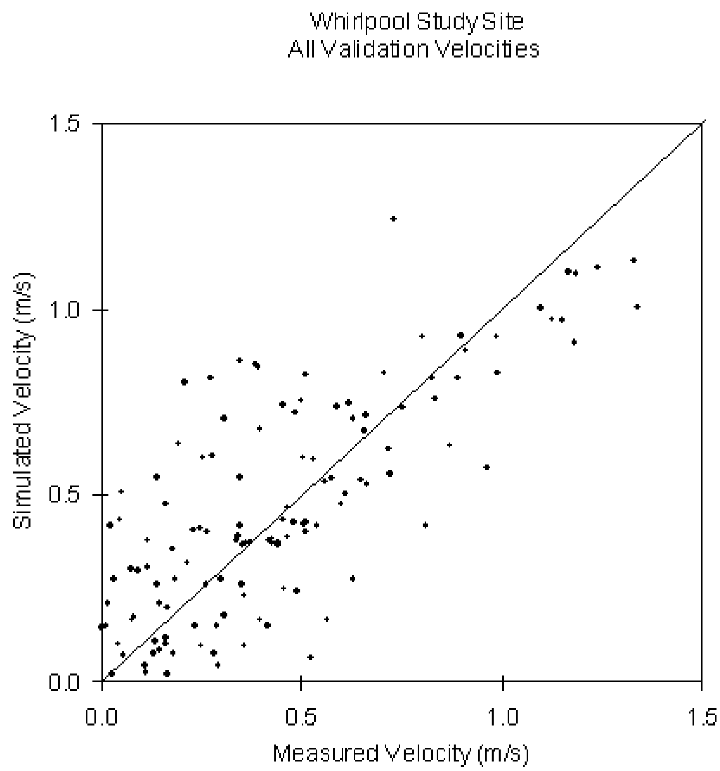
Whirlpool Study Site
All Validation Velocities
Simulated Velocity (m/s)
Measured Velocity (m/s)
0.0
0.5
1.0
1.5

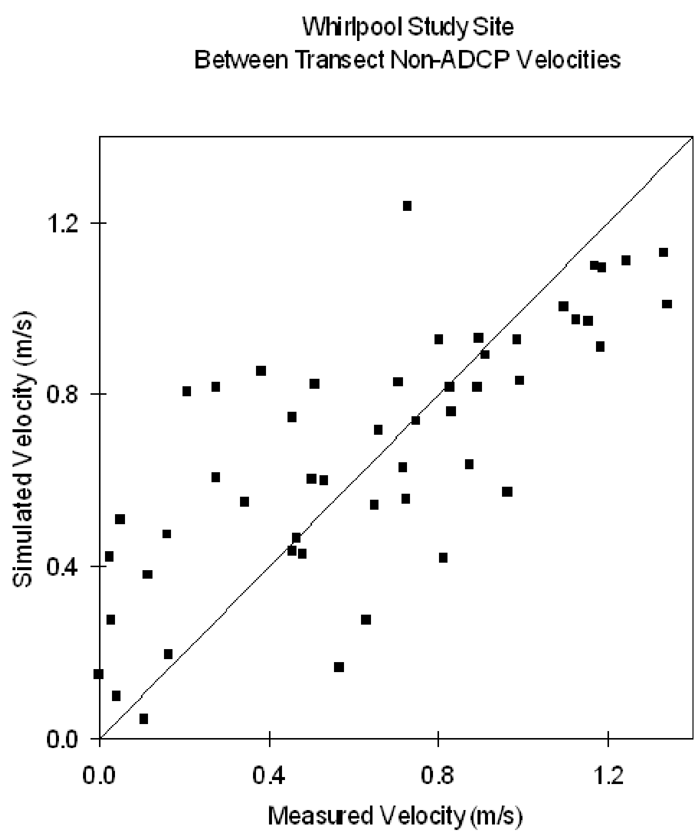
Whirlpool Study Site
Between Transect Non-ADCP Velocities
Simulated Velocity (m/s)
Measured Velocity (m/s)
0.0
0.4
0.8
1.2

Side-Channel Site

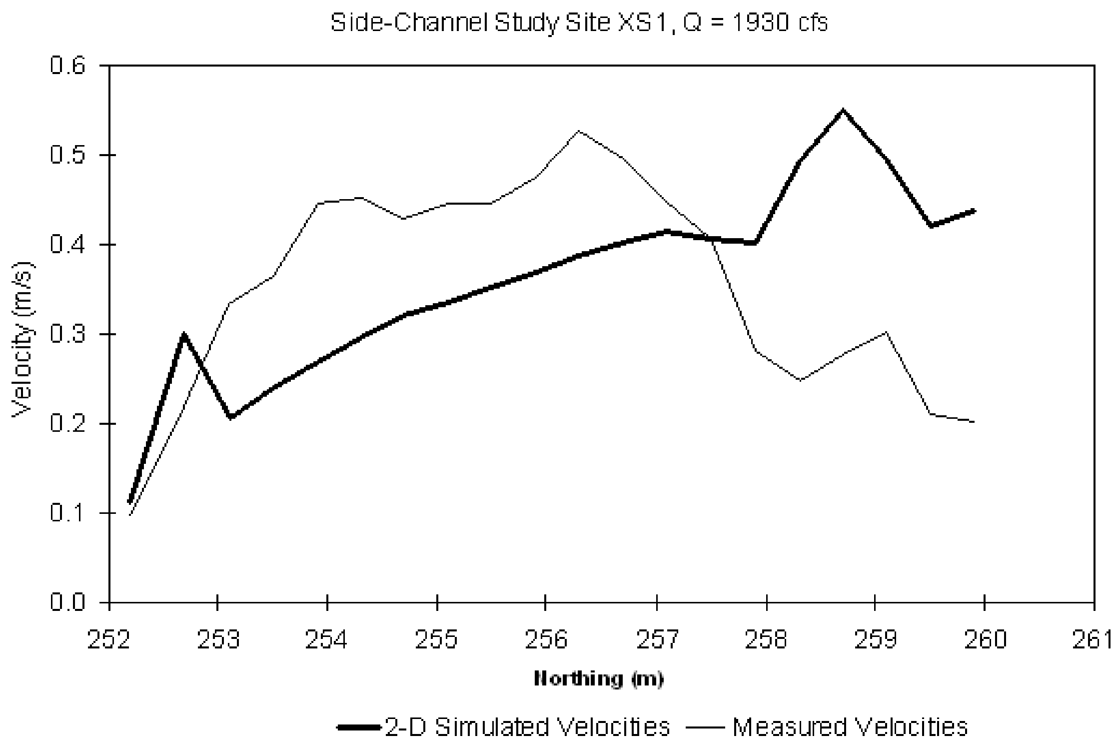

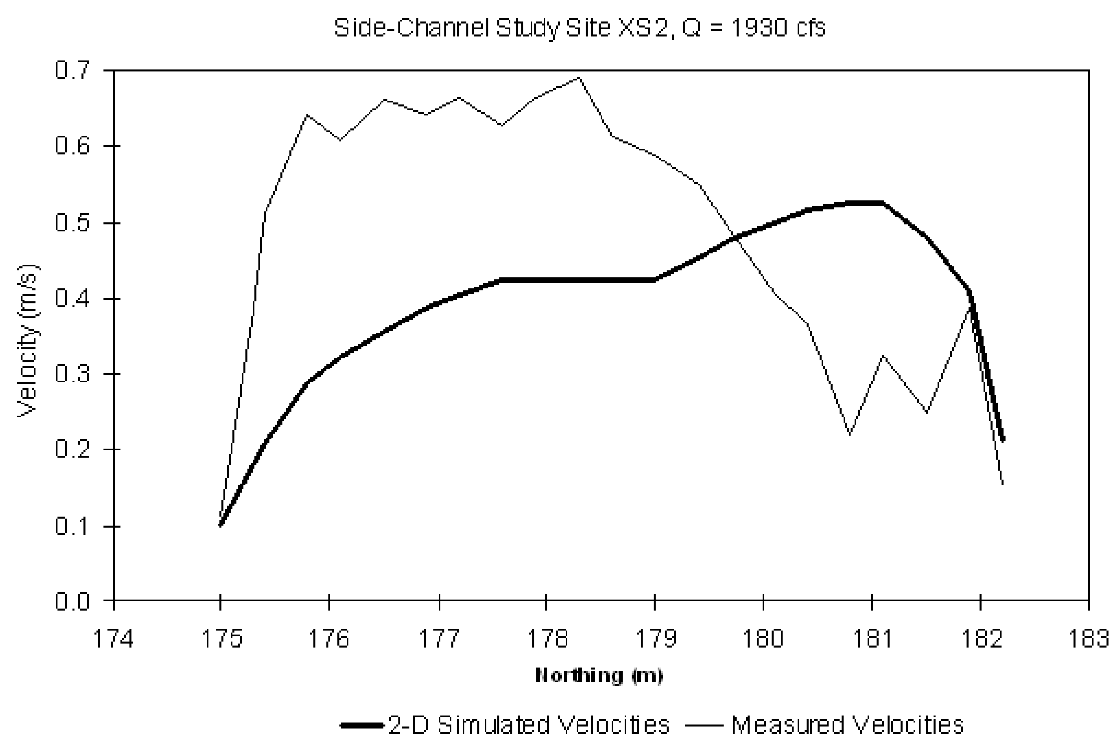

Side-Channel Study Site
All Validation Velocities

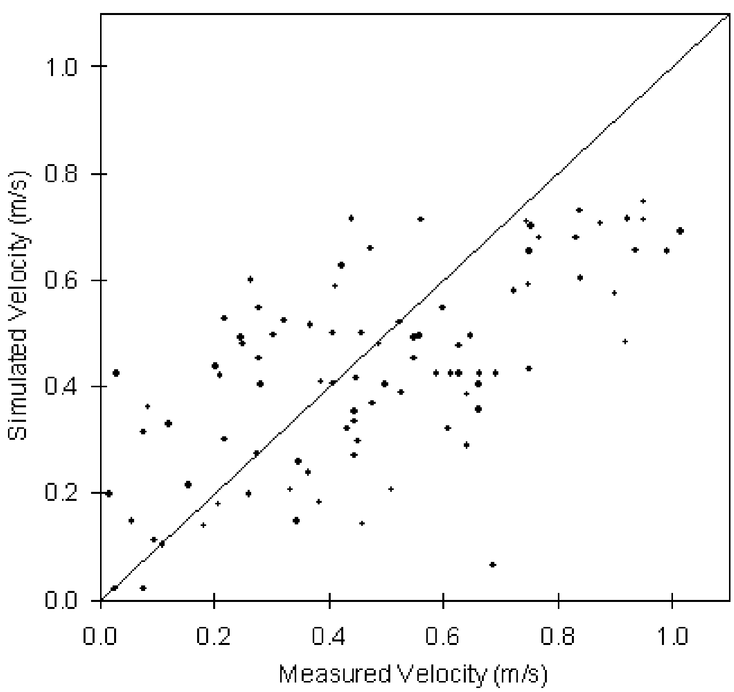

Side-Channel Study Site
Between Transect Non-ADCP Validation Velocities

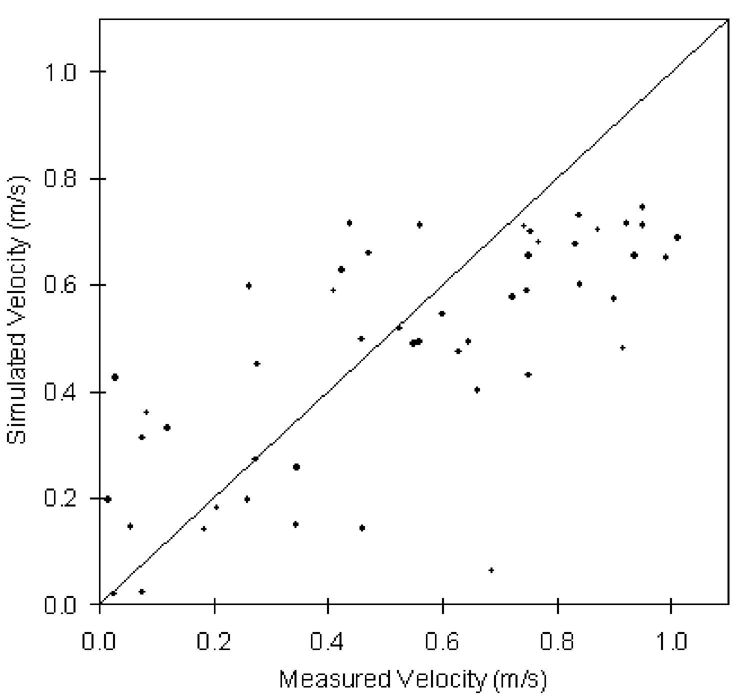

Sucker Glide Study Site

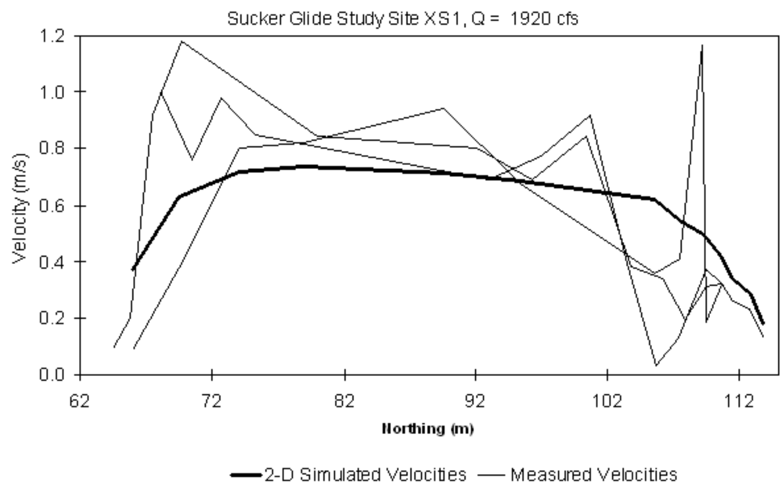

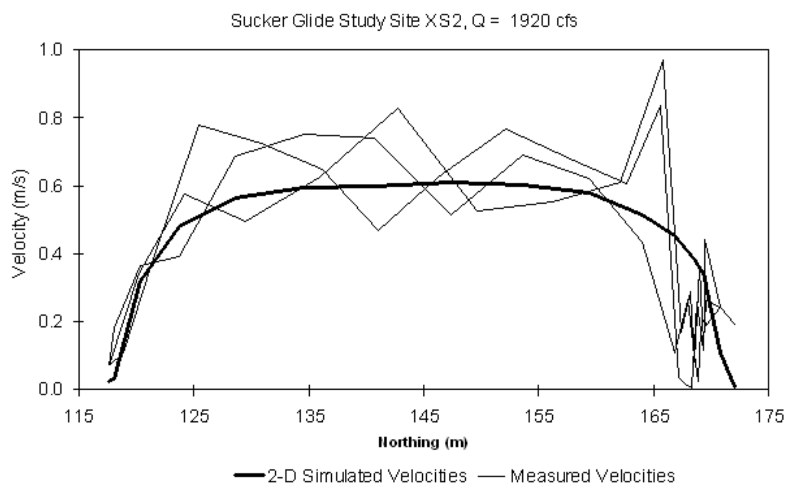

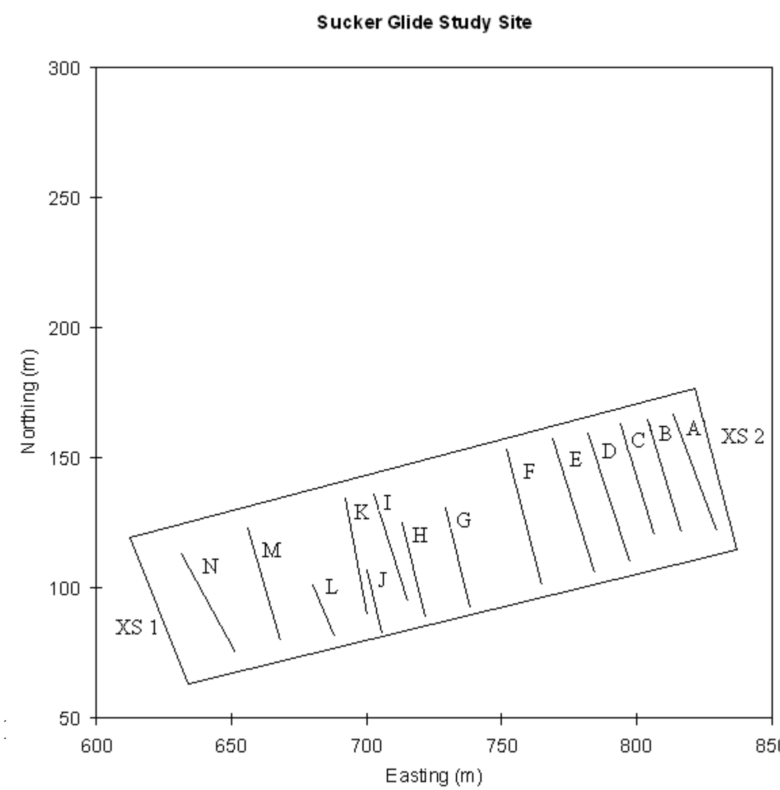

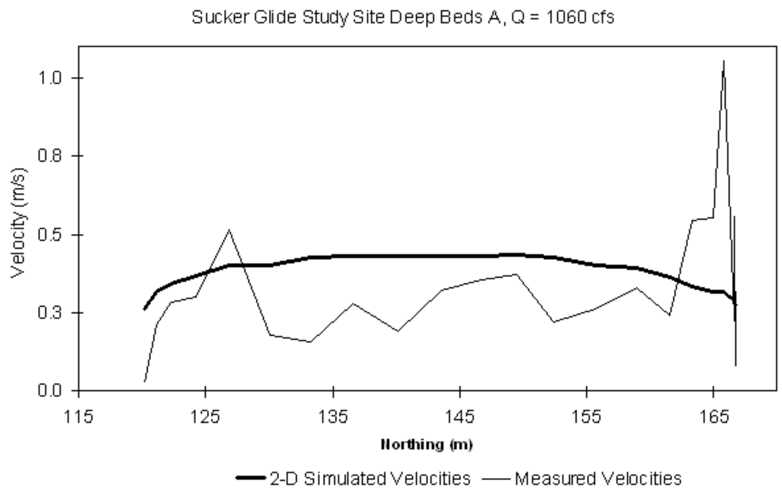
Sucker Glide Study Site Deep Beds A, Q = 1060 cfs
Velocity (m/s)
Northing (m)
2-D Simulated Velocities
Measured Velocities

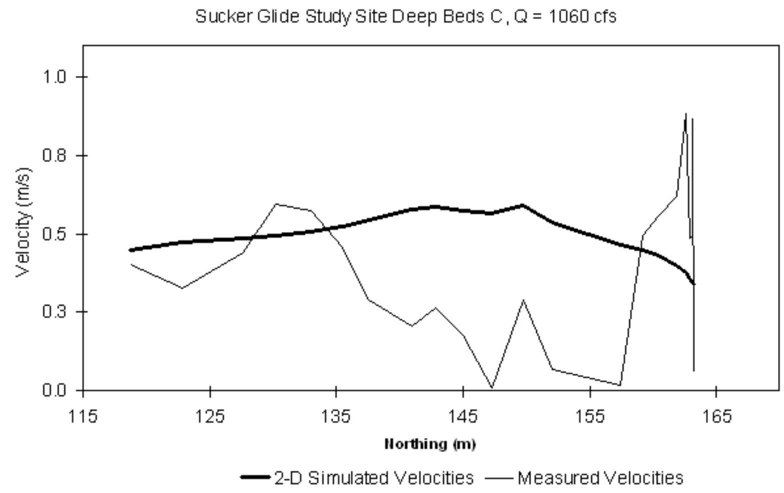
Sucker Glide Study Site Deep Beds C, Q = 1060 cfs
Velocity (m/s)
Northing (m)
2-D Simulated Velocities
Measured Velocities

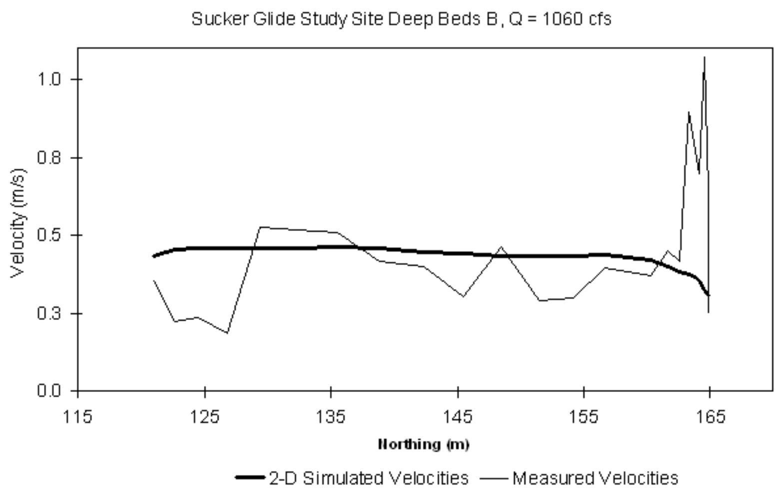
Sucker Glide Study Site Deep Beds B, Q = 1060 cfs
Velocity (m/s)
Northing (m)
2-D Simulated Velocities
Measured Velocities

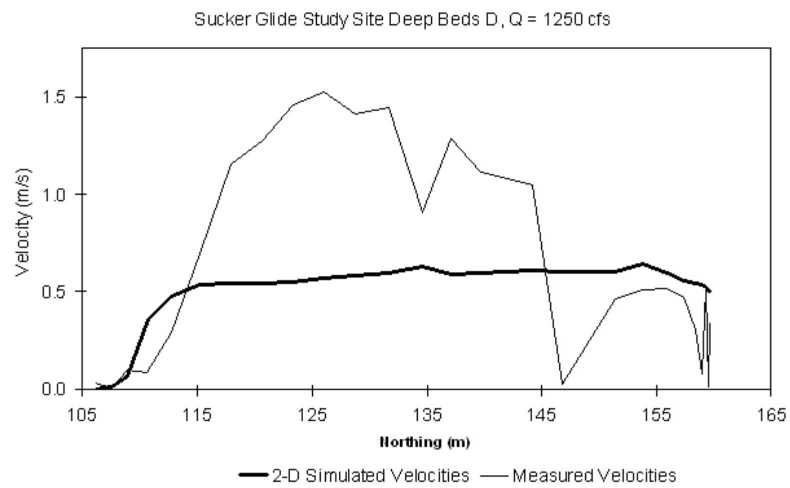
Sucker Glide Study Site Deep Beds D, Q = 1250 cfs
Velocity (m/s)
Northing (m)
2-D Simulated Velocities
Measured Velocities

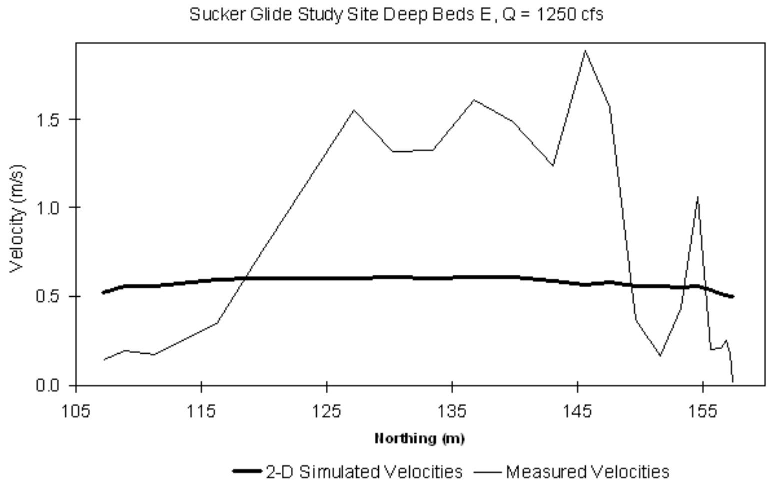

Sucker Glide Study Site Deep Beds E, Q = 1250 cfs
Velocity (m/s)
Northing (m)
2-D Simulated Velocities
Measured Velocities

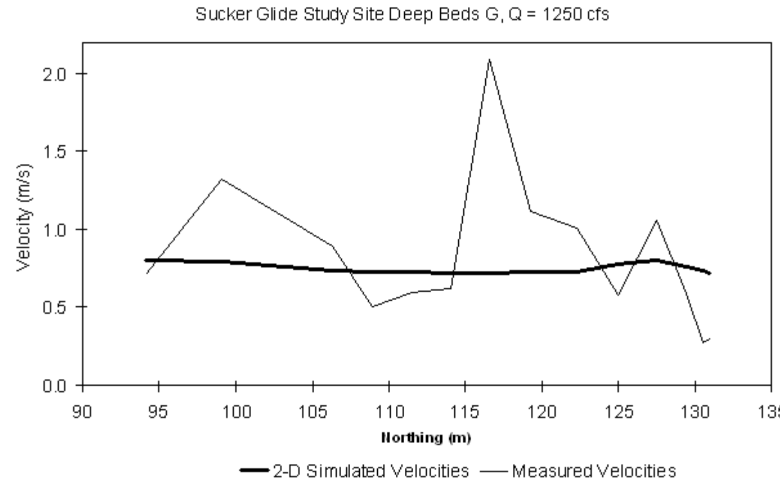

Sucker Glide Study Site Deep Beds G, Q = 1250 cfs
Velocity (m/s)
Northing (m)
2-D Simulated Velocities
Measured Velocities

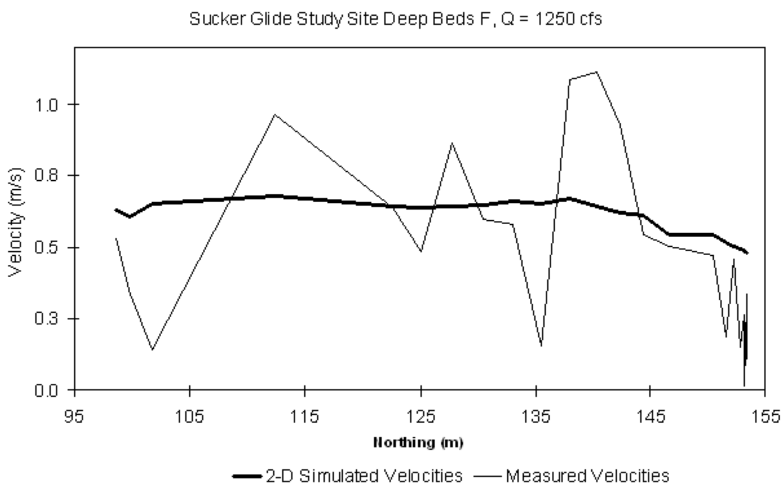

Sucker Glide Study Site Deep Beds F, Q = 1250 cfs
Velocity (m/s)
Northing (m)
2-D Simulated Velocities
Measured Velocities

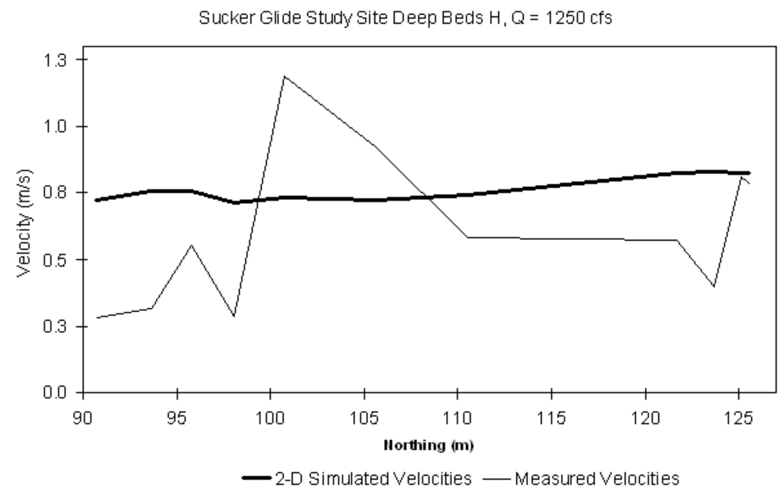

Sucker Glide Study Site Deep Beds H, Q = 1250 cfs
Velocity (m/s)
Northing (m)
2-D Simulated Velocities
Measured Velocities

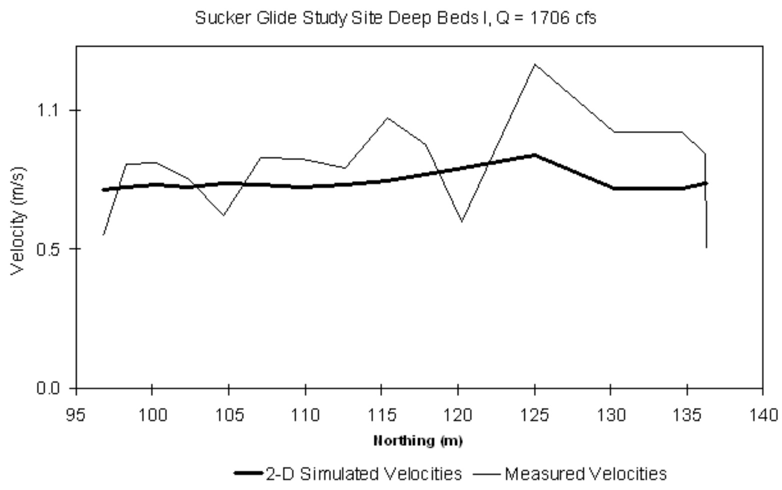
Sucker Glide Study Site Deep Beds I, Q = 1706 cfs
Velocity (m/s)
Northing (m)
2-D Simulated Velocities
Measured Velocities

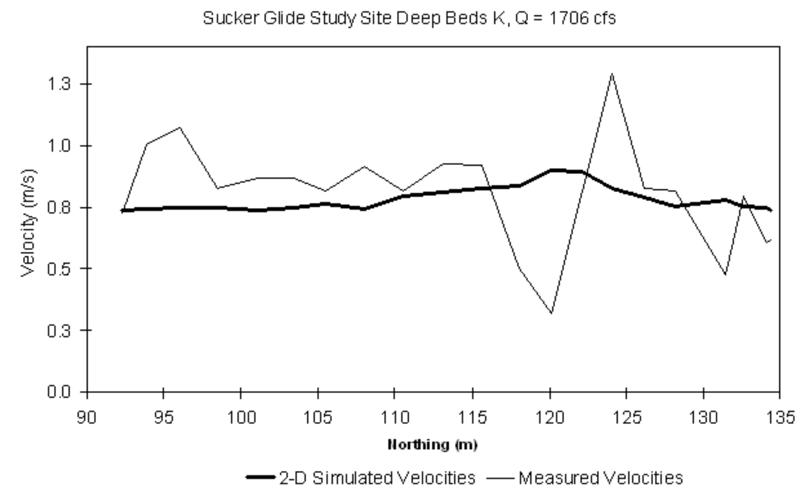
Sucker Glide Study Site Deep Beds K, Q = 1706 cfs
Velocity (m/s)
Northing (m)
2-D Simulated Velocities
Measured Velocities

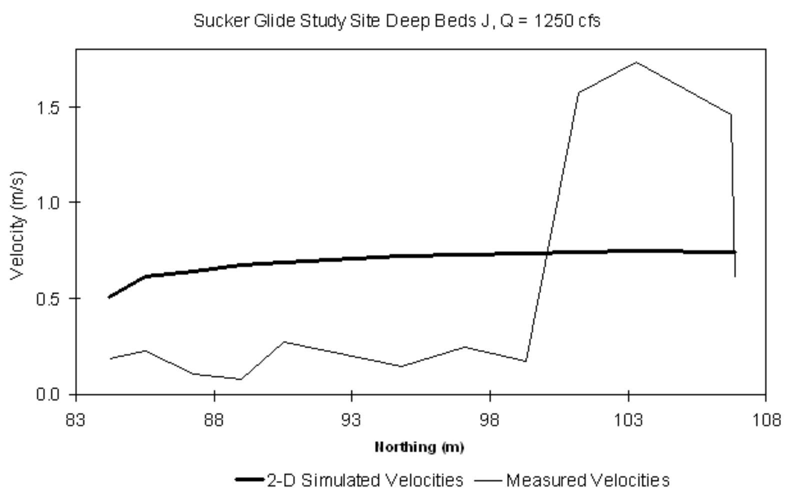
Sucker Glide Study Site Deep Beds J, Q = 1250 cfs
Velocity (m/s)
Northing (m)
2-D Simulated Velocities
Measured Velocities

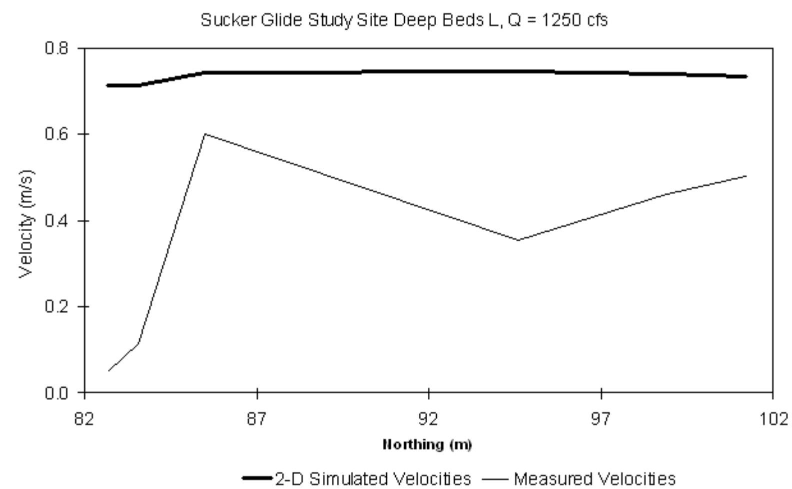
Sucker Glide Study Site Deep Beds L, Q = 1250 cfs
Velocity (m/s)
Northing (m)
2-D Simulated Velocities
Measured Velocities

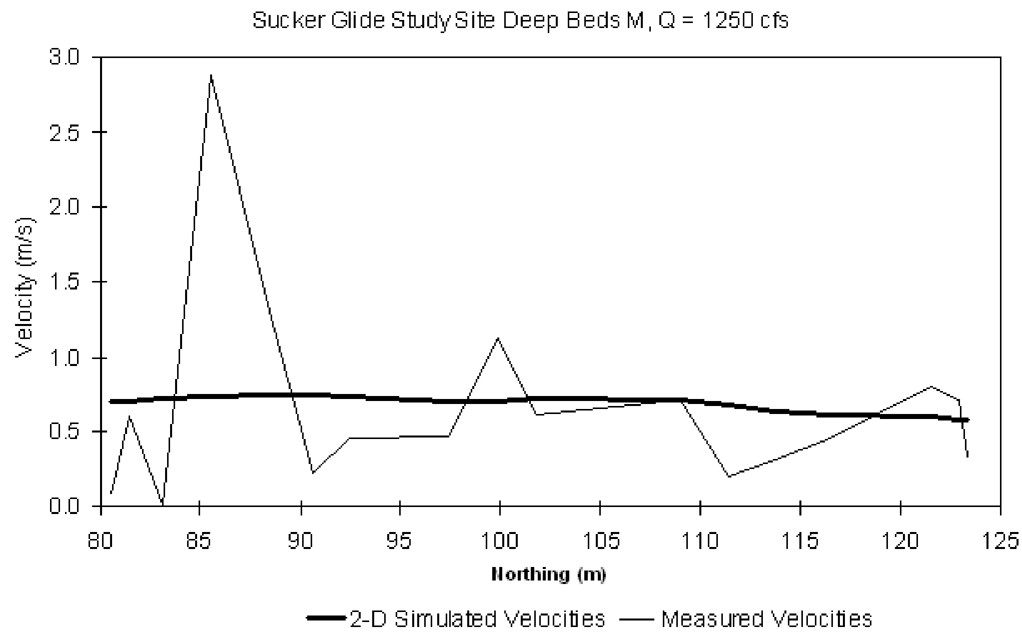
Sucker Glide Study Site Deep Beds M, Q = 1250 cfs
3.0
2.5
2.0
1.5
1.0
0.5
0.0
Velocity (m/s)
80
85
90
95
100
105
110
115
120
125
Northing (m)
2-D Simulated Velocities
Measured Velocities

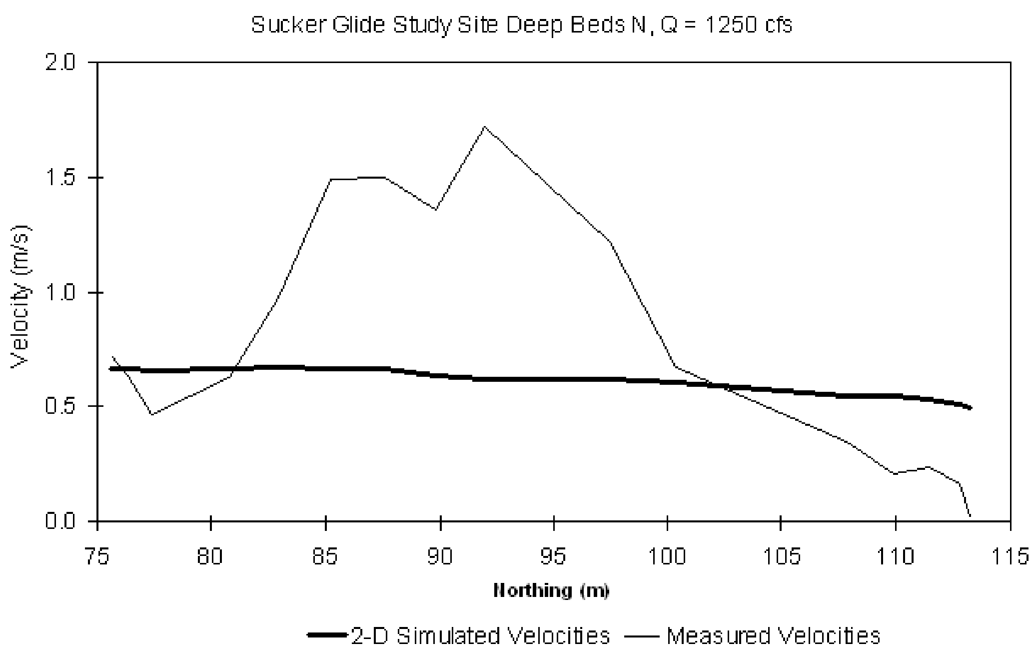
Sucker Glide Study Site Deep Beds N, Q = 1250 cfs
2.0
1.5
1.0
0.5
0.0
Velocity (m/s)
75
80
85
90
95
100
105
110
115
Northing (m)
2-D Simulated Velocities
Measured Velocities

Sucker Glide Study Site
All Validation Velocities

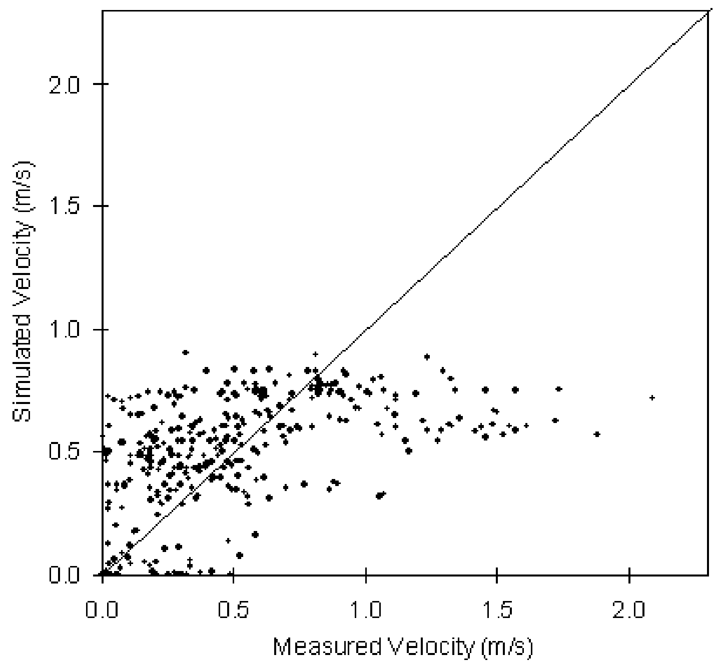

Sucker Glide Study Site
Between Transect Non-ADCP Velocities

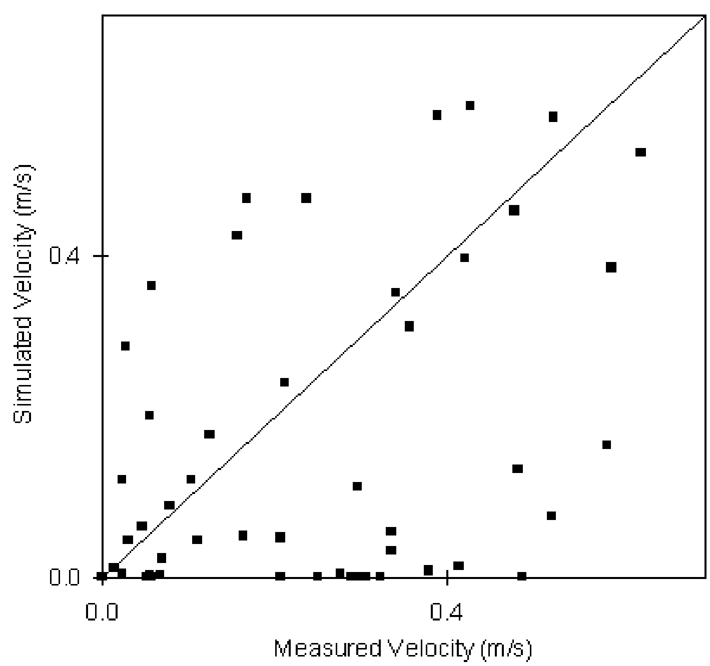

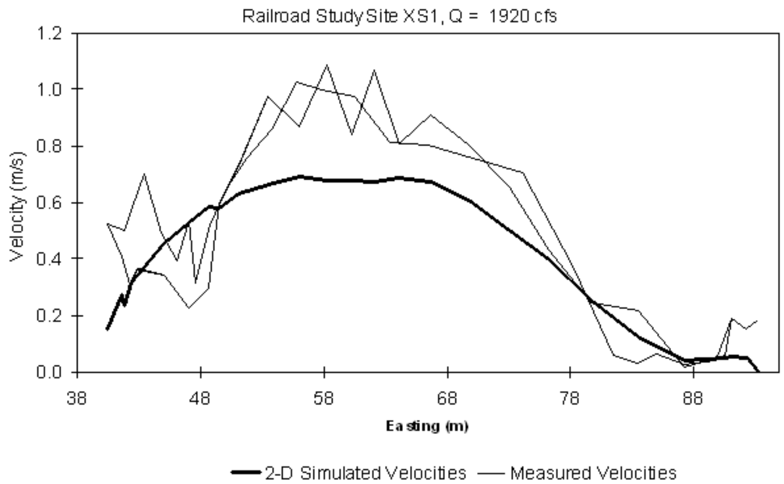
Railroad Study Site XS1, Q = 1920 cfs
Velocity (m/s)
Easting (m)
2-D Simulated Velocities
Measured Velocities

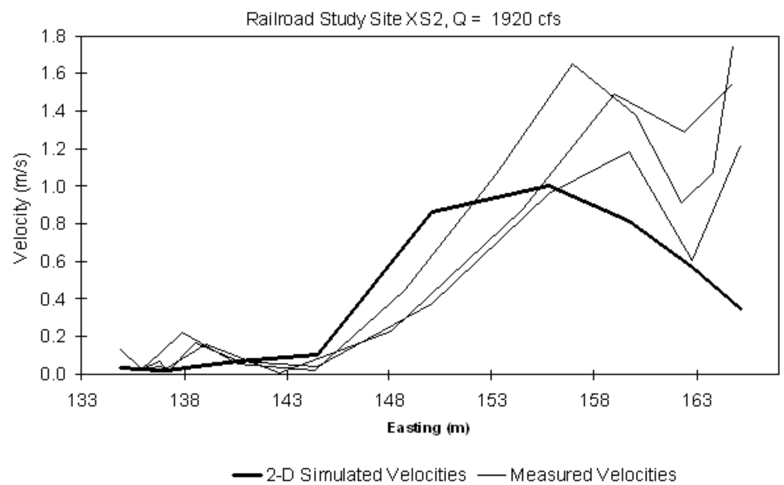
Railroad Study Site XS2, Q = 1920 cfs
Velocity (m/s)
Easting (m)
2-D Simulated Velocities
Measured Velocities

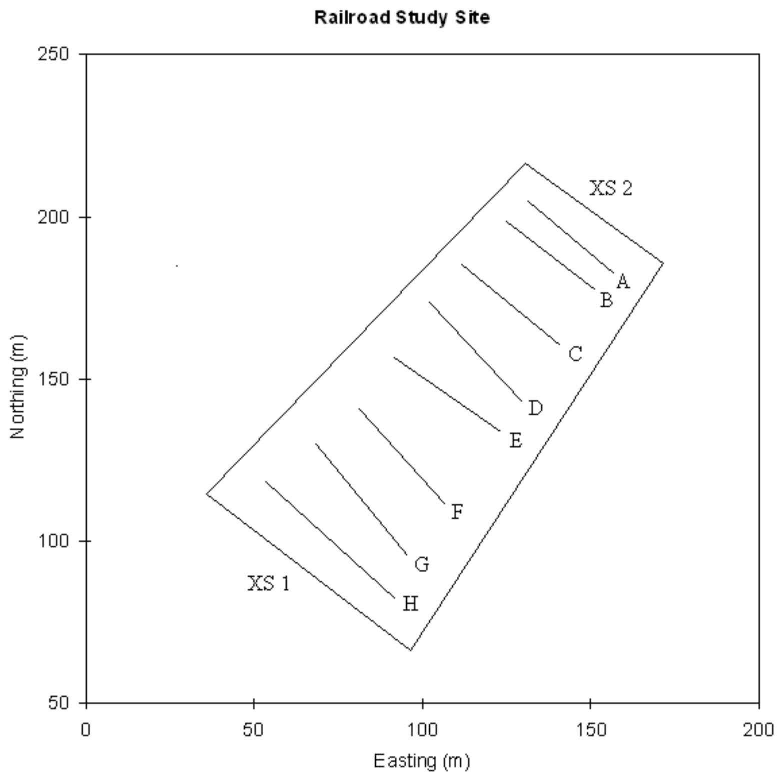
Railroad Study Site
Northing (m)
Easting (m)
XS 2
XS 1
A
B
C
D
E
F
G
H

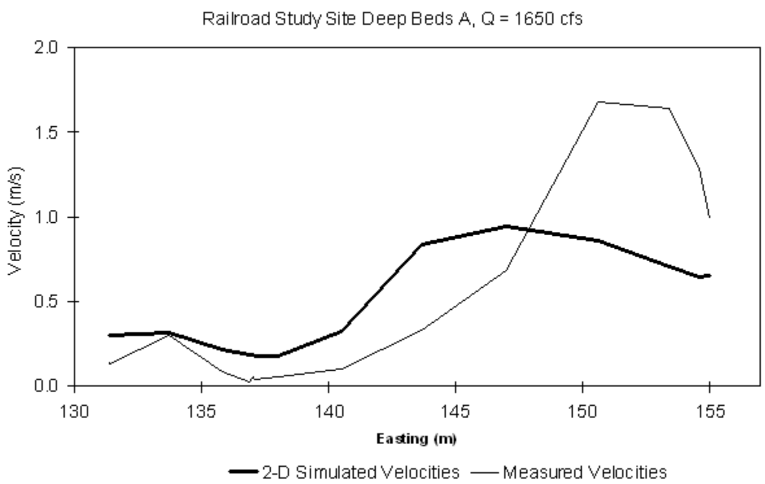
Railroad Study Site Deep Beds A, Q = 1650 cfs
Velocity (m/s)
Easting (m)
2-D Simulated Velocities
Measured Velocities

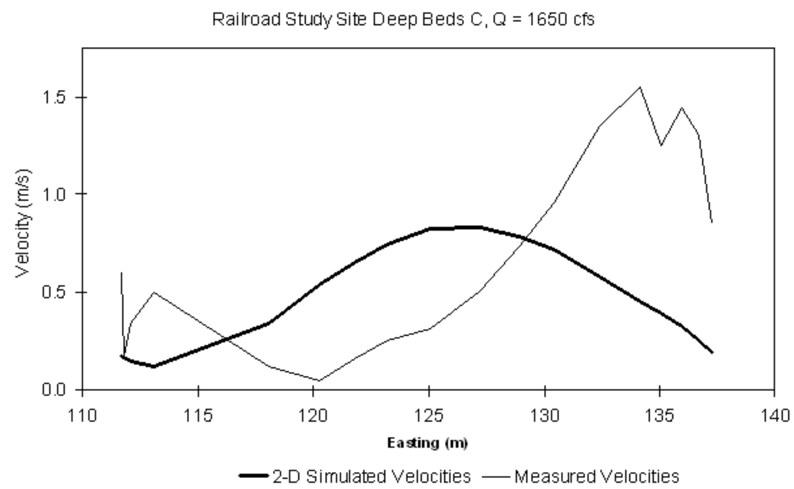
Railroad Study Site Deep Beds C, Q = 1650 cfs
Velocity (m/s)
Easting (m)
2-D Simulated Velocities
Measured Velocities

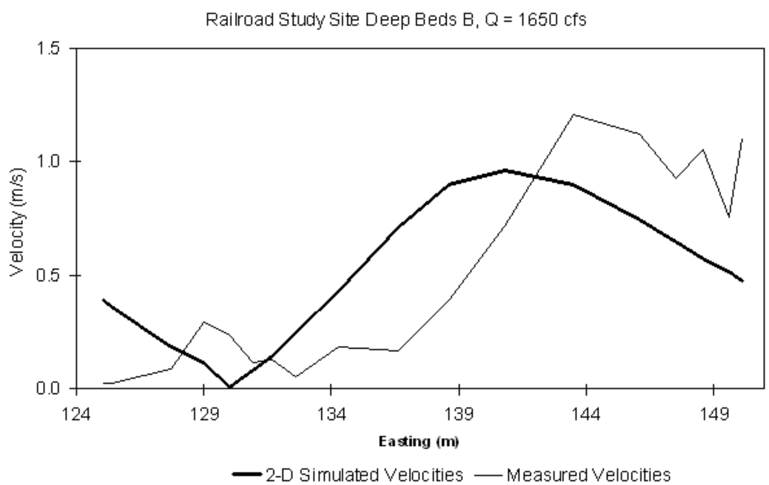
Railroad Study Site Deep Beds B, Q = 1650 cfs
Velocity (m/s)
Easting (m)
2-D Simulated Velocities
Measured Velocities

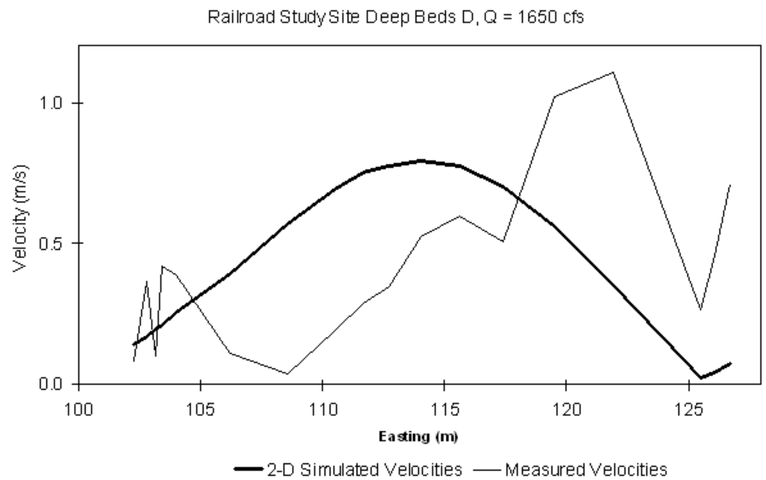
Railroad Study Site Deep Beds D, Q = 1650 cfs
Velocity (m/s)
Easting (m)
2-D Simulated Velocities
Measured Velocities

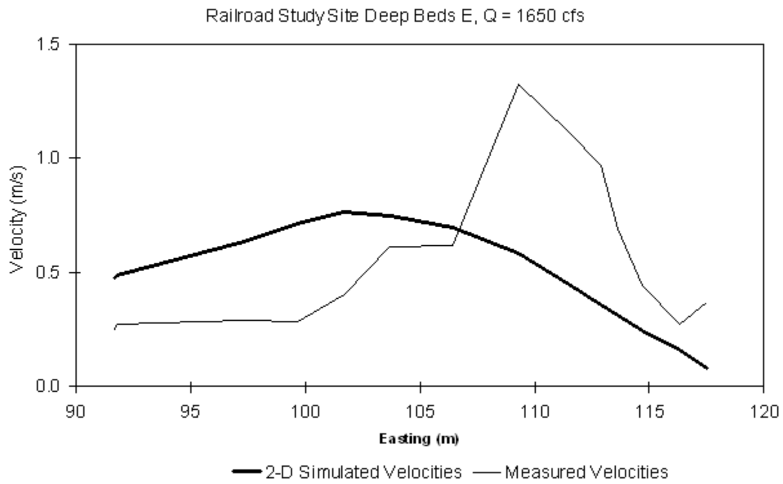
Railroad Study Site Deep Beds E, Q = 1650 cfs
Velocity (m/s)
Easting (m)
2-D Simulated Velocities
Measured Velocities

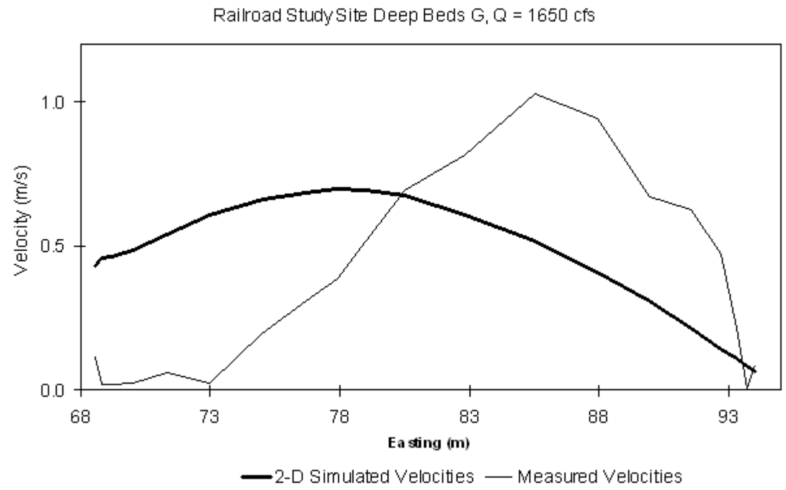
Railroad Study Site Deep Beds G, Q = 1650 cfs
Velocity (m/s)
Easting (m)
2-D Simulated Velocities
Measured Velocities

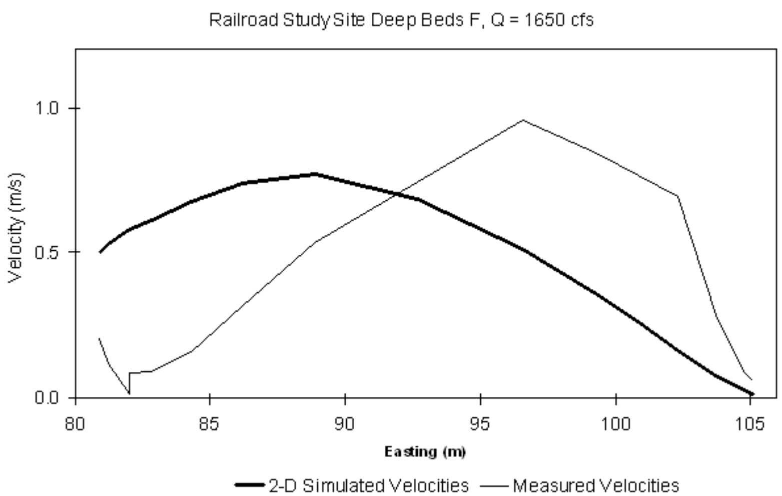
Railroad Study Site Deep Beds F, Q = 1650 cfs
Velocity (m/s)
Easting (m)
2-D Simulated Velocities
Measured Velocities

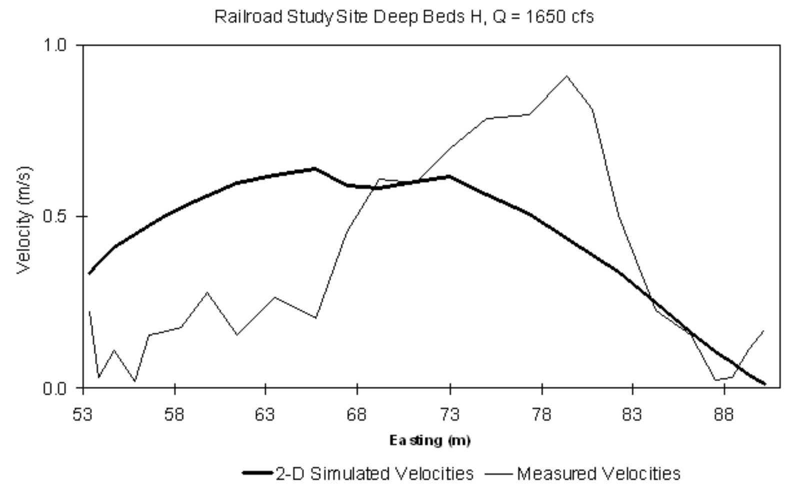
Railroad Study Site Deep Beds H, Q = 1650 cfs
Velocity (m/s)
Easting (m)
2-D Simulated Velocities
Measured Velocities

Railroad Study Site
Between Transect Non-ADCP Velocities

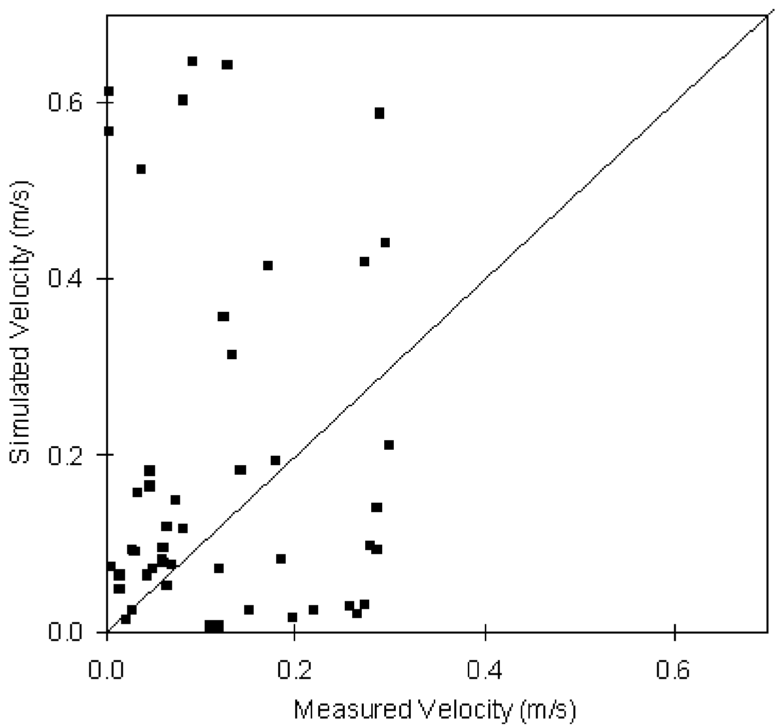

Railroad Study Site
All Validation Velocities

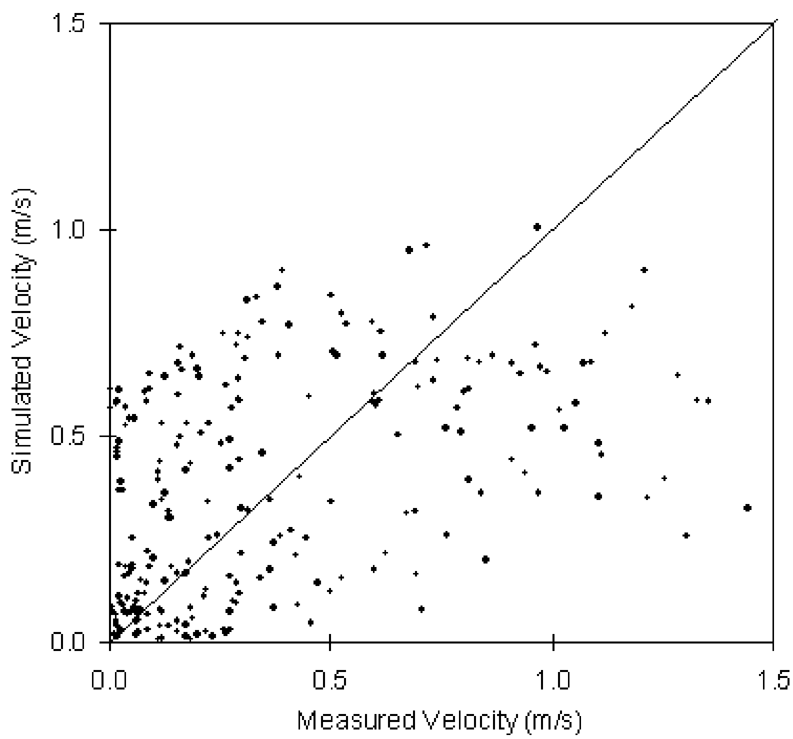

APPENDIX I
EXAMPLE HYDRAULIC MODEL OUTPUT

Narrows Site at 400 cfs

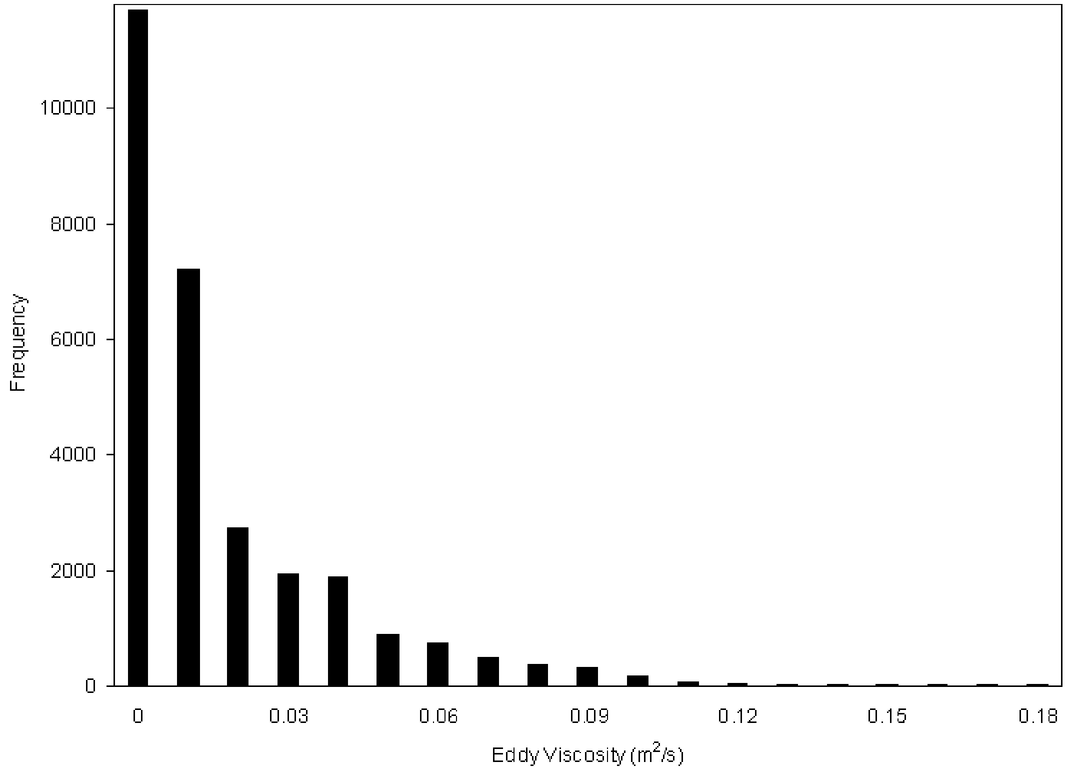

Narrows Site at 4,500 cfs

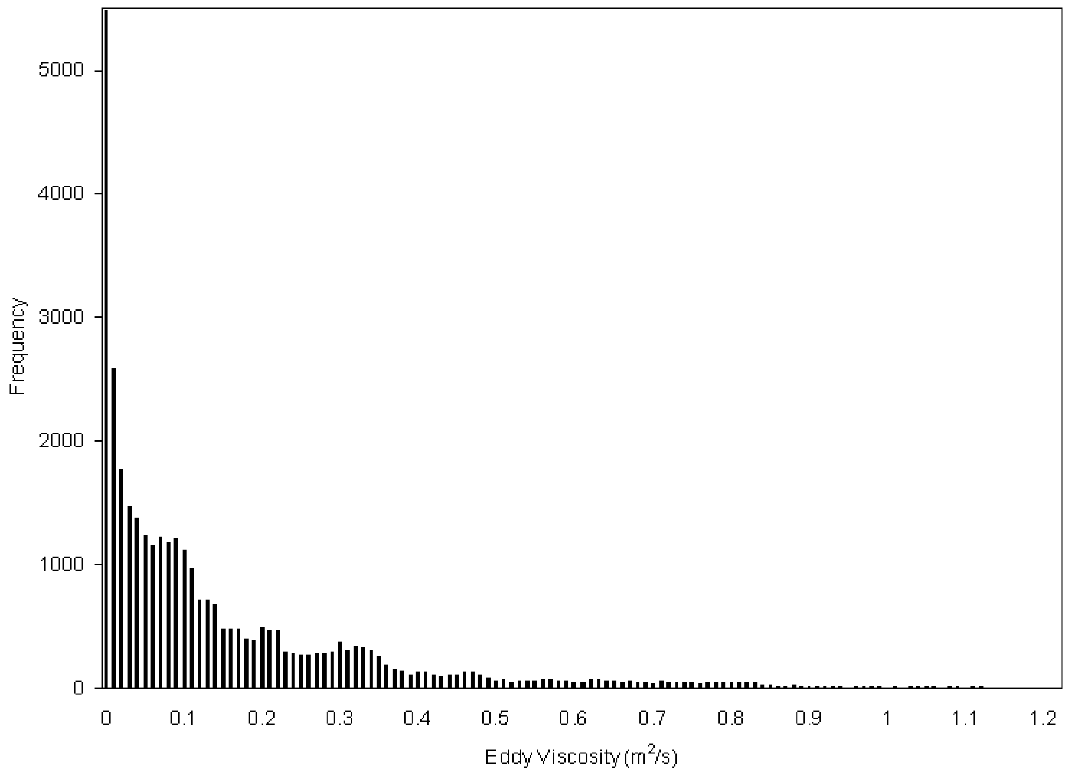

Rosebar Site at 400 cfs

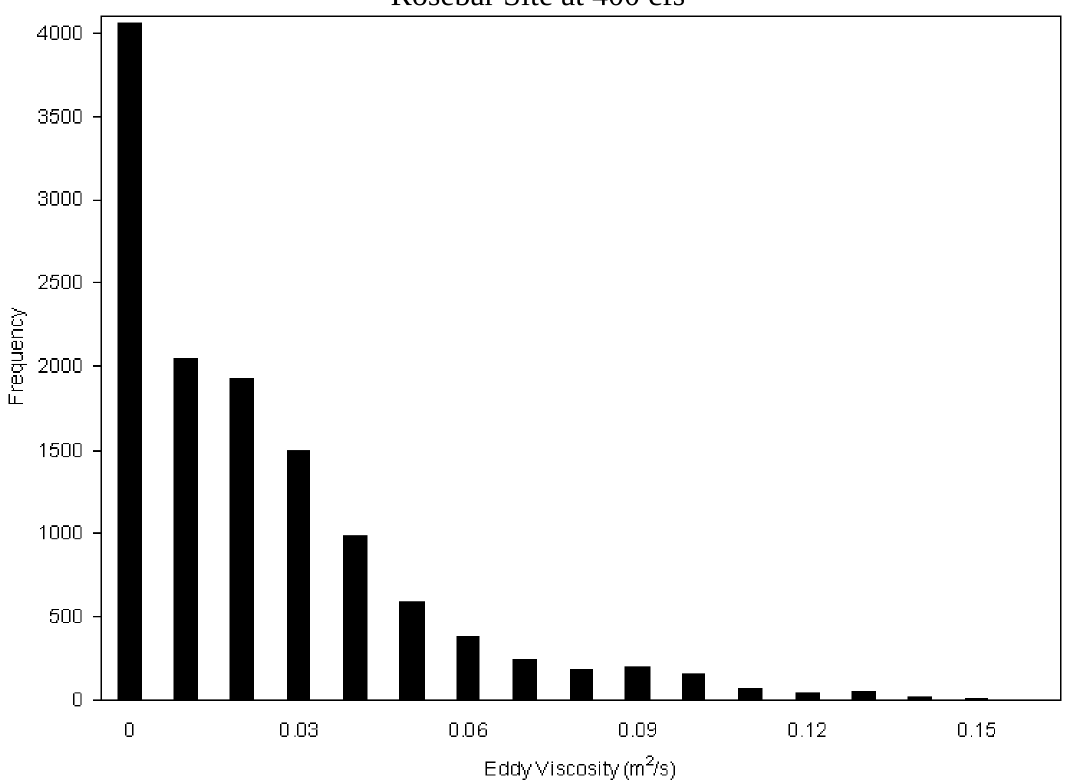

Rosebar Site at 4,500 cfs

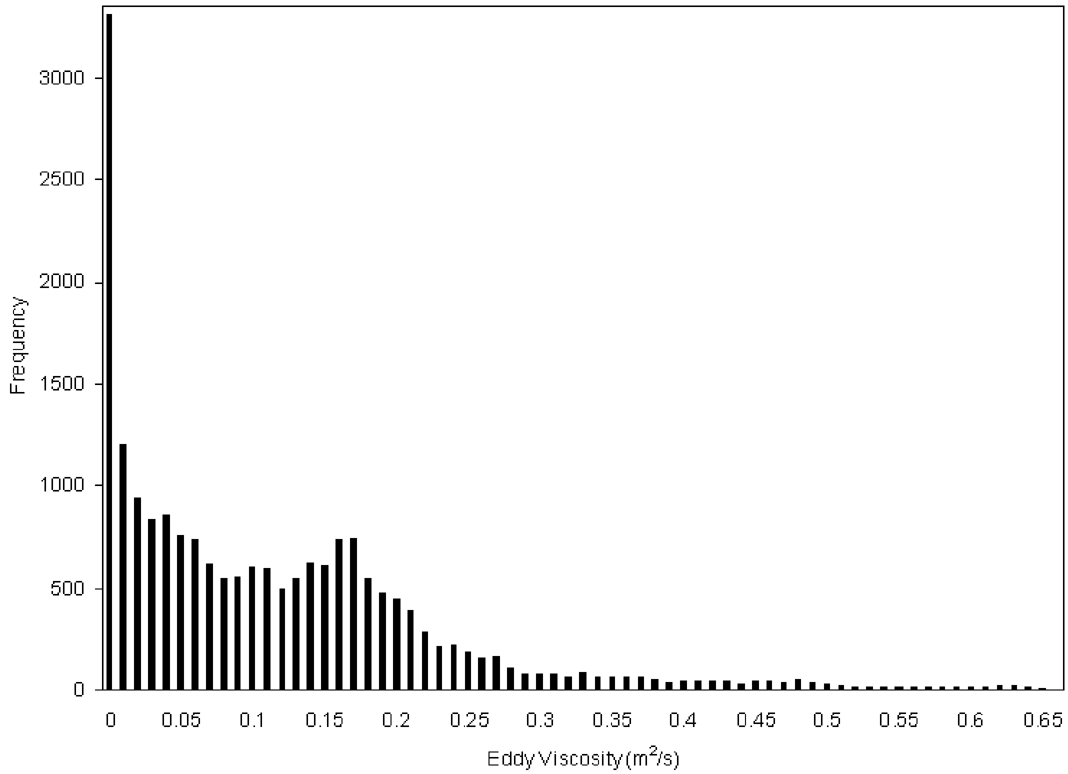

Diversion Site at 400 cfs

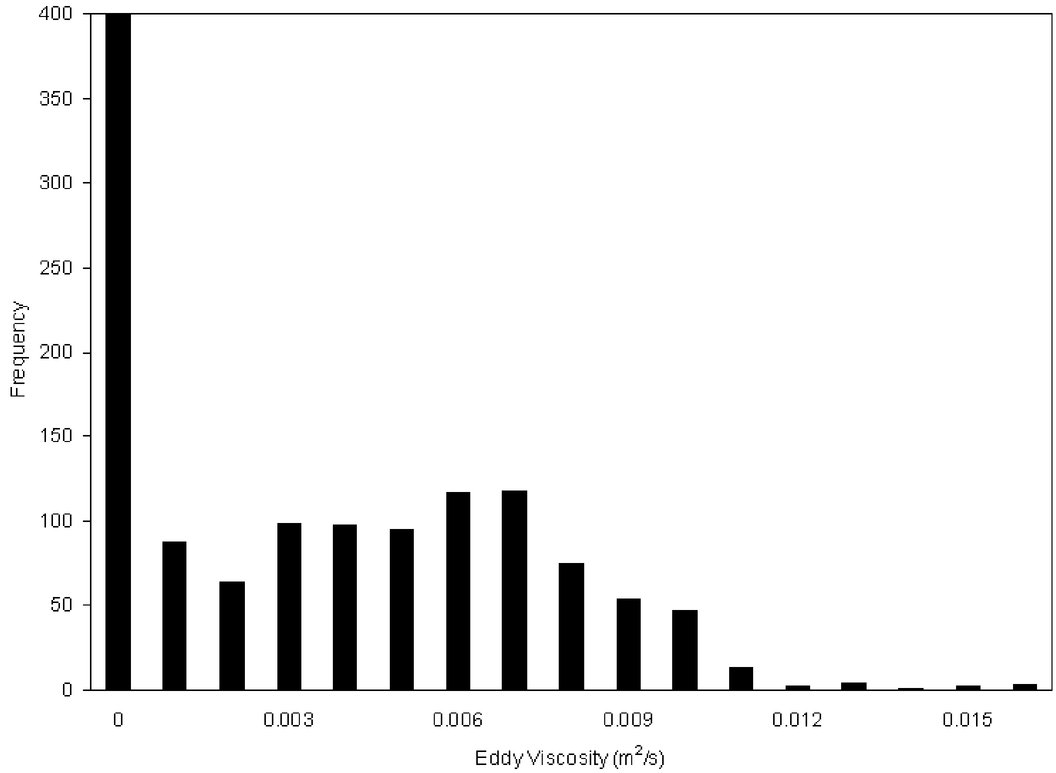

Diversion Site at 4,500 cfs

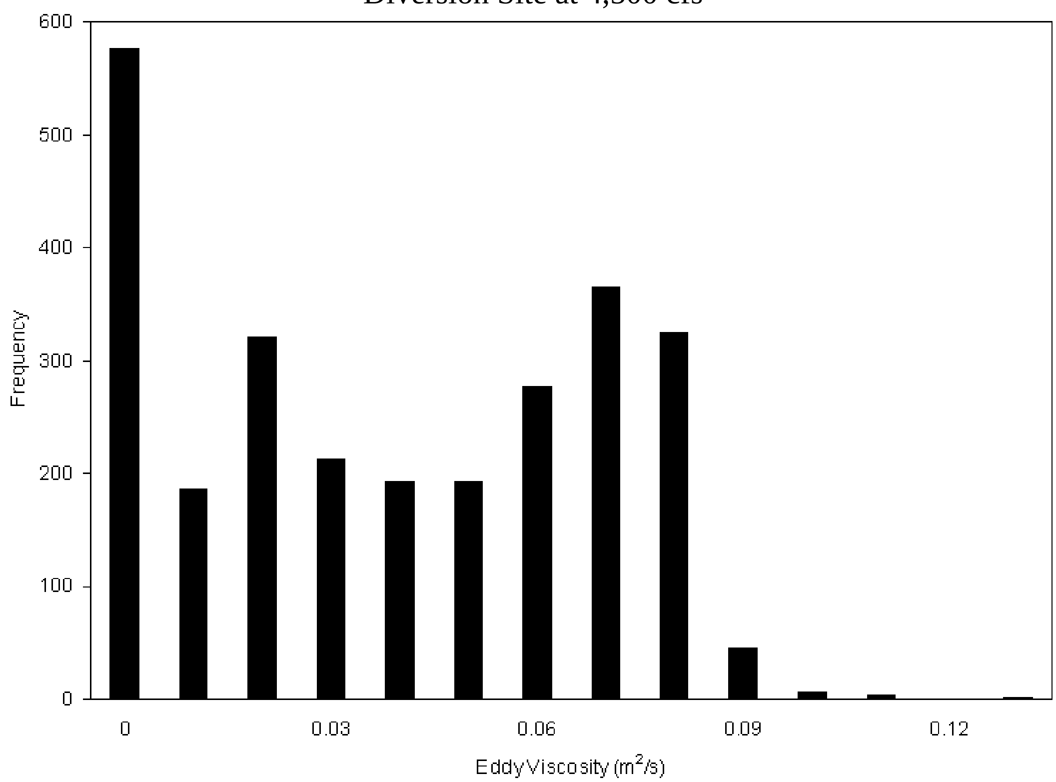

Lower Hallwood Site at 150 cfs

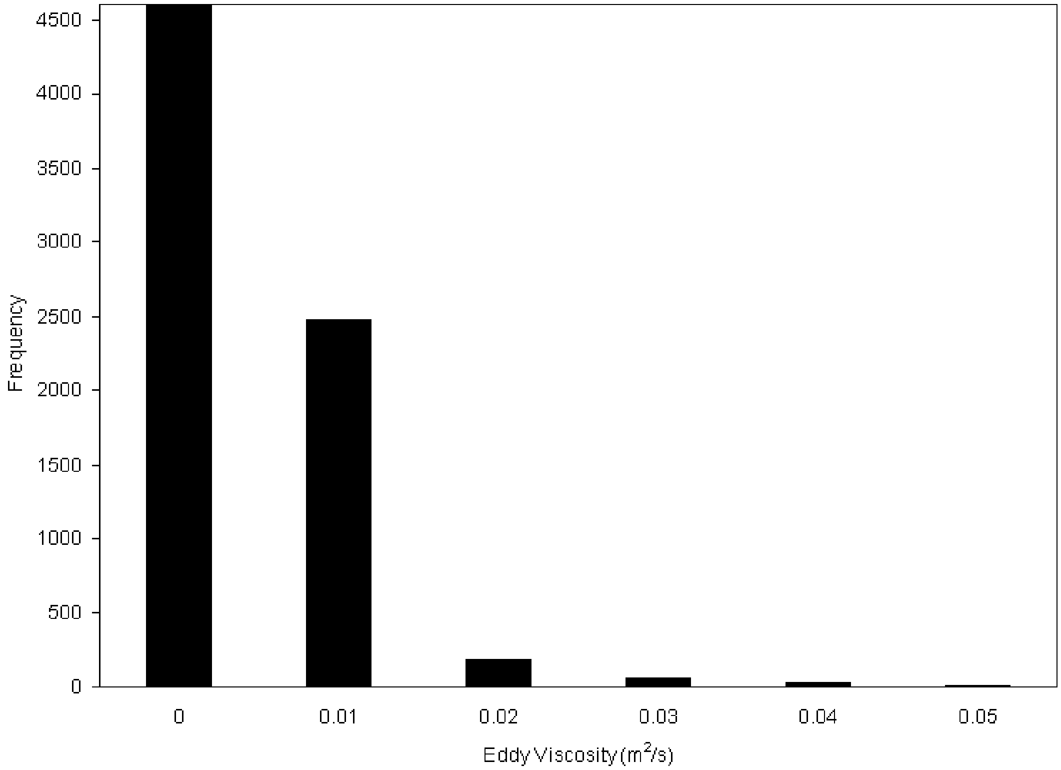

Lower Hallwood Site at 4,500 cfs

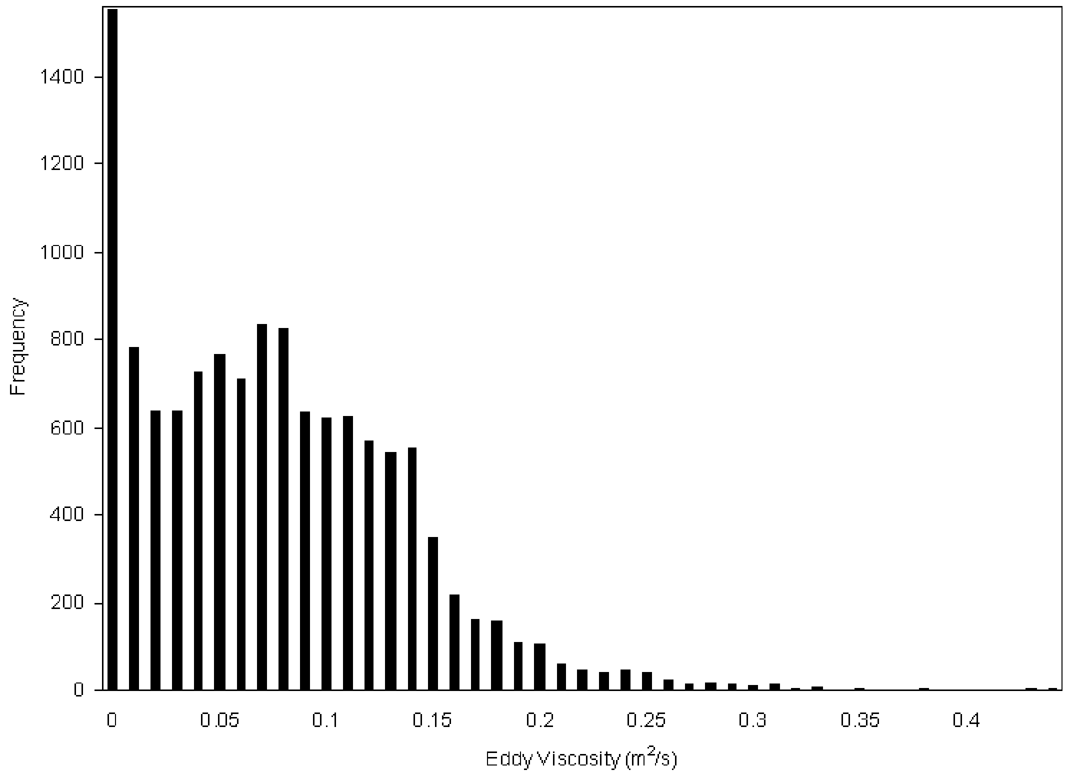

Whirlpool Site at 300 cfs

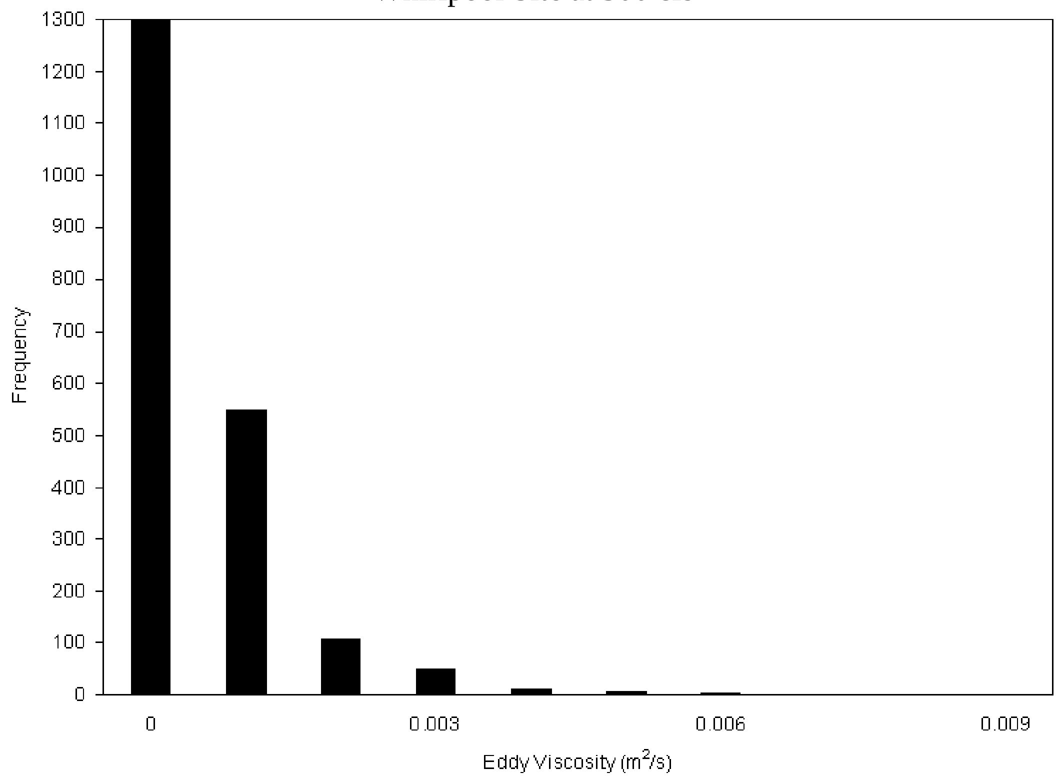

Whirlpool Site at 4,500 cfs

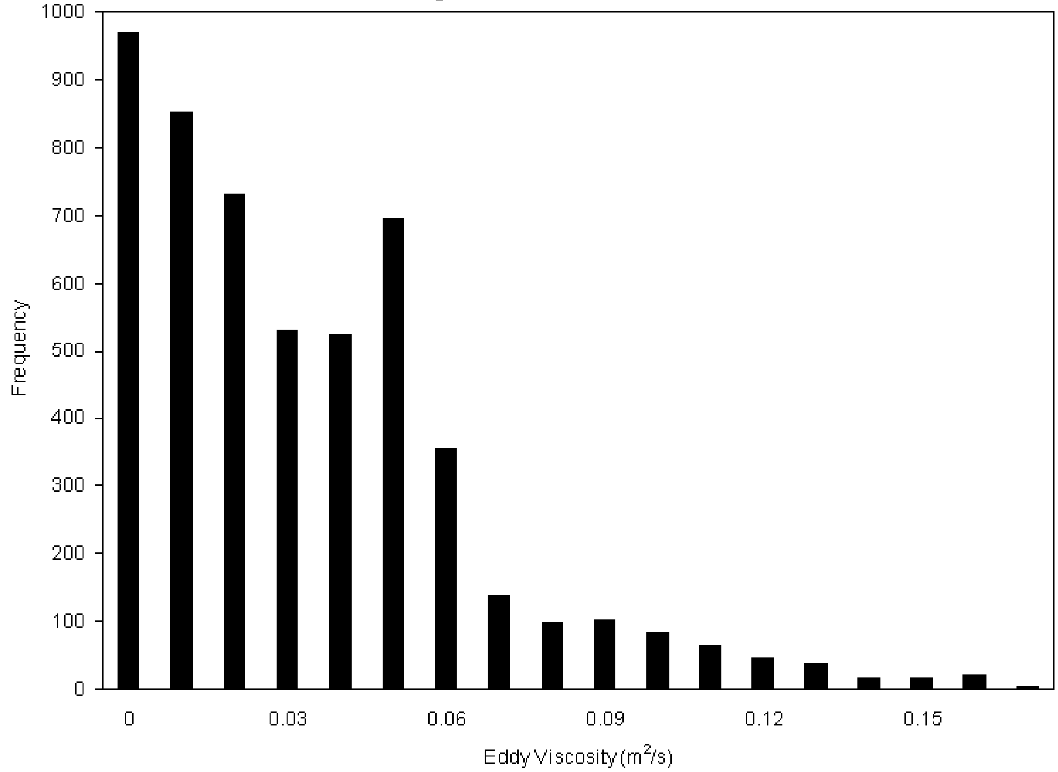

Side-Channel Site at 900 cfs

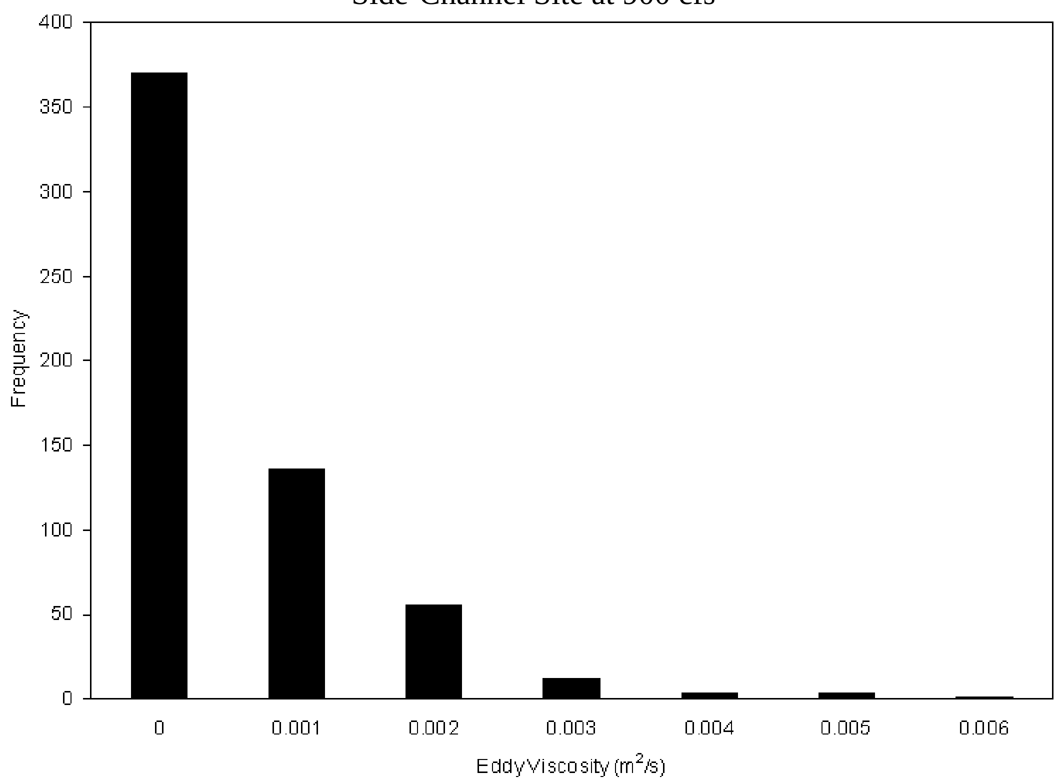

Side-Channel Site at 4,500 cfs

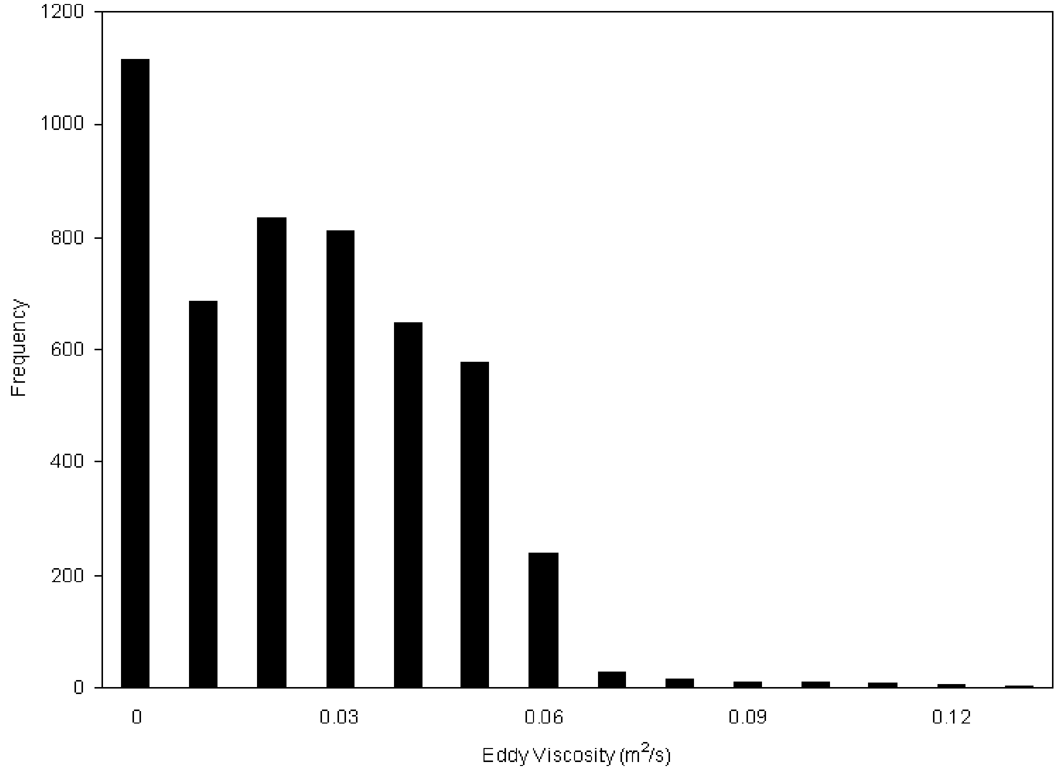

Sucker Glide Site at 150 cfs

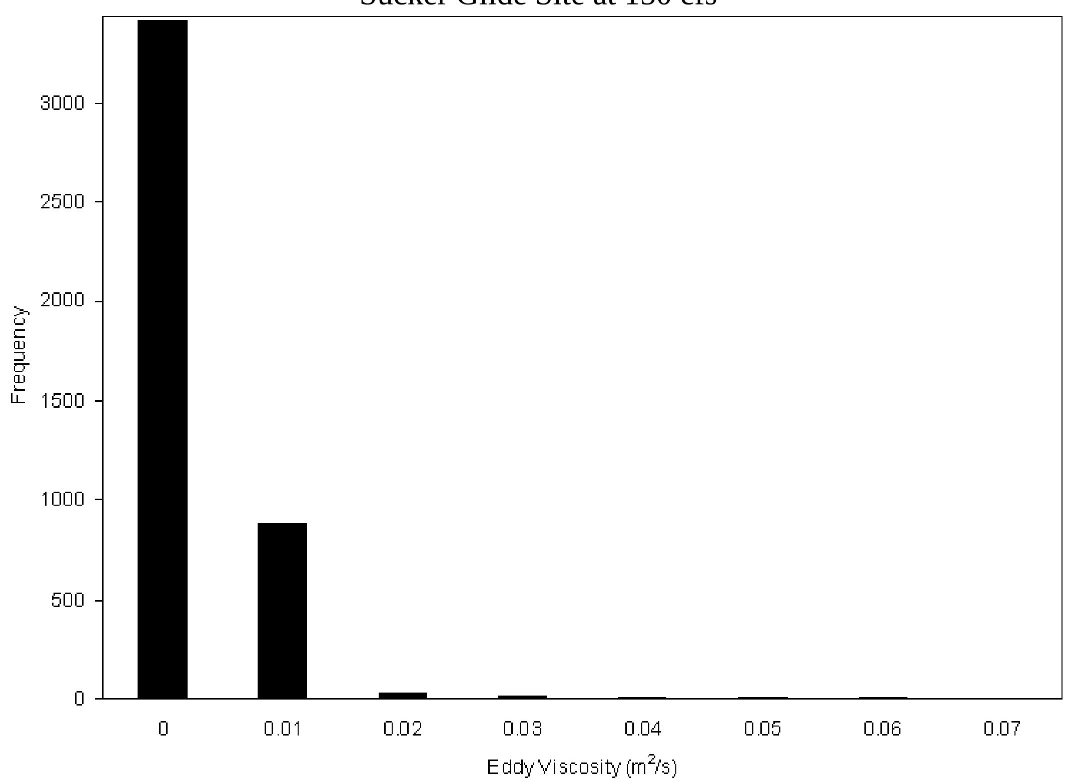

Sucker Glide Site at 4,500 cfs

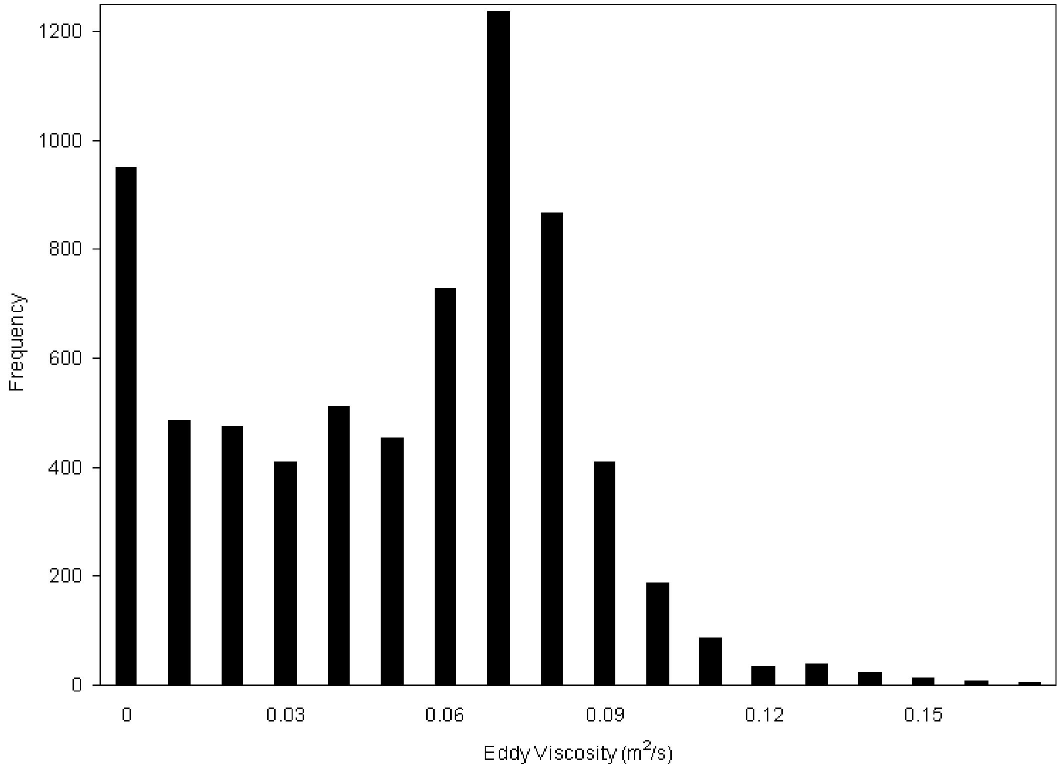

Railroad Site at 150 cfs

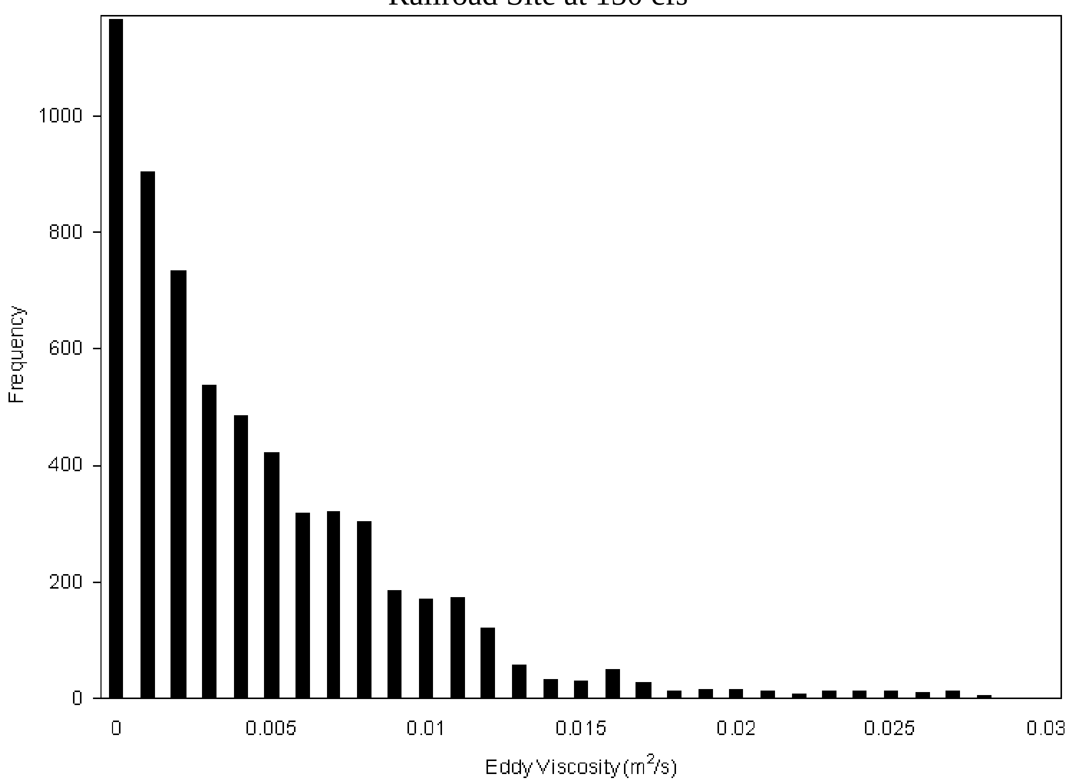

Railroad Site at 4,500 cfs

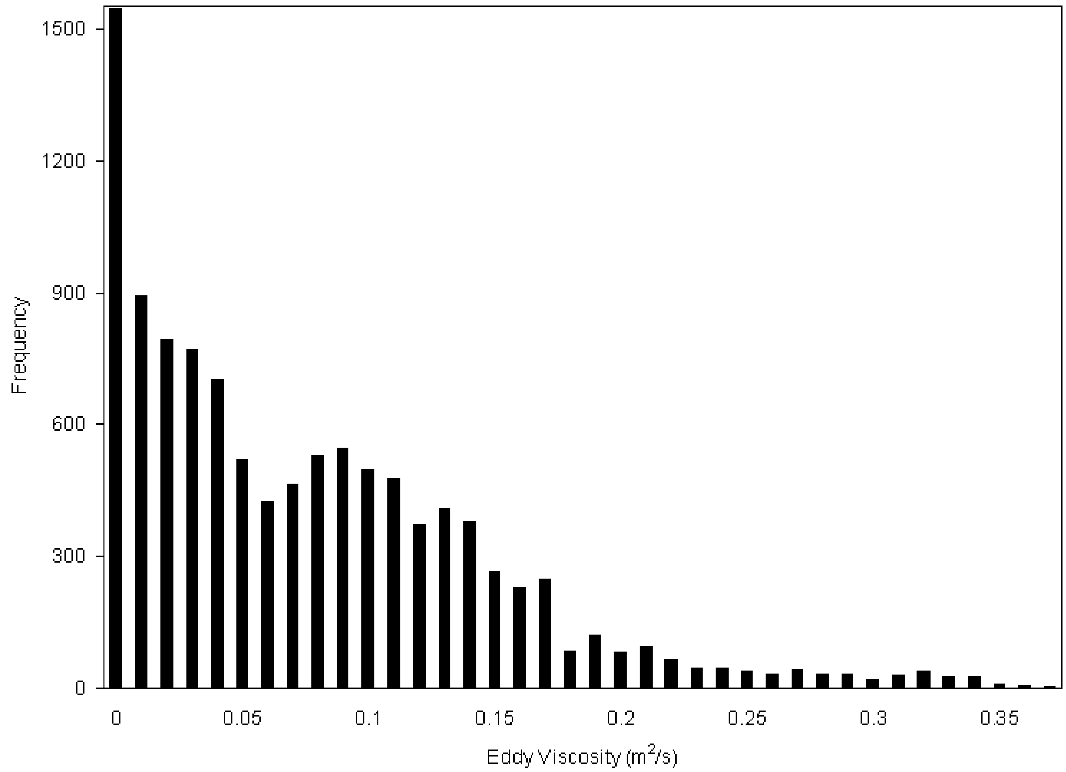

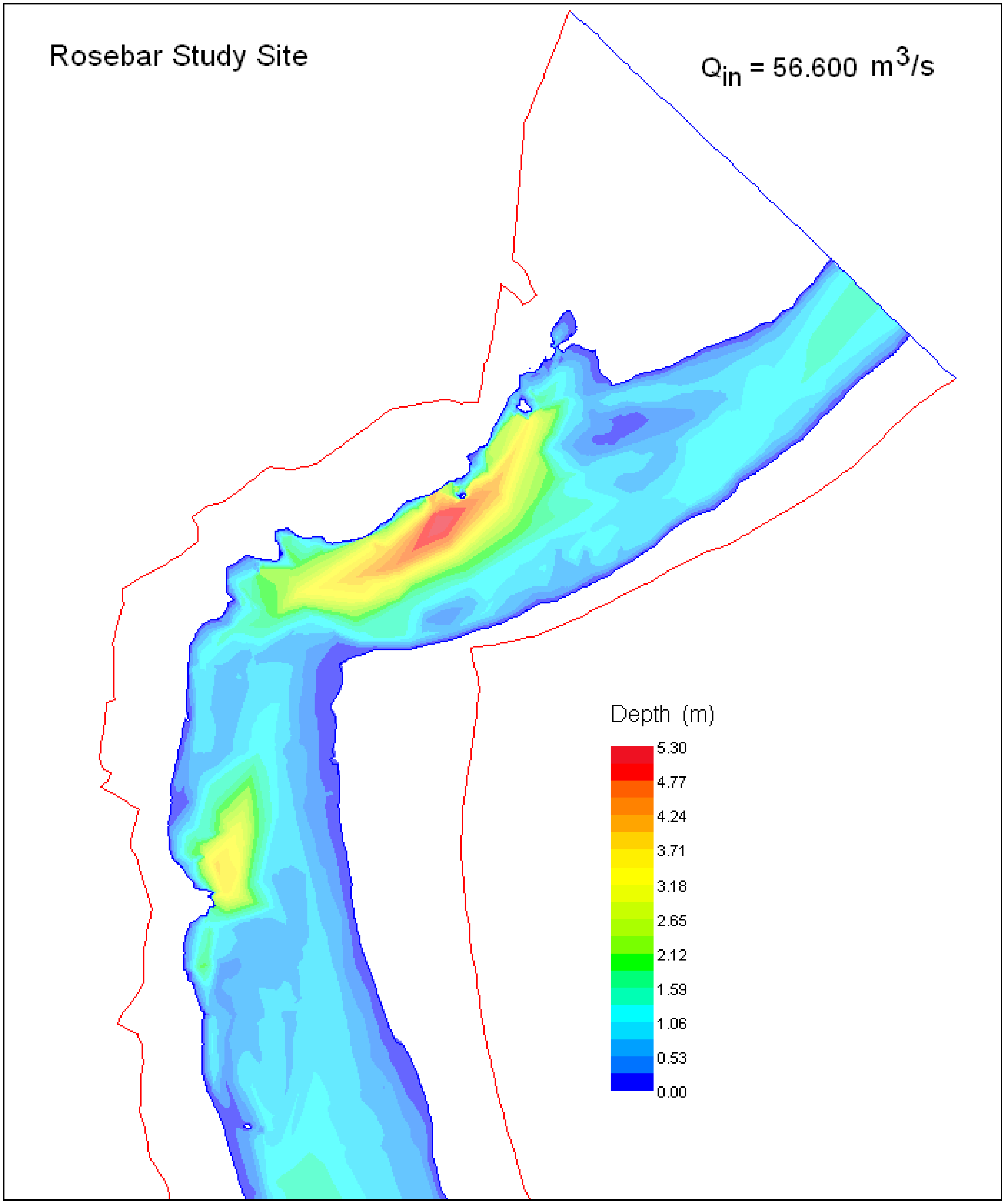

Rosebar Study Site
Q_{in} = 56.600 m^3/s
Depth (m)
5.30
4.77
4.24
3.71
3.18
2.65
2.12
1.59
1.06
0.53
0.00

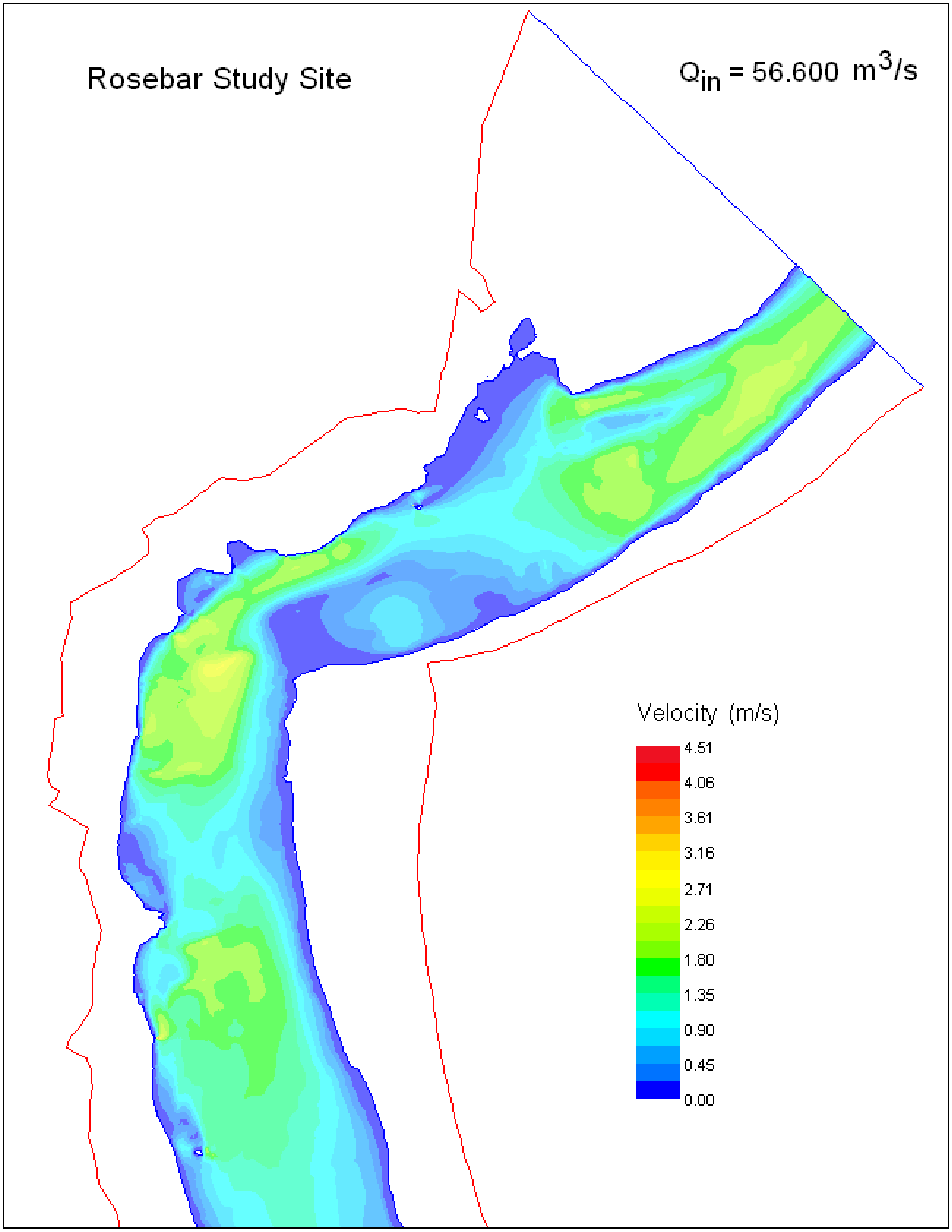
Rosebar Study Site
Q_{in} = 56.600 m^3/s
Velocity (m/s)
4.51
4.06
3.61
3.16
2.71
2.26
1.80
1.35
0.90
0.45
0.00

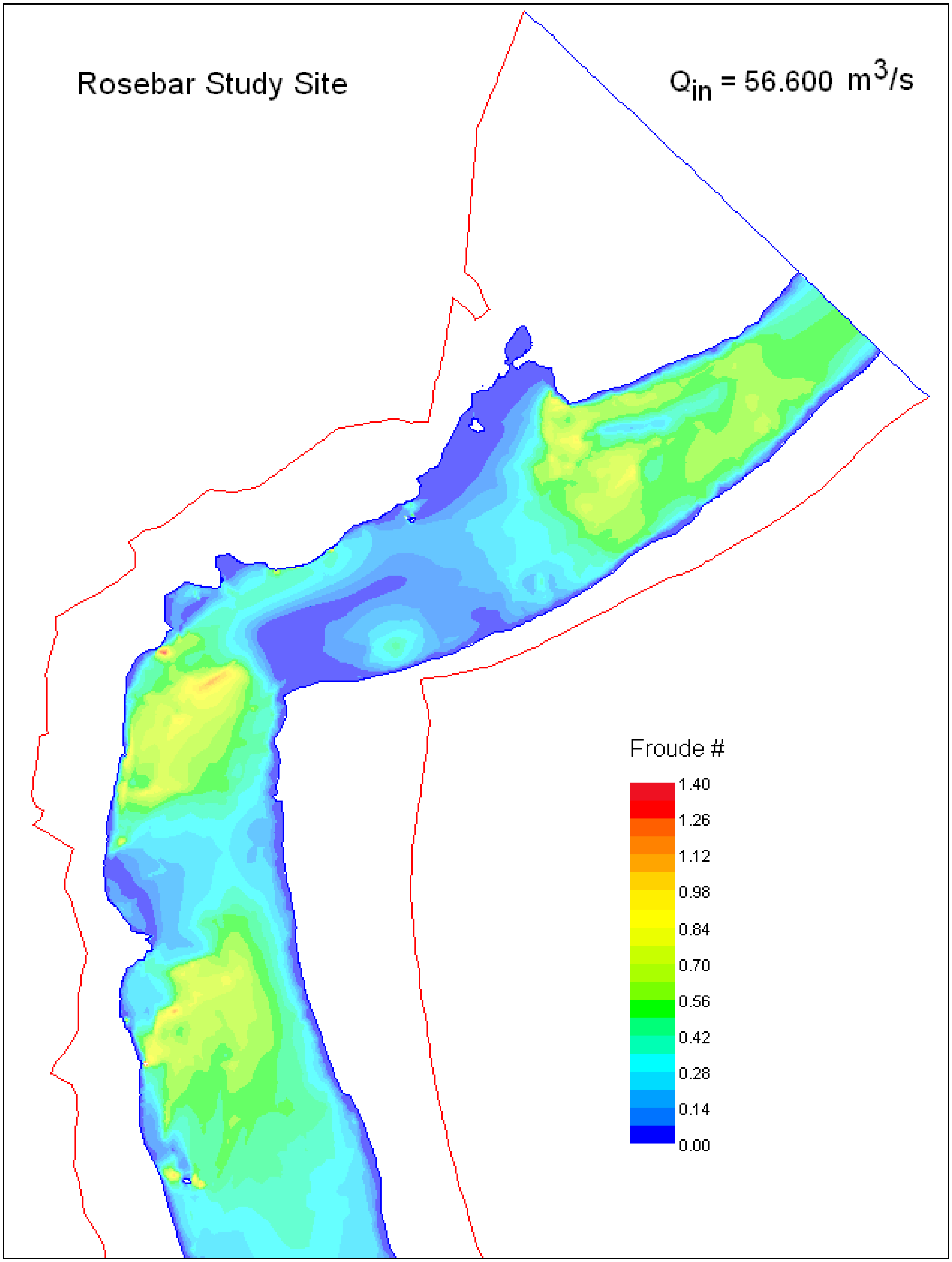

Rosebar Study Site
Q_{in} = 56.600 m^3/s
Froude #
1.40
1.26
1.12
0.98
0.84
0.70
0.56
0.42
0.28
0.14
0.00

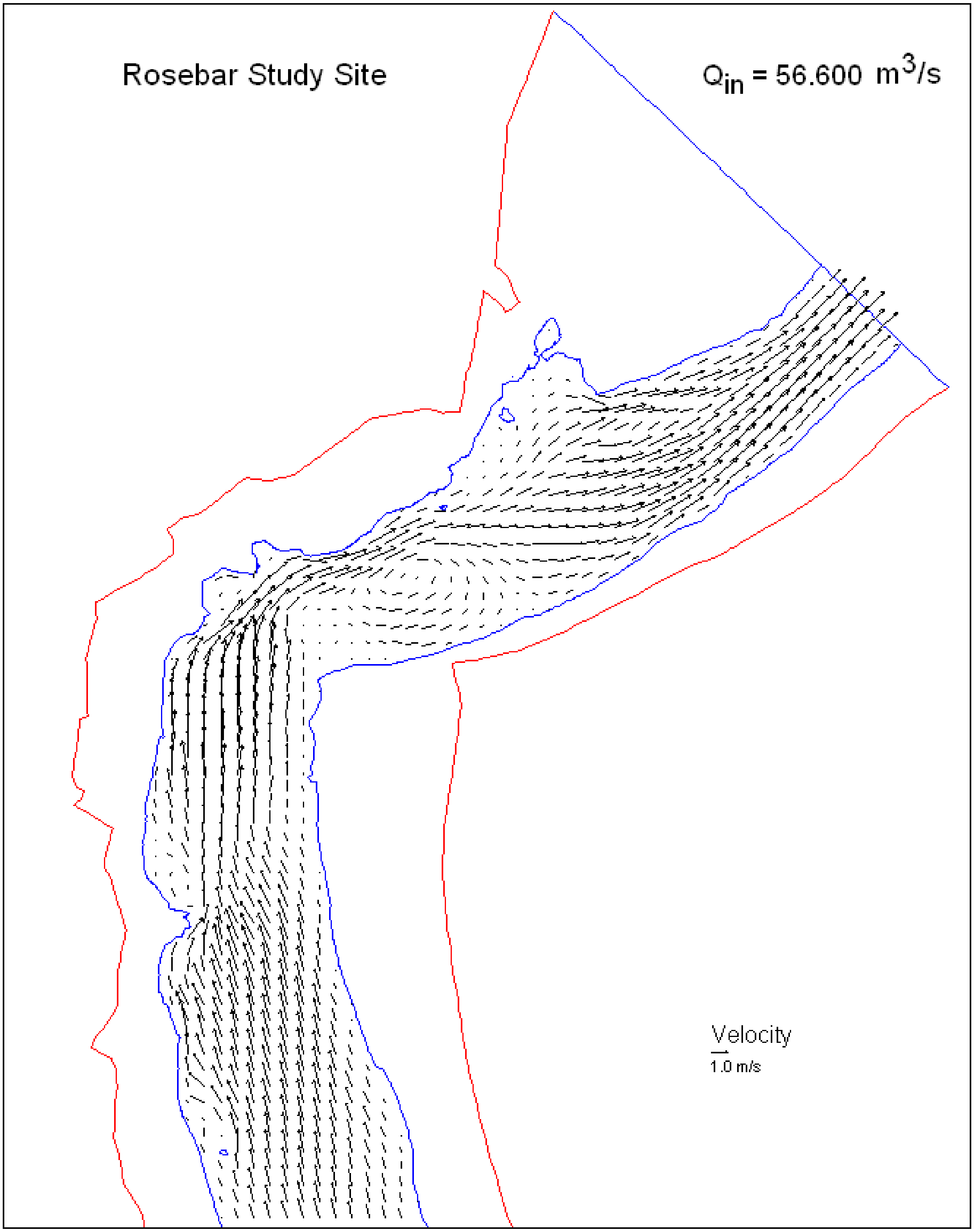

Rosebar Study Site
Q_{in} = 56.600 m^3/s
Velocity
1.0 m/s

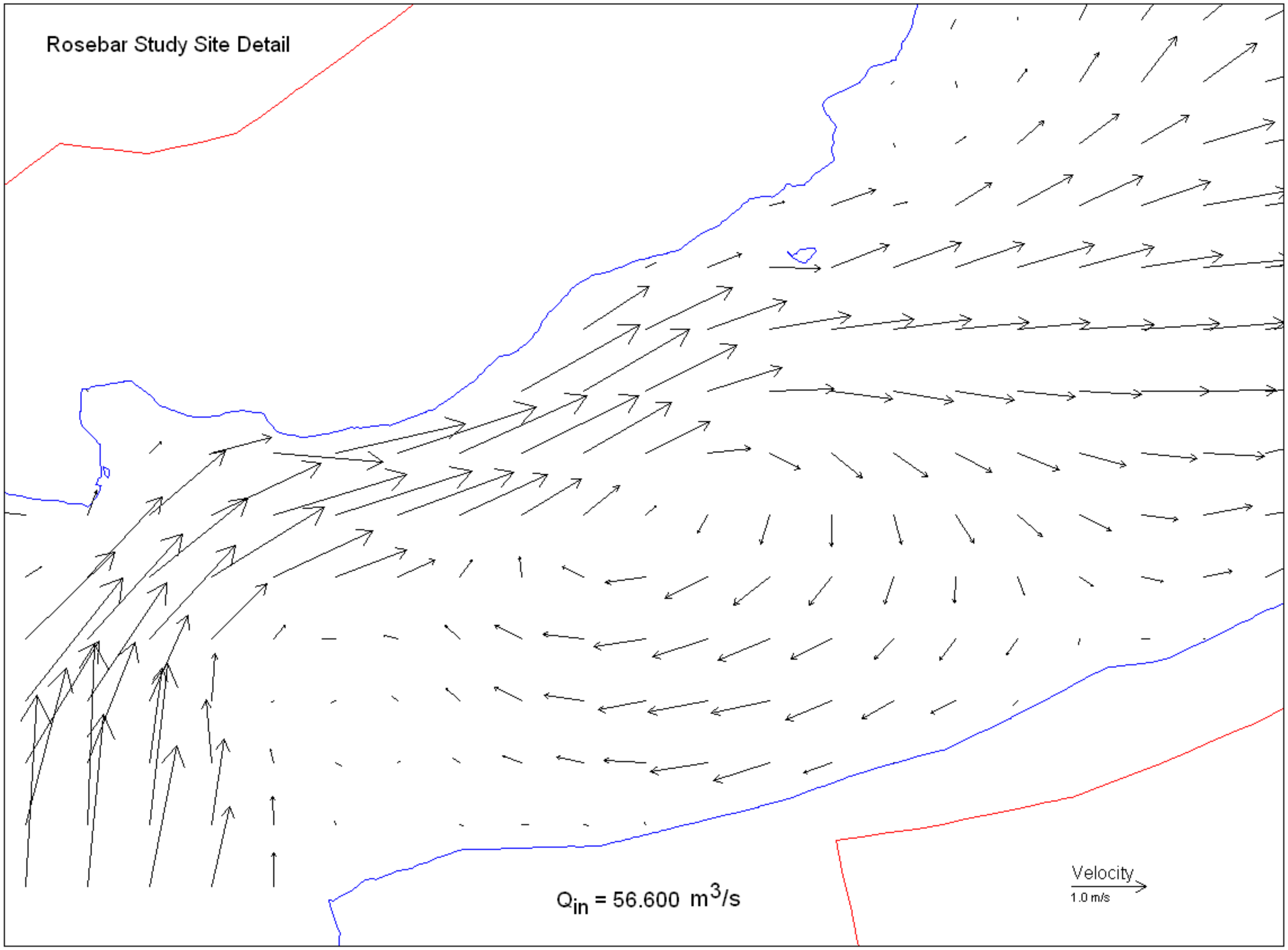
Rosebar Study Site Detail
Q$_{in}$ = 56.600 m^3/s
Velocity
1.0 m/s

APPENDIX J
SIMULATION STATISTICS

Narrows Site

Flow (cfs)	Net Q	Sol Δ	Max F
400	0.03%	.000003	74.21
500	10.99%	.000005	9.40
600	0.03%	< .000001	0.85
700	1.11%	.000008	3.47
800	20.18%	.000007	6.95
900	2.43%	.000006	3.21
1,000	12.54%	.000002	7.81
1,100	14.76%	.000004	15.75
1,200	1.88%	.000001	1.75
1,300	0.02%	.000002	1.99
1,400	0.02%	< .000001	1.59
1,500	0.02%	< .000001	1.50
1,600	0.00%	< .000001	1.43
1,700	0.00%	< .000001	2.56
1,800	0.00%	< .000001	7.48
1,900	0.00%	.000004	5.05
2,000	0.00%	< .000001	3.45
2,100	0.01%	.000007	2.31
2,300	0.00%	.000006	12.29
2,500	0.01%	< .000001	4.22
2,700	0.17%	.000001	32.72
2,900	0.01%	< .000001	10.28
3,100	0.00%	< .000001	15.01
3,300	0.00%	.000005	4.81
3,500	0.02%	< .000001	4.27
3,700	0.00%	.000008	6.12
3,900	0.00%	.000004	5.82
4,100	0.00%	< .000001	8.75
4,300	0.00%	< .000001	6.92
4,500	0.00%	< .000001	9.65

Rosebar Site

Flow (cfs)	Net Q	Sol Δ	Max F
400	0.53%	.000004	1.53
500	0.35%	< .000001	1.65
600	0.29%	< .000001	2.87
700	0.25%	< .000001	3.96
800	0.18%	.000006	2.52
900	0.20%	< .000001	2.24
1,000	0.14%	.000002	2.06
1,100	0.16%	< .000001	1.96
1,200	0.12%	< .000001	5.16
1,300	0.11%	.000001	6.15
1,400	0.13%	.000001	3.71
1,500	0.09%	< .000001	6.74
1,600	0.09%	< .000001	7.66
1,700	0.08%	.000001	6.95
1,800	0.08%	< .000001	5.73
1,900	0.09%	.000001	5.31
2,000	0.07%	.000001	5.86
2,100	0.05%	.000001	4.74
2,300	0.05%	.000001	3.31
2,500	0.04%	.000001	2.51
2,700	0.09%	< .000001	2.59
2,900	0.12%	.000001	2.20
3,100	0.15%	.000002	2.09
3,300	0.15%	.000001	9.25
3,500	0.16%	< .000001	9.50
3,700	0.16%	.000001	4.23
3,900	0.18%	< .000001	4.41
4,100	0.11%	< .000001	3.80
4,300	0.15%	.000003	9.52
4,500	0.15%	.000002	6.00

Diversion Site

Flow (cfs)	Net Q	Sol Δ	Max F
400	0.51%	.000006	0.79
500	0.38%	.000005	0.84
600	0.30%	.000003	0.80
700	0.24%	.000004	0.93
800	0.20%	.000004	1.09
900	0.17%	.000009	1.07
1,000	0%	.000003	1.01
1,100	0%	.000001	1.36
1,200	0%	.000003	1.26
1,300	0.11%	.000008	1.18
1,400	0.10%	.000007	1.12
1,500	0%	.000003	1.07
1,600	0%	.000005	1.04
1,700	0%	.000006	1.01
1,800	0.07%	.000005	0.99
1,900	0.06%	.000003	0.96
2,000	0.06%	.000005	0.95
2,100	0.06%	.000003	0.93
2,300	0.10%	.000008	0.90
2,500	0.04%	.000004	0.86
2,700	0.08%	.000009	0.84
2,900	0.07%	.000004	0.83
3,100	0.10%	.000006	0.82
3,300	0.06%	.000005	0.81
3,500	0%	.000004	0.81
3,700	0.05%	.000004	0.80
3,900	0.10%	.000007	0.79
4,100	0.07%	.000001	0.79
4,300	0.11%	.000008	0.79
4,500	0.06%	.000003	1.50

Lower Hallwood Site

Flow (cfs)	Net Q	Sol Δ	Max F
150	1.94%	.000008	0.86
250	0.78%	.000009	0.97
300	0.53%	.000003	0.94
350	0.50%	.000009	0.90
400	0.49%	.000003	0.91
500	0.31%	.000003	0.88
600	0.21%	.000004	0.90
700	0.16%	.000001	1.55
800	0.06%	< .000001	1.55
900	0.05%	.000001	2.62
1,000	0.05%	< .000001	2.28
1,100	0.05%	< .000001	2.54
1,200	0.13%	< .000001	4.30
1,300	0.10%	.000003	2.62
1,400	0.06%	.000002	3.91
1,500	0.07%	.000004	3.33
1,600	0.07%	.000001	2.85
1,700	0.07%	.000001	2.35
1,800	0.06%	.000001	2.10
1,900	0.07%	.000001	1.66
2,000	0.08%	.000001	1.43
2,100	0.11%	.000001	1.54
2,300	0.10%	.000006	1.84
2,500	0.12%	.000002	1.27
2,700	0.14%	< .000001	1.99
2,900	0.21%	.000008	1.41
3,300	0.18%	.000005	1.22
3,700	0.14%	.000005	1.43
4,100	0.13%	.000005	1.44
4,500	0.18%	.000006	1.51

Whirlpool Site

Flow (cfs)	Net Q	Sol Δ	Max F
150	--	--	--
250	--	--	--
300	0.04%	000001	0.44
350	0.05%	.000005	1.07
400	0.04%	.000008	0.83
500	0.04%	.000005	1.02
600	0.04%	.000004	0.96
700	0.01%	.000009	0.92
800	0.01%	.000005	0.92
900	0.01%	.000003	0.93
1,000	0.01%	.000003	1.02
1,100	0.02%	.000001	0.94
1,200	0.02%	000008	0.90
1,300	0.02%	.000005	0.89
1,400	0.06%	.000006	0.93
1,500	0.092%	.000004	0.91
1,600	0.11%	.000005	1.03
1,700	0.12%	.000003	0.99
1,800	0.08%	.000002	1.35
1,900	0.07%	< .000001	2.57
2,000	0.05%	< .000001	2.64
2,100	0.05%	.000003	2.33
2,300	0.03%	.000007	1.65
2,500	0.03%	.000002	1.35
2,700	0.04%	.000001	1.16
2,900	0.03%	.000002	1.02
3,300	0.03%	.000003	0.99
3,700	0.03%	.000001	1.04
4,100	0.02%	< .000001	1.63
4,500	0.46%	.000006	1.23

Side-Channel Site

Flow (cfs)	Net Q	Sol Δ	Max F
150	--	--	--
250	--	--	--
300	--	--	--
350	--	--	--
400	--	--	--
500	--	--	--
600	--	--	--
700	--	--	--
800	--	--	--
900	20.67%	.000007	0.25
1,000	3.43%	.000003	0.42
1,100	2.86%	.000002	0.44
1,200	2.38%	.000008	0.49
1,300	1.00%	.000007	0.50
1,400	1.03%	.000002	0.48
1,500	1.20%	.000003	0.52
1,600	1.48%	.000003	0.53
1,700	1.08%	.000004	0.94
1,800	0.80%	.000001	0.83
1,900	0.99%	.000003	0.46
2,000	0.95%	.000002	0.53
2,100	0.83%	.000004	0.49
2,300	1.33%	.000003	0.43
2,500	1.28%	.000001	0.45
2,700	0.41%	.000001	0.59
2,900	0.35%	.000001	0.56
3,300	0.26%	< .000001	0.66
3,700	0.01%	.000004	0.70
4,100	0.04%	< .000001	0.55
4,500	0.02%	.000005	0.50

Sucker Glide Site

Flow (cfs)	Net Q	Sol Δ	Max F
150	16.69%	.000002	1.00
250	2.12%	.000005	1.00
300	1.65%	.000006	1.00
350	4.24%	.000006	1.00
400	5.83%	.000007	1.00
500	6.44%	.000007	1.02
600	6.36%	.000006	1.01
700	5.97%	.000008	1.00
800	5.59%	.000004	1.00
900	5.81%	.000002	1.00
1,000	6.36%	.000009	1.00
1,100	0.05%	.000003	0.36
1,200	0.22%	.000006	0.35
1,300	0.10%	.000003	0.34
1,400	0.04%	.000008	0.34
1,500	0.15%	.000007	0.39
1,600	0.09%	.000003	0.40
1,700	0.03%	.000006	0.39
1,800	0.14%	.000003	0.37
1,900	0.10%	.000006	0.41
2,000	0.05%	.000004	0.64
2,100	0.15%	.000005	0.66
2,300	0.07%	.000005	0.60
2,500	0.12%	.000005	0.54
2,700	0.14%	.000005	0.49
2,900	0.10%	.000006	0.47
3,300	0.05%	.000005	0.43
3,700	0.09%	.000005	1.03
4,100	0.04%	.000007	0.90
4,500	0.04%	.000006	0.89

Railroad Site

Flow (cfs)	Net Q	Sol Δ	Max F
150	1.19%	.000002	1.19
250	0.42%	.000008	0.24
300	0.23%	.000001	0.24
350	0.61%	.000002	0.21
400	0.44%	.000001	0.21
500	0.35%	.000005	0.30
600	1.35%	.000003	0.29
700	0.20%	.000004	0.36
800	2.07%	.000008	0.36
900	0%	.000004	0.46
1,000	0.56%	.000001	0.41
1,100	0.61%	.000005	0.33
1,200	0.04%	.000001	0.53
1,300	0.06%	.000006	0.52
1,400	0.10%	.000007	0.47
1,500	0.37%	.000001	0.59
1,600	0.09%	< .000001	0.54
1,700	0.59%	.000001	0.50
1,800	0.38%	.000001	0.57
1,900	0%	.000007	0.56
2,000	0.04%	< .000001	0.51
2,100	0.07%	< .000001	0.62
2,300	0.03%	< .000001	0.45
2,500	0.01%	.000002	0.62
2,700	0.05%	.000002	0.52
2,900	0.20%	.000002	0.56
3,300	0.25%	.000003	0.74
3,700	0.39%	.000003	0.66
4,100	0.62%	.000003	0.77
4,500	1.49%	.000004	0.64

APPENDIX K
HABITAT SUITABILITY CRITERIA

Fall/spring-run Chinook Salmon Fry Rearing

Water Velocity (ft/s)	SI Value	Water Depth (ft)	SI Value	Cover	SI Value	Adjacent Velocity (ft/s)	SI Value
0.00	1.00	0.0	0.00	0	0.00	0.00	0.36
0.10	0.99	0.1	0.00	0.1	0.10	3.60	1.00
0.20	0.95	0.2	0.80	1	0.25	100	1.00
0.30	0.89	0.3	0.84	2	0.10		
0.40	0.81	0.5	0.90	3	0.54		
0.60	0.65	0.6	0.92	3.7	1.00		
0.70	0.56	0.7	0.95	4	1.00		
0.80	0.49	0.8	0.96	4.7	1.00		
0.90	0.42	0.9	0.98	5	1.00		
1.10	0.30	1.1	1.00	5.7	1.00		
1.30	0.22	1.4	1.00	7	0.25		
1.40	0.19	1.7	0.97	8	1.00		
1.70	0.13	2.2	0.87	9	0.25		
2.00	0.10	2.5	0.78	9.7	0.10		
2.10	0.10	2.6	0.76	10	0.54		
2.20	0.09	2.7	0.73	11	0.00		
2.70	0.09	2.8	0.69	100	0.00		
2.80	0.10	3.5	0.48				
2.90	0.10	3.6	0.46				
3.00	0.11	3.8	0.40				
3.10	0.11	3.9	0.38				
3.20	0.12	4.0	0.35				
3.40	0.12	4.6	0.23				
3.50	0.13	4.7	0.22				
3.62	0.13	4.8	0.20				
3.63	0.00	4.9	0.19				
100	0.00	5.0	0.17				
		5.7	0.10				
		5.8	0.10				
		6.0	0.08				
		6.1	0.08				
		6.2	0.07				
		6.3	0.07				
		6.4	0.06				
		6.5	0.06				
		6.6	0.05				
		6.9	0.05				
		7.0	0.04				
		7.3	0.04				
		7.4	0.03				
		8.0	0.03				
		8.1	0.02				
		18.4	0.02				
		18.5	0.00				
		100	0.00				

Fall/spring-run Chinook Salmon Juvenile Rearing

Water Velocity (ft/s)	SI Value	Water Depth (ft)	SI Value	Cover	SI Value	Adjacent Velocity (ft/s)	SI Value
0.00	1.00	0.0	0.00	0	0.00	0.00	0.02
0.10	1.00	0.7	0.00	0.1	0.24	5.50	1.00
0.20	0.99	0.8	0.03	1	0.24	100	1.00
0.30	0.98	1.0	0.05	2	0.24		
0.40	0.97	1.2	0.09	3	0.24		
0.50	0.96	1.4	0.15	3.7	1.00		
0.60	0.94	1.6	0.23	4	1.00		
0.70	0.92	1.9	0.38	4.7	1.00		
0.80	0.89	2.4	0.68	5	1.00		
0.90	0.87	2.5	0.73	5.7	1.00		
1.00	0.84	2.6	0.79	7	0.24		
1.10	0.81	2.9	0.91	8	1.00		
1.20	0.78	3.1	0.97	9	0.24		
1.30	0.74	3.4	1.00	9.7	0.24		
1.40	0.71	3.5	1.00	10	0.24		
1.50	0.67	3.8	0.97	11	0.00		
1.60	0.63	4.0	0.93	100	0.00		
1.70	0.60	4.1	0.90				
1.80	0.56	4.2	0.88				
1.90	0.52	4.4	0.82				
2.00	0.48	4.5	0.78				
2.10	0.45	5.4	0.51				
2.20	0.41	5.5	0.49				
2.30	0.38	5.6	0.46				
2.40	0.34	6.2	0.34				
2.50	0.31	6.3	0.33				
2.55	0.30	6.4	0.31				
3.98	0.30	7.0	0.25				
3.99	0.00	7.1	0.25				
100	0.00	7.2	0.24				
		7.3	0.23				
		7.5	0.23				
		7.6	0.22				
		11.8	0.22				
		11.9	0.00				
		100	0.00				

Steelhead/Rainbow Trout Fry Rearing

Water Velocity (ft/s)	SI Value	Water Depth (ft)	SI Value	Cover	SI Value	Adjacent Velocity (ft/s)	SI Value
0.00	1.00	0.0	0.00	0	0.00	0.00	0.17
0.10	1.00	0.1	0.00	0.1	0.12	4.70	1.00
0.20	0.99	0.2	0.47	1	0.57	100	1.00
0.30	0.98	0.4	0.57	2	0.28		
0.40	0.97	0.5	0.63	3	0.28		
0.50	0.96	0.6	0.67	3.7	1.00		
0.60	0.94	0.7	0.72	4	0.57		
0.70	0.92	0.8	0.77	4.7	1.00		
0.80	0.89	1.0	0.85	5	1.00		
0.90	0.87	1.1	0.88	5.7	1.00		
1.00	0.84	1.2	0.91	7	0.28		
1.10	0.81	1.3	0.94	8	1.00		
1.20	0.78	1.5	0.98	9	0.12		
1.30	0.74	1.7	1.00	9.7	0.12		
1.40	0.71	1.9	1.00	10	1.00		
1.50	0.67	2.2	0.97	11	0.00		
1.60	0.63	2.4	0.93	100	0.00		
1.70	0.60	2.5	0.90				
1.80	0.56	2.9	0.78				
1.90	0.52	3.0	0.75				
2.00	0.48	3.1	0.71				
2.10	0.45	3.2	0.67				
2.20	0.41	3.3	0.64				
2.30	0.38	3.4	0.60				
2.40	0.34	3.5	0.57				
2.50	0.31	3.6	0.53				
2.60	0.28	3.7	0.50				
2.70	0.25	3.8	0.46				
2.80	0.23	4.2	0.34				
2.90	0.20	4.3	0.32				
3.00	0.18	4.4	0.29				
3.10	0.16	4.5	0.27				
3.20	0.14	4.6	0.24				
3.30	0.12	4.8	0.20				
3.40	0.11	4.9	0.19				
3.50	0.09	5.0	0.17				
3.60	0.08	5.1	0.16				
3.66	0.07	5.2	0.14				
3.67	0.00	5.9	0.07				
100	0.00	6.0	0.07				
		6.1	0.06				
		6.2	0.06				
		6.3	0.05				
		6.4	0.00				
		100	0.00				

Steelhead/Rainbow Trout Juvenile Rearing

Water Velocity (ft/s)	SI Value	Water Depth (ft)	SI Value	Cover	SI Value	Adjacent Velocity (ft/s)	SI Value
0.00	1.00	0	0.00	0	0.00	0.00	0.02
0.10	1.00	0.4	0.00	0.1	0.24	5.50	1.00
0.20	0.99	0.5	0.45	1	0.24	100	1.00
0.30	0.98	1.6	0.90	2	0.24		
0.40	0.97	2.0	0.98	3	0.24		
0.50	0.96	2.2	1.00	3.7	1.00		
0.60	0.94	2.5	1.00	4	1.00		
0.70	0.92	3.0	0.94	4.7	1.00		
0.80	0.89	3.5	0.84	5	1.00		
0.90	0.87	5.5	0.32	5.7	1.00		
1.00	0.84	6.5	0.17	7	0.24		
1.10	0.81	8.0	0.07	8	1.00		
1.20	0.78	9.5	0.04	9	0.24		
1.30	0.74	10.5	0.03	9.7	0.24		
1.40	0.71	13.5	0.03	10	0.24		
1.50	0.67	15.0	0.04	11	0.00		
1.60	0.63	15.1	0.00	100	0.00		
1.70	0.60	100	0.00				
1.80	0.56						
1.90	0.52						
2.00	0.48						
2.10	0.45						
2.20	0.41						
2.30	0.38						
2.40	0.34						
2.50	0.31						
2.55	0.30						
3.98	0.30						
3.99	0.00						
100	0.00						

APPENDIX L
HABITAT MODELING RESULTS

Narrows Site WUA (ft^2)

	Fall/Spring-Run Chinook		Steelhead/Rainbow Trout	
Flow (cfs)	Fry	Juvenile	Fry	Juvenile
400	1,422	852	1,155	618
500	1,302	719	1,033	510
600	1,401	371	958	290
700	1,364	397	947	306
800	1,300	734	1,032	519
900	1,286	727	1,042	525
1,000	1,276	683	1,026	495
1,100	1,260	611	994	452
1,200	1,264	435	947	341
1,300	1,251	440	946	346
1,400	1,251	440	948	349
1,500	1,255	440	948	353
1,600	1,237	443	949	359
1,700	1,229	449	950	366
1,800	1,225	454	1,619	372
1,900	1,247	457	958	376
2,000	1,296	459	974	379
2,100	1,346	462	992	383
2,300	1,466	470	1,035	395
2,500	1,543	478	1,072	409
2,700	1,584	487	1,108	425
2,900	1,605	497	1,142	447
3,100	1,740	506	1,233	466
3,300	1,792	516	1,295	486
3,500	1,806	527	1,331	518
3,700	1,813	540	1,358	542
3,900	1,805	554	1,373	558
4,100	1,800	568	1,391	576
4,300	1,785	583	1,400	594
4,500	1,788	598	1,414	602

Rosebar Site WUA (ft^2)

	Fall/Spring-Run Chinook		Steelhead/Rainbow Trout	
Flow (cfs)	Fry	Juvenile	Fry	Juvenile
400	1,088	519	1,382	788
500	1,073	584	1,434	854
600	1,038	643	1,449	914
700	997	695	1,453	949
800	980	729	1,476	938
900	948	767	1,503	959
1,000	916	799	1,528	976
1,100	886	820	1,538	979
1,200	873	844	1,559	989
1,300	837	858	1,557	990
1,400	818	876	1,540	992
1,500	789	862	1,489	963
1,600	787	870	1,469	962
1,700	793	880	1,446	963
1,800	788	887	1,413	957
1,900	776	889	1,379	949
2,000	768	885	1,350	936
2,100	758	882	1,325	924
2,300	767	876	1,291	896
2,500	783	856	1,269	852
2,700	1,008	830	1,312	806
2,900	1,168	818	1,349	787
3,100	1,285	797	1,385	769
3,300	1,409	781	1,433	768
3,500	1,539	772	1,479	763
3,700	1,680	752	1,538	754
3,900	1,808	742	1,597	750
4,100	1,907	731	1,646	746
4,300	2,046	725	1,707	746
4,500	2,166	716	1,772	749

U.C. Sierra Site WUA (ft^2)

	Fall/Spring-Run Chinook		Steelhead/Rainbow Trout	
Flow (cfs)	Fry	Juvenile	Fry	Juvenile
400	7,516	2,709	14,365	6,150
500	7,161	3,173	14,723	6,688
600	7,285	3,584	15,148	7,103
700	7,244	3,935	15,443	7,492
800	7,167	4,204	15,605	7,771
900	7,114	4,385	15,702	7,924
1,000	7,187	4,553	15,905	8,105
1,100	7,127	4,688	15,919	8,219
1,200	7,066	4,773	15,862	8,273
1,300	7,115	4,892	15,820	8,363
1,400	6,929	4,990	15,819	8,438
1,500	7,269	5,025	15,570	8,407
1,600	7,513	5,135	15,507	8,484
1,700	7,760	5,229	15,453	8,540
1,800	7,833	5,370	15,361	8,647
1,900	7,874	5,496	15,158	6,373
2,000	8,005	5,635	15,021	8,807
2,100	8,125	5,769	14,881	8,906
2,300	8,547	6,067	14,701	9,153
2,500	8,621	6,248	14,396	9,251
2,700	9,166	6,393	14,078	9,323
2,900	10,274	6,416	14,074	9,308
3,100	10,538	6,348	13,828	9,200
3,300	10,931	6,162	13,699	9,037
3,500	11,430	5,628	13,712	8,607
3,700	10,589	5,312	13,754	8,541
3,900	10,482	5,071	13,689	8,506
4,100	10,157	4,941	13,567	8,550
4,300	10,013	4,801	13,341	8,538
4,500	9,949	4,551	13,196	8,395

Timbuctoo Site WUA (ft^2)

Flow (cfs)	Fall/Spring-Run Chinook Fry	Fall/Spring-Run Chinook Juvenile	Steelhead/Rainbow Trout Fry	Steelhead/Rainbow Trout Juvenile
400	25,869	7,618	47,526	17,166
500	26,082	8,742	48,260	18,693
600	26,487	9,666	48,836	19,845
700	26,862	10,566	48,994	20,892
800	27,182	11,386	48,853	21,744
900	27,225	12,074	48,474	22,359
1,000	27,135	12,564	47,999	22,738
1,100	27,219	12,990	47,647	23,043
1,200	27,021	13,177	47,150	23,032
1,300	26,827	13,491	46,673	23,117
1,400	26,802	13,711	46,201	23,067
1,500	26,807	13,985	45,631	23,213
1,600	27,530	14,045	46,875	23,122
1,700	28,076	14,052	45,291	22,976
1,800	29,073	14,124	45,441	22,959
1,900	30,572	14,175	45,643	22,915
2,000	32,442	14,236	46,218	23,052
2,100	34,227	14,430	46,947	23,405
2,300	37,647	14,759	48,332	24,227
2,500	40,283	15,094	49,779	25,062
2,700	43,768	15,581	51,652	26,145
2,900	45,728	16,150	53,373	27,581
3,100	47,147	16,766	54,706	29,177
3,300	49,497	17,251	55,962	30,698
3,500	51,100	17,780	57,397	32,068
3,700	52,085	18,144	58,337	32,986
3,900	52,863	18,535	59,034	34,050
4,100	55,164	18,846	59,662	35,017
4,300	56,468	19,220	60,054	36,005
4,500	56,207	19,770	60,185	37,232

Highway 20 Site WUA (ft^2)

Flow (cfs)	Fall/Spring-Run Chinook Fry	Fall/Spring-Run Chinook Juvenile	Steelhead/Rainbow Trout Fry	Steelhead/Rainbow Trout Juvenile
400	4,806	1,816	9,187	3,804
500	5,075	2,145	9,309	4,344
600	5,220	2,478	9,552	4,820
700	5,378	2,801	9,955	5,277
800	5,278	3,066	10,177	5,630
900	5,153	3,265	10,328	5,886
1,000	5,151	3,248	10,516	5,922
1,100	5,356	3,298	10,523	5,952
1,200	5,487	3,449	10,748	6,123
1,300	5,676	3,568	10,938	6,253
1,400	5,734	3,664	11,024	6,344
1,500	5,939	3,776	11,037	6,433
1,600	6,375	3,882	11,082	6,499
1,700	7,069	3,933	11,285	6,530
1,800	7,410	4,063	11,394	6,639
1,900	7,590	4,173	11,398	6,729
2,000	8,019	4,246	11,432	6,768
2,100	8,535	4,301	11,506	6,863
2,300	9,412	4,500	11,730	7,162
2,500	9,753	4,669	11,717	7,424
2,700	9,599	4,700	11,665	7,668
2,900	9,641	4,505	11,634	7,652
3,100	9,660	4,337	11,625	7,662
3,300	9,700	4,193	11,539	7,655
3,500	9,750	4,209	11,467	7,827
3,700	9,438	4,146	11,353	7,957
3,900	9,549	4,048	11,367	8,016
4,100	9,139	3,965	11,435	8,170
4,300	9,194	3,849	11,293	8,360
4,500	9,126	4,173	11,078	8,600

Island Site WUA (ft^2)

	Fall/Spring-Run Chinook		Steelhead/Rainbow Trout	
Flow (cfs)	Fry	Juvenile	Fry	Juvenile
400	11,103	5,085	14,363	8,004
500	11,271	5,726	14,595	8,760
600	11,298	6,249	15,242	9,617
700	11,220	6,697	15,885	10,355
800	11,214	7,034	16,372	10,907
900	11,214	7,272	16,678	11,276
1,000	11,077	7,491	16,773	11,661
1,100	10,961	7,477	16,673	11,666
1,200	10,738	7,509	16,640	11,780
1,300	10,620	7,571	16,509	11,887
1,400	10,517	7,645	16,283	11,951
1,500	10,421	7,719	16,060	11,996
1,600	10,338	7,739	15,759	12,022
1,700	10,191	7,801	15,378	11,978
1,800	10,158	7,828	14,992	11,908
1,900	10,204	7,933	14,736	11,930
2,000	10,360	8,004	14,554	11,942
2,100	10,351	8,035	14,169	11,842
2,300	10,408	8,197	13,625	11,767
2,500	10,312	8,309	13,092	11,596
2,700	10,387	8,345	12,436	11,434
2,900	10,588	8,518	12,042	11,463
3,100	10,753	7,625	11,177	10,678
3,300	10,843	7,632	10,936	10,605
3,500	10,873	7,521	10,706	10,362
3,700	10,789	7,398	10,462	10,206
3,900	10,978	7,159	10,330	9,872
4,100	11,050	6,716	10,316	9,485
4,300	10,668	6,317	10,391	9,215
4,500	10,491	6,011	10,292	9,006

Hammond Site WUA (ft^2)

	Fall/Spring-Run Chinook		Steelhead/Rainbow Trout	
Flow (cfs)	Fry	Juvenile	Fry	Juvenile
400	6,761	3,151	13,881	7,515
500	6,722	3,550	13,204	7,637
600	6,828	3,872	12,398	7,736
700	7,085	4,197	11,724	7,966
800	7,311	4,609	11,274	8,292
900	7,375	4,958	10,858	8,545
1,000	7,489	5,252	10,373	8,603
1,100	7,452	5,385	9,775	8,441
1,200	7,399	5,600	9,294	8,395
1,300	7,258	5,527	8,867	8,087
1,400	7,075	5,383	8,665	7,716
1,500	6,911	4,874	8,420	6,917
1,600	6,858	4,496	8,265	6,393
1,700	6,927	4,140	8,097	5,931
1,800	6,938	3,876	7,982	5,611
1,900	6,943	3,769	7,822	5,419
2,000	6,916	3,622	7,687	5,276
2,100	6,956	3,550	7,542	5,185
2,300	7,006	3,325	7,269	4,927
2,500	7,123	3,179	7,010	4,716
2,700	7,413	3,158	7,006	4,689
2,900	7,500	3,053	6,899	4,546
3,100	7,593	2,946	6,854	4,447
3,300	7,936	2,831	6,911	4,408
3,500	8,254	2,821	6,973	4,522
3,700	8,076	2,786	7,123	4,634
3,900	8,175	2,747	7,166	4,650
4,100	8,725	2,760	7,418	4,753
4,300	8,719	2,760	7,658	4,937
4,500	8,518	2,744	7,752	5,051

Diversion Site WUA (ft^2)

Flow (cfs)	Fall/Spring-Run Chinook Fry	Fall/Spring-Run Chinook Juvenile	Steelhead/Rainbow Trout Fry	Steelhead/Rainbow Trout Juvenile
400	2,125	305	1,872	1,216
500	2,096	424	2,081	1,476
600	2,030	553	2,251	1,724
700	2,044	667	2,379	1,896
800	2,076	778	2,504	2,053
900	2,201	889	2,641	2,195
1,000	2,282	981	2,753	2,309
1,100	2,334	1,060	2,831	2,400
1,200	2,408	1,130	2,897	2,480
1,300	2,449	1,194	2,969	2,572
1,400	2,494	1,253	3,007	2,632
1,500	2,566	1,324	3,064	2,729
1,600	2,614	1,407	3,144	2,840
1,700	2,712	1,497	3,207	2,948
1,800	2,797	1,583	3,277	3,040
1,900	2,841	1,689	3,331	3,171
2,000	2,830	1,772	3,393	3,270
2,100	2,785	1,838	3,420	3,331
2,300	2,744	1,961	3,485	3,456
2,500	2,802	2,071	3,504	3,532
2,700	2,990	2,049	3,536	3,476
2,900	3,064	1,943	3,518	3,371
3,100	3,106	1,685	3,496	3,136
3,300	3,057	1,538	3,492	3,026
3,500	2,906	1,415	3,380	2,913
3,700	2,901	1,352	3,264	2,843
3,900	3,000	1,318	3,221	2,802
4,100	3,155	1,239	3,208	2,741
4,300	3,119	1,254	3,145	2,727
4,500	3,154	1,210	3,077	2,653

Upper Daguerre Site WUA (ft^2)

Flow (cfs)	Fall/Spring-Run Chinook Fry	Fall/Spring-Run Chinook Juvenile	Steelhead/Rainbow Trout Fry	Steelhead/Rainbow Trout Juvenile
150	3,931	855	7,618	2,220
250	3,342	1,334	8,040	2,885
300	3,244	1,542	8,171	3,144
350	3,155	1,715	8,164	3,302
400	3,012	1,865	8,059	3,417
500	2,780	2,122	7,663	3,607
600	2,647	2,270	7,191	3,614
700	2,597	2,389	6,790	3,628
800	2,542	2,401	6,406	3,492
900	2,535	2,442	6,069	3,441
1,000	2,473	2,474	5,706	3,397
1,100	2,379	2,496	5,420	3,400
1,200	2,296	2,500	5,203	3,346
1,300	2,678	2,455	5,114	3,245
1,400	2,854	2,479	4,969	3,251
1,500	3,123	2,461	4,840	3,208
1,600	3,191	2,421	4,665	3,133
1,700	3,346	2,397	4,563	3,095
1,800	3,624	2,353	4,517	3,040
1,900	3,728	2,299	4,408	3,037
2,000	3,802	2,287	4,373	3,047
2,100	3,824	2,201	4,295	2,996
2,300	3,939	2,079	4,196	2,983
2,500	4,091	2,023	4,142	3,000
2,700	4,277	1,925	4,173	2,999
2,900	4,518	1,776	4,191	2,882
3,300	4,509	1,488	4,325	2,804
3,700	4,759	1,266	4,487	2,770
4,100	4,781	1,145	4,709	2,745
4,500	4,807	1,195	4,700	2,878

Lower Daguerre Site WUA (ft^2)

	Fall/Spring-Run Chinook		Steelhead/Rainbow Trout	
Flow (cfs)	Fry	Juvenile	Fry	Juvenile
150	8,481	892	15,891	4,936
250	8,062	1,548	17,454	6,129
300	8,098	1,869	17,787	6,527
350	8,215	2,048	17,925	6,800
400	8,336	2,316	17,993	7,141
500	8,850	2,832	17,803	7,692
600	9,466	3,260	17,648	7,981
700	9,748	3,684	17,506	8,422
800	10,085	3,776	17,235	8,481
900	10,283	3,781	17,152	8,533
1,000	10,642	3,680	17,188	8,536
1,100	11,435	3,743	17,387	8,755
1,200	11,718	3,658	17,358	8,752
1,300	12,398	3,725	17,370	8,841
1,400	13,153	3,768	17,409	8,966
1,500	13,885	3,815	17,706	9,064
1,600	15,025	3,873	18,190	9,209
1,700	16,084	3,915	18,863	9,490
1,800	17,052	3,969	19,554	9,792
1,900	17,805	3,936	20,172	10,022
2,000	18,587	3,984	21,011	10,699
2,100	18,654	3,988	21,071	10,724
2,300	19,943	3,996	22,188	11,325
2,500	19,857	4,151	22,726	12,093
2,700	20,078	4,418	23,633	13,072
2,900	19,703	4,745	23,997	13,852
3,300	19,009	5,656	24,189	15,309
3,700	17,811	6,507	23,494	16,211
4,100	17,161	7,281	22,345	16,556
4,500	16,626	8,117	21,289	16,946

Pyramids Site WUA (ft^2)

Flow (cfs)	Fall/Spring-Run Chinook Fry	Fall/Spring-Run Chinook Juvenile	Steelhead/Rainbow Trout Fry	Steelhead/Rainbow Trout Juvenile
150	6,831	383	11,761	2,775
250	6,059	674	13,799	3,857
300	5,628	808	14,247	4,277
350	5,343	935	14,492	4,580
400	5,069	1,054	14,593	4,816
500	4,800	1,276	14,570	5,200
600	4,785	1,467	14,283	5,462
700	4,810	1,639	13,828	5,675
800	5,015	1,800	13,289	5,897
900	5,092	1,947	12,810	6,118
1,000	5,215	2,084	12,371	6,303
1,100	5,157	2,219	11,832	6,531
1,200	4,994	2,343	10,993	6,685
1,300	4,964	2,477	10,342	6,796
1,400	4,775	2,580	9,604	6,724
1,500	4,747	2,663	8,943	6,623
1,600	4,809	2,749	8,467	6,475
1,700	4,714	2,794	7,956	6,228
1,800	4,758	2,831	7,476	6,004
1,900	4,817	2,877	7,067	5,841
2,000	4,889	2,943	6,746	5,797
2,100	4,820	2,941	6,459	5,564
2,300	4,599	2,878	5,845	5,144
2,500	4,437	2,767	5,287	4,696
2,700	4,210	2,440	4,733	4,207
2,900	4,198	2,146	4,440	3,819
3,300	4,067	1,072	4,143	2,714
3,700	3,880	831	3,996	2,415
4,100	3,699	822	3,884	2,350
4,500	3,677	782	3,905	2,294

Hallwood Site WUA (ft^2)

	Fall/Spring-Run Chinook		Steelhead/Rainbow Trout	
Flow (cfs)	Fry	Juvenile	Fry	Juvenile
150	2,290	157	3,929	890
250	2,447	296	4,803	1,184
300	2,755	365	5,248	1,293
350	3,040	431	5,722	1,404
400	3,065	494	6,077	1,519
500	3,276	620	6,656	1,720
600	3,281	744	7,076	1,958
700	3,119	907	7,370	2,304
800	2,995	1,087	7,425	2,626
900	2,850	1,243	7,336	2,854
1,000	2,814	1,409	7,192	3,060
1,100	2,878	1,579	7,012	3,250
1,200	2,813	1,724	6,710	3,387
1,300	2,742	1,832	6,361	3,469
1,400	2,671	1,896	6,041	3,510
1,500	2,710	1,890	5,714	3,473
1,600	2,832	1,878	5,438	3,456
1,700	2,922	1,832	5,147	3,420
1,800	3,014	1,797	4,856	3,422
1,900	2,995	1,785	4,599	3,434
2,000	2,861	1,756	4,370	3,426
2,100	2,788	1,636	4,160	3,290
2,300	2,781	1,596	3,758	3,236
2,500	2,699	1,562	3,469	3,190
2,700	2,761	1,620	3,267	3,212
2,900	2,788	1,704	3,165	3,257
3,300	2,501	1,704	2,744	3,020
3,700	2,415	1,615	2,507	2,735
4,100	2,454	1,405	2,345	2,385
4,500	2,299	1,297	2,241	2,207

Lower Hallwood Site WUA (ft^2)

	Fall/Spring-Run Chinook		Steelhead/Rainbow Trout	
Flow (cfs)	Fry	Juvenile	Fry	Juvenile
150	6,480	2,113	6,682	4,510
250	5,548	3,217	7,395	6,016
300	5,152	3,674	7,617	6,553
350	4,843	4,113	7,781	6,992
400	4,562	4,479	7,870	7,331
500	4,159	5,043	7,887	7,742
600	3,931	5,462	7,771	7,915
700	3,801	5,692	7,583	7,901
800	3,733	5,820	7,367	7,779
900	3,754	5,863	7,145	7,597
1,000	3,755	5,809	6,868	7,370
1,100	3,736	5,877	6,619	7,261
1,200	3,743	6,006	6,349	7,260
1,300	3,870	6,221	6,083	7,342
1,400	4,067	6,462	5,892	7,470
1,500	4,210	6,731	5,692	7,616
1,600	4,326	6,986	5,526	7,751
1,700	4,433	7,225	5,382	7,857
1,800	4,600	7,455	5,233	7,965
1,900	4,819	7,670	5,150	8,068
2,000	5,080	7,844	5,098	8,096
2,100	5,192	7,804	5,014	8,014
2,300	6,186	7,239	4,984	7,470
2,500	5,731	6,246	4,961	6,617
2,700	6,373	4,992	5,172	5,558
2,900	7,005	3,884	5,457	4,647
3,300	7,873	3,243	6,111	4,418
3,700	8,624	3,030	6,821	4,546
4,100	9,104	2,971	7,738	4,993
4,500	9,116	3,035	8,325	5,374

Plantz Site WUA (ft^2)

	Fall/Spring-Run Chinook		Steelhead/Rainbow Trout	
Flow (cfs)	Fry	Juvenile	Fry	Juvenile
150	2,145	374	2,452	2,010
250	2,251	675	2,788	2,527
300	2,355	822	2,809	2,699
350	2,408	981	2,879	2,908
400	2,415	1,113	2,876	3,081
500	2,357	1,428	2,930	3,457
600	2,335	1,664	2,864	3,690
700	2,279	1,907	2,795	3,905
800	2,276	2,064	2,718	3,946
900	2,251	2,021	2,611	3,738
1,000	2,218	2,086	2,533	3,706
1,100	2,216	2,159	2,485	3,668
1,200	2,277	2,206	2,463	3,629
1,300	2,353	2,302	2,434	3,676
1,400	2,349	2,343	2,359	3,640
1,500	2,404	2,425	2,331	3,712
1,600	2,470	2,432	2,275	3,685
1,700	2,579	2,435	2,247	3,648
1,800	2,692	2,471	2,243	3,691
1,900	3,105	2,463	2,321	3,663
2,000	3,544	2,459	2,384	3,648
2,100	3,785	2,462	2,462	3,648
2,300	3,589	2,385	2,472	3,583
2,500	3,723	2,328	2,497	3,534
2,700	3,642	2,142	2,569	3,357
2,900	3,465	1,998	2,590	3,212
3,300	3,424	1,816	2,889	3,167
3,700	3,842	1,592	3,124	3,108
4,100	4,749	1,302	3,487	2,843
4,500	4,748	1,328	3,786	3,058

Whirlpool Site WUA (ft^2)

	Fall/Spring-Run Chinook		Steelhead/Rainbow Trout	
Flow (cfs)	Fry	Juvenile	Fry	Juvenile
150	0	0	0	0
250	0	0	0	0
300	1,288	20	586	129
350	1,510	68	939	436
400	1,554	101	1,100	627
500	1,553	152	1,333	944
600	1,533	205	1,485	1,183
700	1,521	264	1,601	1,390
800	1,506	325	1,695	1,576
900	1,495	382	1,763	1,736
1,000	1,428	434	1,848	1,874
1,100	1,435	488	1,887	1,999
1,200	1,457	543	1,927	2,107
1,300	1,539	612	1,969	2,215
1,400	1,652	692	1,999	2,318
1,500	1,830	763	2,024	2,403
1,600	2,089	826	2,086	2,479
1,700	2,580	902	2,219	2,564
1,800	3,105	978	2,370	2,648
1,900	3,513	1,049	2,513	2,737
2,000	3,845	1,108	2,662	2,800
2,100	4,228	1,172	2,829	2,900
2,300	4,742	1,309	3,088	3,111
2,500	5,137	1,435	3,371	3,306
2,700	5,491	1,574	3,814	3,557
2,900	5,721	1,712	4,346	3,818
3,300	5,849	2,010	5,105	4,329
3,700	5,931	2,244	5,693	4,787
4,100	5,946	2,488	6,084	5,198
4,500	5,846	2,706	6,370	5,519

Side-Channel Site WUA (ft^2)

	Fall/Spring-Run Chinook		Steelhead/Rainbow Trout	
Flow (cfs)	Fry	Juvenile	Fry	Juvenile
150	0	0	0	0
250	0	0	0	0
300	0	0	0	0
350	0	0	0	0
400	0	0	0	0
500	0	0	0	0
600	0	0	0	0
700	0	0	0	0
800	0	0	0	0
900	417	2	148	16
1,000	661	5	256	42
1,100	767	10	334	84
1,200	856	15	409	139
1,300	952	23	490	195
1,400	1,016	31	557	245
1,500	1,101	42	636	297
1,600	1,180	53	710	346
1,700	1,247	66	790	400
1,800	1,293	80	862	452
1,900	1,357	97	909	495
2,000	1,386	114	977	547
2,100	1,447	134	1,050	598
2,300	1,625	177	1,201	699
2,500	1,725	223	1,323	785
2,700	1,880	273	1,467	877
2,900	2,051	326	1,622	971
3,300	2,261	442	1,925	1,150
3,700	2,423	557	2,188	1,313
4,100	2,804	678	2,460	1,475
4,500	3,168	801	2,727	1,635

Sucker Glide Site WUA (ft^2)

	Fall/Spring-Run Chinook		Steelhead/Rainbow Trout	
Flow (cfs)	Fry	Juvenile	Fry	Juvenile
150	3,690	548	3,501	2,648
250	3,225	977	4,063	3,585
300	3,065	1,314	4,382	4,091
350	2,969	1,707	4,602	4,493
400	2,891	2,165	4,701	4,790
500	2,691	3,134	4,664	5,134
600	2,499	4,010	4,473	5,236
700	2,367	4,666	4,180	5,163
800	2,187	5,079	3,800	4,981
900	2,044	5,245	3,421	4,729
1,000	1,908	5,217	3,061	4,438
1,100	1,885	4,747	3,891	5,172
1,200	1,826	4,902	3,653	5,000
1,300	1,771	4,973	3,421	4,809
1,400	1,736	4,981	3,202	4,609
1,500	1,695	4,928	2,989	4,404
1,600	1,670	4,855	2,802	4,223
1,700	1,621	4,759	2,620	4,044
1,800	1,558	4,646	2,304	3,877
1,900	1,529	4,526	2,303	3,718
2,000	1,544	4,408	2,169	3,574
2,100	1,532	4,294	2,046	3,447
2,300	1,483	4,079	1,851	3,240
2,500	1,514	3,871	1,689	3,042
2,700	1,559	3,681	1,571	2,864
2,900	1,514	3,503	1,457	2,703
3,300	1,445	3,166	1,292	2,390
3,700	1,533	2,912	1,259	2,182
4,100	1,681	2,723	1,285	2,045
4,500	1,745	2,540	1,365	1,943

Railroad Site WUA (ft^2)

	Fall/Spring-Run Chinook		Steelhead/Rainbow Trout	
Flow (cfs)	Fry	Juvenile	Fry	Juvenile
150	1,486	579	999	578
250	1,397	643	903	562
300	1,357	705	884	598
350	1,304	736	851	595
400	1,283	848	866	678
500	1,227	961	845	745
600	1,192	1,049	840	801
700	1,202	1,064	805	781
800	1,180	1,098	794	789
900	1,228	1,028	760	710
1,000	1,186	1,096	767	758
1,100	1,160	1,163	772	817
1,200	1,153	1,156	759	806
1,300	1,137	1,142	755	796
1,400	1,154	1,144	766	800
1,500	1,176	1,140	769	788
1,600	1,204	1,089	762	754
1,700	1,189	1,122	773	778
1,800	1,186	1,102	768	761
1,900	1,185	1,095	768	757
2,000	1,196	1,077	770	741
2,100	1,191	1,071	775	739
2,300	1,194	1,074	787	741
2,500	1,218	1,055	795	733
2,700	1,231	1,056	807	739
2,900	1,239	1,023	821	734
3,300	1,254	978	837	726
3,700	1,264	944	842	722
4,100	1,297	892	876	717
4,500	1,361	825	868	676

Englebright Dam to Daguerre Dam WUA (ft^2)

Flow (cfs)	Fall/Spring-Run Chinook Fry	Fall/Spring-Run Chinook Juvenile	Steelhead/Rainbow Trout Fry	Steelhead/Rainbow Trout Juvenile
400	302,123	122,133	599,581	260,145
500	298,488	138,895	585,381	276,824
600	298,825	152,572	572,320	289,943
700	299,466	166,013	560,190	302,568
800	299,897	178,300	547,332	312,547
900	298,926	186,977	534,750	318,355
1,000	298,855	191,242	522,707	319,124
1,100	298,278	192,140	508,900	315,375
1,200	294,824	192,367	495,958	311,980
1,300	291,956	192,771	485,318	309,000
1,400	288,384	192,045	475,847	304,243
1,500	288,495	187,724	465,245	295,824
1,600	292,850	184,288	464,076	289,786
1,700	296,860	180,222	452,584	283,168
1,800	301,645	178,457	452,388	279,370
1,900	308,573	178,478	444,168	271,911
2,000	317,521	177,265	442,151	275,250
2,100	325,632	177,260	439,185	274,506
2,300	343,055	177,837	435,226	274,694
2,500	357,312	177,681	432,375	273,868
2,700	378,930	178,032	433,345	274,816
2,900	393,057	176,603	435,121	275,553
3,100	400,940	169,937	435,021	273,544
3,300	414,559	166,561	439,016	275,456
3,500	426,434	164,062	444,541	278,187
3,700	423,915	161,574	447,457	281,146
3,900	427,090	160,021	449,583	283,580
4,100	438,631	158,840	454,010	288,168
4,300	441,907	157,479	456,710	293,258
4,500	438,048	158,711	456,399	298,668

Daguerre Dam to Feather River WUA (ft^2)

	Fall/Spring-Run Chinook		Steelhead/Rainbow Trout	
Flow (cfs)	Fry	Juvenile	Fry	Juvenile
150	242,018	5,462	314,630	141,898
250	222,201	7,839	345,955	179,981
300	226,323	9,078	362,156	197,410
350	222,330	10,208	366,499	212,152
400	217,173	11,494	376,984	226,030
500	209,470	13,617	377,907	244,499
600	206,211	15,275	373,177	254,079
700	203,798	16,509	366,091	259,719
800	202,380	17,162	355,400	259,289
900	204,501	17,380	346,278	256,295
1,000	205,468	17,516	338,222	254,003
1,100	206,984	17,820	338,334	262,834
1,200	206,595	18,105	327,971	262,338
1,300	211,182	18,516	319,380	263,390
1,400	216,501	18,873	311,249	264,171
1,500	224,117	19,166	304,079	264,193
1,600	232,810	19,410	299,066	264,575
1,700	241,316	19,627	295,295	264,932
1,800	250,981	19,797	290,876	265,610
1,900	260,571	19,948	289,350	266,711
2,000	270,629	20,089	289,465	268,750
2,100	274,353	19,874	286,122	265,692
2,300	299,096	19,192	284,554	260,481
2,500	290,583	18,121	282,427	252,130
2,700	304,038	16,693	286,519	241,954
2,900	313,680	15,453	291,831	233,586
3,300	319,929	13,929	300,517	227,165
3,700	328,309	13,483	308,800	228,394
4,100	337,756	13,195	319,888	232,181
4,500	338,686	13,214	327,529	237,185

APPENDIX M
COMBINED HABITAT SUITABILITY OF FRY AND JUVENILES

Timbuctoo Steelhead/Rainbow Trout Fry, Q = 917 cfs

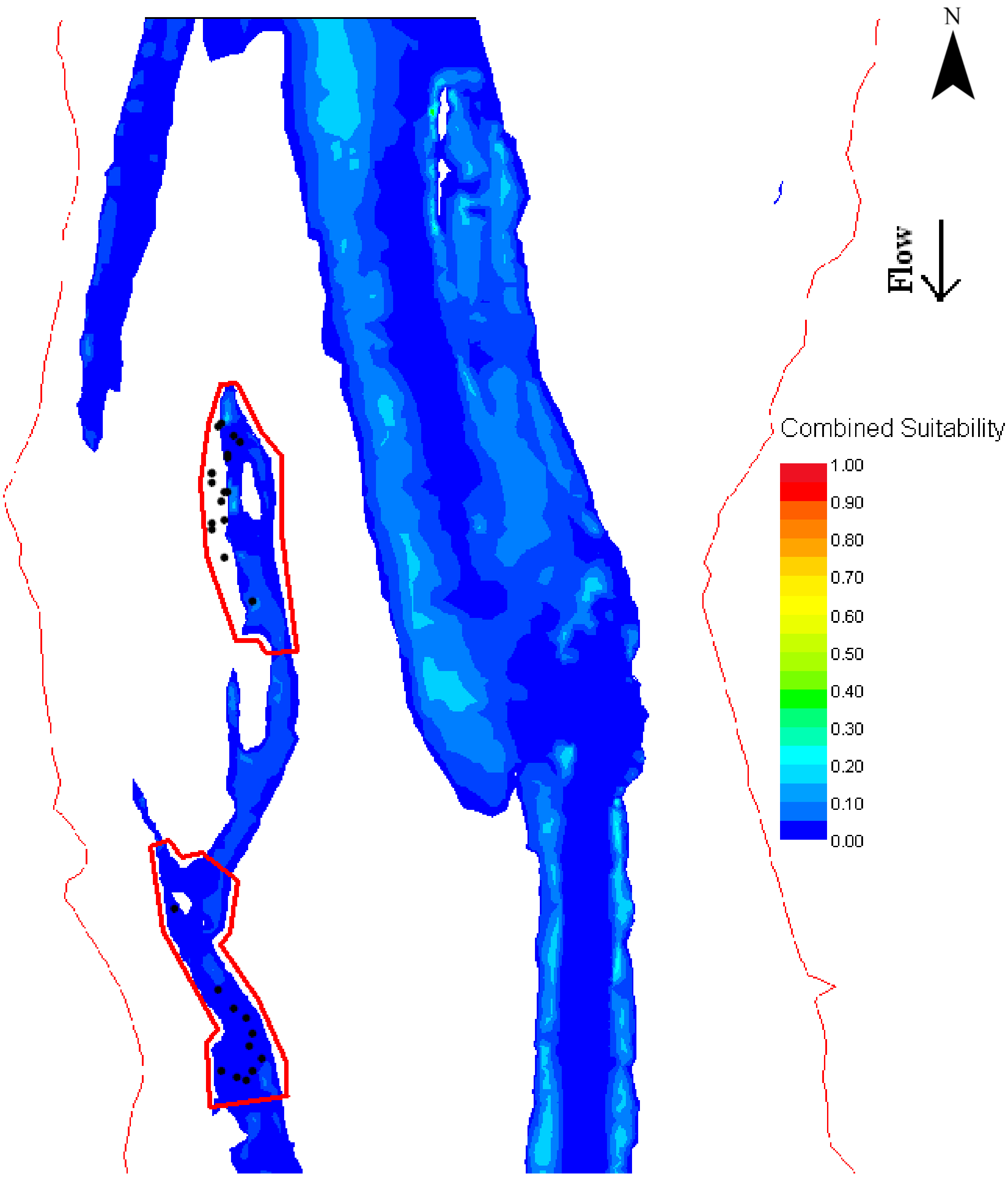

Scale: 1: 2304

• = fry locations. Red boxes delineate areas sampled.

Timbuctoo Steelhead/Rainbow Trout Fry, Q = 917 cfs

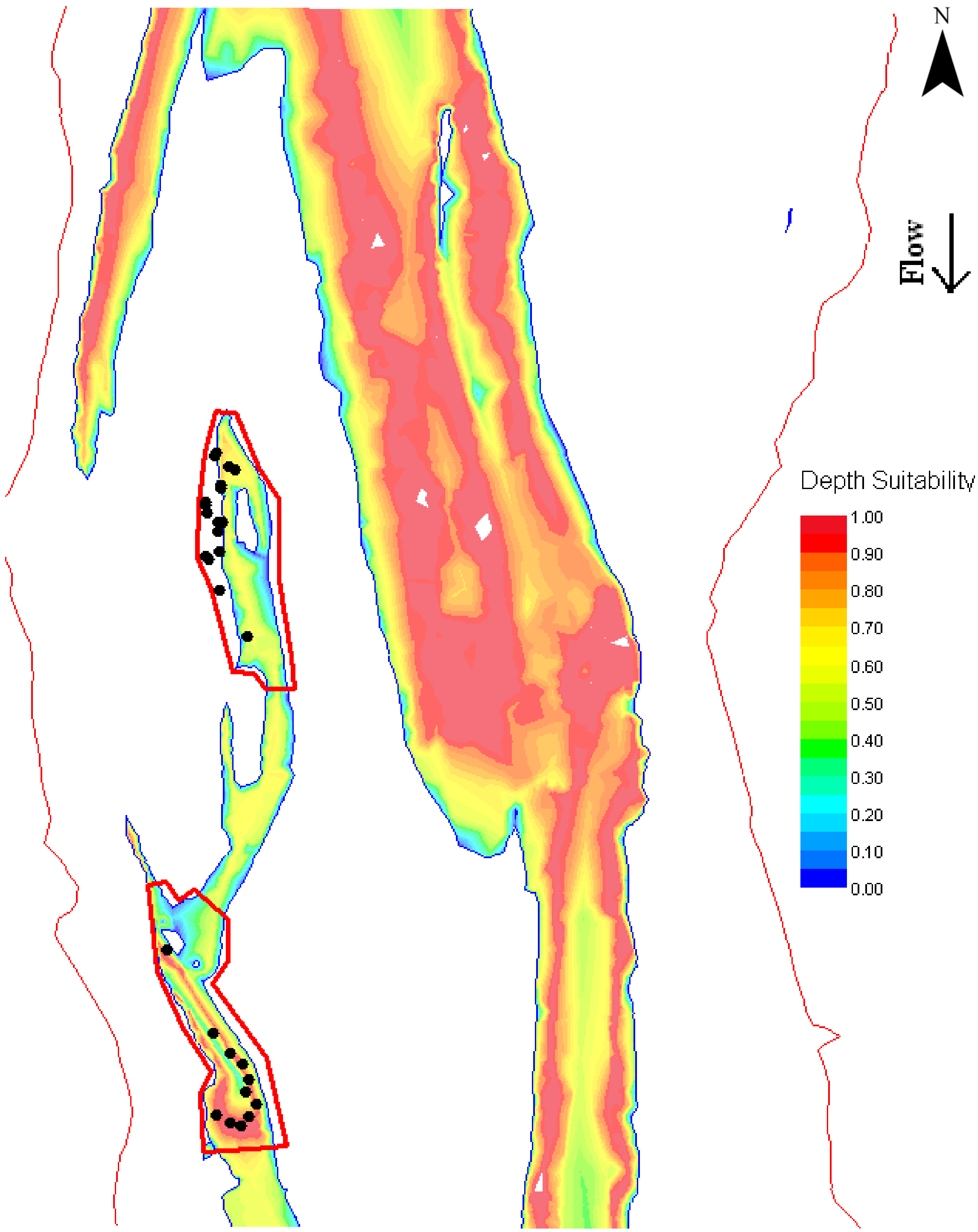

Scale: 1: 2304

• = fry locations. Red boxes delineate areas sampled.

Timbuctoo Steelhead/Rainbow Trout Fry, Q = 917 cfs

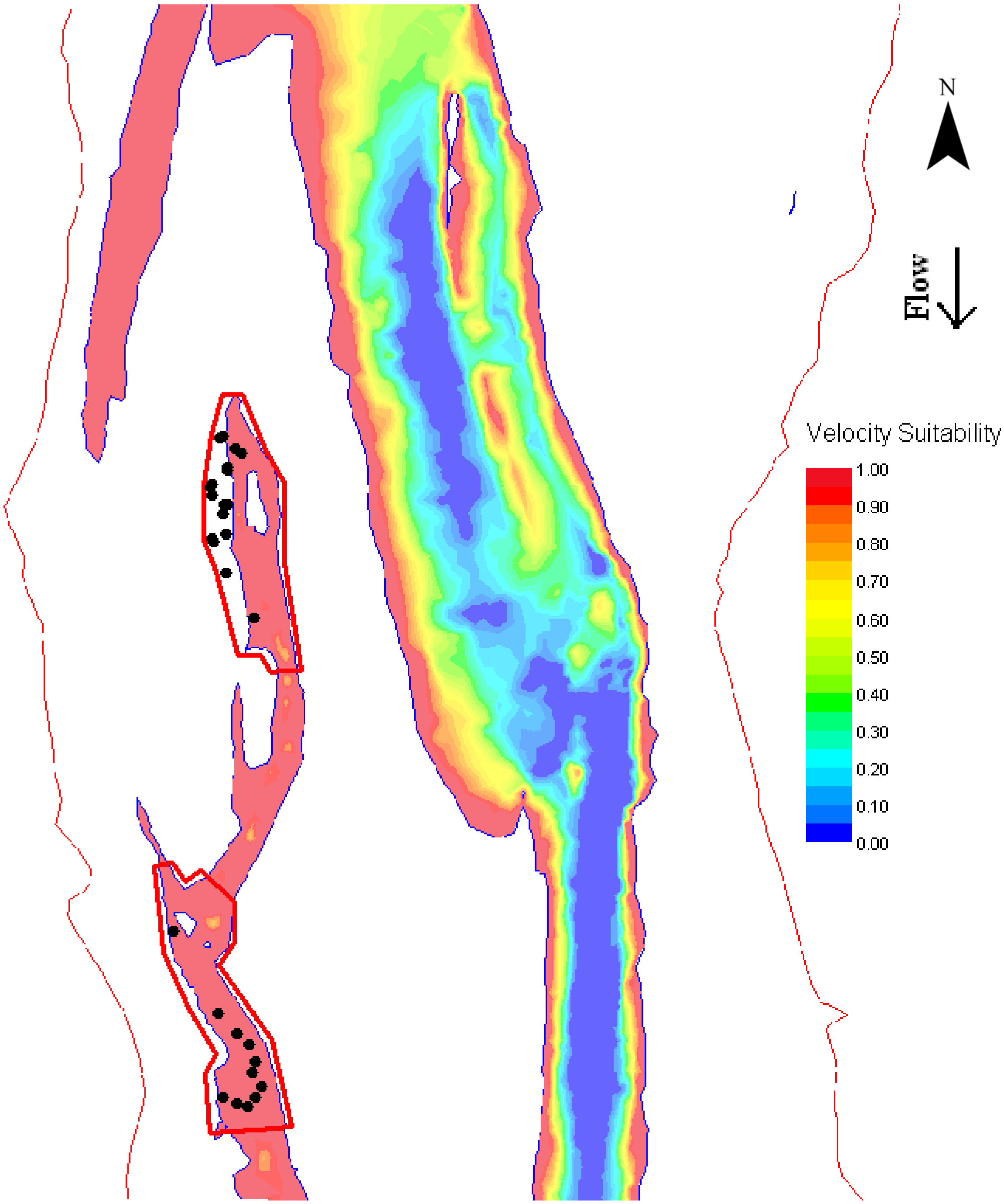

Scale: 1: 2304

• = fry locations. Red boxes delineate areas sampled.

Timbuctoo Steelhead/Rainbow Trout Fry, Q = 917 cfs

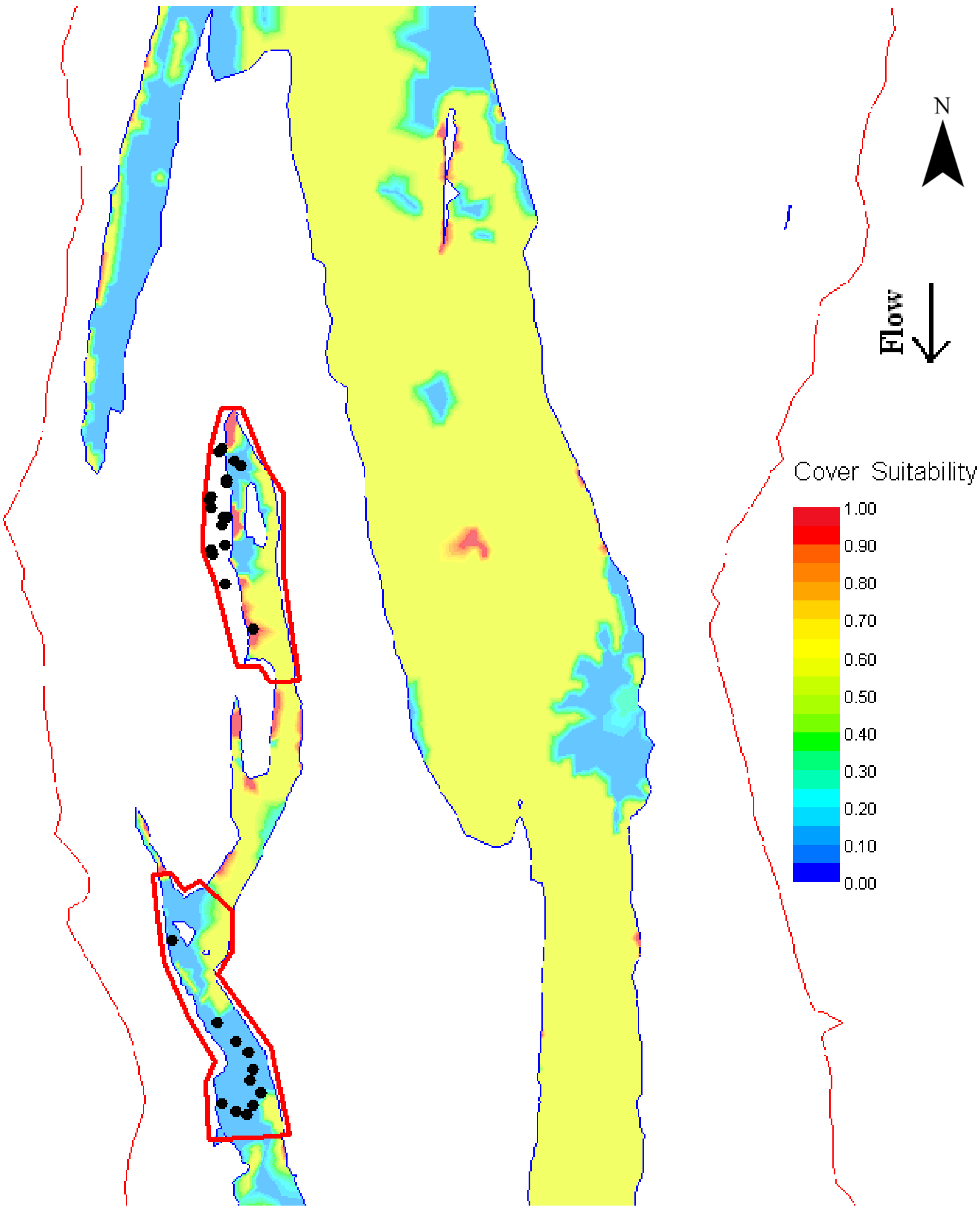

Scale: 1: 2304

• = fry locations. Red boxes delineate areas sampled.

Timbuctoo Steelhead/Rainbow Trout Fry, Q = 917 cfs

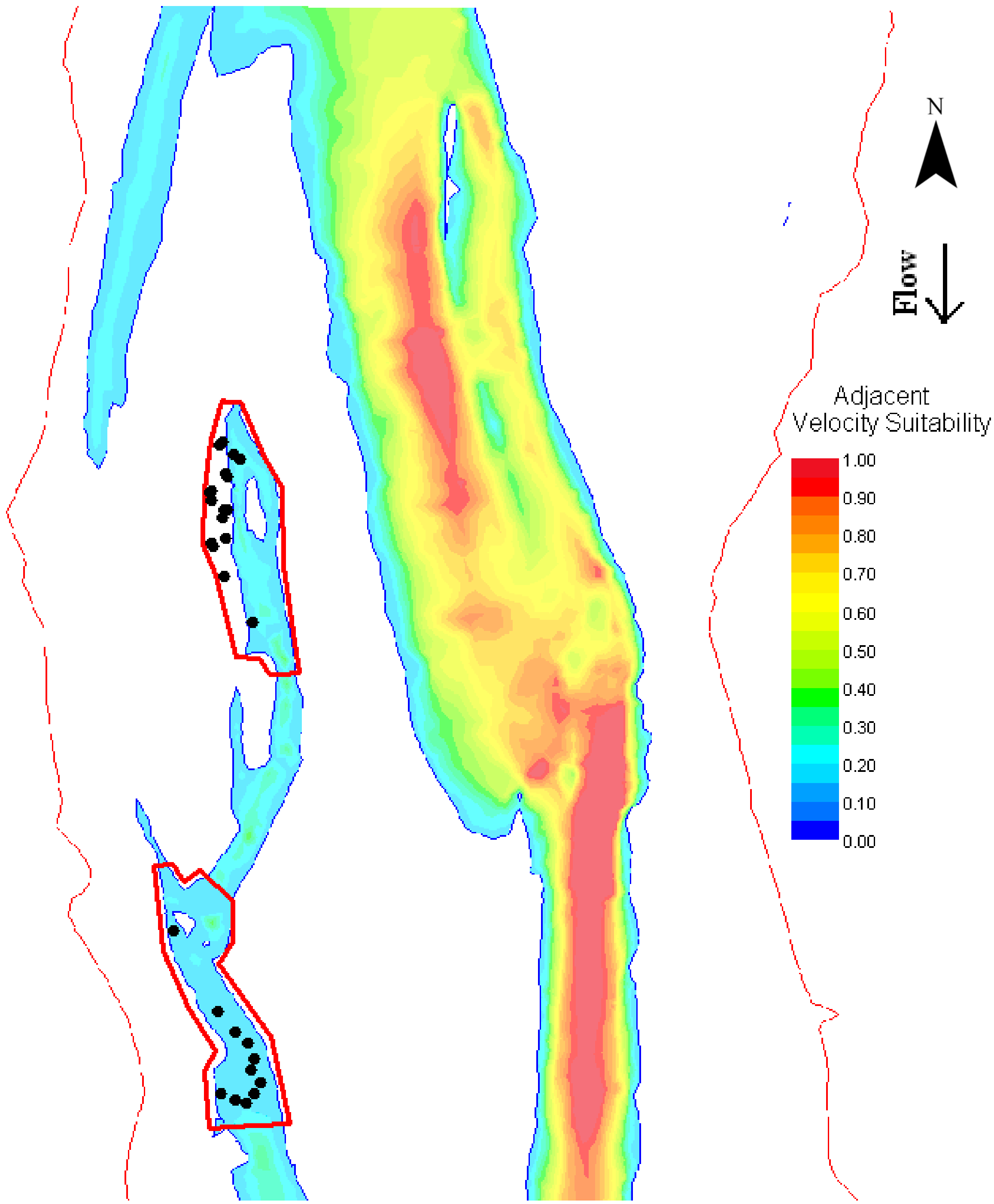

Scale: 1: 2304

• = fry locations. Red boxes delineate areas sampled.

Timbuctoo Steelhead/Rainbow Trout Juvenile, Q = 917 cfs

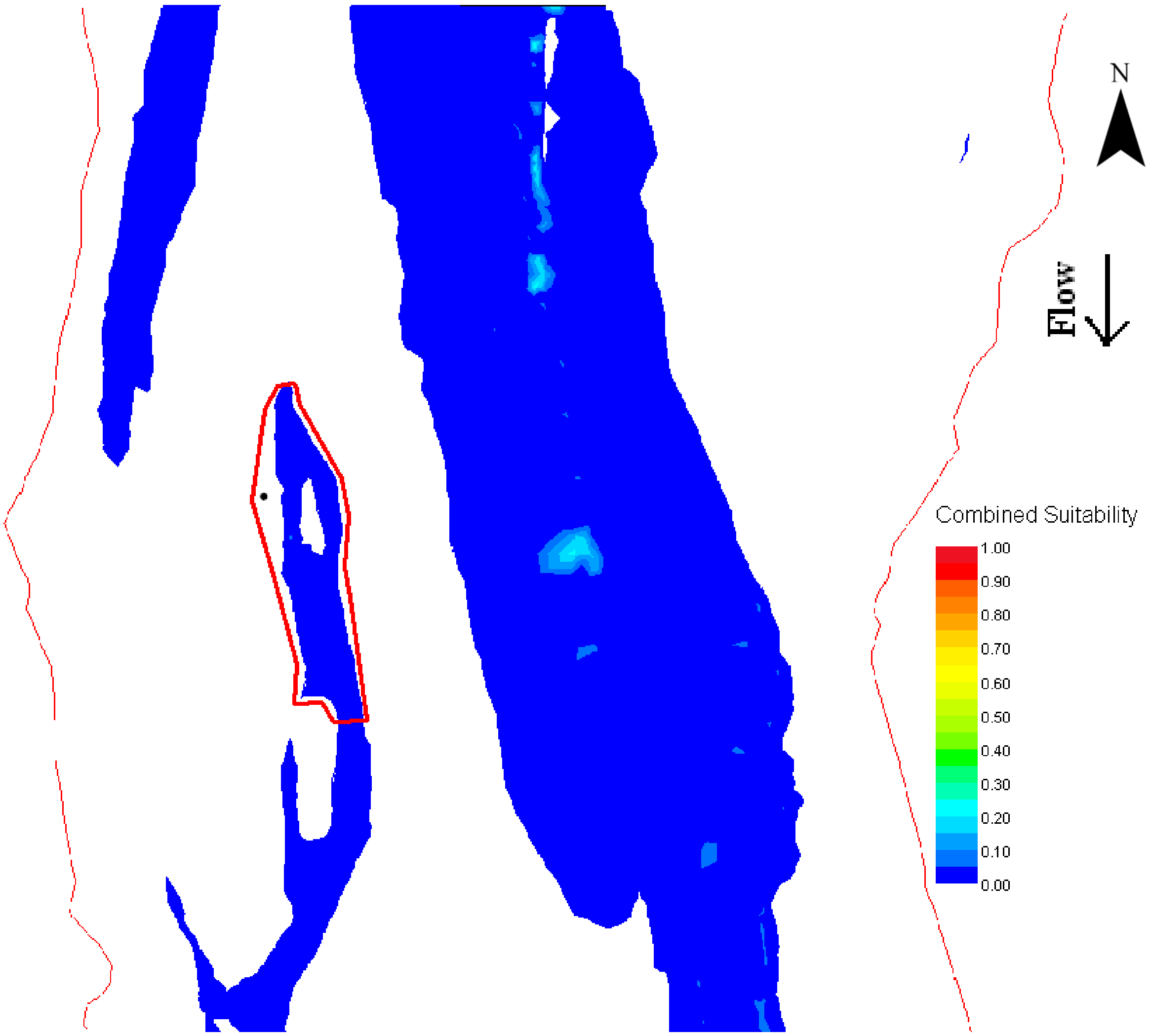

Scale: 1: 2304

• = juvenile locations. Red box delineates area sampled.

Timbuctoo Steelhead/Rainbow Trout Fry, Q = 2,022 cfs

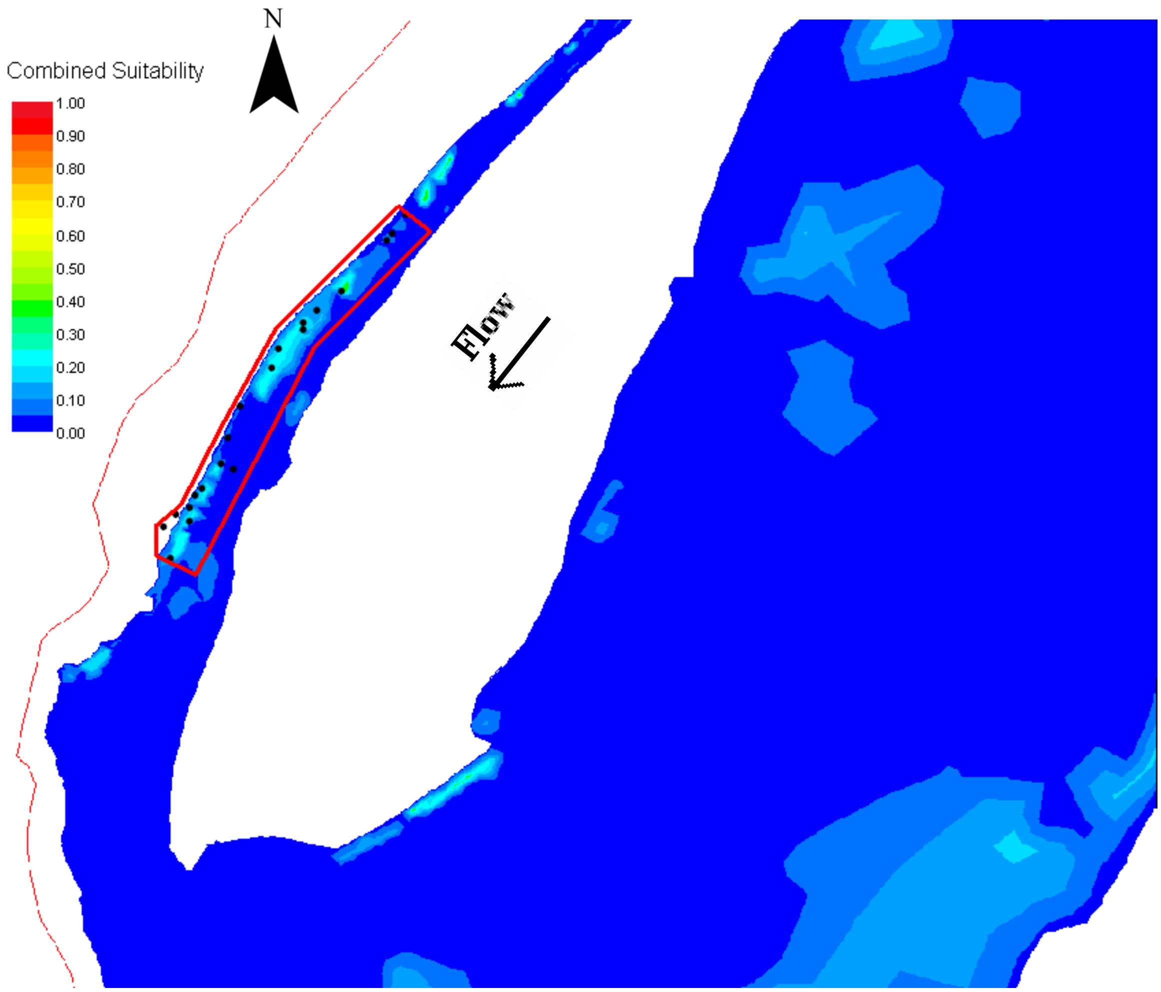

Scale: 1: 1350

• = fry locations. Red box delineates area sampled.

Timbuctoo Steelhead/Rainbow Trout Fry, Q = 2,022 cfs

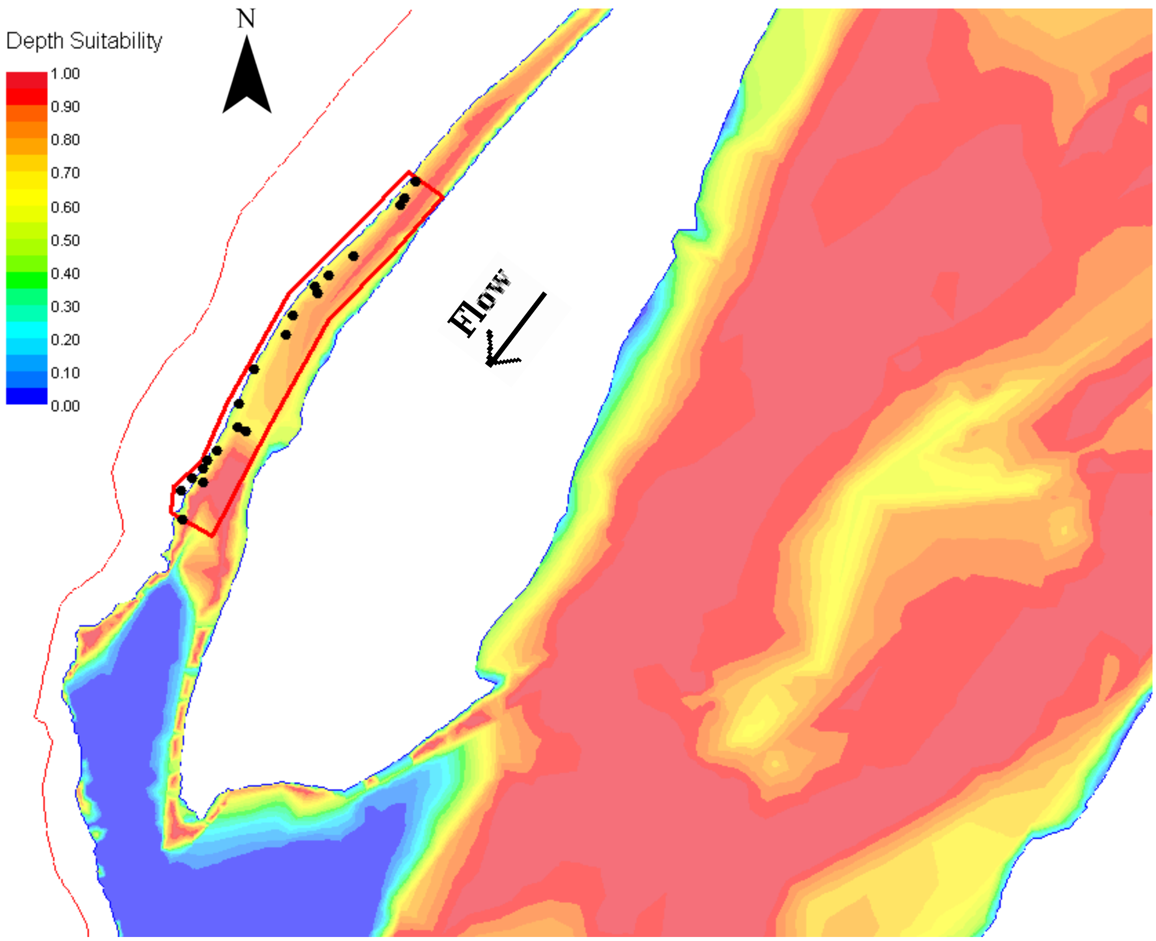

Scale: 1: 1350

• = fry locations. Red box delineates area sampled.

Timbuctoo Steelhead/Rainbow Trout Fry, Q = 2,022 cfs

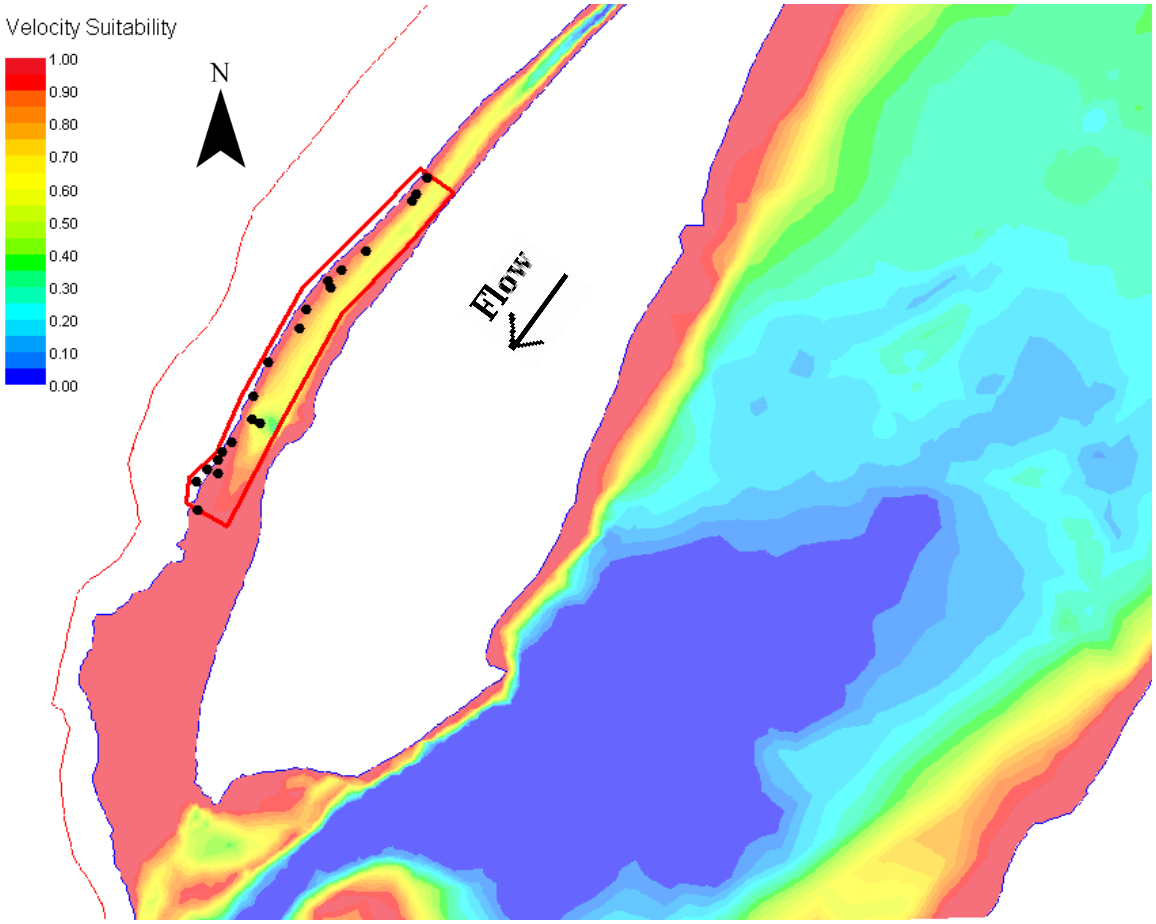

Scale: 1: 1392

• = fry locations. Red box delineates area sampled.

Timbuctoo Steelhead/Rainbow Trout Fry, Q = 2,022 cfs

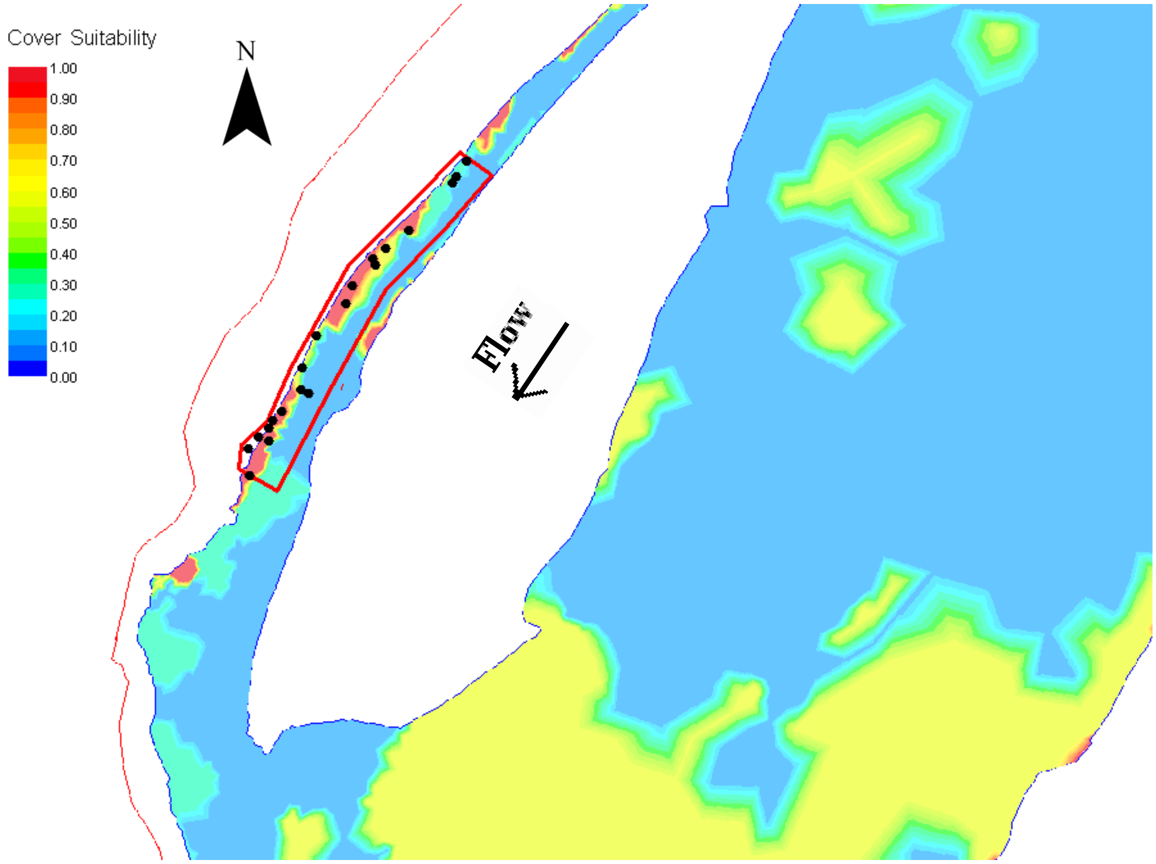

Scale: 1: 1392

• = fry locations. Red box delineates area sampled.

Timbuctoo Steelhead/Rainbow Trout Fry, Q = 2,022 cfs

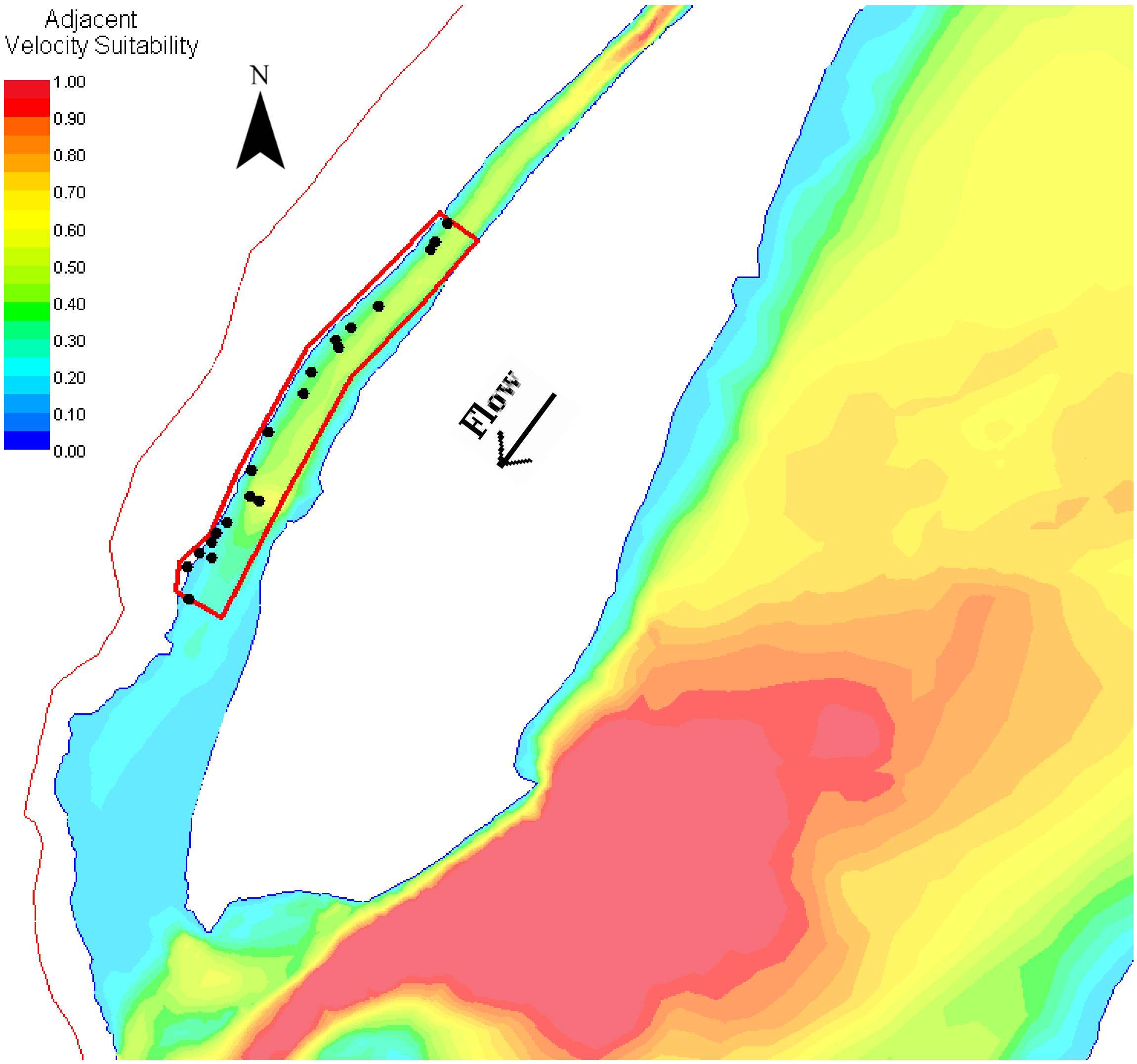

Scale: 1: 1392

• = fry locations. Red box delineates area sampled.

Timbuctoo Steelhead/Rainbow Trout Fry, Q = 1,963 cfs

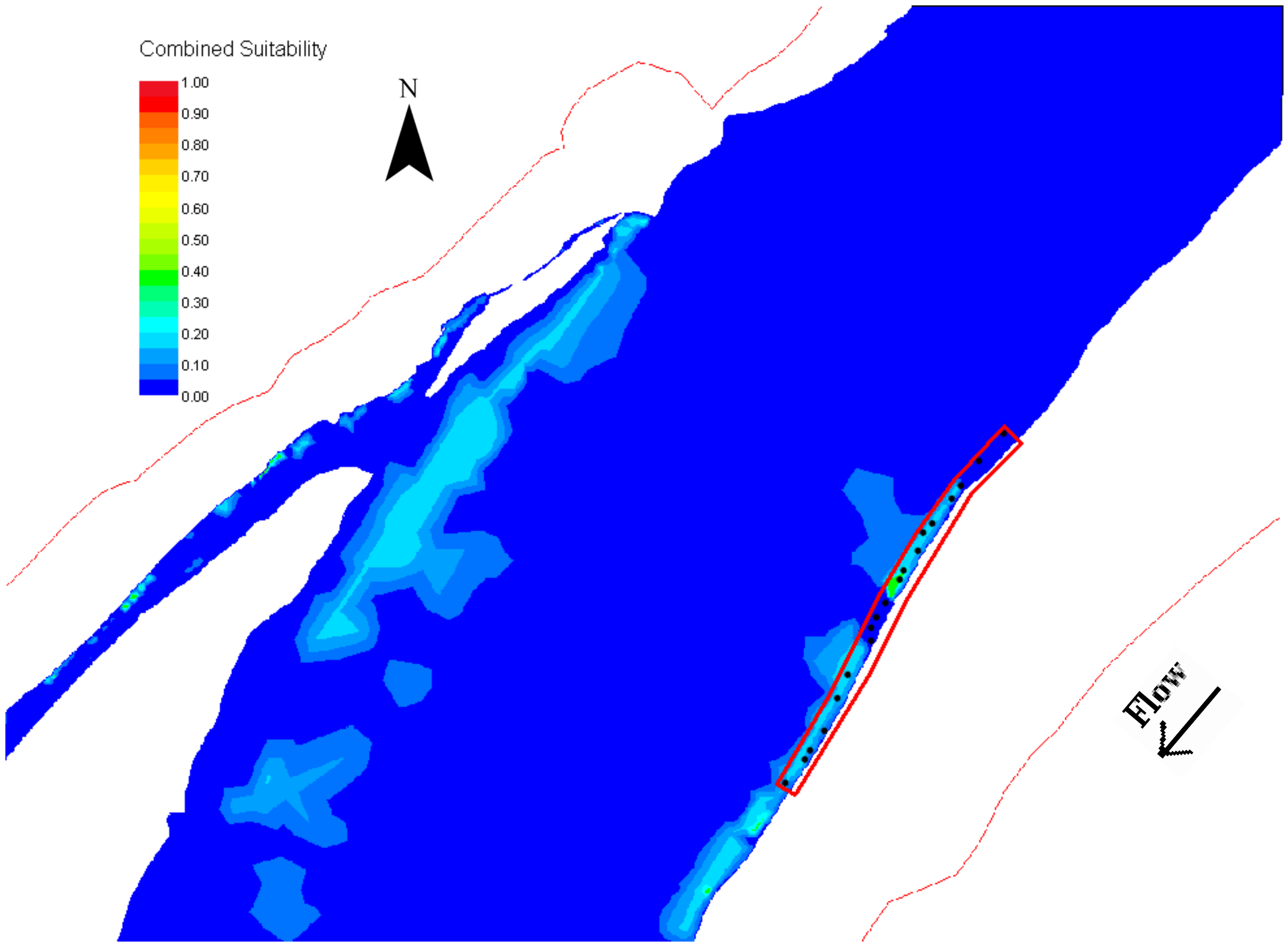

Scale: 1: 1600

• = fry locations. Red box delineates area sampled.

Hammond Fall/spring-Run Chinook Fry, Q = 2,207 cfs

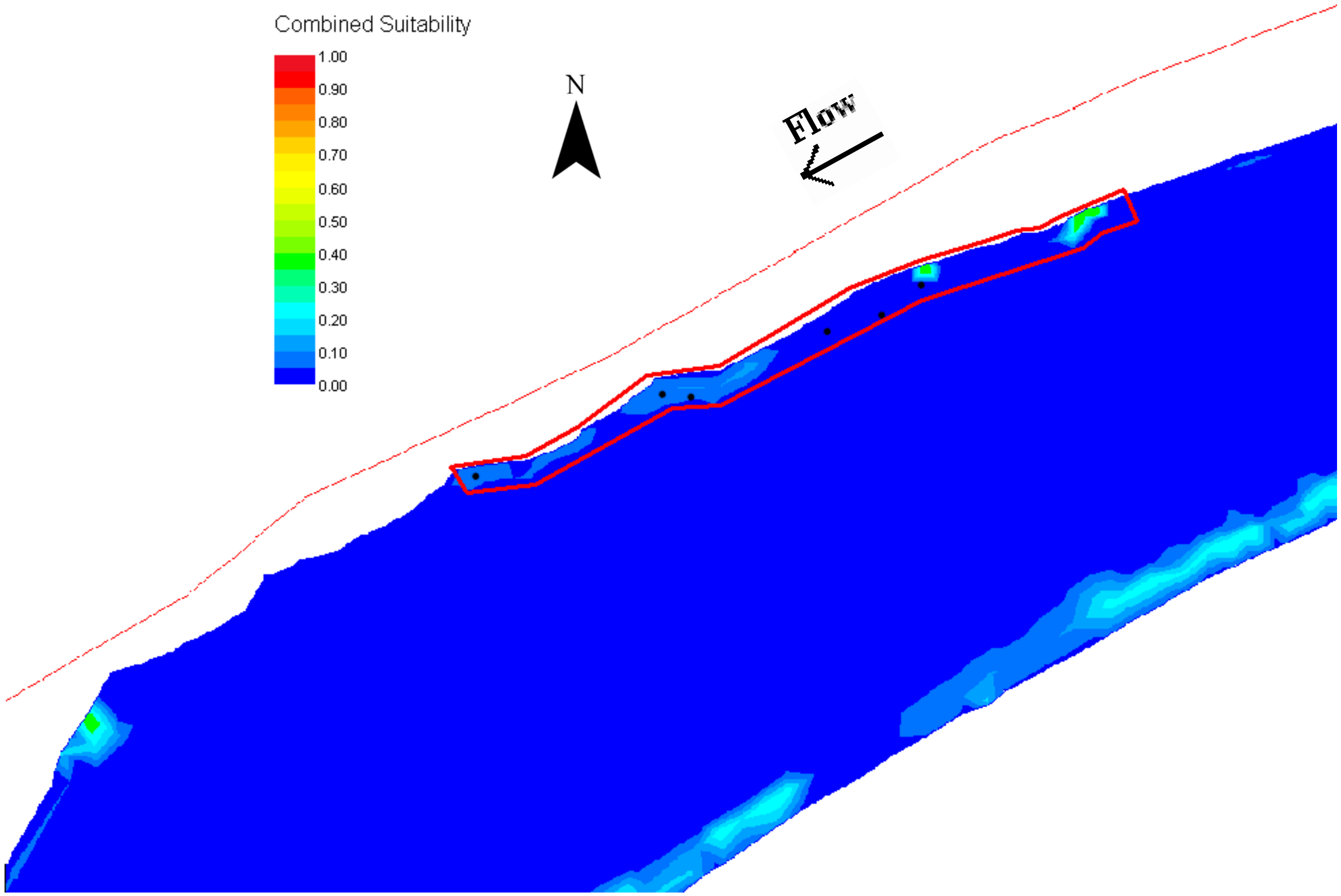

Scale: 1:944

• = fry locations. Red box delineates area sampled.

Hammond Fall/spring-Run Chinook Juvenile, Q = 2,207 cfs

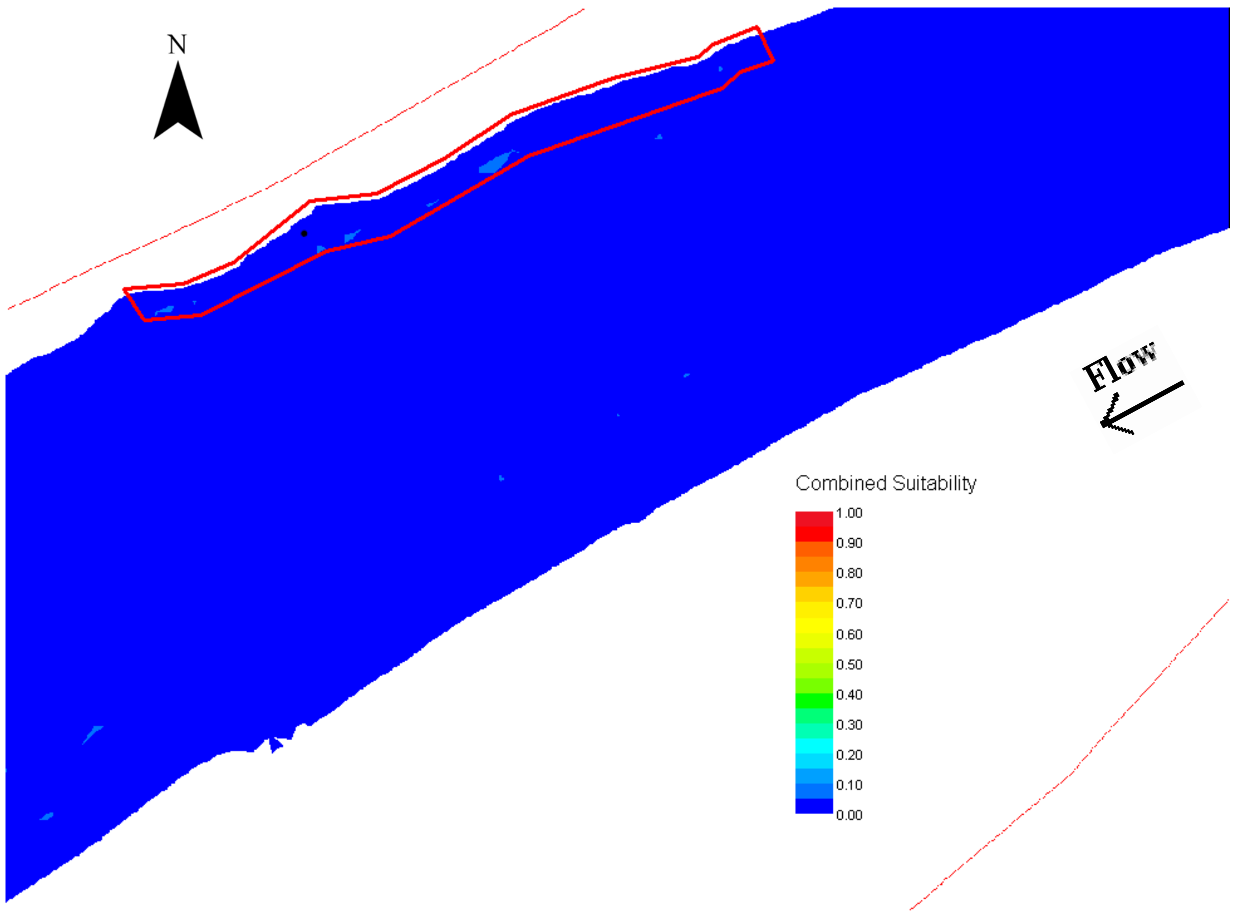

Scale: 1:1011

• = juvenile locations. Red box delineates area sampled.

Hammond Steelhead/Rainbow Trout Fry, Q = 2,207 cfs

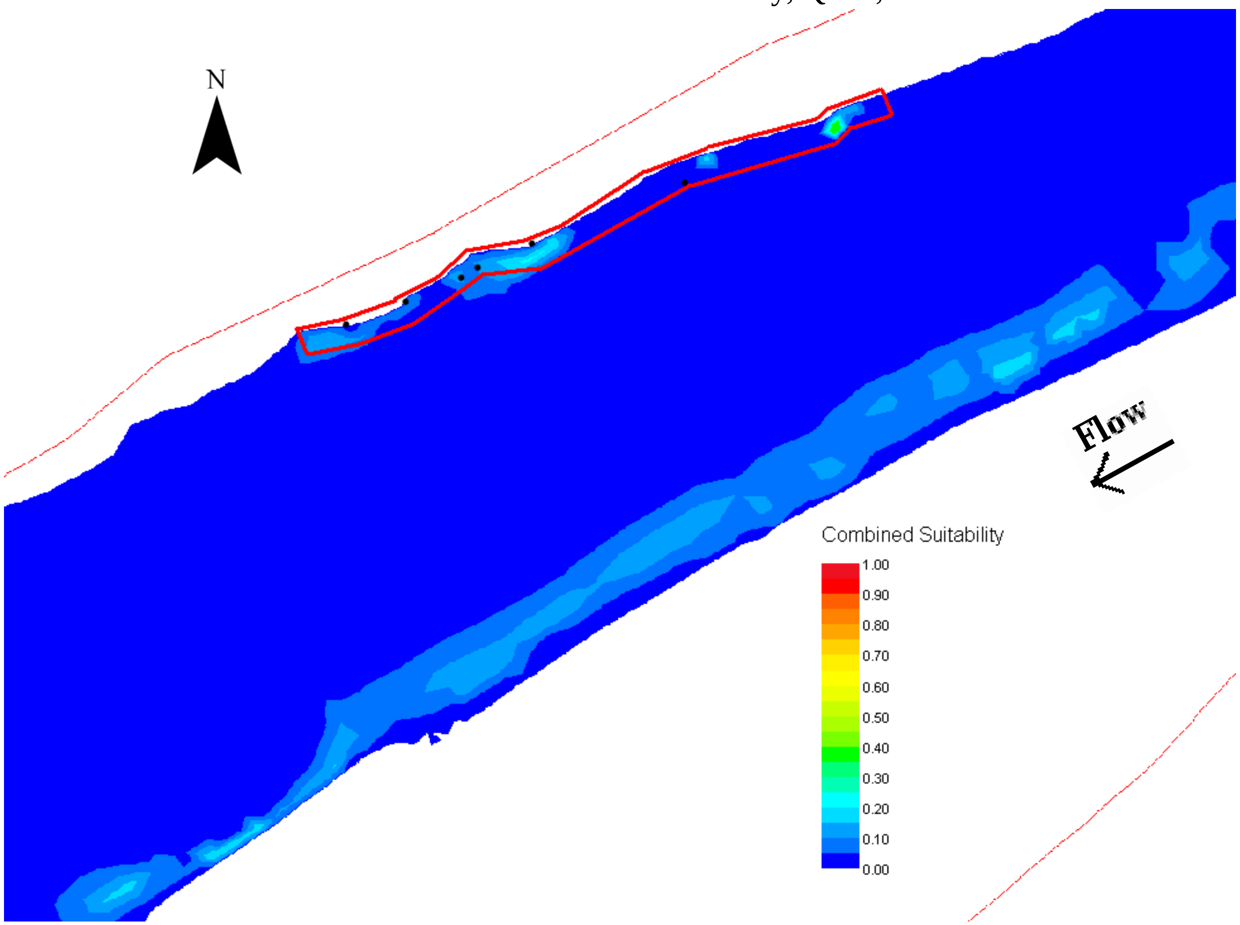

Scale: 1:1087

• = fry locations. Red box delineates area sampled.

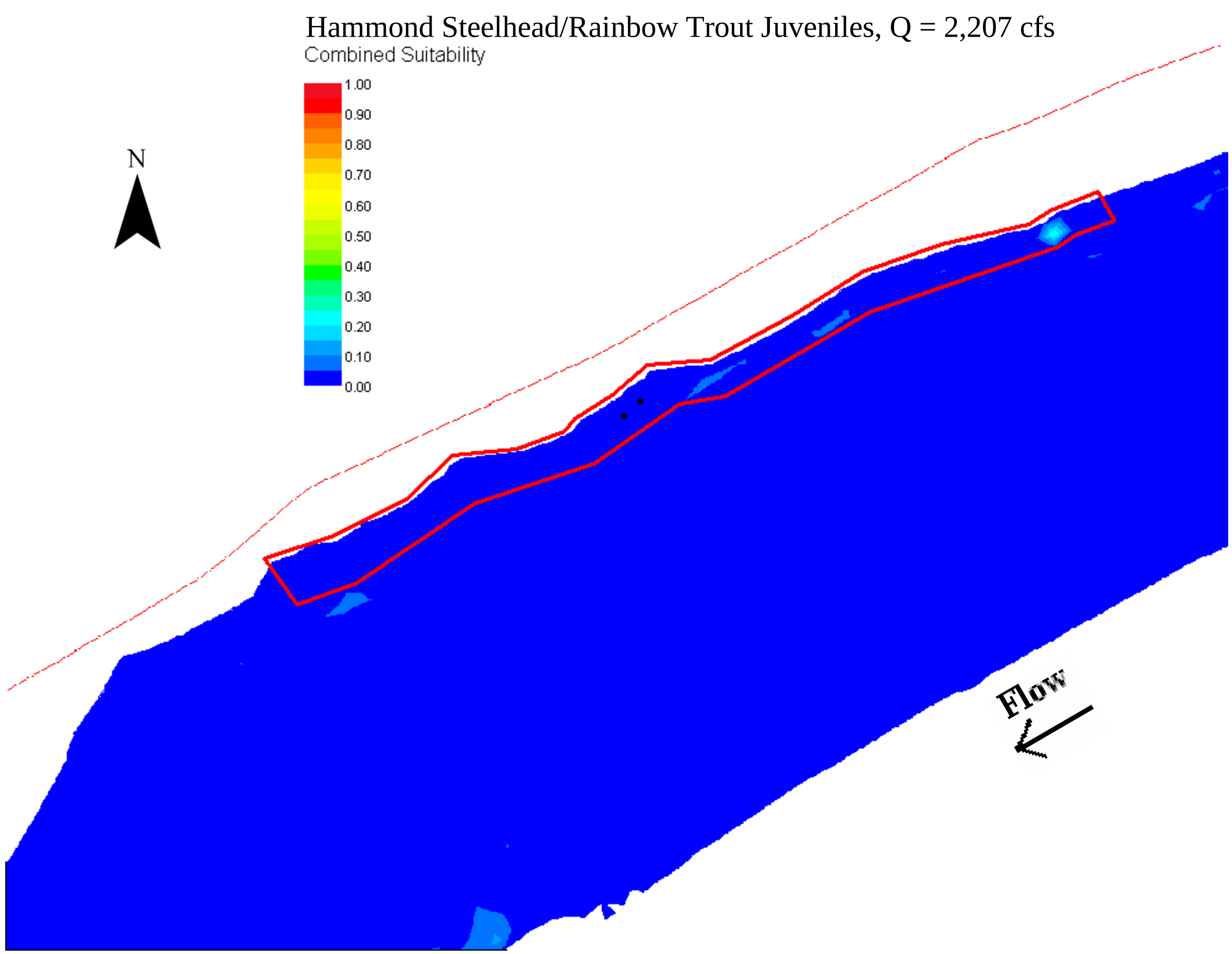

Scale: 1:720

• = juvenile locations. Red box delineates area sampled.

Hammond Steelhead/Rainbow Trout Fry, Q = 708 cfs

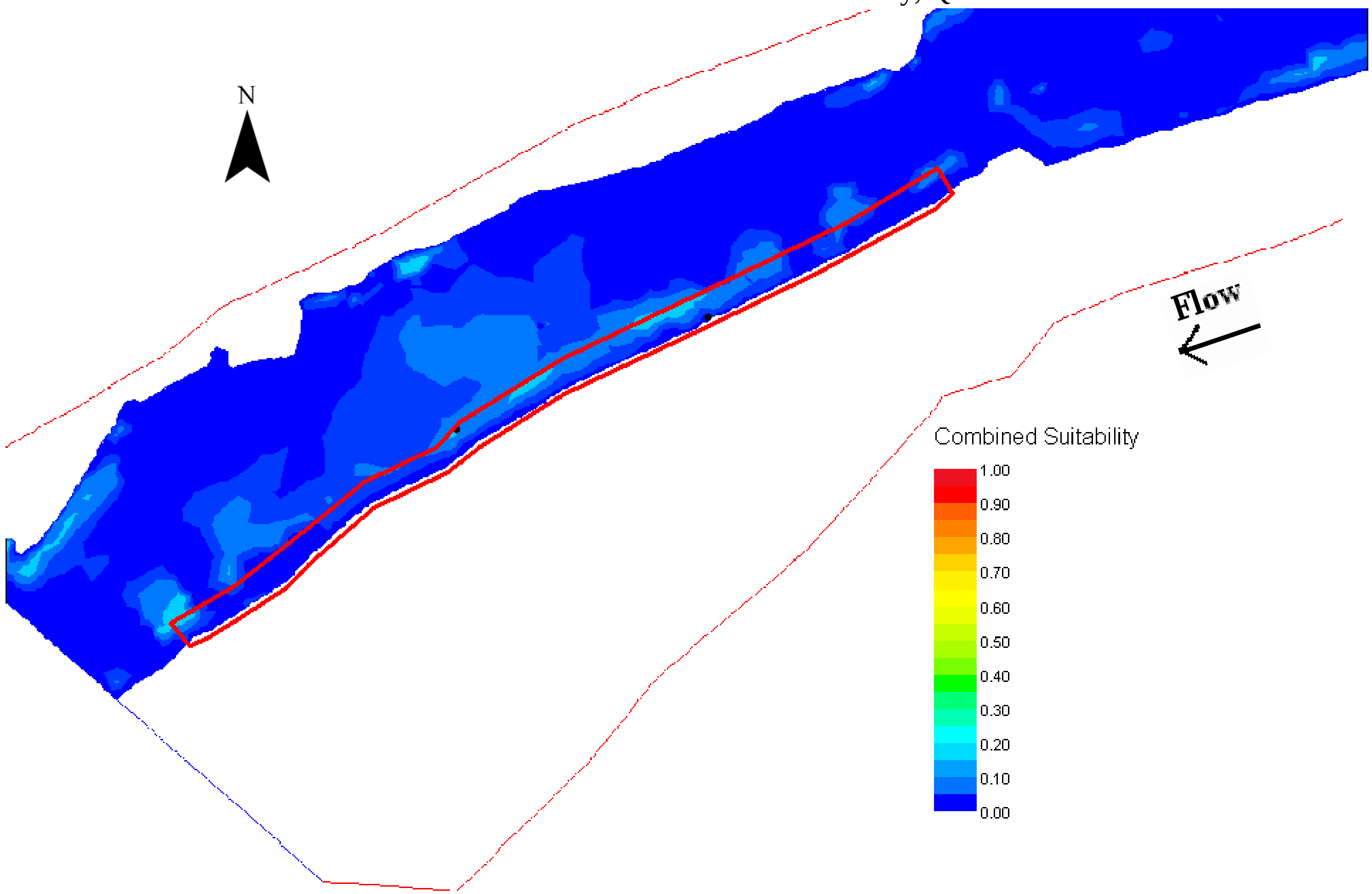

Scale: 1:720

• = fry locations. Red box delineates area sampled.

Lower Daguerre Fall/spring-Run Chinook Fry, Q = 1,560 cfs

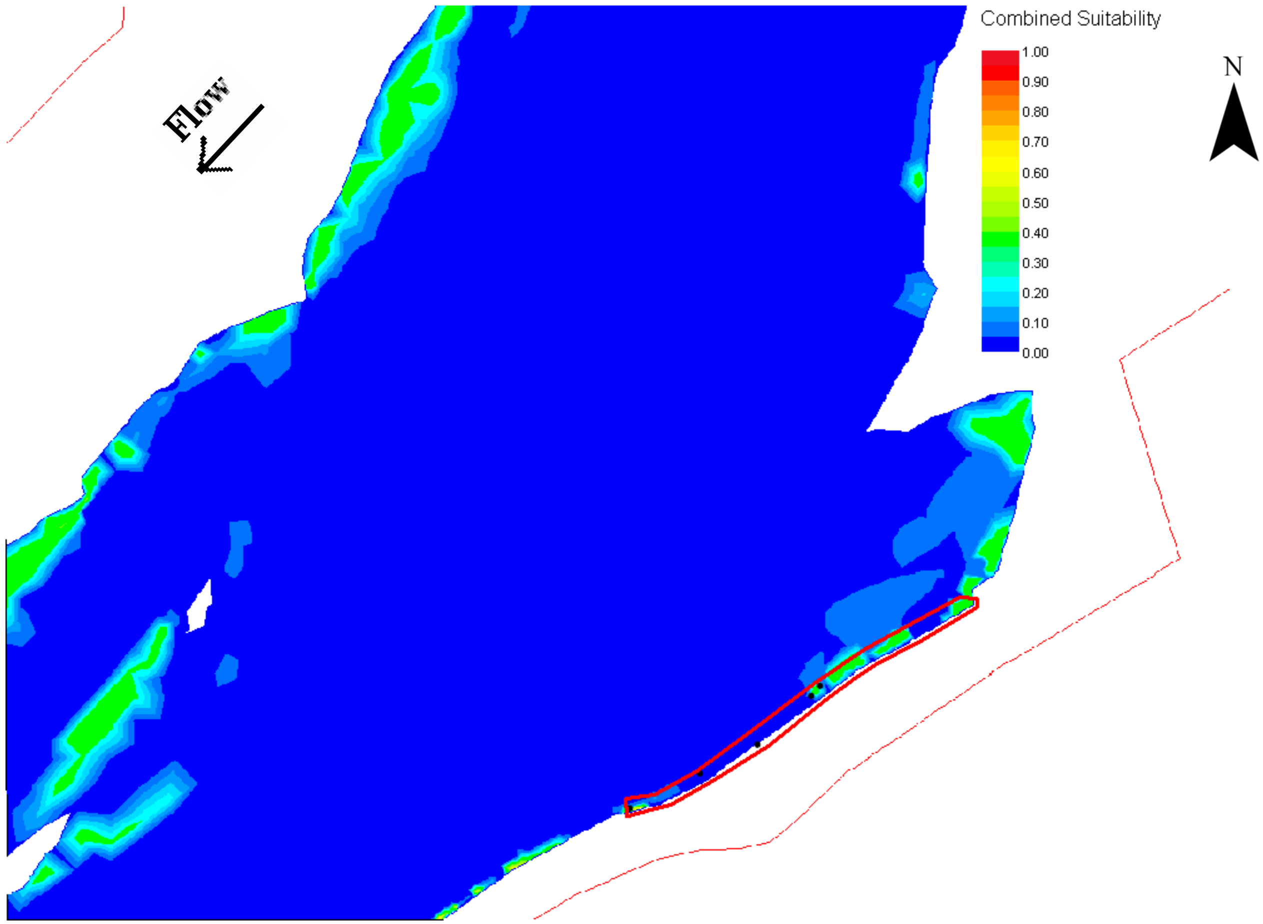

Scale: 1:1158

• = fry locations. Red box delineates area sampled.

Lower Daguerre Fall/spring-Run Chinook Juvenile, Q = 1,560 cfs

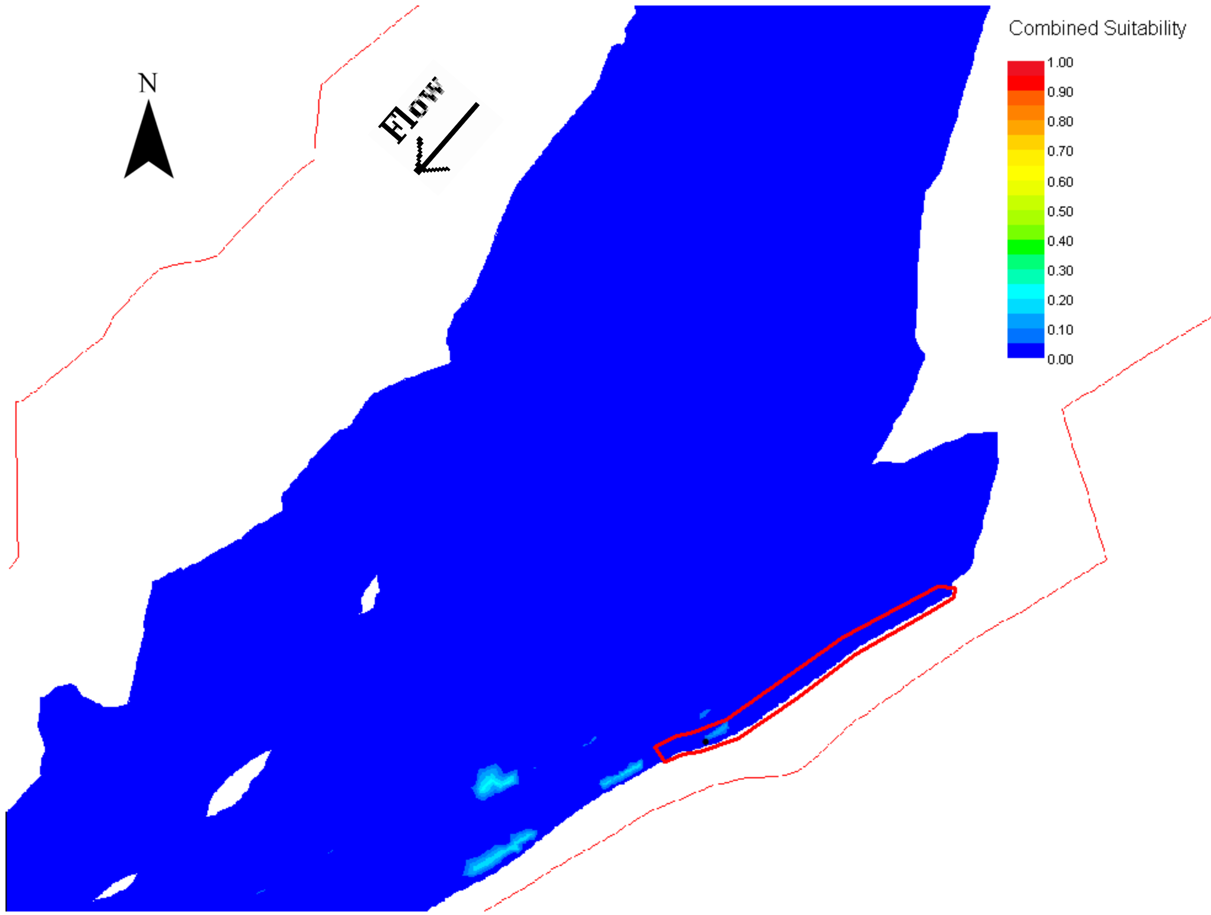

Scale: 1:1406

• = juvenile locations. Red box delineates area sampled.

Side-Channel Fall/spring-Run Chinook Fry, Q = 2,430 cfs

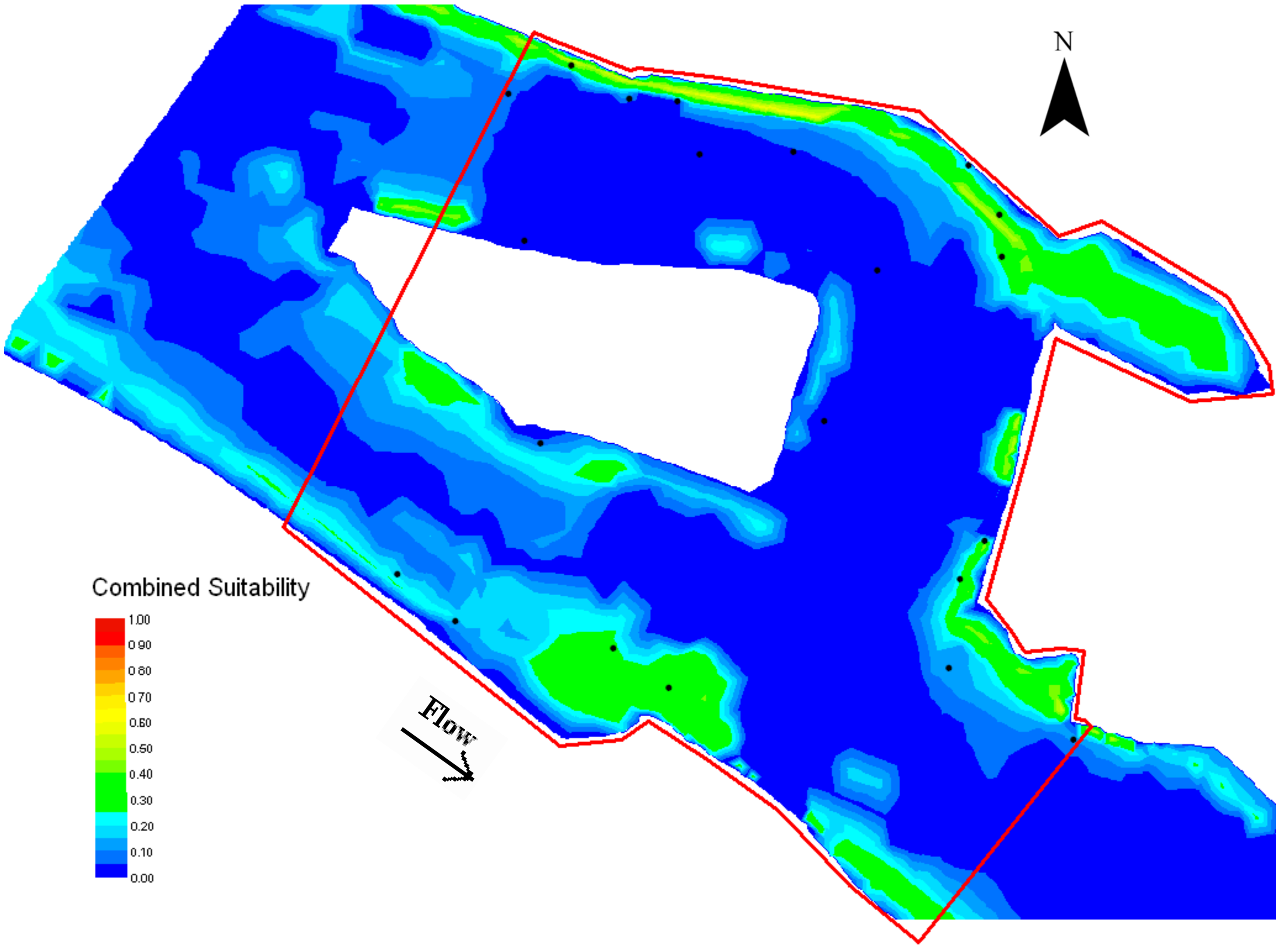

Scale: 1:274

• = juvenile locations. Red box delineates area sampled.

Side-Channel Fall/spring-Run Chinook Juveniles, Q = 2,430 cfs

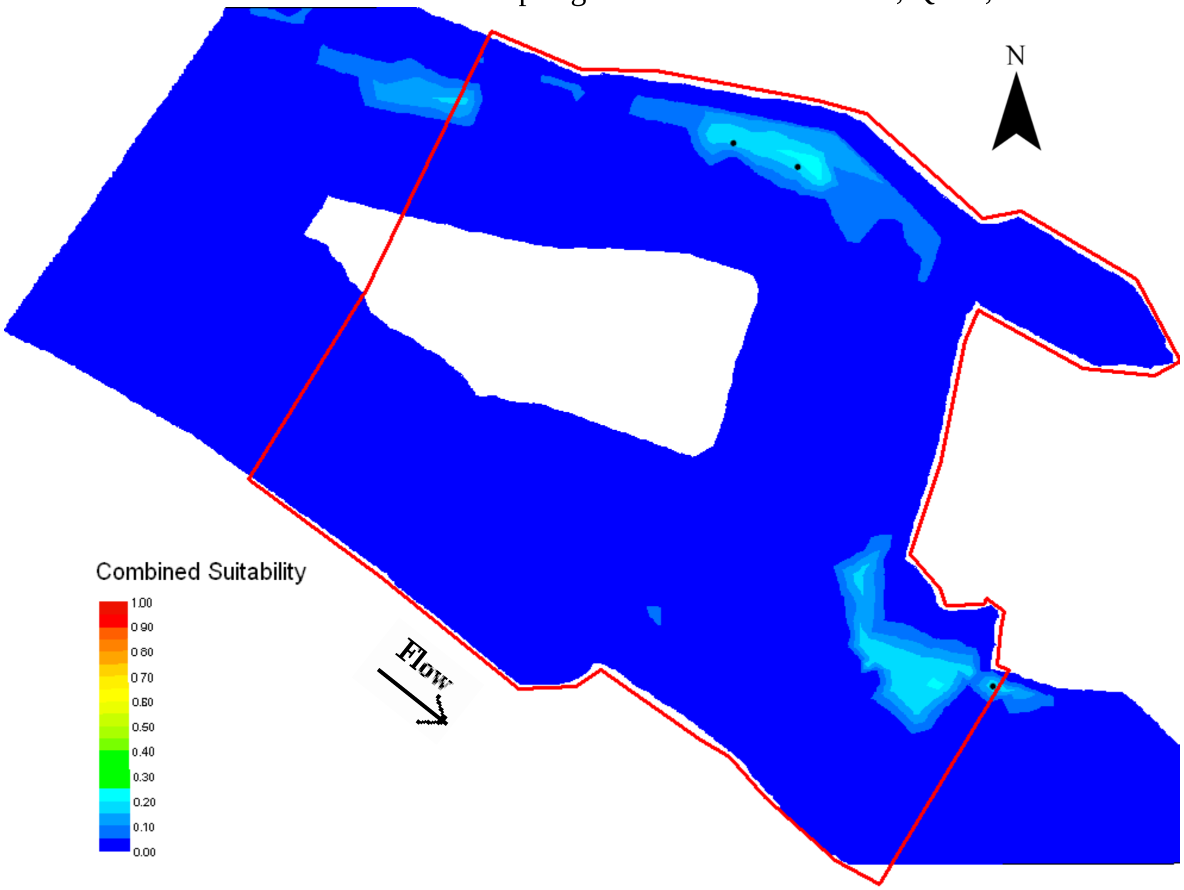

Scale: 1:279

• = juvenile locations. Red box delineates area sampled.

APPENDIX N
ACRONYMS

LIST OF ACRONYMS

2-D	Two dimensional
ACE	U.S. Army Corps of Engineers
ADCP	Acoustic Doppler Current Profiler
ASCII	American Standard Code for Information Interchange
AV	Adjacent Velocity
BCG	Bar Complex Glide
BCP	Bar Complex Pool
BCRi	Bar Complex Riffle
BCRu	Bar Complex Run
C	Contingency coefficient
CDFG	California Department of Fish and Game
cdg	Computational Mesh file
CFG	Configuration File
cfs	cubic feet per second
CSI	Combined Habitat Suitability Index
d85	median diameter for which 85 percent of the particles are smaller
Exp	exponential function
FLOMANN	Flow Manning's n
ft/s	feet per second
FWG	Flat Water Glide
FWP	Flat Water Pool
FWRi	Flat Water Riffle
FWRu	Flat Water Run
GIS	Geographic Information System
GPS	Global Positioning System
h	depth
HABTAV	Adjacent Velocity Habitat Analysis
HSC	Habitat Suitability Criteria
HSI	Habitat Suitability Index
IFG4	Instream Flow Group Program 4
IFIM	Instream Flow Incremental Methodology
m	meter
m/s	meters per second
MANSQ	Mannings Equation Discharge (Q) Simulation Program
Max F	maximum Froude Number
MHU	mesohabitat unit
n	number
p	probability
PHABSIM	Physical Habitat Simulation Model
PVC	Poly Vinyl Chloride

q	unit discharge
QI	Quality Index
R^2	coefficient of determination
RHABSIM	Riverine Habitat Simulation Model
River2D	Two dimensional depth averaged model of river hydrodynamics and fish habitat
RM	River Mile
SCG	Side Channel Glide
SCP	Side Channel Pool
SCRi	Side Channel Riffle
SCRu	Side Channel Run
SCUBA	Self-Contained Underwater Breathing Apparatus
SI	Suitability Index
Sol Δ	solution change
SL	Standard Length
SZF	stage of zero flow
T	Chi-squared test statistic
TIN	Triangulated Irregular Network
U	Mann-Whitney U test statistic
USFWS	U.S. Fish and Wildlife Service
USGS	U.S. Geological Survey
VAF	Velocity Adjustment Factors
WSEL	Water Surface Elevation
WSP	Water Surface Profile Program
WUA	Weighted Useable Area
XS1	downstream transect
XS2	upstream transect
YOY	Young of Year